Non-small Cell Lung Cancer
Current Therapies and New Targeted Treatments

Edited by
Junji Uchino

MDPI

Non-small Cell Lung Cancer: Current Therapies and New Targeted Treatments

Non-small Cell Lung Cancer: Current Therapies and New Targeted Treatments

Editor

Junji Uchino

MDPI

This is a reprint of articles from the Special Issue published online in the open access journal *Journal of Clinical Medicine* (ISSN 2077-0383) (available at: https://www.mdpi.com/journal/jcm/special_issues/Cell_Lung_Cancer).

For citation purposes, cite each article independently as indicated on the article page online and as indicated below:

LastName, A.A.; LastName, B.B.; LastName, C.C. Article Title. *Journal Name* **Year**, *Volume Number*, Page Range.

Contents

About the Editor

Junji Uchino (M.D., Ph.D.) is currently working as an associate professor in the Department of Respiratory Medicine, Kyoto Prefectural University of Medicine. He graduated from Nagasaki University in 1999, admitted to Kyushu University Graduate School of Medicine in 2002 to engage in gene therapy research, and in 2006, he was awarded a PhD due to the results of research on adenovirus-induced lung cancer gene therapy. He has been studying at the University of Washington, St. Louis for 2 years since 2012, to develop gene therapy research for lung cancer. He has been working with the Department of Respiratory Medicine, Kyoto Prefectural University of Medicine, since 2016. He has set up a clinical trial group that is leading a multi-center clinical trial, has drafted a multi-investigator-initiated trial, and has gained a total of $5 million for consigned study as a principal investigator. Since 2020, he has also served as a guest editor in the journal *Frontiers Oncology*.

Preface to "Non-small Cell Lung Cancer: Current Therapies and New Targeted Treatments"

Conventional lung cancer treatments were once limited to surgery, radiation, and chemotherapy. However, gefitinib, a targeted drug, was launched in 2004, and the situation changed. Cancer cases that were highly responsive to gefitinib were later discovered to have epithelial growth factor receptor (EGFR) mutations. This discovery opened the door for biomarker-based treatment strategies. Subsequently, several EGFR-tyrosine kinase inhibitors (TKI) were developed, and they became a new mainstay of treatment for non-small cell lung cancer. In recent years, many mechanisms of resistance to EGFR-TKI have been elucidated; a mutation in the *T790M* gene at exon 20 is found in half of the resistant cases. Hence, osimertinib, which specifically inhibits EGFR despite this *T790*M gene mutation, was developed to achieve long-term progression-free survival. Other driver mutations that are similar to the EGFR mutation were discovered, including the *EML4-ALK* fusion gene (discovered in 2007), *ROS1* gene, and BRAF gene mutations. The TKIs for each of these fusion genes were developed and are used as therapeutic agents.

Another advancement in advanced non-small cell lung cancer is the development of immune checkpoint inhibitors. Four PD-1/PD-L1 inhibitors, including nivolumab, are currently available for treatment of lung cancer. These drugs prevent an escape from the cancer immunity cycle. This ensures that cancer cells will express cancer antigens, causing an anticancer immune response. Due to cancer immunotherapy, long-term survival is possible. The biomarker development for cancer immunotherapy and its side effects is actively being studied.

This Special Issue on "Non-Small Cell Lung Cancer: Current Therapies and New Targeted Treatments" aims to update researchers and clinicians by summarizing the remarkable progress made recently in the field of targeted therapy, immunotherapy, and cancer biology for non-small cell lung cancer.

Junji Uchino
Editor

Article

Negative Effect of Reduced NME1 Expression on Recurrence-Free Survival in Early Stage Non-Small Cell Lung Cancer

Dohun Kim [1], Yujin Kim [2], Bo Bin Lee [2], Dongho Kim [2], Ok-Jun Lee [3], Pildu Jeong [4], Wun-Jae Kim [4], Eun Yoon Cho [5], Joungho Han [5], Young Mog Shim [6] and Duk-Hwan Kim [2],*

[1] Department of Thoracic and Cardiovascular Surgery, Chungbuk National University Hospital, College of Medicine, Chungbuk National University, Cheongju 28644, Korea; mwille@naver.com
[2] Department of Molecular Cell Biology, Sungkyunkwan University School of Medicine, Suwon 16419, Korea; yujin0328@hanmail.net (Y.K.); whitebini@hanmail.net (B.B.L.); jindonghao2001@hotmail.com (D.K.)
[3] Department of Pathology, College of Medicine, Chungbuk National University, Cheongju 28644, Korea; ojlee@chungbuk.ac.kr
[4] Department of Urology, College of Medicine, Chungbuk National University, Cheongju 28644, Korea; leo24fly@chungbuk.ac.kr (P.J.); wjkim@chungbuk.ac.kr (W.-J.K.)
[5] Department of Pathology, Samsung Medical Center, Sungkyunkwan University School of Medicine, Seoul 06351, Korea; eunyoon.cho@samsung.com (E.Y.C.); joungho.han@samsung.com (J.H.)
[6] Department of Thoracic and Cardiovascular Surgery, Samsung Medical Center, Sungkyunkwan University, School of Medicine, Seoul 06351, Korea; youngmog.shim@samsung.com
* Correspondence: dukhwan.kim@samsung.com; Tel.: +822-3410-3632

Abstract: This study aimed to understand whether the effect of non-metastatic cells 1 (NME1) on recurrence-free survival (RFS) in early stage non-small cell lung cancer (NSCLC) can be modified by β-catenin overexpression and cisplatin-based adjuvant chemotherapy. Expression levels of NME1 and β-catenin were analyzed using immunohistochemistry in formalin-fixed paraffin-embedded tissues from 425 early stage NSCLC patients. Reduced NME1 expression was found in 39% of samples. The median duration of follow-up was 56 months, and recurrence was found in 186 (44%) of 425 patients. The negative effect of reduced NME1 expression on RFS was worsened by cisplatin-based adjuvant chemotherapy (adjusted hazard ratio = 3.26, 95% CI = 1.16–9.17, $p = 0.03$). β-catenin overexpression exacerbated the effect of reduced NME1 expression on RFS and the negative effect was greater when receiving cisplatin-based adjuvant chemotherapy: among patients treated with cisplatin-based adjuvant chemotherapy, hazard ratios of patients with reduced NME1 expression increased from 5.59 (95% confidence interval (CI) = 0.62–50.91, $p = 0.13$) to 15.52 (95% CI = 2.94–82.38, $p = 0.001$) by β-catenin overexpression, after adjusting for confounding factors. In conclusion, the present study suggests that cisplatin-based adjuvant chemotherapy needs to be carefully applied to early stage NSCLC patients with overexpressed β-catenin in combination with reduced NME1 expression.

Keywords: adjuvant chemotherapy; β-catenin; lung neoplasms; nucleotide-diphosphate kinase; recurrence

1. Introduction

Lung cancer is one of the most common causes of cancer-related deaths in the world. Despite recent advances in the early detection and treatment of lung cancer, the prognosis is very poor, partly because of a high rate of recurrence even after curative resection. Approximately half of the patients diagnosed with non-small cell lung cancer (NSCLC) develop recurrence and die of the disease even after curative

resection. Adjuvant chemotherapy plays an important role in preventing recurrence following curative resection of lung cancer. A survival benefit of platinum-based adjuvant chemotherapy in NSCLC was confirmed by phase III trials and the Lung Adjuvant Cisplatin Evaluation (LACE) meta-analysis [1,2]. However, some NSCLC patients receiving such adjuvant chemotherapy show no progress in survival. Accordingly, it is critically important to identify biomarkers that can select patients who will not respond well to adjuvant therapy so that an appropriate treatment plan can be provided to patients. Given that occult micro-metastatic cancer cells might be present systemically at the time of surgery, altered expression of metastasis-related genes might be useful as molecular biomarkers to distinguish patients at high risk of recurrence after surgery.

Non-metastatic cells 1 (NME1), also known as NM23-H1, was the first metastasis suppressor discovered by its reduced mRNA transcript levels in a murine melanoma cell line exhibiting high metastatic activity [3]. In addition to its known function as a nucleotide-diphosphate kinase that converts nucleoside diphosphates to nucleoside triphosphates at the expense of adenosine triphosphate (ATP), NME1 is involved in several pathological processes such as motility and metastasis of tumor cells [4]. An inverse relationship between metastatic potential and NME1 expression has been reported in several types of cancers, including non-small cell lung cancer [5,6], melanoma [7], breast cancer [8], hepatocellular carcinoma [9], gastric cancer [10], and colorectal cancer [11]. Transfection of the *NME1* gene into different types of cancer cells has resulted in the inhibition of metastatic properties, including migration, invasion, and colonization [12–16]. *NME1* silencing is known to upregulate β-catenin-dependent TCF/LEF-1 (T-cell factor/lymphoid enhancer-binding factor) transactivation through glycogen synthase kinase (GSK)-3β-independent mechanisms by promoting nuclear translocation of β-catenin [17].

Activation of the canonical Wnt signaling pathway inhibits axin-mediated β-catenin phosphorylation and degradation and allows β-catenin to accumulate in the cytoplasm and then translocate into the nucleus. Nuclear β-catenin forms a stable complex with members of the TCF/LEF transcription factor family and induces the expression of target genes such as *c-MYC* and *CCND1*, and influences the metastatic cascade by regulating the expression of genes such as *AXIN2*, *SNAIL*, *ZEB1*, *COX2*, and *S100A4* [18]. It has been reported that the Wnt/β-catenin signaling pathway is involved in the invasion and metastasis of tumor cells in patients with NSCLC [19–22]. In addition to the nuclear translocation of β-catenin by *NME1* silencing, Wnt/β-catenin-mediated resistance to cisplatin has been demonstrated in human cancers [23,24]. Based on these reports, we hypothesized that NME1 and the Wnt signal may cooperatively affect patient prognosis and cisplatin treatment.

In this study, we analyzed whether the effect of NME1 on recurrence-free survival (RFS) can be modified by cisplatin-based adjuvant chemotherapy and β-catenin overexpression in early stage NSCLC.

2. Materials and Method

2.1. Study Population

This was a retrospective study. Formalin-fixed paraffin-embedded (FFPE) tissue specimens stored at room temperature were obtained from 425 patients with pathologic stage I–IIIA NSCLC who had undergone anatomical lung resection with mediastinal lymph node dissection between November 1994 and April 2004 at Samsung Medical Center in Seoul, Korea. Patients with incomplete resection of lung tissue (e.g., positive malignant cell in resection margin) or history of neoadjuvant therapy were excluded from this study. Postoperative follow-up was performed according to a previously described protocol [25]. Information including recurrence, death, and platinum-based adjuvant chemotherapy was obtained from our hospital's electronic medical records (EMRs) and outside medical records as of 31 July 2018. Thirty-two (7.5%) patients received postoperative adjuvant chemotherapy comprising cisplatin combined with vinorelbine, vinblastine, etoposide, fluorouracil, gemcitabine, pemetrexed, or docetaxel. The chemotherapy regimens were selected by medical oncologists responsible for

treatment decisions. This study was approved by the Institutional Review Board of the Samsung Medical Center (2018-04-153), and pre-operative informed consent for the use of samples was obtained from all patients. Pathologic stage was determined according to the guideline of the 7th edition of the tumor-node-metastasis (TNM) staging system maintained by the American Joint Committee on Cancer [26]. Supporting data for this study are available from the corresponding author upon request.

2.2. Immunohistochemistry

Tissue microarrays (TMAs) were constructed from paraffin blocks prepared from 425 NSCLC samples. Expression levels of β-catenin and NME1 proteins were analyzed using immunohistochemistry. In brief, serial sections of 4 μM in thickness were cut from TMA blocks, deparaffinized in xylene, and rehydrated through a series of decreasing concentrations of alcohols. Antigens were recovered by heating these sections in 10 mM (pH 6) citrate buffer for 10 min using a pressure cooker. These sections were then incubated with primary antibody β-catenin clone 17C2 (Leica Biosystems, Buffalo Grove, IL, USA) or NME1 clone 4B2 (GeneTex, Irvine, CA, USA) at 4 °C overnight. Immunoreactivity of each primary antibody was detected with Envision™ + peroxidase (Dako, Carpinteria, CA, USA). Antibody-bound peroxidase activity was visualized after incubating with chromogen 3,3′-diaminobenzidine (DAB) at room temperature for 1–5 min. Normal bronchial epithelial cells were used for positive control of staining, and primary antibody was replaced by immunoglobin for negative control. All sections were counterstained with Mayer's hematoxylin.

2.3. Interpretation of Immunohistochemical Staining

Immunohistochemical staining was interpreted by consensus between two authors (O.-J.L. and D.-H.K.) in a double-blinded fashion to minimize inter-rater variability. Samples with a Cohen's kappa coefficient of less than 0.20 were removed from further analysis. Although immunoreactivity for β-catenin was found in the membrane, cytoplasm, and nucleus, only cytoplasmic staining was assessed for scoring. The expression of NME1 protein in tumor cells was evaluated based on cytoplasmic staining. Cytoplasmic staining of both proteins was semi-quantitatively evaluated using a score calculated by multiplying the intensity score (0, none; 1, weak; 2, moderate; 3, strong) with the proportion score of positive cells (0, absent; 1, 0–10%; 2, 10–50%; 3, 50–80%; 4, >80%). For NME1, its expression was defined as reduced if a composite score was less than two in a tumor. β-catenin expression was considered to be overexpressed in a tumor with a composite score greater than or equal to two. Staining was performed in triplicate and average values of scores were used to determine the expression levels. Cutoff values for the abnormal expression of NME1 and β-catenin were determined considering an internal control consisting of 23 normal lung cores. Representative positive stainings for β-catenin and NME1 expression are shown in adenocarcinoma and squamous cell carcinoma (Figure 1A). Details of the immunohistochemical staining procedure and interpretation for Ki-67 (MKI67) proteins were reported previously [27].

2.4. Study Design

Patients were randomly selected without stratification or matching by age. The median duration of follow-up was 56 months. The clinical endpoint of the study was recurrence-free survival (RFS), which was defined as the time from the date of the diagnosis to the first recurrence. Variables such as age, sex, histology, pathologic stage, NME1 expression, and adjuvant chemotherapy were initially considered for the analysis of RFS. FFPE tissue samples were obtained from 425 patients because at least 365 patients were needed for analysis of the effect of NME1 expression on RFS under 2-sided $\alpha = 0.05$ and $\beta = 0.1$ (i.e., 90% power).

2.5. Statistical Analyses

To find factors associated with NME1 reduction in NSCLC, chi-square test (or Fisher's exact test) and Student's *t*-test (or one-way ANOVA) were used for univariate analyses of continuous and categorical variables, respectively. A linear relationship between two continuous variables

was analyzed using Pearson's correlation coefficient. The prognostic significance of NME1 on RFS was evaluated by Kaplan–Meier survival curves. The difference between two survival curves was assessed using the log-rank test. Variables with $P \leq 0.25$ in the univariate analysis were included in the multivariate model. Hazard ratios of predictor variables for survival were estimated using the Cox proportional hazards model after controlling for potential confounding factors. The effect of β-catenin expression and adjuvant chemotherapy on NME1 function was analyzed using a stratified Cox proportional hazards model. No replacement was made for missing values. All statistical analyses were two-sided with a type I error of 5%.

3. Results

3.1. Clinicopathological Characteristics

A total of 425 patients with early stage NSCLC were included in the data analysis without dropout. The mean age of the patients at diagnosis was 61 years (range, 37–82 years), and men accounted for 74% of the cases. Adenocarcinoma and squamous cell carcinoma comprised 46% and 47% of the cases, respectively. Patients at I, II, and IIIA stages accounted for 56%, 43%, and 5%, respectively. The relationship between NME1 expression and clinicopathological characteristics is summarized in Supplementary Table S1. NME1 expression was found to be reduced in 165 (39%) of 425 patients. Reduced NME1 expression was not associated with patient's age, sex, tumor size, or exposure to tobacco smoke. However, reduced NME1 expression was found to have a significantly higher prevalence in squamous cell carcinoma (46%) than in adenocarcinoma (34%), and the difference was statistically significant ($p = 0.01$; Figure 1B).
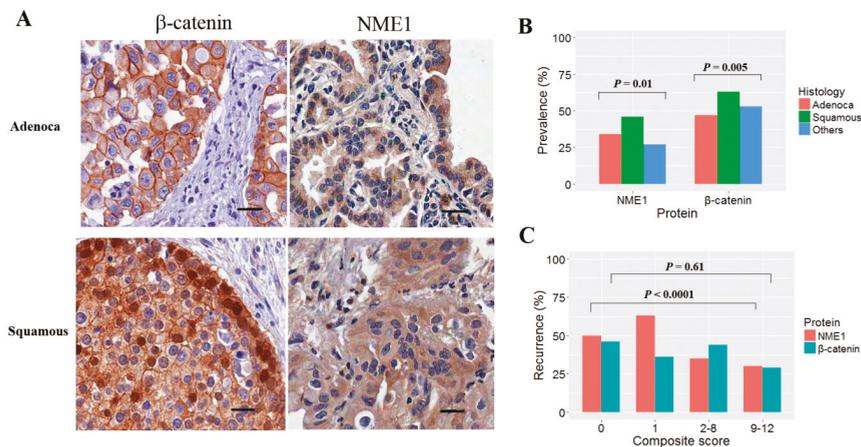
Figure 1. Immunohistochemical staining for non-metastatic cells 1 (NME1) and β-catenin expression in non-small cell lung cancer. (**A**) Expression levels of NME1 and β-catenin were analyzed using immunohistochemical staining (scale bar = 100 μm). Representative images of positive staining are shown in adenocarcinoma (upper) and squamous cell carcinoma (lower) at magnification of ×200. Cytoplasmic staining was considered positive for NME1 and β-catenin expression. (**B**) Prevalence of reduced NME1 expression and β-catenin overexpression was compared according to histologic subtypes. *p*-values were based on Pearson's chi-square test. (**C**) Association between recurrence and the expression levels of NME1 or β-catenin was analyzed in 425 participants.

Postoperative recurrence occurred in 186 (44%) of 425 patients. Patients with reduced NME1 expression had a higher recurrence rate than those without (62% vs. 32%, $p < 0.0001$). β-catenin was overexpressed in 55% of patients, with a higher prevalence in squamous cell carcinoma than that in adenocarcinoma ($p = 0.005$; Figure 1B). Recurrence was found at a high prevalence in patients

with reduced NME1 expression but not β-catenin overexpression irrespective of histologic subtypes (Figure 1C).

3.2. Reduced NME1 Expression Is Significantly Associated with Poor RFS Irrespective of Histology or Pathologic Stage

Univariate analysis was performed to discover prognostic factors that affect RFS in early stage NSCLC. RFS was negatively associated with reduced NME1 expression but not with β-catenin overexpression and cisplatin-based adjuvant chemotherapy (Supplementary Table S2). Patients were stratified according to histology and pathologic stage to analyze whether the relationship between RFS and NME1 expression was modified by histology or pathologic stage. RFS was compared between patients with and without reduced NME1 expression in histologic subtypes. Reduced NME1 expression was significantly associated with RFS ($p < 0.0001$; Supplementary Figure S1A): Five-year RFS rate after surgery was 38% for those with reduced NME1 expression and 68% for those without reduced NME1 expression. Reduced NME1 expression had a negative effect on RFS in adenocarcinoma ($p < 0.0001$; Supplementary Figure S1B) and in squamous cell carcinoma ($p < 0.0001$; Supplementary Figure S1C).

The effect of reduced NME1 expression on RFS was further analyzed based on pathologic stage (Figure 2). The number of patients with stage IIIA NSCLC was five, which was too small to analyze RFS. Therefore, patients with stage IIIA NSCLC were combined with those who had stage IIB NSCLC to analyze RFS. Reduced NME1 expression was significantly associated with poor RFS in stage IA ($p = 0.0005$; Figure 2A), stage IB ($p = 0.001$; Figure 2B), and stage IIA ($p = 0.01$; Figure 2C). It was marginally associated with poor RFS in stage IIB–IIIA ($p = 0.08$; Figure 2D). The relationship between β-catenin overexpression and RFS was also analyzed based on pathologic stage and histology. However, no association was found between them.
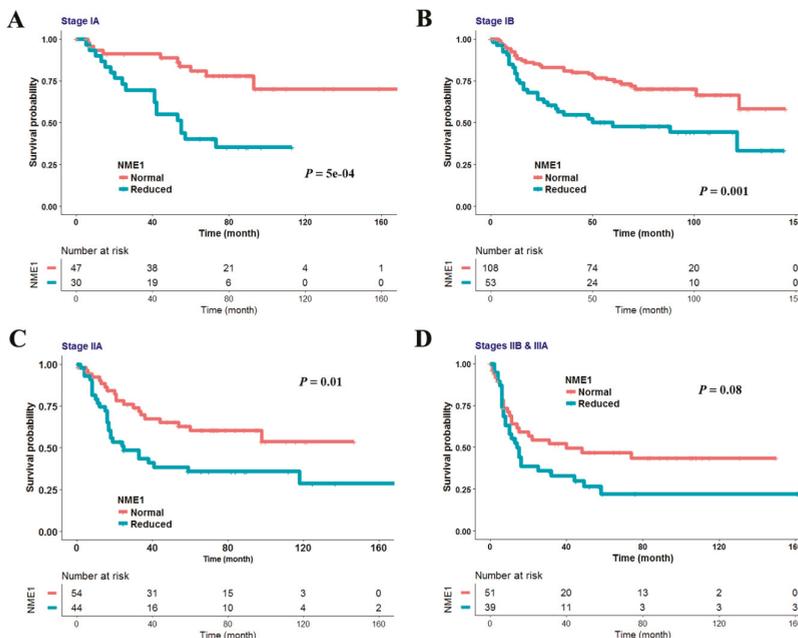
Figure 2. Impact of NME1 on recurrence-free survival (RFS) according to pathologic stages. The effect of reduced NME1 expression on RFS was estimated using the Kaplan–Meier survival curve in 77 patients with stage IA (**A**), 161 with stage IB (**B**), 98 with stage IIA (**C**), and 89 stage IIB–IIIA (**D**). Statistical difference between two survival curves was calculated using the log-rank test.

3.3. Negative Effect of Reduced NME1 Expression on RFS in Patients with Cisplatin-Based Adjuvant Chemotherapy and β-Catenin Overexpression

Cisplatin-based adjuvant chemotherapy was not associated with RFS irrespective of histologic subtypes in univariate analysis. The effect of NME1 or β-catenin on RFS was further analyzed considering cisplatin-based adjuvant chemotherapy. The negative effect of reduced NME1 expression on RFS was worse in patients treated with (Figure 3A) cisplatin-based adjuvant chemotherapy than in those treated without (Figure 3B). Reduced NME1 expression was not associated with β-catenin overexpression in this study. However, it is known that there is a complex interplay between NME1 and β-catenin in a variety of cancers. Therefore, data were further stratified according to β-catenin overexpression. The negative effect of reduced NME1 expression on RFS was much greater in patients with overexpression of β-catenin (Figure 3C) than in those without (Figure 3D).
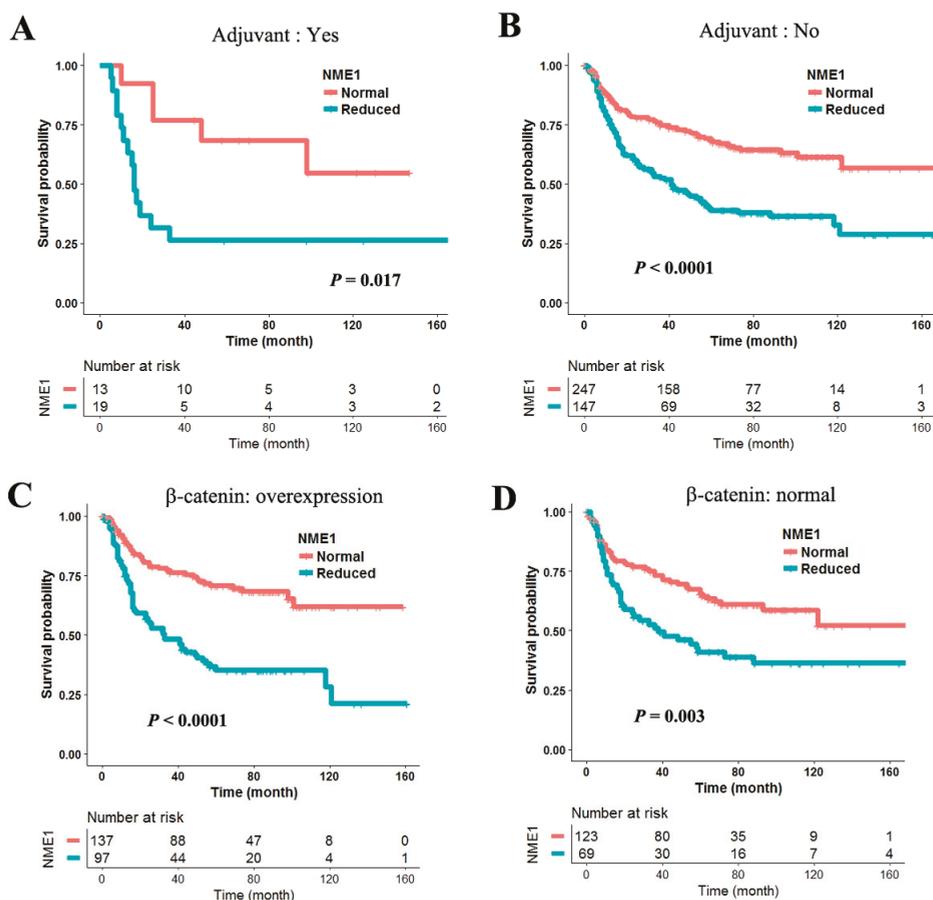
Figure 3. Effect of NME1 on recurrence-free survival, stratified by β-catenin expression and cisplatin-based adjuvant chemotherapy. To understand whether the effect of NME1 on RFS was confounded by β-catenin expression or cisplatin-based adjuvant chemotherapy, data were stratified by β-catenin overexpression (**A,B**) or cisplatin-based adjuvant chemotherapy (**C,D**) and then the survival curves were compared according to NME1. The survival was compared using the log-rank test in 425 non-small cell lung cancers (NSCLCs).

3.4. Multivariate Cox Proportional Hazards Analysis

Multivariate Cox proportional hazards analysis was conducted to measure the effect of reduced NME1 expression on RFS in early stage NSCLC, after adjusting for potential confounding effects of variables. Considering the pathological stage, hazard ratios for RFS ranged from 1.64 to 3.93, after adjusting for patient age, sex, β-catenin expression, adjuvant chemotherapy, and histology (Supplementary Table S3). The hazard ratio for RFS in a total of 425 patients was 2.27 (95% CI = 1.70–3.03, $p < 0.0001$) times worse in patients with reduced NME1 expression than in those without (Supplementary Table S4). However, the hazard ratio was not associated with age (HR = 1.01, 95% CI = 0.99–1.03, $p = 0.18$), sex (HR = 1.02, 95% CI = 0.71–1.47, $p = 0.93$), adjuvant chemotherapy (HR = 1.03, 95% CI = 0.86–2.23, $p = 0.89$), and β-catenin expression (HR = 0.99, 95% CI = 0.75–1.34, $p = 0.99$).

To test our hypothesis that the effect of NME1 expression on RFS may be affected by Wnt signal and cisplatin treatment, we stratified patients according to adjuvant chemotherapy and β-catenin expression. The negative effect of reduced NME1 expression on RFS was exacerbated by cisplatin-based adjuvant chemotherapy (adjusted hazard ratio = 3.26, 95% CI = 1.16–9.17, $p = 0.03$; Supplementary Table S5). For patients who did not receive cisplatin-based adjuvant chemotherapy, the hazard ratio of reduced NME1 expression was increased from 1.89 (95% confidence interval (CI) = 1.21–2.95, $p = 0.005$) to 2.54 (95% CI = 1.66–3.89, $p < 0.0001$; Table 1) by β-catenin overexpression after adjusting for patient age, sex, histology, and pathologic stage. Among patients with β-catenin overexpression who received cisplatin-based adjuvant chemotherapy, patients with reduced NME1 expression were determined to have 15.52 (95% CI = 2.94–82.38, $p = 0.001$; Table 1) times poorer RFS than those without. These results suggest that the negative effect of reduced NME1 expression on RFS may be worsen by cisplatin-based adjuvant chemotherapy and β-catenin overexpression in early stage NSCLC.

Table 1. Cox proportional hazards analysis [a] of RFS according to NME1 in early stage NSCLC stratified by cisplatin-based adjuvant chemotherapy and β-catenin overexpression

Adjuvant Chemotherapy	β-Catenin Overexpression	Reduced NME1 Expression	HR	95% CI	*p*-Value
No	No (*N* = 176)	No	1		
		Yes	1.89	1.21–2.95	0.005
	Yes (*N* = 217)	No	1		
		Yes	2.54	1.66–3.89	<0.0001
Yes	No (*N* = 16)	No	1		
		Yes	5.59	0.62–50.91	0.13
	Yes (*N* = 16)	No	1		
		Yes	15.52	2.94–82.38	0.001

[a] Adjusted for age, sex, histology, and pathologic stage. Abbreviations: HR, hazard ratio; CI, confidence interval.

3.5. Relationship between Ki-67 Labeling Index and Expression of NME1 and β-Catenin

Ki-67 proliferation index was analyzed to investigate whether the effect of NME1 and β-catenin on cisplatin-resistance might be confounded by different cell proliferation activity. Ki-67 proliferation was not significantly different according to abnormal expression of NME1 or β-catenin irrespective of histology (Figure 4A) and cisplatin-based adjuvant chemotherapy (Figure 4B). These observations suggest that NME1 and β-catenin may affect cisplatin-based adjuvant chemotherapy through other mechanisms rather than through any changes in cell proliferation.
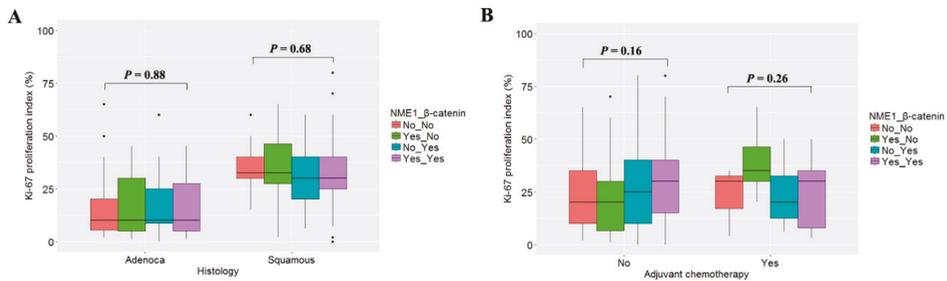
Figure 4. Ki-67 (MKI67) proliferation index according to altered expression of NME1 and β-catenin. Ki-67 proliferation was compared according to expression statuses of NME1 and β-catenin, stratified by histology (**A**) and adjuvant chemotherapy (**B**). "Adenoca" and "Squamous" represent adenocarcinoma and squamous cell carcinoma, respectively. "No" and "Yes" indicate the absence and presence of altered expression, respectively. *p*-values were calculated using one-way ANOVA.

3.6. The Relationship between NME1 and Nuclear β-Catenin Expression

NME1 silencing is known to induce a redistribution of β-catenin from the cell surface into the cytoplasm and nucleus by activating the Wnt pathway [17]. To understand whether NME1 expression affects the nuclear translocation of β-catenin, we analyzed the levels of nuclear β-catenin expression (Figure 5A) according to NME1 expression. The levels of nuclear β-catenin expression showed a linear relationship with those of cytoplasmic β-catenin expression (Pearson's correlation coefficient γ = 0.74, *p* = 0.002; Figure 5B) but not to those of NME1 expression (γ = −0.03, *p* = 0.80; Figure 5C).
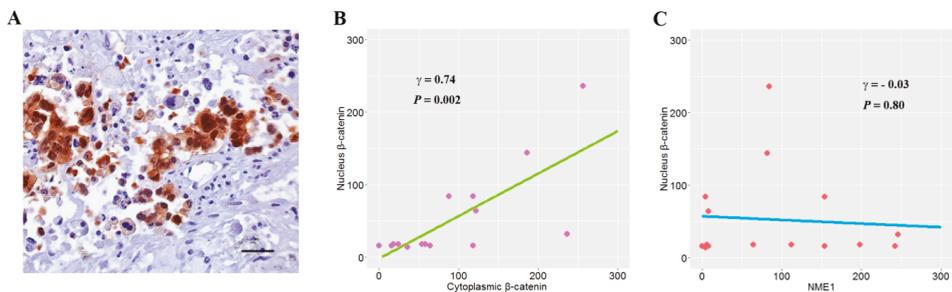
Figure 5. The relationship between NME1 and nuclear β-catenin expression. (**A**) β-catenin expression (scale bar, 100 μm) are shown in nucleus. (**B,C**) X- and Y-axis scores were obtained by multiplying the intensity score of staining with the proportion of positive stained cells. The linear relationship between two variables was calculated using Pearson's correlation coefficient.

4. Discussion

The epithelial–mesenchymal transition (EMT) plays a crucial role in promoting metastasis of carcinoma derived from epithelial cells. Tumor cells lose their epithelial characteristics such as cell polarity and gain mesenchymal features such as increased migratory and invasive potentials during EMT. Our data did not show an association of NME1 expression with tumor growth (Figure 4), consistent with a previous study showing that *NME1* silencing does not provide epithelial cancer cells with a selective growth advantage [17]. A number of groups have reported the relationship between NME1 expression and patient prognosis in NSCLC with different results. Some groups have reported no association between NME1 expression and overall survival [28,29]. In contrast, reduced NME1 expression has been found to be associated with bone metastasis and poor survival in patients with pulmonary adenocarcinoma [30]. Ohta et al. [31] have also reported that NME1 expression is inversely correlated with the microdissemination of tumor cells in stage I NSCLC. In addition, stage

I NSCLC patients with NME1-negative expression show a significantly poorer survival than those without [32,33]. The present study also showed the negative effect of reduced NME1 expression on RFS in early stage NSCLC, consistent with findings from previous groups [30–33].

The negative effect of reduced NME1 expression on RFS in this study was worse in patients with β-catenin overexpression than in those without. How does β-catenin overexpression influence the effect of reduced NME1 expression on RFS? Mechanisms underlying the metastasis suppression of NME1 have been addressed in multiple types of cancer cells. Early efforts have revealed that NME1 may mediate its inhibitory effects on cellular motility and invasion through interactions with signaling cascades [16,34–36]. For example, NME1 negatively regulates Rac1 (Rac family small GTPase 1) and Cdc42 (Cell division cycle 42) GTPase by interacting with Rac1-specific nucleotide exchange factors, TIAM Rac1 associated GEF1 (Tiam1) and TGF_BETA_2 domain-containing protein (Dbl-1), respectively [36]. A splicing variant of *NME1* inhibits the metastasis of lung cancer cells by interacting with Inhibitor of nuclear factor Kappa-B Kinase subunit beta (IKKβ) in an isotype-specific fashion and regulating tumor necrosis factor alpha (TNFα)-stimulated Nuclear Factor kappa-light-chain-enhancer of activated B cells (NF-κB) signaling negatively [16]. In addition, NME1 inhibits the liver metastasis of colon cancer cells by regulating the phosphorylation of myosin light chains in nude mice [35]. *NME1* silencing induces the nuclear translocation of β-catenin by disrupting adherence junction complexes mediated by E-cadherin and promotes extracellular matrix invasion by increasing invadopodia formation and pericellular matrix metalloproteinase (MMP) activity [17].

In addition to its effect on signaling pathways, NME1 is also known to regulate gene transcription by binding to single-stranded DNA. A promoter region between –922 to –846 of Kangai 1 (KAI1) is known to suppress metastasis through the inhibition of cell movement. It responds to NME1 in high-metastatic lung cancer cell line L9981 [37]. NME1 suppresses motile and invasive phenotypes of melanoma cells by inducing the transcription of integrin beta-3 (*ITGβ3*) gene through direct physical interaction with the promoter [38]. NME1 also plays a role as a co-regulator of transcription by regulating expression of metastasis-related genes through direct or indirect interactions with transcription-regulatory elements [39–42]. However, the present study showed no relationship between NME1 expression and nuclear β-catenin expression (Figure 5), suggesting that the adverse effect of NME1 on RFS exacerbated by β-catenin overexpression might not be due to the nuclear translocation of β-catenin by reduced NME1. It is likely that NME1 may interact with β-catenin through other mechanisms such as upregulation of many genes related to cell cycle, apoptosis, and metastasis.

Platinum derivatives such as cisplatin are widely used chemotherapeutic agents for NSCLC. However, cisplatin resistance is a major challenge in the use of these drugs. The molecular mechanism of cisplatin resistance in lung cancer cells is not fully understood. Therefore, there are few efficient strategies to overcome such resistance. Cisplatin-based adjuvant chemotherapy in the present study did not affect RFS in univariate analysis. However, it worsened the RFS in patients with reduced NME1 expression (Supplementary Table S5). A functional link between NME1 expression and responsiveness to cisplatin-based adjuvant chemotherapy has been reported by several groups. Cisplatin increases interstrand DNA cross-links and inhibits pulmonary metastatic colonization in *NME1*-transfected breast cancer cells [43]. NME1 has 3′-5′ exonuclease activity potentially involved in DNA proofreading [44]. Thus, reduced expression of NME1 may contribute to chemoresistance by allowing metastatic cells to escape from apoptosis. Knockdown of *NME1* by shRNA transfection in head and neck squamous carcinoma cells attenuates the chemosensitivity of cells to cisplatin by downregulating cyclins E and A and reducing cisplatin-induced S-phase accumulation [45]. These lines of evidence suggest that reduced NME1 expression might be involved in cisplatin resistance through various mechanisms. Therefore, restoring NME1 expression might be a therapeutic intervention strategy to surmount cisplatin resistance.

Previous studies have demonstrated Wnt/β-catenin-mediated resistance to cisplatin in various types of cancers [23,24]. Transient interference of cytoplasmic GSK-3β increases cisplatin resistance by activating Wnt/β-catenin signaling in cisplatin-resistant A549 cells [23]. Recently, Zhang and

colleagues [24] have reported that the interference of β-catenin expression by siRNA can decrease mRNA and protein levels of anti-apoptotic gene *Bcl-xl* and increase cisplatin sensitivity in A549 wild-type cells. Despite these associations of β-catenin overexpression and cisplatin resistance in various types of cancer cells, β-catenin overexpression alone was not associated with cisplatin resistance in the present study. However, β-catenin overexpression aggravated RFS when patients with reduced NME1 received cisplatin-based adjuvant chemotherapy (Table 1). Further studies are needed to better understand the combined effect of β-catenin and NME1 on RFS of patients receiving platinum-based adjuvant chemotherapy in early stage NSCLC.

This study was limited by several factors. First, this was a retrospective study that was prone to selection and surveillance biases. Second, it is necessary to investigate combined effects of β-catenin and NME1 on apoptosis, migration, invasion, or metastasis in different cell types of lung cancer to clearly understand the molecular mechanisms underlying the effect of β-catenin and NME1 on poor RFS. Third, the lack of a negative effect of β-catenin in the univariate analysis (Supplementary Table S2) in this study might be due to the small sample size and short duration of follow-up. Fourth, *EcoR1* (rs34214448-G/T) polymorphism in *NME1* gene is associated with increased susceptibility to NSCLC [46] and could potentially affect the results of the current analysis, which is based only on expression levels. Fifth, the relationship between the Th1 (T helper cell type 1) and Th 2 (T helper cell type 2) ratio and β-catenin levels were not analyzed in this study. The balance between Th1 and Th2 in the tumor microenvironment is regulated by several factors, and β-catenin may affect the tumor microenvironment. Thus, for the understanding of their relationship and the analysis of β-catenin levels, it may be informative to know the Th1/Th2 ratio of patients. Sixth, the number of patients receiving adjuvant chemotherapy was too small. Accordingly, prospective large-scale studies are needed to validate the effect of β-catenin and cisplatin-based adjuvant chemotherapy on NME1-related RFS in early stage NSCLC.

In conclusion, the present study suggests that the adverse effect of reduced NME1 expression on RFS may be exacerbated by cisplatin-based adjuvant chemotherapy and β-catenin overexpression through other mechanisms rather than through the nuclear translocation of β-catenin in early stage NSCLC. Accordingly, it is recommended that cisplatin-based adjuvant chemotherapy in patients with completely resected stage I–IIIA NSCLC be carefully applied after examining the expression levels of β-catenin and NME1.

Author Contributions: Conceptualization D.K. (Dohun Kim) and D.-H.K.; data curation, Y.K. and W.-J.K.; formal analysis, Y.K., B.B.L., and D.K. (Dongho Kim); methodology, O.-J.L. and P.J.; resources, E.Y.C., J.H., and Y.M.S.; supervision, D.-H.K.; writing—original draft preparation, D.K. (Dohun Kim) and D-H.K.; writing—review and editing, D.K. (Dohun Kim), Y.K., B.B.L., D.K. (Dongho Kim), O.-J.L., P.J., W.-J.K., E.Y.C., J.H., Y.M.S., and D.-H.K.; funding acquisition, D.-H.K. All authors have read and agreed to the published version of the manuscript.

Conflicts of Interest: The authors declare no conflict of interest.

References

1. Pignon, J.-P.; Tribodet, H.; Scagliotti, G.V.; Douillard, J.-Y.; Shepherd, F.A.; Stephens, R.J.; Dunant, A.; Torri, V.; Rosell, R.; Seymour, L.; et al. Lung Adjuvant Cisplatin Evaluation: A Pooled Analysis by the LACE Collaborative Group. *J. Clin. Oncol.* **2008**, *26*, 3552–3559. [CrossRef] [PubMed]

2. Arriagada, R.; Dunant, A.; Pignon, J.-P.; Bergman, B.; Chabowski, M.; Grunenwald, D.; Kozlowski, M.; Le Péchoux, C.; Pirker, R.; Pinel, M.-I.S.; et al. Long-Term Results of the International Adjuvant Lung Cancer Trial Evaluating Adjuvant Cisplatin-Based Chemotherapy in Resected Lung Cancer. *J. Clin. Oncol.* **2010**, *28*, 35–42. [CrossRef] [PubMed]

3. Steeg, P.S.; Bevilacqua, G.; Kopper, L.; Thorgeirsson, U.P.; Talmadge, J.E.; Liotta, L.A.; Sobel, M.E. Evidence for a Novel Gene Associated with Low Tumor Metastatic Potential. *J. Natl. Cancer Inst.* **1988**, *80*, 200–204. [CrossRef]

4. Boissan, M.; Dabernat, S.; Peuchant, E.; Schlattner, U.; Lascu, I.; Lacombe, M.-L. The mammalian Nm23/NDPK family: From metastasis control to cilia movement. *Mol. Cell. Biochem.* **2009**, *329*, 51–62. [CrossRef]

5. Goncharuk, V.N.; Del-Rosario, A.; Kren, L.; Anwar, S.; E Sheehan, C.; Carlson, J.A.; Ross, J.S. Co-downregulation of PTEN, KAI-1, and nm23-H1 tumor/metastasis suppressor proteins in non-small cell lung cancer. *Ann. Diagn. Pathol.* **2004**, *8*, 6–16. [CrossRef] [PubMed]

6. Ayabe, T.; Tomita, M.; Matsuzaki, Y.; Ninomiya, H.; Hara, M.; Shimizu, T.; Edagawa, M.; Onitsuka, T.; Hamada, M. Micrometastasis and expression of nm23 messenger RNA of lymph nodes from lung cancer and the postoperative clinical outcome. *Ann. Thorac. Cardiovasc. Surg.* **2004**, *10*, 152–159.

7. Sarris, M.; Scolyer, R.A.; Konopka, M.; Thompson, J.F.; Harper, C.G.; Lee, C.S. Cytoplasmic expression of nm23 predicts the potential for cerebral metastasis in patients with primary cutaneous melanoma. *Melanoma Res.* **2004**, *14*, 23–27. [CrossRef]

8. Khan, I.; Gril, B.; Steeg, P.S. Metastasis Suppressors NME1 and NME2 Promote Dynamin 2 Oligomerization and Regulate Tumor Cell Endocytosis, Motility, and Metastasis. *Cancer Res.* **2019**, *79*, 4689–4702. [CrossRef]

9. Khera, L.; Paul, C.; Kaul, R. Hepatitis C Virus E1 protein promotes cell migration and invasion by modulating cellular metastasis suppressor Nm23-H1. *Virology* **2017**, *506*, 110–120. [CrossRef]

10. Guan-Zhen, Y.; Ying, C.; Can-Rong, N.; Guo-Dong, W.; Jian-Xin, Q.; Jie-Jun, W. Reduced protein expression of metastasis-related genes (nm23, KISS1, KAI1 and p53) in lymph node and liver metastases of gastric cancer. *Int. J. Exp. Pathol.* **2007**, *88*, 175–183. [CrossRef]

11. Yang, T.; Chen, B.Z.; Li, D.F.; Wang, H.M.; Lin, X.S.; Wei, H.F.; Zeng, Y.M. Reduced NM23 Protein Level Correlates with Worse Clinicopathologic Features in Colorectal Cancers: A Meta-Analysis of Pooled Data. *Medicine (Baltimore)* **2016**, *95*, e2589. [PubMed]

12. Rasool, R.U.; Nayak, D.; Chakraborty, S.; Jamwal, V.L.; Mahajan, V.; Katoch, A.; Faheem, M.M.; Iqra, Z.; Amin, H.; Gandhi, S.G.; et al. Differential regulation of NM23-H1 under hypoxic and serum starvation conditions in metastatic cancer cells and its implication in EMT. *Eur. J. Cell Boil.* **2017**, *96*, 164–171. [CrossRef] [PubMed]

13. Horak, C.; Mendoza, A.; Vega-Valle, E.; Albaugh, M.; Graff-Cherry, C.; McDermott, W.G.; Hua, E.; Merino, M.J.; Steinberg, S.M.; Khanna, C.; et al. Nm23-H1 Suppresses Metastasis by Inhibiting Expression of the Lysophosphatidic Acid Receptor EDG2. *Cancer Res.* **2007**, *67*, 11751–11759. [CrossRef] [PubMed]

14. Khan, I.; Steeg, P.S. The relationship of NM23 (NME) metastasis suppressor histidine phosphorylation to its nucleotide diphosphate kinase, histidine protein kinase and motility suppression activities. *Oncotarget* **2017**, *9*, 10185–10202. [CrossRef]

15. Che, G.; Chen, J.; Liu, L.; Wang, Y.; Li, L.; Qin, Y.; Zhou, Q. Transfection of nm23-H1 increased expression of beta-Catenin, E-Cadherin and TIMP-1 and decreased the expression of MMP-2, CD44v6 and VEGF and inhibited the metastatic potential of human non-small cell lung cancer cell line L9981. *Neoplasma* **2006**, *53*, 530–537.

16. You, D.-J.; Park, C.R.; Lee, H.B.; Moon, M.J.; Kang, J.-H.; Lee, C.; Oh, S.-H.; Ahn, C.; Seong, J.Y.; Hwang, J.-I. A Splicing Variant of NME1 Negatively Regulates NF-κB Signaling and Inhibits Cancer Metastasis by Interacting with IKKβ. *J. Boil. Chem.* **2014**, *289*, 17709–17720. [CrossRef]

17. Boissan, M.; De Wever, O.; Lizarraga, F.; Wendum, D.; Poincloux, R.; Chignard, N.; Desbois-Mouthon, C.; Dufour, S.; Nawrocki-Raby, B.; Birembaut, P.; et al. Implication of Metastasis Suppressor NM23-H1 in Maintaining Adherens Junctions and Limiting the Invasive Potential of Human Cancer Cells. *Cancer Res.* **2010**, *70*, 7710–7722. [CrossRef]

18. Hansen, M.T.; Forst, B.; Cremers, N.; Quagliata, L.; Ambartsumian, N.; Grum-Schwensen, B.; Klingelhöfer, J.; Abdul-Al, A.; Herrmann, P.; Osterland, M.; et al. A link between inflammation and metastasis: Serum amyloid A1 and A3 induce metastasis, and are targets of metastasis-inducing S100A4. *Oncogene* **2014**, *34*, 424–435. [CrossRef]

19. He, W.; He, S.; Wang, Z.; Shen, H.; Fang, W.; Zhang, Y.; Qian, W.; Lin, M.; Yuan, J.; Wang, J.; et al. Astrocyte elevated gene-1(AEG-1) induces epithelial-mesenchymal transition in lung cancer through activating Wnt/β-catenin signaling. *BMC Cancer* **2015**, *15*, 107. [CrossRef]

20. Shukla, S.; Sinha, S.; Khan, S.; Kumar, S.; Singh, K.; Mitra, K.; Maurya, R.; Meeran, S.M. Cucurbitacin B inhibits the stemness and metastatic abilities of NSCLC via downregulation of canonical Wnt/β-catenin signaling axis. *Sci. Rep.* **2016**, *6*, 21860. [CrossRef]

21. Lu, J.; Du, C.; Yao, J.; Wu, B.; Duan, Y.; Zhou, L.; Xu, N.; Zhou, F.; Gu, L.; Zhou, H.; et al. C/EBPα Suppresses Lung Adenocarcinoma Cell Invasion and Migration by Inhibiting β-Catenin. *Cell. Physiol. Biochem.* **2017**, *42*, 1779–1788. [CrossRef] [PubMed]

22. Yang, S.; Liu, Y.; Li, M.-Y.; Ng, C.S.H.; Yang, S.-L.; Wang, S.S.; Zou, C.; Dong, Y.; Du, J.; Long, X.; et al. FOXP3 promotes tumor growth and metastasis by activating Wnt/β-catenin signaling pathway and EMT in non-small cell lung cancer. *Mol. Cancer* **2017**, *16*, 124. [CrossRef]

23. Gao, Y.; Liu, Z.; Zhang, X.; He, J.; Pan, Y.; Hao, F.; Xie, L.; Li, Q.; Qiu, X.; Wang, E. Inhibition of cytoplasmic GSK 3β increases cisplatin resistance through activation of Wnt/β catenin signaling in A549/DDP cells. *Cancer Lett.* **2013**, *336*, 231–239. [CrossRef] [PubMed]

24. Zhang, J.; Liu, J.; Li, H.; Wang, J. β-Catenin signaling pathway regulates cisplatin resistance in lung adenocarcinoma cells by upregulating Bcl-xl. *Mol. Med. Rep.* **2016**, *13*, 2543–2551. [CrossRef] [PubMed]

25. Kim, J.S.; Kim, J.-W.; Han, J.; Shim, Y.M.; Park, J.; Kim, D.-H. Cohypermethylation of p16 and FHIT Promoters as a Prognostic Factor of Recurrence in Surgically Resected Stage I Non–Small Cell Lung Cancer. *Cancer Res.* **2006**, *66*, 4049–4054. [CrossRef]

26. Edge, S.B.; Byrd, D.R.; Compton, C.C.; Fritz, A.G.; Greene, F.L.; Troth, A. American Joint Committee on Cancer. In *AJCC Cancer Staging Manual*, 7th ed.; Springer: New York, NY, USA, 2010; pp. 253–270.

27. Kim, J.S.; Han, J.; Shim, Y.M.; Park, J.; Kim, D.H. Aberrant methylation of H-cadherin (CDH13) promoter is associated with tumor progression in primary nonsmall cell lung cancer. *Cancer* **2005**, *104*, 1825–1833.

28. MacKinnon, M. p53, c-erbB-2 and nm23 expression have no prognostic significance in primary pulmonary adenocarcinoma. *Eur. J. Cardio-Thoracic Surg.* **1997**, *11*, 838–842. [CrossRef]

29. Tomita, M.; Ayabe, T.; Matsuzaki, Y.; Onitsuka, T. Immunohistochemical analysis of nm23-H1 gene product in node-positive lung cancer and lymph nodes. *Lung Cancer* **1999**, *24*, 11–16. [CrossRef]

30. Yang, M.; Sun, Y.; Sun, J.; Wang, Z.; Zhou, Y.; Yao, G.; Gu, Y.; Zhang, H.; Zhao, H. Differentially expressed and survival-related proteins of lung adenocarcinoma with bone metastasis. *Cancer Med.* **2018**, *7*, 1081–1092. [CrossRef]

31. Ohta, Y.; Nozawa, H.; Tanaka, Y.; Oda, M.; Watanabe, Y. Increased vascular endothelial growth factor and vascular endothelial growth factor–c and decreased nm23 expression associated with microdissemination in the lymph nodes in stage i non–small cell lung cancer. *J. Thorac. Cardiovasc. Surg.* **2000**, *119*, 804–813. [CrossRef]

32. Katakura, H.; Tanaka, F.; Oyanagi, H.; Miyahara, R.; Yanagihara, K.; Otake, Y.; Wada, H. Clinical significance of nm23 expression in resected pathologic-stage I, non-small cell lung cancer. *Ann. Thorac. Surg.* **2002**, *73*, 1060–1064. [CrossRef]

33. Liu, C.; Liu, J.; Wang, X.; Mao, W.; Jiang, L.; Ni, H.; Mo, M.; Wang, W. Prognostic impact of nm23-H1 and PCNA expression in pathologic stage I non-small cell lung cancer. *J. Surg. Oncol.* **2011**, *104*, 181–186. [CrossRef] [PubMed]

34. Otsuki, Y.; Tanaka, M.; Yoshii, S.; Kawazoe, N.; Nakaya, K.; Sugimura, H. Tumor metastasis suppressor nm23H1 regulates Rac1 GTPase by interaction with Tiam1. *Proc. Natl. Acad. Sci. USA* **2001**, *98*, 4385–4390. [CrossRef] [PubMed]

35. Suzuki, E.; Ota, T.; Tsukuda, K.; Okita, A.; Matsuoka, K.; Murakami, M.; Doihara, H.; Shimizu, N. nm23-H1 reduces in vitro cell migration and the liver metastatic potential of colon cancer cells by regulating myosin light chain phosphorylation. *Int. J. Cancer* **2004**, *108*, 207–211. [CrossRef] [PubMed]
36. Murakami, M.; Meneses, P.I.; Lan, K.; Robertson, E.S. The suppressor of metastasis Nm23-H1 interacts with the Cdc42 Rho family member and the pleckstrin homology domain of oncoprotein Dbl-1 to suppress cell migration. *Cancer Boil. Ther.* **2008**, *7*, 677–688. [CrossRef]
37. You, J.; Chang, R.; Liu, B.; Zu, L.; Zhou, Q. Nm23-H1 was involved in regulation of KAI1 expression in high-metastatic lung cancer cells L9981. *J. Thorac. Dis.* **2016**, *8*, 1217–1226. [CrossRef]
38. Leonard, M.K.; Novak, M.; Snyder, D.; Snow, G.; Pamidimukkala, N.; McCorkle, J.R.; Yang, X.H.; Kaetzel, D. The metastasis suppressor NME1 inhibits melanoma cell motility via direct transcriptional induction of the integrin beta-3 gene. *Exp. Cell Res.* **2019**, *374*, 85–93. [CrossRef]
39. Subramanian, C.; Robertson, E.S. The Metastatic Suppressor Nm23-H1 Interacts with EBNA3C at Sequences Located between the Glutamine- and Proline-Rich Domains and Can Cooperate in Activation of Transcription. *J. Virol.* **2002**, *76*, 8702–8709. [CrossRef]
40. Curtis, C.D.; Likhite, V.S.; McLeod, I.X.; Yates, J.R.; Nardulli, A.M. Interaction of the Tumor Metastasis Suppressor Nonmetastatic Protein 23 Homologue H1 and Estrogen Receptor Alters Estrogen-Responsive Gene Expression. *Cancer Res.* **2007**, *67*, 10600–10607. [CrossRef]
41. Horak, C.; Lee, J.H.; Elkahloun, A.G.; Boissan, M.; Dumont, S.; Maga, T.K.; Arnaud-Dabernat, S.; Palmieri, D.; Stetler-Stevenson, W.G.; Lacombe, M.-L.; et al. Nm23-H1 Suppresses Tumor Cell Motility by Down-regulating the Lysophosphatidic Acid Receptor EDG2. *Cancer Res.* **2007**, *67*, 7238–7246. [CrossRef]
42. Choudhuri, T.; Murakami, M.; Kaul, R.; Sahu, S.K.; Mohanty, S.; Verma, S.; Kumar, P.; Robertson, E.S. Nm23-H1 can induce cell cycle arrest and apoptosis in B cells. *Cancer Boil. Ther.* **2010**, *9*, 1065–1078. [CrossRef]
43. Ferguson, A.W.; Flatow, U.; Macdonald, N.J.; Larminat, F.; A Bohr, V.; Steeg, P.S. Increased sensitivity to cisplatin by nm23-transfected tumor cell lines. *Cancer Res.* **1996**, *56*, 2931–2935.
44. Ma, D.; McCorkle, J.R.; Kaetzel, D. The Metastasis Suppressor NM23-H1 Possesses 3′-5′ Exonuclease Activity. *J. Boil. Chem.* **2004**, *279*, 18073–18084. [CrossRef] [PubMed]
45. Wang, Y.-F.; Chang, C.-J.; Chiu, J.-H.; Lin, C.-P.; Li, W.-Y.; Chang, S.-Y.; Chu, P.-Y.; Tai, S.-K.; Chen, Y.-J. NM23-H1 expression of head and neck squamous cell carcinoma in association with the response to cisplatin treatment. *Oncotarget* **2014**, *5*, 7392–7405. [CrossRef] [PubMed]
46. Shi, X.; Jin, H.; Peng, M.; Li, B.; She, M.; Zhu, T.; Wen, S.; Qin, D.-C. Association between NME1 polymorphisms and cancer susceptibility: A meta-analysis based on 1644 cases and 2038 controls. *Pathol. Res. Pract.* **2018**, *214*, 467–474. [CrossRef] [PubMed]

Article

Predicting the Role of DNA Polymerase β Alone or with *KRAS* Mutations in Advanced NSCLC Patients Receiving Platinum-Based Chemotherapy

Maria Francesca Alvisi [1,†], Monica Ganzinelli [2,†], Helena Linardou [3,†], Elisa Caiola [4,†], Giuseppe Lo Russo [2], Fabiana Letizia Cecere [5], Anna Cecilia Bettini [6], Amanda Psyrri [7], Michele Milella [8], Eliana Rulli [1], Alessandra Fabbri [9], Marcella De Maglie [10,11], Pierpaolo Romanelli [10,11], Samuel Murray [12], Gloriana Ndembe [4], Massimo Broggini [4,*], Marina Chiara Garassino [2,‡] and Mirko Marabese [4,*,‡]

[1] Laboratory of Methodology for Clinical Research, Department of Oncology, Istituto di Ricerche Farmacologiche Mario Negri IRCCS, 20156 Milan, Italy; mariafrancesca.alvisi@marionegri.it (M.F.A.); eliana.rulli@marionegri.it (E.R.)
[2] Unit of Thoracic Oncology, Medical Oncology Department 1, Fondazione IRCCS Istituto Nazionale dei Tumori, 20133 Milan, Italy; monica.ganzinelli@istitutotumori.mi.it (M.G.); Giuseppe.LoRusso@istitutotumori.mi.it (G.L.R.); marina.garassino@istitutotumori.mi.it (M.C.G.)
[3] 4th Oncology Department, Metropolitan Hospital, 18547 Athens, Greece; elinardou@otenet.gr
[4] Laboratory of Molecular Pharmacology, Department of Oncology, Istituto di Ricerche Farmacologiche Mario Negri IRCCS, 20156 Milan, Italy; elisa.caiola@marionegri.it (E.C.); gloriana.ndembe@marionegri.it (G.N.)
[5] Division of Medical Oncology 1, IRCCS Regina Elena National Cancer Institute, 00144 Rome, Italy; fabianacecere@gmail.com
[6] UO Oncologia Medica, ASST Papa Giovanni XXIII, 24127 Bergamo, Italy; abettini@asst-pg23.it
[7] Section of Oncology, Department of Internal Medicine, Attikon Hospital, National Kapodistrian University of Athens, 12462 Athens, Greece; psyrri237@yahoo.com
[8] Department of Medicine, Section of Medical Oncology, University and Hospital Trust of Verona, 37126 Verona, Italy; michele.milella@aovr.veneto.it
[9] Department of Pathology and Laboratory Medicine, Fondazione IRCCS Istituto Nazionale dei Tumori, 20133 Milan, Italy; Alessandra.fabbri@istitutotumori.mi.it
[10] Mouse & Animal Pathology Lab, Fondazione Filarete, 20139 Milan, Italy; marcellademaglie@libero.it (M.D.M.); pierpaolo.romanelli.medvet@gmail.com (P.R.)
[11] Department of Veterinary Medicine, University of Milan, 20122 Milan, Italy
[12] Biomarker Solutions Ltd., London EC1V 2NX, UK; smgenedb@gmail.com
* Correspondence: massimo.broggini@marionegri.it (M.B.); mirko.marabese@marionegri.it (M.M.); Tel.: +39-0239014585 (M.B.); +39-0239014236 (M.M.)
† Shared first authors.
‡ Shared last authors.

Abstract: Clinical data suggest that only a subgroup of non-small cell lung cancer (NSCLC) patients has long-term benefits after front-line platinum-based therapy. We prospectively investigate whether KRAS status and DNA polymerase β expression could help identify patients responding to platinum compounds. Prospectively enrolled, advanced NSCLC patients treated with a first-line regimen containing platinum were genotyped for KRAS and centrally evaluated for DNA polymerase β expression. Overall survival (OS), progression-free survival (PFS), and the objective response rate (ORR) were recorded. Patients with KRAS mutations had worse OS (hazard ratio (HR): 1.37, 95% confidence interval (95% CI): 0.70–2.27). Negative DNA polymerase β staining identified a subgroup with worse OS than patients expressing the protein (HR: 1.43, 95% CI: 0.57–3.57). The addition of KRAS to the analyses further worsened the prognosis of patients with negative DNA polymerase β staining (HR: 1.67, 95% CI: 0.52–5.56). DNA polymerase β did not influence PFS and ORR. KRAS may have a negative role in platinum-based therapy responses in NSCLC, but its impact is limited.

DNA polymerase β, when not expressed, might indicate a group of patients with poor outcomes. KRAS mutations in tumors not expressing DNA polymerase β further worsens survival. Therefore, these two biomarkers together might well identify patients for whom alternatives to platinum-based chemotherapy should be used.

1. Introduction

Over the last 40 years, several million lung cancer patients have received platinum-based regimens, and despite the clinical use of an impressive variety of targeted agents, these drugs are still one of the main therapeutic options for certain patients [1]. Platinum compounds are also the best choice in first-line immunotherapy combinations [2]. However, despite the good impact of platinum-based therapies, only a small proportion of patients have durable benefits [3]. Therefore, biomarkers to explain the resistance mechanisms to platinum compounds are urgently needed.

KRAS mutations have long been considered potential biomarkers to predict the outcome of platinum-based chemotherapy in NSCLC [4]. The TAILOR trial data shed light on the possibility that there was a small negative prognostic effect of *KRAS* mutations in advanced NSCLC patients treated with a platinum-based doublet when EGFR-mutant patients were excluded from the analysis [5].

Platinum adducts are repaired by different DNA repair systems. The Fanconi anemia (FA) pathway is thought to coordinate these systems, including homologous recombination (HR), nucleotide excision repair (NER), and translesion synthesis (TLS) repair [6,7]. Other DNA repair systems, such as base excision repair (BER), are involved in cisplatin-induced DNA damage, but so far, they have been assigned only a marginal role in repairing this damage [8].

Our group recently reported in a preclinical study that DNA polymerase β, an important component of the BER pathway, could be involved in platinum-based chemotherapy responses. Our results suggested a different pattern of sensitivity/resistance to cisplatin, dependent on *KRAS* mutational status [9].

The present work explores whether DNA polymerase β, alone or in combination with *KRAS* mutational status, can identify tumors with different abilities to respond to platinum compounds. This is the first study to prospectively assess the combined role of the selected biomarkers to identify patients who could benefit from platinum-based therapy.

2. Material and Methods

2.1. Study Population and Samples

The Fondazione IRCCS Istituto Nazionale dei Tumori (Milan, Italy), the Regina Elena National Cancer Institute (Rome, Italy), the Hospital Papa Giovanni XXIII (Bergamo, Italy), and the Metropolitan and Attikon Hospitals (Athens, Greece) were the centers involved. Consecutive patients with metastatic NSCLC who received platinum-based chemotherapy in combination with either vinorelbine, gemcitabine, or pemetrexed, according to the physician's choice, as first-line therapy between February 2014 and April 2017 were included in the BioRaRe prospective multicenter trial.

All patients had an Eastern Cooperative Oncology Group (ECOG) Performance Status (PS) between 0 and 2 and were at least 18 years of age. Exclusion criteria included any evidence of serious comorbidities that the investigator judged as a contraindication to the participation in the study, pregnancy, and breast-feeding.

Patients evaluable for tumor response according to the RECIST 1.1 criteria were examined, and their demographics and clinical and pathological characteristics were retrieved. E-CRF and medical records were used to collect data.

The study was approved by the Fondazione IRCCS Istituto Nazionale dei Tumori Institutional Review Board (INT18/13) and conducted according to the Declaration of Helsinki ethical principles for medical research involving human subjects. All patients gave signed written informed consent.

2.2. Mutational Analysis

KRAS mutational status was determined by Sanger sequencing at each center, following the protocol already used in a clinical trial by our group [10]. Briefly, DNA extraction was performed on histological tumor specimens by using standard phenol–chloroform procedure after macro/microdissection in order to recovery most of the cancer cells and to reduce contamination by normal ones. DNA preparations were verified for their concentration and quality by spectrophotometric measurement. Genomic DNAs were amplified by polymerase chain reaction (PCR) using high-fidelity Taq polymerase and specific primers encompassing intronic regions for KRAS exons 2–4. PCR products were then analyzed electrophoretically on agarose gel, and automated bidirectional sequencing was performed using BigDye Terminator chemistry. Sequences were then automatically compared with wild-type KRAS gene profiles by software analysis to assess the presence of possible mutations.

2.3. Immunohistochemical Analysis (IHC)

IHC was done centrally on single slides at the Fondazione Filarete, as previously reported [11]. Sections were immune-stained with anti-DNA polymerase β antibody ab26343 (Abcam, Cambridge, UK), and incubated with biotinylated secondary goat anti-rabbit antibody (VC-BA-1000-MM15, Vector Laboratories, Burlingame, CA, USA). Sections were labeled by the avidin–biotin–peroxidase (ABC) procedure with a commercial immunoperoxidase kit (VECTASTAIN Elite ABC-Peroxidase Kit Standard, VC-PK-6100-KI01, Vector Laboratories, Burlingame, CA, USA). The immune reaction was visualized with 3,3′-diaminobenzidine peroxidase DAB substrate kit (VC-SK-4100-KI01, Vector Laboratories, Burlingame, CA, USA) substrate and sections were counterstained with Mayer's hematoxylin. Figure S1 shows representative images of negative and positive DNA polymerase β staining.

A semiquantitative H-score (percentage of positive tumoral cells x intensity: 0 = negative, 1 = slight, 2 = moderate, 3 = strong) was calculated independently by two pathologists. In case of disagreement, a third opinion was requested.

2.4. Outcomes

The primary outcome of the study was progression-free survival (PFS). Secondary outcomes were objective response rate (ORR) and overall survival (OS). PFS was defined as the time from the start of the platinum-based first-line therapy to the date of progression or death from any cause, whichever came first. ORR was defined as the proportion of patients with a complete or partial response to treatment. OS was defined as the time from the platinum-based first-line therapy to the date of death from any cause.

2.5. Statistical Methods

Chi-squared and Kruskal–Wallis tests were used to analyze the relations between the DNA polymerase β H-score (Polβ) and categorical clinical variables. The Spearman correlation coefficient was used to measure the correlation between Polβ and continuous clinical variables. Polβ was analyzed as a continuous and dichotomous variable (Polβ = 0 as negative and Polβ > 0 as positive).

Patients who had not died or had no disease progression were censored at their last available information on status. Survival curves were calculated with the Kaplan–Meier method and tested by the log-rank test. Cox proportional hazard models were used to analyze the impact of DNA polymerase β on PFS and OS, adjusting for clinical and pathological characteristics such as ECOG-PS, age, histology, smoking, therapy, and, only for OS, immunotherapy. Results were expressed as hazard ratios (HRs) with their 95% confidence intervals (95% CIs).

The impact of DNA polymerase β on ORR was analyzed with logistic regression models and expressed as odds ratios (ORs) with their 95% CIs, while for dichotomized analysis, the chi-square test was used. A subgroup analysis was done for patients with both Polβ and KRAS mutational status available.

All statistical tests were two-sided, and $p < 0.05$ was considered statistically significant. Statistical analyses were done using SAS version 9.4 (SAS Institute, Cary, NC, USA).

3. Results

Of the 120 patients registered in the trial with material available, 109 had a DNA polymerase β H-score (Polβ) and 74 had both Polβ and *KRAS* mutational status. Figure 1 reports the flowchart of the study.
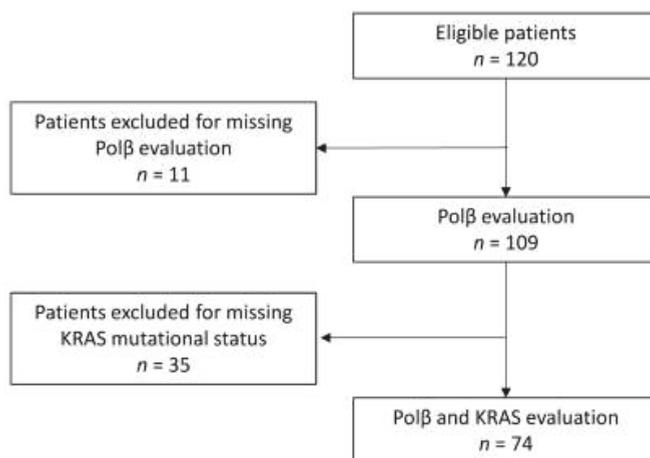
Figure 1. CONSORT diagram showing the flow of participants.

The main demographic characteristics of the population ($n = 109$) and the relationships between characteristics and Polβ are reported in Table 1.

3.1. Progression-Free Survival

The median PFS was, respectively, 5.9 and 7.2 months in the mutated (mut) and wild-type (wt) KRAS groups (adjusted HR mut vs. wt: 1.09, 95% CI: 0.56–2.08, $p = 0.815$).

Polβ, considered a continuous variable, did not have any significant impact on PFS in a multivariable Cox model. HR was 0.99 for each 10-unit increment of the score, with 95% CI 0.97–1.02 and $p = 0.579$. The inclusion of KRAS mutational status in the statistical model did not modify the impact of Polβ on progression or death risk (HR: 0.99, 95% CI: 0.96–1.02, $p = 0.501$). Considering Polβ as a dichotomous variable, median PFS were, respectively, 4 and 6.3 months for negative (neg) and positive (pos) staining. The absence or presence of DNA polymerase β had no impact on the risk of PFS, considering the multivariable models, either including KRAS status or not in the analysis (HR pos vs. neg: 1.10, 95% CI: 0.44–2.70, $p = 0.847$; HR pos vs. neg: 1.08, 95% CI: 0.49–2.38, $p = 0.857$). Detailed results of the multivariable analysis for PFS are reported in Table 2, and the Kaplan–Meier curves for PFS are shown in Figure 2A. The forest plot in Figure 2B graphically shows the effect of KRAS status on the relationship between Polβ and PFS.

3.2. Overall Survival

The median OS was, respectively, 12.4 and 20.5 months in the mutated and wild-type KRAS groups (adjusted HR mut vs. wt: 1.27, 95% CI: 0.70–2.27, $p = 0.441$).

Polβ, analyzed as a continuous variable, had no impact on survival in the multivariable models including KRAS status or not (HR: 0.99, 95% CI: 0.96–1.01, $p = 0.39$; HR = 0.99, 95% CI: 0.95–1.02, p-value = 0.388).

Patients who were negative for DNA polymerase β staining had a median OS of 11.6 months compared to 20.6 months in the positive group. The absence of DNA polymerase β caused a worse but not statistically significant OS compared to DNA polymerase β-expressing patients (HR pos vs. neg: 1.43, 95% CI: 0.57–3.57, $p = 0.439$). With the inclusion of KRAS mutational status in the statistical model, the effect on survival with Polβ was stronger (HR pos vs. neg: 1.67, 95% CI: 0.52–5.56, $p = 0.386$). The results of the multivariate analyses for OS are reported in Table 3. Kaplan–Meier curves for OS, reported in Figure 3A,B, show the effect of KRAS status on the relationship between Polβ and OS.

Table 1. Baseline characteristics of patients ($n = 109$) and their relation with Polβ as a continuous or dichotomous variable. Pos, positive; neg, negative.

		n (%)		p Polβ Continuous	p Polβ pos vs. neg
Age of diagnosis	Median(Q1–Q3)	66.8 (60.0–71.4)		0.448 *	0.788 [†]
	Missing	3			
Gender	Male	70	65.4	0.717 [†]	0.366 **
	Female	37	34.6		
	Missing	2			
ECOG-PS	0	78	81.3	0.157 [†]	0.443 **
	1	17	17.7		
	2	1	1		
	Missing	13			
Smoking	Never	21	20	0.618 [†]	1.000 **
	Former smokers	42	40		
	Smokers	42	40		
	Missing	4			
Stage at diagnosis	IIIB	28	26.2	0.038 [†]	0.507 **
	IV	79	73.8		
	Missing	2			
Histotype	Adenocarcinoma	90	82.6	0.291 [†]	0.184 **
	Squamous	17	15.6		
	Other	2	1.8		
Platinum-based therapy	Cisplatin	33	34.7	0.726 [†]	0.486 **
	Carboplatin	62	65.3		
	Missing	14			
Immunotherapy	No	62	58.5	0.248 [†]	0.352 **
	Yes	44	41.5		
	Missing	3			
Polβ	Median(Q1-Q3)	160.0 (60.0–200.0)		-	-
	negative	13	11.9	-	-
	positive	96	88.1		
KRAS	Mutated	35	47.3	0.053 [†]	0.125 **
	Wild-Type	39	52.7		
	Missing	35			

At a median follow-up of 18.8 months (Q1–Q3: 8.3–48.9), there were 90 progressions, 62 deaths, and 100 deaths or progressions. Q1–Q3: first–third quartile, pos: positive, neg: negative, [†]: Kruskal–Wallis test, *: Spearman correlation, **: Fisher test.

Table 2. Multivariable Cox models adjusted for ECOG-PS, age, histology, smoking, and therapy for progression-free survival, considering Polβ continuous or Polβ positive vs. negative. Pos, positive; neg, negative.

	Polβ Continuous		Polβ pos vs. neg	
	HR (95% CI)	*p*	HR (95% CI)	*p*
Polβ (10-unit increment)	0.99 (0.97–1.02)	0.579	-	-
Polβ				
Positive	-	-	reference	
Negative	-	-	1.07 (0.49–2.38)	0.857
Age at metastasis diagnosis (5 years increment)	0.82 (0.72–0.94)	0.005	0.82 (0.72–0.95)	0.006
Histology				
Adenocarcinoma	reference		reference	
Squamous	1.10 (0.60–2.03)	0.755	1.12 (0.60–2.10)	0.728
Nos or other	2.26 (0.27–18.6)	0.449	2.34 (0.28–19.5)	0.432
Smoke				
Never	reference		reference	
Previous	1.25 (0.69–2.26)	0.463	1.27 (0.70–2.29)	0.434
Current	0.79 (0.40–1.56)	0.495	0.81 (0.41–1.59)	0.543
ECOG-PS	1.51 (0.78–2.94)	0.223	1.51 (0.76–3.00)	0.244
Therapy				
Cisplatin	reference		reference	
Carboplatin	1.73 (1.02–2.92)	0.041	1.69 (1.01–2.85)	0.046

Table 3. Multivariable Cox models adjusted for ECOG-PS, age, histology, smoking, therapy, and immunotherapy for OS, considering Polβ continuous and Polβ positive or negative. Pos: positive, neg: negative.

	Polβ Continuous		Polβ pos vs. neg	
	HR (95% CI)	*p*	HR (95% CI)	*p*
Polβ (10-unit increment)	0.99 (0.96–1.01)	0.390	-	-
Polβ				
Positive	-	-	reference	
Negative	-	-	1.43 (0.57–3.57)	0.439
Age at metastasis diagnosis (5 years increments)	0.87 (0.75–1.01)	0.066	0.87 (0.75–1.01)	0.065
Histology				
Adenocarcinoma	reference		reference	
Squamous	0.94 (0.46–1.95)	0.877	0.98 (0.47–2.06)	0.960
Nos or other	7.67 (0.83–70.6)	0.072	8.86 (0.94–83.3)	0.056
Smoke				
Never	reference		reference	
Previous	2.65 (1.15–6.12)	0.022	2.76 (1.21–6.30)	0.016
Current	1.58 (0.61–4.11)	0.350	1.63 (0.63–4.26)	0.316
ECOG-PS	1.18 (0.48–2.90)	0.724	1.12 (0.44–2.87)	0.812
Therapy				
Cisplatin	reference		reference	
Carboplatin	1.74 (0.94–3.21)	0.075	1.70 (0.93–3.12)	0.084
Immunotherapy				
No	reference		reference	
Yes	0.57 (0.32–1.03)	0.063	0.55 (0.31–0.98)	0.041
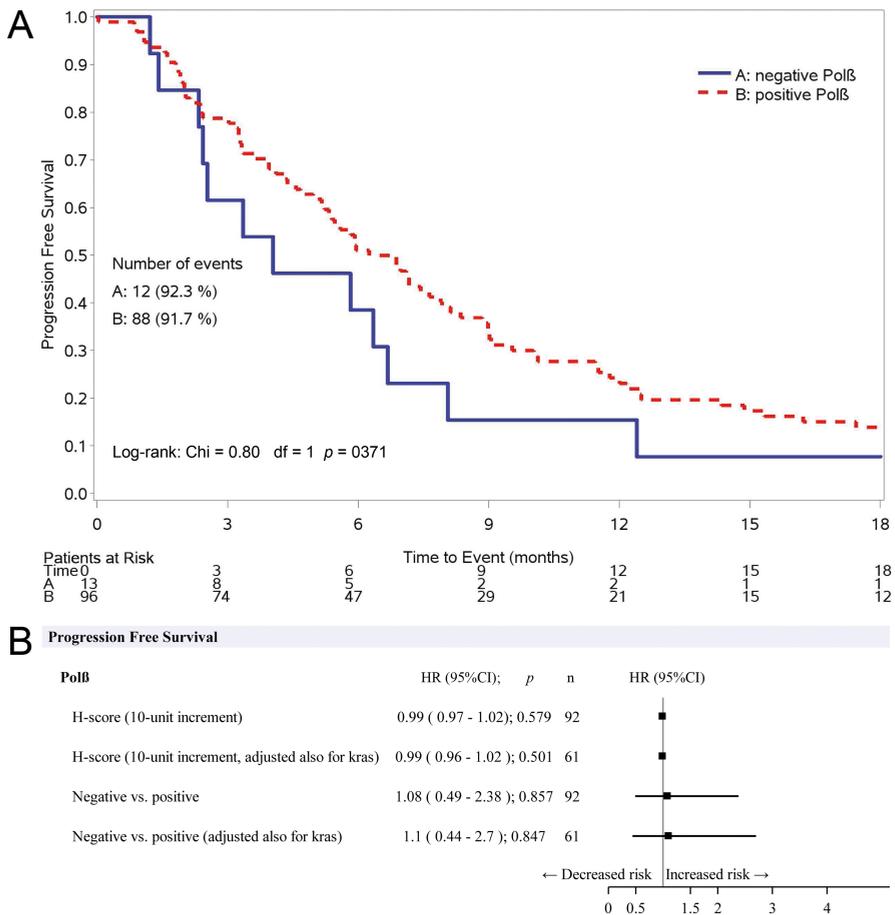
Figure 2. (**A**) Kaplan–Meier curves for PFS according to the positive or negative DNA polymerase β staining. (**B**) Effect of KRAS status on the relationship between Polβ and PFS adjusted for ECOG-PS, age, histology, smoking, and therapy.
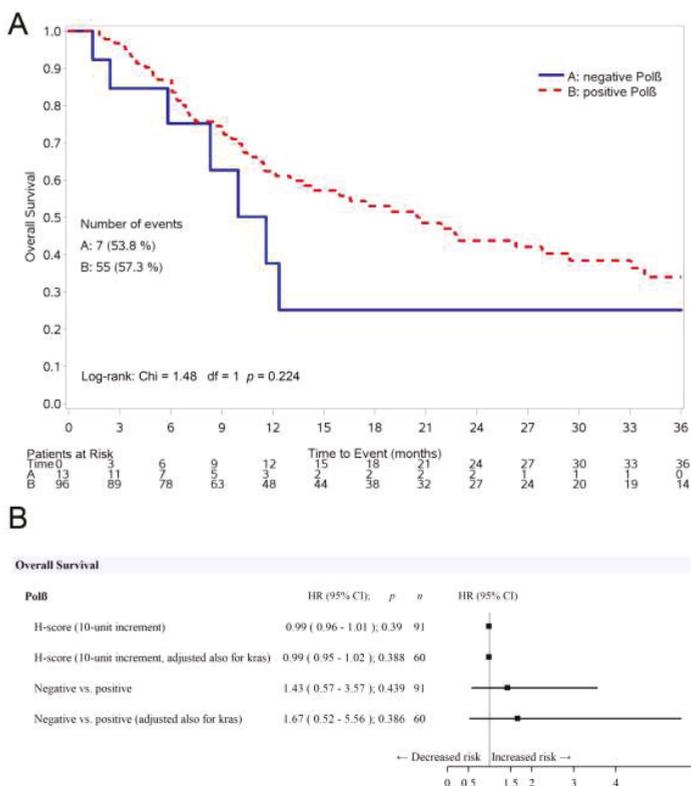
Figure 3. (**A**) Kaplan–Meier curves for OS, according to the positive or negative DNA polymerase β staining. (**B**) Effect of KRAS status on the relationship between Polβ and PFS adjusted for ECOG-PS, age, histology, smoking, therapy, and immunotherapy.

3.3. Overall Response Rate

There were no differences between the DNA polymerase β negative and positive staining groups, or among different Polβ as a continuous variable in ORR to platinum-based first-line therapy (Table 4).

Table 4. Objective response rates by DNA Polymerase β H-score (Polβ). CR, complete response; PR, partial response; SD, stable disease; PD, progressive disease.

	Polβ neg $n = 12$	Polβ pos $n = 64$	Chi-Squared Test	Logistic Regression Model
CR + PR −n (%)	4 (33.3)	23 (35.9)	Chi = 0.03	OR = 1.002
95% CI	34.9–90.1	51.1–75.7	Df = 1	95%CI = 0.997–1.006
SD + PD −n (%)	8 (66.7)	41 (64.1)	$p = 0.864$	$p = 0.505$
95% CI	9.9–65.1	24.3–48.9		

4. Discussion

KRAS mutations have often been investigated as possible biomarkers for selecting chemotherapy, but results have varied, casting doubt on the true utility of this protein. In a previously published randomized prospective trial from our group, an analysis of 247 patients showed that those carrying KRAS mutations and treated with a first-line platinum-based regimen had worse PFS than patients with wild-type KRAS [5]. The present study detected a not-statistically-significant effect for OS,

KRAS-mutated patients having a worse prognosis than KRAS wild-type patients. A possible explanation, although the trend is in line with previous observations, is that the statistical power of this cohort of patients was half that in our earlier study, where KRAS status was significantly associated with survival. On the other hand, the LACE-Bio pooled analysis, including data of 1543 patients participating in four clinical trials, showed that there is no difference in terms of outcomes in early-stage lung cancer patients with either wild-type or mutated KRAS [12]. Our different result may suggest that KRAS mutations could play different roles in early and advanced disease. In advanced stages, KRAS could be a condition necessary, but not sufficient, to explain a more aggressive phenotype.

There is preclinical evidence that KRAS and its mutated versions modulate DNA repair, hence the cellular response to genotoxic agents. Oncogenic RAS can inactivate BRCA-1 dependent homologous recombination (HR) by favoring the dissociation of BRCA-1 from chromatin [13]. Moreover, activated KRAS can suppress the expression of DNA repair genes (including BRCA1, BRCA2, EXO-1, and TP53) [14]. In leukemic cells, mutant KRAS promoted the upregulation of components of the alternative nonhomologous end-joining (NHEJ) pathway, such as DNA ligase IIIα, PARP1, and XRCC1, and the inhibition of the alternative NHEJ pathway selectively sensitized KRAS-mutated cells to chemotherapy [15].

Our group also suggested KRAS-dependent specific alterations in the BER system, where we found DNA polymerase β as a possible selection factor. We demonstrated at the preclinical level that DNA polymerase β could play a role in the response to cisplatin-based chemotherapy, and the data indicated a pattern of sensitivity or resistance depending on the KRAS mutational status [9]. These findings support the hypothesis that the combination of mutant-KRAS status with DNA repair could be a predictive biomarker for response to platinum-based therapy.

On the basis of these assumptions, we planned a translational study to clinically validate KRAS and DNA polymerase β as "biomarkers" for poor response and outcome to platinum-based first-line chemotherapy. We investigated DNA polymerase β as a possible selection marker, alone or in combination with KRAS status. DNA polymerase β expression, summarized in the H-score and considered as a continuous variable, was meaningless to both PFS and OS, alone or with KRAS.

When we compared negative or positive DNA polymerase β staining patients, we detected an interesting, though not statistically significant, difference: OS patients negative for DNA polymerase β staining had worse outcomes than the positive staining group. This result was confirmed even when KRAS status was considered in the analysis.

These data, although interesting and calling for further analysis, are not supported by the literature, where DNA polymerase β upregulation was described as causing resistance to cisplatin in an ovarian cancer model [16]. In a colorectal cancer model expressing high levels of DNA polymerase β, cisplatin was ineffective compared to the same model in which DNA polymerase β was downregulated. In the same paper, 5-year OS curves showed that patients with high DNA polymerase β expression had a significantly poorer prognosis than those with low expression [17]. However, DNA polymerase β has been investigated as a selection marker in very few, only retrospective studies, and our is the first attempt to investigate it, prospectively, in NSCLC.

A recent report suggests that if cells are not able to repair DNA single-strand break lesions through BER (as should be the case here for cells negative for DNA polymerase β), these lesions are channeled to the HR system [18]. We do not know whether this is also true for cisplatin-induced DNA lesions and whether these patients have HR alterations, but it does suggest an intriguing explanation for the worse outcome observed in DNA polymerase β-negative patients.

To our knowledge, this is the first investigation of the role and value of DNA polymerase β, alone or in combination with KRAS status, as a marker of response to platinum-based therapy in NSCLC. Besides the results, this paper also stimulates the idea to further investigate the combination of biomarkers that indicate how different biological pathways coexist or work together in those scenarios, where no single biomarker has been shown to have strong value.

In conclusion, KRAS may have a negative role in platinum-based therapy responses in NSCLC, but its impact is limited. The absence of DNA polymerase β might indicate a group of patients with poor outcomes compared to patients positively staining for this protein. In addition, a mutated form of KRAS in tumors not expressing DNA polymerase β further worsens survival. Therefore, these two biomarkers together might well identify patients for whom alternatives to platinum-based chemotherapy should be used.

References

1. Schirrmacher, V. From chemotherapy to biological therapy: A review of novel concepts to reduce the side effects of systemic cancer treatment (Review). *Int. J. Oncol.* **2018**, *54*, 407–419. [PubMed]
2. Gandhi, L.; Rodriguez-Abreu, D.; Gadgeel, S.; Esteban, E.; Felip, E.; De Angelis, F.; Dómine, M.; Clingan, P.; Hochmair, M.J.; Powell, S.F.; et al. Pembrolizumab plus Chemotherapy in Metastatic Non–Small-Cell Lung Cancer. *N. Engl. J. Med.* **2018**, *378*, 2078–2092. [CrossRef] [PubMed]
3. Schmidt, E.V. Developing combination strategies using PD-1 checkpoint inhibitors to treat cancer. *Semin. Immunopathol.* **2019**, *41*, 21–30. [CrossRef] [PubMed]
4. Piva, S.; Ganzinelli, M.; Garassino, M.C.; Caiola, E.; Farina, G.; Broggini, M.; Marabese, M. Across the universe of K-RAS mutations in non-small-cell-lung cancer. *Curr. Pharm. Des.* **2014**, *20*, 3933–3943. [CrossRef] [PubMed]
5. Marabese, M.; Ganzinelli, M.; Garassino, M.C.; Shepherd, F.A.; Piva, S.; Caiola, E.; Macerelli, M.; Bettini, A.; Lauricella, C.; Floriani, I.; et al. KRAS mutations affect prognosis of non-small-cell lung cancer patients treated with first-line platinum containing chemotherapy. *Oncotarget* **2015**, *6*, 34014–34022. [CrossRef] [PubMed]
6. Deans, A.J.; West, S.C. DNA interstrand crosslink repair and cancer. *Nat. Rev. Cancer* **2011**, *11*, 467–480. [CrossRef] [PubMed]
7. Haynes, B.; Saadat, N.; Myung, B.; Shekhar, M.P. Crosstalk between translesion synthesis, Fanconi anemia network, and homologous recombination repair pathways in interstrand DNA crosslink repair and development of chemoresistance. *Mutat. Res.-Rev. Mutat. Res.* **2015**, *763*, 258–266. [CrossRef] [PubMed]
8. Jung, Y.; Lippard, S.J. Direct cellular responses to platinum-induced DNA damage. *Chem. Rev.* **2007**, *107*, 1387–1407. [CrossRef] [PubMed]
9. Caiola, E.; Salles, D.; Frapolli, R.; Lupi, M.; Rotella, G.; Ronchi, A.; Garassino, M.C.; Mattschas, N.; Colavecchio, S.; Broggini, M.; et al. Base excision repair-mediated resistance to cisplatin in KRAS(G12C) mutant NSCLC cells. *Oncotarget* **2015**, *6*, 30072–30087. [CrossRef] [PubMed]
10. Garassino, M.C.; Martelli, O.; Broggini, M.; Farina, G.; Veronese, S.M.; Rulli, E.; Bianchi, F.; Bettini, A.; Longo, F.; Moscetti, L.; et al. Erlotinib versus docetaxel as second-line treatment of patients with advanced non-small-cell lung cancer and wild-type EGFR tumours (TAILOR): A randomised controlled trial. *Lancet Oncol.* **2013**, *14*, 981–988. [CrossRef]
11. Marabese, M.; Marchini, S.; A Sabatino, M.; Polato, F.; Vikhanskaya, F.; Marrazzo, E.; Riccardi, E.; Scanziani, E.; Broggini, M. Effects of inducible overexpression of DNp73α on cancer cell growth and response to treatment in vitro and in vivo. *Cell Death Differ.* **2005**, *12*, 805–814. [CrossRef] [PubMed]

12. Shepherd, F.A.; Domerg, C.; Hainaut, P.; Jänne, P.A.; Pignon, J.-P.; Graziano, S.; Douillard, J.-Y.; Brambilla, E.; Le Chevalier, T.; Seymour, L.; et al. Pooled analysis of the prognostic and predictive effects of KRAS mutation status and KRAS mutation subtype in early-stage resected non–small-cell lung cancer in four trials of adjuvant chemotherapy. *J. Clin. Oncol.* **2013**, *31*, 2173–2181. [CrossRef] [PubMed]

13. Tu, Z.; Aird, K.M.; Bitler, B.G.; Nicodemus, J.P.; Beeharry, N.; Xia, B.; Yen, T.J.; Zhang, R. Oncogenic RAS regulates BRIP1 expression to induce dissociation of BRCA1 from Chromatin, Inhibit DNA repair, and promote senescence. *Dev. Cell* **2011**, *21*, 1077–1091. [CrossRef] [PubMed]

14. Tsunoda, T.; Takashima, Y.; Fujimoto, T.; Koyanagi, M.; Yoshida, Y.; Doi, K.; Tanaka, Y.; Kuroki, M.; Sasazuki, T.; Shirasawa, S. Three-dimensionally specific inhibition of DNA repair-related genes by activated KRAS in colon crypt model. *Neoplasia* **2010**, *12*, 397–404. [CrossRef] [PubMed]

15. Hahnel, P.S.; Enders, B.; Sasca, D.; Roos, W.P.; Kaina, B.; Bullinger, L.; Theobald, M.; Kindler, T. Targeting components of the alternative NHEJ pathway sensitizes KRAS mutant leukemic cells to chemotherapy. *Blood* **2014**, *123*, 2355–2366. [CrossRef] [PubMed]

16. Bergoglio, V.; Canitrot, Y.; Hogarth, L.; Minto, L.; Howell, S.B.; Cazaux, C.; Hoffmann, J.-S. Enhanced expression and activity of DNA polymerase beta in human ovarian tumor cells: Impact on sensitivity towards antitumor agents. *Oncogene* **2001**, *20*, 6181–6187. [CrossRef] [PubMed]

17. Iwatsuki, M.; Mimori, K.; Yokobori, T.; Tanaka, F.; Tahara, K.; Inoue, H.; Baba, H.; Mori, M. A platinum agent resistance gene, POLB, is a prognostic indicator in colorectal cancer. *J. Surg. Oncol.* **2009**, *100*, 261–266. [CrossRef] [PubMed]

18. Giovannini, S.; Weller, M.C.; Repmann, S.; Moch, H.; Jiricny, J. Synthetic lethality between BRCA1 deficiency and poly(ADP-ribose) polymerase inhibition is modulated by processing of endogenous oxidative DNA damage. *Nucleic Acids Res.* **2019**, *47*, 9132–9143. [CrossRef] [PubMed]

Article

Final Results from a Phase II Trial of Osimertinib for Elderly Patients with Epidermal Growth Factor Receptor t790m-Positive Non-Small Cell Lung Cancer That Progressed during Previous Treatment

Akira Nakao [1,†], **Osamu Hiranuma** [2,†], **Junji Uchino** [3,*,†], **Chikara Sakaguchi** [4], **Tomoyuki Araya** [5], **Noriya Hiraoka** [6], **Tamotsu Ishizuka** [7], **Takayuki Takeda** [8], **Masayuki Kawasaki** [9], **Yasuhiro Goto** [10], **Hisao Imai** [11], **Noboru Hattori** [12], **Keita Nakatomi** [13], **Hidetaka Uramoto** [14], **Kiyoaki Uryu** [15], **Minoru Fukuda** [16], **Yasuki Uchida** [17], **Toshihide Yokoyama** [18], **Masaya Akai** [19], **Tadashi Mio** [20], **Seiji Nagashima** [21], **Yusuke Chihara** [3], **Nobuyo Tamiya** [3], **Yoshiko Kaneko** [3], **Takako Mouri** [3], **Tadaaki Yamada** [3], **Kenichi Yoshimura** [22], **Masaki Fujita** [1] and **Koichi Takayama** [3]

1   Department of Respiratory Medicine, Faculty of Medicine, Fukuoka University, Fukuoka 814-0180, Japan; akiran@fukuoka-u.ac.jp (A.N.); mfujita@fukuoka-u.ac.jp (M.F.)
2   Department of Respiratory Medicine, Otsu City Hospital, Shiga 520-0804, Japan; osamu319@true.ocn.ne.jp
3   Department of Pulmonary Medicine, Kyoto Prefectural University of Medicine, Kyoto 602-8566, Japan; c1981311@koto.kpu-m.ac.jp (Y.C.); koma@koto.kpu-m.ac.jp (N.T.); kaneko-y@koto.kpu-m.ac.jp (Y.K.); tmouri@koto.kpu-m.ac.jp (T.M.); tayamada@koto.kpu-m.ac.jp (T.Y.); takayama@koto.kpu-m.ac.jp (K.T.)
4   Department of Pulmonary Medicine, Rakuwakai Otowa Hospital, Kyoto 607-8062, Japan; rakuwadr1141@rakuwadr.com
5   Department of Respiratory Medicine, National Hospital Organization, Kanazawa Medical Center, Ishikawa 920-8650, Japan; komatsu_alone@yahoo.co.jp
6   Department of Respiratory Medicine, Japanese Red Cross Kyoto Daiichi Hospital, Kyoto 605-0981, Japan; noriya-hiraoka@kyoto1-jrc.org
7   Third Department of Internal Medicine, Faculty of Medical Sciences, University of Fukui, Fukui 910-1193, Japan; tamotsui@u-fukui.ac.jp
8   Department of Respiratory Medicine, Japanese Red Cross Society Kyoto Daini Hospital, Kyoto 602-8026, Japan; dyckw344@yahoo.co.jp
9   Department of Respiratory Medicine, National Hospital Organization, Omuta National Hospital, Fukuoka 837-0911, Japan; kawasaki.masayuki.hx@mail.hosp.go.jp
10 Department of Respiratory Medicine, Fujita Health University, Aichi 470-1192, Japan; gotoyasu@fujita-hu.ac.jp
11 Division of Respiratory Medicine, Gunma Prefectural Cancer Center, Gunma 373-8550, Japan; hi-imai@gunma-cc.jp
12 Department of Molecular and Internal Medicine, Graduate School of Biomedical & Health Sciences, Hiroshima University, Hiroshima 734-8553, Japan; nhattori@hiroshima-u.ac.jp
13 Department of Respiratory Medicine, Kyushu Central Hospital of the Mutual Aid Association of Public School Teachers, Fukuoka 815-8588, Japan; keita.nakatomi@icloud.com
14 Department of Thoracic Surgery, Kanazawa Medical University, Ishikawa 920-0293, Japan; hidetaka@kanazawa-med.ac.jp
15 Department of Respiratory Medicine, Yao Tokushukai General Hospital, Osaka 581-0011, Japan; kiyoaki.uryuu@tokushukai.jp
16 Second Department of Internal Medicine, Nagasaki University Hospital, Nagasaki 852-8523, Japan; mifukuda@nagasaki-u.ac.jp
17 Department of Respiratory Medicine, Shiga University of Medical Science Hospital, Shiga 520-2192, Japan; uchiy@belle.shiga-med.ac.jp
18 Department of Respiratory Medicine, Kurashiki Central Hospital, Okayama 710-8602, Japan; ty14401@kchnet.or.jp
19 Department of Respiratory Medicine, Japanese Red Cross Fukui Hospital, Fukui 918-8501, Japan; makai-0314@fukui-med.jrc.or.jp

[20]   Division of Respiratory Medicine, Center for Respiratory Diseases, National Hospital Organization Kyoto Medical Center, Kyoto 612-8555, Japan; tmio.kmc@gmail.com

[21]   Department of Respiratory Medicine, National Hospital Organization Nagasaki Medical Center, Nagasaki 856-0835, Japan; nagashima.seiji.kg@mail.hosp.go.jp

[22]   Center for Integrated Medical Research, Hiroshima University Hospital, Hiroshima University, Hiroshima 734-8553, Japan; keyoshim@hiroshima-u.ac.jp

*   Correspondence: uchino@koto.kpu-m.ac.jp; Tel.: +81-75-251-5513

†   Contributed equally.

Abstract: Epidermal growth factor receptor tyrosine kinase inhibitors (EGFR-TKIs) are used for treating EGFR-mutated lung cancer, and osimertinib is effective in cases that acquired T790M mutations after treatment with the first- and second-generation EGFR-TKIs. However, no study has evaluated its safety and efficacy in older patients. This phase II trial (jRCTs071180002) evaluated osimertinib in T790M mutation-positive Japanese patients who were ≥75 years old and had experienced relapse or progression after previous EGFR-TKI treatment. Our previous report that enrolled 36 patients showed the overall response rate (58.3%) and disease control rate (97.2%), while this report describes the results for the progression-free survival (PFS), overall survival (OS), and safety analyses. The median PFS was 11.9 months (95% confidence interval (CI): 7.9–17.5), and the median OS was 22.0 months (95% CI: 16.0 months–not reached). The most frequent adverse events were anemia/hypoalbuminemia (27 patients, 75.0%), thrombocytopenia (21 patients, 58.3%), and paronychia/anorexia/diarrhea/neutropenia (15 patients, 41.7%). Pneumonitis was observed in four patients (11.1%), including two patients (5.6%) with Grade 3–4 pneumonitis. These results suggest that osimertinib was relatively safe and effective for non-small cell lung cancer that acquired T790M mutations after previous EGFR-TKI treatment, even among patients who were ≥75 years old.

Keywords: non-small cell lung cancer; EGFR-TKI; T790M; osimertinib

1. Introduction

Treatment for epidermal growth factor receptor (EGFR)-mutated non-small cell lung cancer (NSCLC) typically involves EGFR tyrosine kinase inhibitors (EGFR-TKIs). Gefitinib and erlotinib are the first-generation EGFR-TKIs that provide significant survival benefits compared with platinum-based chemotherapy in clinical trials [1–6]. Afatinib and dacomitinib are the second-generation EGFR-TKIs that provide significantly longer progression-free survival (PFS) compared to that of platinum-based chemotherapy and first-generation EGFR-TKIs, although the second-generation EGFR-TKIs did not significantly improve overall survival (OS) [7–11]. In addition, these drugs are associated with more severe toxicity profiles, such as skin disorders, relative to the first-generation EGFR-TKIs.

Various mechanisms are responsible for resistance to the first-generation and second-generation EGFR-TKIs, with more than one-half of the cases involving the EGFR exon 20 T790M mutation [12]. Osimertinib is a third-generation EGFR-TKI that was developed to address this issue [12], and he AURA3 study revealed that it provided significantly longer PFS compared to platinum-based chemotherapy among patients with T790M-mutated lung cancer [13]. Moreover, the FLAURA trial conducted on first-line treatment revealed that osimertinib administered as an initial treatment for EGFR-mutated cases significantly prolonged PFS and OS compared with the first-generation EGFR-TKIs, with a median OS of >3 years [14,15]. Furthermore, osimertinib is expected to have good central nervous system translocation and a limited inhibition of the wild-type EGFR, which may make it less toxic, and therefore, the first choice for EGFR-mutated NSCLC [16–18]. Nevertheless, additional evidence is needed to support this application based on various patient populations. We have performed a phase II study to investigate the efficacy and safety of osimertinib in elderly Japanese patients (≥75 years old)

with NSCLC containing the T790M mutation who progressed or experienced a relapse while receiving the first- and second- generations of EGFR-TKI treatment. In our previous report, the response rate was the primary endpoint, and the disease control rate was the secondary endpoint [19]. This report presents the results from our final analyses of PFS, OS, and safety events, which were the additional secondary endpoints in that trial.

2. Experimental Section

2.1. Patients

The study eligibility and exclusion criteria have been previously reported [19,20]. Patients were enrolled in this study between July 2016 and May 2018 if they met the following eligibility criteria: recurrence of NSCLC after achieving stable disease or better as their best overall response after treatment with the first- and second-generation of EGFR-TKIs; harboring an EGFR mutation (activating) and being T790M-positive; aged over 75 years; performance status of ≤1 based on the Eastern Cooperative Oncology Group (ECOG) scale; adequate bone marrow function (leukocyte count 3000–12,000/μL, platelet count ≥100,000/μL, and hemoglobin level ≥9.0 g/dL), adequate hepatic function (bilirubin level ≤1.5 mg/dL, aspartate aminotransferase of ≤100 IU/L, alanine aminotransferase of ≤100 IU/L), and adequate renal function (serum creatinine ≤2.0 mg/dL); a measurable lesion according to the Response Evaluation Criteria in Solid Tumors (RECIST) guidelines version 1.1; and provision of written informed consent. The exclusion criteria were pulmonary disorders; including idiopathic pulmonary fibrosis; interstitial pneumonia; pneumoconiosis; active radiation pneumonitis and drug-induced pneumonia, active infection; symptomatic brain metastasis; uncontrollable diabetes mellitus or severe comorbidities such as heart disease or renal disease; watery diarrhea; active concomitant malignancy; pregnancy or other medical problems that could prevent compliance with the protocol. The trial protocol was registered at Japan Registry of Clinical Trials (jRCTs071180002) and was approved by the ethical review board of Clinical Research Network Fukuoka Certified Review Board (CRB7180004). All patients provided written informed consent before enrollment.

2.2. Study Design, Treatments, and Endpoints

This single-arm-multicenter study involved daily oral administration of osimertinib (80 mg/day). Osimertinib had to be started at 80 mg/day, and if adverse events (AEs) occurred, dose reduction was performed according to the dose reduction criteria. Administration of osimertinib was continued until the patient met the discontinuation criteria or disease progression. Tumor assessments were performed at baseline, every 6 weeks (± 2 weeks) for 6 months, and then every 9 weeks (± 2 weeks) until disease progression. Baseline brain imaging was performed on a similar schedule. Among patients with T790M mutations, the objective response rate (ORR) was 62% (95% confidence interval [CI]: 54–68) in the AURA extension study (201 patients). In the AURA2 study (210 patients) the ORR was 70% (95% CI: 64–77) and the median PFS was 9.9 months (95% CI: 9.5–12.3) [21–23]. Docetaxel is the standard treatment for elderly patients based on the Japanese guidelines, as it provided an ORR of 22.7% in a study that compared docetaxel to vinorelbine [24]. Another recent study evaluated carboplatin plus pemetrexed for elderly Japanese patients and revealed an ORR of 41.2% [25]. Based on these findings, a required sample size of 31 patients was calculated according to the normal approximation method, with an expected response rate of 60%, a threshold response rate of 35%, two-sided alpha = 0.05, and 1 – beta = 0.8. However, the target sample size was increased to 35 patients to account for potential dropout cases. The primary endpoint for the trial was the overall response rate (ORR), while the secondary endpoints were PFS, OS, disease control rate (DCR), and safety events.

2.3. Statistical Methods

The ORR was calculated as the proportion of subjects with complete response or partial response as their best treatment responses. The DCR was calculated as the proportion of subjects who achieved

stable disease (or better) as their best treatment response. The PFS interval was calculated from the date of enrollment to the first instance of disease progression, death from any cause, or the last follow-up without evidence of progression (for surviving patients with no evidence of progression). The OS interval was calculated from the date of enrollment to the date of death from any cause. Adverse events were evaluated from the first drug administration to 30 days after the last drug administration and were graded based on the Japanese JCOG translation of version 4.0 of the Common Terminology Criteria for Adverse Events.

The Wilson method was used to estimate the ORR and DCR with their two-sided 95% CIs. Statistical significance was considered present when the lower limit of the estimated 95% CI was above the threshold of 35% for ORR. The Kaplan–Meier method was used to evaluate the survival curves for PFS and OS, as well as the median and annual values. The Brookmeyer and Crowley method was used to estimate the CI values for median values, and Greenwood's formula was used to estimate the standard error for annual values.

3. Results

3.1. Patient Characteristics

The study enrolled 36 patients between July 2016 and May 2018, with 23 female patients (63.9%) with a median age of 80 years, and 19 patients (52.8%) who were ≥80 years old. The histological types were adenocarcinoma in 35 patients (97.2%) and a mixed type with small cell lung cancer in only 1 patient. Based on the 7th edition of the AJCC system for staging lung cancer, 25 cases (69.4%) were considered stage IV, 10 cases (27.8%) involved relapse after surgery, and 1 case (2.8%) was considered stage IIIB. Among the enrolled patients, 30.6% were former smokers. The EGFR gene mutations involved the exon 20 T790M mutation in all cases, as well as exon 19 deletion in 22 cases (61.1%) and the exon 21 L858R point mutation in 11 cases (30.6%). Brain metastasis was detected in 15 patients (41.7%) (Table 1).

Table 1. Patient characteristics.

		n (%)
Sex	Male	13 (36.1)
	Female	23 (63.9)
Age	Median (range)	80 (75–92)
	≥80 years	52.8 %
	>85 years	11.1 %
PS	0	8 (22.2)
	1	28 (77.8)
Histology	Adenocarcinoma	35 (97.2)
	Adenocarcinoma + SCLC	1 (2.8)
Stage	IIIB	1 (2.8)
	IV	25 (69.4)
	Relapse after surgery	10 (27.8)
EGFR mutation	T790M	36 (100.0)
	Exon 19 deletion	22 (61.1)
	L858R	11 (30.6)
	G719X	1 (2.8)
Smoking status	Ex-smoker	11(30.6)
Pre-treatment	Surgery	12 (33.3)

Table 1. *Cont.*

		n (%)
	Chemotherapy	13 (36.1)
	EGFR-TKI	36 (100.0)
	Afatinib	5 (13.9)
	Erlotinib	10 (27.8)
	Gefitinib	21 (58.3)
	Radiotherapy	10 (27.8)
	Thoracic drainage	4 (11.1)
Metastasis site	Lung	18 (50.0)
	Pleural dissemination	12 (33.3)
	Brain	15 (41.7)
	Bone	12 (33.3)
	Liver	8 (22.2)

PS: performance status, SCLC: small cell lung cancer.

3.2. Efficacy

The ORR from our previous report was 58.3% (95% CI: 42.2–72.9), which included a complete response rate of 2.8% and a partial response rate of 55.6%. The stable disease rate was 38.9%, and the DCR was 97.2%. The median response duration was 54.9 weeks (95% CI: 26.9–69.1), and a waterfall plot revealed that 33 patients (91.6%) experienced tumor shrinkage, which indicated favorable antitumor activity. Sixteen patients (44.4%) continued treatment beyond progression.

The median PFS was 11.9 months (95% CI: 7.9–17.5), with 1-year PFS rate of 50.0% and 2-year PFS rate of 18.3% (Figure 1). The median OS was 22.0 months (95% CI: 16.0–not reached), with 1-year OS rate of 77.8% and 2-year OS rate of 49.5% (Figure 2).

No. of patients at risk

| 36 | 28 | 18 | 10 | 5 | 2 | 0 |
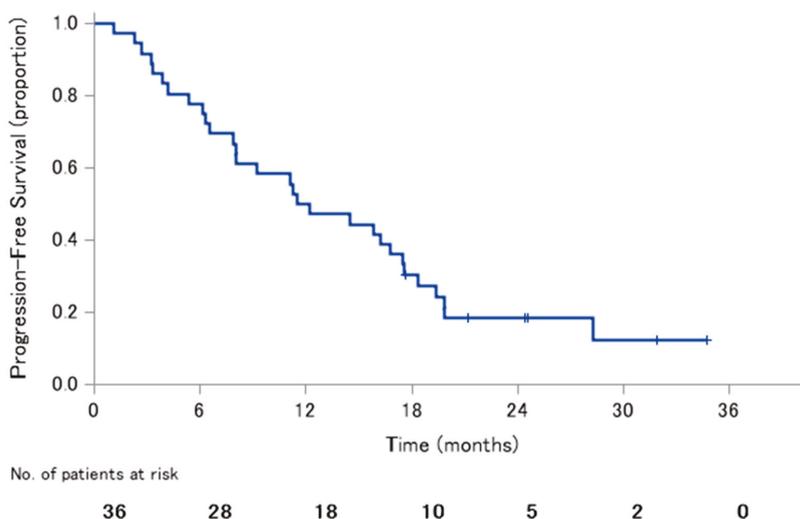
Figure 1. Progression-free survival.
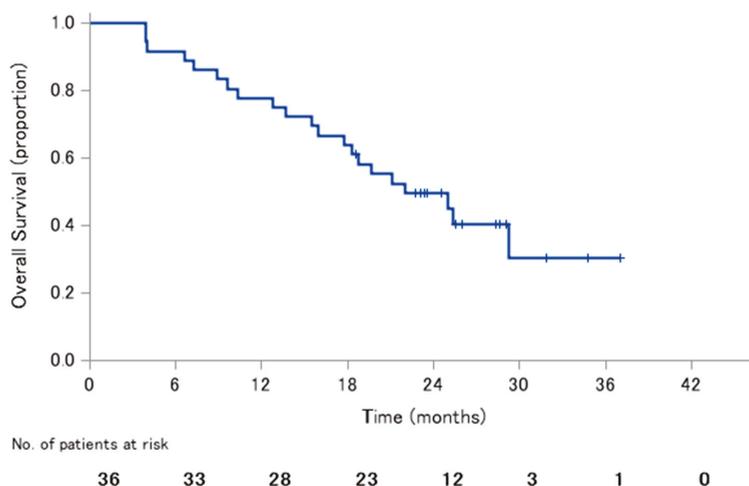
Figure 2. Overall survival.

3.3. Safety

Adverse events occurred in 31 cases (86.1%), with Grade 3 or higher adverse events observed in 10 cases (27.8%). Seven patients (19.4%) required dose reductions, 10 patients (27.8%) discontinued treatment because of adverse events, and 1 patient died (2.8%). The adverse event leading to death was a pulmonary infection, although this was judged unlikely to have been caused by the osimertinib treatment. There were no death events caused by drug-induced lung injury. The most frequent adverse event was anemia/hypoalbuminemia (27 patients, 75.0%), which was followed by thrombocytopenia (21 patients, 58.3%), paronychia/anorexia/diarrhea/neutropenia (15 patients, 41.7%), leukopenia/aspartate aminotransferase increase (14 patients, 38.9%), fatigue/acneiform eruption (13 patients, 36.1%), and alanine aminotransferase increase/alkaline phosphatase increase/creatinine increase (11 patients, 30.6%). The Grade 3–4 adverse events included fatigue, anorexia, diarrhea, cardiac ejection fraction decreased, prolonged QT, leukopenia, neutropenia, and aspartate aminotransferase increase. The cases of cardiac ejection fraction were decreased and the cases of prolonged QT were different cases, and delirium and hallucinations were observed in the same patient. Pneumonitis was observed in four patients (11.1%), including two patients (5.6%) with Grade 3–4 pneumonitis (Table 2).

Table 2. Adverse events.

	Any Grade	Grade 3–4
All adverse events > 15%, *n* (%)		
Anemia	27 (75.0)	0 (0.0)
Hypoalbuminemia	27 (75.0)	0 (0.0)
Platelet count decreased	21 (58.3)	0 (0.0)
Neutrophil count decreased	15 (41.7)	1 (2.8)
Paronychia	15 (41.7)	0 (0.0)
Decreased appetite	15 (41.7)	4 (11.1)
Diarrhea	15 (41.7)	1 (2.8)
White blood cell decreased	14 (38.9)	1 (2.8)
Aspartate aminotransferase increased	14 (38.9)	2 (5.6)

Table 2. *Cont.*

	Any Grade	Grade 3–4
Fatigue	13 (36.1)	3 (8.3)
Dermatitis acneiform	13 (36.1)	0 (0.0)
Alanine aminotransferase increased	11 (30.6)	0 (0.0)
Alkaline phosphatase increased	11 (30.6)	2 (5.6)
Creatinine increased	11 (30.6)	0 (0.0)
Pruritus	8 (22.2)	0 (0.0)
Mucositis oral	8 (22.2)	0 (0.0)
Grade 3–4 adverse events, *n* (%)		
Pneumonitis	4 (11.1)	2 (5.6)
Left ventricular systolic dysfunction	1 (2.8)	1 (2.8)
Electrocardiogram QT prolongation	1 (2.8)	1 (2.8)
Delirium	1 (2.8)	1 (2.8)
Hallucination	1 (2.8)	1 (2.8)
Dyspnea	1 (2.8)	1 (2.8)
Dehydration	1 (2.8)	1 (2.8)
Lung infection	2 (5.6)	1 (2.8)
Sinusitis	1 (2.8)	1 (2.8)

4. Discussion

Treatment of NSCLC has advanced dramatically after the introduction of molecularly targeted drugs, such as EGFR-TKIs for EGFR-mutated cases. The first- and second-generation of EGFR-TKIs proved to be highly effective in several studies, although the effects tended to only last for approximately 1 year [1–11]. Approximately one-half of the resistant cases involved a gatekeeper mutation in exon 20 (T790M), and osimertinib was developed and approved for the treatment of these cases [12,13]. The results of the FLAURA trials positioned osimertinib as a standard treatment option, and even as an initial treatment option [14,15]. However, many cases still involve treatment in the second line or later, as the T790M mutation was identified via re-biopsy in patients who received first-generation or second-generation EGFR-TKIs as their initial treatment. When the T790M mutation was identified in these cases, patients typically received osimertinib.

Aging populations are becoming increasingly common worldwide, and many lung cancer cases involve older patients [26,27]. There are concerns that older patients have a higher risk of developing adverse events, which may necessitate dose reduction or treatment discontinuation, and subsequently result in decreased efficacy. Thus, this phase II study aimed to evaluate the safety and efficacy of osimertinib in elderly patients with EGFR-mutated lung cancer involving the T790M mutation. The primary endpoint was the ORR, and our previous report found that the ORR was 58.3% (95% CI: 42.2–72.9), which fulfilled the efficacy criterion (the lower limit of the CI exceeded the threshold response rate of 35%) [19]. This report describes the secondary endpoints, which include the DCR (97.2%), median PFS (11.9 months), and median OS (22.0 months). In terms of efficacy, the pooled results from the AURA expansion and AURA2 studies revealed an ORR of 66%, a DCR of 91%, a median PFS of 9.9 months, and a median OS of 26.8 months [23]. In addition, phase 3 AURA3 studies revealed an ORR of 70.6%, a DCR of 93.2%, a median PFS of 10.1 months, and a median OS of 26.8 months [13,28]. Thus, while our ORR was lower than that shown in the previous studies, it agrees with the slightly lower ORR (61.1%) that was retrospectively observed in another sample of elderly Japanese patients [29]. Furthermore, our findings regarding PFS and OS do not appear inferior to the results from previous studies, thereby suggesting that osimertinib was effective in elderly Japanese patients. Regarding the effects based on the PS, the ORR of PS0 and PS1 was 75% and 53.6%, respectively, and the PFS was 13.7 months and 11.9 months, respectively. Since there were few cases, it was impossible to discuss the significant differences, but the PS0 group tended to be superior.

It is also important to compare the results from osimertinib treatment to those from cytotoxic anticancer drugs, which are the alternative options if osimertinib is not used for T790M-positive

cases. For example, the control group for the AURA3 study received platinum plus pemetrexed, which provided an ORR of 31%, a DCR of 74%, a median PFS of 4.4 months, and a median OS of 22.5 months [13,28]. A subgroup analysis of ≥70-year-old Japanese patients from the JACAL study evaluated carboplatin plus pemetrexed and revealed an ORR of 24%, a DCR of 68%, a median PFS of 5.2 months, and a median OS of 16.8 months [30,31]. Thus, our OS findings may be comparable to the results from the entire AURA3 population, although our ORR, DCR, and PFS outcomes are comparable or even slightly better. Interestingly, 71% of the patients in the group that received platinum plus pemetrexed subsequently received additional treatment, with 60% experiencing a greater effect after crossing over to osimertinib treatment. Therefore, while the JACAL study had only included EGFR-mutated cases and did not specifically consider older patients, we believe that osimertinib may provide good outcomes among older patients with EGFR-mutated (T790M) NSCLC.

Safety is also an important consideration in this setting, given the concerns regarding the potentially higher risk of adverse events among older patients. In the AURA3 study, it appears that Japanese patients had a higher risk of paronychia, diarrhea, and skin pruritus, although no clear increase was observed among elderly patients. However, elderly patients had a clearly increased frequency of myelosuppression events, such as anemia (75% in this study vs. 8% in AURA3 study), leukopenia (38.9% in this study vs. 8% in AURA3 study), neutropenia (41.7% in this study vs. 8% in AURA3 study), and thrombocytopenia (58.3% in this study vs. 10% in AURA3 study), although the frequencies of Grade 3–4 adverse events were generally comparable. Osimertinib has also been reported to be more frequently myelosuppressed than in other EGFR-TKI in a pivotal study [13,14]. In addition, myelosuppression was reported to be stronger in the analysis of the Japanese population [32]. Although the obvious mechanism was unclear, it was suggested that racial differences might be involved. Since myelosuppression was observed more frequently in the present study than in the aforementioned analysis of the Japanese population, caution should be exercised in the elderly Japanese. Fiala et al. reported that pre-treatment hypoalbuminemia correlated with poor prognosis in advanced NSCLC patients treated with erlotinib [33]. The present study also revealed that anorexia and exhaustion were common (30–40% of cases vs. 16-18% of cases in AURA3 study, including some Grade 3–4 cases), as well as hypoalbuminemia (75% of cases vs. N/A in AURA3 study). Therefore, careful follow-up is needed for elderly patients who are receiving osimertinib. Elevated alkaline phosphatase and creatinine values were also observed, albeit not serious cases, and related follow-up testing is also important. Cardiac adverse events, such as decreased left heart ejection fraction and QT prolongation, were observed in some cases, although only one patient experienced a Grade 3–4 cardiac adverse event. Central nervous system events, such as delirium and hallucination, may be explained by the large proportion of cases with brain metastasis (41.7%), although caution should be exercised if these events present in conjunction with sinusitis and pulmonary infection. Regarding AE by PS, no clear difference was observed between PS0 and PS1.

All-grade pneumonitis was observed in 11.1% of cases, and Grade 3–4 pneumonitis was observed in 5.6% of cases. The rates after conventional EGFR-TKI treatment were 4% in the AURA3 study and 7.3% in the Japanese subset of patients, which suggests that Japanese patients may have a higher rate of pneumonitis [13,34]. The difference between our findings and the previous findings may be related to differences in the proportions of patients with a history of smoking (69.4% for the present study, 32.2% for the AURA3 study, and 31.7% for the Japanese subset of the AURA3 population). In addition, the Japanese subset of the FLAURA study population had a higher frequency of pulmonary disorders (all grades: 12%, Grade 3 or higher: 2%); it should be noted that this is a first-line trial. Other reports have also suggested that osimertinib may be associated with an increased incidence of pulmonary disorders relative to other EGFR-TKIs [32]. Nevertheless, the odds ratio for pulmonary disorders after gefitinib treatment was 1.92-fold higher among Japanese patients who were ≥55 years old, which suggests that careful follow-up is required for patients who are ≥75 years old [35].

The present study revealed all-grade AEs in 86.1%, Grade 3 or worse AEs in 27.8%, and fatal AEs in 2.8% of the patients. These rates did not appear to be substantially elevated among elderly

patients, based on results from the AURA3 study and its Japanese subgroup (all-grade: 97.8% and 100%, Grade 3 or higher: 22.6% and 31.7%, and fatal AEs: 1.4% and 0%). However, AEs leading to treatment discontinuation occurred in 12 patients (33.3%) in our study, which was more common than the rates of 6.8% in the AURA3 study and 7.3% in the Japanese subgroup. For example, we observed drug-induced lung injury in four patients (11.1%), and these patients needed to stop treatment. In addition, three patients (8.3%) discontinued treatment because of Grade 4 AEs (pulmonary infection, hallucinations, and hepatic dysfunction), although those events were judged unlikely to be associated with their treatment. One patient (2.8%) required a two-step dose reduction, and two patients (5.6%) were unable to continue the treatment protocol because of a ≥4-week treatment disruption. Treatment was also stopped in one case involving Grade 3 aspiration pneumonia, one case at the attending physician's discretion, and one case because the patient refused to continue treatment. Thus, although the safety of osimertinib outside the study protocol has not been evaluated, most of these AEs and treatment discontinuations were likely not to have been caused by a drug-induced pulmonary injury.

Most all-grade adverse events involved anorexia, fatigue, myelosuppression, and gastrointestinal symptoms. These complications were generally not serious and could be addressed using conventional management strategies. However, it is important to note that the frequency of drug-induced lung injury may increase, which highlights the importance of a careful follow-up in this population. Despite the potential need for a careful follow-up and the small sample size, which was the limitation in this study, it appears that osimertinib can be a standard treatment even for the elderly patients harboring T790M mutation.

While the present study provided encouraging data, we are conducting an additional phase II study (SPIRAL-0) to confirm the safety and efficacy of osimertinib in ≥75-year-old patients with untreated NSCLC harboring EGFR-activating mutations [36]. This may provide further information to guide the increasing use of osimertinib treatment in this setting.

Author Contributions: Conceptualization, J.U.; validation, J.U., A.N., and K.T.; formal analysis, K.Y.; investigation, O.H., C.S., T.A., N.H., T.I., T.T., M.K., Y.G., H.I., N.H., K.N., H.U., K.U., M.F. (Minoru Fukuda), Y.U., T.Y. (Toshihide Yokoyama), M.A., T.M. (Tadashi Mio), S.N., Y.C., N.T., Y.K., T.M. (Takako Mouri), T.Y. (Tadaaki Yamada) and M.F. (Masaki Fujita); data curation, K.Y.; writing—original draft preparation, A.N.; writing—review and editing, J.U.; supervision, K.T.; project administration, J.U.; funding acquisition, J.U. All authors have read and agreed to the published version of the manuscript.

References

1. Mok, T.S.; Wu, Y.L.; Thongprasert, S.; Yang, C.H.; Chu, D.T.; Saijo, N.; Sunpaweravong, P.; Han, B.; Margono, B.; Ichinose, Y.; et al. Gefitinib or carboplatin-paclitaxel in pulmonary adenocarcinoma. *N. Engl. J. Med.* **2009**, *361*, 947–957. [CrossRef] [PubMed]

2. Maemondo, M.; Inoue, A.; Kobayashi, K.; Sugawara, S.; Oizumi, S.; Isobe, H.; Gemma, A.; Harada, M.; Yoshizawa, H.; Kinoshita, I.; et al. Gefitinib or chemotherapy for non-small-cell lung cancer with mutated EGFR. *N. Engl. J. Med.* **2010**, *362*, 2380–2388. [CrossRef] [PubMed]

3. Mitsudomi, T.; Morita, S.; Yatabe, Y.; Negoro, S.; Okamoto, I.; Tsurutani, J.; Seto, T.; Satouchi, M.; Tada, H.; Hirashima, T.; et al. Gefitinib versus cisplatin plus docetaxel in patients with non-small-cell lung cancer harbouring mutations of the epidermal growth factor receptor (WJTOG3405): An open label, randomised phase 3 trial. *Lancet Oncol.* **2010**, *11*, 121–128. [CrossRef]

4. Zhou, C.; Wu, Y.L.; Chen, G.; Feng, J.; Liu, X.Q.; Wang, C.; Zhang, S.; Wang, J.; Zhou, S.; Ren, S.; et al. Erlotinib versus chemotherapy as first-line treatment for patients with advanced EGFR mutation-positive non-small-cell lung cancer (OPTIMAL, CTONG-0802): A multicentre, open-label, randomised, phase 3 study. *Lancet Oncol.* **2011**, *12*, 735–742. [CrossRef]

5. Rosell, R.; Carcereny, E.; Gervais, R.; Vergnenegre, A.; Massuti, B.; Felip, E.; Palmero, R.; Garcia-Gomez, R.; Pallares, C.; Sanchez, J.M.; et al. Erlotinib versus standard chemotherapy as first-line treatment for European patients with advanced EGFR mutation-positive non-small-cell lung cancer (EURTAC): A multicentre, open-label, randomised phase 3 trial. *Lancet Oncol.* **2012**, *13*, 239–246. [CrossRef]

6. Wu, Y.L.; Zhou, C.; Liam, C.K.; Wu, G.; Liu, X.; Zhong, Z.; Lu, S.; Cheng, Y.; Han, B.; Chen, L.; et al. First-Line erlotinib versus gemcitabine/cisplatin in patients with advanced EGFR mutation-positive non-small-cell lung cancer: Analyses from the phase III, randomized, open-label, ENSURE study. *Ann. Oncol.* **2015**, *26*, 1883–1889. [CrossRef] [PubMed]

7. Sequist, L.V.; Yang, J.C.; Yamamoto, N.; O'Byrne, K.; Hirsh, V.; Mok, T.; Geater, S.L.; Orlov, S.; Tsai, C.M.; Boyer, M.; et al. Phase III study of afatinib or cisplatin plus pemetrexed in patients with metastatic lung adenocarcinoma with EGFR mutations. *J. Clin. Oncol.* **2013**, *31*, 3327–3334. [CrossRef]

8. Wu, Y.L.; Zhou, C.; Hu, C.P.; Feng, J.; Lu, S.; Huang, Y.; Li, W.; Hou, M.; Shi, J.H.; Lee, K.; et al. Afatinib versus cisplatin plus gemcitabine for first-line treatment of Asian patients with advanced non-small-cell lung cancer harbouring EGFR mutations (LUX-Lung 6): An open-label, randomised phase 3 trial. *Lancet Oncol.* **2014**, *15*, 213–222. [CrossRef]

9. Park, K.; Tan, E.H.; O'Byme, K.; Zhang, L.; Boyer, M.; Mok, T.; Hirsh, V.; Yang, J.C.; Lee, K.H.; Lu, S.; et al. Afatinib versus gefitinib as first-line treatment of patients with EGFR mutation-positive non-small-cell lung cancer (LUX-Lung 7): A phase 2B, open-label, randomised controlled trial. *Lancet Oncol.* **2016**, *17*, 577–589. [CrossRef]

10. Paz-Ares, L.; Tan, E.H.; O'Byme, K.; O'Byrne, K.; Zhang, L.; Hirsh, V.; Boyer, M.; Yang, J.C.; Mok, T.; Lee, K.H.; et al. Afatinib versus gefitinib in patients with EGFR mutation-positive advanced non-small-cell lung cancer: Overall survival data from the phase IIb LUX-Lung 7 trial. *Ann. Oncol.* **2017**, *28*, 270–277. [CrossRef]

11. Wu, Y.L.; Cheng, Y.; Zhou, X.; Lee, K.H.; Nakagawa, K.; Niho, S.; Tsuji, F.; Linke, R.; Rosell, R.; Corral, J.; et al. Dacomitinib versus gefitinib as first-line treatment for patients with EGFR-mutation-positive non-small-cell lung cancer (ARCHER 1050): A randomised, open-label, phase 3 trial. *Lancet Oncol.* **2017**, *18*, 1454–1466. [CrossRef]

12. Yu, H.A.; Arcila, M.E.; Rekhtman, N.; Sima, C.S.; Zakowski, M.F.; Pao, W.; Kris, M.G.; Miller, V.A.; Ladanyi, M.; Riely, G.J. Analysis of tumor specimens at the time of acquired resistance to EGFR-TKI therapy in 155 patients with EGFR-mutant lung cancers. *Clin. Cancer Res.* **2013**, *19*, 2240–2247. [CrossRef] [PubMed]

13. Mok, T.S.; Wu, Y.L.; Ahn, M.J.; Garassino, M.C.; Kim, H.R.; Ramalingam, S.S.; Shepherd, F.A.; He, Y.; Akamatsu, H.; Theelen, W.S.; et al. Osimertinib or platinum-pemetrexed in EGFR T790M-positive lung cancer. *N. Engl. J. Med.* **2017**, *376*, 629–640. [CrossRef] [PubMed]

14. Soria, J.C.; Ohe, Y.; Vansteenkiste, J.; Reungwetwattana, T.; Chewaskulyong, B.; Lee, K.H.; Dechaphunkul, A.; Imamura, F.; Nogami, N.; Kurata, T.; et al. Osimertinib in untreated EGFR-mutated advanced non-small-cell lung cancer. *N. Engl. J. Med.* **2018**, *378*, 113–125. [CrossRef]

15. Ramalingam, S.S.; Vanteenkiste, J.; Planchard, D.; Cho, B.C.; Gray, J.E.; Ohe, Y.; Zhou, C.; Reungwetwattana, T.; Cheng, Y.; Chewaskulyong, B.; et al. Overall survival with Osimertinib in untreated, EGFR-mutated advanced NSCLC. *N. Engl. J. Med.* **2020**, *382*, 41–50. [CrossRef]

16. Nanjo, S.; Ebi, H.; Takeuchi, S.; Takeuchi, S.; Yamada, T.; Mochizuki, S.; Okada, Y.; Nakada, M.; Murakami, T.; Yano, S. High efficacy of third generation EGFR inhibitor AZD9291 in a leptomeningeal carcinomatosis model with EGFR-mutant lung cancer cells. *Oncotarget* **2016**, *7*, 3847–3856. [CrossRef]

17. Nanjo, S.; Hata, A.; Okuda, C.; Kaji, R.; Okada, H.; Tamura, D.; Irie, K.; Okada, H.; Fukushima, S.; Katakami, N. Standard-Dose osimertinib for refractory leptomeningeal metastases in T790M-positive EGFR-mutant non-small cell lung cancer. *Br. J. Cancer* **2018**, *118*, 32–37. [CrossRef]

18. Cross, D.A.; Ashton, S.E.; Ghiorghlu, S.; Eberlein, C.; Nebhan, C.A.; Spitzler, P.J.; Orme, J.P.; Finlay, M.R.; Ward, R.A.; Mellor, M.J.; et al. AZD9291, an irreversible EGFR TKI, overcomes T790M-mediated resistance to EGFR inhibitors in lung cancer. *Cancer Discov.* **2014**, *4*, 1046–1061. [CrossRef]

19. Nakao, A.; Hiranuma, O.; Uchino, J.; Sakaguchi, C.; Kita, T.; Hiraoka, N.; Ishizuka, T.; Kubota, Y.; Kawasaki, M.; Goto, Y.; et al. Osimertinib in elderly patients with epidermal growth factor receptor T790M-positive non-small-cell lung cancer who progressed during prior treatment: A phase II trial. *Oncologist* **2019**, *24*, 593-e170. [CrossRef]

20. Uchino, J.; Nakao, A.; Tamiya, N.; Kaneko, Y.; Yamada, T.; Yoshimura, K.; Fujita, M.; Takayama, K. Treatment rationale and design of the SPIRAL study: A phase II trial of osimertinib in elderly epidermal growth factor receptor T790M-positive nonsmall-cell lung cancer patients who progressed during prior EGFR-TKI treatment. *Medicine* **2018**, *97*, e11081. [CrossRef]

21. Yang, J.C.; Ahn, M.J.; Kim, D.W.; Ramalingam, S.S.; Sequist, L.V.; Su, W.C.; Kim, S.W.; Kim, J.H.; Planchard, D.; Felip, E.; et al. Osimertinib in pretreated T790M-positive advanced non-small-cell lung cancer: AURA study phase II extension component. *J. Clin. Oncol.* **2017**, *35*, 1288–1296. [CrossRef] [PubMed]

22. Goss, G.; Tsai, C.M.; Shepherd, F.A.; Bazhenova, L.; Lee, J.S.; Chang, G.C.; Crino, L.; Satouchi, M.; Chu, Q.; Hida, T.; et al. Osimertinib for pretreated EGFR Thr790Met-positive advanced non-small-cell lung cancer (AURA2): A multicentre, open-label, single-arm, phase 2 study. *Lancet Oncol.* **2016**, *17*, 1643–1652. [CrossRef]

23. Ahn, M.J.; Tsai, C.M.; Shepherd, F.A.; Bazhenova, L.; Sequist, L.V.; Hida, T.; Yang, J.; Ramalingam, S.S.; Mitsudomi, T.; Jänne, P.A.; et al. Osimertinib in patients with T790M mutation-positive, advanced non-small cell lung cancer: Long-term follow-up from a pooled analysis of 2 phase 2 studies. *Cancer* **2019**, *125*, 892–901. [CrossRef] [PubMed]

24. Kudoh, S.; Takeda, K.; Nakagawa, K.; Takada, M.; Katakami, N.; Matsui, K.; Shinkai, T.; Sawa, T.; Goto, I.; Semba, H.; et al. Phase III study of docetaxel compared with vinorelbine in elderly patients with advanced non-small-cell lung cancer: Results of the West Japan Thoracic Oncology Group Trial (WJTOG 9904). *J. Clin. Oncol.* **2006**, *24*, 3657–3663. [CrossRef]

25. Tamiya, M.; Tamiya, A.; Kaneda, H.; Nakagawa, K.; Yoh, K.; Goto, K.; Okamoto, H.; Shimokawa, T.; Abe, T.; Tanaka, H.; et al. A phase II study of pemetrexed plus carboplatin followed by maintenance pemetrexed as first-line chemotherapy for elderly patients with advanced non-squamous non-small cell lung cancer. *Med. Oncol.* **2016**, *33*, 2. [CrossRef]

26. Barta, J.A.; Zinner, R.G.; Unger, M. Lung cancer in the older patient. *Clin. Geriatr. Med.* **2017**, *33*, 563–577. [CrossRef]

27. Torre, L.A.; Siegel, R.L.; Ward, E.M.; Jemal, A. Global cancer incidence and mortality rates and trends—An update. *Cancer Epidemiol. Biomark. Prev.* **2016**, *25*, 16–27. [CrossRef]

28. Wu, Y.L.; Mok, T.S.; Han, J.; Ahn, M.J.; Delmonte, A.; Ramalingam, S.S.; Kim, S.; Shepherd, F.A.; Laskin, J.; He, Y.; et al. Overall Survival (OS) from the AURA3 phase III study: Osimertinib vs Platinum-Pemetrexed (PLT-PEM) in Patients (PTS) with EGFR T790M advanced Non-Small Cell Lung Cancer (NSCLC) and progression on a prior EGFR-tyrosine kinase inhibitor (TKI). *Ann. Oncol.* **2019**, *20* (Suppl. 9), ix157–ix181.

29. Furuta, H.; Uemura, T.; Yoshida, T.; Kobara, M.; Yamaguchi, T.; Watanabe, N.; Shimizu, J.; Horio, Y.; Kuroda, H.; Sakao, Y.; et al. Efficacy and safety data of Osimertinib in elderly patients with NSCLC who harbor the EGFR T790M mutation after failure of initial EGFR-TKI treatment. *Anticancer Res.* **2018**, *38*, 5231–5237. [CrossRef]

30. Okamoto, I.; Aoe, K.; Kato, T.; Hosomi, Y.; Yokoyama, A.; Imamura, F.; Kiura, K.; Hirashima, T.; Nishio, M.; Nogami, N.; et al. Pemetrexed and carboplatin followed by pemetrexed maintenance therapy in chemo-naïve patients with advanced nonsquamous non-small-cell lung cancer. *Investig. New Drugs* **2013**, *31*, 1275–1282. [CrossRef]

31. Nogami, N.; Nishio, M.; Okamoto, I.; Enatsu, S.; Suzukawa, K.; Takai, H.; Nakagawa, K.; Tamura, T. Pemetrexed and carboplatin combination therapy followed by pemetrexed maintenance in Japanese patients with non-squamous non-small cell lung cancer: A subgroup analysis of elderly patients. *Respir. Investig.* **2019**, *57*, 27–33. [CrossRef] [PubMed]

32. Ohe, Y.; Imamura, F.; Nogami, N.; Okamoto, I.; Kurata, T.; Kato, T.; Sugawara, S.; Ramalingam, S.S.; Uchida, H.; Hodge, R.; et al. Osimertinib versus standard-of-care EGFR-TKI as first-line treatment for EGFRm advanced NSCLC: FLAURA Japanese subset. *Jpn. J. Clin. Oncol.* **2019**, *49*, 29–36. [CrossRef] [PubMed]

33. Fiala, O.; Pesek, M.; Finek, J.; Racek, J.; Minarik, M.; Benesova, L.; Bortlicek, Z.; Sorejs, O.; Kucera, R.; Topolcan, O. Serum albumin is a strong predictor of survival in patients with advanced-stage non-small cell lung cancer treated with erlotinib. *Neoplasma* **2016**, *63*, 471–476. [CrossRef] [PubMed]

34. Akamatsu, H.; Katakami, N.; Okamoto, I.; Kato, T.; Kim, Y.H.; Imamura, F.; Shinkai, M.; Hodge, R.A.; Uchida, H.; Hida, T. Osimertinib in Japanese patients with EGFR T790M mutation-positive advanced non-small-cell lung cancer: AURA3 trial. *Cancer Sci.* **2018**, *109*, 1930–1938. [CrossRef] [PubMed]

35. Kudoh, S.; Kato, H.; Nishiwaki, Y.; Fukuoka, M.; Nakata, K.; Ichinose, Y.; Tsuboi, M.; Yokota, S.; Nakagawa, K.; Suga, M. Interstitial lung disease in Japanese patients with lung cancer: A cohort and nested case-control study. *Am. J. Respir. Crit. Care Med.* **2008**, *177*, 1348–1357. [CrossRef]

36. Chihara, Y.; Yamada, T.; Uchino, J.; Tamiya, N.; Kaneko, Y.; Kishimoto, J.; Takayama, K. Rationale and design of a phase II trial of osimertinib as first-line treatment for elderly patients with epidermal growth factor receptor mutation-positive advanced non-small cell lung cancer (SPIRAL-0 study). *Transl. Lung Cancer Res.* **2019**, *8*, 1086–1090. [CrossRef]

Article

Clinicopathological Significance of *RUNX1* in Non-Small Cell Lung Cancer

Yujin Kim [1], Bo Bin Lee [1], Dongho Kim [1], Sangwon Um [2], Eun Yoon Cho [3], Joungho Han [3], Young Mog Shim [4] and Duk-Hwan Kim [1],*

[1]   Department of Molecular Cell Biology, Sungkyunkwan University School of Medicine, Suwon 440-746, Korea; yujin0328@hanmail.net (Y.K.); whitebini@hanmail.net (B.B.L.); jindonghao2001@hotmail.com (D.K.)
[2]   Department of Internal Medicine, Samsung Medical Center, Sungkyunkwan University School of Medicine, Seoul 135-710, Korea; sangwon72.um@samsung.com
[3]   Department of Pathology, Samsung Medical Center, Sungkyunkwan University School of Medicine, Seoul 135-710, Korea; eunyoon.cho@samsung.com (E.Y.C.); joungho.han@samsung.com (J.H.)
[4]   Department of Thoracic and Cardiovascular Surgery, Samsung Medical Center, Sungkyunkwan University, School of Medicine, Seoul 135-710, Korea; youngmog.shim@samsung.com
*   Correspondence: dukhwan.kim@samsung.com

Abstract: This study aimed to understand the clinicopathological significance of runt-related transcription factor 1 (*RUNX1*) in non-small cell lung cancer (NSCLC). The methylation and mRNA levels of *RUNX1* in NSCLC were determined using the Infinium HumanMethylation450 BeadChip and the HumanHT-12 expression BeadChip. RUNX1 protein levels were analyzed using immunohistochemistry of formalin-fixed paraffin-embedded tissues from 409 NSCLC patients. Three CpGs (cg04228935, cg11498607, and cg05000748) in the CpG island of *RUNX1* showed significantly different methylation levels (Bonferroni corrected $p < 0.05$) between tumor and matched normal tissues obtained from 42 NSCLC patients. Methylation levels of the CpGs in the tumor tissues were inversely related to mRNA levels of *RUNX1*. A logistic regression model based on cg04228935 showed the best performance in predicting NSCLCs in a test dataset (N = 28) with the area under the receiver operating characteristic (ROC) curve (AUC) of 0.96 (95% confidence interval (CI) = 0.81–0.99). The expression of RUNX1 was reduced in 125 (31%) of 409 patients. Adenocarcinoma patients with reduced RUNX1 expression showed 1.97-fold (95% confidence interval = 1.16–3.44, $p = 0.01$) higher hazard ratio for death than those without. In conclusion, the present study suggests that abnormal methylation of *RUNX1* may be a valuable biomarker for detection of NSCLC regardless of race. And, reduced RUNX1 expression may be a prognostic indicator of poor overall survival in lung adenocarcinoma.

Keywords: lung cancer; RUNX1; methylation; biomarker; survival

---

1. Introduction

Lung cancer is the leading cause of cancer-related death in the world. Despite significant advances in the diagnosis and treatment of the disease over the past 20 years, its prognosis is still very poor, with the overall 5-year survival rate staying at 15%–20% [1]. The prognosis of cancer patients is mostly determined by disease stage. The occult metastatic spread of cancer cells to surrounding tissues in more than 50% of lung cancer patients at the time of diagnosis affects a poor prognosis. The majority of patients undergoing curative surgical resection at an early stage and, if necessary, adjuvant chemotherapy have achieved favorable long-term survival. Patients with surgically resected stage IA, stage IB, and stage II non-small cell lung cancers (NSCLCs) had an overall five-year survival rate of 83%, 69%, and 48%, respectively [2]. Targeted therapy has a great effect on the prognosis

of specific patients; however, it is applicable to only about 10%–20% of patients. Accordingly, it is important to identify novel diagnostic and therapeutic biomarkers for the detection of early-stage lung cancer and for the development of new molecular-targeted therapies for NSCLC.

Runt-related transcription factor 1 (RUNX1) is one of the RUNX family proteins (RUNX1, RUNX2, and RUNX3), which forms a heterodimeric complex with the core binding factor β (CBFβ), resulting in enhanced transcription of the RUNX gene family by stimulating the DNA binding ability and stability of the family proteins [3,4]. RUNX1 is essential for hematopoiesis and is involved in the generation of hematopoietic stem cells. Mutations and translocations in *RUNX1* are well established as causes of myelodysplastic syndrome or acute myelogenous leukemia [5–7]. Gain- or loss-of-function mutations of *RUNX1* have also been reported in various solid tumors. Missense mutations of *RUNX1* were reported in luminal-type breast cancer [8], and loss-of-function somatic mutations or deletion of *RUNX1* have been reported in breast cancer and lung cancer [9,10].

To understand the clinicopathological significance of *RUNX1* in NSCLC, we analyzed the methylation status of *RUNX1* in different types of samples from a total of 118 NSCLC patients and 60 healthy individuals. The prediction performance of classifiers was validated in The Cancer Genome Atlas (TCGA) lung cancer. Expression levels of RUNX1 were also analyzed using HT-12 array and immunohistochemistry in tissue specimens from 42 and 409 NSCLC patients, respectively.

2. Materials and Methods

2.1. Study Population

Formalin-fixed paraffin-embedded tumor tissues were obtained from 409 NSCLC patients who underwent curative surgical resection at the Department of Thoracic and Cardiovascular Surgery, Samsung Medical Center, Seoul, Korea, between August 1994 and May 2014. All samples were obtained from operative patients. Follow-up of patients for the detection of recurrence or death following curative resection was conducted by a nurse specialized in oncology as described previously [11]. The pathological stage of NSCLC was determined using the tumor/node/metastasis (TNM) system provided by the American Joint Committee on Cancer (AJCC) [12]. This study was conducted in accordance with the ethical principles stated in the Declaration of Helsinki and approved by the Institutional Review Board (IRB#: 2010-07-204) of the Samsung Medical Center. Written informed consent to use pathological specimens for research was obtained from all patients prior to surgery. All data are not publicly available due to privacy and ethical restriction.

2.2. Analysis of RUNX1 Methylation and mRNA Levels

We previously analyzed the DNA methylation and mRNA expression at the level of genome using the Infinium HumanMethylation450 BeadChip and the HumanHT-12 expression BeadChips (Illumina, San Diego, CA, USA), respectively, in 42 surgically resected tumor and matched normal tissues, 136 bronchial washings, 12 sputums, or 6 bronchial biopsy specimens obtained from a total of 118 NSCLC patients and 60 cancer-free patients [13]. We used the reported data for the analysis of methylation and mRNA levels of *RUNX1*. Preprocessing such as background or batch effect correction, probe filtering, and adjustment of the background signal difference between types I and II probes was conducted using the R software package called wateRmelon [14]. Methylation level (β-value), ranging from 0 (no methylation) to 1 (100% methylation), was estimated as the ratio of fluorescence signal intensity between methylated alleles and the sum of methylated and unmethylated alleles at each CpG locus. The levels of mRNA expression from HT-12 chips were normalized using the R lumi package (https://bioconductor.org/biocLite.R).

2.3. Feature Selection for Prediction of Lung Cancer

To select candidate CpGs for lung cancer prediction among differentially methylated CpGs and to build models for lung cancer prediction, we divided the normal and tumor tissues from 42 patients

into training and test datasets, according to a 7:3 ratio. Supervised machine learning algorithms were applied to select features in the training dataset. Age-related CpGs or any CpGs that were significantly correlated in the normal or tumor tissues were removed during the model building. Supervised machine learning algorithms for feature selection and model building were applied using RapidMiner Studio version 8.2 (RapidMiner Inc, Boston, MA, USA).

2.4. Evaluation of Prediction Performance of Models in The Cancer Genome Atlas (TCGA) Lung Cancer

Prediction performance of selected models was further tested using 899 TCGA lung cancers, including 75 normal and 824 tumor tissues. The performance was tested without distinction between adenocarcinoma and squamous cell carcinoma. The prediction performance of models was evaluated using receiver operating characteristic (ROC) curves, plotted using the MedCalc statistical Software version 19.0.5 (MedCalc Softward bvba, Ostend, Belgium).

2.5. Immunohistochemistry

The expression of RUNX1, Ki-67, phospho-pRb (Ser-807/811) proteins in the 409 NSCLC patients was determined using immunohistochemistry of tissue microarrays (TMAs). In brief, the 4-mm–thick TMA tissue sections on glass slide were deparaffinized in xylene and rehydrated in a series of decreasing concentrations of alcohol. Antigens were recovered by putting sections into 10 mmol/L citrate buffer solution (pH 6.0) and by heating in a microwave oven for 10 min. The sections were then incubated overnight at 4 °C with a mouse monoclonal antibody to RUNX1 (AML1/RUNX1 Antibody (clone 3A1) IHC-plus™ LS-B5382, LifeSpan BioSciences, Seattle, WA, USA), a polyclonal anti-phospho-pRb (Ser-807/811) antibody (Cell Signaling, Danvers, MA, USA), and a mouse monoclonal anti-Ki-67 (DAKO; clone MIB-1) antibody. Immunoreactivity of the proteins was detected using the Envision-Plus/horseradish peroxidase system (Dako, Carpinteria, CA, USA), and the antibody-bound peroxidase activity was visualized by incubating in 0.05% 3,3′-diaminobenzidine tetrahydrochloride (DAB) for 3 min at room temperature. All sections were counterstained with Mayer's hematoxylin and a negative control was included by excluding the primary antibody each time. Three samples with RUNX1 expression in normal bronchial epithelial cells were used as a positive control for RUNX1 staining, and IHC was performed in duplicate.

2.6. Interpretation of Immunohistochemical Staining

The immunohistochemical stainings were interpreted by two authors (EY Cho and D-H Kim) in a double-blinded fashion, and samples showing poor inter-rater reliability ($\kappa < 0.20$) were removed from data analysis. RUNX1 expression was considered positive when nuclear staining was present, and the intensity and proportion of positive nuclear staining was assessed for scoring. A composite score of RUNX1 protein expression was semi-quantitatively calculated by multiplying the proportion score of positive cells (0, absent; 1, 0%–10%; 2, 10%–50%; 3, 50%–80%; and 4, >80%) with the staining intensity score (0, none; 1, weak; 2, moderate; and 3, strong). A cutoff for the reduced expression of RUNX1 protein was determined by taking into account the distribution of the composite scores between normal and tumor tissues and by comparing both false-negative and false-positive rates at different cutoffs. RUNX1 expression was considered reduced in a tumor with a composite score less than two. To score for phospho-pRb (Ser-807/811) and Ki-67, positive staining was determined according to the percentage of positively stained nuclei.

2.7. Statistical Analysis

Univariate analysis was performed using the *t*-test (or Wilcoxon rank sum test) and the chi-square test (or Fisher's exact test) for continuous and categorical variables, respectively. The correlation between methylation levels of CpGs in the *RUNX1* gene was analyzed using Spearman's rank correlation coefficient. The effect of reduced RUNX1 expression on survival was estimated using the Kaplan–Meier survival curves, and the difference between the survival curves of any two groups

was evaluated by the log-rank test. Cox proportional hazards analysis was conducted to estimate the hazard ratios of reduced RUNX1 expression for survival after controlling for potential confounding factors. Statistical analysis was conducted using R software version 3.3.3. (R Foundation for Statistical Computing, Vienna, Austria).

3. Results

3.1. RUNX1 Hypermethylation Is Inversely Associated with Its Expression

Data reported previously were used to identify differentially methylated CpGs in *RUNX1* gene in tumor and matched normal tissues from 42 NSCLC patients. The Wilcoxon rank-sum test was applied because the distribution of β-values obtained from tumor tissues using a 450 K array was negatively skewed and did not follow a normal distribution (Shapiro-Wilk test, $p < 0.05$). Three CpGs with a p-value less than or equal to 1.03×10^{-7} (Bonferroni significance threshold) were identified from the 450K array: three CpGs (cg11498607, cg04228935, cg05000748) at the CpG island of *RUNX1* showed hypermethylation in tumor tissues compared with normal tissues (Figure 1A). The methylation levels of the three CpGs did not vary significantly with histology (Figure 1B). Altered methylation of three CpGs was not significantly correlated with a patient's age (Figure 1C).The methylation levels were not also associated with smoking status (Figure 1D) and recurrence (Figure 1E). However, the methylation levels were found to be higher in the poorly differentiated type of NSCLC than in the well differentiated type (Figure S1). The *RUNX1* mRNA levels were analyzed using the HT-12 array to determine the association between methylation changes and changes in *RUNX1* gene expression. The methylation levels of individual CpGs were negatively associated with the mRNA levels of *RUNX1* ($p < 0.05$; Figure 1F).
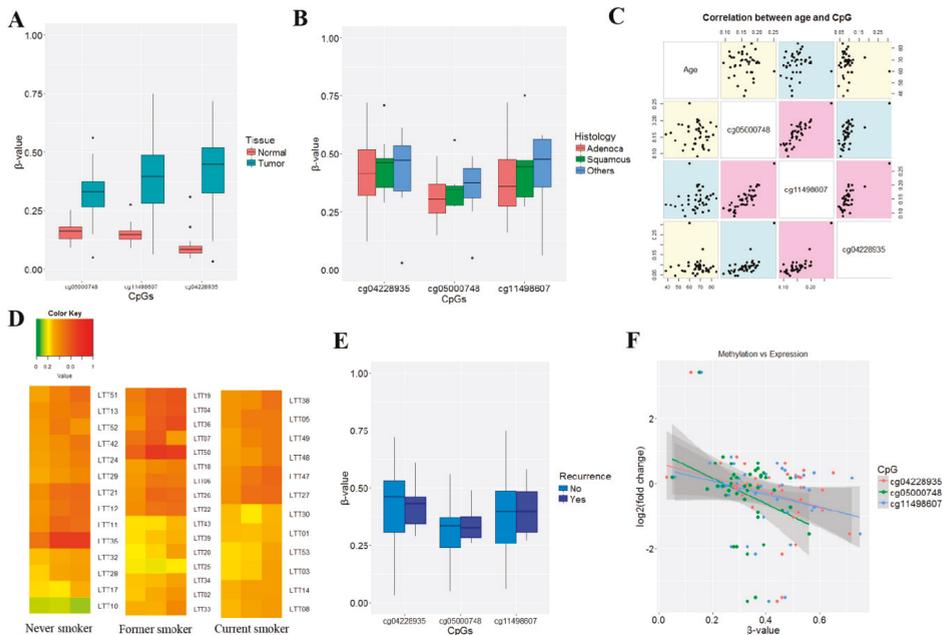
Figure 1. Relationship between methylation and mRNA levels of runt-related transcription factor 1 (*RUNX1*) in 42 lung tumor and matched normal tissues. (**A**) Methylation levels of three CpGs at the CpG island of *RUNX1* gene were compared between the tumor and matched normal tissues obtained from 42 NSCLC patients. Y-axis indicates β-values. (**B**) Methylation levels of the three CpGs were compared according to histologic subtypes. (**C**) Correlations between the patient's age and the methylation levels of the three CpGs were analyzed in 42 tumor tissues. Spearman's correlation coefficient was used to calculate *p*-values. Magenta color indicates $p < 0.05$. (**D**) Methylation levels of three CpGs at a CpG island of *RUNX1* were compared in never-smokers, former smokers, and current smokers. Y-axis indicates sample identification numbers. Methylation levels are represented using gradient-based colors from green (0%–20%) to yellow (21%–50%) to red (51%–100%). (**E**) The association between recurrence and the methylation levels at three CpGs were analyzed in 42 NSCLCs. (**F**) The correlation between methylation levels of three CpGs and the mRNA expression of *RUNX1* was analyzed in 42 tumor tissues from patients with NSCLC. Y-axis indicates the log2 fold change (= log2(tumor/normal)) between tumor and matched normal tissues. X-axis indicates β-values in tumor tissues.

3.2. Prediction of Non-Small Cell Lung Cancer (NSCLC) Using Abnormal Methylation Levels of RUNX1

Features for prediction of NSCLC were selected in 42 tumors and matched normal tissues. Lung tumor and matched normal tissues were divided into training and test datasets at a ratio of 7:3, respectively. We built models using the training dataset and tested the performance of the models using the test dataset. Supervised machine learning algorithms such as k-nearest neighbor (kNN), support vector machine (SVM), neural network, logistic regression, and decision tree were applied for feature selection. Since individual CpGs were correlated with each other, only one CpG was included in the models. Among the applied algorithms, a logistic regression model based on cg04228935 showed the best performance in classifying NSCLCs in a test dataset (N = 28) with a sensitivity of 92.9% and a specificity of 92.9% (area under the curve (AUC) = 0.96; 95% confidence interval (CI) = 0.81–0.99, $p < 0.0001$; Figure 2A).
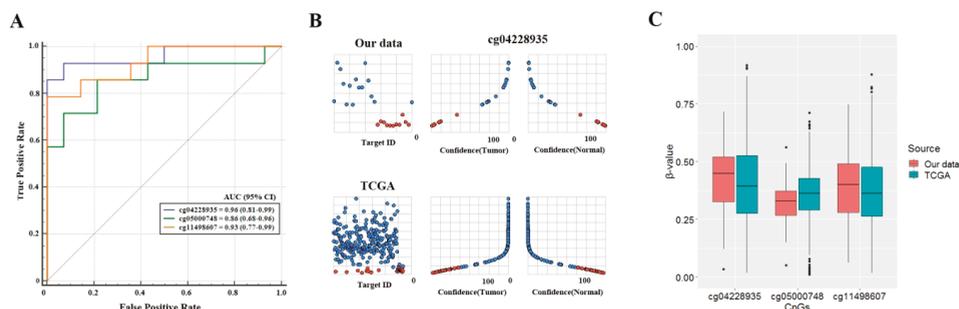
Figure 2. Evaluation of prediction performance of five supervised machine learning algorithms in non-small cell lung cancer (NSCLC). (**A**) The true and false positive rates of logistic regression model based on three CpGs were evaluated in a test dataset (N = 28) of 42 NSCLCs, and the receiver operating characteristic (ROC) curves were plotted using the MedCalc software. (**B**) The prediction certainty of the support vector machine model was evaluated in the test dataset of our data and TCGA lung cancer. The X-axis indicates the degree (0% to 100%) of certainty for prediction of our and TCGA tissues as normal or tumor for each β-value on the Y-axis. The sky blue and red orange circles indicate tumor and normal tissues, respectively. (**C**) The β-values of the three CpGs in our and TCGA data were compared to understand the difference of *RUNX1* hypermethylation among other ethnic groups or populations.

To determine if *RUNX1* hypermethylation may be a biomarker for the detection of NSCLC in other races, we tested *RUNX1* hypermethylation in the 899 TCGA primary lung cancers (75 normal tissues and 824 tumor tissues). As with our data, the TCGA data was divided into a training dataset (N = 630) and a test dataset (N = 269), and the performance of logistic regression model based on three CpGs was evaluated on the test dataset (Table S1). The sensitivity and specificity of the model based on cg04228935 in a test dataset (N = 269) were 91.8% and 96.4%, respectively. AUC was 0.95 (95% confidence interval = 0.93–0.98, $p < 0.0001$). The degree of prediction certainty of NSCLC in the test datasets was high in our data and TCGA lung cancer data (Figure 2B). We finally compared the methylation levels of three CpGs at a CpG island of *RUNX1* between our data and TCGA lung cancer data. No significant difference was found between the two data (Figure 2C).

3.3. Methylation Pattern of RUNX1 in Tumor Tissue Is Similar to that in Bronchial Biopsy Specimen

To test if bronchial washing, sputum, and bronchial biopsy specimens could be used as surrogate samples for analyzing *RUNX1* methylation in the lung, we compared the methylation levels of the CpG (cg04228935) in 42 tumors and matched normal tissues, 136 bronchial washings, 12 sputum samples, and 6 bronchial biopsy specimens. The clinical and pathological characteristics of the NSCLC patients were previously reported [13]. The methylation levels of the CpG in lung tumor tissues were not significantly different from those in bronchial biopsy specimens from lung cancer patients ($p > 0.05$, Wilcoxon rank sum test), unlike bronchial washings and sputum samples (Figure 3A). The CpG methylation levels were further compared between paired bronchial washing and sputum samples from 12 NSCLC patients (Figure 3B) and between bronchial washing and paired bronchial biopsies from 6 NSCLC patients (Figure 3C). The methylation levels of the CpG were found to be similar between bronchial washings and sputum samples but significantly higher in bronchial biopsy than in bronchial washing ($p < 0.05$, Wilcoxon signed-rank test). These findings suggest that a detection model for NSCLC using abnormal methylation of *RUNX1* is applicable to bronchial biopsy specimens.
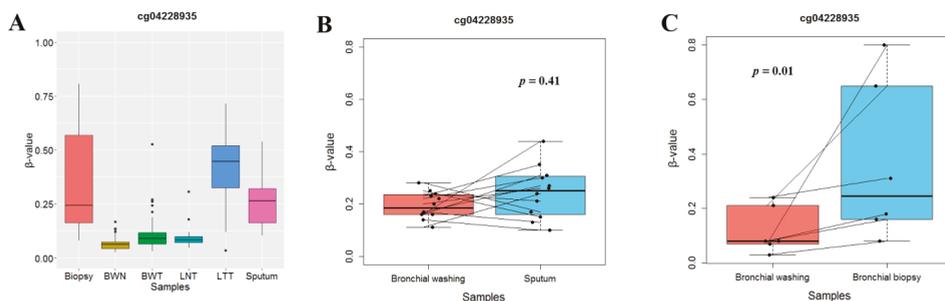
Figure 3. Comparison of *RUNX1* methylation levels among different types of specimens. (**A**) The methylation levels of a CpG (cg04228935) selected for NSCLC prediction were compared among bronchial biopsies from 6 lung cancer patients (biopsy), bronchial washing samples from 60 healthy individuals (bronchial washing normal, BWN) and 76 lung cancer patients (bronchial washing tumor, BWT), tumor (lung tumor tissue, LTT) and matched normal (lung normal tissue, LNT) tissues from 42 NSCLC patients, and sputum specimens from 12 lung cancer patients (sputum). (**B,C**) Methylation levels of a CpG (cg04228935) were compared using parallel coordinate plots between paired bronchial washing and sputum specimens from 12 NSCLC patients (**B**) and between paired bronchial washing and biopsy samples from six NSCLC patients (**C**). Methylation levels in bronchial washings were similar to those in sputum samples but were significantly low compared with those in bronchial biopsy (Wilcoxon signed-rank test). Y-axis indicates β-values from the 450 K array.

3.4. RUNX1 Affects Overall Survival in Adenocarcinoma

To elucidate the effect of RUNX1 expression on survival of NSCLC patient, we analyzed the expression of RUNX1 using immunohistochemistry of formalin-fixed paraffin-embedded tumor tissues from 409 NSCLCs. Representative positive staining patterns of RUNX1 are shown in adenocarcinoma and squamous cell carcinoma (Figure 4A). Clinicopathological characteristics of 409 non-small cell lung cancer patients are listed in Table S2. The median follow-up period of patients was 5.2 years. RUNX1 expression was reduced in 31% of the samples. Reduced RUNX1 expression was not related to pathologic stage (Figure S2), but was found more frequently in woman (Figure 4B) and in adenocarcinoma (Figure 4C) and was significantly associated with poor overall survival in adenocarcinoma ($p = 0.005$; Figure 4D) but not in squamous cell carcinoma ($p = 0.87$). The median survival of adenocarcinoma patients with and without reduced RUNX1 expression was 41 and 81 months, respectively. Cox proportional hazards analysis also showed that overall survival of adenocarcinoma patients with reduced RUNX1 expression was approximately 1.97 (95% CI = 1.16–3.44; $p = 0.01$) times poorer than in those without, after controlling for age, recurrence, and pathologic stage (Table 1). However, RUNX1 expression was not associated with recurrence-free survival irrespective of histology in NSCLC ($p = 0.21$).

Table 1. Cox proportional hazards analysis of overall survival according to RUNX1 expression.

Histology	RUNX1 Expression	HR	95% CI	*p*-Value
Adeno (N = 189)	Normal	1.00		
	Reduced	1.97	1.16–3.44	0.01
Squamous (N = 192)	Normal	1.00		
	Reduced	1.46	0.78–5.32	0.21

Abbreviations: Adeno, adenocarcinoma; squamous, squamous cell carcinoma; HR, hazard ratio; CI, confidence interval; RUNX1, runt-related transcription factor 1.
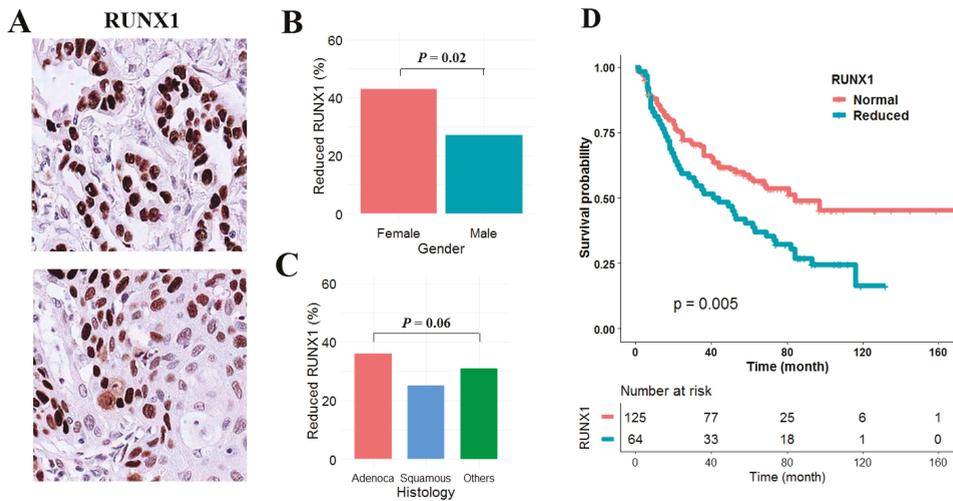
Figure 4. The effect of RUNX1 expression on overall survival in NSCLC. (**A**) RUNX1 expression was analyzed using immunohistochemistry in 409 NSCLC patients. Positive staining occurred in the nucleus of adenocarcinoma (upper) and squamous cell carcinoma. (X200). (**B**,**C**) Reduced expression levels were compared according to gender (**B**) and histologic subtypes (**C**). *p*-values are based on Student *t*-test. (**D**) The effect of reduced RUNX1 expression on overall survival of patients with adenocarcinoma was analyzed using Kaplan-Meier survival curve. *p*-value was calculated using log-rank test.

3.5. No Correlation between Reduced RUNX1 Expression and Expression Levels of Phospho-Rb and Ki67 Proliferation Index

RUNX proteins are implicated in diverse signaling pathways and cellular processes, including the cell cycle and stress response. In order to elucidate the effect of RUNX1 on the cell cycle and cell proliferation in NSCLC, we analyzed the phospho-pRb (Ser-807/811) levels and Ki-67 proliferation index according to the expression status of RUNX1. The average phospho-pRb (Ser-807/811) levels were 2.7% in tumor tissues with reduced RUNX1 expression and 2.1% in tumor tissues without reduced RUNX1 expression. The difference was not statistically significant ($p = 0.18$), irrespective of histology (Figure 5A). The Ki-67 proliferation index in tumor tissues with reduced RUNX1 expression was slightly higher than in tumor tissues without reduced RUNX1 expression, but the difference was also not statistically significant (28.8% vs. 22.3%, $p = 0.18$), irrespective of histology (Figure 5B).

A

B
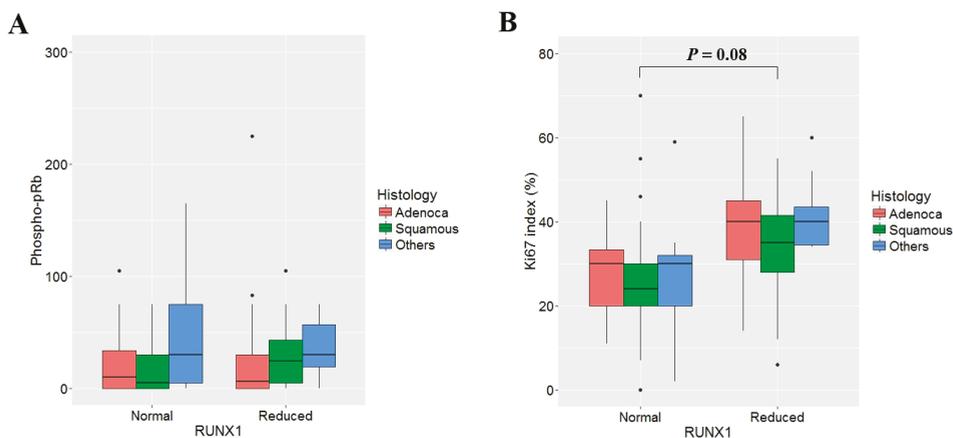
Figure 5. The effect of RUNX1 expression on phospho-pRb (Ser-807/811) level and Ki-67 proliferation index. The expression levels of phosphorylated pRb stained using polyclonal anti-phospho-pRb (Ser-807/811) antibody (Cell Signaling, Danvers, MA, USA) (**A**) and Ki-67 proliferation index (**B**) were compared according to the expression status of RUNX1 using Student *t*-test. The phospho-pRb levels and Ki-67 proliferation index were not significantly different between tumor tissues with normal or reduced RUNX1 expression irrespective of histologic subgroup.

4. Discussion

RUNX1 causes a wide range of leukemias through translocation with genes such as eight-twenty-one (ETO) [7] and acts as an oncogene in various solid tumors such as ovarian cancer [15], and endometrial cancer [16], as well as in the mouse mammary tumor virus-polyoma middle tumor-antigen (MMTV-PyMT) transgenic mouse model of breast cancer [17], and in the transgenic adenocarcinoma of mouse prostate (TRAMP) model of prostate cancer [18]. RUNX1 is also known to function as a tumor suppressor in different types of cancer. For example, the ectopic expression of RUNX1 in esophageal adenocarcinoma cells reduced the anchorage-independent growth [19], and the knockdown of *RUNX1* by siRNAs enhanced androgen-independent proliferation of prostate cancer cells [20]. In addition, the inhibition of endogenous *RUNX1* using short-hairpin RNA targeting RUNX1 (shRunx1) in breast cancer cells resulted in loss of epithelial morphology and promotion of epithelial-mesenchymal transition [9], and the ectopic expression of RUNX1 reduced the population of breast cancer stem cells [21]. RUNX1 also inhibited the migration and stemness of mammary epithelial cells [22]. Ramsay et al. [10] reported that lentiviral-mediated RNAi knockdown of *RUNX1* increased the proliferation and migration of lung cancer cells. In the present study, *RUNX1* showed abnormal methylation in primary NSCLCs, and the reduced expression of RUNX1 was associated with poor overall survival, suggesting that RUNX1 may play a role as a tumor suppressor in normal bronchial epithelial cells.

Functional disruption of RUNX1 usually occurs by chromosomal translocation, point mutation, or deletion in leukemia and some solid tumors. *RUNX1* mutation has been reported rarely in lung cancer [23], although changes in its methylation have been reported by a couple of studies [24,25]. In this study, *RUNX1* was found to be abnormally methylated at the CpG island of *RUNX1* in NSCLC tumor tissues, and the methylation and mRNA levels of *RUNX1* showed a linear negative correlation. Unlike most genes whose transcription is regulated by a single promoter, *RUNX1* is regulated by two promoters in the upstream region of 5′ UTR [26]. The three hypermethylated CpGs in this study might affect the transcription of *RUNX1*, which may also be affected by tissue-specific control factors. Further studies are needed to understand the mechanisms underlying transcriptional repression mediated by abnormal methylation of *RUNX1* in NSCLC.

A CpG (cg04228935) for the prediction of NSCLC was identified using tumor and matched normal tissues obtained from 42 NSCLC patients. Although the number of normal samples in the TCGA lung cancer data is small and the prevalence of lung cancer is not the exact same between Koreans and Americans, the present study suggests that RUNX1 hypermethylation may be a useful biomarker for the early detection of NSLC in other populations worldwide. Screening of lung cancer using low-dose computed tomography (LDCT) reduces mortality; however, approximately 20% of pulmonary nodules were found to be false positive [27,28]. A biopsy is needed for a more accurate diagnosis of lung cancer, but it is very difficult to obtain tissue in some patients. Methylation levels of a CpG (cg04228935) from bronchial biopsy were comparable to those from surgically resected lung tumor tissues. Accordingly, bronchial biopsy specimens may be used for the molecular analysis of *RUNX1*, and advances in technology such as electromagnetic navigation bronchoscopy (ENB) and endobronchial ultrasonography using a guided sheath (EBUS-GS) may provide more adequate specimens with fewer complications.

The association of *RUNX1* mutations or changes in expression with the prognosis of patients has been reported in various carcinomas, and the effect of RUNX1 on prognosis varies considerably depending on the type of cancer. *RUNX1* mutations are associated with poor overall survival in adult acute myelogenous leukemia (AML) as well as in pediatric AML [29,30]. The RUNX1 expression in prostate cancer tissues was negatively associated with poor prognosis [20]. The low RUNX1 expression in breast cancers is associated with metastasis to lymph nodes and poor survival [9,21]. In addition, the RUNX1-RUNX3 expression showed a significant effect on the survival of breast cancer patients with high YAP-signature expression levels [22]. Lung adenocarcinomas with low RUNX1 expression were associated with poor overall survival compared to tumors with high RUNX1 expression [10]. Our data also showed that reduced RUNX1 expression was associated with poor overall survival in adenocarcinomas. Based on these observations, it is likely that the reduced expression of RUNX1 may serve as an indicator of poor prognosis in patients with lung adenocarcinoma.

RUNX proteins are known to regulate a wide range of biological processes via various interacting proteins in human cancer and to be implicated in carcinogenesis mediated via TGF-β and Wnt signaling pathways, and in cell cycle or stress response. For example, RUNX1 promoter is regulated by EZH2 (enhancer of zeste homolog 2)-dependent histone H3 lysine 27 (K27) trimethylation in prostate cancer cells [20]. RUNX1 directly regulates E-cadherin, and rescues TGFβ-induced EMT phenotype in breast cancer cells [9]. RUNX1 suppresses breast cancer growth by repressing the activity of breast cancer stem cells and inhibiting ZEB1 expression directly [21]. RUNX1 acts as a negative regulator of oncogenic function of YAP that is involved in solid tumor progression [22]. The effect of RUNX1 on cell cycle in lung cancer differs between study groups. RUNX1 stimulated G1 to S progression in hematopoietic cells, partly via transcriptional induction of cyclin D2 promoter [31], whereas RUNX1 depletion resulted in an increased E2F1 mRNA levels in lung cancer cells [10]. In this study, tumor tissues with reduced RUNX1 expression did not show high levels of pRb phosphorylation (Ser-807/811) or the Ki67 proliferation index, suggesting that the reduced expression of RUNX1 may be involved in lung carcinogenesis through other mechanisms rather than cell-cycle regulation and growth control.

This study was limited by several factors. First, the effect of the two promoters on abnormal methylation of three CpGs in *RUNX1* gene and the tissue-specific factors affecting the expression of RUNX1 were not fully elucidated. Second, we failed to analyze *RUNX1* methylation in circulating cell-free DNA and to evaluate the prediction performance of the model due to assay failure. Third, the present study was a retrospective case-control study, which can result in a biased estimate of the population prevalence of NSCLC. In addition, sputum analysis was limited to the very few specimens from NSCLC patients only. Accordingly, the prediction performance of the model needs to be validated using several molecular techniques such as droplet digital polymerase chain reaction (ddPCR) in sputums and cell-free DNAs from a large cohort. Fourth, it is unclear the abnormal methylation of RUNX1 as a predictive biomarker can also be applied to tissue samples from metastatic lesions because the data from the present study and TCGA was from surgical specimens of early stage

tumors. Fifth, methylation levels from benign lung tumors such as localized organizing pneumonia and hamartoma were not analyzed due to lack of samples.

In conclusion, the present study suggests that abnormal methylation at the CpG island of the *RUNX1* gene may be a valuable biomarker for the detection of NSCLC regardless of races. Reduced expression of RUNX1 may be associated with poor overall survival in patients with lung adenicarcinoma.

References

1. Siegel, R.L.; Miller, K.D.; Jemal, A. Cancer statistics, 2016. *CA Cancer J. Clin.* **2016**, *66*, 7–30. [CrossRef] [PubMed]

2. Yamamoto, K.; Ohsumi, A.; Kojima, F.; Imanishi, N.; Matsuoka, K.; Ueda, M.; Miyamoto, Y. Long-term survival after video-assisted thoracic surgery lobectomy for primary lung cancer. *Ann. Thorac. Surg.* **2010**, *89*, 353–359. [CrossRef]

3. Warren, A.J.; Bravo, J.; Williams, R.L.; Rabbitts, T.H. Structural basis for the heterodimeric interaction between the acute leukaemia-associated transcription factors AML1 and CBFbeta. *EMBO J.* **2000**, *19*, 3004–3015. [CrossRef] [PubMed]

4. Yan, J.; Liu, Y.; Lukasik, S.M.; Speck, N.A.; Bushweller, J.H. CBFbeta allosterically regulates the Runx1 Runt domain via a dynamic conformational equilibrium. *Nat. Struct. Mol. Biol.* **2004**, *11*, 901–906. [CrossRef] [PubMed]

5. Langabeer, S.E.; Gale, R.E.; Rollinson, S.J.; Morgan, G.J.; Linch, D.C. Mutations of the AML1 gene in acute myeloid leukemia of FAB types M0 and M7. *Genes Chromosomes Cancer* **2002**, *34*, 24–32. [CrossRef]

6. Harada, H.; Harada, Y.; Niimi, H.; Kyo, T.; Kimura, A.; Inaba, T. High incidence of somatic mutations in the AML1/RUNX1 gene in myelodysplastic syndrome and low blast percentage myeloid leukemia with myelodysplasia. *Blood* **2004**, *103*, 2316–2324. [CrossRef]

7. Lam, K.; Zhang, D.E. RUNX1 and RUNX1-ETO: Roles in hematopoiesis and leukemogenesis. *Front Biosci.* **2012**, *17*, 1120–1139. [CrossRef]

8. Ellis, M.J.; Ding, L.; Shen, D.; Luo, J.; Suman, V.J.; Wallis, J.W.; Van Tine, B.A.; Hoog, J.; Goiffon, R.J.; Goldstein, T.C.; et al. Whole-genome analysis informs breast cancer response to aromatase inhibition. *Nature* **2012**, *486*, 353–360. [CrossRef]

9. Hong, D.; Messier, T.L.; Tye, C.E.; Dobson, J.R.; Fritz, A.J.; Sikora, K.R.; Browne, G.; Stein, J.L.; Lian, J.B.; Stein, G.S. Runx1 stabilizes the mammary epithelial cell phenotype and prevents epithelial to mesenchymal transition. *Oncotarget* **2017**, *8*, 17610–17627. [CrossRef]

10. Ramsey, J.; Butnor, K.; Peng, Z.; Leclair, T.; van der Velden, J.; Stein, G.; Lian, J.; Kinsey, C.M. Loss of RUNX1 is associated with aggressive lung adenocarcinoma. *J. Cell Physiol.* **2018**, *233*, 3487–3497. [CrossRef]

11. Kim, J.S.; Han, J.; Shim, Y.M.; Park, J.; Kim, D.H. Aberrant methylation of H-cadherin (CDH13) promoter is associated with tumor progression in primary nonsmall cell lung carcinoma. *Cancer* **2005**, *104*, 1825–1833. [PubMed]

12. Edge, S.B.; Byrd, D.R.; Compton, C.C.; Fritz, A.G.; Greene, F.L.; Troth, A. American Joint Committee on Cancer. In *AJCC Cancer Staging Manual*, 7th ed.; Springer: New York, NY, USA, 2010; pp. 253–270.

13. Um, S.W.; Kim, H.K.; Kim, Y.; Lee, B.B.; Kim, D.; Han, J.; Kim, H.; Shim, Y.M.; Kim, D.H. Bronchial biopsy specimen as a surrogate for DNA methylation analysis in inoperable lung cancer. *Clin. Epigenetics* **2017**, *9*, 131. [CrossRef] [PubMed]

14. Pidsley, R.; Y Wong, C.C.; Volta, M.; Lunnon, K.; Mill, J.; Schalkwyk, L.C. A data-driven approach to preprocessing Illumina 450K methylation array data. *BMC. Genomics* **2013**, *14*, 293. [CrossRef] [PubMed]

15. Ketia, M.; Bachvarova, M.; Morin, C.; Plante, M.; Gregoire, J.; Renaud, M.C.; Sebastianelli, A.; Trinh, X.B.; Bachvarov, D. The RUNX1 transcription factor is expressed in serous epithelial ovarian carcinoma and contributes to cell proliferation, migration and invasion. *Cell Cycle* **2013**, *12*, 972–986.

16. Planagumà, J.; Díaz-Fuertes, M.; Gil-Moreno, A.; Abal, M.; Monge, M.; García, A.; Baró, T.; Thomson, T.M.; Xercavins, J.; Alameda, F.; et al. A differential gene expression profile reveals overexpression of RUNX1/AML1 in invasive endometrioid carcinoma. *Cancer Res.* **2004**, *64*, 8846–8853. [CrossRef] [PubMed]

17. Browne, G.; Taipaleenmaki, H.; Bishop, N.M.; Madasu, S.C.; Shaw, L.M.; van Wijnen, A.J.; Stein, J.L.; Stein, G.S.; Lian, J.B. Runx1 is associated with breast cancer progression in MMTV-PyMT transgenic mice and its depletion in vitro inhibits migration and invasion. *J. Cell Physiol.* **2015**, *230*, 2522–2532. [CrossRef]

18. Farina, N.H.; Zingiryan, A.; Akech, J.A.; Callahan, C.J.; Lu, H.; Stein, J.L.; Languino, L.R.; Stein, G.S.; Lian, J.B. A microRNA/Runx1/Runx2 network regulates prostate tumor progression from onset to adenocarcinoma in TRAMP mice. *Oncotarget* **2016**, *7*, 70462–70474. [CrossRef]

19. Dulak, A.M.; Schumacher, S.; van Lieshout, J.; Imamura, Y.; Fox, C.; Shim, B.; Ramos, A.H.; Saksena, G.; Baca, S.C.; Baselga, J.; et al. Gastrointestinal adenocarcinomas of the esophagus, stomach and colon exhibit distinct patterns of genome instability and oncogenesis. *Cancer Res.* **2012**, *72*, 4383–4393. [CrossRef]

20. Takayama, K.; Suzuki, T.; Tsutsumi, S.; Fujimura, T.; Urano, T.; Takahashi, S.; Homma, Y.; Aburatani, H.; Inoue, S. RUNX1, an androgen- and EZH2-regulated gene, has differential roles in AR-dependent and -independent prostate cancer. *Oncotarget* **2015**, *6*, 2263–2276. [CrossRef]

21. Hong, D.; Fritz, A.J.; Finstad, K.H.; Fitzgerald, M.P.; Weinheimer, A.; Viens, A.L.; Ramsey, J.; Stein, J.L.; Lian, J.B.; Stein, G.S. Suppression of breast cancer stem cells and tumor growth by the RUNX1 transcription factor. *Mol. Cancer Res.* **2018**, *16*, 1952–1964. [CrossRef]

22. Kulkarni, M.; Tan, T.Z.; Syed Sulaiman, N.B.; Lamar, J.M.; Bansal, P.; Cui, J.; Qiao, Y.; Ito, Y. RUNX1 and RUNX3 protect against YAP-mediated EMT, stem-ness and shorter survival outcomes in breast cancer. *Oncotarget* **2018**, *9*, 14175–14192. [CrossRef] [PubMed]

23. Hao, C.; Wang, L.; Peng, S.; Cao, M.; Li, H.; Hu, J.; Huang, X.; Liu, W.; Zhang, H.; Wu, S.; et al. Gene mutations in primary tumors and corresponding patient-derived xenografts derived from non-small cell lung cancer. *Cancer Lett.* **2015**, *357*, 179–185. [CrossRef]

24. Feng, Q.; Hawes, S.E.; Stern, J.E.; Wiens, L.; Lu, H.; Dong, Z.M.; Jordan, C.D.; Kiviat, N.B.; Vesselle, H. DNA methylation in tumor and matched normal tissues from non-small cell lung cancer patients. *Cancer Epidemiol. Biomarkers Prev.* **2008**, *17*, 645–654. [CrossRef] [PubMed]

25. Rauch, T.A.; Wang, Z.; Wu, X.; Kernstine, K.H.; Riggs, A.D.; Pfeifer, G.P. DNA methylation biomarkers for lung cancer. *Tumour Biol.* **2012**, *33*, 287–296. [CrossRef] [PubMed]

26. Ghozi, M.C.; Bernstein, Y.; Negreanu, V.; Levanon, D.; Groner, Y. Expression of the human acute myeloid leukemia gene AML1 is regulated by two promoter regions. *Proc. Natl. Acad. Sci. USA* **1996**, *93*, 1935–1940. [CrossRef]

27. National Lung Screening Trial Research Team; Aberle, D.R.; Adams, A.M.; Berg, C.D.; Black, W.C.; Clapp, J.D.; Fagerstrom, R.M.; Gareen, I.F.; Gatsonis, C.; Marcus, P.M.; et al. Reduced lung-cancer mortality with low-dose computed tomographic screening. *N. Engl. J. Med.* **2011**, *365*, 395–409.

28. Bach, P.B.; Mirkin, J.N.; Oliver, T.K.; Azzoli, C.G.; Berry, D.A.; Brawley, O.W.; Byers, T.; Colditz, G.A.; Gould, M.K.; Jett, J.R.; et al. Benefits and harms of CT screening for lung cancer: A systematic review. *JAMA* **2012**, *307*, 2418–2429. [CrossRef]

29. Jalili, M.; Yaghmaie, M.; Ahmadvand, M.; Alimoghaddam, K.; Mousavi, S.A.; Vaezi, M.; Ghavamzadeh, A. Prognostic Value of RUNX1 Mutations in AML: A Meta-Analysis. *Asian Pac. J. Cancer Prev.* **2018**, *19*, 325–332.

30. Yamato, G.; Shiba, N.; Yoshida, K.; Hara, Y.; Shiraishi, Y.; Ohki, K.; Okubo, J.; Park, M.J.; Sotomatsu, M.; Arakawa, H.; et al. RUNX1 mutations in pediatric acute myeloid leukemia are associated with distinct genetic features and an inferior prognosis. *Blood* **2018**, *131*, 2266–2270. [CrossRef]
31. Strom, D.K.; NiP, J.; Westendorf, J.J.; Linggi, B.; Lutterbach, B.; Downing, J.R.; Lenny, N.; Hiebert, S.W. Expression of the AML-1 oncogene shortens the G(1) phase of the cell cycle. *J. Biol. Chem.* **2002**, *275*, 3438–3445. [CrossRef]

Article

HIP1R Expression and Its Association with PD-1 Pathway Blockade Response in Refractory Advanced NonSmall Cell Lung Cancer: A Gene Set Enrichment Analysis

Young Wha Koh [1],*, Jae-Ho Han [1], Seokjin Haam [2] and Hyun Woo Lee [3]

[1] Department of Pathology, Ajou University School of Medicine, Suwon 16499, Korea; hanpathol@naver.com
[2] Department of Thoracic and Cardiovascular Surgery, Ajou University School of Medicine,
    Suwon 16499, Korea; haamsj@aumc.ac.kr
[3] Department of Hematology-Oncology, Ajou University School of Medicine, Suwon 16499, Korea;
    leehw@ajou.ac.kr
*   Correspondence: youngwha9556@gmail.com; Tel.: +82-31-219-7055

Abstract: Huntingtin-interacting protein 1-related protein (HIP1R) plays an important role in the regulation of programmed death-ligand 1 (PD-L1). The aim of this study was to investigate the expression of HIP1R and confirm its predictive or prognostic roles in anti-PD-1 therapy in nonsmall cell lung cancer (NSCLC) patients. HIP1R and PD-L1 immunohistochemical expression was examined in 52 refractory advanced NSCLC patients treated with anti-PD-1 inhibitors. We performed gene set enrichment analysis (GSEA) to detect HIP1R-specific gene sets. Patients in the PD-1 inhibitor responder group had lower HIP1R expression by univariate logistic regression analysis (odds ratio (OR) = 0.235, $p = 0.015$) and multivariate logistic regression analysis (OR = 0.209, $p = 0.014$). Patients with high HIP1R expression had poorer progression-free survival (PFS) than patients with low HIP1R expression in univariate analysis ($p = 0.037$) and multivariate Cox analysis (hazard ratio = 2.098, $p = 0.019$). The web-based mRNA dataset also showed that high HIP1R expression correlated with inferior overall survival in lung adenocarcinoma ($p = 0.026$). GSEA revealed that HIP1R levels correlate with a set of genes that reflect PD-L1-related immune pathways. HIP1R expression may be a promising predictor for determination of patient responses to anti-PD-1 treatment.

Keywords: nonsmall cell lung cancer; HIP1R; PD-L1; biomarker

1. Introduction

Emergence of immune checkpoint inhibitors was a turning point in the treatment of advanced nonsmall cell lung cancer (NSCLC). Therapies targeting the programmed cell death protein 1 (PD-1) checkpoint, such as nivolumab and pembrolizumab, have yielded impressive responsive rates in advanced NSCLC patients otherwise refractory to multiples lines of therapy [1–3]. However, the overall response rate for PD-1 inhibitor therapy is approximately 15–20% in unselected patients with NSCLC, and between 15% and 45% in patients with PD-L1-expressing NSCLC [4]. We need a biomarker that can more accurately predict the response to PD-1 inhibitors.

Expression of programmed death ligand-1 (PD-L1), the PD-1 ligand, is currently the most widely used biomarker for PD-1 inhibition. To identify patients who preferentially respond to PD-1 blockade, we need to better understand how the PD-1 pathway is regulated. Recently, several mechanisms have been reported to underlie PD-1 pathway regulation. CKLF-like MARVEL transmembrane-domain-containing 6 (CMTM6) regulates the PD-1 pathway by maintaining the expression of PD-L1, and CMTM6 is a predictor of the response to PD-1 inhibitors [5,6]. F-box only

protein 38 (FBXO38) mediates PD-1 ubiquitination of T cells, and knockout of FBXO38 in such cells induces tumor progression in a mouse model due to increased PD-1 expression by tumor-infiltrating T cells [7]. AXL expression displays a positive correlation with PD-L1 expression in lung adenocarcinoma with epidermal growth factor receptor (EGFR) mutation, and abolition of AXL kinase activity inhibits *PD-L1* mRNA expression in a lung adenocarcinoma cell line with EGFR mutation [8].

Recent research has uncovered new strategies to remove specific unwanted proteins by using cellular protein degradation mechanisms, including lysosome-targeting molecules [9], proteolysis-targeting chimeras (PROTACs) [10], and tag-based degradation systems (dTAG) [11]. Wang et al. reported that Huntingtin-interacting protein 1-related protein (HIP1R) promotes lysosomal degradation of PD-L1, inhibits HIP1R-induced PD-L1 accumulation, and alters T cell–mediated cytotoxicity in a human colorectal cancer cell line [12]. A chimeric peptide including a lysosomal sorting signal and the HIP1R PD-L1-binding sequence significantly inhibits PD-L1 protein expression [12]. Although immune checkpoint inhibition is the most popular treatment for lung cancer, relationships involving HIP1R and immune checkpoint inhibitors in lung cancer have not been studied.

The present study was conducted to determine whether HIP1R protein expression affects the response of NSCLC patients to anti-PD-1 inhibitors and their prognosis. The relationship between HIP1R and PD-L1 was also evaluated, employing immunohistochemical and web-based mRNA expression data. In addition, we performed gene set enrichment analysis (GSEA) on RNA-sequencing data from The Cancer Genome Atlas (TCGA) to confirm the molecular pathways associated with HIP1R expression.

2. Materials and Methods

2.1. Patients

We retrospectively selected 52 advanced NSCLC patients who were administered PD-1 inhibitor from 2016 to 2019, and they previously received one or two lines of chemotherapy. This study was approved by the Institutional Review Board of Ajou University School of Medicine. Informed consent was waived due to the retrospective nature of the study (AJIRB-BMR-KSP-19-050 and 2019-03-26).

Patients treated with PD-1 inhibitor were assigned to either a responder group (complete response, partial response, or stable disease) or a nonresponder group (disease progression), according to the response evaluation criteria for solid tumors (RECIST) version 1.1 [13].

2.2. Immunohistochemical Staining and HIP1R Expression Scoring

One board-certified pathologist (YWK) reviewed hematoxylin and eosin (H&E)-stained tissue samples to determine a definitive pathologic diagnosis according to the 2015 World Health Organization Classification of Lung Tumors [14]. All patients were pathologically staged according to the eighth edition of the TNM classification.

HIP1R immunohistochemical (IHC) staining was performed with a Benchmark XT automatic IHC staining device (Ventana Medical Systems, Tucson, AZ, USA). The samples were incubated with an anti-HIP1R antibody (dilution 1:1000, 16814-1-AP, polyclonal, Proteintech, Rosemont, IL, USA). We used a human placenta tissue as positive control according to the manufacturer's recommendations (Figure S1). We also evaluated the intensity of HIP1R staining on a four-point intensity scale: 0 (no staining), 1 (light yellow = faint staining), 2 (yellow-brown = moderate staining), and 3 (brown = strong staining) (Figure 1). We also evaluated the percentages (0–100%) of cytoplasmic versus membranous localization of HIP1R. We used H-scores to interpret HIP1R staining [15], where H-score = [1 × (% cells 1+) + 2 × (% cells 2+) + 3 × (% cells 3+)]. H-scores (0–300) were obtained by multiplying the percentage of cells by the intensity score.
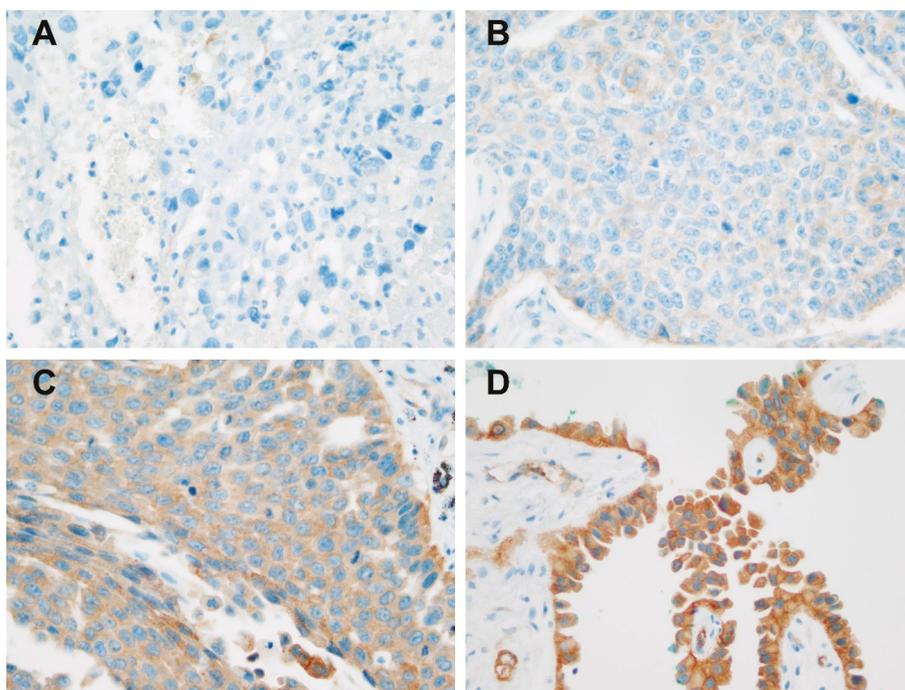
Figure 1. Huntingtin-interacting protein 1-related protein (HIP1R) expression in nonsmall cell carcinoma.
(**A**) No staining of HIP1R, x400. (**B**) Faint HIP1R staining, X400. (**C**) Moderate HIP1R staining, X400.
(**D**) Strong HIP1R staining, X400.

2.3. Immunohistochemical Staining and PD-L1 Expression Scoring

Two PD-L1 antibodies (clone name SP263 or 22C3) were used to detect PD-L1 expression. Sp263 was a companion diagnostic assay for OPDIVO® (nivolumab), and 22c3 was a companion diagnostic assay for KEYTRUDA® (pembrolizumab). We performed SP263 and/or 22C3 assays prior to PD-1 inhibitor treatment for all NSCLC patients. Thirteen (25%) of the 52 specimens were tested for both SP263 and 22C3, 27 (51.9%) for only SP263, and 12 (23.1%) for only 22C3. Two PD-L1 tests used prediluted antibody (ready to use) according to the protocol. The SP263 assay was performed using a VENTANA BenchMark ULTRA instrument (Roche, Basel, Switzerland), and the 22C3 assay was conducted using the Dako Link-48 platform (Dako, Carpinteria, California, US), as recommended by the manufacturers [16]. PD-L1 intensity was also evaluated on a four-point intensity scale (0, none; 1, faint; 2, moderate; and 3, strong), and the percentage of membranous expression of PD-L1 was determined (Figures S2 and S3). When both the 22C3 and SP263 tests were conducted, mean values were used. High PD-L1 expression was defined as $\geq$ 50% of definitive tumor cells exhibiting PD-L1 staining, because 50% was the cut-off used for NSCLC [17].

2.4. Web-Based mRNA Profiling, GSEA, and Kaplan Meier Analysis

The mRNA sequencing data of 517 lung adenocarcinoma patients and 501 lung squamous cell carcinoma patients were downloaded from The Cancer Genome Atlas (TCGA) cBioportal (http://cbioportal.org) [18]. We conducted correlation analysis involving PD-L1 and HIP1R mRNA sequencing data.

GSEA is a method of analyzing associations between gene expression and biological information. We conducted GSEA using GSEA version 4.0.3 from the Broad Institute at MIT and Harvard (http:

//www.broadinstitute.org/gsea/index.jsp) [19]. TCGA mRNA sequencing data derived from lung adenocarcinoma and lung squamous cell carcinoma patients was used. Depending on the median value, it is divided into low and high HIP1R. Hallmark gene sets representing well-defined biological states or processes were used for GSEA. 1000 permutations were used for estimating nominal *p* values. If the *p* value was less than 0.05 and the False Discovery Rate (FDR) was less than 0.25, the findings were considered statistically significant.

We conducted survival analyses using an online Kaplan Meier plotter tool [20]. The online Kaplan Meier plotter tool provides mRNA expression data of cancer patients and allows for survival analysis. Survival analyses were performed in 719 patients with lung adenocarcinoma and 524 lung squamous cell carcinoma cases according to their HIP1R mRNA expression.

2.5. Statistical Analyses

Spearman's rank order correlation coefficient analysis was used to measure monotonic relationships between continuous variables. Mann Whitney U-tests were used to compare differences between two independent groups. Univariate and multivariate logistic regression analyses were performed to determine factors that predicted a response to PD-1 inhibitors. Receiver operating curve (ROC) analysis was used to determine the cut-off values for HIP1R expression. The progression-free survival (PFS) or overall survival (OS) difference between the cohorts was determined using the log-rank test. Univariate and multivariate prognostic analyses were performed for PFS using a Cox proportional hazards regression model. SPSS Statistics for Windows (Version 25.0, IBM, Armonk, NY, USA) was used for all analyses, and *p* values <0.05 were considered to be statistically significant.

3. Results

3.1. Patient Demographics

Detailed patient and tumor characteristics are summarized in Table 1. Forty-six tissues were collected from lung lesions, and six were obtained from metastatic sites. Twenty-seven (51.9%) patients had been treated with nivolumab, and 25 (48.1%) patients received pembrolizumab. All patients were refractory to conventional treatments such as chemotherapy, radiotherapy, or target therapy. Therefore, they received PD-1 inhibitor as a second line or later setting. Twenty-seven (51.9%) patients were classified as responders, and 25 (48.1%) were classified as nonresponders. Four patients were treated with epidermal growth factor receptor (EGFR) inhibitors before PD-1 inhibitor administration. Patients with anaplastic lymphoma kinase (ALK) fusion were not identified in the present study.

3.2. Relationships Between HIP1R and PD-L1 Analyzed by IHC and mRNA Expression

We performed correlation analysis of HIP1R and PD-L1 expression using IHC techniques. There was no statistically significant correlation between HIP1R and PD-L1 expression ($p = 0.905$, Figure 2A).

Correlation analyses of HIP1R and PD-L1 expression were performed using mRNA data. From the TCGA dataset, HIP1R mRNA expression levels were negatively correlated with PD-L1 mRNA levels in adenocarcinoma and squamous cell carcinoma. (Spearman's rho = −0.233, $p < 0.001$, Figure 2B; Spearman's rho = −0.224, $p < 0.001$, Figure 2C).

Table 1. Demographic and clinical characteristics of patients.

Variable	Number (%)
Age, Median (Range) (Years)	64 (38–85)
Male Sex	43 (82.7%)
Smoking Sistory	31 (73.8%)
Histologic Subtype	
Adenocarcinoma	22 (42.3%)
Squamous Cell Carcinoma	19 (36.5%)
Pleomorphic Carcinoma	4 (7.7%)
NSCLC, NOS	7 (13.5%)
Clinical Stage at Diagnosis	
III	13 (25%)
IV	39 (75%)
Genetic Alteration Status	
EGFR-Mutated	4 (9.1%)
ALK-Rearranged	0 (0%)
Wild Type	44 (92.3%)
Type of PD-1 Blockade	
Nivolumab	27 (51.9%)
Pembrolizumab	25 (48.1%)
PD-L1 Expression	
Low (<50%)	17 (32.7%)
High (≥50%)	35 (67.3%)
Response to PD-1 Blockade	
Responder	27 (51.9%)
Nonresponder	25 (48.1%)

Smoking history was collected for 42 patients. EGFR test was performed in 44 patients. ALK test was performed in 47 patients. Abbreviations: epidermal growth factor receptor; EGFR, nonsmall-cell lung cancer—not otherwise specified; NSCLC, NOS, programmed cell death protein 1, PD-1; programmed death-ligand 1, PD-L1.
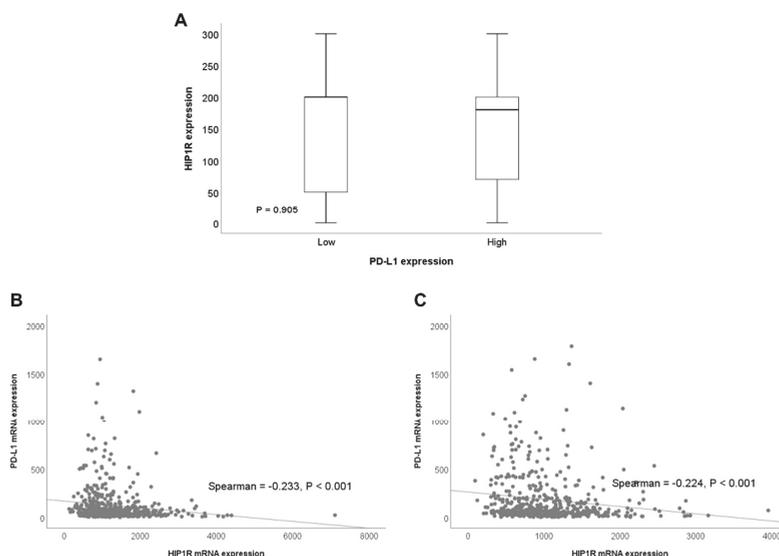
Figure 2. Correlation analyses involving Huntingtin-interacting protein 1-related protein (HIP1R) and programmed death-ligand 1 (PD-L1) expression. (**A**) Correlation between HIP1R and PD-L1 detected immunohistochemically. (**B**) Correlation between HIP1R and PD-L1 mRNA expression in lung adenocarcinoma. (**C**) Correlation between HIP1R and PD-L1 mRNA expression in lung squamous cell carcinoma.

3.3. Associations Involving HIP1R, PD-L1, Clinicopathologic Parameters, and Response to PD-1 Inhibitors

ROC analysis was performed to determine the cut-off value for HIP1R expression. Cut-off was determined as the value corresponding to the maximum joint sensitivity and specificity of the ROC curve. The area under the curve (AUC) was 0.659 for the expression of HIP1R, and the cut-off value was 180 (66% sensitivity and 68% specificity, Figure 3).
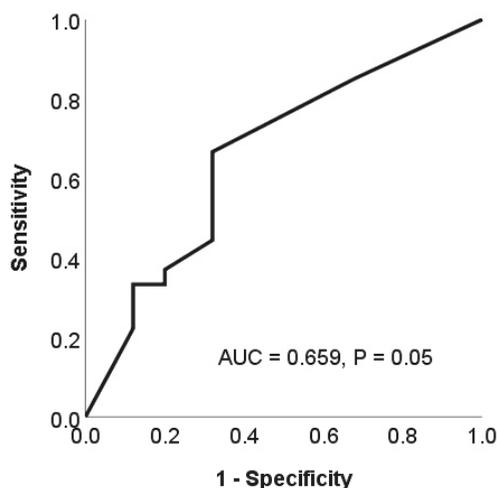
Figure 3. Receiver operating characteristic (ROC) and area under the curve (AUC) analysis of HIP1R expression.

We explored the predictive capacity of HIP1R, PD-L1, and clinicopathologic factors in terms of responses to PD-1 inhibition. By univariate analysis, the expression of HIP1R was found to be a predictor of the response to anti-PD-1 therapy (OR) = 0.235, p = 0.015; Table 2). PD-L1 expression was also found to be a predictor of the response to anti-PD-1 therapy (OR = 4.062, p = 0.028; Table 2). By multivariate analysis, the expression of HIP1R was an independent predictor of anti-PD-1 therapy response (OR = 0.209, p = 0.014, Table 2).

Table 2. Univariate and multivariate logistic regression analysis for predicting clinical response to PD-1 blockade.

Covariate	Univariate Analysis			Multivariate Analysis		
	OR	95% CI	*p*-Value [†]	OR	95% CI	*p*-Value [†]
Age (≥65 Years vs. <65 Years)	1.591	0.532–4.757	0.406			
Sex (Male vs. Female)	2.526	0.558–11.44	0.229			
Smoking History (+ vs. −)	3.238	0.720–14.56	0.126			
Presence of EGFR Mutation (+ vs. −)	0.222	0.021–2.330	0.210			
Type of PD-1 Blockade (Nivolumab vs. Pembrolizumab)	1.875	0.622–5.649	0.264			
PD-L1 (>50% vs. ≤50%)	4.062	1.166–14.15	0.028	4.664	1.198–18.15	0.026
HIP1R (>180 vs. ≤180)	0.235	0.074–0.751	0.015	0.209	0.060–0.731	0.014

[†] logistic regression analysis. Abbreviations: confidence interval; CI, epidermal growth factor receptor; EGFR, Huntingtin Interacting Protein 1 Related; HIP1R, odd ratio; OR, programmed cell death protein 1, PD-1; programmed death-ligand 1, PD-L1.

3.4. GSEA According to HIP1R mRNA Expression

We performed GSEA to identify gene sets associated with HIP1R mRNA expression in the TCGA mRNA data of lung adenocarcinoma and lung squamous cell carcinoma cases. In lung adenocarcinoma, we identified the top 20 most prominent pathways that were upregulated in the low HIP1R mRNA expression group (Table S1). Four of the 20 were immune-related gene sets and were statistically

significant (HALLMARK_ALLOGRAFT_REJECTION, HALLMARK_INFLAMMATORY_RESPONSE, HALLMARK_IL6_JAK_STAT3_SIGNALING, and HALLMARK_IL2_STAT5_SIGNALING) (Figure 4). HALLMARK_INTERFERON_GAMMA_RESPONSE is also upregulated in the low HIP1R mRNA expression group, although the statistical significance was marginal ($p = 0.063$). Core enrichment gene lists for HALLMARK_ALLOGRAFT_REJECTION, HALLMARK_INFLAMMATORY_RESPONSE, HALLMARK_IL6_JAK_STAT3_SIGNALING and HALLMARK_IL2_STAT5_SIGNALING are summarized in Tables S2–S5. In lung squamous cell carcinoma, there were no statistically significant immune-related gene sets associated with HIP1R mRNA expression (Table S6).
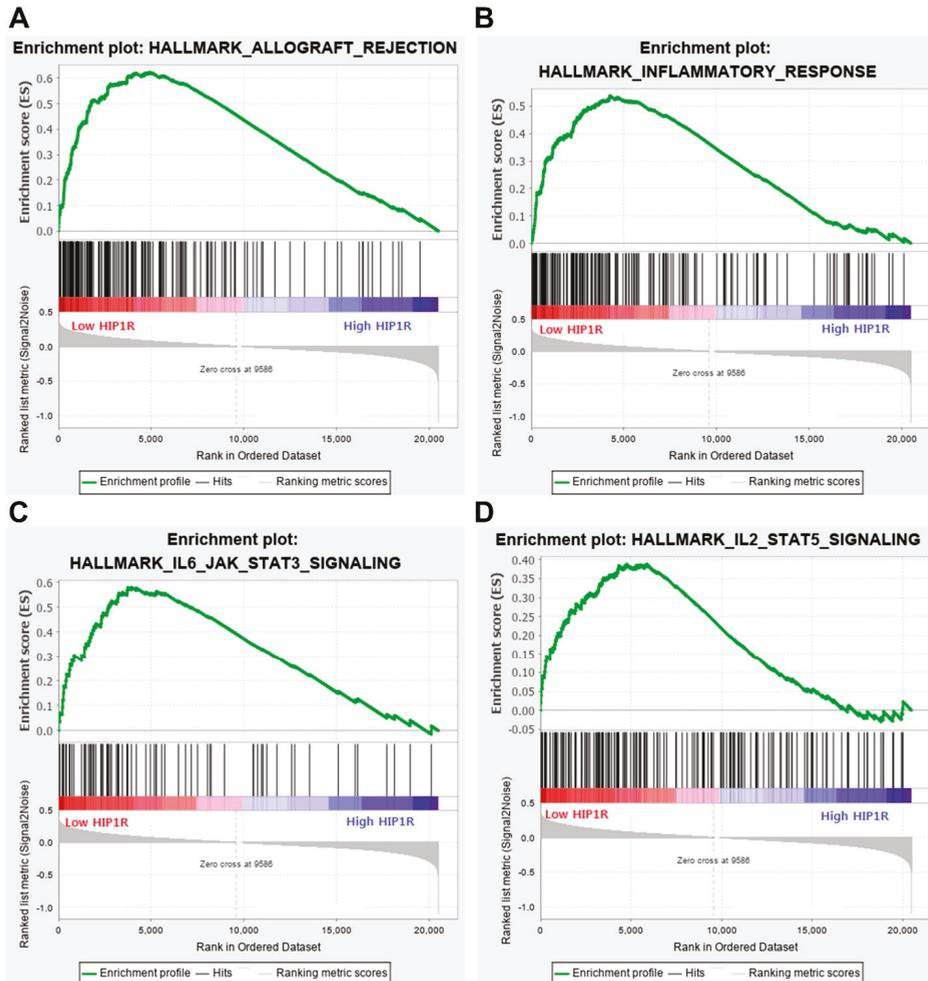
Figure 4. Gene set enrichment analysis (GSEA) according to HIP1R mRNA expression. (**A**) HALL MARK_ALLOGRAFT_REJECTION pathway; (**B**) HALLMARK_INFLAMMATORY_RESPONSE pathway; (**C**) HALLMARK_IL6_JAK_STAT3_SIGNALING pathway; (**D**) HALLMARK _IL2_STAT5_SIGNALING pathway.

3.5. Prognostic Significance of HIP1R and PD-L1

Patients with high HIP1R expression had inferior PFS to patients with low HIP1R expression ($p = 0.037$, Figure 5A). Patients with high HIP1R expression also showed an inferior OS than patients with low HIP1R expression, however the statistical significance was not reached ($p = 0.11$, Figure 5B). Patients with high PD-L1 expression had superior PFS or OS than patients with low PD-L1 expression ($p = 0.028$, Figure 5C and $p = 0.031$, Figure 5D, respectively). Furthermore, patients with high HIP1R expression and low PD-L1 expression had lower PFS or OS than patients with other expression patterns ($p < 0.001$, Figure 5E and $p = 0.001$, Figure 5F, respectively). In multivariate analysis, high HIP1R expression was an independent prognostic factor for PFS (HR = 2.098, $p = 0.019$, Table 3).
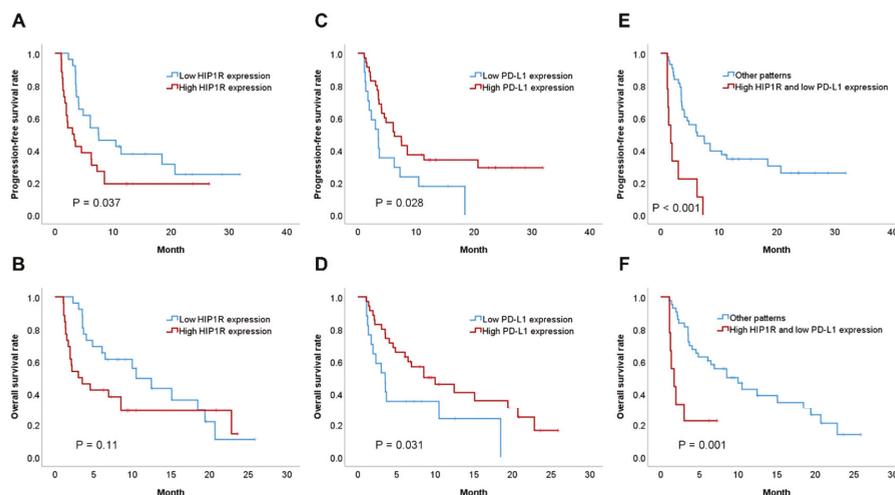
Figure 5. Comparison of survival rates according to HIP1R and PD-L1 expression. (**A**) Progression-free survival (PFS) and expression of HIP1R. (**B**) Overall survival (OS) and expression of HIP1R (**C**) PFS and PD-L1. (**D**) OS and PD-L1. (**E**) PFS, HIP1R, and PD-L1. (**F**) OS, HIP1R, and PD-L1.

Table 3. Univariate and multivariate analyses of progression-free survival.

Covariate	Univariate Analysis			Multivariate Analysis		
	HR	95% CI	*p*-Value [†]	HR	95% CI	*p*-Value [†]
Age (≥65 Years vs. <65 Years)	1.120	0.597–2.101	0.724			
Sex (Male vs. Female)	0.553	0.251–1.218	0.141			
Smoking History (+ vs. −)	1.121	0.517–2.429	0.773			
Presence of EGFR Mutation (+ vs. −)	1.603	0.482–5.329	0.441			
Type of PD-1 Blockade (Nivolumab vs. Pembrolizumab)	1.482	0.785–2.800	0.225			
PD-L1 (>50% vs. ≤50%)	0.489	0.254–0.942	0.032	0.432	0.222–0.844	0.014
HIP1R (>180 vs. ≤180)	1.935	1.027–3.648	0.041	2.098	1.136–4.133	0.019

[†] Cox proportional hazards regression model. Abbreviations: CI, confidence interval; EGFR, epidermal growth factor receptor; HIP1R, Huntingtin Interacting Protein 1 Related; HR, hazard ratio; PD-1, programmed cell death protein 1; PD-L1, programmed death-ligand 1.

We used a Kaplan Meier plotter tool and performed survival analysis according to HIP1R mRNA expression in lung adenocarcinoma and lung squamous cell carcinoma patients. The group with high HIP1R mRNA expression exhibited poorer OS in patients with adenocarcinoma ($p = 0.026$, Figure S4A). However, in lung squamous cell carcinoma, HIP1R mRNA expression was not correlated with OS ($p = 0.63$, Figure S4B)

4. Discussion

This study had several novel discoveries. First, we found that the expression of HIP1R was an independent predictive factor for anti-PD-1 treatment response by NSCLC patients. Second, the expression of HIP1R was an independent prognostic factor of PFS in patients treated with anti-PD-1 inhibitors. Third, GSEA revealed that *HIP1R* mRNA expression was tightly correlated with immune-related gene sets in lung adenocarcinoma. These GSEA results suggested that *HIP1R* mRNA expression plays an important role in regulating the expression of PD-L1.

GSEA revealed that low *HIP1R* mRNA expression was closely associated with allograft rejection, inflammatory responses, IL6-JAK-STAT3, IL2-STAT5, and interferon gamma response pathways in lung adenocarcinoma. PD-L1 expression is correlated with marked expression of adaptive immune responses (CD8+ T-cells) [21]. In our study, CD8 was also included in the core enrichment gene list of HALLMARK_ALLOGRAFT_REJECTION. Previous studies have also reported that the IL6-JAK-STAT3 pathway induces PD-L1 upregulation. IL-6 is positively correlated with PD-L1 expression in human hepatocellular carcinoma (HCC) cells, and IL-6 induces PD-L1 stability through glycosylation in a HCC cell line [22]. Glioblastoma-derived IL6 is required for up-regulation of myeloid PD-L1 in glioblastoma through a STAT3-dependent mechanism [23]. Combined blockade of IL6 and PD-L1 signaling achieves synergistic antitumor immune responses in colon carcinoma and murine melanoma models [24]. PD-L1 expression is also regulated by interferon gamma signaling in a melanoma cell line [25]. GSEA suggested that HIP1R expression plays an important role in adaptive immune responses associated with PD-L1.

In the present study, no correlation was identified between HIP1R and PD-L1 protein expression, However, HIP1R mRNA expression was negatively correlated with the mRNA expression level of PD-L1 in adenocarcinoma and squamous cell carcinoma. There are several possible explanations for this discrepancy. Post-transcriptional and post-translational modifications affect the level of protein expression [26]. Proteins can have significantly different half-lives in vivo [27]. There were no cases of surgery in our study, therefore the only sample we received was a biopsy. We cannot conduct additional experiments for mRNA testing of HIP1R and PD-L1, because very little tumor tissue remains in paraffin tissue.

Patients with high HIP1R mRNA expression exhibited poor clinical outcomes in web-based mRNA data of adenocarcinoma cases; however, HIP1R mRNA expression was not correlated with OS in squamous cell carcinoma. From our IHC data, HIP1R expression was correlated with poor clinical outcomes. However, we did perform subgroup analysis according to histologic type because of our small sample size. HIP1R levels also correlate with a set of genes that reflect PD-L1-related immune pathways in GSEA analysis of adenocarcinoma cases; however, there were no statistically significant immune-related gene sets associated with HIP1R mRNA expression in squamous cell carcinoma. Currently, lung adenocarcinoma and squamous cell carcinoma are known to involve different biologic mechanisms and prognoses. Therefore, the role of HIP1R in adaptive immune responses and its effect on clinical outcomes may vary depending on the histological type.

Despite some surprising discoveries, our study has certain limitations. First, our cohort was small. We performed multivariate logistic regression and prognostic analyses on only 52 samples. However, the web-based mRNA dataset also revealed results similar to ours. These results encourage further investigations involving larger populations. Second, we used an IHC method to detect HIP1R protein expression. There is no information regarding standardization, reliability, and reproducibility of IHC staining. We used the same antibody that Wang et al. used [12]. However, Wang et al. used HIP1R antibody (16814-1-AP) in Western Blott (WB) and immunofluorescence alone. Only recently has HIP1R attracted attention in cancer research, so few studies have been done on HIP1R. Therefore, there are no antibodies that are commonly used in immunohistochemistry. In the catalog of HIP1R antibody (16814-1-AP), it can be used in IHC, immunoprecipitation (IP), WB, and ELISA. According to the manufacturer's guidelines, this antibody was validated by western blot in HeLa cells and human liver tissue. We used a human placenta tissue as positive control as recommended. An automatic IHC staining

device (Benchmark XT) may improve the reproducibility of IHC staining. The H-scoring method is widely used for immunochemical staining, and is known to have relatively high reproducibility among pathologists [28,29]. Third, we examined the protein expression of HIP1R and PD-L1 in refractory advanced NSCLC; however, the mRNA profiles of HIP1R and PD-L1 were not evaluated. Because protein expression of HIP1R did not correlate with PD-L1 expression, the relationship between HIP1R and PD-L1 mRNA expression profile is very important. To verify the results of GSEA, we should evaluate the mRNA expression profiles of HIP1R. However, the sample we have is a small biopsy, and we have already performed several immunohistochemical stainings for diagnosis and ALK and EGFR mutation tests. Therefore, currently, very little tumor tissue remains in paraffin tissue and we cannot conduct additional experiments for mRNA testing. To confirm our experiments, future research should measure the mRNA expression level of HIP1R on many samples and investigate the relationship with the PD-1 blocker and PD-L1 expression.

In conclusion, we examined the expression of HIP1R in 52 refractory NSCLC samples from patients treated with PD-1 inhibitors. HIP1R expression was an independent biomarker predicting patient response to PD-1 inhibitors. High HIP1R expression was an independent predictor of poor PFS. In addition, HIP1R mRNA expression was significantly correlated with immune-related gene sets in lung adenocarcinoma. These immune-related gene sets are known to play important roles in PD-L1 regulation. Based on our findings, HIP1R expression may be a promising predictor for the therapeutic determination of responses to anti-PD-1 treatment.

References

1. Garon, E.B.; Rizvi, N.A.; Hui, R.; Leighl, N.; Balmanoukian, A.S.; Eder, J.P.; Patnaik, A.; Aggarwal, C.; Gubens, M.; Horn, L.; et al. Pembrolizumab for the treatment of nonsmall-cell lung cancer. *New Engl. J. Med.* **2015**, *372*, 2018–2028. [CrossRef] [PubMed]

2. Gettinger, S.; Rizvi, N.A.; Chow, L.Q.; Borghaei, H.; Brahmer, J.; Ready, N.; Gerber, D.E.; Shepherd, F.A.; Antonia, S.; Goldman, J.W.; et al. Nivolumab Monotherapy for First-Line Treatment of Advanced NonSmall-Cell Lung Cancer. *J. Clin. Oncol. Off. J. Am. Soc. Clin. Oncol.* **2016**, *34*, 2980–2987. [CrossRef] [PubMed]

3. Herbst, R.S.; Baas, P.; Kim, D.W.; Felip, E.; Perez-Gracia, J.L.; Han, J.Y.; Molina, J.; Kim, J.H.; Arvis, C.D.; Ahn, M.J.; et al. Pembrolizumab versus docetaxel for previously treated, PD-L1-positive, advanced nonsmall-cell lung cancer (KEYNOTE-010): A randomised controlled trial. *Lancet* **2016**, *387*, 1540–1550. [CrossRef]

4. Shukuya, T.; Carbone, D.P. Predictive Markers for the Efficacy of Anti-PD-1/PD-L1 Antibodies in Lung Cancer. *J. Thorac. Oncol. Off. Publ. Int. Assoc. Study Lung Cancer* **2016**, *11*, 976–988. [CrossRef] [PubMed]

5. Mezzadra, R.; Sun, C.; Jae, L.T.; Gomez-Eerland, R.; de Vries, E.; Wu, W.; Logtenberg, M.E.W.; Slagter, M.; Rozeman, E.A.; Hofland, I.; et al. Identification of CMTM6 and CMTM4 as PD-L1 protein regulators. *Nature* **2017**, *549*, 106–110. [CrossRef]

6. Koh, Y.W.; Han, J.H.; Haam, S.; Jung, J.; Lee, H.W. Increased CMTM6 can predict the clinical response to PD-1 inhibitors in nonsmall cell lung cancer patients. *Oncoimmunology* **2019**, *8*, e1629261. [CrossRef]

7. Meng, X.; Liu, X.; Guo, X.; Jiang, S.; Chen, T.; Hu, Z.; Liu, H.; Bai, Y.; Xue, M.; Hu, R.; et al. FBXO38 mediates PD-1 ubiquitination and regulates anti-tumour immunity of T cells. *Nature* **2018**, *564*, 130–135. [CrossRef]

8. Tsukita, Y.; Fujino, N.; Miyauchi, E.; Saito, R.; Fujishima, F.; Itakura, K.; Kyogoku, Y.; Okutomo, K.; Yamada, M.; Okazaki, T.; et al. Axl kinase drives immune checkpoint and chemokine signalling pathways in lung adenocarcinomas. *Mol. Cancer* **2019**, *18*, 24. [CrossRef]

9. Bauer, P.O.; Goswami, A.; Wong, H.K.; Okuno, M.; Kurosawa, M.; Yamada, M.; Miyazaki, H.; Matsumoto, G.; Kino, Y.; Nagai, Y.; et al. Harnessing chaperone-mediated autophagy for the selective degradation of mutant huntingtin protein. *Nat. Biotechnol.* **2010**, *28*, 256–263. [CrossRef]

10. Sakamoto, K.M.; Kim, K.B.; Kumagai, A.; Mercurio, F.; Crews, C.M.; Deshaies, R.J. Protacs: Chimeric molecules that target proteins to the Skp1-Cullin-F box complex for ubiquitination and degradation. *Proc. Natl. Acad. Sci. USA* **2001**, *98*, 8554–8559. [CrossRef]

11. Nabet, B.; Roberts, J.M.; Buckley, D.L.; Paulk, J.; Dastjerdi, S.; Yang, A.; Leggett, A.L.; Erb, M.A.; Lawlor, M.A.; Souza, A.; et al. The dTAG system for immediate and target-specific protein degradation. *Nat. Chem. Biol.* **2018**, *14*, 431–441. [CrossRef] [PubMed]

12. Wang, H.; Yao, H.; Li, C.; Shi, H.; Lan, J.; Li, Z.; Zhang, Y.; Liang, L.; Fang, J.Y.; Xu, J. HIP1R targets PD-L1 to lysosomal degradation to alter T cell-mediated cytotoxicity. *Nat. Chem. Biol.* **2019**, *15*, 42–50. [CrossRef] [PubMed]

13. Eisenhauer, E.A.; Therasse, P.; Bogaerts, J.; Schwartz, L.H.; Sargent, D.; Ford, R.; Dancey, J.; Arbuck, S.; Gwyther, S.; Mooney, M.; et al. New response evaluation criteria in solid tumours: Revised RECIST guideline (version 1.1). *Eur. J. Cancer* **2009**, *45*, 228–247. [CrossRef]

14. Travis, W.D.; Brambilla, E.; Nicholson, A.G.; Yatabe, Y.; Austin, J.H.; Beasley, M.B.; Chirieac, L.R.; Dacic, S.; Duhig, E.; Flieder, D.B.; et al. The 2015 World Health Organization Classification of Lung Tumors: Impact of Genetic, Clinical and Radiologic Advances Since the 2004 Classification. *J. Thorac. Oncol. Official Publ. Int. Assoc. Study Lung Cancer* **2015**, *10*, 1243–1260. [CrossRef] [PubMed]

15. McCarty, K.S., Jr.; Szabo, E.; Flowers, J.L.; Cox, E.B.; Leight, G.S.; Miller, L.; Konrath, J.; Soper, J.T.; Budwit, D.A.; Creasman, W.T.; et al. Use of a monoclonal anti-estrogen receptor antibody in the immunohistochemical evaluation of human tumors. *Cancer Res.* **1986**, *46*, 4244s–4248s.

16. Munari, E.; Rossi, G.; Zamboni, G.; Lunardi, G.; Marconi, M.; Sommaggio, M.; Netto, G.J.; Hoque, M.O.; Brunelli, M.; Martignoni, G.; et al. PD-L1 Assays 22C3 and SP263 are Not Interchangeable in NonSmall Cell Lung Cancer When Considering Clinically Relevant Cutoffs: An Interclone Evaluation by Differently Trained Pathologists. *Am. J. Surg. Pathol.* **2018**, *42*, 1384–1389. [CrossRef]

17. Büttner, R.; Gosney, J.R.; Skov, B.G.; Adam, J.; Motoi, N.; Bloom, K.J.; Dietel, M.; Longshore, J.W.; López-Ríos, F.; Penault-Llorca, F.; et al. Programmed Death-Ligand 1 Immunohistochemistry Testing: A Review of Analytical Assays and Clinical Implementation in NonSmall-Cell Lung Cancer. *J. Clin. Oncol. Off. J. Am. Soc. Clin. Oncol.* **2017**, *35*, 3867–3876. [CrossRef]

18. Cerami, E.; Gao, J.; Dogrusoz, U.; Gross, B.E.; Sumer, S.O.; Aksoy, B.A.; Jacobsen, A.; Byrne, C.J.; Heuer, M.L.; Larsson, E.; et al. The cBio cancer genomics portal: An open platform for exploring multidimensional cancer genomics data. *Cancer Discov.* **2012**, *2*, 401–404. [CrossRef]

19. Subramanian, A.; Tamayo, P.; Mootha, V.K.; Mukherjee, S.; Ebert, B.L.; Gillette, M.A.; Paulovich, A.; Pomeroy, S.L.; Golub, T.R.; Lander, E.S.; et al. Gene set enrichment analysis: A knowledge-based approach for interpreting genome-wide expression profiles. *Proc. Natl. Acad. Sci. USA* **2005**, *102*, 15545–15550. [CrossRef]

20. Gyorffy, B.; Surowiak, P.; Budczies, J.; Lanczky, A. Online survival analysis software to assess the prognostic value of biomarkers using transcriptomic data in nonsmall-cell lung cancer. *PLoS ONE* **2013**, *8*, e82241. [CrossRef]

21. Huang, C.Y.; Wang, Y.; Luo, G.Y.; Han, F.; Li, Y.Q.; Zhou, Z.G.; Xu, G.L. Relationship between PD-L1 Expression and CD8+ T-cell Immune Responses in Hepatocellular Carcinoma. *J. Immunother.* **2017**, *40*, 323–333. [CrossRef] [PubMed]

22. Chan, L.C.; Li, C.W.; Xia, W.; Hsu, J.M.; Lee, H.H.; Cha, J.H.; Wang, H.L.; Yang, W.H.; Yen, E.Y.; Chang, W.C.; et al. IL-6/JAK1 pathway drives PD-L1 Y112 phosphorylation to promote cancer immune evasion. *J. Clin. Investig.* **2019**, *129*, 3324–3338. [CrossRef] [PubMed]

23. Lamano, J.B.; Lamano, J.B.; Li, Y.D.; DiDomenico, J.D.; Choy, W.; Veliceasa, D.; Oyon, D.E.; Fakurnejad, S.; Ampie, L.; Kesavabhotla, K.; et al. Glioblastoma-Derived IL6 Induces Immunosuppressive Peripheral Myeloid Cell PD-L1 and Promotes Tumor Growth. *Clin. Cancer Res. Off. J. Am. Assoc. Cancer Res.* **2019**, *25*, 3643–3657. [CrossRef] [PubMed]

24. Tsukamoto, H.; Fujieda, K.; Miyashita, A.; Fukushima, S.; Ikeda, T.; Kubo, Y.; Senju, S.; Ihn, H.; Nishimura, Y.; Oshiumi, H. Combined Blockade of IL6 and PD-1/PD-L1 Signaling Abrogates Mutual Regulation of Their Immunosuppressive Effects in the Tumor Microenvironment. *Cancer Res.* **2018**, *78*, 5011–5022. [CrossRef]

25. Garcia-Diaz, A.; Shin, D.S.; Moreno, B.H.; Saco, J.; Escuin-Ordinas, H.; Rodriguez, G.A.; Zaretsky, J.M.; Sun, L.; Hugo, W.; Wang, X.; et al. Interferon Receptor Signaling Pathways Regulating PD-L1 and PD-L2 Expression. *Cell Rep.* **2017**, *19*, 1189–1201. [CrossRef]

26. Greenbaum, D.; Colangelo, C.; Williams, K.; Gerstein, M. Comparing protein abundance and mRNA expression levels on a genomic scale. *Genome Biol.* **2003**, *4*, 117. [CrossRef]

27. Nie, L.; Wu, G.; Zhang, W. Correlation of mRNA expression and protein abundance affected by multiple sequence features related to translational efficiency in Desulfovibrio vulgaris: A quantitative analysis. *Genetics* **2006**, *174*, 2229–2243. [CrossRef]

28. Aviles-Salas, A.; Muniz-Hernandez, S.; Maldonado-Martinez, H.A.; Chanona-Vilchis, J.G.; Ramirez-Tirado, L.A.; HernaNdez-Pedro, N.; Dorantes-Heredia, R.; Rui, Z.M.J.M.; Motola-Kuba, D.; Arrieta, O. Reproducibility of the EGFR immunohistochemistry scores for tumor samples from patients with advanced nonsmall cell lung cancer. *Oncol. Lett.* **2017**, *13*, 912–920. [CrossRef]

29. Detre, S.; Jotti, G.S.; Dowsett, M. A "quickscore" method for immunohistochemical semiquantitation: Validation for oestrogen receptor in breast carcinomas. *J. Clin. Pathol.* **1995**, *48*, 876–878. [CrossRef]

Article

Prognostic Value of Tumor Size in Resected Stage IIIA-N2 Non-Small-Cell Lung Cancer

Chih-Yu Chen [1,2], Bing-Ru Wu [1,2], Chia-Hung Chen [1,2], Wen-Chien Cheng [1,2], Wei-Chun Chen [1,3,4], Wei-Chih Liao [1,2,4,*], Chih-Yi Chen [5], Te-Chun Hsia [1,3,4] and Chih-Yen Tu [1,2]

[1] Division of Pulmonary and Critical Care Medicine, Department of Internal Medicine, China Medical University Hospital, Taichung 40447, Taiwan; cychen0808@gmail.com (C.-Y.C.); d18351@mail.cmuh.org.tw (B.-R.W.); d7996@mail.cmuh.org.tw (C.-H.C.); d14321@mail.cmuh.org.tw (W.-C.C.); d8040@mail.cmuh.org.tw (W.-C.C.); d1914@mail.cmuh.org.tw (T.-C.H.); d7855@mail.cmuh.org.tw (C.-Y.T.)
[2] School of Medicine, China Medical University, Taichung 40402, Taiwan
[3] Department of Respiratory Therapy, China Medical University, Taichung 40402, Taiwan
[4] Hyperbaric oxygen therapy center, China Medical University Hospital, Taichung 40447, Taiwan
[5] Department of Surgery, Chung Shan Medical University Hospital, Taichung 40201, Taiwan; cshy1566@csh.org.tw
* Correspondence: weichih.liao@gmail.com; Tel.: +886-4-2205-2121 (ext. 4661)

Abstract: The eighth edition of the American Joint Committee on Cancer (AJCC) staging system for lung cancer was introduced in 2017 and included major revisions, especially of stage III. For the subgroup stage IIIA-N2 non-small-cell lung cancer (NSCLC), surgical resection remains controversial due to heterogeneous disease entity. The aim of this study was to evaluate the clinicopathologic features and prognostic factors of patients with completely resected stage IIIA-N2 NSCLC. We retrospectively evaluated 77 consecutive patients with pathologic stage IIIA-N2 NSCLC (AJCC eighth edition) who underwent surgical resection with curative intent in China Medical University Hospital between 2006 and 2014. Survival analysis was conducted, using the Kaplan–Meier method. Prognostic factors predicting overall survival (OS) and disease-free survival (DFS) were analyzed, using log-rank tests and multivariate Cox proportional hazards models. Of the 77 patients with pathologic stage IIIA-N2 NSCLC examined, 35 (45.5%) were diagnosed before surgery and 42 (54.5%) were diagnosed unexpectedly during surgery. The mean age of patients was 59 years, and the mean length of follow-up was 38.1 months. The overall one-, three-, and five-year OS rates were 91.9%, 61.3%, and 33.5%, respectively. Multivariate analysis showed that tumor size <3 cm (hazards ratio (HR): 0.373, $p = 0.003$) and video-assisted thoracoscopic surgery (VATS) approach (HR: 0.383, $p = 0.014$) were significant predictors for improved OS. For patients with surgically treated, pathologic stage IIIA-N2 NSCLC, tumor size <3 cm and the VATS approach seemed to be associated with better prognosis.

Keywords: non-small-cell lung cancer; stage IIIA-N2; surgery

1. Introduction

Lung cancer is the most commonly diagnosed cancer and the leading cause of cancer death in the world. In 2018, an estimated 2.1 million new cases (1,368,524 in men and 725,352 in women) of lung and bronchial cancer were diagnosed, and 1.8 million individuals (1,184,947 in men and 576,060 in women) were expected to die of the tumor [1]. Despite recent advances in molecularly targeted therapy and immunotherapy, the long-term survival of patients with lung cancer remains poor, and the five-year-survival rate is below 20% [2,3]. While more than 80% of tumors were unresectable, surgical resection is the major treatment modality for curative intent, with the five-year survival rate being about 60% [4].

The most important prognostic factor for lung cancer is the stage at presentation, which also guides the clinical management of these patients. Based on a global database of lung-cancer cases assembled by the International Association for the Study of Lung Cancer (IASLC) [5], the eighth edition of the American Joint Committee on Cancer (AJCC) staging system for lung cancer was published in 2017 [6], and it was implemented in clinical practice worldwide in 2018 [7]. In addition to the reclassification of extra-thoracic disease into M1b and M1c, the most significant change distinguishing the eighth edition from the seventh edition is the modification of T classification, which may result in different stage allocations. In the eighth edition, stages T1–T4 are redefined according to tumor size (T1a ≤ 1 cm; 1 cm < T1b < 2 cm; 2 cm < T1c < 3 cm; 3 cm < T2a < 4 cm; 4 cm < T2b < 5 cm; 5 cm < T3 < 7 cm; T4 > 7 cm). For patients with former stage IIIA-N2 disease, the reclassification of tumor size more than 5 cm shifting from T2b to T3 (> 5 cm but < 7 cm) and from T3 to T4 (> 7 cm) results in a change of stage from IIIA to IIIB.

Due to heterogeneous disease entity, the role of surgical resection for patients with former stage IIIA-N2 non-small-cell lung cancer (NSCLC) remains controversial. According to the guidelines [7,8], multidisciplinary team assessment prior to treatment is warranted to evaluate the resectability, depending on single N2 lymph node station involvement and/or small lymph node size (<3 cm). The treatment options include resection, followed by adjuvant chemotherapy; induction therapy, followed by surgery; definitive concurrent chemoradiation; and consolidation therapy with Durvalumab. However, despite the complexity in treatment planning and major changes in T description and stage allocation of the eighth edition, the guidelines do not address the consequent changes to treatment algorithms for patients with clinical stage IIIA-N2 NSCLC. Furthermore, the role of surgical resection with curative intent in such patients has not been well evaluated. Hence, the aim of this study was to evaluate the clinical features and surgical–pathological factors that affect the prognosis of patients with resected stage IIIA-N2 NSCLC.

2. Materials and Methods

This study was approved by the Institutional Review Board of China Medical University Hospital (CMUH109-REC1-037, date of approval: 11 March 2020), and informed consent was waived because of the retrospective nature of the study.

2.1. Inclusion Criteria

From 1 January 2006 to 31 December 2014, 748 patients with lung cancer underwent surgical resection with mediastinal lymph node dissection or sampling at China Medical University Hospital. The tumor-node-metastasis (TNM) staging system was reclassified according to the eighth edition of the AJCC staging system. A total of 77 (10.3%) patients with stage IIIA-N2 NSCLC who underwent surgical resection with curative intent were enrolled in the study. Smoking status was classified as ever (including current and former smoker) or never smoker. Family history of cancer was defined as any first-degree relative diagnosed with any form of cancer. The preoperative staging workup included complete blood count, serum biochemistry, carcinoembryonic antigen (CEA), chest radiography, chest computed tomography (CT) scan, bronchoscopy, and nuclear medicine exam. Patients with positive surgical tumor margin and incomplete medical record were excluded. There were weekly multidisciplinary lung cancer meetings where thoracic radiologists, radiation oncologist, surgeons, and pulmonologists from the China Medical University Hospital jointly reviewed and discussed the management plan of patients with lung cancer.

2.2. Surgical Technique

Only patients having the Eastern Cooperative Oncology Group (ECOG) performance of 0 or 1 were considered as surgical candidates, and all surgery was performed with curative intent. All patients underwent surgery either with preoperatively clinical N2 disease or unexpectedly during surgery. Tumor location was analyzed as dichotomous variables (lower versus upper or middle lobes; peripheral

(outer one-third of lung field) versus central (inner two-thirds of lung fields)). Induction therapy was defined as preoperative chemotherapy and/or radiotherapy. Adjuvant therapy was defined as treatment with either chemotherapy, radiotherapy, or a combination of both after surgical resection. The type of surgery included standard (pneumonectomy, bilobectomy, or lobectomy) and limited resection (wedge resection or segmentectomy). Mediastinal lymph node dissection or sampling with a minimum of three different stations was performed according to the surgeon's experience, and all resected lymph nodes were labeled separately. All pulmonary resections were performed either through open thoracotomy or video-assisted thoracoscopic surgery (VATS).

2.3. Histopathological Evaluation

All surgical specimens were evaluated for pathologic staging. Histological typing was performed according to the World Health Organization classification. The recorded variables included tumor size, differentiation grade, visceral pleural involvement, lymphovascular permeation, perineural invasion, multiple N2 station, and N2 ratio. Multiple N2 station was defined as lymph node metastasis involving more than one N2 station. N2 ratio was calculated by dividing the total number of metastatic by the total number of N2 lymph nodes examined.

2.4. Statistical Analysis

All statistical analyses were performed by using MedCalc Statistical Software version 19.0.7 (MedCalc Software bvba, Ostend, Belgium; https://www.medcalc.org; 2019). Normally and non-normally distributed continuous data were expressed as mean (standard deviation (SD)) and median (interquartile range (IQR)), respectively. Categorical variables were reported as number (%). Overall survival (OS) was defined as the time from the date of pathological diagnosis until the date of death or last follow-up. Disease-free survival (DFS) was defined as the time from the date of pathological diagnosis until the date of recurrence, death, or last follow-up. Survival curves were estimated by using the Kaplan–Meier method. The prognostic factor analyses were performed by log-rank tests and Cox proportional-hazards regression model. Statistical analysis was considered to be significant when the *p*-value was < 0.05.

3. Results

3.1. Demographic and Clinicopathologic Characteristics

Of the 77 patients with pathologic stage IIIA-N2 NSCLC, 35 were male, and 42 were female, with a mean age of 59 years (SD, 12.2 years; range, 34 to 82 years). Thirty-five (45.5%) patients were diagnosed as N2 disease before surgery, and 42 (54.5%) were diagnosed unexpectedly during surgery. Forty-one (53.2%) patients underwent VATS, and 36 (46.8%) underwent open thoracotomy. The most common histology was adenocarcinoma (62, 80.5%), followed by squamous cell carcinoma (9, 11.7%). The mean size of tumor was 2.9 cm (SD, 1.0 cm). Forty-five (58.4%) patients had tumors of 3 cm or less in diameter, and 32 (41.6%) patients had tumors greater than 3 cm. With respect to lymph node involvement, multiple N2 station was seen in 21 (27.3%) patients and median N2 ratio was 33.3% (IQR, 13.8–50%). Sixty-five (84.4%) patients received adjuvant chemotherapy, of which 23 patients received postoperative radiotherapy. Demographic and clinicopathologic characteristics of the patients are shown in Table 1.

Table 1. Demographic and clinicopathologic characteristics of 77 patients with resected stage IIIA-N2 non-small-cell lung cancer.

Parameter	Value
Age, Mean (SD), y	59 (12.2)
Male, No. (%)	35 (45.5)
Ever smoker, No. (%)	29 (37.7)
Family History of Cancer, No. (%)	14 (18.2)
Comorbidities, No. (%)	
Hypertension	24 (31.2)
Cardiovascular Disease	8 (10.4)
Chronic Obstructive Pulmonary DiseaseLiver Disease	6 (7.8)
Chronic Kidney Disease	6 (7.8)
Diabetes Mellitus	4 (5.2)
	10 (13.0)
Performance status, No. (%)	
ECOG 0	39 (50.6)
ECOG 1	38 (49.4)
Clinical N2, No. (%)	35 (45.5)
Surgical Procedure, No. (%)	
Limited Resection	8 (10.4)
Standard Resection	69 (89.6)
Surgical Approach, No. (%)	
VATS	41 (53.2)
Open Thoracotomy	36 (46.8)
Tumor size, mean (SD), cm	2.9 (1.0)
Tumor Size, No. (%)	
≤3 cm	45 (58.4)
3–5 cm	32 (41.6)
Histology, No. (%)	
Adenocarcinoma	62 (80.5)
Squamous Cell Carcinoma	9 (11.7)
Others	6 (7.8)
Differentiation, No. (%)	
Well–moderate	48 (62.3)
Poor	27 (35.1)
Unknown	2 (2.6)
CEA, Median (IQR), ng/mL	4.0 (2.3–13.1)
Visceral Pleural Involvement, No. (%)	35 (45.5)
Lymphovascular Permeation, No. (%)	66 (85.7)
Perineural Invasion, No. (%)	12 (15.6)
Number of Examined Lymph Nodes, Median (IQR)	14 (9–20)
Number of Positive Lymph Nodes, Median (IQR)	3 (1–6)
N2 Ratio, Median (IQR), %	33.3 (13.8–50.0)
Tumor Location, No. (%)	
Central Location	44 (57.1)
Lower Lobe Location	31 (40.3)
Multiple N2 Station, No. (%)	21 (27.3)
Induction therapy, No. (%)	10 (13.0)
Adjuvant Therapy, No. (%)	65 (84.4)
Postoperative Radiotherapy, No. (%)	23 (29.9)

SD, standard deviation; IQR, interquartile range; ECOG, Eastern Cooperative Oncology Group; VATS, video-assisted thoracoscopic surgery; CEA, carcinoembryonic antigen; y, years.

3.2. Overall Survival

Figure 1 depicts that the one-, three-, and five-year OS rates were 91.9%, 61.3%, and 33.5%, respectively. The mean length of follow-up was 38.1 months.
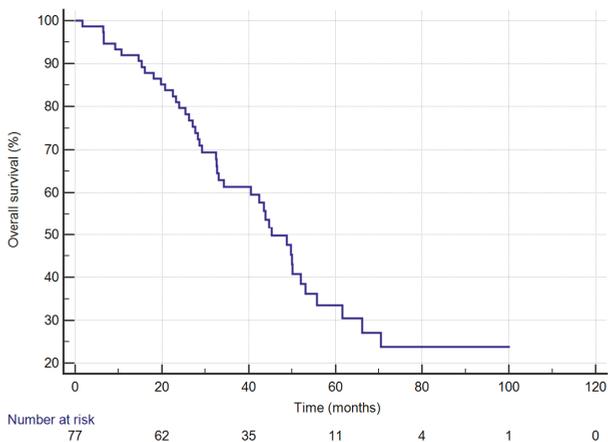
Figure 1. Overall-survival curves of 77 patients with completely resected stage IIIA-N2 non-small-cell lung cancer.

In univariate analysis, the median OS was significantly influenced by tumor size. The median OS was 52.0 months (95% CI: 45.3–66.1) in patients with tumors of 3 cm or less, worsening to 32.6 months (95% CI: 23.2–43.6) in patients with tumors greater than 3 cm (log-rank $p = 0.002$) and corresponding to a five-year OS rate of 43.3% and 21.7%, respectively (Figure 2). Moreover, patients with VATS approach had significantly better OS compared with those who received open thoracotomy (five-year OS: 63.5% vs. 18.3%; log-rank $p = 0.009$). On the other hand, OS rates were significantly worse in patients with elder age (versus those with age under 65 years, five-year OS: 24.2% vs. 39.0%; log-rank $p = 0.031$) and those with ECOG 1 (versus those with ECOG 0, 5-year OS: 19.3% vs. 49.4%; log-rank $p = 0.016$).
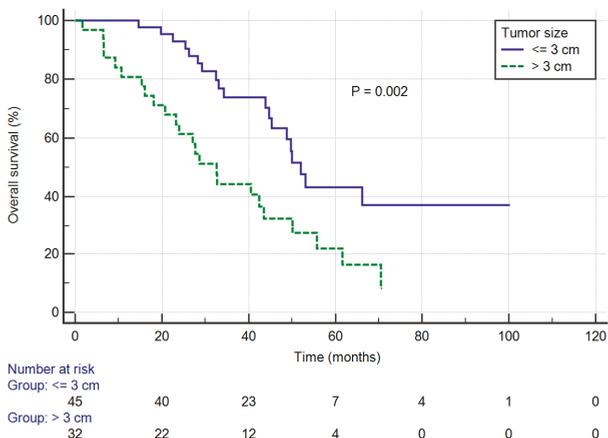
Figure 2. Overall survival curves of patients stratified by tumor size.

Multivariate analysis showed that tumor size <3 cm (HR: 0.373, 95% CI: 0.194–0.714, $p = 0.003$) and VATS approach (HR: 0.383, 95% CI: 0.178–0.824, $p = 0.014$) were significant predictors for OS. Univariate and multivariate data are shown in Tables 2 and 3.

Table 2. Univariate analysis of factors associated with overall survival.

Parameter	Hazard Ratio (95% CI)	*p*-Value
Age (≥65 y versus <65)	1.939 (1.050–3.582)	0.034
Gender (Male versus Female)	1.084 (0.582–2.020)	0.799
Ever Smoker (Yes versus No)	0.987 (0.526–1.851)	0.967
Family History of Cancer (Yes versus No)	0.681 (0.302–1.532)	0.352
Hypertension (Yes versus No)	0.630 (0.310–1.279)	0.201
Cardiovascular Disease (Yes versus No)	0.523 (0.161–1.692)	0.279
Chronic Obstructive Pulmonary Disease (Yes versus No)	2.094 (0.741–5.916)	0.163
Liver Disease (Yes versus No)	1.662 (0.698–3.960)	0.251
Chronic Kidney Disease (Yes versus No)	0.395 (0.054–2.877)	0.359
Diabetes Mellitus (Yes versus No)	1.040 (0.438–2.469)	0.930
Performance Status (ECOG 1 versus ECOG 0)	2.093 (1.133–3.867)	0.018
Clinical N2 (Yes versus Unsuspected)	0.963 (0.525–1.767)	0.903
Limited Resection (Yes versus Anatomical)	1.453 (0.612–3.449)	0.397
VATS (Yes versus Open Thoracotomy)	0.429 (0.223–0.824)	0.011
Tumor Size (≤3 versus 3–5)	0.390 (0.213–0.715)	0.002
Histology (Adenocarcinoma versus Others)	1.442 (0.689–3.018)	0.332
Differentiation (Poor versus Others)	0.618 (0.311–1.226)	0.168
CEA (≥3 versus <3)	1.593 (0.729–3.482)	0.243
Visceral Pleural Involvement (Yes versus No)	1.359 (0.743–2.486)	0.319
Lymphovascular Permeation (Yes versus No)	1.314 (0.513–3.352)	0.567
Perineural Invasion (Yes versus No)	0.483 (0.173–1.354)	0.166
N2 Ratio (≥40% versus <40%)	1.167 (0.632–2.154)	0.622
Central Location (Yes versus Peripheral)	1.061 (0.576–1.955)	0.848
Lower Lobe Location (Yes versus Upper or Middle)	1.408 (0.757–2.619)	0.280
Multiple N2 Station (Yes versus No)	1.056 (0.550–2.028)	0.870
Induction Therapy (Yes versus No)	0.793 (0.281–2.236)	0.660
Adjuvant Therapy (Yes versus No)	1.147 (0.483–2.725)	0.756
Postoperative Radiotherapy (Yes versus No)	0.551 (0.263–1.151)	0.113

Variables with *p*-values of less than 0.2 were tested in multivariate analysis. CI, confidence interval; ECOG, Eastern Cooperative Oncology Group; VATS, video-assisted thoracoscopic surgery; CEA, carcinoembryonic antigen.

Table 3. Multivariate analysis of factors associated with overall survival.

Parameter	Hazard Ratio (95% CI)	*p*-Value
Age (≥65 y versus <65)	1.576 (0.799–3.111)	0.190
Performance Status (ECOG 1 versus ECOG 0)	1.669 (0.878–3.173)	0.118
VATS (Yes versus Open Thoracotomy)	0.383 (0.178–0.824)	0.014
Tumor Size (≤3 versus 3–5)	0.373 (0.194–0.714)	0.003
Differentiation (Poor versus Others)	0.732 (0.358–1.499)	0.394
Perineural Invasion (Yes versus No)	0.681 (0.229–2.023)	0.489
Postoperative Radiotherapy (Yes versus No)	1.173 (0.501–2.745)	0.713

CI, confidence interval; ECOG, Eastern Cooperative Oncology Group; VATS, video-assisted thoracoscopic surgery.

3.3. Disease-Free Survival

The one-, three-, and five-year DFS rates were 53.4%, 24.5%, and 12.5%, respectively.

In univariate analysis, the median DFS was significantly influenced by tumor size. The median DFS was 18.4 months (95% CI: 11.9–33.6) in patients with tumors of 3 cm or less, worsening to 11.0 months (95% CI: 7.1–15.6) in patients with tumors greater than 3 cm (log-rank *p* = 0.016) and corresponding to a three-year DFS rate of 33.4% and 12.5%, respectively (Supplementary Materials Figure S1). There was a non-significant trend between poor prognosis and both clinical N2 disease (versus unsuspected N2 disease, three-year DFS: 16.2% vs. 31.1%; log-rank *p* = 0.077) and elevated CEA level (versus CEA level less than 3 ng/mL, three-year DFS: 18.2% vs. 33.3%; log-rank *p* = 0.053).

Multivariate analysis showed that tumor size <3 cm (HR: 0.451, 95% CI: 0.235–0.865, *p* = 0.017) and clinical N2 versus unsuspected N2 disease (HR: 2.525, 95% CI: 1.340–4.757, *p* = 0.004) were significant

predictors for DFS. Both univariate and multivariate data are shown in Supplementary Materials Tables S1 and S2.

4. Discussion

The AJCC TNM staging system is the global standard for lung cancer staging [8]. Compared with the seventh edition, the eighth edition has been validated in several cohorts [9,10], demonstrating better survival stratification and prognosis prediction. With regard to the major changes in the T classification, former stage IIIA-N2 disease is further separated into stage IIIA and IIIB, based on tumor size, which is suggestive of distinct prognosis between the two subgroups. Sui et al. [9] retrospectively analyzed a Chinese cohort including 3599 patients with pathological stage IA to IIIA between 2005 and 2012. Of 772 former stage IIIA patients, stage migration to IIIB was found in 180 (23.3%) patients, and associated with lower five-year survival rate (26.1% vs. 41.7%, *p* < 0.001). Therefore, we focused on updated stage IIIA-N2 NSCLC, which represents a heterogenic group of patients and complex treatment modalities, including surgical resection.

The role of surgical resection for patients with stage IIIA-N2 NSCLC remains controversial, with different management preferences between Europe and America [11]. In Europe, surgeons tend to perform upfront resection, without induction therapy, for single-station, non-bulky N2 disease. The European Society for Medical Oncology (ESMO) guideline recommends that surgical resection, followed by adjuvant chemotherapy, is a reasonable treatment option for single-station N2 disease [8]. By contrast, in America, the standard treatment has been induction chemotherapy or chemoradiation, followed by surgical resection. A Cardiothoracic Surgery Network survey [12] demonstrated that more than 80% of thoracic surgeon preferred induction therapy for stage IIIA-N2 NSCLC, whereas only 12% preferred surgical resection followed by adjuvant therapy. For macroscopic single station N2 disease, 62% would consider surgical resection only if N2 clearance was achieved, whereas 18% considered this inoperable and offer definitive concurrent chemoradiation. Regarding the preference of induction therapy followed by surgical resection in America, considerations include better tolerance to full-dose chemotherapy preoperatively, better control of the systemic micro-metastases, assessment of treatment response before decision of surgery, and possible parenchymal sparing surgery [13]. Therefore, the approach of induction therapy is supported by the National Comprehensive Cancer Center Network (NCCN) guideline [7]. However, despite the high agreement and guideline recommendation, substantial variation in clinical practice existed in The Society of Thoracic Surgeons General Thoracic Surgery Database [14]. Of 3319 clinical stage III-N2 patients, 54% received direct surgical resection and 46% received induction therapy, with five-year survival rates of 36% and 35%, respectively. Considering the controversial role of surgical resection for patients with updated stage IIIA-N2 NSCLC, our study was aimed to investigate prognostic factors to guide therapeutic decisions.

For former stage IIIA-N2 NSCLC, previous studies have well demonstrated prognostic factors, including number of positive lymph nodes [15], microscopic N2 [16], single-station N2 [17–20], VATS approach [21], lobectomy approach [22], postoperative radiotherapy [23,24], and pathological response after induction therapy [25,26]. However, there is still some concern about changes of T classification and stage migration in the eighth edition. In the study, we presented a single-center retrospective study of 77 surgically resected IIIA-N2 NSCLC patients, staged according to the eighth edition of the AJCC staging system. Our first finding is that tumor size <3 cm was associated with better prognosis (HR: 0.373, *p* = 0.003). The possible reason is that tumor size was correlated with occult systemic micro-metastases. Yang et al. [27] reported that the proportions of cases with N0M0 status with tumor size <2 cm and >7 cm were 70.79% and 33.33%, respectively. Cho et al. [28] analyzed the data of 1821 patients with clinical N0-1 NSCLC, in which they found that tumor size >3 cm was a common predictor for unsuspected N2 and multiple-station N2 disease. Based on our finding and major changes of T classification, further large-scale studies are warranted to confirm the role of tumor size in patient selection and treatment strategy. Our second finding is that VATS approach was associated with better prognosis (HR: 0.383, *p* = 0.014). Previous studies showed similar results [21,26]. Despite the possible

selection bias of our study, the consistency of these findings suggests that the VATS approach can be employed safely, without compromised prognosis.

Our 33.5% five-year OS rate is slightly lower than that of the IASLC database [5], in which the five-year OS rates for clinical and pathological stage IIIA disease are 36% and 41%, respectively. The relatively poorer prognosis in our patients highlights the importance of patient selection and the multimodality treatment approach. First, in patients with stage IIIA-N2 NSCLC undergoing surgical resection, the prognostic value of degree of lymph node involvement has been well documented. The ESMO guideline [8] highlights that single-station N2 disease is the most important features while evaluating resectability. Several studies [17–20] have also demonstrated that multiple-station N2 involvement indicates a poorer prognosis, regardless of whether the induction therapy is given: five-year OS rate is usually below 25%. Given the poorer prognosis and higher risk of systemic micro-metastases, upfront surgical resection should be avoided in patients with multiple-station N2 disease. However, in our study, 21 (27.3%) patients with multiple-station N2 disease received surgical resection, whereas only 10 (13%) patients received induction therapy. Second, regardless of whether to offer surgical resection, the implementation of multimodality treatment is of most importance [7,8]. There is pooled evidence in a network meta-analysis [29] where patients with stage IIIA-N2 NSCLC treated with single modality treatment of either surgery or radiotherapy alone seemed to have the worst outcomes. Nevertheless, in our study, 12 (15.6%) patients received surgical resection, only without adjuvant therapy. The lack of multimodality treatment would also explain the poorer outcome of the study.

Our study has some limitations. First, given the nature of retrospective analysis, patients in our study were highly selected by multidisciplinary team screening and not representative of all patients with stage IIIA-N2 NSCLC. In addition, it is not possible to answer the question whether upfront surgical resection is superior to other multimodality approaches. Second, the number of cases in our study was small. The uneven distribution of clinicopathologic characteristics (e.g., single- or multiple-station N2) and treatment approaches (e.g., induction therapy) complicated the interpretation, and the statistical power could be limited.

5. Conclusions

In conclusion, we retrospectively reviewed the clinical and pathological characteristics of patients with completely resected stage IIIA-N2 NSCLC, according to the eighth edition of the AJCC staging system. Tumor size <3 cm was the only independent factor for better OS and DFS. In addition, the VATS approach was also a good prognostic factor regarding OS rate. These findings may be helpful to identify patients with stage IIIA-N2 NSCLC eligible to surgical resection.

Author Contributions: Conceptualization, Chih-Yu Chen; Data curation, Wen-Chien Cheng and Wei-Chun Chen; Formal analysis, B.-R.W. and C.-H.C.; Methodology, C-H.C.; Software, Chih-Yu Chen; Supervision, T.-C.H. and C.-Y.T.; Validation, Chih-Yi Chen; Visualization, C-H.C.; Writing—original draft, Chih-Yu Chen; Writing—review & editing, W.-C.L. All authors have read and agreed to the published version of the manuscript.

References

1. Bray, F.; Ferlay, J.; Soerjomataram, I.; Siegel, R.L.; Torre, L.A.; Jemal, A. Global cancer statistics 2018: GLOBOCAN estimates of incidence and mortality worldwide for 36 cancers in 185 countries. *CA Cancer J. Clin.* **2018**, *68*, 394–424. [CrossRef] [PubMed]

2. Wang, B.Y.; Huang, J.Y.; Cheng, C.Y.; Lin, C.H.; Ko, J.; Liaw, Y.P. Lung cancer and prognosis in taiwan: A population-based cancer registry. *J. Thorac. Oncol.* **2013**, *8*, 1128–1135. [CrossRef] [PubMed]

3. Howlader, N.; Noone, A.; Krapcho, M.; Miller, D.; Brest, A.; Yu, M.; Ruhl, J.; Tatalovich, Z.; Mariotto, A.; Lewis, D.J.N.C.I. *SEER Cancer Statistics Review, 1975–2016*; National Cancer Institute: Bethesda, MD, USA, 2019.

4. Goya, T.; Asamura, H.; Yoshimura, H.; Kato, H.; Shimokata, K.; Tsuchiya, R.; Sohara, Y.; Miya, T.; Miyaoka, E. Prognosis of 6644 resected non-small cell lung cancers in Japan: A Japanese lung cancer registry study. *Lung Cancer* **2005**, *50*, 227–234. [CrossRef] [PubMed]

5. Goldstraw, P.; Chansky, K.; Crowley, J.; Rami-Porta, R.; Asamura, H.; Eberhardt, W.E.; Nicholson, A.G.; Groome, P.; Mitchell, A.; Bolejack, V. The IASLC Lung Cancer Staging Project: Proposals for Revision of the TNM Stage Groupings in the Forthcoming (Eighth) Edition of the TNM Classification for Lung Cancer. *J. Thorac. Oncol.* **2016**, *11*, 39–51. [CrossRef]

6. Detterbeck, F.C.; Boffa, D.J.; Kim, A.W.; Tanoue, L.T. The Eighth Edition Lung Cancer Stage Classification. *Chest* **2017**, *151*, 193–203. [CrossRef]

7. Ettinger, D.S.; Aisner, D.L.; Wood, D.E.; Akerley, W.; Bauman, J.; Chang, J.Y.; Chirieac, L.R.; D'Amico, T.A.; Dilling, T.J.; Dobelbower, M.; et al. NCCN Guidelines Insights: Non-Small Cell Lung Cancer, Version 5.2018. *J. Natl. Compr. Canc. Netw.* **2018**, *16*, 807–821. [CrossRef]

8. Postmus, P.E.; Kerr, K.M.; Oudkerk, M.; Senan, S.; Waller, D.A.; Vansteenkiste, J.; Escriu, C.; Peters, S. Early and locally advanced non-small-cell lung cancer (NSCLC): ESMO Clinical Practice Guidelines for diagnosis, treatment and follow-up. *Ann. Oncol.* **2017**, *28*, 1–21. [CrossRef]

9. Sui, X.; Jiang, W.; Chen, H.; Yang, F.; Wang, J.; Wang, Q. Validation of the Stage Groupings in the Eighth Edition of the TNM Classification for Lung Cancer. *J. Thorac. Oncol.* **2017**, *12*, 1679–1686. [CrossRef]

10. Yang, L.; Wang, S.; Zhou, Y.; Lai, S.; Xiao, G.; Gazdar, A.; Xie, Y. Evaluation of the 7(th) and 8(th) editions of the AJCC/UICC TNM staging systems for lung cancer in a large North American cohort. *Oncotarget* **2017**, *8*, 66784–66795. [CrossRef]

11. Rocco, G.; Nason, K.; Brunelli, A.; Varela, G.; Waddell, T.; Jones, D.R. Management of stage IIIA (N2) non-small cell lung cancer: A transatlantic perspective. *J. Thorac. Cardiovasc. Surg.* **2016**, *151*, 1235–1238. [CrossRef]

12. Veeramachaneni, N.K.; Feins, R.H.; Stephenson, B.J.; Edwards, L.J.; Fernandez, F.G. Management of stage IIIA non-small cell lung cancer by thoracic surgeons in North America. *Ann. Thorac. Surg.* **2012**, *94*, 922–926, discussion 926–928. [CrossRef] [PubMed]

13. Mehran, R. The role of surgery in patients with clinical n2 disease. *Thorac. Surg. Clin.* **2013**, *23*, 327–335. [CrossRef] [PubMed]

14. Boffa, D.; Fernandez, F.G.; Kim, S.; Kosinski, A.; Onaitis, M.W.; Cowper, P.; Jacobs, J.P.; Wright, C.D.; Putnam, J.B.; Furnary, A.P. Surgically Managed Clinical Stage IIIA-Clinical N2 Lung Cancer in The Society of Thoracic Surgeons Database. *Ann. Thorac. Surg.* **2017**, *104*, 395–403. [CrossRef] [PubMed]

15. Yoo, C.; Yoon, S.; Lee, D.H.; Park, S.I.; Kim, D.K.; Kim, Y.H.; Kim, H.R.; Choi, S.H.; Kim, W.S.; Choi, C.M.; et al. Prognostic Significance of the Number of Metastatic pN2 Lymph Nodes in Stage IIIA-N2 Non-Small-Cell Lung Cancer After Curative Resection. *Clin. Lung Cancer* **2015**, *16*, 203–212. [CrossRef] [PubMed]

16. Garelli, E.; Renaud, S.; Falcoz, P.-E.; Weingertner, N.; Olland, A.; Santelmo, N.; Massard, G. Microscopic N2 disease exhibits a better prognosis in resected non-small-cell lung cancer. *Eur. J. Cardiothorac. Surg.* **2016**, *50*, 322–328. [CrossRef]

17. Cerfolio, R.J.; Bryant, A.S. Survival of patients with unsuspected N2 (stage IIIA) nonsmall-cell lung cancer. *Ann. Thorac. Surg.* **2008**, *86*, 362–366, discussion 366–367. [CrossRef]

18. Decaluwe, H.; De Leyn, P.; Vansteenkiste, J.; Dooms, C.; Van Raemdonck, D.; Nafteux, P.; Coosemans, W.; Lerut, T. Surgical multimodality treatment for baseline resectable stage IIIA-N2 non-small cell lung cancer. Degree of mediastinal lymph node involvement and impact on survival. *Eur. J. Cardiothorac. Surg.* **2009**, *36*, 433–439. [CrossRef]

19. Yoshino, I.; Yoshida, S.; Miyaoka, E.; Asamura, H.; Nomori, H.; Fujii, Y.; Nakanishi, Y.; Eguchi, K.; Mori, M.; Sawabata, N.; et al. Surgical outcome of stage IIIA- cN2/pN2 non-small-cell lung cancer patients in Japanese lung cancer registry study in 2004. *J. Thorac. Oncol.* **2012**, *7*, 850–855. [CrossRef]

20. Tsitsias, T.; Boulemden, A.; Ang, K.; Nakas, A.; Waller, D.A. The N2 paradox: Similar outcomes of pre- and postoperatively identified single-zone N2a positive non-small-cell lung cancer. *Eur. J. Cardiothorac. Surg.* **2014**, *45*, 882–887. [CrossRef]

21. Wang, S.; Zhou, W.; Zhang, H.; Zhao, M.; Chen, X. Feasibility and long-term efficacy of video-assisted thoracic surgery for unexpected pathologic N2 disease in non-small cell lung cancer. *Ann. Thorac. Med.* **2013**, *8*, 170–175. [CrossRef]

22. Jimenez, M.F.; Varela, G.; Novoa, N.M.; Aranda, J.L. Results of surgery for non-small cell lung cancer with N2 involvement unsuspected before thoracotomy. *Arch. Bronconeumol.* **2008**, *44*, 65–69. [CrossRef]

23. Robinson, C.G.; Patel, A.P.; Bradley, J.D.; DeWees, T.; Waqar, S.N.; Morgensztern, D.; Baggstrom, M.Q.; Govindan, R.; Bell, J.M.; Guthrie, T.J.; et al. Postoperative radiotherapy for pathologic N2 non-small-cell lung cancer treated with adjuvant chemotherapy: A review of the National Cancer Data Base. *J. Clin. Oncol.* **2015**, *33*, 870–876. [CrossRef] [PubMed]

24. Yang, C.F.; Kumar, A.; Gulack, B.C.; Mulvihill, M.S.; Hartwig, M.G.; Wang, X.; D'Amico, T.A.; Berry, M.F. Long-term outcomes after lobectomy for non-small cell lung cancer when unsuspected pN2 disease is found: A National Cancer Data Base analysis. *J. Thorac. Cardiovasc. Surg.* **2016**, *151*, 1380–1388. [CrossRef]

25. Cerfolio, R.J.; Maniscalco, L.; Bryant, A.S. The treatment of patients with stage IIIA non-small cell lung cancer from N2 disease: Who returns to the surgical arena and who survives. *Ann. Thorac. Surg.* **2008**, *86*, 912–920, discussion 912–920. [CrossRef] [PubMed]

26. Yang, C.F.; Adil, S.M.; Anderson, K.L.; Meyerhoff, R.R.; Turley, R.S.; Hartwig, M.G.; Harpole, D.H., Jr.; Tong, B.C.; Onaitis, M.W.; D'Amico, T.A.; et al. Impact of patient selection and treatment strategies on outcomes after lobectomy for biopsy-proven stage IIIA pN2 non-small cell lung cancer. *Eur. J. Cardiothorac. Surg.* **2016**, *49*, 1607–1613. [CrossRef] [PubMed]

27. Yang, F.; Chen, H.; Xiang, J.; Zhang, Y.; Zhou, J.; Hu, H.; Zhang, J.; Luo, X. Relationship between tumor size and disease stage in non-small cell lung cancer. *BMC Cancer* **2010**, *10*, 474. [CrossRef]

28. Cho, H.J.; Kim, S.R.; Kim, H.R.; Han, J.O.; Kim, Y.H.; Kim, D.K.; Park, S.I. Modern outcome and risk analysis of surgically resected occult N2 non-small cell lung cancer. *Ann. Thorac. Surg.* **2014**, *97*, 1920–1925. [CrossRef]

29. Zhao, Y.; Wang, W.; Liang, H.; Yang, C.J.; D'Amico, T.; Ng, C.S.H.; Liu, C.C.; Petersen, R.H.; Rocco, G.; Brunelli, A.; et al. The Optimal Treatment for Stage IIIA-N2 Non-Small Cell Lung Cancer: A Network Meta-Analysis. *Ann. Thorac. Surg.* **2019**, *107*, 1866–1875. [CrossRef]

Article

Comparative Efficacy of Targeted Therapies in Patients with Non-Small Cell Lung Cancer: A Network Meta-Analysis of Clinical Trials

Tung Hoang [1], Seung-Kwon Myung [1,2,3,*], Thu Thi Pham [4,5], Jeongseon Kim [1] and Woong Ju [6,7]

[1] Department of Cancer Biomedical Science, National Cancer Center Graduate School of Cancer Science and Policy, Goyang 10408, Korea; 75256@ncc.re.kr (T.H.); jskim@ncc.re.kr (J.K.)

[2] Division of Cancer Epidemiology and Management, National Cancer Center Research Institute, Goyang 10408, Korea

[3] Department of Family Medicine and Center for Cancer Prevention and Detection, National Cancer Center Hospital, Goyang 10408, Korea

[4] Health Data Science Program, Institute of Public Health, Charité Universitätsmedizin Berlin, 10117 Berlin, Germany; thuphamhup@gmail.com

[5] Molecular Epidemiology Research Group, Max Delbrück Center for Molecular Medicine (MDC), 13125 Berlin, Germany

[6] Department of Obstetrics and Gynecology, Ewha Womans University College of Medicine, Seoul 07804, Korea; goodmorning@ewha.ac.kr

[7] Medical Research Institute, Ewha Womans University College of Medicine, Seoul 07804, Korea

*   Correspondence: msk@ncc.re.kr; Tel.: +82-31-920-0479

Abstract: This study aims to investigate the efficacy of targeted therapies in the treatment of non-small cell lung cancer (NSCLC) by using a network meta-analysis of clinical trials. PubMed, EMBASE, Cochrane Library, and Clinicaltrials.gov were searched by using keywords related to the topic on 19 September 2018. Two investigators independently selected relevant trials by pre-determined criteria. A pooled response ratio (RR) for overall response rate (ORR) and a hazard ratio (HR) for progression-free survival (PFS) were calculated based on both the Bayesian and frequentist approaches. A total of 128 clinical trials with 39,501 participants were included in the final analysis of 14 therapeutic groups. Compared with chemotherapy, both ORR and PFS were significantly improved for afatinib, alectinib, and crizotinib, while only PFS was significantly improved for cabozantinib, ceritinib, gefitinib, and osimertinib. Consistency was observed between the direct and indirect comparisons based on the Bayesian approach statistically and the frequentist approach visually. Cabozantinib and alectinib showed the highest probability for the first-line treatment ranking in ORR (62.5%) and PFS (87.5%), respectively. The current network meta-analysis showed the comprehensive evidence-based comparative efficacy of different types of targeted therapies, which would help clinicians use targeted therapies in clinical practice.

Keywords: non-small cell lung cancer; targeted therapy; network meta-analysis

1. Introduction

Lung cancer is the most common cancer and the leading cause of cancer death worldwide, with approximately 2.1 million new cases (11.6% of the total new cases) and 1.76 million deaths (18.4% of the total deaths) [1,2]. Of the two major types of lung cancer, non-small cell lung cancer (NSCLC) accounts for about 85% to 90% of all lung cancers, which typically has a slower rate and double time than small cell lung cancer [3,4].

Among several treatment options for NSCLC treatment recommended by the latest updated National Comprehensive Cancer Network (NCCN) guideline, targeted cancer therapy with various pathways is one of the new generations of cancer treatments [5]. Some cell surface receptors such as epidermal growth factor receptor (EGFR), anaplastic lymphoma kinase (ALK), and receptor of silencing 1 (ROS1) are overactive in the pathology of NSCLC [6,7]. Also, B-Raf proto-oncogene (BRAF), kirsten rat sarcoma 2 viral oncogene homolog (KRAS) and a kinase upstream of mitogen-activated protein kinase (MEK) have generated recent interest [8]. Other inhibitors of human epidermal growth factor receptor 2 (HER2), 'rearranged during transfection' proto-oncogene (RET), and tyrosine-protein kinase Met (MET) have also been approved for the treatment of NSCLC [9–11]. Although the efficacy of targeted therapies has been evaluated through large-scale randomized controlled trials and has already been approved by the Food and Drug Administration (FDA), their comparative efficacy has not been investigated.

Therefore, we performed a network meta-analysis (NMA) of clinical trials to compare and rank targeted therapies for the treatment of patients with NSCLC.

2. Materials and Methods

2.1. Search Strategy and Keywords

Eligible studies were identified by searching PubMed, EMBASE, Cochrane library, and Clinicaltrials.gov databases from their inception until September 19, 2018, limiting to human subjects and a clinical trial. The keywords for literature search were as follows: 'ado-trastuzumab', 'afatinib', 'alectinib', 'bevacizumab', 'brigatinib', 'cabozantinib', 'ceritinib', 'cetuximab', 'crizotinib', 'dabrafenib', 'erlotinib', 'gefitinib', 'osimertinib', 'ramucirumab', 'trametinib', 'vandetanib', and 'vemurafenib' for intervention factors; 'non-small cell lung cancer' for an outcome factor; and 'clinical trial' and 'randomized controlled trial' for type of study. The bibliographies of relevant articles were also reviewed to identify additional studies related to this topic. The literature search was restricted to studies published in English.

2.2. Selection of Relevant Studies

We included head-to-head or controlled trials that: compared the efficacy of FDA-approved targeted drugs with chemotherapy or placebos in the treatment of NSCLC; reported the outcomes on overall response rates (ORRs) and/or hazard ratios (HRs) for progression-free survival (PFS).

Two investigators (Hoang and Myung) independently selected relevant trials searched from the databases. The following variables were extracted from all the included studies: study name (first author, published year, and specific trial title, if possible), period and country, regimen of the intervention and the comparison, number of participants, and main outcomes.

2.3. Data Analysis

The pooled response ratio (RR) for ORRs based on an arm-based approach, HR for PFS based on a contrast-based approach, and their 95% confidence intervals (95% CIs) were calculated for estimating the differences between treatment groups.

We measured inconsistency, which implies statistical disagreement between direct and indirect comparisons [12,13]. The generalized linear model was applied for the Bayesian NMA [14]. Binomial likelihood and logit link function were applied for arm-based data of ORR, while normal likelihood and identity link function were used for contrast-based data of natural logarithm HR in the Bayesian approach [14]. Also, Bayesian model assumptions in the Bayesian analysis were assessed by the convergence diagnostics of the Markov chain Monte Carlo [14].

Based on the ranking probabilities of each therapy in different treatment lines, we calculated the surface under the cumulative ranking line (SUCRA) value and performed k-means clustering analysis to group the similar treatments [15,16].

For the statistical analysis of this NMA, we used different packages including pcnetmeta, gemtc, and netmeta in the R statistical environment [17–19]. Results from both the Bayesian approach (pcnetmeta and gemtc packages) and the frequentist approach (netmeta package) and were presented.

Finally, we calculated a decremental hazard-response ratio (DHRR) to obtain a decreased amount of HR per a unit of RR (compared to a dummy group) as in the following formula:

$$\mathrm{DHRR} = -\frac{\mathrm{HR} - \mathrm{HR_o}}{\mathrm{RR} - \mathrm{RR_o}}$$

where $\mathrm{HR_o}$ and $\mathrm{RR_o}$ are a baseline hazard ratio and a response ratio of chemotherapy vs. a dummy group, respectively.

3. Results

3.1. Selection of Relevant Studies

Figure S1 shows the flow diagram for selection of relevant studies. We identified 7279 articles from four different databases (PubMed, EMBASE, Cochrane Library, and Clinicaltrials.gov) using the keywords and hand-search from relevant bibliographies. After excluding 845 duplicated records and 5815 irrelevant studies, the full text of the remaining 619 articles were reviewed. Overall, a total of 128 parallel clinical trials were included in the current network meta-analysis.

3.2. Study Characteristics

The general characteristics of the included studies (eReferences in the Supplement) were summarized in Table S1. A total of 39,501 study participants were assigned to receive 14 different treatments including 12 targeted therapies, 1 chemotherapy, and 1 dummy. Sixty-four % of all the studies involved the comparisons between EGFR-targeted drugs and other treatments.

3.3. Network Geometry

Figure 1 shows the network geometry for ORR and PFS to represent graphical comparisons among various treatments. The comparative efficacy between erlotinib vs. chemotherapy/bevacizumab vs. dummy/erlotinib vs. dummy was frequently investigated for ORR, while the comparative efficacy between erlotinib vs. chemotherapy/gefitinib vs. chemotherapy/gefitinib vs. dummy/bevacizumab vs. dummy/erlotinib vs. dummy was done for PFS.
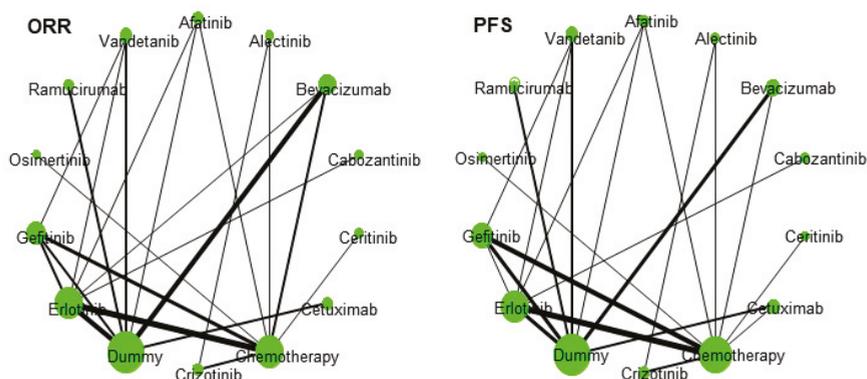
Figure 1. Network geometry of comparisons for overall response rate (ORR) and progression-free survival (PFS).

3.4. Assumption Checking

Figures S2 and S3 show a heat map, which provides visual inconsistency between direct and indirect comparisons in the frequentist approach. There was a big difference between inconsistency before and after the detachment in some treatment comparisons. However, no inconsistency was observed in the Bayesian approach (Figures S4 and S5).

Substantial heterogeneity was detected in both ORR and PFS, with the global $I^2 = 78\%$ for both outcomes as well as for either a pairwise pooled effect or a consistency effect (Table S2).

The width of every line reflects the number of studies. The size of the circles is proportional to the number of study participants. A dummy group is a placebo or a control group without additional treatment.

3.5. Comparative Efficacy

Compared to chemotherapy, afatinib, alectinib, ceritinib, and crizotinib were found to have a higher ORR with RRs ranging between 2.26 (95% CI, 1.34–3.82) for crizotinib and 3.75 (95% CI, 1.80–7.94) for ceritinib (Figure 2). Also, cabozantinib, gefitinib, and osimertinib vs. chemotherapy were found to improve PFS with HRs ranging from 0.17 (95% CI, 0.10–0.29) for alectinib to 0.78 (0.67–0.91) for gefitinib (Figure 3).
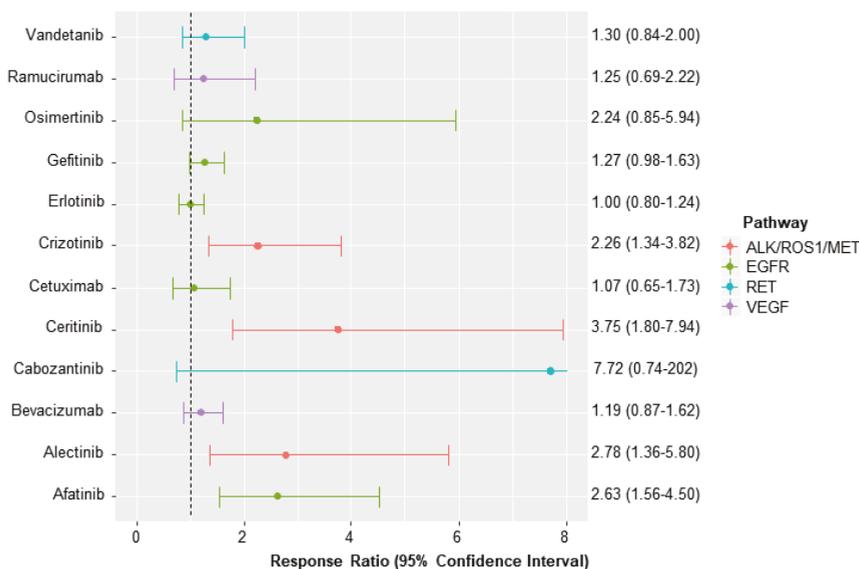
Figure 2. Response ratio for overall response rate of each targeted therapy vs. chemotherapy.
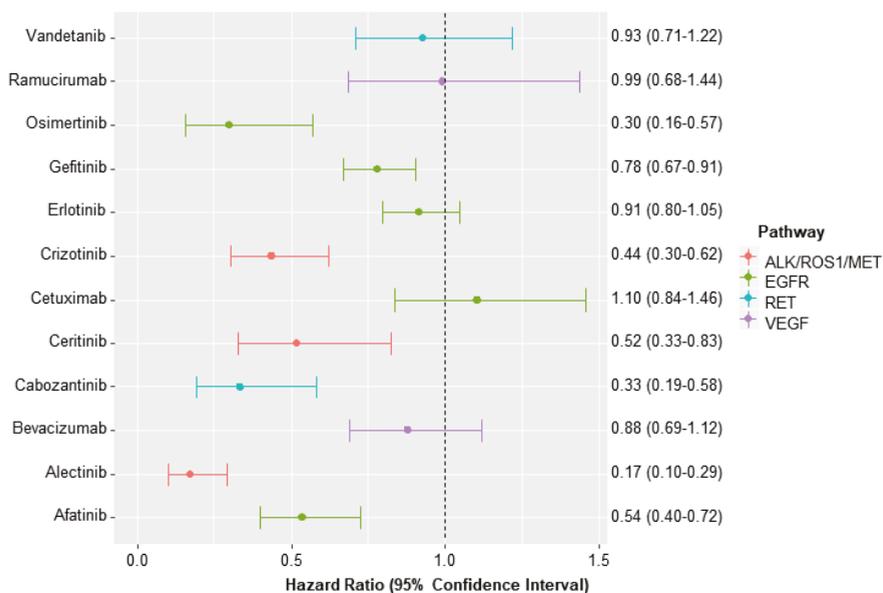
Figure 3. Hazard ratio for progression-free survival of each targeted therapy vs. chemotherapy.

Tables 1 and 2 show the league tables representing the comparative efficacy of targeted therapies for ORR and PFS in the network meta-analysis based on the Bayesian approach.

Among EGFR inhibitors, ORR was found to be significantly higher in afatinib treatment, compared to cetuximab (RR, 2.46; 95% CI, 1.25–4.90), erlotinib (RR, 2.64; 95% CI, 1.54–4.58), and gefitinib (RR, 2.08; 95% CI, 1.18-3.68) (Table 1). Also, afatinib had a significantly longer PFS, compared to cetuximab (HR, 0.49; 95% CI, 0.33–0.71), erlotinib (HR, 0.59; 95% CI 0.44–0.80), and gefitinib (HR, 0.69; 95% CI, 0.50–0.95) (Table 2). Osimertinib was found to improve PFS, compared to cetuximab (HR, 0.27; 95% CI, 0.14–0.55), erlotinib (HR, 0.33; 95% CI, 0.17–0.64), and gefitinib (HR, 0.39; 95% CI, 0.20–0.75) (Table 2). Gefitinib showed a better PFS compared to cetuximab (HR, 0.70; 95% CI, 0.53–0.94) (Table 2).

Regarding ALK/ROS1/MET targeted drugs, there were no significant differences in ORR between each pair of crizotinib, ceritinib, and alectinib (Table 1). However, alectinib showed a superior efficacy compared to either crizotinib (HR, 0.40; 95% CI, 0.25–0.64) or ceritinib (HR, 0.33; 0.17–0.67) for PFS (Table 2).

As for VEGF pathway (bevacizumab and ramucizumab) and RET targeted therapy (cabozantinib and vandetanib), only cabozantinib was found to improve PFS compared to vandetanib (HR, 0.36; 95% CI, 0.20–0.66) (Table 2).

3.6. Sensitivity Analysis

Findings of the direct pairwise meta-analysis and the relative effect estimates for ORR and PFS using the frequentist approach are presented in Tables S3–S5. The findings were similar to those by using the Bayesian approach (Tables 1 and 2).

Table 1. Comparative efficacy of targeted therapies for overall response rate in the network meta-analysis based on the Bayesian approach.

Afat	Alec	Beva	Cabo	Ceri	Cetu	Chem	Criz	Dum	Erlo	Gefi	Osim	Ramu	Vand
Afat	0.95 (0.38–2.31)	2.22 (1.25–3.98)	0.34 (0.01–3.81)	0.71 (0.28–1.73)	2.46 (1.25–4.90)	2.63 (1.56–4.50)	1.18 (0.55–2.46)	3.53 (2.06–6.15)	2.64 (1.54–4.58)	2.08 (1.18–3.68)	1.18 (0.39–3.51)	2.11 (1.00–4.49)	2.03 (1.07–3.88)
1.06 (0.43–2.62)	Alec	2.34 (1.08–5.22)	0.36 (0.01–4.26)	0.74 (0.26–2.10)	2.60 (1.10–6.27)	2.78 (1.36–5.80)	1.24 (0.67–2.27)	3.74 (1.75–8.22)	2.79 (1.32–6.02)	2.20 (1.03–4.78)	1.24 (0.37–4.21)	2.24 (0.90–5.71)	2.15 (0.93–5.03)
0.45 (0.25–0.80)	0.42 (0.19–0.93)	Beva	0.15 (0.01–1.63)	0.31 (0.14–0.70)	1.11 (0.70–1.78)	1.19 (0.87–1.62)	0.52 (0.28–0.96)	1.59 (1.25–2.05)	1.19 (0.87–1.63)	0.94 (0.66–1.32)	0.53 (0.19–1.46)	0.95 (0.54–1.69)	0.92 (0.59–1.41)
2.93 (0.26–76.6)	2.79 (0.23–76.6)	6.49 (0.62–170)	Cabo	2.08 (0.17–57.3)	7.21 (0.67–193)	7.72 (0.74–202)	3.45 (0.30–92.0)	10.36 (0.99–272)	7.74 (0.75–201)	6.09 (0.58–162)	3.45 (0.27–104)	6.20 (0.56–166)	5.95 (0.56–157)
1.43 (0.58–3.57)	1.35 (0.48–3.78)	3.16 (1.43–7.12)	0.49 (0.02–5.78)	Ceri	3.51 (1.45–8.60)	3.75 (1.80–7.94)	1.66 (0.68–4.13)	5.04 (2.30–11.2)	3.76 (1.74–8.25)	2.96 (1.36–6.54)	1.68 (0.50–5.65)	3.02 (1.18–7.83)	2.89 (1.23–6.89)
0.41 (0.20–0.80)	0.38 (0.16–0.91)	0.90 (0.56–1.44)	0.14 (0.01–1.49)	0.28 (0.12–0.69)	Cetu	1.07 (0.65–1.73)	0.47 (0.23–0.96)	1.44 (0.96–2.14)	1.07 (0.67–1.72)	0.84 (0.51–1.38)	0.48 (0.16–1.41)	0.86 (0.45–1.65)	0.82 (0.48–1.41)
0.38 (0.22–0.64)	0.36 (0.17–0.74)	0.84 (0.62–1.15)	0.13 (0.00–1.35)	0.27 (0.13–0.56)	0.93 (0.58–1.53)	Chem	0.44 (0.26–0.75)	1.34 (1.03–1.77)	1.00 (0.80–1.25)	0.79 (0.61–1.02)	0.45 (0.17–1.17)	0.80 (0.45–1.45)	0.77 (0.50–1.19)
0.86 (0.41–1.82)	0.81 (0.44–1.49)	1.90 (1.04–3.51)	0.29 (0.01–3.28)	0.60 (0.24–1.48)	2.11 (1.04–4.34)	2.26 (1.34–3.82)	Criz	3.03 (1.69–5.50)	2.26 (1.29–4.03)	1.78 (0.99–3.20)	1.01 (0.34–3.03)	1.81 (0.84–3.99)	1.74 (0.89–3.45)
0.28 (0.16–0.49)	0.26 (0.12–0.57)	0.63 (0.49–0.80)	0.10 (0.00–1.01)	0.20 (0.09–0.43)	0.70 (0.47–1.04)	0.75 (0.57–0.98)	0.33 (0.18–0.59)	Dum	0.75 (0.58–0.96)	0.59 (0.44–0.78)	0.33 (0.12–0.91)	0.60 (0.36–1.00)	0.57 (0.40–0.82)
0.38 (0.22–0.65)	0.36 (0.17–0.76)	0.84 (0.61–1.15)	0.13 (0.00–1.33)	0.26 (0.12–0.57)	0.93 (0.58–1.50)	1.00 (0.80–1.24)	0.44 (0.25–0.78)	1.34 (1.05–1.72)	Erlo	0.79 (0.59–1.04)	0.45 (0.16–1.19)	0.80 (0.46–1.42)	0.77 (0.51–1.16)
0.48 (0.27–0.85)	0.45 (0.21–0.98)	1.07 (0.76–1.51)	0.16 (0.01–1.72)	0.34 (0.15–0.74)	1.19 (0.73–1.94)	1.27 (0.98–1.63)	0.56 (0.31–1.01)	1.70 (1.28–2.27)	1.27 (0.96–1.68)	Gefi	0.57 (0.21–1.53)	1.02 (0.57–1.83)	0.98 (0.63–1.51)
0.85 (0.29–2.56)	0.80 (0.24–2.70)	1.88 (0.68–5.22)	0.29 (0.01–3.75)	0.59 (0.18–2.01)	2.09 (0.71–6.26)	2.24 (0.85–5.94)	0.99 (0.33–2.97)	3.01 (1.10–8.30)	2.24 (0.84–6.07)	1.77 (0.65–4.84)	Osim	1.80 (0.59–5.63)	1.73 (0.60–5.02)
0.47 (0.22–1.00)	0.44 (0.18–1.12)	1.05 (0.59–1.85)	0.16 (0.01–1.79)	0.33 (0.13–0.84)	1.16 (0.61–2.23)	1.25 (0.69–2.22)	0.55 (0.25–1.19)	1.67 (1.00–2.78)	1.25 (0.71–2.20)	0.98 (0.55–1.76)	0.56 (0.18–1.70)	Ramu	0.96 (0.51–1.79)
0.49 (0.26–0.94)	0.46 (0.20–1.07)	1.09 (0.71–1.69)	0.17 (0.01–1.77)	0.34 (0.15–0.81)	1.21 (0.71–2.09)	1.30 (0.84–2.00)	0.57 (0.29–1.13)	1.74 (1.22–2.51)	1.30 (0.86–1.59)	1.02 (0.66–1.59)	0.58 (0.20–1.67)	1.04 (0.56–1.96)	Vand

Drugs are reported in alphabetical order. Data in the right-upper triangle are RRs (95% confidence interval, CI) in the row-defining treatment compared with the column-defining treatment. RRs higher than 1 favor the row-defining treatment (the first drug in alphabetical order). RRs for the opposite comparison of ORR are in the left-lower triangle. Each comparison is shown twice in the table, once with drug A vs. drug B and once with drug B vs. drug A. Significant results are in italic and underscored. RR, response ratio; CI, confidence interval; ORR: overall response rate; Afat, afatinib; Alec, alectinib; Beva, bevacizumab; Cabo, cabozantinib; Ceri, ceritinib; Cetu, cetuximab; Chem, chemotherapy; Criz, crizotinib; Dum, dummy; Erlo, erlotinib; Gefi, gefitinib; Osim, osimertinib; Ramu, ramucirumab; Vand, vandetanib.

Table 2. Comparative efficacy of targeted therapies for progression-free survival in the network meta-analysis based on the Bayesian approach.

Afat	Alec	Beva	Cabo	Ceri	Cetu	Chem	Criz	Dum	Erlo	Gefi	Osim	Ramu	Vand
Afat	3.10 (1.69–5.65)	0.61 (0.43–0.87)	1.61 (0.87–2.98)	1.03 (0.60–1.79)	0.49 (0.33–0.71)	0.54 (0.40–0.72)	1.23 (0.78–1.96)	0.43 (0.32–0.58)	0.59 (0.44–0.80)	0.69 (0.50–0.95)	1.79 (0.88–3.63)	0.54 (0.35–0.84)	0.58 (0.40–0.84)
0.32 (0.18–0.59)	Alec	0.20 (0.11–0.35)	0.52 (0.24–1.11)	0.33 (0.17–0.67)	0.16 (0.09–0.28)	0.17 (0.10–0.29)	0.40 (0.25–0.64)	0.14 (0.08–0.24)	0.19 (0.11–0.33)	0.22 (0.13–0.38)	0.58 (0.25–1.33)	0.17 (0.09–0.33)	0.19 (0.10–0.33)
1.64 (1.15–2.33)	5.08 (2.87–9.04)	Beva	2.63 (1.46–4.76)	1.69 (1.01–2.86)	0.80 (0.59–1.08)	0.88 (0.69–1.12)	2.02 (1.32–3.10)	0.71 (0.58–0.86)	0.96 (0.76–1.23)	1.13 (0.88–1.45)	2.93 (1.47–5.82)	0.89 (0.60–1.30)	0.95 (0.70–1.28)
0.62 (0.34–1.15)	1.93 (0.90–4.12)	0.38 (0.21–0.69)	Cabo	0.64 (0.31–1.32)	0.30 (0.16–0.55)	0.33 (0.19–0.58)	0.77 (0.40–1.49)	0.27 (0.15–0.47)	0.37 (0.21–0.63)	0.43 (0.24–0.76)	1.11 (0.48–2.60)	0.34 (0.18–0.65)	0.36 (0.20–0.66)
0.97 (0.56–1.67)	3.00 (1.50–6.02)	0.59 (0.35–0.99)	1.55 (0.76–3.20)	Ceri	0.47 (0.27–0.81)	0.52 (0.33–0.83)	1.19 (0.67–2.14)	0.42 (0.26–0.68)	0.57 (0.35–0.92)	0.67 (0.41–1.09)	1.73 (0.78–3.85)	0.52 (0.29–0.95)	0.56 (0.33–0.96)
2.05 (1.41–2.99)	6.37 (3.54–11.5)	1.26 (0.92–1.71)	3.30 (1.80–6.07)	2.12 (1.24–3.64)	Cetu	1.10 (0.84–1.46)	2.54 (1.62–3.98)	0.89 (0.70–1.13)	1.21 (0.91–1.59)	1.42 (1.06–1.89)	3.68 (1.83–7.39)	1.11 (0.74–1.67)	1.19 (0.85–1.66)
1.86 (1.38–2.51)	5.77 (3.42–9.73)	1.14 (0.89–1.44)	2.99 (1.72–5.21)	1.92 (1.21–3.06)	0.91 (0.69–1.20)	Chem	2.30 (1.61–3.29)	0.81 (0.68–0.95)	1.09 (0.96–1.25)	1.29 (1.10–1.50)	3.33 (1.75–6.34)	1.01 (0.70–1.46)	1.08 (0.82–1.41)
0.81 (0.51–1.29)	2.51 (1.57–4.00)	0.50 (0.32–0.76)	1.30 (0.67–2.52)	0.84 (0.47–1.50)	0.39 (0.25–0.62)	0.44 (0.30–0.62)	Criz	0.35 (0.24–0.52)	0.48 (0.33–0.70)	0.56 (0.38–0.83)	1.45 (0.69–3.04)	0.44 (0.26–0.73)	0.47 (0.30–0.73)
2.30 (1.71–3.11)	7.15 (4.14–12.4)	1.41 (1.16–1.71)	3.71 (2.12–6.49)	2.38 (1.46–3.91)	1.12 (0.88–1.43)	1.24 (1.05–1.46)	2.85 (1.92–4.22)	Dum	1.36 (1.16–1.59)	1.59 (1.34–1.89)	4.13 (2.12–8.02)	1.25 (0.90–1.73)	1.33 (1.05–1.68)
1.70 (1.26–2.30)	5.27 (3.07–9.07)	1.04 (0.82–1.32)	2.73 (1.60–4.68)	1.76 (1.09–2.85)	0.83 (0.63–1.09)	0.91 (0.80–1.05)	2.10 (1.44–3.07)	0.74 (0.63–0.86)	Erlo	1.17 (0.98–1.40)	3.05 (1.57–5.88)	0.92 (0.64–1.33)	0.98 (0.76–1.28)
1.45 (1.05–1.99)	4.49 (2.62–7.75)	0.88 (0.69–1.13)	2.33 (1.32–4.10)	1.50 (0.92–2.44)	0.70 (0.53–0.91)	0.78 (0.67–0.91)	1.79 (1.21–2.63)	0.63 (0.53–0.74)	0.85 (0.67–1.02)	Gefi	2.59 (1.33–5.03)	0.78 (0.54–1.14)	0.84 (0.64–1.10)
0.56 (0.28–1.14)	1.73 (0.75–3.97)	0.34 (0.17–0.68)	0.90 (0.38–2.10)	0.58 (0.26–1.28)	0.27 (0.14–0.55)	0.30 (0.16–0.57)	0.69 (0.33–1.44)	0.24 (0.12–0.47)	0.33 (0.17–0.64)	0.39 (0.20–0.75)	Osim	0.30 (0.14–0.64)	0.32 (0.16–0.65)
1.84 (1.18–2.89)	5.72 (3.02–10.9)	1.13 (0.77–1.66)	2.97 (1.55–5.68)	1.91 (1.06–3.47)	0.90 (0.60–1.36)	0.99 (0.68–1.44)	2.28 (1.37–3.82)	0.80 (0.58–1.12)	1.09 (0.75–1.56)	1.27 (0.88–1.85)	3.31 (1.56–6.94)	Ramu	1.07 (0.71–1.61)
1.73 (1.19–2.50)	5.36 (2.99–9.67)	1.06 (0.78–1.43)	2.78 (1.53–5.06)	1.79 (1.04–3.06)	0.84 (0.60–1.17)	0.93 (0.71–1.22)	2.13 (1.36–3.33)	0.75 (0.59–0.95)	1.02 (0.78–1.32)	1.19 (0.91–1.57)	3.10 (1.54–6.23)	0.94 (0.62–1.40)	Vand

Drugs are reported in alphabetical order. Data in the right-upper triangle are HRs (95% CI) in the row-defining treatment compared with the column-defining treatment. HRs lower than 1 favour the row-defining treatment (the first drug in alphabetical order). HRs for the opposite comparison of PFS are in the left-lower triangle. Each comparison is shown twice in the table, once with drug A vs. drug B and once with drug B vs. drug A. Significant results are in italic and underscored. HR, hazard ratio; CI, confidence interval; PFS: progression-free survival. Afat, afatinib; Alec, alectinib; Beva, bevacizumab; Cabo, cabozantinib; Ceri, ceritinib; Cetu, cetuximab; Chem, chemotherapy; Criz, crizotinib; Dum, dummy; Erlo, erlotinib; Gefi, gefitinib; Osim, osimertinib; Ramu, ramucirumab; Vand, vandetanib.

3.7. Treatment Ranking

The Gelman plot for checking Bayesian model assumption shows a low chain reduction over time for both ORR and PFS outcomes, and the chains seem roughly converged after maximum 10,000 iterations in chain (Figures S6 and S7). Also, cabozantinib and alectinib were found to become the first-line therapies with the highest treatment ranking probabilities of 62.5% for ORR and 87.5% for PFS, respectively (Tables S6 and S7 and Figure S8). In the k-means clustering analysis of SUCRA, ceritinib, alectinib, crizotinib, osimertinib, cabozantinib, and afatinib showed the more efficacy compared with the remaining treatment (Figure S9).

Figure S10 reports the two-dimensional graphs about RR for ORR and HR for PFS in the comparison with dummy group. DHRR indicated the decrease of HR obtained per 1 unit increase of RR for osimertinib (0.34), alectinib (0.28), bevacizumab (0.38), and vandetanib (0.14), which are higher than that for other drugs relating to EGFR, ALK/ROS1/MET, VEGF, and RET pathways.

4. Discussion

4.1. Summary of Findings

In the current comprehensive network meta-analysis, compared to chemotherapy, most of the targeted drugs including afatinib, alectinib, cabozantinib, ceritinib, crizotinib, gefitinib, and osimertinib showed a significantly higher efficacy in ORR and PFS. Among EGFR inhibitors, afatinib was found to improve both ORR and PFS, vs. cetuximab, erlotinib, or gefitinib treatment. Furthermore, alectinib and cabozantinib also showed the lower risk of disease progression, compared to other drugs in the ALK/ROS1/MET and RET pathways.

There was no inconsistency between direct and indirect comparisons in most treatments based on the Bayesian approach. The findings of the NMA based on both the frequentist and Bayesian approach were similar in pooled effect sizes as well as a significant direction. Also, Bayesian assumptions were ensured by convergence diagnostics.

4.2. Comparison with Previous Studies

Previous reports related to EGFR inhibitors showed consistent findings with the current study. A recent meta-analysis of 90 retrospective or prospective cohort studies and clinical trials showed the comparable effect of gefitinib vs. erlotinib [20]. The RR (95% CI) for ORR and HR (95% CI) for PFS were 1.05 (1.00–1.11) and 1.00 (0.95–1.04), respectively [20]. Another network meta-analysis of 11 clinical trials also showed the similar PFS between gefitinib and erlotinib [21]. However, unlike our findings, the third-generation EGFR inhibitor osimertinib was found to have a longer PFS (HR 0.71, 95% CI 0.54–0.95), and the significant difference between the second-generation EGFR inhibitor afatinib and standard of care (either gefitinib or erlotinib) was not observed (HR 0.96, 95% CI, 0.86–1.17) [21].

In a large medical chart review of 1471 participants with ALK-positive NSCLC among a total of 27,375 recorded subjects from seven countries, crizotinib showed a significant improvement in complete response (odds ratio (OR) = 2.65, 95% CI = 1.69–4.15) and reduction of recurrence/progression (odds ratio = 0.38, 95% CI = 0.24–0.59) compared to controls [22]. Also, a recent network meta-analysis of ALK inhibitors showed consistent findings among treatments in both ORR and PFS outcomes [23]. In Fan et al.'s study, a remarkable improvement in ORR was shown: the ORs (95%CI) for crizotinib, ceritinib, and alextinib were 11.69 (4.29–36.56), 7.85 (3.44–19.27), and 6.04 (3.33–11.71), compared to chemotherapy, respectively [23]. The superior efficacy of alectinib in PFS might be associated with the resistance to crizotinib among ALK-positive NSCLC patients, which reduces therapeutic response to crizotinib [24,25]. Although ceritinib is also a second-generation ALK inhibitor, our study showed that there is no signicant difference in the efficacy between ceritinib and crizotinib. Similarly, the recent meta-analyses of pooled estimates reported that crizotinib might have higher ORR [66% (58–74%) vs. 52% (38–66%)] and longer PFS [9.27 months (8.28–10.26) vs. 5.92 months (4.36–7.48)] than ceritinib,

although no statistical test was performed [26]. It remains unclear why ceritinib did not show a superior efficacy unlike alectinib.

4.3. Strengths and Limitations

To the best of our knowledge, this is the first network meta-analysis which summarized the direct and indirect evidence on the comparative efficacy of targeted therapies in the treatment of NSCLC. Also, this compiled a large dataset, and the method was valid by checking several assumptions. In addition, this network meta-analysis included clinical trials only, which had a higher level of evidence than observational studies and allowed us to obtain the precise estimates.

Despite the strengths, there are several limitations in the current study. The efficacy of targeted therapies was evaluated through ORR and PFS surrogates only. We did not perform subgroup analyses by different treatment lines and patients of different mutations as well. Also, the potential heterogeneity was observed with approximately 78% for both ORR and PFS outcomes. Finally, among 34,969 subjects included for the analysis of ORR outcome, the small number of patients received cabozatinib (38 subjects, Table S1). Also, a big difference in ORRs between the two arms (10.5% for cabozatinib vs. 2.6% erlotinib) might lead to the large error margins for the comparative effect of cabozantinib and other treatments (Figure 2 and Table 1).

5. Conclusions

In summary, the current study showed the comprehensive evidence-based comparative efficacy of different types of targeted therapies, which would help clinicians use targeted therapies in clinical practice. Cabozantinib and alectinib showed the highest probability for the first-line treatment ranking in ORR and PFS, respectively.

References

1. Bray, F.; Ferlay, J.; Soerjomataram, I.; Siegel, R.L.; Torre, L.A.; Jemal, A. Global cancer statistics 2018: GLOBOCAN estimates of incidence and mortality worldwide for 36 cancers in 185 countries. *CA Cancer J. Clin.* **2018**, *68*, 394–424. [CrossRef] [PubMed]
2. International Agency for Research on Cancer: GLOBOCAN. Fact Sheet by Cancer Type: Lung Cancer. Available online: http://gco.iarc.fr/today/fact-sheets-cancers (accessed on 4 July 2019).

3. Dai, L.; Lin, Z.; Cao, Y.; Chen, Y.; Xu, Z.; Qin, Z. Targeting EIF4F complex in non-small cell lung cancer cells. *Oncotarget* **2017**, *8*, 55731–55735. [CrossRef] [PubMed]

4. Zappa, C.; Mousa, S.A. Non-small cell lung cancer: Current treatment and future advances. *Transl. Lung Cancer Res.* **2016**, *5*, 288–300. [CrossRef] [PubMed]

5. National Comprehensive Cancer Network (NCCN). Non-Small Cell Lung Cancer. *Clinical Practice Guidelines in Oncology (Version 1.2018).* Available online: https://www.nccn.org (accessed on 4 July 2019).

6. Prabhu, V.V.; Devaraj, N. Epidermal growth factor receptor tyrosine kinase: A potential target in treatment of non-small-cell lung carcinoma. *J. Environ. Pathol. Toxicol. Oncol.* **2017**, *36*, 151–158. [CrossRef] [PubMed]

7. Toschi, L.; Rossi, S.; Finocchiaro, G.; Santoro, A. Non-small cell lung cancer treatment (r)evolution: Ten years of advances and more to come. *Ecancermedicalscience* **2017**, *11*, 787. [CrossRef] [PubMed]

8. Brustugun, O.T.; Khattak, A.M.; Tromborg, A.K.; Beigi, M.; Beiske, K.; Lund-Iversen, M.; Helland, A. BRAF-mutations in non-small cell lung cancer. *Lung Cancer* **2014**, *84*, 36–38. [CrossRef] [PubMed]

9. Gainor, J.F.; Shaw, A.T. Novel targets in non-small cell lung cancer: ROS1 and RET fusions. *Oncologist* **2013**, *18*, 865–875. [CrossRef] [PubMed]

10. Gelsomino, F.; Facchinetti, F.; Haspinger, E.R.; Garassino, M.C.; Trusolino, L.; De Braud, F.; Tiseo, M. Targeting the MET gene for the treatment of non-small-cell lung cancer. *Crit. Rev. Oncol. Hematol.* **2014**, *89*, 284–299. [CrossRef] [PubMed]

11. Mar, N.; Vredenburgh, J.J.; Wasser, J.S. Targeting HER2 in the treatment of non-small cell lung cancer. *Lung Cancer* **2015**, *87*, 220–225. [CrossRef] [PubMed]

12. Rouse, B.; Chaimani, A.; Li, T. Network meta-analysis: An introduction for clinicians. *Intern. Emerg. Med.* **2017**, *12*, 103–111. [CrossRef] [PubMed]

13. Shim, S.; Yoon, B.H.; Shin, I.S.; Bae, J.M. Network meta-analysis: Application and practice using Stata. *Epidemiol. Health* **2017**, *39*, e2017047. [CrossRef] [PubMed]

14. Neupane, B.; Richer, D.; Bonner, A.J.; Kibret, T.; Beyene, J. Network meta-analysis using R: A review of currently available automated packages. *PLoS ONE* **2014**, *9*, e115065. [CrossRef] [PubMed]

15. Kassambara, A.; Fabian, M. Factoextra: Extract and Visualize the Results of Multivariate Data Analyses. Available online: http://www.sthda.com/english/rpkgs/factoextra (accessed on 12 December 2019).

16. Salanti, G.; Ades, A.E.; Ioannidis, J.P. Graphical methods and numerical summaries for presenting results from multiple-treatment meta-analysis: An overview and tutorial. *J. Clin. Epidemiol.* **2011**, *64*, 163–171. [CrossRef] [PubMed]

17. Lin, L.; Zhang, J.; Chu, H. Pcnetmeta: Methods for Patient-Centered Network Meta-Analysis. Available online: https://cran.r-project.org/web/packages/pcnetmeta/pcnetmeta.pdf (accessed on 9 November 2019).

18. Rucker, G.; Schwarzer, G.; Krahn, U.; Konig, J. Netmeta: Network Meta-Analysis Using Frequentist Methods. Available online: https://cran.r-project.org/web/packages/netmeta/netmeta.pdf (accessed on 9 November 2019).

19. Van Valkenhoef, G.; Kuiper, J. Gemtc: Network Meta-Analysis Using Bayesian Methods. Available online: https://cran.r-project.org/web/packages/gemtc/gemtc.pdf (accessed on 9 November 2019).

20. Yang, Z.; Hackshaw, A.; Feng, Q.; Fu, X.; Zhang, Y.; Mao, C.; Tang, J. Comparison of gefitinib, erlotinib and afatinib in non-small cell lung cancer: A meta-analysis. *Int. J. Cancer* **2017**, *140*, 2805–2819. [CrossRef] [PubMed]

21. Lin, J.Z.; Ma, S.K.; Wu, S.X.; Yu, S.H.; Li, X.Y. A network meta-analysis of nonsmall-cell lung cancer patients with an activating EGFR mutation: Should osimertinib be the first-line treatment? *Medicine* **2018**, *97*, e11569. [CrossRef] [PubMed]

22. DiBonaventura, M.; Higginbottom, K.; Meyers, A.; Morimoto, Y.; Ilacqua, J. Comparative effectiveness of crizotinib among ALK+ NSCLC patients across the United States, Western Europe, and Japan. *Value Health* **2016**, *19*, A711. [CrossRef]

23. Fan, J.; Fong, T.; Xia, Z.; Zhang, J.; Luo, P. The efficacy and safety of ALK inhibitors in the treatment of ALK-positive non-small cell lung cancer: A network meta-analysis. *Cancer Med.* **2018**, *7*, 4993–5005. [CrossRef] [PubMed]

24. Dagogo-Jack, I.; Shaw, A.T. Crizotinib resistance: Implications for therapeutic strategies. *Ann. Oncol.* **2016**, *27*, iii42–iii50. [CrossRef] [PubMed]

25. Gainor, J.F.; Dardaei, L.; Yoda, S.; Friboulet, L.; Leshchiner, I.; Katayama, R.; Dagogo-Jack, I.; Gadgeel, S.; Schultz, K.; Singh, M.; et al. Molecular mechanisms of resistance to first- and second-generation ALK inhibitors in ALK-rearranged lung cancer. *Cancer Discov.* **2016**, *6*, 1118–1133. [CrossRef] [PubMed]
26. Hoang, T.; Myung, S.K.; Pham, T.T.; Park, B. Efficacy of Crizotinib, Ceritinib, and Alectinib in ALK-Positive Non-Small Cell Lung Cancer Treatment: A Meta-Analysis of Clinical Trials. *Cancers* **2020**, *12*, 526. [CrossRef] [PubMed]

Article

Concomitant *TP53* Mutation Confers Worse Prognosis in *EGFR*-Mutated Non-Small Cell Lung Cancer Patients Treated with TKIs

Matteo Canale [1], Elisabetta Petracci [2], Angelo Delmonte [3], Giuseppe Bronte [3], Elisa Chiadini [1], Vienna Ludovini [4], Alessandra Dubini [5], Maximilian Papi [6], Sara Baglivo [4], Nicoletta De Luigi [7], Alberto Verlicchi [3], Rita Chiari [8], Lorenza Landi [9], Giulio Metro [4], Marco Angelo Burgio [3], Lucio Crinò [3] and Paola Ulivi [1,*]

[1] Biosciences Laboratory, Istituto Scientifico Romagnolo per lo Studio e la Cura dei Tumori (IRST) IRCCS, 47014 Meldola, Italy; matteo.canale@irst.emr.it (M.C.); elisa.chiadini@irst.emr.it (E.C.)

[2] Biostatistics and Clinical Trials Unit, Istituto Scientifico Romagnolo per lo Studio e la Cura dei Tumori (IRST) IRCCS, 47014 Meldola, Italy; elisabetta.petracci@irst.emr.it

[3] Department of Medical Oncology, Istituto Scientifico Romagnolo per lo Studio e la Cura dei Tumori (IRST) IRCCS, 47014 Meldola, Italy; angelo.delmonte@irst.emr.it (A.D.); giuseppe.bronte@irst.emr.it (G.B.); alberto.verlicchi@irst.emr.it (A.V.); marco.burgio@irst.emr.it (M.A.B.); lucio.crino@irst.emr.it (L.C.)

[4] Department of Medical Oncology, Santa Maria della Misericordia Hospital, 06129 Perugia, Italy; oncolab@hotmail.com (V.L.); baglivosara@gmail.com (S.B.); giulio.metro@yahoo.com (G.M.)

[5] Department of Pathology, Morgagni-Pierantoni Hospital, 47121 Forlì, Italy; alessandra.dubini@auslromagna.it

[6] Department of Medical Oncology, Per gli Infermi Hospital, Rimini 47923, Italy; maximilianpapi@libero.it

[7] UOS Oncology, Istituto per la Sicurezza Sociale, State Hospital, Cailungo 47893, San Marino, Italy; nicolettadeluigi@hotmail.com

[8] Department of Medical Oncology, Ospedali Riuniti Padova Sud "M. Teresa di Calcutta", ULSS6 Euganea, 35131 Padova, Italy; rita.chiari@aulss6.veneto.it

[9] Department of Medical Oncology, S. Maria delle Croci Hospital, 48121 Ravenna, Italy; landi.lorenza@gmail.com

* Correspondence: paola.ulivi@irst.emr.it; Tel.: +39–0543–739980

Abstract: Background: Non-small cell lung cancer (NSCLC) is the primary cause of cancer-related deaths worldwide. Epidermal Growth Factor Receptor (*EGFR*)-mutated patients usually benefit from TKIs treatment, but a significant portion show unresponsiveness due to primary resistance mechanisms. We investigated the role of *TP53* mutations in predicting survival and response to *EGFR*-TKIs in EGFR-mutated NSCLC patients, to confirm, on an independent case series, our previous results. Methods: An independent retrospective cohort study was conducted, on a case series of 136 *EGFR*-mutated NSCLC patients receiving first or second generation TKIs as a first line therapy, and a smaller fraction of patients who acquired the T790M resistance mutation and were treated with third generation TKIs in the second or further line of treatment. *TP53* mutations were evaluated in relation to disease control rate (DCR), objective response rate (ORR), progression-free survival (PFS) and overall survival (OS) of the patients. Results: Forty-two patients (30.9%) showed a *TP53* mutation. Considered together, *TP53* mutations had no significant impact on time-to-event endpoints. Considering the different *TP53* mutations separately, exon 8 mutations confirmed their negative effect on PFS (HR 3.16, 95% 1.59–6.28, $p = 0.001$). In patients who developed the T790M resistance mutation, treated with third generation TKIs, the *TP53* exon 8 mutations predicted worse PFS (even though not statistically significant), and OS (HR 4.86, 95% CI: 1.25–18.90, $p = 0.023$). Conclusions: *TP53* exon 8 mutations confirmed their negative prognostic impact in patients treated with first and second generation TKIs and demonstrated a role in affecting clinical outcome in patients treated with third generation TKIs.

1. Introduction

Epidermal growth factor receptor (*EGFR*)-tyrosine kinase inhibitors (TKIs) have changed the natural history of non-small-cell lung cancer (NSCLC) patients harboring specific *EGFR* mutations at exons 18, 19 and 21. Randomized trials have demonstrated a median progression-free survival (PFS) of 9.7 and 9.5 months in patients harboring sensitizing *EGFR* mutations treated with first-generation *EGFR*-TKIs versus platinum-based chemotherapy [1,2], and 11.1 months for second generation TKIs [3]. Third generation TKI osimertinib, initially designed to overcome the arising of T790M resistance mutation in *EGFR* pre-treated patients [4], has recently become the gold standard for *EGFR*-mutated patients, reaching a median PFS of 18.9 months [5].

Despite the high sensitivity of *EGFR*-mutated patients to *EGFR*-TKIs, the objective response rate is of about 70–80% for 1st, 2nd and 3rd generation TKIs [2,3,5], meaning that a portion of patients do not respond to *EGFR*-TKI treatment, notwithstanding the presence of sensitizing *EGFR* mutation, suggesting the presence of primary resistance mechanisms.

Our previous study and several others showed that the concomitant presence of *TP53* mutation confers a worse prognosis in *EGFR*-mutated patients treated with first and second generation TKIs [6–8]. Subsequent studies performed using next generation sequencing methodologies showed that the presence of concomitant mutation in different genes is associated with a lower response to *EGFR*-TKIs and, however, *TP53* mutation confirms to be the most significant predictor of worse outcome. In particular, it seems that specific *TP53* mutations are more implicated in predicting the worse prognosis [6,9,10], confirming that different *TP53* mutations confer different p53 functions. Within the coding region of the *TP53* gene, several studies have reported that a higher frequency of mutations occurs in the exons 5–8, and that mutations in these exons are associated to differential functions of p53 protein [9,10]. As the different published studies have analyzed principally patients treated with first and second generation TKIs, few data are available with regard to the role of *TP53* mutation in relation to response to third generation TKIs.

The main purpose of this research was to confirm our previously published results on the role of *TP53* mutations, in an independent cohort of advanced *EGFR*-mutated patients treated with first or second generation TKIs in the first line setting, and to investigate the role of *TP53* mutations in predicting prognosis of patients with acquired T790M mutation treated with third generation TKIs.

2. Materials and Methods

To confirm our previous results on the role of *TP53* mutations in relation to the effectiveness of TKIs, an independent retrospective cohort study was conducted. All consecutive patients with advanced *EGFR*-mutated NSCLC receiving a first line TKI treatment (i.e., gefitinib, erlotinib, or afatinib) from July 2010 to May 2018 at the Medical Oncology Units of the Romagna catchment area (Area Vasta Romagna, AVR) and at the S. Maria della Misericordia Hospital of Perugia, Italy, were included in this study. Demographic and clinical characteristics of the patients were obtained using a medical and radiographic records review including age, gender, smoking history, histology, and information on death and response to treatment. *EGFR* status had been routinely determined at the Biosciences Laboratory of IRST-IRCCS and the Laboratory of Molecular Biology of the S. Maria della Misericordia Hospital, Perugia, by MassARRAY, pyrosequencing, direct sequencing or Next-Generation Sequencing (NGS) methodologies.

To evaluate the independent role of *TP53* mutations, that is, eventually adjusting for other covariates, and to obtain a more accurate estimate of their prognostic effect, an analysis combining the data of the present work with those from our previous one [6], was also performed, updating follow-ups of the previous case series to 30 June 2018.

Moreover, considering the two cohorts together, we identified a subgroup of 42 patients who developed the T790M resistance mutation and were treated with third generation TKI, osimertinib. All patients provided an informed consent, and the study was approved by the AVR Ethical Committee (study code IRST-B053).

2.1. EGFR and TP53 Mutation Analysis

EGFR mutation analyses were performed on both cytologic and histologic samples, accurately selected by a dedicated expert pathologist from each center at the time of diagnosis. The same DNA specimens were used for the determination of *TP53* mutation status, blindly to the clinical outcomes. Quality controls were periodically performed during the course of the study to ensure concordance of molecular results.

DNA was extracted by macro-dissection of an area comprising at least 50% of tumor cells. Cells were lysed in a digestion buffer of 50 mmol/L KCl, 10 mmol/L Tris-HCl pH 8.0, 2.5 mmol/L MgCl$_2$, and Tween-20 0.45%; proteinase K at 1.25 mg/mL were added to each specimen, with an overnight incubation at 56 °C. After proteinase K inactivation at 95 °C for 10 min, samples were centrifuged twice to eliminate debris and supernatant DNA quantity and quality was assessed by Nanodrop (Celbio) before molecular analyses.

Mutation status for exons 5–8 of *TP53* gene was performed by PCR amplification and Direct Sequencing using 3130 Genetic Analyzer (Applied Biosystems, Monza, Italy), or Next-Generation Sequencing by Ion S5 platform (Thermofisher, Monza, Italy), or MySeq platform (Illumina, San Diego, CA, USA).

2.2. Response Evaluation

Best clinical response to treatment with TKI was classified on the basis of interval CT scans as complete response (CR), partial response (PR), stable disease (SD), or progressive disease (PD) using standard Response Evaluation Criteria in Solid Tumors criteria (RECIST) version 1.1. Patients with both baseline imaging and at least one repeated evaluation after continuous *EGFR*-TKI monotherapy were evaluable for radiographic response. The same criteria for response evaluation and periodicity were used by all centers taking part in the study.

2.3. Statistical Analyses

Data were summarized by mean ± standard deviation (SD) for continuous variables and through natural frequencies and percentages for categorical ones.

Treatment responses were reported as objective response rate (ORR) and disease control rate (DCR). The time-to-event endpoints examined were progression-free survival (PFS) and overall survival (OS). PFS was defined as the time from start of first line treatment (or from start of osimertinib for the subgroup analysis) to disease progression or death for any cause, whichever occurred first. Patients who were alive and progression-free at 30 June 2018, the last follow-up update, were censored at that date.

OS was defined as the time from start of first line treatment to death for any cause. Alive patients were censored at the date of the last follow-up update. PFS and OS functions were estimated using the Kaplan–Meier method, and the log-rank test was used to assess differences between groups. Median PFS and OS were reported as point estimates and 95% confidence intervals (CI) in round brackets. The Cox proportional hazards regression model was used to quantify the association between specific covariates and the time-to-event endpoints. Results are reported as HR and 95% CI in round brackets. To assess the association between mutations and the duration of response to TKIs, patients were divided into short-term responders (PFS less than 6 months), intermediate-term responders (PFS ≥6 months and ≤24 months) or long-term responders (PFS >24 months). The association between categorical variables was tested by the Pearson's χ^2 test or Fisher exact test, when appropriate, whereas those between a continuous variable and a categorical one was tested by means of the Student *t*-test or *F* test for more than two categories. To evaluate the independent role of *TP53* mutations in a multivariate analysis and to obtain more accurate estimates of their prognostic effect, a combined analysis including

data of the present work with those from our previous one, was performed. Follow-up of our previous cohort was updated on 30 June 2018. A multivariable model was obtained using backward stepwise variable selection, setting the significance level for variable removal from the model equal to 0.10. In a perspective of parsimonious modelling, when appropriate, categories of some study variables were grouped. The proportional hazards assumption was evaluated using a statistical test based on Schoenfeld residuals. In case of non-proportional hazards for a specific variable, a Cox model with time-dependent coefficient, $\beta(t)$, was fitted. To simplify model interpretation, a step function for $\beta(t)$ was used, dividing the follow-up period in three time periods since treatment started: the first 6 months, 6–12 months, and greater than 12 months.

Overall and when not otherwise specified, a two-sided *p*-value (*p*) <0.05 was considered statistically significant. All statistical analyses were performed using STATA 15.0 software (College Station, TX, USA) and R version 3.6.1.

3. Results

3.1. Clinico-Pathologic and Molecular Features of Patients

Patients characteristics, *EGFR* mutations, type of TKI received and *TP53* mutations are reported in Table 1. All 136 patients carried an *EGFR* mutation (exon 19 deletions 53.7%, exon 21 L858R 35.3%, other *EGFR* mutations 11.0%) and received a first line *EGFR*-TKI (36.7% Erlotinib, 5.1% Erlotinib plus bevacizumab, 30.9% gefitinib, 27.2% afatinib). Of the patients with available information on smoking habit, half were never smokers (50.8%), and half were former or current smokers (28.8% and 20.3%, respectively). We found *TP53* mutations in 42 (30.9%) of the 136 analyzed patients: 12 mutations were in exon 5 (28.6%), 6 in exon 6 (14.3%), 13 in exon 7 (31.0%) and 11 in exon 8 (26.2%). Following the classification of *TP53* mutations into disruptive and non-disruptive ones [6], 11 patients had a disruptive mutation whereas 31 had a non-disruptive one (26.2% and 73.8%, respectively).

Table 1. Demographic, clinicopathological and molecular characteristics of patients (*n* = 136).

Characteristic	*n*	(%)
Gender		
Female	86	(62.2)
Male	50	(36.8)
Age at first line TKI		
Mean ± SD		67.6 ± 11.2
Smoking habit †		
Never smoker	60	(50.9)
Former smoker	34	(28.8)
Current smoker	24	(20.3)
Type of *EGFR* mutation		
Exon 19 deletion	73	(53.7)
Exon 21 L858R	48	(35.3)
Other uncommon mutations	15	(11.0)
Type of *EGFR* exon 19 deletion		
No exon 19 deletion	63	(46.3)
Deletion starts at codon 746	62	(45.6)
Deletion starts at codon 747	11	(8.1)
Type of TKI received in first line setting		
Erlotinib *	57	(41.9)
Gefitinib	42	(30.9)
Afatinib	37	(27.2)
***TP53* mutation**		
Wild type	94	(69.1)
Exon 5	12	(8.8)
Exon 6	6	(4.4)
Exon 7	13	(9.6)
Exon 8	11	(8.1)
Type of *TP53* mutation		
Wild type	94	(69.1)
Disruptive	11	(8.1)
Non-disruptive	31	(22.8)

† The sum does not add up to the total due to missing values. * Of these patients, 7 received Erlotinib plus Bevacizumab as a first line therapy, as provided in the Beverly clinical trial.

While for patients with exon 19 deletion the three different TKIs were used in an almost similar proportion (32.9% patients received erlotinib, 30.1% gefitinib, and 37.0% afatinib), patients with a mutation in exon 21 L858R were predominantly treated with erlotinib or gefitinib (52.1% and 39.6% of the patients, respectively), and those with uncommon mutations received predominantly erlotinib or afatinib (53.3% and 40.0%, respectively, Table S1).

No statistically significant associations were observed between type of *TP53* mutation, type of *EGFR* mutation and patient characteristics (Table S2).

3.2. Patients Outcome in Relation to EGFR Mutations

Overall, ORR and DCR were 67.4%, and 89.3%, respectively. Considering the clinical responses by type of *EGFR* mutation, ORR was considerably higher in the subgroup of patients with exon 19 deletion (77.5%), with respect to patients with L585R mutation (55.3%), and the subgroup with other mutations (54.6%), *p* = 0.029. A higher percentage of long responders was observed in patients carrying exon 19 deletion (12.3%), with respect to patients with L858R point mutation (7.3%), or patients with the other *EGFR* mutations (6.6%), Table 2.

Table 2. Best clinical response according to *EGFR* mutations.

	All *EGFR* Mutations (*n* = 136)		Exon 19 Deletion (*n* = 73)		Exon 21 L858R (*n* = 48)		Other *EGFR* Mutations (*n* = 15)		*p*
	n	(%)	*n*	(%)	*n*	(%)	*n*	(%)	
Best response [†]									0.026
CR	13	(9.9)	8	(11.3)	4	(8.5)	1	(7.1)	
PR	76	(57.6)	47	(66.2)	22	(46.8)	7	(50.0)	
SD	29	(22.0)	7	(9.9)	17	(36.2)	5	(35.7)	
PD	14	(10.6)	9	(12.7)	4	(8.5)	1	(7.1)	
ORR	89	(67.4)	55	(77.5)	26	(55.3)	6	(54.6)	0.029
DCR	118	(89.4)	62	(87.3)	43	(91.5)	11	(100.0)	0.844
Duration of response									0.260
Short-term responders	36	(26.4)	19	(26.0)	10	(20.8)	7	(46.7)	
Medium-term responders	87	(64.0)	45	(61.6)	35	(72.9)	7	(46.7)	
Long-term responders	13	(9.6)	9	(12.3)	2	(6.3)	1	(6.6)	

[†] The sum does not add up to the total due to missing values.

Median PFS and OS were 12.3 (95% CI: 9.9–13.8) and 27.3 (95% CI: 21.9–52.9) months, respectively. No statistically significant association between PFS, OS and type of *EGFR* mutations was found (*p* = 0.282 and *p* = 0.207, respectively).

3.3. Patients Outcome in Relation to TP53 Mutations

No statistically significant associations were found between *TP53* mutations and ORR and DCR (Table S3). When considering any type of *TP53* mutation with regard to PFS, no association was found; however, significant results were observed considering only *TP53* exon 8 mutations. As previously reported [6], patients with this gene mutation showed a shorter median PFS than non-exon 8 mutated and wild type *TP53* patients: 5.8 months (95% CI: 2.4–10.2) vs. 14.4 (95% CI: 6.7–21.8) and 12.4 (95% CI: 10.0–15.0), respectively (Figure 1A). These patients also showed a poorer OS as compared with the other groups, even though this result was not statistically significant: median OS were 18.53 months (95% CI: 7.3–NR), 34.8 (95% CI: 21.6–NR), 27.3 (95% CI: 20.2–52.9), respectively (Figure 1B).

The presence of *TP53* exon 8 mutation seemed to be associated with a worse prognosis in a similar way in the patients with the different *EGFR* mutations, both in terms of PFS and OS.

In particular, patients with wild type *TP53* exon 8 had a better clinical outcome independently by *EGFR* status: median PFS and OS were 12.9 (95% CI: 10.0–16.3) and 29.7 months (95% CI: 23.0–60.5) for patients with *EGFR* exon 19 deletion vs. 12.4 months (95% CI: 7.9–15.0) and 23.2 months (95% CI: 19.2–63.7) for those with other *EGFR* mutations, respectively; in the subgroup of patients with *TP53* exon 8 mutations, median PFS and OS were 5.8 months (95% CI: 2.5–NR) and 21.9 months (95% CI: 7.3–NR)

for patients with *EGFR* exon 19 deletion vs. 6.4 (95% CI: 2.4–NR) and 18.5 months (95% CI: 7.6–NR) for those with other *EGFR* mutations. In Table S4, the univariate Cox analysis results are reported.
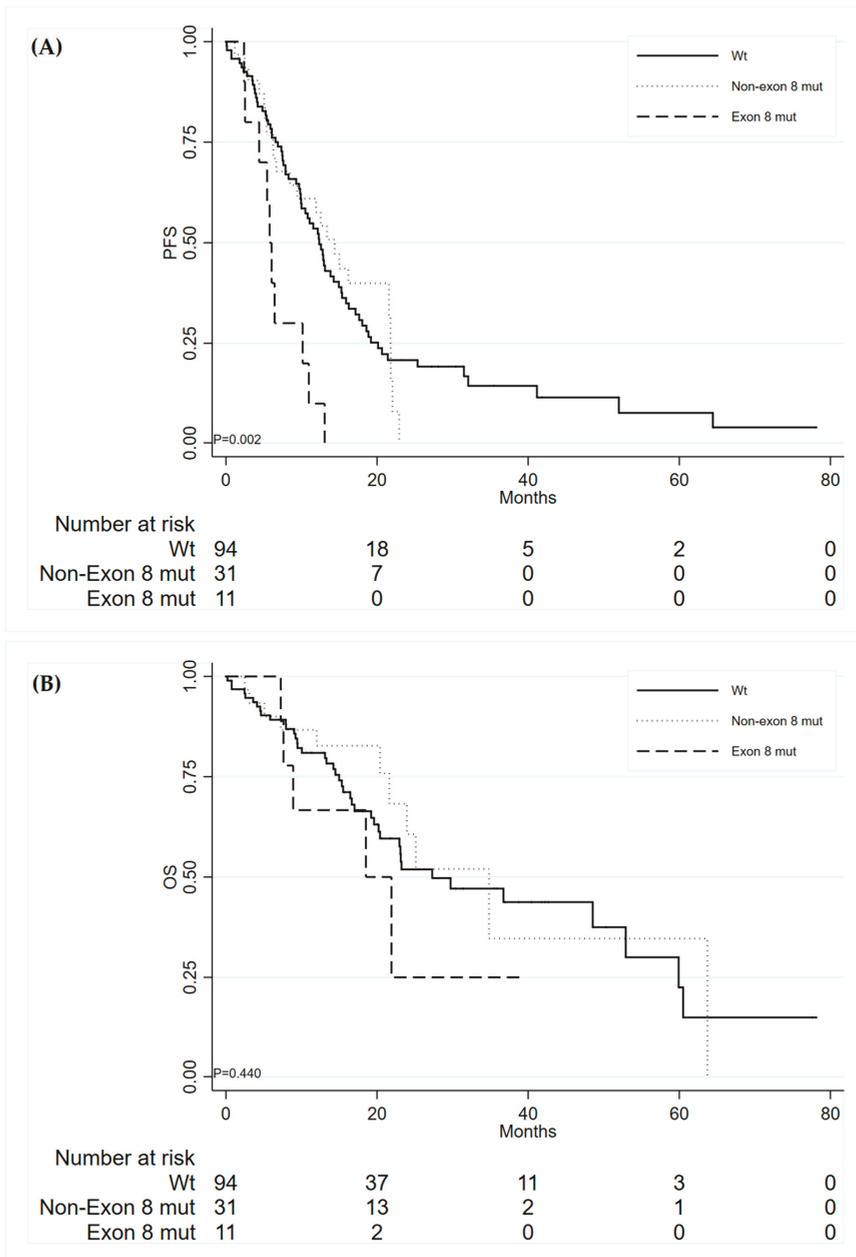
Figure 1. Progression-free survival (**A**) and Overall Survival (**B**) of patients according to *TP53*.

3.4. Multivariate Analysis of the Role of TP53 Mutation: Combined Cohorts of Patients

To obtain a more precise estimate of the effect of *TP53* exon 8 mutation on PFS and OS, and to determine its potential independent role considering other information, a pooled analysis considering either data from our previously analyzed cohort and the one described in the present study, was performed.

The final multivariate model for PFS included both *EGFR* exon 19 deletion as well as TP53 mutation. As soon as the effect of exon 19 deletion on the hazard of disease progression or death is not constant over time, that is, the proportional hazards assumption underlying the Cox model was violated, to obtain a better model fit, this variable was entered into the model with a time-dependent coefficient. Table 3 shows that the effect of exon 19 mutation changes over time, showing a strong protective effect over the first six months that vanishes afterward.

Table 3. Multivariate Cox analysis of progression-free survival (PFS) (*n* = 272).

		PFS	
	HR	**95% CI**	*p*
Exon 19 deletion			
No	1		
Yes			
0–6 months	0.56	(0.35–0.89)	0.014
6–12 months	0.67	(0.40–1.12)	0.123
>12 months	1.27	(0.80–2.03)	0.314
TP53 **exon 8 mutations**			
Wild-type *TP53*	1		
Non-Exon 8 mutations	1.02	0.73–1.42	0.905
Exon 8 mutations	1.81	1.13–2.92	0.014

Adjusting for presence of *EGFR* exon 19 deletion, *TP53* mutations affecting exon 8 demonstrated to be the unique independent negative prognostic factor for PFS (HR 1.81, 95% CI: 1.13–2.92, Table 3). With regard to OS, only deletion in *EGFR* Exon 19 resulted associated to OS, probably due to data from our previous cohort (HR 0.52 (95% CI: 0.26–1.03) for the first 6 months of follow-up, HR 0.44 (95% CI: 0.22–0.90), for successive 6 months, and HR 1.08 (95% CI: 0.72–1.61) after 12 months).

3.5. TP53 Mutations in Relation to Responsiveness to Third Generation TKIs: Combined Cohorts of Patients

Considering both patients' cohorts (*n* = 272 patients), we considered 42 patients who developed a T790M resistance mutation and were treated with third generation TKI osimertinib, in the second or further lines of therapy. Of these, 41 were evaluable for *TP53* mutation status; we found 10 *TP53* mutated patients (24.4%): 3 mutations in exon 5 (30%), 1 in exon 6 (10%), 2 in exon 7 (20%) and 4 in exon 8 (40%). Within the 41 patients with available clinical information, median PFS and OS were 13.86 (95% CI: 5.5–18.53) and 44.38 months (95% CI: 10.64–24.28), respectively. Median PFS of exon 8 *TP53* mutated patients was 2.83 (2.17–NR) months, with respect to a median PFS of 16.79 (5.55–22.31) and 15.28 (1.91–NR) months, for wt *TP53* and patients with mutations in other exons of the gene, respectively (Figure 2A). Even though a good separation, the difference among curves was not statistically significant (*p* = 0.304), due to small numbers of the exon 8 mutated patients. On the other hand, exon 8 *TP53* gene mutations significantly affected the survival of the patients, with a median OS for exon 8 *TP53* mutated patients of 18.53 (7.26–NR) months, with respect to 42.15 (29.43–NR) and 59.92 (29.73–NR) months of patients with mutations in other exons of *TP53* and wt *TP53*, respectively (*p* = 0.044) (Figure 2B). Table 4 shows the univariate hazard ratios for PFS and OS with respect to the presence of *TP53* exon 8 mutation.
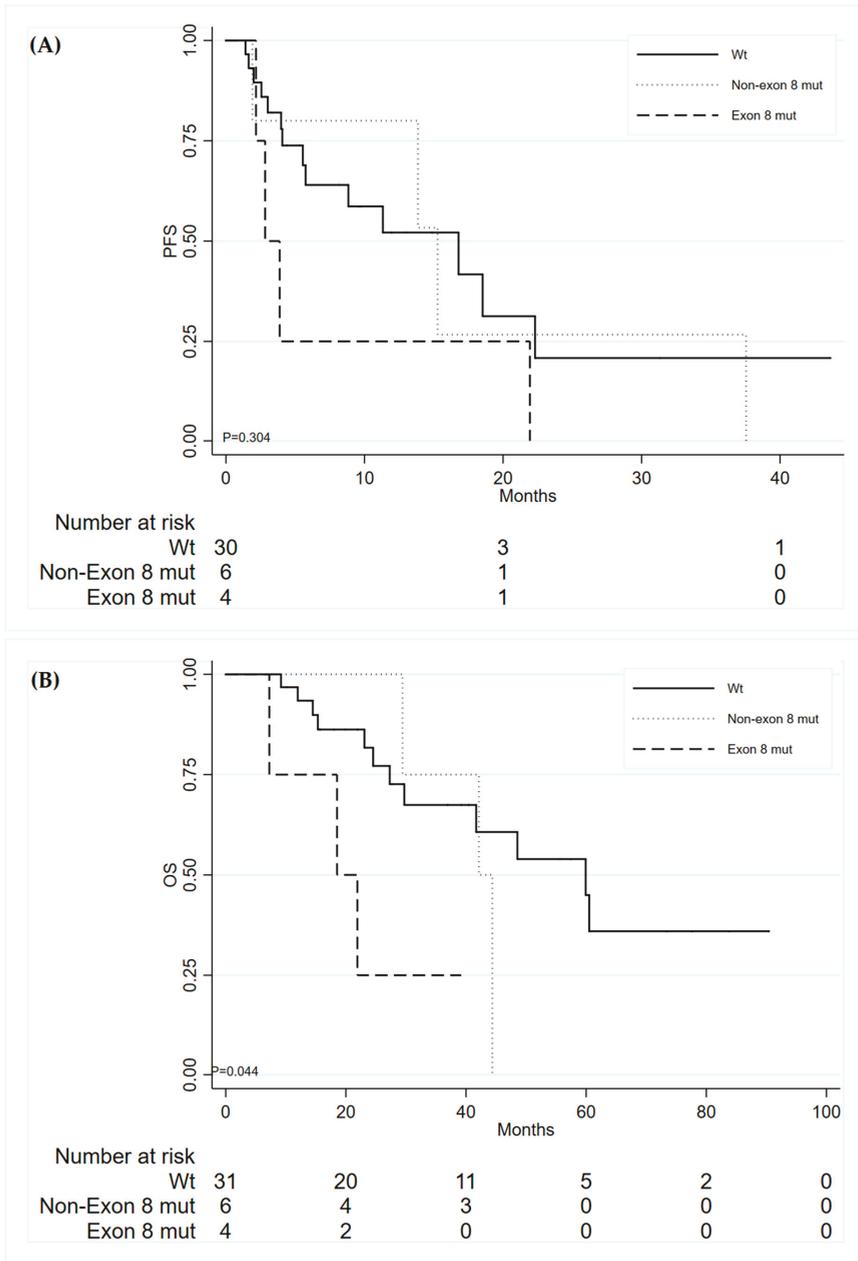
Figure 2. Progression-free survival (**A**) and Overall Survival (**B**) in relation to *TP53* mutations of patients with acquired T790M treated with third generation TKIs.

Table 4. *TP53* mutations in relation to progression-free survival (PFS) and overall survival (OS) of patients receiving osimertinib in second or further lines of treatment.

	PFS			OS		
	HR	**(95% CI)**	*p*	**HR**	**(95% CI)**	*p*
TP53 Exon 8						
Wild type	1			1		
Non-Exon 8 mutations	1.15	(0.37–3.59)	0.811	1.55	(0.42–5.76)	0.514
Exon 8 mutations	2.39	(0.77–7.45)	0.134	4.86	(1.25–18.90)	0.023

4. Discussion

In this study, we analyzed *TP53* mutations in relation to clinical outcome in a large cohort of *EGFR*-mutated NSCLC patients receiving first or second generation TKIs as a first line therapy. Our results confirm that exon 8 *TP53* mutations are associated with a shorter PFS, in all settings of treatment.

Moreover, such a negative effect was also observed in the subgroup of patients treated with third generation after the development of T790M mutation.

Numerous studies demonstrated the role of *TP53* mutations in predicting poor prognosis of advanced NSCLC patients [9,11–15], and this was confirmed also in the subgroup of NSCLC patients carrying *EGFR* mutations [8,9,16]. In particular, different recent studies showed that the concurrent presence of *TP53* mutations negatively affects response to TKIs in *EGFR*-mutated NSCLC patients, suggesting a role for these gene mutations in determining primary resistance to these drugs [6,7,17–20]. *TP53* is the most frequently mutated gene in lung adenocarcinoma, with mutation rates reported up to 55% [13,21–23], with a predominantly clonal expression [24]. In our case series, we found 30% of patients carrying a *TP53* mutation in the exons 5–8, the same percentage we previously reported in an independent case series. It is well known that different *TP53* mutations lead to changes in the P53 protein that may have diverse biological significance [9,10,25], and mutations in the DNA-binding domain (exons 5–8), are frequently associated with gain-of-function properties, resulting in pro-oncogenic features of the P53 protein [26]. In our previous work, we found that exon 8 *TP53* mutations were able to predict worse response to *EGFR* TKIs, especially in the subgroup of patients with *EGFR* exon 19 deletion. In the present study we confirmed the negative prognostic value of *TP53* exon 8 mutation in an independent cohort of *EGFR*-mutated NSCLC treated with both first and second generation TKIs in the first line setting. In the present study, the prognostic value of exon 8 *TP53* mutation was evident independently from the type of *EGFR* mutation. In a combined analysis, we showed that the effect was evident on overall survival in *EGFR*-mutated patients who developed T790M at progression after first line TKIs and osimertinib.

These results, in agreement with those reported by Kim et al. [7], suggest a negative predictive role of *TP53* mutation in all lines of therapy and in relation to all TKIs. Furthermore, our results are consistent with a recent study that found that *TP53* mutations in exon 8 are associated with shorter OS of patients receiving a TKI as a first line treatment [27].

In another study, missense mutations in *TP53* gene resulted in shorter PFS in *EGFR* mutated patients treated with TKIs but showed no associations with PFS and OS in patients undergoing surgical resection [28]. According to Xu et al., who reported *TP53* mutations in 88% of NSCLC *EGFR*-mutated patients that responded for <6 months to an *EGFR* TKIs, with respect to 13% of responders for >24 months [29], our results show a higher rate of *TP53* mutations in non-responders group, with no *TP53* mutated patients in the long responder group.

To investigate the role of *TP53* mutations in predicting clinical outcome of patients treated with third generation TKIs, we considered 42 patients' developed T790M mutation to first line treatment with first or second generation TKI and received a third generation drug in the second or further line of therapy. In this subgroup, we found a diminished PFS in patients carrying *TP53* mutations in exon 8, even though without statistical significance, probably due to the small number of analyzed

patients; exon 8 *TP53* mutated patients had a significantly shorter OS, with respect to wt *TP53* patients and patients with mutations in other exons of *TP53*. This observation is consistent with previous observations, that identified *TP53* mutations (not only in exon 8) as a negative prognostic predictor [7,16]. This result was not confirmed by a study from Labbé et al., that found no differences in ORR of patients treated with third generation TKIs, based on *TP53* mutation status; this could be for the small size of the analyzed case series [28]. In the light of the paradigm shift brought by FLAURA trial [5], there is a need to identify which biomarkers could predict primary resistance to osimertinib as a first line therapy; if confirmed in a larger case series treated with third generation TKI in the first line, these results could help to better stratify patients, suggesting an *EGFR*-independent mechanism of resistance, as others have already highlighted [30].

5. Conclusions

In conclusion, we confirmed that *TP53* exon 8 mutations identify a subgroup of patients with primary resistance to *EGFR* TKIs, and that this is true also in relation to third generation TKIs such as osimertinib. These data suggest that patients with concomitant *EGFR* and exon 8 *TP53* mutations should be candidates for more aggressive therapeutic schemes and should be monitored with a stricter follow-up.

References

1. Rosell, R.; Carcereny, E.; Gervais, R.; Vergnenègre, A.; Massuti, B.; Felip, E.; Palmero, R.; Garcia-Gomez, R.; Pallares, C.; Sanchez, J.M.; et al. Erlotinib versus standard chemotherapy as first-line treatment for European patients with advanced EGFR mutation-positive non-small-cell lung cancer (EURTAC): a multicentre, open-label, randomised phase 3 trial. *Lancet Oncol.* **2012**, *13*, 239–246. [CrossRef]

2. Mok, T.S.; Wu, Y.-L.; Thongprasert, S.; Yang, J.C.-H.; Chu, D.-T.; Saijo, N.; Sunpaweravong, P.; Han, B.; Margono, B.; Ichinose, Y.; et al. Gefitinib or Carboplatin–Paclitaxel in Pulmonary Adenocarcinoma. *N. Engl. J. Med.* **2009**, *361*, 947–957. [CrossRef]

3. Yang, J.C.-H.; Wu, Y.-L.; Schuler, M.; Sebastian, M.; Popat, S.; Yamamoto, N.; Zhou, C.; Hu, C.-P.; O'Byrne, K.; Feng, J.; et al. Afatinib versus cisplatin-based chemotherapy for EGFR mutation-positive lung adenocarcinoma (LUX-Lung 3 and LUX-Lung 6): analysis of overall survival data from two randomised, phase 3 trials. *Lancet Oncol.* **2015**, *16*, 141–151. [CrossRef]

4. Mok, T.S.; Wu, Y.-L.; Ahn, M.-J.; Garassino, M.C.; Kim, H.R.; Ramalingam, S.R.; Shepherd, F.A.; He, Y.; Akamatsu, H.; Theelen, W.S.; et al. Osimertinib or Platinum-Pemetrexed in EGFR T790M-Positive Lung Cancer. *N. Engl. J. Med.* **2016**, *376*, 629–640. [CrossRef]

5. Soria, J.-C.; Ohe, Y.; Vansteenkiste, J.; Reungwetwattana, T.; Chewaskulyong, B.; Lee, K.H.; Dechaphunkul, A.; Imamura, F.; Nogami, N.; Kurata, T.; et al. Osimertinib in UntreatedEGFR-Mutated Advanced Non–Small-Cell Lung Cancer. *N. Engl. J. Med.* **2018**, *378*, 113–125. [CrossRef]

6. Canale, M.; Petracci, E.; Delmonte, A.; Chiadini, E.; Dazzi, C.; Papi, M.; Capelli, L.; Casanova, C.; De Luigi, N.; Mariotti, M.; et al. Impact of TP53 Mutations on Outcome in EGFR-Mutated Patients Treated with First-Line Tyrosine Kinase Inhibitors. *Clin. Cancer Res.* **2016**, *23*, 2195–2202. [CrossRef]

7. Kim, Y.; Lee, B.; Shim, J.H.; Lee, S.-H.; Park, W.-Y.; Choi, Y.-L.; Sun, J.-M.; Ahn, J.S.; Ahn, M.-J.; Park, K. Concurrent Genetic Alterations Predict the Progression to Target Therapy in EGFR-Mutated Advanced NSCLC. *J. Thorac. Oncol.* **2019**, *14*, 193–202. [CrossRef]

8. VanderLaan, P.A.; Rangachari, D.; Mockus, S.M.; Spotlow, V.; Reddi, H.V.; Malcolm, J.; Costa, D.B. Mutations in TP53, PIK3CA, PTEN and other genes in EGFR mutated lung cancers: Correlation with clinical outcomes. *Lung Cancer* **2018**, *106*, 17–21. [CrossRef]

9. Molina-Vila, M.A.; Bertran-Alamillo, J.; Gascó, A.; Mayo-de-las-Casas, C.; Sánchez-Ronco, M.; Pujantell-Pastor, L.; Majem, M. Nondisruptive p53 Mutations Are Associated with Shorter Survival in Patients with Advanced Non–Small Cell Lung Cancer. *Clin. Cancer Res.* **2014**, *2*, 4647–4660. [CrossRef]

10. Poeta, M.L.; Manola, J.; Goldwasser, M.A.; Forastiere, A.; Benoit, N.; Califano, J.A.; Ridge, J.A.; Goodwin, J.; Kenady, D.; Saunders, J.; et al. TP53 mutations and survival in squamous-cell carcinoma of the head and neck. *N. Engl. J. Med.* **2007**, *357*, 2552–2561. [CrossRef]

11. La Fleur, L.; Falk-Sörqvist, E.; Smeds, P.; Berglund, A.; Sundström, M.; Mattsson, J.S.; Brandén, E.; Koyi, H.; Isaksson, J.; Brunnström, H.; et al. Mutation patterns in a population-based non-small cell lung cancer cohort and prognostic impact of concomitant mutations in KRAS and TP53 or STK11. *Lung Cancer* **2019**, *130*, 50–58. [CrossRef]

12. Zhao, J.; Han, Y.; Li, J.; Chai, R.; Bai, C. Prognostic value of KRAS/TP53/PIK3CA in non-small cell lung cancer. *Oncol Lett.* **2019**, *17*, 3233–3240. [CrossRef]

13. Volckmar, A.-L.; Leichsenring, J.; Kirchner, M.; Christopoulos, P.; Neumann, O.; Budczies, J.; De Oliveira, C.M.M.; Rempel, E.; Buchhalter, I.; Brandt, R.; et al. Combined targeted DNA and RNA sequencing of advanced NSCLC in routine molecular diagnostics: Analysis of the first 3,000 Heidelberg cases. *Int. J. Cancer* **2019**, *145*, 649–661. [CrossRef]

14. Jiao, X.-D.; Qin, B.-D.; You, P.; Cai, J.; Zang, Y.-S. The prognostic value of TP53 and its correlation with EGFR mutation in advanced non-small cell lung cancer, an analysis based on cBioPortal data base. *Lung Cancer* **2018**, *123*, 70–75. [CrossRef]

15. Gu, J.; Zhou, Y.; Huang, L.; Ou, W.; Wu, J.; Li, S.; Xu, J.; Feng, J.; Liu, B. TP53 mutation is associated with a poor clinical outcome for non-small cell lung cancer: Evidence from a meta-analysis. *Mol. Clin. Oncol.* **2016**, *5*, 705–713. [CrossRef]

16. Aggarwal, C.; Davis, C.W.; Mick, R.; Thompson, J.C.; Ahmed, S.; Jeffries, S.; Bagley, S.; Gabriel, P.; Evans, T.L.; Bauml, J.M.; et al. Influence of TP53 Mutation on Survival in Patients With Advanced EGFR-Mutant Non–Small-Cell Lung Cancer. *JCO Precis. Oncol.* **2018**, 1–29. [CrossRef]

17. Yu, H.A.; Arcila, M.E.; Rekhtman, N.; Sima, C.S.; Zakowski, M.F.; Pao, W.; Kris, M.; Miller, V.A.; Ladanyi, M.; Riely, G.J. Analysis of tumor specimens at the time of acquired resistance to EGFR-TKI therapy in 155 patients with EGFR-mutant lung cancers. *Clin. Cancer Res.* **2013**, *19*, 2240–2247. [CrossRef]

18. Hou, H.; Qin, K.; Liang, Y.; Zhang, C.; Liu, N.; Jiang, H.; Liu, K.; Zhu, J.; Lv, H.; Li, T.; et al. Concurrent TP53 mutations predict poor outcomes of EGFR-TKI treatments in Chinese patients with advanced NSCLC. *Cancer Manag. Res.* **2019**, *11*, 5665–5675. [CrossRef]

19. Jin, Y.; Shi, X.; Zhao, J.; He, Q.; Chen, M.; Yan, J.; Ou, Q.; Wu, X.; Shao, Y.W.; Yu, X. Mechanisms of primary resistance to EGFR targeted therapy in advanced lung adenocarcinomas. *Lung Cancer* **2018**, *124*, 110–116. [CrossRef]

20. Chen, M.; Xu, Y.; Zhao, J.; Zhong, W.; Zhang, L.; Bi, Y.; Wang, M. Concurrent Driver Gene Mutations as Negative Predictive Factors in Epidermal Growth Factor Receptor-Positive Non-Small Cell Lung Cancer. *EBioMedicine* **2019**, *42*, 304–310. [CrossRef]

21. Comprehensive molecular characterization of gastric adenocarcinoma. *Nature* **2014**, *513*, 202–209. [CrossRef] [PubMed]

22. Corrigendum: Comprehensive molecular profiling of lung adenocarcinoma. *Nature* **2014**, *514*, 262. [CrossRef]

23. Shi, J.; Hua, X.; Zhu, B.; Ravichandran, S.; Wang, M.; Nguyen, C.; Brodie, S.A.; Palleschi, A.; Alloisio, M.; Pariscenti, G.; et al. Somatic Genomics and Clinical Features of Lung Adenocarcinoma: A Retrospective Study. *PLoS Med.* **2016**, *13*, 1–24. [CrossRef] [PubMed]

24. Jamal-Hanjani, M.; Wilson, G.A.; McGranahan, N.; Birkbak, N.J.; Watkins, T.B.; Veeriah, S.; Shafi, S.; Johnson, D.H.; Mitter, R.; Rosenthal, R.; et al. Tracking the Evolution of Non-Small-Cell Lung Cancer. *N. Engl. J. Med.* **2017**, *376*, 2109–2121. [CrossRef]

25. Brosh, R.; Rotter, V. When mutants gain new powers: news from the mutant p53 field. *Nat. Rev. Cancer* **2009**, *9*, 701. [CrossRef]

26. Muller, P.A.J.; Vousden, K.H. P53 mutations in cancer. *Nat. Cell Biol.* **2013**, *15*, 2–8. [CrossRef]

27. Liu, Y.; Xu, F.; Wang, Y.; Wu, Q.; Wang, B.; Yao, Y.; Zhang, Y.; Han-Zhang, H.; Ye, J.; Zhang, L.; et al. Mutations in exon 8 of TP53 are associated with shorter survival in patients with advanced lung cancer. *Oncol. Lett.* **2019**, *18*, 3159–3169. [CrossRef]

28. Labbé, C.; Cabanero, M.; Korpanty, G.J.; Tomasini, P.; Doherty, M.K.; Mascaux, C.; Leighl, N.B. Lung Cancer Prognostic and predictive e ff ects of TP53 co-mutation in patients with EGFR-mutated non-small cell lung cancer (NSCLC). *Lung Cancer* **2017**, *111*, 23–29. [CrossRef]

29. Xu, Y.; Tong, X.; Yan, J.; Wu, X.; Shao, Y.W.; Fan, Y. Short-Term Responders of Non–Small Cell Lung Cancer Patients to EGFR Tyrosine Kinase Inhibitors Display High Prevalence of TP53 Mutations and Primary Resistance Mechanisms. *Transl. Oncol.* **2018**, *11*, 1364–1369. [CrossRef]

30. Leonetti, A.; Sharma, S.; Minari, R.; Perego, P.; Giovannetti, E.; Tiseo, M. Resistance mechanisms to osimertinib in EGFR-mutated non-small cell lung cancer. *Br. J. Cancer* **2019**, *121*, 725–737. [CrossRef]

Article

Prediction of Anti-Cancer Drug-Induced Pneumonia in Lung Cancer Patients: Novel High-Resolution Computed Tomography Fibrosis Scoring

Hiroshi Gyotoku [1], Hiroyuki Yamaguchi [1,*], Hiroshi Ishimoto [1], Shuntaro Sato [2], Hirokazu Taniguchi [1], Hiroaki Senju [1], Tomoyuki Kakugawa [1,3], Katsumi Nakatomi [1], Noriho Sakamoto [1], Minoru Fukuda [1,4], Yasushi Obase [1], Hiroshi Soda [5], Kazuto Ashizawa [4] and Hiroshi Mukae [1]

[1] Department of Respiratory Medicine, Nagasaki University Graduate School of Biomedical Sciences, Nagasaki University, Nagasaki 852-8523, Japan; hirokazu_pc@hotmail.co.jp
[2] Clinical Research Center, Nagasaki University Hospital, Nagasaki 852-8501, Japan
[3] Department of Pulmonology and Gerontology, Yamaguchi University Graduate School of Medicine, Ube 755-0046, Japan
[4] Clinical Oncology Center, Nagasaki University Hospital, Nagasaki 852-8501, Japan
[5] Department of Respiratory Medicine, Sasebo City General Hospital, Nagasaki 857-8511, Japan
* Correspondence: yamaguchi-hiroyuki@umin.ac.jp

Abstract: Background and objective: Pre-existing interstitial lung disease (ILD) in lung cancer patients is considered a risk factor for anti-cancer drug-induced pneumonia; however, a method for evaluating ILD, including mild cases, has not yet been established. We aimed to elucidate whether the quantitative high-resolution computed tomography fibrosis score (HFS) is correlated with the risk of anti-cancer drug-induced pneumonia in lung cancer patients, even in those with mild pre-existing ILD. Methods: The retrospective single-institute study cohort comprised 214 lung cancer patients who underwent chemotherapy between April 2013 and March 2016. The HFS quantitatively evaluated the grade of pre-existing ILD. We extracted data regarding age, sex, smoking history, and coexisting factors that could affect the incidence of anti-cancer drug-induced pneumonia. Cox proportional hazard models were used to analyze the effects of the HFS and other factors on the risk of anti-cancer drug-induced pneumonia. Results: Pre-existing ILD was detected in 61 (29%) of 214 patients, while honeycombing and traction bronchiectasis were observed in only 15 (7.0%) and 10 (4.7%) patients, respectively. Anti-cancer drug-induced pneumonia developed in 19 (8.9%) patients. The risk of anti-cancer drug-induced pneumonia increased in proportion to the HFS (hazard ratio, 1.16 per point; 95% confidence interval, 1.09–1.22; $p < 0.0001$). Conclusions: The quantitative HFS was correlated with the risk of developing anti-cancer drug-induced pneumonia in lung cancer patients, even in the absence of honeycombing or traction bronchiectasis. The quantitative HFS may lead to better management of lung cancer patients with pre-existing ILD.

Keywords: lung cancer; interstitial lung disease; pulmonary fibrosis; radiology and other imaging

1. Introduction

Anti-cancer drug-induced pneumonia is a potentially fatal disease in lung cancer patients. Pre-existing chronic interstitial lung disease (ILD) is considered a risk factor for anti-cancer drug-induced pneumonia, as is being male, being elderly, having a poor Eastern Cooperative Oncology Group performance status (ECOG-PS), a history of smoking, and low forced vital capacity [1–4]. The American Thoracic Society/European Respiratory Society/Japanese Respiratory Society/Latin American Thoracic

Association guidelines for the classification of idiopathic interstitial pneumonia (IIP) are often employed for evaluating ILD [5–7]. Several clinical trials of anti-cancer drugs have included lung cancer patients with ILD, which was evaluated according to the IIP guidelines [8–12].

However, the IIP guidelines do not include and evaluate mild pre-existing ILD without honeycombing or traction bronchiectasis. The 2018 idiopathic pulmonary fibrosis (IPF) guidelines define mild ILD as "indeterminate for usual interstitial pneumonia (UIP) HRCT pattern" [13]. Nevertheless, few studies regarding anti-cancer drug-induced pneumonia have referred to mild pre-existing ILD [1,2]. Thus, a quantitative method for evaluating pre-existing ILD, including mild ILD, has not yet been established.

The quantitative high-resolution computed tomography (HRCT) scores of acute interstitial pneumonia and acute respiratory distress syndrome (ARDS) have been reported to correlate with pathology and prognosis [14–17]. The HRCT fibrosis score (HFS) was modified from this score in order to evaluate lung fibrosis easily, with an increased HFS over the course of 6 months indicating poor prognosis [18]. We hypothesized that the HFS could reflect the degree of the lung fibrosing process, resulting in the exact evaluation of the risk of anti-cancer drug-induced pneumonia in lung cancer patients with pre-existing ILD. This retrospective cohort study was designed to determine whether the quantitative HFS correlates with the risk of anti-cancer drug-induced pneumonia in lung cancer patients, including those with mild pre-existing ILD.

2. Methods

2.1. Study Design

This retrospective, single-institute, cohort study was performed at the Department of Respiratory Medicine, Nagasaki University Hospital. Patients were enrolled based on the following three inclusion criteria: admitted to our department between April 2013 and March 2016; pathologically diagnosed with lung cancer; and receiving anti-cancer drugs, including cytotoxic drugs and molecular-target agents. Patients were excluded from the analysis if they irregularly received adjuvant chemotherapy with oral tegafur–uracil alone or if >50% of the lung fields could not be evaluated primarily due to the extensive cancer lesions or postoperative status.

Eligible patients were extracted from lung cancer patients using the hospital's electronic medical record system. Anti-cancer drugs were administered in various clinical conditions, including conventional or adjuvant chemotherapy, and concurrent or sequential radiotherapy. All patients were followed up with until December 2017. A systemic follow-up survey of the lesions was performed by physical examination, chest radiography, and blood tests at least once a month. Chest HRCT was routinely conducted as scheduled for outpatient follow-up. The censored cases were defined as death, transferring hospital, lost to follow-up, or the initiation of immune checkpoint inhibitors.

2.2. Chest HRCT Scoring System

HRCT (Aquilion ONE^{TM}, Canon Medical Systems, Ohtawara, Japan) scans were obtained with 0.5 mm collimation and a 1 mm slice thickness at 1 mm intervals from the lung apices to the bases in the supine position at full inspiration. Two experienced pulmonologists (H.G. and H.I. with 11 and 19 years of experience, respectively), who were blinded to the clinical data, individually assessed the degree of pre-existing ILD using the HFS.

In detail, the HFS was calculated in three areas of each lung before the first administration of anti-cancer drugs: the level of the carina, the level of the right inferior pulmonary vein, and the middle of the two levels. First, the HRCT findings were scored as follows: normal attenuation (score 1), reticular abnormality (score 2), both reticular abnormality and traction bronchiectasis (score 3), and honeycombing (score 4). We did not evaluate extensive pure ground glass opacity, and we organized the lesions after pneumonia, operation, and radiotherapy. Second, the extent of the interstitial

abnormalities was estimated as the percentage of the 5% intervals. We multiplied the score and the extent percentage and summed the points for each of the six areas. Finally, we averaged the summed points of the six areas. ILD was categorized as no ILD (HFS = 100), mild ILD (HFS = 101–200), moderate ILD (HFS = 201–300), and severe ILD (HFS = 301–400).

Furthermore, the two independent pulmonologists also evaluated the degree of emphysema using the Goddard score (GS) for the six areas analyzed above [19]. The extent of LAA (low-attenuation areas) was scored as follows: < 5% LAA (score of 0), 6%–25% LAA (score of 1), 26%–50% LAA (score of 2), 51%–75% (score of 3), and > 75% LAA (score of 4). The six scores were summed, and emphysema was graded as no emphysema (GS = 0), mild emphysema (GS = 1–7), moderate emphysema (GS = 8–15), and severe emphysema (GS = 16–24).

2.3. Examples of HFS and GS in Lung Cancer Patients with Pre-Existing ILD

Two representative patients were evaluated using the HFS (Figure 1). Regarding the HFS, Patient A scored 104 points, and patient B scored 122.5 points. The details are provided in Figure 1. Regarding the GS, patient A scored 0 points according to the two pulmonologists. Patient B was awarded 18 points by Dr. H.G. Each of six lung fields was evaluated as score 3; $3 \times 6 = 18$. In contrast, Patient B was awarded 15 points by Dr. H.I. Overall, patient B received an average GS of 16.5, indicating severe emphysema.
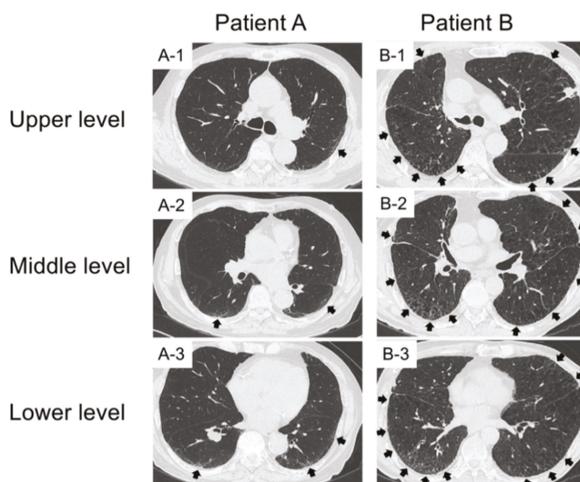
Figure 1. Imaging findings in two representative patients evaluated using the high-resolution computed tomography fibrosis score. The black arrows indicate reticular abnormality (score 2). Patient A scored 104 points, and patient B scored 122.5 points. The scoring of each patient was as follows: Patient A scored 105 points, as evaluated by Dr. H.G. In detail, the (**A-1**) right field was evaluated as 100% of score 1; $100 \times 1 = 100$. The A-1 left, (**A-2**) right, (**A-2**) left, and (**A-3**) right fields were evaluated as 95% of score 1 and 5% of score 2; $(95 \times 1) + (5 \times 2) = 105$. The (**A-3**) left field was evaluated as 90% of score 1 and 10% of score 2; $(90 \times 1) + (10 \times 2) = 110$. Thus, the HFS was $(100 \times 1 + 105 \times 4 + 110 \times 1)/6 = 105$. In contrast, patient A scored 103 points, as evaluated by Dr. H.I. Overall, patient A received an average high-resolution computed tomography fibrosis score (HFS) of 104. Patient B scored 125 points, as evaluated by Dr. H.G. In detail, the (**B-1**) left were evaluated as 80% of score 1 and 20% of score 2; $(80 \times 1) + (20 \times 2) = 120$. The (**B-1**) right, (**B-2**) right and left, and (**B-3**) left were evaluated as 75% of score 1 and 25% of score 2; $(75 \times 1) + (25 \times 2) = 125$. The (**B-3**) right was evaluated as 70% of score 1 and 30% of score 2; $(70 \times 1) + (30 \times 2) = 130$. Thus, the HFS was $(120 \times 1 + 125 \times 4 + 130 \times 1)/6 = 125$. In contrast, patient B scored 120 points, as evaluated by Dr. H.I. Overall, patient A received an average HFS of 122.5.

2.4. Anti-Cancer Drug-Induced Pneumonia

The definition of anti-cancer drug-induced pneumonia was interstitial lung disease developed from anti-cancer drug exposure to 60 days after the final anti-cancer treatment. We determined the diagnosis based on clinical and radiological findings and excluded apparent pulmonary infection, radiation-induced lung injury, and heart failure. The evaluation of anti-cancer drug-induced pneumonia was defined according to the Common Terminology Criteria for Adverse Events (CTCAE) version 4.0 from the National Cancer Institute (Bethesda, MD) [20]. The time to onset of anti-cancer drug-induced pneumonia was defined as the interval between the first administration of anti-cancer drugs and the diagnosis of anti-cancer drug-induced pneumonia.

2.5. Clinical Data Collection

We collected other clinical data, including age; sex; ECOG-PS; smoking history; tumor histology; clinical stage; epidermal growth factor receptor mutations; anaplastic lymphoma kinase rearrangements; and previous chemotherapy, thoracic surgery, and thoracic radiation.

2.6. Statistical Analysis

The inter-observer variations in the HFS and GS were assessed using intra-class correlation coefficients (ICC). The prevalence of pre-existing ILD and anti-cancer drug-induced pneumonia was accompanied by 95% confidence intervals (CIs), and the difference was evaluated by chi-square test. The cumulative incidence of anti-cancer drug-induced pneumonia, which was stratified by HFS of >110, 110 ≥ HFS > 100, and HFS = 100, was assessed via the Kaplan–Meier method and the trend log-rank test. We evaluated the hazard ratio (HR) and 95% CI of each potential risk factor for anti-cancer drug-induced pneumonia by simple Cox proportional hazard analysis. We selected variables according to a literature review and clinical expertise. We confirmed whether HFS (per point) may be affected by another potential risk factor using replaced multiple Cox proportional hazards analyses.

The plotting of Kaplan–Meier curves and the trend log-rank test were conducted using GraphPad Prism version 7 (GraphPad Software Inc., La Jolla, CA, USA). The other statistical analyses were performed using JMP pro version 14 (SAS Institute, Cary, NC, USA). A two-tailed *p* value of < 0.05 was considered statistically significant.

2.7. Ethical Considerations

This study was performed in accordance with the Declaration of Helsinki. The institutional review board of Nagasaki University Hospital approved this study protocol (approval number 17032713-3). Informed consent was obtained from the patients by an opt-out system on the hospital website, in accordance with the ethical guideline presented by the Ministry of Health, Labor, and Welfare in Japan. This trial was registered with the University Hospital Medical Information Network in Japan (UMIN), registry number UMIN000026964.

3. Results

3.1. Patient Characteristics and HFS

A total of 214 lung cancer patients were extracted and analyzed from 1280 patients with respiratory diseases (Figure 2). The study population was composed of approximately 70% males and ever smokers (Table 1). The inter-observer agreement on the HRCT findings was high for the HFS (ICC = 0.96) and GS (ICC = 0.97) between the two pulmonologists. The prevalence of pre-existing ILD was 28.5% (61/214 cases; 95% CI, 22.5–34.5) in lung cancer patients undergoing anti-cancer drug therapy. Incidentally, all pre-existing ILDs scored by the HFS were mild grade. Honeycombing and traction bronchiectasis were observed in only 15 (7.0%) and 10 (4.7%) of 214 cases, respectively.

```
┌─────────────────────────────────────┐
│ Admitted our respiratory medicine    │
│ department from April 2013 to        │
│ March 2016 (n = 1280)                │
└─────────────────────────────────────┘
          │        ┌──────────────────────────────────────────┐
          │        │ · Infectious disease (n = 396)            │
          │        │ · Diffuse alveolar disease (n = 211)      │
          ├────────│ · Sarcoidosis (n = 68)                    │
          │        │ · Allergic disease (n = 30)               │
          │        │ · Others (n = 76)                         │
          │        └──────────────────────────────────────────┘
┌─────────────────────────────┐
│ Thoracic tumor disease       │
│ (n = 499)                    │
└─────────────────────────────┘
          │        ┌──────────────────────────────────────────┐
          │        │ · Other oncology (n = 78)                 │
          ├────────│ · Benign tumor (n = 15)                   │
          │        │ · Lung cancer suspected (n = 15)          │
          │        └──────────────────────────────────────────┘
┌─────────────────────────────┐
│ Lung cancer                  │
│ (n = 391)                    │
└─────────────────────────────┘
          │        ┌──────────────────────────────────────────┐
          │        │ · Operation only (n = 74)                 │
          │        │ · Radiation only (n = 33)                 │
          ├────────│ · Best supportive care only (n = 49)      │
          │        │ · Hospital transfer before undergoing     │
          │        │   anti-caner drugs (n = 6)                │
          │        └──────────────────────────────────────────┘
┌───────────────────────────────────────────────┐
│ Underwent anti-cancer drugs (cytotoxic          │
│ anticancer drugs and molecular-target drugs)    │
│ (n = 229)                                       │
└───────────────────────────────────────────────┘
          │        ┌──────────────────────────────────────────┐
          ├────────│ · Not evaluated (n = 2)                   │
          │        │ · Underwent tegafur-uracil only (n = 13)  │
          │        └──────────────────────────────────────────┘
┌─────────────────────────────┐
│ Analysis                     │
│ (n = 214)                    │
└─────────────────────────────┘
```

Figure 2. Study flow diagram.

Table 1. Characteristics of lung cancer patients who underwent anti-cancer drugs.

	Total (*n* = 214)
Age, range	67 (25–85)
Gender	
Male	144 (67%)
Female	70 (33%)
Smoking history	
Ever-smoker	148 (69%)
Never-smoker	66 (31%)
ECOG-PS	
0–1	209 (98%)
2–4	5 (2%)
Histology	
Adenocarcinoma	136 (64%)
Squamous cell carcinoma	35 (16%)
Small-cell lung cancer	31 (14%)
Others	12 (6%)
Clinical stage	
I	4 (2%)
II	14 (7%)
III	53 (25%)
IV, Recurrence	143 (67%)
Genetic abnormalities	
Wild type	151 (71%)
EGFR mutations	56 (26%)
ALK rearrangements	7 (3%)
GS	
Normal	93 (43%)
Mild	77 (36%)
Moderate	36 (17%)
Severe	8 (4%)

ECOG-PS, Eastern Cooperative Oncology Group performance status; EGFR, epidermal growth factor receptor; ALK, anaplastic lymphoma kinase; GS, Goddard score.

The prevalence of anti-cancer drug-induced pneumonia was 8.9% (19/214 cases; 95% CI: 5.0–12.8). Anti-cancer drug-induced pneumonia was likely to develop in patients with pre-existing ILD (Figure 3). Although anti-cancer drug-induced pneumonia occurred twice in two patients with mild ILD, we analyzed the first event only. The prevalence of anti-cancer drug-induced pneumonia was 24.6% (15/61 cases; 95% CI, 13.9–35.3) in patients with pre-existing ILD, and 2.6% (4/153 cases; 95% CI, −0.4–5.6) in those without ILD. The development of anti-cancer drug-induced pneumonia was more frequent in patients with pre-existing ILD than in those without ILD ($p < 0.0001$).
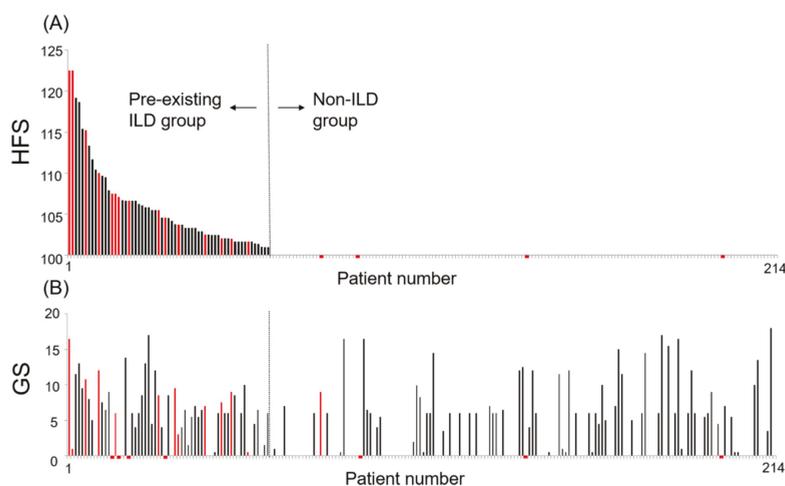
Figure 3. Bar graph of the incidence of anti-cancer drug induced pneumonia according to the high-resolution computed tomography fibrosis score and Goddard score. (**A**) Relationship between the high-resolution computed tomography fibrosis score (HFS) and the development of anti-cancer drug-induced pneumonia in 214 patients with lung cancer. The red bars represent the patients with anti-cancer drug-induced pneumonia, and the black bars represent those without. An HFS of >100 indicates the presence of pre-existing interstitial lung disease (ILD). (**B**) Relationship between the Goddard score (GS) and the development of anti-cancer drug-induced pneumonia in lung cancer patients. The red and black bars are defined as described above. Each pair of upper and lower panels represents the same patient.

3.2. Potential Risk Factors of Anti-Cancer Drug-Induced Pneumonia

The cumulative risk of anti-cancer drug-induced pneumonia was significantly increased in patients with a higher HFS ($p < 0.0001$, Figure 4). The simple Cox proportional hazard analysis showed a risk factor for anti-cancer drug-induced pneumonia (Table 2A); a high HFS and being male were significant risk factors for anti-cancer drug-induced pneumonia. The HFS in particular was a prominent risk factor; an increase of one HFS point was associated with a 16% increased risk of developing anti-cancer drug-induced pneumonia (HR, 1.16; 95% CI, 1.09–1.22; $p < 0.001$). Smoking history and high GS (indicating severe emphysema) were not associated with a risk of anti-cancer drug-induced pneumonia. The robustness of the HFS as a risk factor remained constant in the replaced multiple Cox proportional hazard analyses of other potential risk factors (Table 2B). A multivariate Cox proportional hazard analysis was not performed, because the simple and replaced multiple Cox proportional hazards analyses revealed that the HFS was a prominent risk factor of anti-cancer drug-induced pneumonia.
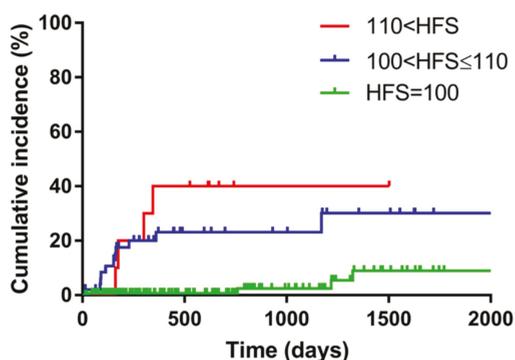
Figure 4. Kaplan–Meier estimated curves of the incidence of anti-cancer drug-induced pneumonia stratified by the high-resolution computed tomography fibrosis score. The Kaplan–Meier estimated curves indicated that the incidence of anti-cancer drug-induced pneumonia is increased in patients with higher high-resolution computed tomography fibrosis scores (HFSs) ($p < 0.0001$ according to the log-rank test).

Table 2. (**A**) Potential risk factors for anti-cancer drug induced pneumonia ($n = 214$) by the simple Cox proportional hazards analysis. (**B**) Influence of other clinical factors to the hazard ratio of HFS by the simple and replaced multiple Cox proportional hazards analyses.

	HR	95% CI	*p*-value
Age			
< 70	1.00		
≥ 70	1.37	0.51–3.42	0.51
Gender			
Female	1.00		
Male	3.29	1.09-14.18	0.034
ECOG-PS			
0–1	1.00		
2–4	3.61	0.20–17.67	0.30
Histology			
Adenocarcinoma	1.00		
Squamous-cell carcinoma	0.70	0.11–2.53	0.62
Small-cell carcinoma	0.72	0.11–2.62	0.65
Others	1.03	0.06–5.22	0.97
Clinical Stage			
I–II	n/c		
III	1.00		
IV, Recurrence	0.91	0.36–2.60	0.86

Table 2. *Cont.*

	HR	95% CI	*p*-value
Smoking history			
No	1		
Yes	2.97	0.99-12.80	0.053
Genetic abnormalities [†]			
No	1		
Yes	0.65	0.21–1.73	0.40
GS (per point)	1.06	0.97–1.15	0.20
HFS (per point)	1.16	1.09–1.22	< 0.0001
Operation			
No	1		
Yes	0.49	0.16–1.30	0.16
Radiation			
No	1		
Yes	1.66	0.66–4.14	0.28

(A) [†] Gene abnormalities includes anaplastic lymphoma kinase (ALK) and epidermal growth factor receptor (EGFR). HR, hazard ratio; CI, confidence interval; ECOG-PS, Eastern Cooperative Oncology Group performance status; n/c, not calculated; GS, Goddard score; HFS, HRCT fibrosis score.

	HFS		
Variables	**HR**	**95% CI**	***p***
Simple HFS	1.16	1.09–1.22	< 0.0001
Replaced multiple Variable to adjust the effect of HFS			
Age	1.15	1.08–1.22	<0.0001
Gender	1.14	1.07–1.21	0.0002
ECOG-PS	1.16	1.09–1.22	<0.0001
Histology	1.16	1.09–1.23	<0.0001
Clinical stage	1.15	1.08–1.22	<0.0001
Smoking history	1.15	1.08–1.22	0.0001
Gene abnormalities	1.16	1.08–1.23	<0.0001
GS	1.16	1.08–1.23	<0.0001
Operation	1.16	1.09–1.22	<0.0001
Radiation	1.16	1.09–1.23	<0.0001

(B) HFS, HRCT fibrosis score; HR, hazard ratio; CI, confidence interval; ECOG-PS, Eastern Cooperative Oncology Group performance status; GS, Goddard score.

3.3. Characteristics of Patients with Anti-Cancer Drug-Induced Pneumonia

The characteristics of the 19 patients with anti-cancer drug-induced pneumonia are listed in Table S1. Although previous radiotherapy did not confer a risk for anti-cancer drug-induced pneumonia (Table 2A), 10 of 19 these patients had received radiotherapy. The development of radiological interstitial abnormalities in the ten patients did not correspond to the exposure to radiation. The HFS did not correlate with the grade of anti-cancer drug-induced pneumonia. Specific regimens were not associated with the risk of anti-cancer drug-induced pneumonia.

4. Discussion

To the best of our knowledge, the present study is the first to provide the following important findings. The quantitative HFS is positively correlated with the risk of anti-cancer drug-induced pneumonia in lung cancer patients. In particular, the HFS was associated with a risk of anti-cancer

drug-induced pneumonia in patients with mild pre-existing ILD, even in the absence of honeycombing or traction bronchiectasis.

The current IIP guidelines do not assess the severity of pre-existing ILD, particularly mild ILD. IPF diagnosed using the IIP guidelines was observed in 2%–8% of lung cancer patients [21–23]. In contrast, 28.5% of lung cancer patients that were administered anti-cancer drugs had mild pre-existing ILD confirmed by the HFS in the present study. In two computed tomography lung cancer screening trials that defined the patterns of mild interstitial lung abnormalities, ILD was detected in 15.7%–21.2% of patients with a history of smoking [24,25]. Since the IIP guidelines do not necessarily consider the radiological process of pulmonary fibrosis, mild ILD may have been overlooked. Precise evaluation of the risk of anti-cancer drug-induced pneumonia requires a quantitative method capable of detecting all levels of ILD, including mild ILD.

In the present study, the quantitative HFS was significantly correlated with the risk of anti-cancer drug-induced pneumonia. Little is known of the relationship between anti-cancer drugs and mild pre-existing ILD [1,2]. A nested case-control study investigated the risk factors for pre-existing ILD associated with chemotherapy and gefitinib [1]. Although this study referred to the severity of ILD, including mild grade, the severity was not clearly defined. The adjusted odds ratios indicated that patients with mild and moderate–severe ILD had an approximately five-fold increased risk of developing acute ILD compared to patients without ILD, suggesting no difference between mild and moderate–severe ILD. Another prospective cohort study identified the risk factors for pre-existing ILD associated with erlotinib [2]. This study evaluated only the extent of interstitial abnormalities, but not the fibrous pattern on HRCT. The study population of patients with pre-existing ILD predominantly comprised patients with mild ILD, in which abnormalities involved <5% of the bilateral lower lobes. The multivariate logistic regression analysis yielded an odds ratio of 4.0 (95% CI, 1.3–12.1) between the presence and absence of ILD. Thus, the present study first revealed that an increase of HFS point was associated with a 16% increased risk of anti-cancer drug-induced pneumonia, even in mild ILD without honeycombing and traction bronchiectasis.

Pre-existing mild ILD might induce drug-induced pneumonia because a histological UIP pattern may be involved. The 2018 IPF guidelines categorize mild ILD as an indeterminate for the UIP HRCT pattern (early UIP pattern) [13]. This category includes the subset of patients with reticular patterns in the absence of honeycombing and traction bronchiectasis, predominantly in the subpleural and basal fields. Lung cancer patients with UIP HRCT patterns exhibited exacerbation of ILD more frequently than did those with non-UIP HRCT patterns [3]. In precision medicine, many novel anti-cancer drugs have been developed, some of which are likely to cause drug-induced pneumonia. The early recognition of the subtle fibrosing findings on HRCT may enable physicians to provide better management of lung cancer patients receiving anti-cancer drugs.

The present study had several limitations. First, all cases of pre-existing ILD incidentally included mild cases. Thus, we did not necessarily verify the utility of the HFS for moderate and severe ILD. However, a previous case-control study revealed that the odds ratio of the development of anti-cancer drug-induced pneumonia was high in patients with moderate/severe pre-existing ILD as well as those with mild ILD [1]. Second, the pulmonary function test results could not be evaluated, due to missing values in clinical practice. Another quantitative HRCT scoring system has been replaced by the diffusion capacity of carbon monoxide test for the prognosis with IPF patients [26]. Third, this was a single institutional analysis, and the number of anti-cancer drug-induced pneumonia cases was small. The present findings are therefore potentially subject to selection bias. Further prospective investigations involving large cohorts are required to confirm our findings.

In conclusion, HFS may correlate with the risk of anti-cancer drug-induced pneumonia in lung cancer patients, even in the absence of honeycombing or traction bronchiectasis. This quantitative HFS could be a predictor of anti-cancer drug-induced pneumonia, which could improve the management of lung cancer patients with ILD.

References

1. Kudoh, S.; Kato, H.; Nishiwaki, Y.; Fukuoka, M.; Nakata, K.; Ichinose, Y.; Tsuboi, M.; Yokota, S.; Nakagawa, K.; Suga, M.; et al. Interstitial Lung Disease in Japanese Patients with Lung Cancer. *Am. J. Respir. Crit. Care Med.* **2008**, *177*, 1348–1357. [CrossRef] [PubMed]

2. Johkoh, T.; Sakai, F.; Kusumoto, M.; Arakawa, H.; Harada, R.; Ueda, M.; Kudoh, S.; Fukuoka, M. Association Between Baseline Pulmonary Status and Interstitial Lung Disease in Patients With Non–Small-Cell Lung Cancer Treated With Erlotinib—A Cohort Study. *Clin. Lung Cancer* **2014**, *15*, 448–454. [CrossRef] [PubMed]

3. Kenmotsu, H.; Naito, T.; Kimura, M.; Ono, A.; Shukuya, T.; Nakamura, Y.; Tsuya, A.; Kaira, K.; Murakami, H.; Takahashi, T.; et al. The Risk of Cytotoxic Chemotherapy-Related Exacerbation of Interstitial Lung Disease with Lung Cancer. *J. Thorac. Oncol.* **2011**, *6*, 1242–1246. [CrossRef] [PubMed]

4. Kobayashi, H.; Naito, T.; Omae, K.; Omori, S.; Nakashima, K.; Wakuda, K.; Ono, A.; Kenmotsu, H.; Murakami, H.; Endo, M.; et al. ILD-NSCLC-GAP index scoring and staging system for patients with non-small cell lung cancer and interstitial lung disease. *Lung Cancer* **2018**, *121*, 48–53. [CrossRef] [PubMed]

5. American Thoracic, S.; European Respiratory, S. American Thoracic Society/European Respiratory Society International Multidisciplinary Consensus Classification of the Idiopathic Interstitial Pneumonias. This joint statement of the American Thoracic Society (ATS), and the European Respiratory Society (ERS) was adopted by the ATS board of directors, June 2001 and by the ERS Executive Committee, June 2001. *Am. J. Respir. Crit. Care Med.* **2002**, *165*, 277–304.

6. Raghu, G.; Collard, H.R.; Egan, J.J.; Martinez, F.J.; Behr, J.; Brown, K.K.; Colby, T.V.; Cordier, J.F.; Flaherty, K.R.; Lasky, J.A.; et al. An official ATS/ERS/Japanese Respiratory Society (JRS)/ Latin American Thoracic Association (ALAT) statement: Idiopathic pulmonary fibrosis: Evidence-based guidelines for diagnosis and management. *Am. J. Respir. Crit. Care Med.* **2011**, *183*, 788–824. [CrossRef]

7. Travis, W.D.; Costabel, U.; Hansell, D.M.; King, T.E.; Jr Lynch, D.A.; Nicholson, A.G.; Ryerson, C.J.; Ryu, J.H.; Selman, M.; Wells, A.U.; et al. An official ATS/ERS statement: Update of the international multidisciplinary classification of the idiopathic interstitial pneumonias. *Am. J. Respir. Crit. Care Med.* **2013**, *188*, 733–748. [CrossRef]

8. Minegishi, Y.; Sudoh, J.; Kuribayasi, H.; Mizutani, H.; Seike, M.; Azuma, A.; Yoshimura, A.; Kudoh, S.; Gemma, A. The safety and efficacy of weekly paclitaxel in combination with carboplatin for advanced non-small cell lung cancer with idiopathic interstitial pneumonias. *Lung Cancer* **2011**, *71*, 70–74. [CrossRef]

9. Minegishi, Y.; Kuribayashi, H.; Kitamura, K.; Mizutani, H.; Kosaihira, S.; Okano, T.; Seike, M.; Azuma, A.; Yoshimura, A.; Kudoh, S.; et al. The Feasibility Study of Carboplatin Plus Etoposide for Advanced Small Cell Lung Cancer with Idiopathic Interstitial Pneumonias. *J. Thorac. Oncol.* **2011**, *6*, 801–807. [CrossRef]

10. Sekine, A.; Satoh, H.; Baba, T.; Ikeda, S.; Okuda, R.; Shinohara, T.; Komatsu, S.; Hagiwara, E.; Iwasawa, T.; Ogura, T.; et al. Safety and efficacy of S-1 in combination with carboplatin in non-small cell lung cancer patients with interstitial lung disease: A pilot study. *Cancer Chemother. Pharmacol.* **2016**, *77*, 1245–1252. [CrossRef]

11. Yasuda, Y.; Hattori, Y.; Tohnai, R.; Ito, S.; Kawa, Y.; Kono, Y.; Urata, Y.; Nogami, M.; Takenaka, D.; Negoro, S.; et al. The safety and efficacy of carboplatin plus nanoparticle albumin-bound paclitaxel in the treatment of non-small cell lung cancer patients with interstitial lung disease. *Jpn. J. Clin. Oncol.* **2017**, *48*, 89–93. [CrossRef] [PubMed]

12. Shimizu, R.; Fujimoto, D.; Kato, R.; Otoshi, T.; Kawamura, T.; Tamai, K.; Matsumoto, T.; Nagata, K.; Otsuka, K.; Nakagawa, A.; et al. The safety and efficacy of paclitaxel and carboplatin with or without bevacizumab for treating patients with advanced nonsquamous non-small cell lung cancer with interstitial lung disease. *Cancer Chemother. Pharmacol.* **2014**, *74*, 1159–1166. [CrossRef] [PubMed]

13. Raghu, G.; Remy-Jardin, M.; Myers, J.L.; Richeldi, L.; Ryerson, C.J.; Lederer, D.; Behr, J.; Cottin, V.; Danoff, S.K.; Morell, F.; et al. Diagnosis of Idiopathic Pulmonary Fibrosis. An Official ATS/ERS/JRS/ALAT Clinical Practice Guideline. *Am. J. Respir. Crit. Care Med.* **2018**, *198*, e44–e68. [CrossRef] [PubMed]

14. Ichikado, K.; Johkoh, T.; Ikezoe, J.; Takeuchi, N.; Kohno, N.; Arisawa, J.; Nakamura, H.; Nagareda, T.; Itoh, H.; Ando, M. Acute interstitial pneumonia: High-resolution CT findings correlated with pathology. *Am. J. Roentgenol.* **1997**, *168*, 333–338. [CrossRef]

15. Ichikado, K.; Suga, M.; Gushima, Y.; Johkoh, T.; Iyonaga, K.; Yokoyama, T.; Honda, O.; Shigeto, Y.; Tomiguchi, S.; Takahashi, M.; et al. Hyperoxia-induced Diffuse Alveolar Damage in Pigs: Correlation between Thin-Section CT and Histopathologic Findings. *Radiology* **2000**, *216*, 531–538. [CrossRef]

16. Ichikado, K.; Suga, M.; Müller, N.L.; Taniguchi, H.; Kondoh, Y.; Akira, M.; Johkoh, T.; Mihara, N.; Nakamura, H.; Takahashi, M.; et al. Acute Interstitial Pneumonia. *Am. J. Respir. Crit. Care Med.* **2002**, *165*, 1551–1556. [CrossRef]

17. Ichikado, K.; Suga, M.; Muranaka, H.; Gushima, Y.; Miyakawa, H.; Tsubamoto, M.; Johkoh, T.; Hirata, N.; Yoshinaga, T.; Kinoshita, Y.; et al. Prediction of Prognosis for Acute Respiratory Distress Syndrome with Thin-Section CT: Validation in 44 Cases. *Radiol.* **2006**, *238*, 321–329. [CrossRef]

18. Oda, K.; Ishimoto, H.; Yatera, K.; Naito, K.; Ogoshi, T.; Yamasaki, K.; Imanaga, T.; Tsuda, T.; Nakao, H.; Kawanami, T.; et al. High-resolution CT scoring system-based grading scale predicts the clinical outcomes in patients with idiopathic pulmonary fibrosis. *Respir. Res.* **2014**, *15*, 10. [CrossRef]

19. Goddard, P.R.; Nicholson, E.; Laszlo, G.; Watt, I. Computed tomography in pulmonary emphysema. *Clin. Radiol.* **1982**, *33*, 379–387. [CrossRef]

20. US Department of Health and Human Services. Common terminology criteria for adverse events (CTCAE). In *NIH publication. no. 10-5410*; US Department of Health and Human Services, National Institutes of Health, National Cancer Institute: Bethesda, MD, USA, 2010.

21. Isobe, K.; Hata, Y.; Sakamoto, S.; Takai, Y.; Shibuya, K.; Homma, S. Clinical characteristics of acute respiratory deterioration in pulmonary fibrosis associated with lung cancer following anti-cancer therapy. *Respirol.* **2010**, *15*, 88–92. [CrossRef]

22. Hironaka, M.; Fukayama, M. Pulmonary fibrosis and lung carcinoma: A comparative study of metaplastic epithelia in honeycombed areas of usual interstitial pneumonia with or without lung carcinoma. *Pathol. Int.* **1999**, *49*, 1060–1066. [CrossRef] [PubMed]

23. Kawasaki, H.; Nagai, K.; Yoshida, J.; Nishimura, M.; Nishiwaki, Y. Postoperative morbidity, mortality, and survival in lung cancer associated with idiopathic pulmonary fibrosis. *J. Surg. Oncol.* **2002**, *81*, 33–37. [CrossRef] [PubMed]

24. Jin, G.Y.; Lynch, D.; Chawla, A.; Garg, K.; Tammemagi, M.; Sahin, H.; Misumi, S.; Kwon, K.S. Interstitial lung abnormalities in a CT lung cancer screening population: Prevalence and progression rate. *Radiol.* **2013**, *268*, 563–571. [CrossRef] [PubMed]

25. Sverzellati, N.; Guerci, L.; Randi, G.; Calabrò, E.; La Vecchia, C.; Marchianò, A.; Pesci, A.; Zompatori, M.; Pastorino, U. Interstitial lung diseases in a lung cancer screening trial. *Eur. Respir. J.* **2011**, *38*, 392–400. [CrossRef] [PubMed]

26. Ley, B.; Elicker, B.M.; Hartman, T.E.; Ryerson, C.J.; Vittinghoff, E.; Ryu, J.; Lee, J.S.; Jones, K.D.; Richeldi, L.; King, T.E.; et al. Idiopathic pulmonary fibrosis: CT and risk of death. *Radiol.* **2014**, *273*, 570–579. [CrossRef] [PubMed]

Article

RAD51B^{me} Levels as a Potential Predictive Biomarker for PD-1 Blockade Response in Non-Small Cell Lung Cancer

Inês Maria Guerreiro [1,*,†], **Daniela Barros-Silva** [2,†], **Paula Lopes** [2,3], **Mariana Cantante** [2,3], **Ana Luísa Cunha** [2,3], **João Lobo** [2,3,4], **Luís Antunes** [5], **Ana Rodrigues** [1], **Marta Soares** [1], **Rui Henrique** [2,3,4] and **Carmen Jerónimo** [2,4,*]

[1] Department of Medical Oncology, Portuguese Oncology Institute of Porto (IPO-Porto), R. Dr. António Bernardino de Almeida, 4200-072 Porto, Portugal; rodriguesana@me.com (A.R.); martasoares71@gmail.com (M.S.)

[2] Cancer Biology and Epigenetics Group, IPO Porto Research Center (GEBC CI-IPOP), Portuguese Oncology Institute of Porto (IPO Porto) & Porto Comprehensive Cancer Center (P.CCC), R. Dr. António Bernardino de Almeida, 4200-072 Porto, Portugal; daniela.barros.silva94@gmail.com (D.B.-S.); lopesanapaula.s@gmail.com (P.L.); marianacantantecf@gmail.com (M.C.); analuisa.cunha@ipoporto.min-saude.pt (A.L.C.); jpedro.lobo@ipoporto.min-saude.pt (J.L.); henrique@ipoporto.min-saude.pt (R.H.)

[3] Department of Pathology, Portuguese Oncology Institute of Porto (IPOP), R. Dr. António Bernardino de Almeida, 4200-072 Porto, Portugal

[4] Department of Pathology and Molecular Immunology, Institute of Biomedical Sciences Abel Salazar, University of Porto (ICBAS-UP), Rua Jorge de Viterbo Ferreira, 228, 4050-313 Porto, Portugal

[5] Cancer Epidemiology Group, IPO Porto Research Center (CI-IPOP), Portuguese Oncology Institute of Porto (IPO-Porto), R. Dr. António Bernardino de Almeida, 4200-072 Porto, Portugal; luis.antunes@ipoporto.min-saude.pt

* Correspondence: ines.m.guerreiro@gmail.com (I.M.G.); carmenjeronimo@ipoporto.min-saude.pt (C.J.); Tel.: +351-225-084-000 (I.M.G.); Fax: +351-225-084-001 (I.M.G.)

† Joint first authors.

Abstract: Lung cancer (LC) cells frequently express high levels of programmed death-ligand 1 (PD-L1). Although these levels grossly correlate with the likelihood of response to specific checkpoint inhibitors, the response prediction is rather imperfect, and more accurate predictive biomarkers are mandatory. We examined the methylation profile of *RAD51B* (*RAD51B^{me}*) as a candidate predictive biomarker for anti-PD-1 therapy efficacy in non-small cell lung cancer (NSCLC), correlating with patients' outcome. PD-L1 immunoexpression and *RAD51B^{me}* levels were analysed in NSCLC samples obtained from patients not treated with anti-PD-1 (Untreated Cohort (#1)) and patients treated with PD-1 blockade (Treated Cohort (#2)). Of a total of 127 patients assessed, 58.3% depicted PD-L1 positivity (PD-L1$^+$). *RAD51B^{me}* levels were significantly associated with PD-L1 immunoexpression. Patients with PD-1 blockade clinical benefit disclosed higher *RAD51B^{me}* levels ($p = 0.0390$) and significantly lower risk of disease progression (HR 0.37; 95% CI: 0.15–0.88; $p = 0.025$). Combining *RAD51B^{me+}* with PD-L1$^+$ improved the sensitivity of the test to predict immunotherapy response. PD-L1$^+$ was also associated with lower risk of death (HR 0.35; 95% CI: 0.15–0.81; $p = 0.014$). Thus, *RAD51B^{me}* levels might be combined with validated predictive biomarker PD-L1 immunostaining to select patients who will most likely experience clinical benefit from PD-1 blockade. The predictive value of *RAD51B^{me}* should be confirmed in prospective studies.

Keywords: *RAD51B* methylation; PD-L1 expression; predictive biomarker; PD-1 blockade

1. Introduction

Lung cancer is the leading cause of cancer death in Europe, with an estimated 470,000 new cases (311,000 in men and 158,200 in women) in 2018 [1]. The estimated mortality in 2018 was 20.1% in both genders, being the most common cause of death from cancer in men (267,000 deaths, 24.8%) and the second most frequent in women (121,000 deaths, 14.2%) [1]. Most patients are diagnosed at advanced stages, with an overall 5-year survival rate of 4–17% depending on the stage and regional differences [2]. The incidence of lung cancer is directly related to tobacco smoking, which is the primary cause of lung cancer, accounting for about 80% to 90% of cases [3]. The risk of lung cancer increases with the extent of smoking measured by the number of packs of cigarettes smoked per day and with the number of years of smoking (pack-years of smoking history) [4].

Since the emergence of personalised targeted therapies, pathology plays a critical role because histologic and genetic features of lung cancer are important determinants of molecular testing and treatment decisions [5–7]. Lung cancer can be classified in non-small cell lung cancer (NSCLC) and small-cell lung cancer [5]. NSCLC is the most frequent class of lung cancer, representing 80% of all cases [4] and includes non-squamous carcinoma and squamous cell carcinoma as major types [5]. Non-squamous carcinoma includes adenocarcinoma, which is the most common subtype of lung cancer [4]. When clear adenocarcinoma, squamous or neuroendocrine morphology or staining pattern is not present, NSCLC is generally classified as not otherwise specified (NOS) [5].

Several predictive biomarkers indicative of therapeutic efficacy have emerged in lung cancer [6]. Immunotherapy, mainly immune checkpoint inhibitors, has changed the treatment paradigm of NSCLC. Immune checkpoints are important to control the immune responses in order to protect tissues from damage when the immune system is activated [8]. The expression of immune checkpoint proteins can be dysregulated by cancer cells, enabling immune evasion, a cancer hallmark [8,9]. Programmed cell death protein 1 (PD-1) is an immune checkpoint receptor expressed on the surface of activated T cells, including a large proportion of tumour-infiltrating lymphocytes from many tumours [8,10]. The binding to its ligands, PD-L1 and PD-L2, inhibits the response of cytotoxic T cells, hence the activation of the pathway PD-1/PD-L1 is a mechanism of immune-escape [11]. PD-L1 is commonly upregulated at the tumour cell surface [8] and is generally expressed in 20% to 40% of NSCLC [12]. There is evidence that infiltrating lymphocytes, mutational burden, and the expression of PD-L1 [13,14] are predictive biomarkers for treatment with checkpoint inhibitors. However, prediction of response is rather imperfect and, thus, more accurate predictive biomarkers are mandatory.

Genome instability leading to the accumulation of genomic aberrations is another characteristic of cancer cells [9]. Double-strand DNA breaks (DSB) may lead to mutations, chromosomal translocations, cell senescence and apoptosis [15,16]; hence, repair mechanisms are essential to maintain genome stability. Homologous recombination repair (HRR) is the leading DNA repair mechanism of double-strand DNA breaks (DSB) that uses the homologous region of the sister chromatid as the replicative template in order to reliably repair DSB [16]. *RAD51* protein has an important activity in HRR, promoting the insertion of the broken ends of the DSB into the sister chromatid [17,18]. Its action is dependent on *RAD51*-like proteins: *RAD51B*, *RAD51C*, *RAD51D*, *XRCC2* and *XRCC3* [17–19]. Defects in the HRR pathway entail cell proliferation despite DNA damage, promoting cancer development [20]. HRR pathway deficiencies seem to be associated with higher expression of PD-L1 and linked to an immune-evasive tumour phenotype [16]. Rieke et al. found that HRR genes hypermethylation is inversely correlated with mRNA transcription and associated with PD-L1 expression in head and neck, lung, and cervix squamous cell carcinomas [18]. As such, the methylation status of these genes could represent new predictive biomarkers for immune checkpoint inhibition.

The aim of this study is to investigate the association of immune checkpoint PD-L1 expression and the status of DNA repair gene *RAD51B* promoter methylation (*RAD51B^{me}*) in advanced NSCLC, correlating with patients' outcome. Additionally, the potential of *RAD51B^{me}* levels as a candidate predictive biomarker for PD-1 blockade response in NSCLC was also assessed.

2. Materials and Methods

2.1. Patient Selection

We retrospectively analysed patients ≥18 years old, diagnosed with advanced NSCLC (adenocarcinoma, squamous cell carcinoma, and non-small cell lung cancer, not otherwise specified), at the Portuguese Oncology Institute of Porto (IPO-Porto) between 2014 and 2019. All tissue samples were obtained at the time of diagnosis. Samples were routinely fixed, and paraffin-embedded for standard pathological examination by haematoxylin and eosin (H&E) and specific immunostaining for tumour classification, grading, and staging, according to World Health Organization (WHO) Classification of Tumours of the Lung, Pleura, Thymus and Heart (4th Edition, Volume 7). Specimens were evaluated by two lung pathology proficient pathologists (ALC and RH). Biopsy samples available at the archive of the Department of Pathology were obtained for the "Untreated" cohort (Cohort #1, patients not exposed to anti-PD-1 blockade) and "Treated" cohort (Cohort #2, patients exposed to anti-PD-1 blockade anytime during the course of the disease) and were included after approval by the ethics committee of IPO-Porto (CES 15R1/2017).

2.2. Clinical and Pathological Data Collection

Relevant clinical and pathological variables were retrospectively collected for patients' characterisation, including pathological diagnosis (adenocarcinoma, squamous cell carcinoma, not otherwise specified), gender (female, male), age, smoking habits (never smoker, smoker, previous smoker), stage of the disease (stages IIIA to IVB were considered as advanced disease) and type of anti-PD-1 treatment (nivolumab, pembrolizumab, according to the current practice at the time).

All patients whose tumours displayed ≥50% PD-L1 expression did pembrolizumab as a first-line treatment [21], patients whose tumours had 1–49% PD-L1 expression did pembrolizumab [22] or nivolumab as second line treatment, and those with negative PD-L1 expression did nivolumab as a second-line treatment after progression of disease on or after standard platinum-based chemotherapy [23,24]. In patients whose tumours presented a driver mutation (epidermal growth factor receptor (*EGFR*) tyrosine kinase mutation, anaplastic lymphoma kinase (*ALK*) gene rearrangement or c-ROS oncogene 1 (*ROS1*) translocations), treatment with anti-PD-1 was done after progression on or after tyrosine kinase inhibitors and platinum-based chemotherapy.

Response to treatment was assessed by using the Response Evaluation Criteria in Solid Tumours (RECIST): complete response (CR)—disappearance of all target lesions, pathological lymph nodes must have reduction in short axis to <10 mm; partial response (PR)—at least a 30% decrease in the sum of diameters of target lesions, taking as reference the baseline sum diameters; progressive disease (PD)—at least a 20% increase in the sum of diameters of target lesions, taking as reference the smallest sum on study which must demonstrate an absolute increase of at least 5 mm; stable disease (SD)—neither sufficient shrinkage to qualify for PR nor sufficient increase to qualify for PD. Clinical benefit was considered if CR, PR or SD were present.

All procedures performed were in accordance with the ethical standards of the institutional and national research committees and with the 1964 Helsinki declaration and its later amendments or comparable ethical standards.

2.3. Assessment of PD-L1 Expression by Immunohistochemistry

PD-L1 (dilution 1:100, clone 22C3, DAKO) immunostaining was performed on a BenchMark Ultra platform (Ventana, Tucson, AZ, USA) using OptiView DAB detection kit (Ventana, Tucson, AZ, USA) and high pH buffer solution (CC1, Ventana, Tucson, AZ, USA for 40 min at 95 °C) was used for antigen retrieval. Appropriate positive controls were used for each antibody and negative controls consisted of omission of primary antibody. PD-L1 expression was assessed by a proficient pathologist (ALC) who determined the tumour proportion score (TPS), according to the European Society for Medical

Oncology (ESMO) guidelines. TPS was considered negative if <1%, positive intermediate if 1–49%, and positive strong if ≥50%.

2.4. Methylation Analysis

DNA and RNA were extracted from all clinical samples and cell lines using an FFPE RNA/DNA Purification Plus Kit (Norgen, Thorold, ON, Canada), according to the manufacturer's instructions. The bisulfide modification was accomplished using an EZ DNA Methylation-Gold™ Kit (Zymo Research, Orange, CA, USA) that integrates DNA denaturation and the bisulfide conversion processes into one-step, according to the recommended protocol. Evaluation of the DNA repair genes' methylation status was done by quantitative methylation-specific PCR (qMSP) assays and was performed using Xpert Fast SYBR (GRiSP, Porto, Portugal), according to the recommended protocol, in 384-well plates using a Roche LightCycler 480 II. Primers addressing the informative CpG sites within the promoter region were designed using Methyl Primer Express v1 and are described in Table 1. *β-actin* (ACTB) was used as an internal reference gene for normalization.

Table 1. Primer sequences for *ß-Actin* and *RAD51B^{me}*.

Gene	Forward (5′–3′)	Reverse (5′–3′)
ß-Actin	TGGTGATGGAGGAGGTTTAGTAAGT	AACCAATAAAACCTACTCCTCCCTTAA
RAD51B^{me}	AGATTTTTAGGGTCGAGAGC	CGCCCGACTAATTTTTTTAT

2.5. Statistical Analysis

Statistical analysis was conducted separately for each cohort.

Categorical variables are presented as counts and proportions and continuous variables are displayed as mean (standard deviation). Median (interquartile range) is used to describe variables with a highly skewed distribution.

Chi-square test was used to test the association between categorical variables; the Mann–Whitney U test was used to compare continuous variables with skewed distribution. A logistic regression analysis was carried out to identify predictors of PD-L1 expression. The variables considered in the logistic regression model were *RAD51B^{me}* (continuous), sex, age, smoking status and histological subtype.

The area under the receiver operating characteristics curve (AUC, 95% CI) was analysed to assess the performance of the *RAD51B* promotor methylation level as a predictive biomarker for PD-1 blockade response. Specificity, sensitivity, positive predictive value (PPV), negative predictive value (NPV), and accuracy were determined for PD-L1, according to positive vs. negative immune scores and for *RAD51B* methylation by applying an empirical cut-off obtained by ROC curve analysis (sensitivity + (1-specificity)). This cut-off value combines the maximum sensitivity and specificity, ensuring the perfect categorization of the samples as positive and negative for the methylation test. For the analysis of combined *RAD51B^{me+}*/PD-L1$^+$, the test was considered positive when at least one of the variables was plotted, as positive in individual analysis. Diagnostic biomarker performance was calculated, taking into consideration that all the patients included were subjected to anti-PD-1 treatment.

Progression-free survival (PFS) and overall survival (OS) were estimated by means of the Kaplan–Meier method for the Treated Cohort (#2). PFS was defined as the length of time from the beginning of anti-PD-1 blockade until disease progression or death from the disease and OS as the length of time from the beginning of anti-PD-1 blockade until death from any cause. The differences between groups were tested using the log-rank test. Hazard ratios (HRs) from multivariable Cox regression were used to quantify the association between clinicopathological features and survival. *RAD51B* promoter methylation level was considered positive if the quantitative value was above the 75th percentile. A *p*-value smaller than 0.05 (two-sided) indicated statistical significance.

All analyses were performed using IBM SPSS Statistics version 26.0 (SPSS, Chicago, IL, USA) and GraphPad Prism 7.01 (GraphPad Software, La Jolla, CA, USA).

3. Results

Between 2014 and 2019, 293 patients fulfilling the inclusion criteria were analysed. The median age was 64 years, 79.9% were male, and most of the patients (70%) presented adenocarcinoma. A biopsy sample was available in 127 (43.3%) patients (*n* = 64 in Untreated Cohort (#1) and *n* = 63 in Treated Cohort (#2)). PD-L1 expression was deemed positive in 58.3% cases (*n* = 31 in Untreated Cohort (#1) and *n* = 43 in Treated Cohort (#2)). Table 2 depicts patients' characteristics in the Untreated and Treated cohorts.

Table 2. Clinical and pathological data according to the testing cohorts.

Characteristics	Untreated Cohort (#1) *n* = 64	Treated Cohort (#2) *n* = 63
Gender, (*n*, %)		
Male	51 (79.7)	49 (77.8)
Female	13 (20.3)	14 (22.2)
Age (year), median (IQR)	62.5 (29.0–84.0)	62.0 (32.0–77.0)
Histologic subtype (*n*, %)		
Adenocarcinoma	41 (64.1)	46 (73.0)
Squamous	22 (34.4)	17 (27.0)
NOS	1 (1.6)	-
Smoking habits (*n*, %)		
Never	16 (25.0)	10 (15.9)
Smoker	20 (31.3)	20 (31.7)
Previous smoker	28 (43.7)	33 (53.4)
PD-L1 immunoexpression (*n*, %)		
Negative	33 (51.6)	20 (31.7)
Intermediate (1–49%)	18 (28.1)	14 (22.2)
Strong (≥ 50%)	13 (20.3)	29 (46.0)
Anti-PD-1 agent (*n*, %)		
Pembrolizumab	n.a.	38 (60.3)
Nivolumab		25 (39.7)
PD-1 blockade (*n*, %)		
Clinical benefit	n.a.	13 (20.6)
Non-clinical benefit		50 (79.4)
End of PD-1 blockade treatment (*n*, %)		
Not applicable		18 (28.6)
Disease progression	n.a.	39 (61.9)
Toxicity		6 (9.5)
Progression-free survival since PD-1 blockade, months median (IQR)	n.a.	8.1 (5.1–11.1)
Overall survival since PD-1 blockade, months median (IQR)	n.a.	21.3 (13.7–28.9)
RAD51B^{me} levels (normalized to β-actin), median (IQR)	0.54 (0.16–1.34)	1.08 (0.25–2.06)

n.a.—not applicable; IQR – Interquartil Range.

In the Treated Cohort (#2), 18 patients whose tumours showed ≥50% PD-L1 expression were treated with pembrolizumab in first-line; 19 and 3 patients whose tumours had 1–49% PD-L1 expression were treated with pembrolizumab and nivolumab, respectively, in second-line after progression on chemotherapy. Eighteen patients with PD-L1 negative tumours were treated with nivolumab as a second-line treatment. Four patients with adenocarcinoma carried driver mutations (3 had an *EGFR* tyrosine kinase mutation and 1 had an *ALK* gene rearrangement). As such, anti-PD-1 therapy was

administered as a third-line treatment, after progression on tyrosine kinase inhibitors (first-line) and chemotherapy (second-line).

Regarding molecular analysis, $RAD51B^{me}$ levels were significantly higher in PD-L1 positive vs. negative cases in both cohorts (Untreated Cohort (#1)—$p = 0.0216$; Treated Cohort (#2)—$p < 0.0001$) (Figure 1). Patients presenting higher $RAD51B^{me}$ levels showed a higher chance of having a positive PD-L1 immunoexpression (Untreated cohort (#1) OR: 51.68, 95% CI: 1.77–1512.04, $p = 0.022$; Treated cohort (#2) OR: 45.51, 95% CI: 5.29–391.20, $p = 0.001$), adjusting for sex, age, smoking status and histological subtype (detailed information in Table S1). No differences in $RAD51B^{me}$ levels were found between squamous cell carcinoma and adenocarcinoma cases in both cohorts (Untreated Cohort (#1)—$p = 0.774$; Treated Cohort (#2)—$p = 0.520$).
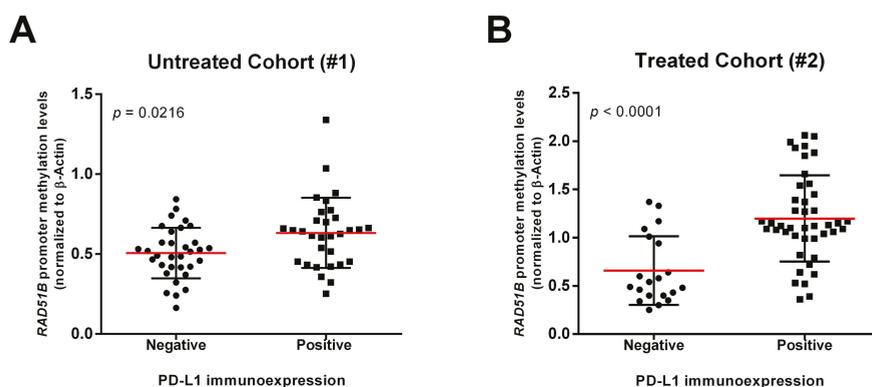
Figure 1. $RAD51B$ promoter methylation levels within PD-L1 negative and PD-L1 positive immunoexpression among NSCLC samples. Scatter plot representing $RAD51B$ promoter methylation levels distribution obtained by qMSP for (**A**) Untreated Cohort (#1) and (**B**) Treated Cohort (#2) patients, according to negative and positive PD-L1 immunoexpression. Mann–Whitney U-test. Red horizontal line represents the median methylation levels.

$RAD51B^{me}$ levels were significantly higher in patients submitted to immunotherapy, which demonstrated clinical benefit ($p = 0.0390$; Figure 2A). Moreover, patients with positive $RAD51B^{me}$ levels ($RAD51B^{me+}$ was consider when methylation levels >P75) disclosed clinical benefit independently from PD-L1 expression (Figure 2B). Additionally, $RAD51B^{me}$ discriminated between PD-1 blockade clinical benefit and no clinical benefit with 85% specificity and 90% positive predictive value (AUC: 0.758, 95% CI: 0.626–0.889, $p = 0.0015$; Figure 2C and Table 3). Remarkably, combining $RAD51B^{me+}$ with PD-L1$^+$ improved the sensitivity of the test (68%) to predict immunotherapy response, maintaining high specificity (85%) and increasing positive predictive value (94%).

Table 3. $RAD51B^{me}$, PD-L1 staining and the combination of the two variables performances as predictive biomarkers of PD-1 blockade response in the Treated Cohort (#2).

	Predictive Biomarkers of PD-1 Blockade Response		
	$RAD51B^{me+}$	PD-L1$^+$	$RAD51B^{me+}$/PD-L1$^+$
Sensitivity	38%	74%	68%
Specificity	85%	54%	85%
Accuracy	48%	70%	71%
PPV	90%	86%	94%
NPV	26%	35%	41%

Abbreviations: PPV: positive predictive value, NPV: negative predictive value.
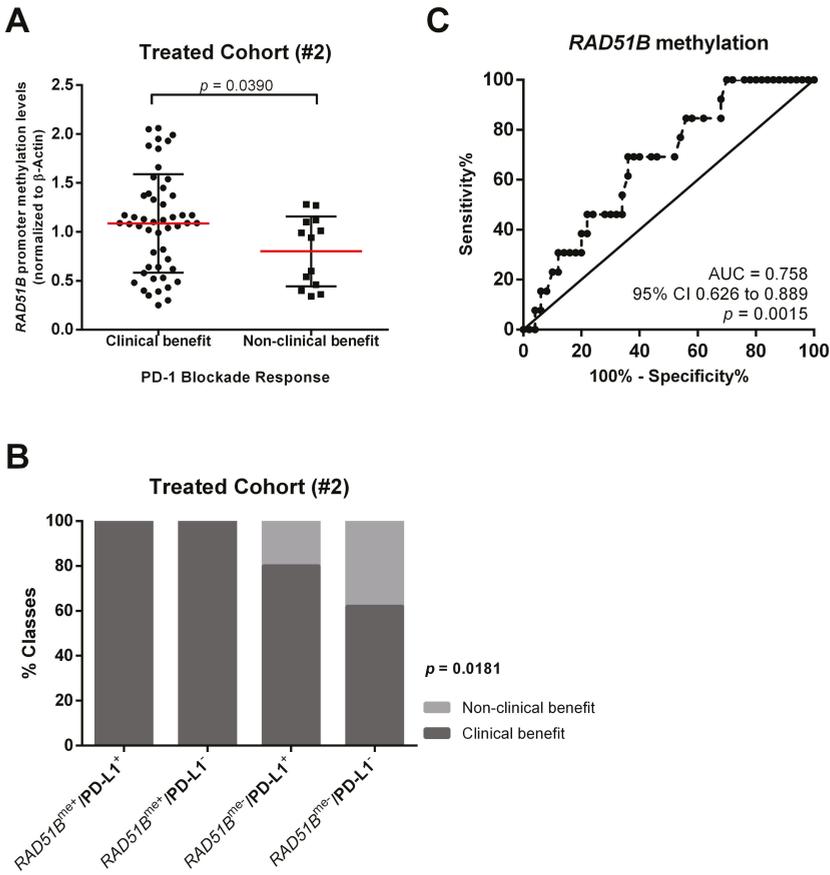
Figure 2. *RAD51B^me* levels and PD-L1 positivity associate with PD-1 blockade clinical benefit. (**A**) Scatter plot representing *RAD51B* promoter methylation levels distribution obtained by qMSP in patients with and without clinical benefit from immunotherapy. Mann–Whitney U-test. Red horizontal line represents the median methylation levels; (**B**) Contingency graph displaying the percentage of patients with and without PD-1 blockade clinical benefit, according to *RAD51B* promoter methylation and PD-L1 status. Chi-square test. *RAD51B^me* were considered positive when promoter methylation levels >P75; (**C**) Receiver operator characteristic (ROC) curve for discrimination between patients with and without clinical benefit from immunotherapy based on *RAD51B* promoter methylation levels distribution in the Treated Cohort (#2).

The median follow-up time for the Treated Cohort (#2) was 18 months (95% CI: 15.1–20.9). The median PFS was significantly higher in *RAD51B^{me+}* patients (*p* = 0.0216; Figure 3A). Furthermore, patients with *RAD51B^{me+}* disclosed a lower risk of disease progression (HR 0.37; 95% CI: 0.15–0.88; *p* = 0.025) compared with *RAD51B^{me-}*. Considering the PD-L1 expression, no significant differences were depicted for PFS (*p* = 0.2023), although PD-L1^+ patients disclosed a trend for higher PFS (Figure 3B). Nonetheless, PD-L1^+ associated with a longer OS (*p* = 0.0307) and a lower risk of death (HR 0.35; 95% CI: 0.15–0.81; *p* = 0.014). For *RAD51B*, lower methylation levels tend to associate with shorter OS, despite not being statistically significant. Also, no significant differences were observed for PFS or OS, when combining in panel PD-L1 expression and *RAD51B^me* levels.
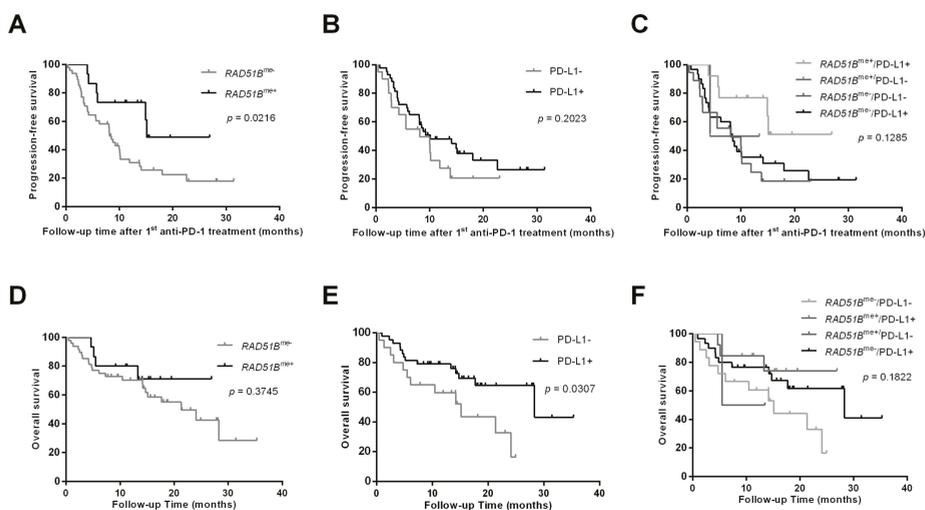
Figure 3. Kaplan–Meier survival curves for progression-free survival (after first anti-PD-1 treatment) of patients according to (**A**) *RAD51B^{me}* status; (**B**) PD-L1 status; and (**C**) combined *RAD51B^{me}* and PD-L1 status. Kaplan–Meier survival curves for patients' overall survival according to (**D**) *RAD51B^{me}* status, (**E**) PD-L1 status, and (**F**) combined *RAD51B^{me}* and PD-L1 status. Log-rank test. *RAD51B^{me}* was considered positive when promoter methylation levels >P75.

4. Discussion

Despite the improvement in lung cancer treatment over the last years, it remains a lethal disease in most cases, mostly due to diagnosis at advanced stages and suboptimal effectiveness of standard therapy. Nonetheless, the emergence of novel therapeutic strategies, including immune-based cancer therapies, has improved the prospects of patients diagnosed at advanced stages of the disease. Indeed, anti-PD-1 treatment for advanced NSCLC has improved the survival of patients [22]. Currently, the most commonly used biomarker to predict this response to anti-PD-1 therapy is PD-L1 immunostaining, although a substantial number of patients with PD-L1 positive immunostaining do not respond [21], highlighting the need for new biomarkers. In NSCLC, similar to other tumours, a higher tumour mutation burden was a strong predictor of immunotherapy efficacy [25–28]. Additionally, defects in the HRR pathway have been associated with higher expression of co-regulatory molecules such as PD-L1, suggesting that deficient homologous recombination, by disabling repair of DNA defects, may lead to neoantigens production with the recruitment of T-cells to the tumour microenvironment. This engages tumour cells to upregulate the expression of PD-L1 as an adaptive resistance mechanism [29]. A recent study demonstrated that DNA methylation profile of NSCLC might also be determinant for the efficacy of anti-PD-1 treatment in stage IV patients [30]. Furthermore, epigenetic alterations in *RAD51B*, specifically DNA promoter methylation, were associated with PD-L1 expression in squamous cell carcinomas [18]. This is a *RAD51* paralog, essential for DSB repair in the homologous recombinant pathway [17]. Thus, we sought to investigate the association of immune checkpoint PD-L1 expression and DNA methylation status of DNA repair gene *RAD51B* in non-small cell lung cancer (NSCLC), correlating with patient outcome.

Overall, the chances of positive PD-L1 expression in advanced NSCLC increased with the level of *RAD51^{me+}*. Remarkably, a link between *RAD51B^{me}* and the immune response in NSCLC has been previously suggested [29]. Furthermore, *Rieke et al.* demonstrated that methylation was associated with low mRNA expression levels and with homologous recombination deficiency [18]. Additionally, a significant positive correlation between *RAD51B* methylation status and the inflammatory gene signature, particularly, interferon-gamma (IFN-γ) was disclosed [18]. Interestingly, IFN-γ is an

important inducer of PD-L1 expression, which acts via the JAK/STAT1/interferon regulatory factor (IRF) [31] in various types of cancers, including NSCLC. Furthermore, the depletion of *RAD51B* was shown to induce immune response through activation of the STAT3 pathway [32], which activates *CD274* gene/PD-L1 induction [31,33]. Therefore, our results further support the link between homologous repair deficiency by epigenetic regulation and immune checkpoint players, specifically PD-L1. Considering the available literature, assessing the inflammatory profile of these tumours might be useful to determine whether there is a direct effect between DNA repair candidate genes hypermethylation and the expression of immune checkpoint proteins.

Remarkably, *RAD51B^{me+}* associated with better clinical response to treatment with PD-1 blockade and to a reduction of disease progression by 60%. Conversely, *RAD51B^{me-}* associated with the absence of clinical benefit, which was even more relevant in negative PD-L1 expression cases. Hence, *RAD51B^{me}* might constitute a potential biomarker of response to anti-PD-1 therapy. Although *RAD51B^{me}* depicted lower sensitivity than PD-L1$^+$ as a predictive biomarker for treatment with anti-PD-1, it displayed higher specificity.

Although PD-L1 expression has not been described as a strong prognostic factor mostly due to methodological approaches variations, including diverse immunohistochemistry antibodies, dissimilar evaluation for PD-L1 positivity (cut-off % or H-score) and patients' selection [13,34], in our study, both PD-L1$^+$ and *RAD51B^{me+}* associated with better overall survival. Conversely, another research team suggested that *RAD51B* overexpression associates with improved OS in NSCLC patients [35]. Notwithstanding higher promoter methylation levels might entail expression downregulation, several other genetic and epigenetic mechanisms may contribute to this apparent inconsistency. Furthermore, higher *RAD51B* methylation status was depicted in patients with longer progression-free survival after anti-PD-1 treatment, supporting once more the clinical benefit of PD-1 blockade when *RAD51B* promoter is methylated. The shorter overall survival of non-smokers patients may be partially explained by the fact that these patients had a longer median time (higher than 20 months) between diagnosis and the treatment with PD-L1 inhibitors than smokers.

Therefore, PD-L1$^+$ and *RAD51B^{me+}* are promising biomarkers to predict response to PD-1 blockade rather than overall prognostic factors in NSCLC's patients. As such, *RAD51B^{me}* might represent a new predictive marker potentially assessable in liquid biopsies, allowing for a better selection of patients for anti-PD-1 treatment and eventually for monitoring patients' immunotherapy response throughout the course of the disease. Although our study paves the way for new prospective studies on the *RAD51B* promoter methylation's predictive role in patients with NSCLC treated with anti-PD-1, the retrospective design and small sample size are not neglectable limitations. Nevertheless, all the patients and samples enrolled in the study were analysed using the same criteria both for molecular biology strategies or clinical and pathological data collection. Importantly, other strengths of our research work are the fact that all patients were uniformly treated at the same institution, and all were evaluated by computed tomographic scans at specific timepoints during the course of treatment.

5. Conclusions

Herein, we confirm that higher *RAD51B^{me}* levels associate with PD-L1 immunoexpression, as well as with immunotherapy's efficacy, in an independent advanced NSCLC patient cohort. Prospective studies, with larger cohorts of patients and extended follow-up periods, are warranted to validate these results and determine whether the methylation profile of this gene might be a predictive tool for selecting patients that will benefit from anti-PD-1 therapy.

Author Contributions: I.M.G. and D.B.-S. collected clinical and pathological data, performed the methylation analysis and the statistical analysis and original draft preparation. P.L. and M.C. did the immunohistochemical staining for PD-L1. A.L.C. and J.L., and R.H. assessed PD-L1 immunoexpression. L.A. contributed to the statistical analysis and interpretation of data. A.R., M.S. and R.H. contributed to the design of the work. C.J. contributed to the conception of the work, review and editing. All authors have read and agreed to the published version of the manuscript.

Conflicts of Interest: The authors declare no conflict of interest.

References

1. Ferlay, J.; Colombet, M.; Soerjomataram, I.; Dyba, T.; Randi, G.; Bettio, M.; Gavin, A.; Visser, O.; Bray, F. Cancer incidence and mortality patterns in Europe: Estimates for 40 countries and 25 major cancers in 2018. *Eur. J. Cancer* **2018**, *103*, 356–387. [CrossRef] [PubMed]

2. Hirsch, F.R.; Scagliotti, G.V.; Mulshine, J.L.; Kwon, R.; Curran, W.J., Jr.; Wu, Y.-L.; Paz-Ares, L. Lung cancer: Current therapies and new targeted treatments. *Lancet* **2017**, *389*, 299–311. [CrossRef]

3. Ettinger, D.S.; Wood, D.E.; Akerley, W.; Bazhenova, L.A.; Borghaei, H.; Camidge, D.R.; Cheney, R.T.; Chirieac, L.R.; D'Amico, T.A.; Dilling, T.J. NCCN guidelines insights: Non–small cell lung cancer, version 4.2016. *J. Natl. Compr. Cancer Netw.* **2016**, *14*, 255–264. [CrossRef] [PubMed]

4. Travis, W.D.; Brambilla, E.; Nicholson, A.G.; Yatabe, Y.; Austin, J.H.; Beasley, M.B.; Chirieac, L.R.; Dacic, S.; Duhig, E.; Flieder, D.B. The 2015 World Health Organization classification of lung tumors: Impact of genetic, clinical and radiologic advances since the 2004 classification. *J. Thorac. Oncol.* **2015**, *10*, 1243–1260. [CrossRef] [PubMed]

5. Mok, T.S. Personalized medicine in lung cancer: What we need to know. *Nat. Rev. Clin. Oncol.* **2011**, *8*, 661–668. [CrossRef]

6. Kerr, K.M.; Bubendorf, L.; Edelman, M.J.; Marchetti, A.; Mok, T.; Novello, S.; O'Byrne, K.; Stahel, R.; Peters, S.; Felip, E. Second ESMO consensus conference on lung cancer: Pathology and molecular biomarkers for non-small-cell lung cancer. *Ann. Oncol.* **2014**, *25*, 1681–1690. [CrossRef]

7. Pardoll, D.M. The blockade of immune checkpoints in cancer immunotherapy. *Nat. Rev. Cancer* **2012**, *12*, 252–264. [CrossRef]

8. Hanahan, D.; Weinberg, R.A. Hallmarks of cancer: The next generation. *Cell* **2011**, *144*, 646–674. [CrossRef]

9. Garon, E.B.; Rizvi, N.A.; Hui, R.; Leighl, N.; Balmanoukian, A.S.; Eder, J.P.; Patnaik, A.; Aggarwal, C.; Gubens, M.; Horn, L. Pembrolizumab for the treatment of non–small-cell lung cancer. *N. Engl. J. Med.* **2015**, *372*, 2018–2028. [CrossRef]

10. Petrelli, F.; Maltese, M.; Tomasello, G.; Conti, B.; Borgonovo, K.; Cabiddu, M.; Ghilardi, M.; Ghidini, M.; Passalacqua, R.; Barni, S. Clinical and Molecular Predictors of PD-L1 Expression in Non–Small-Cell Lung Cancer: Systematic Review and Meta-analysis. *Clin. Lung Cancer* **2018**, *19*, 315–322. [CrossRef]

11. Syn, N.L.; Teng, M.W.; Mok, T.S.; Soo, R.A. De-novo and acquired resistance to immune checkpoint targeting. *Lancet Oncol.* **2017**, *18*, e731–e741. [CrossRef]

12. Shi, Y. Regulatory mechanisms of PD-L1 expression in cancer cells. *Cancer Immunol. Immunother.* **2018**, *67*, 1–9. [CrossRef] [PubMed]

13. Wang, A.; Wang, H.; Liu, Y.; Zhao, M.; Zhang, H.; Lu, Z.; Fang, Y.; Chen, X.; Liu, G. The prognostic value of PD-L1 expression for non-small cell lung cancer patients: A meta-analysis. *Eur. J. Surg. Oncol. (EJSO)* **2015**, *41*, 450–456. [CrossRef] [PubMed]

14. Iarovaia, O.V.; Rubtsov, M.; Ioudinkova, E.; Tsfasman, T.; Razin, S.V.; Vassetzky, Y.S. Dynamics of double strand breaks and chromosomal translocations. *Mol. Cancer* **2014**, *13*, 249. [CrossRef] [PubMed]

15. O'Kane, G.M.; Connor, A.A.; Gallinger, S. Characterization, detection, and treatment approaches for homologous recombination deficiency in cancer. *Trends Mol. Med.* **2017**, *23*, 1121–1137. [CrossRef] [PubMed]

16. Rodrigue, A.; Lafrance, M.; Gauthier, M.C.; McDonald, D.; Hendzel, M.; West, S.C.; Jasin, M.; Masson, J.Y. Interplay between human DNA repair proteins at a unique double-strand break in vivo. *EMBO J.* **2006**, *25*, 222–231. [CrossRef] [PubMed]

17. Gachechiladze, M.; Škarda, J.; Soltermann, A.; Joerger, M. RAD51 as a potential surrogate marker for DNA repair capacity in solid malignancies. *Int. J. Cancer* **2017**, *141*, 1286–1294. [CrossRef]

18. Rieke, D.T.; Ochsenreither, S.; Klinghammer, K.; Seiwert, T.Y.; Klauschen, F.; Tinhofer, I.; Keilholz, U. Methylation of RAD51B, XRCC3 and other homologous recombination genes is associated with expression of immune checkpoints and an inflammatory signature in squamous cell carcinoma of the head and neck, lung and cervix. *Oncotarget* **2016**, *7*, 75379–75393. [CrossRef]

19. Thacker, J. The RAD51 gene family, genetic instability and cancer. *Cancer Lett.* **2005**, *219*, 125–135. [CrossRef]

20. Suwaki, N.; Klare, K.; Tarsounas, M. RAD51 paralogs: Roles in DNA damage signalling, recombinational repair and tumorigenesis. *Semin. Cell Dev. Biol.* **2011**, *22*, 898–905. [CrossRef]

21. Reck, M.; Rodríguez-Abreu, D.; Robinson, A.G.; Hui, R.; Csőszi, T.; Fülöp, A.; Gottfried, M.; Peled, N.; Tafreshi, A.; Cuffe, S. Pembrolizumab versus chemotherapy for PD-L1–positive non–small-cell lung cancer. *N. Engl. J. Med.* **2016**, *375*, 1823–1833. [CrossRef] [PubMed]

22. Herbst, R.S.; Baas, P.; Kim, D.-W.; Felip, E.; Pérez-Gracia, J.L.; Han, J.-Y.; Molina, J.; Kim, J.-H.; Arvis, C.D.; Ahn, M.-J. Pembrolizumab versus docetaxel for previously treated, PD-L1-positive, advanced non-small-cell lung cancer (KEYNOTE-010): A randomised controlled trial. *Lancet* **2016**, *387*, 1540–1550. [CrossRef]

23. Brahmer, J.; Reckamp, K.L.; Baas, P.; Crinò, L.; Eberhardt, W.E.; Poddubskaya, E.; Antonia, S.; Pluzanski, A.; Vokes, E.E.; Holgado, E. Nivolumab versus docetaxel in advanced squamous-cell non–small-cell lung cancer. *N. Engl. J. Med.* **2015**, *373*, 123–135. [CrossRef] [PubMed]

24. Borghaei, H.; Paz-Ares, L.; Horn, L.; Spigel, D.R.; Steins, M.; Ready, N.E.; Chow, L.Q.; Vokes, E.E.; Felip, E.; Holgado, E. Nivolumab versus docetaxel in advanced nonsquamous non–small-cell lung cancer. *N. Engl. J. Med.* **2015**, *373*, 1627–1639. [CrossRef] [PubMed]

25. Hellmann, M.D.; Ciuleanu, T.-E.; Pluzanski, A.; Lee, J.S.; Otterson, G.A.; Audigier-Valette, C.; Minenza, E.; Linardou, H.; Burgers, S.; Salman, P. Nivolumab plus ipilimumab in lung cancer with a high tumor mutational burden. *N. Engl. J. Med.* **2018**, *378*, 2093–2104. [CrossRef] [PubMed]

26. Rizvi, N.A.; Hellmann, M.D.; Snyder, A.; Kvistborg, P.; Makarov, V.; Havel, J.J.; Lee, W.; Yuan, J.; Wong, P.; Ho, T.S. Mutational landscape determines sensitivity to PD-1 blockade in non–small cell lung cancer. *Science* **2015**, *348*, 124–128. [CrossRef]

27. Rizvi, H.; Sanchez-Vega, F.; La, K.; Chatila, W.; Jonsson, P.; Halpenny, D.; Plodkowski, A.; Long, N.; Sauter, J.L.; Rekhtman, N. Molecular determinants of response to anti–programmed cell death (PD)-1 and anti–programmed death-ligand 1 (PD-L1) blockade in patients with non–small-cell lung cancer profiled with targeted next-generation sequencing. *J. Clin. Oncol.* **2018**, *36*, 633–641. [CrossRef]

28. Topalian, S.L.; Drake, C.G.; Pardoll, D.M. Immune checkpoint blockade: A common denominator approach to cancer therapy. *Cancer Cell* **2015**, *27*, 450–461. [CrossRef]

29. Bhattacharya, S.; Srinivasan, K.; Abdisalaam, S.; Su, F.; Raj, P.; Dozmorov, I.; Mishra, R.; Wakeland, E.K.; Ghose, S.; Mukherjee, S. RAD51 interconnects between DNA replication, DNA repair and immunity. *Nucleic Acids Res.* **2017**, *45*, 4590–4605. [CrossRef]

30. Duruisseaux, M.; Martínez-Cardús, A.; Calleja-Cervantes, M.E.; Moran, S.; de Moura, M.C.; Davalos, V.; Piñeyro, D.; Sanchez-Cespedes, M.; Girard, N.; Brevet, M. Epigenetic prediction of response to anti-PD-1 treatment in non-small-cell lung cancer: A multicentre, retrospective analysis. *Lancet Respir. Med.* **2018**, *6*, 771–781. [CrossRef]

31. Abdel-Rahman, O. Correlation between PD-L1 expression and outcome of NSCLC patients treated with anti-PD-1/PD-L1 agents: A meta-analysis. *Crit. Rev. Oncol. Hematol.* **2016**, *101*, 75–85. [CrossRef] [PubMed]

32. Marzec, M.; Zhang, Q.; Goradia, A.; Raghunath, P.N.; Liu, X.; Paessler, M.; Wang, H.Y.; Wysocka, M.; Cheng, M.; Ruggeri, B.A. Oncogenic kinase NPM/ALK induces through STAT3 expression of immunosuppressive protein CD274 (PD-L1, B7-H1). *Proc. Natl. Acad. Sci. USA* **2008**, *105*, 20852–20857. [CrossRef] [PubMed]

33. Akbay, E.A.; Koyama, S.; Carretero, J.; Altabef, A.; Tchaicha, J.H.; Christensen, C.L.; Mikse, O.R.; Cherniack, A.D.; Beauchamp, E.M.; Pugh, T.J. Activation of the PD-1 pathway contributes to immune escape in EGFR-driven lung tumors. *Cancer Discov.* **2013**, *3*, 1355–1363. [CrossRef] [PubMed]

34. Zhou, Z.-J.; Zhan, P.; Song, Y. PD-L1 over-expression and survival in patients with non-small cell lung cancer: A meta-analysis. *Transl. Lung Cancer Res.* **2015**, *4*, 203–208. [CrossRef] [PubMed]
35. Wu, M.; Sheng, Z.; Jiang, L.; Liu, Z.; Bi, Y.; Shen, Y. Overexpression of RAD51B predicts a preferable prognosis for non-small cell lung cancer patients. *Oncotarget* **2017**, *8*, 91471–97480. [CrossRef] [PubMed]

Potential of FDG-PET as Prognostic Significance after anti-PD-1 Antibody against Patients with Previously Treated Non-Small Cell Lung Cancer

Kosuke Hashimoto [1], Kyoichi Kaira [1],*, Ou Yamaguchi [1], Atsuto Mouri [1], Ayako Shiono [1], Yu Miura [1], Yoshitake Murayama [1], Kunihiko Kobayashi [1], Hiroshi Kagamu [1] and Ichiei Kuji [2]

[1] Department of Respiratory Medicine, Comprehensive Cancer Center, International Medical Center, Saitama Medical University, 1397-1 Yamane, Hidaka-City, Saitama 350-1298, Japan; hkosuke@saitama-med.ac.jp (K.H.); ouyamagu@saitama-med.ac.jp (O.Y.); mouria@saitama-med.ac.jp (A.M.); respiratory@hotmail.co.jp (A.S.); you_mi@saitama-med.ac.jp (Y.M.); ymura114@saitama-med.ac.jp (Y.M.); kobakuni@saitama-med.ac.jp (K.K.); kagamu19@saitama-med.ac.jp (H.K.)

[2] Department of Nuclear Medicine, Comprehensive Cancer Center, International Medical Center, Saitama Medical University, 1397-1 Yamane, Hidaka-City, Saitama 350-1298, Japan; kuji@saitama-med.ac.jp

* Correspondence: kkaira1970@yahoo.co.jp; Tel.: +81-42-984-4111; Fax: +81-42-984-4741

Abstract: It remains unclear whether the accumulation of 2-deoxy-2-[^{18}F]fluoro-D-glucose (^{18}F-FDG) before the initiation of anti-programmed death-1 (PD-1) antibody can predict the outcome after its treatment. The aim of this study is to retrospectively examine the prognostic significance of ^{18}F-FDG uptake as a predictive marker of anti-PD-1 antibody. Eighty-five patients with previously treated non-small cell lung cancer (NSCLC) who underwent ^{18}F-FDG-positron emission tomography (PET) just before administration of nivolumab or pembrolizumab monotherapy were eligible in our study, and metabolic tumor volume (MTV), total lesion glycolysis (TLG) and the maximum of standardized under value (SUV$_{max}$) on ^{18}F-FDG uptake were assessed. Objective response rate, median progression-free survival and median overall survival were 36.6%, 161 days and 716 days, respectively. The frequency of any immune-related adverse events was significantly higher in patients with low ^{18}F-FDG uptake on PET than in those with high uptake. By multivariate analysis, the tumor metabolic activity by TLG and MTV was identified as an independent prognostic factor for predicting outcome after anti-PD-1 antibody therapy, but not SUV$_{max}$, predominantly in patients with adenocarcinoma. Metabolic tumor indices as TLG and MTV on ^{18}F-FDG uptake could predict the prognosis after anti-PD-1 antibodies in patients with previously treated NSCLC.

Keywords: FDG-PET; immune checkpoint inhibitor; PD-1; lung cancer; prognosis

1. Introduction

Non-small cell lung cancer (NSCLC) is the leading cause of cancer-related deaths worldwide. Recent studies have proven that anti-programmed death-1 (PD-1)/programmed death ligand-1 (PD-L1) antibodies provide significant survival benefits in patients with advanced NSCLC, when compared with standard chemotherapy [1–4]. Although the efficacy of the anti-PD-1 antibody varies according to the immunohistochemical degree of PD-L1 expression within tumor cells, there are no established biomarkers to predict the outcome after the administration of the anti-PD-1 antibody and the expression of PD-L1. If a useful biomarker is obtained from common modalities, this discovery can be easily adopted into daily practice.

Notably, 2-deoxy-2-[^{18}F]fluoro-D-glucose (^{18}F-FDG) positron emission tomography (PET) is a distinguished radiological modality to distinguish benign lesions from malignant tumors [5]. The uptake

of ^{18}F-FDG is observed in non-malignant lesions such as sarcoidosis, granuloma, pneumonia, and tuberculosis, but it can closely resemble the metabolic activity of malignant tumors [5]. Previous reports demonstrated that the accumulation of ^{18}F-FDG within tumor cells was significantly linked to the presence of glucose transporter 1 (Glut1), hypoxia-inducible factor 1α (HIF-1α), and vascular endothelial growth factor (VEGF)b [6]. Several researchers have described that the accumulation of ^{18}F-FDG exhibited a significant correlation with the expression of PD-L1 in patients with NSCLC [7–9]. Although little is known about the close association between immune environment and glucose metabolism, it is important to discover how metabolic tumor activity can affect the upregulation of PD-L1 expression. Moreover, it has been reported that ^{18}F-FDG-PET is useful for assessing the therapeutic monitoring of anti-PD-1 antibody with regard to the prognosis and overall response rate [10]. Little is known as to whether the uptake of ^{18}F-FDG before the administration of anti-PD-1 antibody can predict the efficacy and prognosis of immune checkpoint inhibitors (ICI) in patients with advanced NSCLC.

The maximum standardized uptake value (SUVmax) is extensively used to evaluate the metabolic degree of ^{18}F-FDG within tumor cells. Since SUVmax reflects the maximal point of glucose metabolism within tumor specimens, it remains unclear whether it can indicate the total metabolic tumor volume (MTV). Recently, total lesion glycolysis (TLG) and MTV—indicators of ^{18}F-FDG accumulation within tumor cells—have been identified as significant prognostic markers for predicting the treatment outcome in patients with NSCLC. A meta-analysis described TLG and MTV as better predictive markers than SUVmax [11]. Moreover, an exploratory study documented that the tumor metabolic activity assessed by TLG and MTV is better than SUVmax in evaluating the therapeutic monitoring of anti-PD-1 antibody in patients with previously treated NSCLC [10]. Recent reports suggested that baseline tumor size could predict adverse outcomes in patients with NSCLC who received ICI [12–14]. However, the detailed mechanism behind tumor burden (TB), determined by baseline tumor size and causing poor efficacy of ICI, is unclear. Tumors possibly suppress the immune response by different mechanisms other than the PD-1/PD-L1 pathway. Tumor hypoxia, determined by HIF-1, induces VEGF, which induces immunosuppressive T-lymphocytes such as regulatory T-cells (Tregs) and myeloid-derived suppressor cells [15,16]. These evidences suggest that the high HIF-1 expression caused by an increased tumor size creates an immunosuppressive environment regardless of ICI treatment and contributes to the poor outcome for patients with NSCLC [15,16]. However, whether morphological assessment, based on baseline tumor size, can accurately reflect the volume of tumor hypoxia or tumor metabolic activity is debatable. Therefore, ^{18}F-FDG uptake is expected to assess tumor activity more accurately than TB on computed tomography (CT).

We conducted this study to investigate whether the degree of ^{18}F-FDG uptake before the administration of anti-PD-1 antibody can predict the prognosis in patients with previously treated advanced NSCLC, by evaluating the correlation between TB and SUVmax, TLG, and MTV.

2. Materials and methods

2.1. Patients

We retrospectively examined the medical records at Saitama Medical University International Medical Center, Saitama, Japan (ethical approval code: 19-225; date of approval: 13 November 2019) and selected patients with previously treated NSCLC who received anti-PD-1 antibody monotherapy, such as nivolumab and pembrolizumab, and underwent ^{18}F-FDG-PET after previous treatment and before the initiation of anti-PD-1 antibody as a recurrent survey. From February 2016 through April 2019, 97 patients with pretreated NSCLC were administered nivolumab and pembrolizumab. Twelve patients were excluded because of inadequate medical information and absence of an evaluable target lesion. Therefore, the final cohort consisted of 85 patients.

This study was approved by the institutional ethics committee of the Saitama Medical University International Medical Center. All procedures performed in studies involving human participants

were in accordance with the ethical standards of the institutional and/or national research committee and with the 1964 Helsinki declaration and its later amendments or comparable ethical standards. The requirement for written informed consent was waived because of the retrospective nature of the study.

2.2. Treatment, Efficacy Evaluation, and Assessment of Baseline Tumor Burden

Nivolumab and pembrolizumab were intravenously administered at 3 mg/kg every 2 weeks and at 200 mg/day every 3 weeks, respectively. Complete blood cell count, differential count, routine chemistry measurements, physical examination, and toxicity assessment were performed weekly. Acute toxicity was graded using the Common Terminology Criteria for Adverse Events version 4.0. Tumor response was evaluated using the Response Evaluation Criteria in Solid Tumors version 1.1 [17]. Baseline TB was evaluated using CT for target lesions [13,14]. TB was defined as the sum of the longest diameter for a maximum of five target lesions and up to two lesions per organ [13,14].

2.3. PET Imaging and Data Analysis

Patients fasted for at least 6 hours before PET imaging, performed using a PET/CT scanner (Biograph 6 or 16, Siemens Healthineers K.K., Japan) with a 585 mm field of view. Three-dimensional data acquisition was initiated 60 minutes after injecting 3.7 MBq/kg of FDG. We acquired eight bed positions (2-minute acquisition per bed position) according to the range of imaging. Attenuation-corrected transverse images obtained with ^{18}F-FDG were reconstructed with the ordered-subsets expectation-maximization algorithm, based on the point spread function into 168×168 matrices with a slice thickness of 2.00 mm.

For the semiquantitative analysis, functional images of SUV were produced using attenuation-corrected transaxial images, injected dosage of ^{18}F-FDG, patient's body weight, and he cross-calibration factor between PET and the dose calibrator. SUV was defined as follows:

SUV = Radioactive concentration in the region of interest (ROI) (MBq/g)/Injected dose (MBq)/Patient's body weight (g).

A nuclear physician conducted the volume of interest (VOI) analysis using CT scans, eliminating the physiological uptake in the heart, urinary tracts, and gastrointestinal tracts. We used GI-PET software (Nihon Medi-physics Co. Ltd., Tokyo, Japan) on a Windows workstation to semi-automatically calculate the MTV and TLG (= $SUV_{mean} \times$ MTV), of each lesion using SUV thresholds in the liver VOI (= $SUV_{mean} + [1.5 \times SUV_{Standard\_Deviation}]$). These SUV thresholds were the optimum values to generate VOIs in which the whole tumor mass is completely enclosed in all cases, with the CT image as the reference. SUV_{max} and SUV_{mean} within the generated VOI were also calculated automatically. VOIs over all measurable lesions on pretreatment PET/CT were automatically registered. In case of multiple lesions in the same organ, a maximum of 100 lesions were measured.

2.4. Statistical Analysis

Statistical significance was indicated by $p < 0.05$. Fisher's exact tests were used to examine the association between two categorical variables. Correlations between SUVmax, MTV, and TLG on ^{18}F-FDG uptake were analyzed using the Pearson rank test. The Kaplan–Meier method was used to estimate survival as a function of time, and survival differences were analyzed by log-rank tests. Progression-free survival (PFS) was defined as the time from the initiation of anti-PD-1 antibody to tumor recurrence or death from any cause, while overall survival (OS) was defined as the time from the initiation of anti-PD-1 antibody to death from any cause. Statistical analyses were performed using GraphPad Prism 7 (Graph Pad Software, San Diego, CA, USA) and JMP 14.0 (SAS Institute Inc., Cary, NC, USA).

3. Results

3.1. Assessment of SUV_{max}, MTV, and TLG on ^{18}F-FDG Uptake

In all 85 patients, the median values of SUVmax, MTV, and TLG on ^{18}F-FDG and TB were 6.0 (range, 3.1–21.0), 17.8 cm^3 (range, 1.1–379 cm^3), 75.4 gcm^3/mL (range, 3.9–2550 g·cm^3/mL), and 65 cm (range, 6.6–230.6 cm), respectively. According to histological types, the median values of SUVmax, MTV, and TLG on ^{18}F-FDG and TB in adenocarcinoma were 6.7 (range, 3.1–21.3), 11.3 cm^3 (range, 1.1–276 cm^3), 58.3 g·cm^3/mL (range, 3.9–1398 g·cm^3/mL), and 53 cm (range, 6.6–230.6 cm), respectively, and those in non-adenocarcinoma displayed 8.4 (range, 3.2–20.4) 24.8 cm^3 (range, 1.1–379 cm^3), 105.6 g·cm^3/mL (range, 4.0–2550 g·cm^3/mL), and 75 cm (range, 18.2–228.3 cm), respectively. The difference of each parameter for SUVmax, MTV, and TLG on ^{18}F-FDG and TB was not significant between adenocarcinoma and non- adenocarcinoma. The SUVmax correlated significantly with MTV ($r = 0.49$, $p < 0.01$), TLG ($r = 0.56$, $p < 0.01$), and TB ($r = 0.33$, $p < 0.01$). Figure 1 is a representative PET image showing the assessment of SUVmax, MTV, and TLG on ^{18}F-FDG.

The discriminative value of various SUVmax, MTV, and TLG cutoffs for ^{18}F-FDG uptake were explored in the context of OS and PFS (Figure 2) [13]. For prognosis in OS and PFS analyses, the most discriminative cutoffs based on log-rank test for SUVmax, MTV, and TLG were 6.0, 5.0, and 20, respectively. The TLG cutoff of 20 was significant in the OS analysis, but not in the PFS analysis, although it was the most favorable TLG cutoff. The SUVmax cutoff of 6 was not significant in either OS or PFS analysis, but still seemed better considering the results of the log-rank test. The 12 cm cutoff for TB was based on a previous study [13].
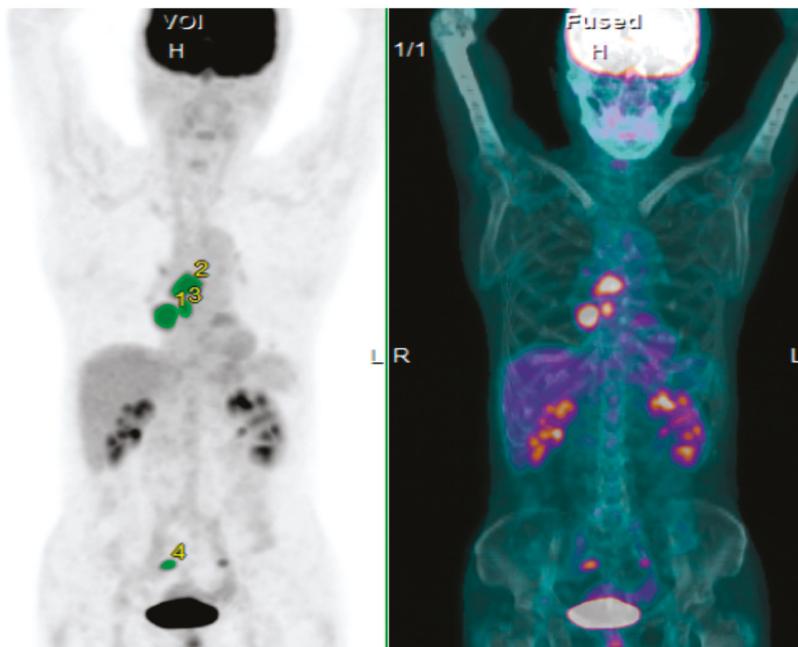
Figure 1. Imaging from a positron emission tomography (PET) scan of non-small cell lung cancer (NSCLC), indicating the measurement of SUVmax, metabolic tumor volume (MTV) and total lesion glycolysis (TLG) on 2-deoxy-2-[^{18}F]fluoro-D-glucose (^{18}F-FDG).

3.2. Patient Demographics

Patient demographics according to the cutoff values of SUVmax, MTV, and TLG on ^{18}F-FDG uptake are listed in Table 1. In the 17 patients harboring epidermal growth factor receptor (*EGFR*) mutation, deletion 19 and L858R were observed in 11 and 6 patients, respectively. High TLG and SUVmax on ^{18}F-FDG uptake were significantly associated with smoking history. The objective response rate and disease control rate were 36.6% [95% confidence internal (CI); 26.2%–47.0%] and 65.9% [95%CI; 55.6%–76.1%]. No significant difference in the response to ICI was observed according to the degree of SUVmax, MTV, and TLG on ^{18}F-FDG uptake. The median time from the date of ^{18}F-FDG-PET scan to the initiation of anti-PD-1 antibodies was 18 days (range, 1–107 days). Next, we analyzed different incidences of immune-related adverse events (irAEs) according to the degree of SUVmax, MTV, and TLG on ^{18}F-FDG uptake and TB. The frequency of any irAE was significantly higher in patients with low values of SUVmax, MTV, and TLG on PET than in those with high values, but not for TB (Table S1, online only). The incidence of grade 3 or 4 irAEs exhibited no close correlation with the degree of ^{18}F-FDG uptake on PET and TB.

Table 1. Patient's demographics according to the assessment of FDG uptake.

Variables	Total (*n* = 85)	TLG			MTV			SUVmax		
		High (*n* = 59)	Low (*n* = 26)	*p*-Value	High (*n* = 58)	Low (*n* = 27)	*p*-Value	High (*n* =5 2)	Low (*n* = 33)	*p*-Value
Age ≤ 70/>70 (range: 38–86 years)	42/43	29/30	13/13	>0.99	25/33	17/10	0.11	26/26	16/17	>099
Gender Male/Female	65/20	47/12	18/8	0.41	46/12	19/8	0.42	42/10	23/10	0.29
Smoking history Yes/No	71/14	51/8	10/16	**<0.01**	50/8	21/6	0.35	47/5	24/9	**0.04**
Performance status 0 or 1/2 or 3	79/6	53/6	26/0	0.17	52/6	27/0	0.17	46/6	33/0	0.07
Histological type AC/Non-AC	51/34	33/26	18/8	0.34	32/26	19/8	0.24	27/25	24/9	0.07
EGFR mutation Yes/No	17/68	12/47	5/21	>0.99	12/47	5/22	>0.99	10/42	7/26	>0.99
Response to ICI [#] CR or PR/SD or PD CR, PR or SD/PD	29/51 53/27	20/35 34/21	9/16 19/6	>0.99 0.31	20/34 36/18	9/17 17/9	>0.99 >0.99	21/27 34/15	8/24 19/12	0.10 0.47

Abbreviations: TLG, total lesion glycolysis; MTV, metabolic tumor volume; SUVmax, the maximum of standardized uptake value; AC, adenocarcinoma; Non-AC, non-adenocarcinoma; EGFR, epidermal growth factor receptor; CR, complete response; PR, partial response; SD, stable disease; PD, progressive disease; ICI, immune checkpoint inhibitor. #, because of 6 patients with no measurable lesion, 82 patients were analyzed according to the uptake of FDG; Bold character shows statistically significance.

3.3. Survival and ^{18}F-FDG-PET:

The median OS and PFS were 716 and 161 days, respectively, and the 2-year OS rate was 44.8%. Among all patients, those with a low TLG exhibited significantly better OS than those with a high TLG. Similarly, the survival analysis of MTV on ^{18}F-FDG uptake demonstrated a significantly worse OS and PFS for patients with a high MTV (Figure 2). No statistically significant difference in the OS and PFS was observed between patients with a low and high SUVmax (Figure 2). However, in 70 patients without an EGFR mutation, a statistically significant difference in OS and PFS was recognized between patients with low and high TLG or low and high MTV, but not between those with low and high SUVmax and low and high TB (Figure 3). Survival analysis results are listed in Table 2. Univariate analysis in all patients identified performance status (PS), TLG, and MTV as significant prognostic markers for OS; the significant predictors for PFS were PS and MTV. Subsequently, we performed a multivariate analysis according to TLG and MTV and confirmed that PS, TLG, and MTV were independent prognostic factors for poor OS and PFS; the significant prognostic marker for PFS was PS (Table 3). In patients without EGFR mutation, a multivariate analysis identified TLG and MTV as independent prognostic factors for predicting poor OS. Histological typing confirmed TLG and MTV as significant prognostic factors in patients with adenocarcinoma, but not in those with non-adenocarcinoma.
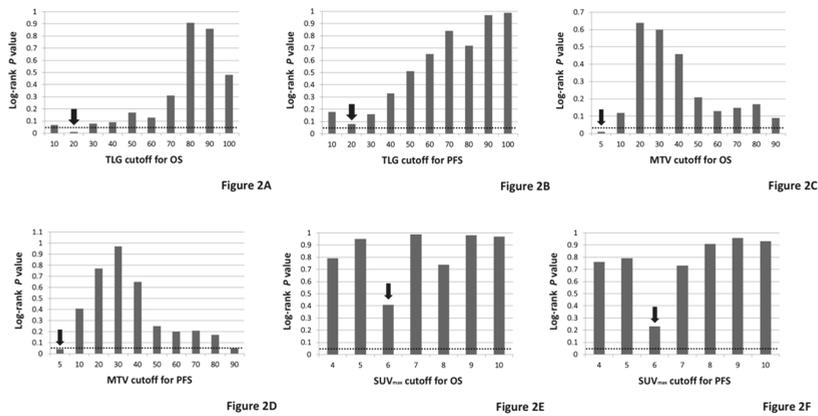
Figure 2. Discriminative value by log-rank test according to various TLG (**A**), MTV (**C**) and SUVmax (**E**) cutoff for OS and TLG (**B**), MTV (**D**) and SUVmax (**F**) cutoff for PFS in 18F-FDG-PET.
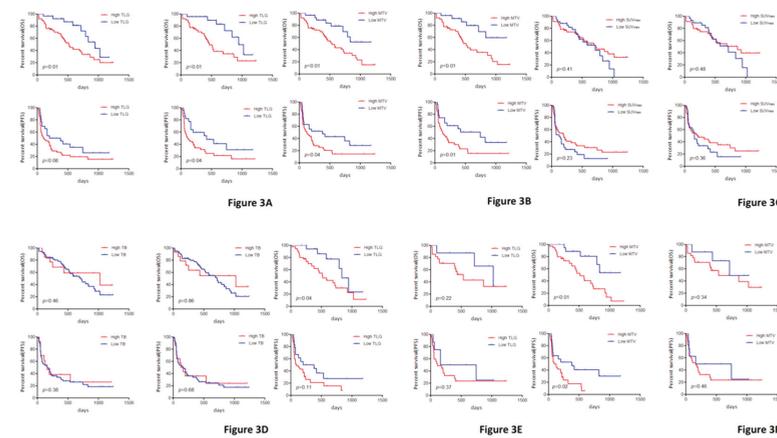
Figure 3. Kaplan–Meier curves according to various TLG (**A**), MTV (**B**), SUVmax (**C**) and TB (**D**) for OS and PFS. (**A**); OS (upper left) and PFS (lower left) in all patients and OS (upper right) and PFS (lower right) in those without EGFR mutation according to TLG. (**B**); OS (upper left) and PFS (lower left) in all patients and OS (upper right) and PFS (lower right) in those without EGFR mutation according to MTV. (**C**); OS (upper left) and PFS (lower left) in all patients and OS (upper right) and PFS (lower right) in those without EGFR mutation according to SUVmax. (**D**); OS (upper left) and PFS (lower left) in all patients and OS (upper right) and PFS (lower right) in those without EGFR mutation according to TB. (**E**); OS (upper left) and PFS (lower left) in patients with AC patients and OS (upper right) and PFS (lower right) in those with non-AC according to TLG. (**F**); OS (upper left) and PFS (lower left) in patients with non-AC patients and OS (upper right) and PFS (lower right) in those with non-AC according to MTV. Abbreviation: TLG, total lesion glycolysis; MTV, metabolic tumor volume; SUVmax: maximal standardized under value; TB, tumor burden; OS, overall survival; PFS, progression-free survival; AC, adenocarcinoma; non-AC, non-adenocarcinoma.

Table 2. Univariate analysis in overall survival and progression-free survival.

	Overall Survival				Progression-Free Survival			
	All Patients (*n* = 85)		Patients without EGFR Mutation (*n* = 70)		All Patients (*n* = 85)		Patients without EGFR Mutation (*n* = 70)	
Variables	MST (days)	*p*-Value	MST (days)	*p*-Value	MST (days)	*p*-Value	MST (days)	*p*-Value
Age (≤70/>70)	737/693	0.73	865/693	0.85	164/161	0.88	181/180	0.92
Gender (Male/Female)	716/737	0.85	693/837	0.59	181/75	0.67	172/420	0.23
Smoking (Yes/No)	716/737	0.53	716/637	0.74	181/72	0.09	181/272	0.85
PS (0 or 1/2 or 3)	724/115	**<0.01**	716/74	**<0.01**	172/40	**<0.01**	200/25	0.10
Histological type (AC/Non-AC)	724/716	0.84	693/716	0.66	146/161	0.76	220/161	0.39
TLG (High/Low)	516/945	**0.01**	465/945	**<0.01**	114/291	0.08	114/420	**0.04**
MTV (High/Low)	536/NR	**<0.01**	465/NR	**<0.01**	125/382	**0.04**	127/382	**0.02**
SUVmax (High/Low)	724/716	0.41	865/716	0.48	201/125	0.23	204/161	0.36
TB (High/Low)	793/693	0.46	837/693	0.86	204/137	0.38	182/181	0.68

Abbreviations: TLG, total lesion glycolysis; MTV, metabolic tumor volume; SUVmax, the maximum of standardized uptake value; AC, adenocarcinoma; Non-AC, non-adenocarcinoma; PS, performance status; HR, hazard ratio; 95% CI, 95% confidence interval; NR, not reached; EGFR, epidermal growth factor receptor; TB, tumor burden; Bold character shows statistically significance.

Table 3. Multivariate analysis of overall survival and progression-free survival.

	Overall Survival				Progression-Free Survival			
	All Patients (*n* = 85)		Patients without EGFR Mutation (*n* = 70)		All Patients (*n* = 85)		Patients without EGFR Mutation (*n* = 70)	
Variables	HR 95% CI	*p*-Value	HR 95% CI	*p*-Value	HR 95% CI	*p*-Value	HR 95% CI	*p*-Value
Survival Analysis Including TLG								
Age (≤ 70/> 70)	1.02 0.74–1.39	0.91	1.02 0.72–1.44	0.90	0.95 0.74–1.23	0.74	0.98 0.73–1.31	0.89
Gender (Male/Female)	1.11 0.76–1.55	0.55	0.95 0.55–1.48	0.85	1.07 0.79–1.41	0.61	0.81 0.49–1.19	0.31
PS (0 or 1/2 or 3)	1.68 1.05–2.51	**0.03**	2.22 1.06–3.93	**0.03**	1.63 1.02–2.36	**0.04**	1.41 0.68–2.43	0.31
TLG (High/Low)	1.47 1.03–2.21	**0.03**	1.63 1.10–2.60	**0.01**	1.21 0.92–1.63	0.16	1.32 0.97–1.86	0.07
Survival Analysis Including MTV								
Age (≤ 70/> 70)	0.92 0.68–1.26	0.64	0.87 0.61–1.25	0.46	0.91 0.71–1.18	0.51	0.91 0.67–1.21	0.51
Gender (Male/Female)	1.09 0.75–1.52	0.61	0.97 0.56–1.51	0.91	1.06 0.78–1.40	0.66	0.80 0.49–1.18	0.28
PS (0 or 1/2 or 3)	1.69 1.06–2.51	**0.02**	2.23 1.06–3.94	**0.03**	1.59 1.02–2.33	**0.04**	1.41 0.68–2.41	0.31
MTV (High/Low)	1.59 1.09–2.45	**0.01**	1.83 1.19–3.04	**<0.01**	1.28 0.97–1.73	0.07	1.45 1.05–2.05	**0.02**

Abbreviations: TLG, total lesion glycolysis; MTV, metabolic tumor volume; PS, performance status; HR, hazard ratio; 95% CI, 95% confidence interval; EGFR, epidermal growth factor receptor.

4. Discussion

To the best of our knowledge, this is the first study to evaluate the prognostic significance of metabolic parameters measured by ^{18}F-FDG-PET for predicting outcomes after the initiation of anti-PD-1 antibodies in patients with previously treated NSCLC. We found that the tumor metabolic volume assessed by TLG and MTV was an independent prognostic factor, but not SUVmax and TB. The roles of TLG and MTV as significant predictive markers after anti-PD-1 antibody therapy may be closely associated with patients with a histology of adenocarcinoma and without EGFR mutation.

Although the value of SUVmax on ^{18}F-FDG uptake within tumor cells was closely correlated with that of TLG and MTV, SUVmax on ^{18}F-FDG uptake before anti-PD-1 antibody could not accurately predict the outcome after the initiation of treatment. Furthermore, we found that low uptake of ^{18}F-FDG was closely associated with the occurrence of irAEs and the incidence of grade 3 or 4 irAEs exhibited no close correlation with the degree of ^{18}F-FDG uptake on PET. In addition, there was no significant correlation between the response to the anti-PD-1 antibody and the degree of ^{18}F-FDG uptake. However, we discovered that MTV of pretreatment ^{18}F-FDG-PET plays a crucial role in the prognostic significance of anti-PD-1 antibody treatment. Unlike previous studies [12,13], our study indicated that TB determined by baseline tumor size was not a significant predictor of ICI or irAEs. Further studies are warranted to investigate whether pretreatment of MTV can predict the outcome of ICI plus ICI or the combination of ICI plus cytotoxic chemotherapy as first-line treatment.

A recent study reported that the metabolic response to ^{18}F-FDG uptake measured by TLG or MTV was a stronger biomarker for the prediction of efficacy and survival at one month after the initiation of nivolumab than SUV_{max} [10]. The predictive probability of partial response (100% versus 29%, $p = 0.021$) and progressive disease (100% versus 22.2%, $p = 0.002$) at one month after nivolumab treatment was significantly higher in ^{18}F-FDG-PET than in CT. Moreover, multivariate analysis confirmed the ^{18}F-FDG uptake measurement by TLG or MTV as an independent prognostic factor. Thus, ^{18}F-FDG-PET may be a useful radiographic modality for immune monitoring to predict the efficacy of ICI. However, a large-scale prospective study is required to confirm these results [10,18]. A recent meta-analysis suggested that in lung cancer, metabolic parameters such as TLG and MTV are better prognostic predictors after any treatment when compared with SUV_{max} [11].

Recently, Jreige et al. described that the metabolic-to-morphological volume ratio (MMVR)—calculated by dividing MTV by morphological tumor volume (MoTV)—was able to predict the radiological response to anti-PD-1/PD-L1 blockade and was negatively correlated with tumor PD-L1 expression and tumor necrosis [18]. Although their study analyzed only 17 patients who received anti-PD-1 therapy, they suggested that anti-PD-1 therapy is effective for tumor tissues with a low ratio of MTV, and the presence of a low MTV contributes to the upregulation of PD-L1 expression by the hypoxic environment in the tumor arising from necrosis and inflammation. However, it remained unclear whether MMVR could predict the outcome after anti-PD-1 therapy. Our study, however, indicated that patients with a low MTV exhibited a favorable prognosis after anti-PD-1 therapy. Several studies have demonstrated that tumor necrosis triggers inflammation, which facilitates the influx of lymphocytes and the upregulation of PD-L1, related to tumor necrosis factor-α, and that necrosis or inflammation was closely linked to tumor recurrence and worse survival [19,20]. Our study could not investigate the relationship between necrosis or inflammation and tumor metabolic volume; therefore, it remains unclear whether low MTV and TLG are associated with necrosis, inflammation, and hypoxic environment in the tumor. Further investigation is warranted to elucidate the prognostic significance of MTV and TLG as predictive markers of anti-PD-1 therapy based on the biological aspect.

The mechanism by which tumor cells uptake ^{18}F-FDG requires glucose metabolism, hypoxia, and angiogenesis, and ^{18}F-FDG is closely associated with the expression of these markers [6]. The expression of PD-L1 is significantly related to Glut1, HIF-1α and SUV_{max} on ^{18}F-FDG uptake in lung cancer [7–9]. However, it is reported that TLG and MTV on ^{18}F-FDG uptake were not closely correlated with PD-L1 expression levels [18], but Foxp3-Tregs are described to be positively associated with TLG and MTV [21]. Considering these evidences, the active environment with high MTV may form an immunosuppressive state, contributing to the resistant situation to ant-PD-1 blockage.

Our study has several limitations. First, we employed a retrospective approach and a small cohort, which may have introduced bias in our results. More than half of the patients with previously treated NSCLC had not undergone ^{18}F-FDG-PET just before the initiation of anti-PD-1 antibody treatment. Therefore, we think that the number of eligible patients was slightly limited. However, the current study is meaningful for the prediction of anti-PD-1 therapy. Second, our study suggests that MTV could be a predictive marker for ICI treatment compared to the morphological tumor volume. However, the

appropriateness of morphological assessment used for calculating the optimal tumor volume of all metastatic lesions using CT scan is debatable. Thus, it may be difficult to perform a concise comparison between metabolic and morphological tumor volumes. Moreover, we had no information about the calculation of MMVR in our study, thus, there were some limitations in discussing the prognostic significance of metabolic tumor volume compared to MMVR. Lastly, an the immunohistochemical analysis of PD-L1, expression within tumor cells using tumor specimens was not performed before anti-PD1 antibody treatment. At our institution, re-biopsy was not done routinely before ICI treatment except for the initial diagnosis. Further study is warranted to investigate the relationship between MTV and the immune environment.

In conclusion, TLG and MTV on ^{18}F-FDG uptake may predict the prognosis after anti-PD-1 antibodies in patients with previously treated NSCLC, but not SUVmax on ^{18}F-FDG uptake. Although MTV may indirectly reflect the presence of morphological tumor volume with active tumor cells, the assessment of TLG and MTV on ^{18}F-FDG uptake is easily executable in daily practice. A prospective study is needed to confirm these results.

References

1. Borghaei, H.; Paz-Ares, L.; Horn, L.; Spigel, D.R.; Steins, M.; Ready, N.E.; Chow, L.Q.; Vokes, E.E.; Felip, E.; Holgado, E.; et al. Nivolumab versus Docetaxel in Advanced Nonsquamous Non-Small-Cell Lung Cancer. *N. Engl. J. Med.* **2015**, *373*, 1627–1639. [CrossRef] [PubMed]

2. Robert, C.; Long, G.V.; Brady, B.; Dutriaux, C.; Maio, M.; Mortier, L.; Hassel, J.C.; Rutkowski, P.; McNeil, C.; Kalinka-Warzocha, E.; et al. Nivolumab in previously untreated melanoma without BRAF mutation. *N. Engl. J. Med.* **2015**, *372*, 320–330. [CrossRef] [PubMed]

3. Reck, M.; Rodríguez-Abreu, D.; Robinson, A.G.; Hui, R.; Csőszi, T.; Fülöp, A.; Gottfried, M.; Peled, N.; Tafreshi, A.; Cuffe, S.; et al. Pembrolizumab versus Chemotherapy for PD-L1-Positive Non-Small-Cell Lung Cancer. *N. Engl. J. Med.* **2016**, *375*, 1823–1833. [CrossRef] [PubMed]

4. Rittmeyer, A.; Barlesi, F.; Waterkamp, D.; Park, K.; Ciardiello, F.; von Pawel, J.; Gadgeel, S.M.; Hida, T.; Kowalski, D.M.; Dols, M.C.; et al. Atezolizumab versus docetaxel in patients with previously treated non-small-cell lung cancer (OAK): A phase 3, open-label, multicentre randomised controlled trial. *Lancet* **2017**, *389*, 255–265. [CrossRef]

5. Kaira, K.; Oriuchi, N.; Otani, Y.; Yanagitani, N.; Sunaga, N.; Hisada, T.; Ishizuka, T.; Endo, K.; Mori, M. Diagnostic usefulness of fluorine-18-alpha-methyltyrosine positron emission tomography in combination with 18F-fluorodeoxyglucose in sarcoidosis patients. *Chest* **2007**, *131*, 1019–1027. [CrossRef]

6. Kaira, K.; Endo, M.; Abe, M.; Nakagawa, K.; Ohde, Y.; Okumura, T.; Takahashi, T.; Murakami, H.; Tsuya, A.; Nakamura, Y.; et al. Biologic correlation of 2-[18F]-fluoro-2-deoxy-D-glucose uptake on positron emission tomography in thymic epithelial tumors. *J. Clin. Oncol.* **2010**, *28*, 3746–3753. [CrossRef]

7. Takada, K.; Toyokawa, G.; Okamoto, T.; Baba, S.; Kozuma, Y.; Matsubara, T.; Haratake, N.; Akamine, T.; Takamori, S.; Katsura, M.; et al. Metabolic characteristics of programmed cell death-ligand 1-expressing lung cancer on ^{18}F-fluorodeoxyglucose positron emission tomography/computed tomography. *Cancer Med.* **2017**, *6*, 2552–2561. [CrossRef]

8. Kasahara, N.; Kaira, K.; Yamaguchi, K.; Masubuchi, H.; Tsurumaki, H.; Hara, K.; Koga, Y.; Sakurai, R.; Higuchi, T.; Handa, T.; et al. Fluorodeoxyglucose uptake is associated with low tumor-infiltrating lymphocyte levels in patients with small cell lung cancer. *Lung Cancer* **2019**, *134*, 180–186. [CrossRef]

9. Kaira, K.; Shimizu, K.; Kitahara, S.; Yajima, T.; Atsumi, J.; Kosaka, T.; Ohtaki, Y.; Higuchi, T.; Oyama, T.; Asao, T.; et al. 2-Deoxy-2-[fluorine-18] fluoro-d-glucose uptake on positron emission tomography is associated with programmed death ligand-1 expression in patients with pulmonary adenocarcinoma. *Eur. J. Cancer* **2018**, *101*, 181–190. [CrossRef]

10. Kaira, K.; Higuchi, T.; Naruse, I.; Arisaka, Y.; Tokue, A.; Altan, B.; Suda, S.; Mogi, A.; Shimizu, K.; Sunaga, N.; et al. Metabolic activity by ^{18}F-FDG-PET/CT is predictive of early response after nivolumab in previously treated NSCLC. *Eur. J. Nucl. Med. Mol. Imaging* **2018**, *45*, 56–66. [CrossRef]

11. Im, H.J.; Pak, K.; Cheon, G.J.; Kang, K.W.; Kim, S.J.; Kim, I.J.; Chung, J.K.; Kim, E.E.; Lee, D.S. Prognostic value of volumetric parameters of ^{18}F-FDG PET in non-small-cell lung cancer: A meta-analysis. *Eur. J. Nucl. Med. Mol. Imaging* **2015**, *42*, 241–251. [CrossRef] [PubMed]

12. Katsurada, M.; Nagano, T.; Tachihara, M.; Kiriu, T.; Furukawa, K.; Koyama, K.; Otoshi, T.; Sekiya, R.; Hazama, D.; Tamura, D.; et al. Baseline tumor size as predictive and prognostic factor of immune checkpoint inhibitor therapy for non-small cell lung cancer. *Anticancer Res.* **2019**, *39*, 815–825. [CrossRef] [PubMed]

13. Sakata, Y.; Kawamura, K.; Ichikado, K.; Shingu, N.; Yasuda, Y.; Eguchi, Y.; Hisanaga, J.; Nitawaki, T.; Iio, M.; Sekido, Y.; et al. Comparisons between tumor burden and other prognostic factors that influence survival of patients with non-small cell lung cancer treated with immune checkpoint inhibitors. *Thorac. Cancer* **2019**, *10*, 2259–2266. [CrossRef] [PubMed]

14. Dercle, L.; Ammari, S.; Champiat, S.; Massard, C.; Ferté, C.; Taihi, L.; Seban, R.D.; Aspeslagh, S.; Mahjoubi, L.; Kamsu-Kom, N.; et al. Rapid and objective CT scan prognostic scoring identifies metastatic patients with long-term clinical benefit on anti-PD-1/L1 therapy. *Eur. J. Cancer* **2016**, *65*, 33–42. [CrossRef]

15. Fukumura, D.; Kloepper, J.; Amoozgar, Z.; Duda, D.G.; Jain, R.K. Enhancing cancer immunotherapy using antiangiogenics; opportunities and challenges. *Nat. Rev. Clin. Oncol.* **2018**, *29*, 325–340. [CrossRef]

16. Schaaf, M.B.; Garg, A.D.; Agostinis, P. Defining the role of the tumor vasculature in antitumor immunity and immunotherapy. *Cell Death Dis.* **2018**, *1*, 115. [CrossRef]

17. Eisenhauer, E.A.; Therasse, P.; Bogaerts, J.; Schwart, L.H.; Sargent, D.; Ford, R.; Dancey, J.; Arbuck, S.; Gwyther, S.; Mooney, M.; et al. New response evaluation criteria in solid tumour: Revised RECIST guideline (version 1.1). *Eur. J. Cancer* **2009**, *45*, 228–247. [CrossRef]

18. Jreige, M.; Letovanec, I.; Chaba, K.; Renaud, S.; Rusakiewicz, S.; Cristina, V.; Peters, S.; Krueger, T.; de Leval, L.; Kandalaft, L.E.; et al. ^{18}F-FDG PET metabolic-to-morphological volume ratio predicts PD-L1 tumour expression and response to PD-1 blockade in non-small-cell lung cancer. *Eur. J. Nucl. Med. Mol. Imaging* **2019**, *46*, 1859–1868. [CrossRef]

19. Garg, A.D.; Agostinis, P. Cell death and immunity in cancer from danger signals to mimicry of pathogen defense responses. *Immmunol. Rev.* **2017**, *280*, 126–148. [CrossRef]

20. Gkogkou, C.; Frangia, K.; Saif, M.W.; Trigidou, R.; Syrigos, K. Necrosis and apoptotic index as prognostic factors in non-small cell lung cancer: A review. *Springerplus* **2014**, *3*, 120. [CrossRef]

21. Wang, Y.; Zhao, N.; Wu, Z.; Pan, N.; Shen, X.; Liu, T.; Wei, F.; You, J.; Xu, W.; Ren, X. New insight on the correlation of metabolic status on ^{18}F-FDG PET/CT with immune marker expression in patients with non-small cell lung cancer. *Eur. J. Nucl. Med. Mol. Imaging* **2019**, in press. [CrossRef] [PubMed]

Article

Identification of Clonality through Genomic Profile Analysis in Multiple Lung Cancers

**Rumi Higuchi [1,†], Takahiro Nakagomi [1,2,†], Taichiro Goto [1,2,*], Yosuke Hirotsu [3,†],
Daichi Shikata [1], Yujiro Yokoyama [1,2], Sotaro Otake [1], Kenji Amemiya [3], Toshio Oyama [4],
Hitoshi Mochizuki [3] and Masao Omata [3,5]**

[1] Lung Cancer and Respiratory Disease Center, Yamanashi Central Hospital, Yamanashi 400-8506, Japan;
lumi.hgc.236@gmail.com (R.H.); nakagomi.takahiro@gmail.com (T.N.); shikarupd@yahoo.co.jp (D.S.);
dooogooodooo@me.com (Y.Y.); sotaro.otake@gmail.com (S.O.)
[2] Department of Surgery, School of Medicine, Keio University, Tokyo 160-8582, Japan
[3] Genome Analysis Center, Yamanashi Central Hospital, Yamanashi 400-8506, Japan;
hirotsu-bdyu@ych.pref.yamanashi.jp (Y.H.); amemiya-bdcd@ych.pref.yamanashi.jp (K.A.);
h-mochiduki2a@ych.pref.yamanashi.jp (H.M.); m-omata0901@ych.pref.yamanashi.jp (M.O.)
[4] Department of Pathology, Yamanashi Central Hospital, Yamanashi 400-8506, Japan;
t-oyama@ych.pref.yamanashi.jp
[5] Department of Gastroenterology, The University of Tokyo Hospital, Tokyo 113-8655, Japan
* Correspondence: taichiro@1997.jukuin.keio.ac.jp; Tel.: +81-55-253-7111
† These authors contributed equally to this work.

Abstract: In cases of multiple lung cancers, individual tumors may represent either a primary lung cancer or both primary and metastatic lung cancers. In this study, we investigated the differences between clinical/histopathological and genomic diagnoses to determine whether they are primary or metastatic. 37 patients with multiple lung cancers were enrolled in this study. Tumor cells were selected from tissue samples using laser capture microdissection. DNA was extracted from those cells and subjected to targeted deep sequencing. In multicentric primary lung cancers, the driver mutation profile was mutually exclusive among the individual tumors, while it was consistent between metastasized tumors and the primary lesion. In 11 patients (29.7%), discrepancies were observed between genomic and clinical/histopathological diagnoses. For the lymph node metastatic lesions, the mutation profile was consistent with only one of the two primary lesions. In three of five cases with lymph node metastases, the lymph node metastatic route detected by genomic diagnosis differed from the clinical and/or pathological diagnoses. In conclusion, in patients with multiple primary lung cancers, cancer-specific mutations can serve as clonal markers, affording a more accurate understanding of the pathology of multiple lung cancers and their lymphatic metastases and thus improving both the treatment selection and outcome.

Keywords: lung cancer; multiple cancers; metastasis; sequencing; mutation; genomic diagnosis

---

1. Introduction

In patients with synchronous or metachronous multiple cancers, individual tumors may appear as either a primary lung cancer or both primary and metastatic lung cancers. The selection of treatment in such cases is dependent on the resulting characteristics. In patients with multiple lung cancers, the nature of a tumor (i.e., whether it is metastatic or primary) can usually be judged on the basis of diagnostic imaging findings, clinical course, and/or pathology. If individual tumors composing multiple lung cancers are histologically inconsistent in terms of histological morphology and/or cellular atypism, the multiple onset of primary cancers is highly likely. However, there are no specific radiological,

clinical or histological features that can be utilized to unambiguously distinguish intrapulmonary metastases from multiple primary cancers and the cut diagnosis can be perplexing in the clinical setting. The differing biological activities of tumors allow for prognostic distinctions to be drawn and patients with intrapulmonary metastasis are supposed to have a poorer prognosis. Therefore, it is critically important to develop improved methods for the identification of tumors by exploring new, practical techniques and markers. We have previously demonstrated that as a more precise and clinically applicable method, a comparison of the driver mutation profiles enables elucidation of the clonal origin of tumors and thus facilitates an accurate discrimination between primary and metastatic tumors [1]. However, this finding was based on only 12 multiple lung cancer cases; hence, validation through a study involving a larger number of such cases was needed. Moreover, the significance of these findings in the clinical setting remained to be determined. In view of this, we extended the case accrual period to 5 years and included 37 patients with multiple lung cancers in the present study. In addition, we analyzed the clinical course in individual patients in detail to examine the use of mutation data for the diagnosis of multiple lung cancers in clinical practice and to determine the actual contribution of this approach to an improvement of clinical practice. Furthermore, we analyzed gene mutations in primary lung cancers as well as metastatic lymph nodes and genetically examined the pathology of the metastatic lymph nodes to accurately understand the pathology of lymphatic metastasis and thus enhance the postoperative treatment outcome.

2. Methods

2.1. Patients and Sample Preparation

The study enrolled 37 patients who had undergone surgery for multiple lung cancers in our department between January 2015 and July 2019. Written informed consent for genetic research was obtained from all patients, which was performed in accordance with protocols approved by the institutional review board in our hospital. Histological typing was performed according to the World Health Organisation (WHO) classification (3rd edition) [2] and clinical staging was performed according to the International Union Against Cancer Tumor-Node-Metastasis (TNM) classification (8th edition) [3].

A serial section from formalin-fixed, paraffin-embedded (FFPE) tissue was stained with hematoxylin-eosin and subsequently microdissected using an ArcturusXT laser capture microdissection system (Thermo Fisher Scientific, Tokyo, Japan). DNA was extracted using the QIAamp DNA FFPE Tissue Kit (Qiagen, Tokyo, Japan). FFPE DNA quality was verified using primers for the ribonuclease P locus. Peripheral blood was drawn from each patient immediately before surgery. A buffy coat was isolated by centrifugation and DNA was extracted from these cells using the QIAamp DNA Blood Mini Kit (Qiagen).

2.2. Targeted Deep Sequencing and Data Analysis

A panel covering the exons of 53 lung cancer-related genes (see Supplementary Table S1) was designed in-house to perform targeted sequencing. These genes were selected after a literature search based on the following criteria: (a) genes involved in lung cancer according to The Cancer Genome Atlas [4,5] and other, similar projects [6–10] or (b) genes frequently mutated in lung cancer according to the Catalogue Of Somatic Mutations In Cancer (COSMIC) database [11]. Ion AmpliSeq designer software (Thermo Fisher Scientific) was utilized for the primer composition, as previously reported [1,12,13]. An Ion AmpliSeq Library kit (Thermo Fisher Scientific) was utilized for the preparation of sequencing libraries. The library samples were bar-coded with an Ion Xpress Barcode Adapters kit (Thermo Fisher Scientific), purified using Agencourt AMPure XP reagent (Beckman Coulter, Tokyo, Japan) and subsequently quantified using an Ion Library Quantitation Kit (Thermo Fisher Scientific). The libraries were templated with an Ion PI Template OT2 200 Kit v3 (Thermo

Fisher Scientific). Sequencing was performed on Ion Proton (Ion Torrent) with an Ion PI Sequencing 200 Kit v3.

The sequence data were processed on standard Ion Torrent Suite Software. Raw signal data were measured using the Torrent Suite version 4.0. The pipeline consisted of signaling processing, base calling, quality score assignment, read alignment to the human genome 19 reference (hg19), mapping quality control and coverage analysis. After the data analysis, the annotation of single-nucleotide variants and indels (insertions and deletions) was performed on the Ion Reporter Server System (Thermo Fisher Scientific). Blood cell DNA extracted from the peripheral blood was used as a normal control to detect variants (Tumor-Normal pair analysis). Sequencing data were visually analyzed using an Integrative Genomics Viewer.

3. Results

3.1. Patient Characteristics

The 37 patients recruited in this study (age range, 54–85 years; mean age, 70.5 ± 7.5 years) were divided into different groups according to the following characteristics (Supplementary Table S2): 31 males, 6 females; 30 smokers, 7 non-smokers; and pathological stage IA (n = 10), IB (n = 15), IIA (n = 2), IIB (n = 4), IIIA (n = 5) and IIIB (n = 1). The maximum tumor diameter ranged from 2 mm to 80 mm (mean tumor diameter, 24.5 ± 15.9 mm).

Twenty nine patients were diagnosed with double or triple primary lung cancers on the basis of histopathological characteristics, including 15 patients with adenocarcinoma–adenocarcinoma, 3 patients with squamous cell carcinoma–squamous cell carcinoma, 5 patients with adenocarcinoma–squamous cell carcinoma and 6 patients with other combinations. In terms of tumor development, tumors developed synchronously and metachronously in 26 and 11 patients, respectively. In patients with metachronous tumors, the tumors were designated as tumor 1 (T1), T2 and T3 in chronological order from the earliest to the latest. In those with synchronous tumors, this designation was based on the order of size from the largest to the smallest.

3.2. Targeted Sequencing Identified Somatic Mutations in the Lung Cancers

Targeted sequencing was performed on 76 surgically resected tumors and 8 lymph nodes obtained from 37 patients, with their blood cell samples utilized as normal controls. The mean coverage depth was 1411-fold for cancer samples (range, 106- to 5096-fold) and 1387-fold for blood cell samples (range, 76- to 6960-fold). Sequence analyses detected 314 somatic mutations with an allele fraction ≥1% from 84 cancer lesions (1–54 mutations per tumor) (Supplementary Table S3). Among these mutations, 137 mutations (44%) were present at an allele fraction ≥20% (Supplementary Table S3).

In 29 patients, the gene, amino-acid substitution and nucleotide changes that were caused by these somatic mutations within individual tumors composing the multiple lung cancers lacked consistency (Figure 1, Supplementary Table S3). Thus, there were no shared or overlapping mutations among the individual lung cancers detected in these patients. This finding demonstrated that the multiple lung cancers in these cases were independently developed primary lung cancers (Figure 1). Meanwhile, in 8 patients, the gene mutation profile was consistent among the individual tumors, suggesting the presence of intrapulmonary metastasis (Figure 2). Importantly, in these cases, nucleotide position and mutation variance were entirely consistent across the tumors (Supplementary Table S3).
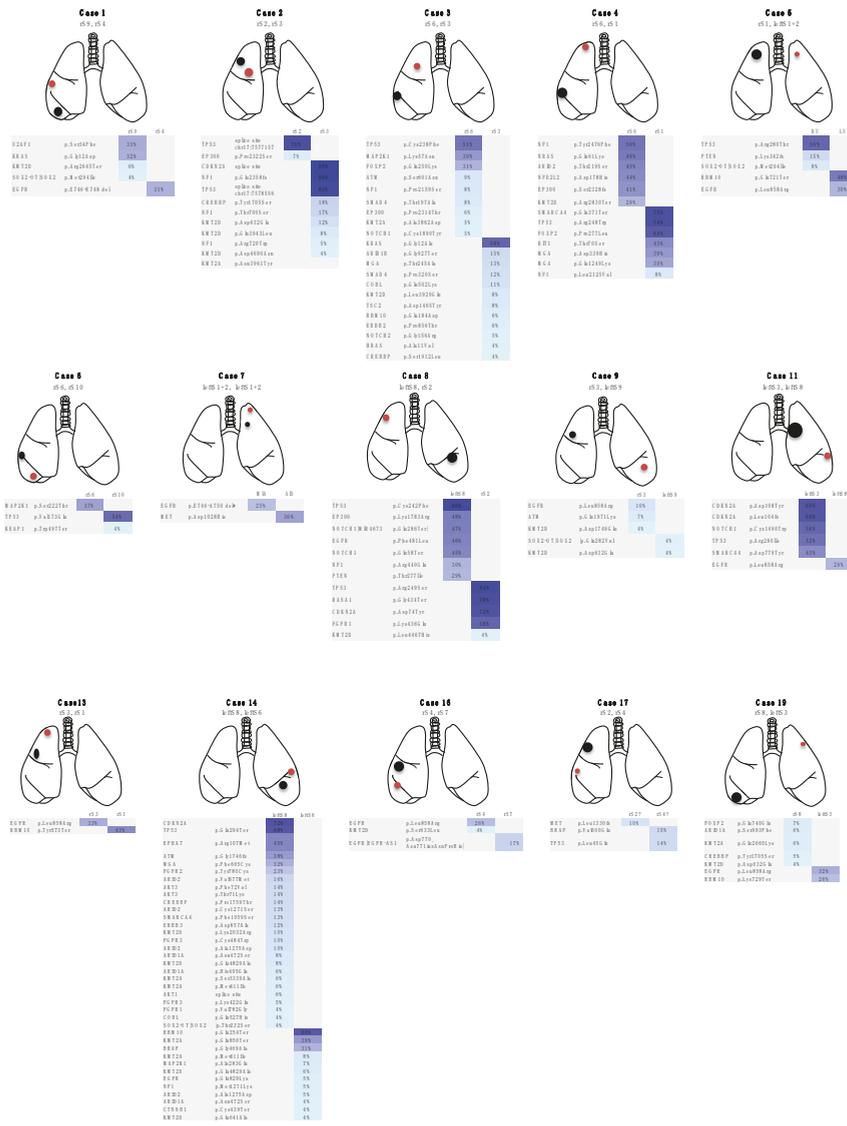
Figure 1. *Cont.*
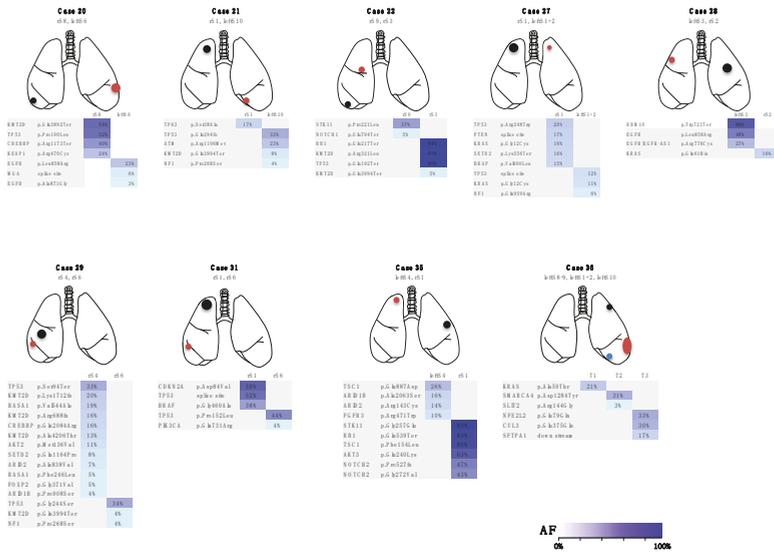
Figure 1. Heatmap of gene mutations in patients with double or triple primary lung cancers. These maps visualize the gene mutations in each cancer. Two or three lung cancers in each patient were characterized by different mutation profiles and all patients were diagnosed with double or triple primary lung cancers. Case 21, 22 and 28 were metachronous cancers, while the other cases in this figure were synchronous cancers. The remaining 5 cases of double primary lung cancers (cases 12, 18, 24, 26 and 34 in Table 1 and Table S2) that are not shown in this figure are described in detail in the Case presentation section. Black, red and blue indicate tumor 1 (T1), T2 and T3, respectively. r, right; S, segment; AF, allele fraction; MIA, microinvasive adenocarcinoma; AIS, adenocarcinoma in situ.
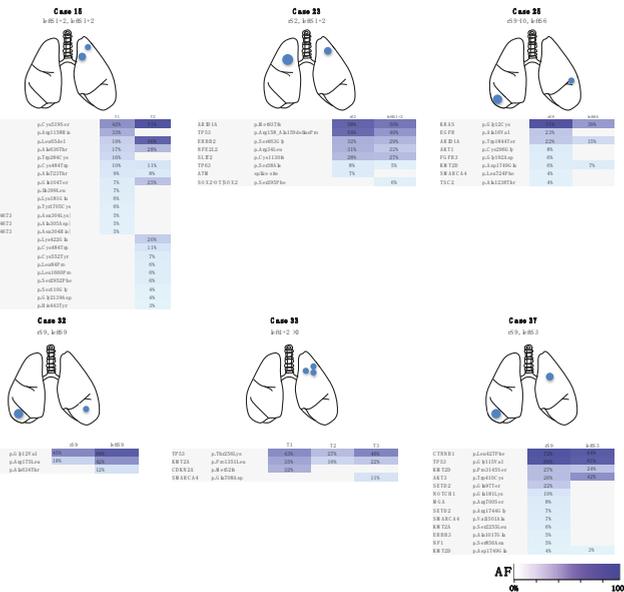
Figure 2. Heatmap of gene mutations in patients with metastatic lung cancers. The mutation profiles were consistent between the individual tumors in each case and the tumors were identified as

intrapulmonary metastasis. Case 33 was synchronous cancers, while the other cases in this figure were metachronous cancers. The remaining 2 cases of metastatic lung cancers (cases 10 and 30 in Table 1 and Table S2) that are not shown in this figure are described in detail in the Case presentation section. r, right; S, segment; AF, allele fraction.

3.3. Case Presentations

Three Representative Cases are Described in Detail Below

Case A (Case 30 in Table 1 and Table S2)

A 74-year-old man had two tumors in the right upper lobe that were resected through right upper lobectomy. Both tumors morphologically had an irregular surface; thus, they were diagnosed as primary lung cancers (Figure 3A,B). Pathologically, the peripheral lesion was identified as an adenosquamous carcinoma comprised of squamous cell carcinoma and acinar-predominant adenocarcinoma, whereas the central lesion was identified as papillary-predominant adenocarcinoma (Figure 3C,D). On the basis of the histopathological differences, the tumors were judged as double primary tumors. Pathologically, the cancer stage was determined to be pT1cN2M0, stage IIIA. However, the genetic mutation profiles were completely consistent between these two tumors, suggesting they are metastases (Figure 3E). Moreover, their mutation profiles were also consistent with the mutation profile of the metastatic lymph node. (Figure 3E). Based on the genetic diagnosis, the cancer stage was ultimately upgraded to T3N2M0, stage IIIB. At the patient's request, he was placed on follow-up without any postoperative adjuvant chemotherapy. The patient has remained alive for 2 years postoperatively without any recurrence.
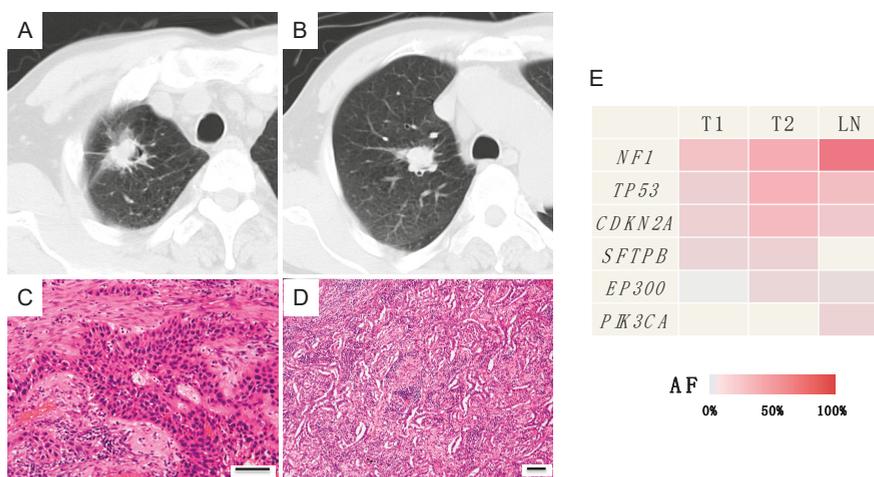
Figure 3. Radiological, histopathological and genomic findings in case A. (**A**,**B**) Right upper lobe nodules: one tumor was located in the peripheral region, whereas the other was located in the central region. (**C**) Histologically, the peripheral tumor (T1) was identified as an adenosquamous carcinoma. (**D**) The central tumor (T2) was histologically identified as an adenocarcinoma. Each scale bar indicates 100 μm. (**E**) The heatmap revealed that the same mutation profiles were shared by the two tumors and the lymph node metastasis. AF, allele fraction; LN, lymph node

Case B (Case 10 in Table 1 and Table S2)

A 59-year-old woman presented with 0.7-cm nodules in the right lower lobe 1.5 years after undergoing right upper lobectomy for cancer. The tumors were round and had a smooth surface. Because of their morphology, they were suspected of being metastatic lesions. After 4 months of follow-up, there was no increase in the number of lung lesions, suggesting solitary intrapulmonary metastasis. Subsequently, wedge resection was performed. Although both tumors were pathologically papillary-predominant adenocarcinoma (Figure 4C,D), a lepidic pattern was observed in the periphery of the smaller nodule (Figure 4E), leading to a diagnosis of double primary lung cancers. However, the genetic mutation profile was consistent between the two tumors, suggesting them to be metastases (Figure 4F). The patient was positive for a mutation in the epidermal growth factor receptor (EGFR) gene (exon 19 deletion); hence, oral administration of an EGFR-tyrosine kinase inhibitor (gefitinib) was continued. The patient has remained alive without recurrence for 4 years after the second surgery.
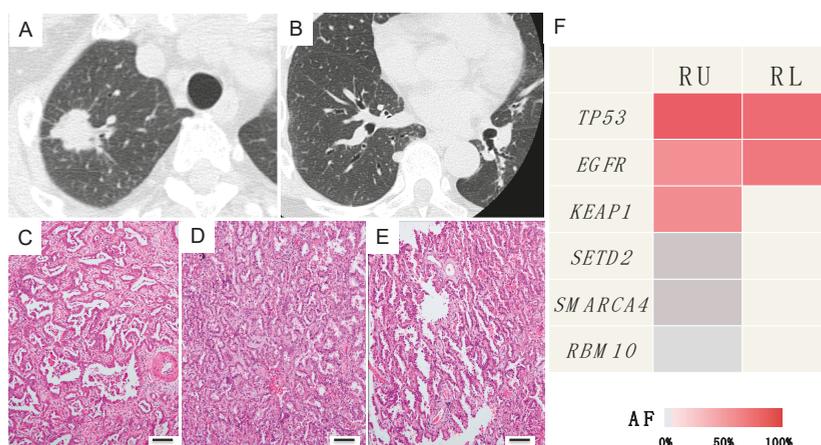
Figure 4. Radiological, histopathological and genomic findings in case B. (**A**) Lung cancer in the right upper lobe. (**B**) A small nodule in the right lower lobe. (**C**) Histology of the lung cancer in the right upper lobe. (**D,E**) Histology of the nodule in the right lower lobe. A lepidic pattern was observed in the periphery of the small nodule. Each scale bar indicates 100 μm. (**F**) Heatmap of the gene mutations of the two lung tumors. The significant mutations identified in the right upper lobe tumor were homologous with those detected in the right lower lobe tumor. RU, right upper lobe; RL, right lower lobe; AF, allele fraction

Case C (Case 18 in Table 1 and Table S2)

A 74-year-old man presented with tumors measuring 4.0 cm and 1.8 cm in the left upper lobe, so left upper lobectomy was performed (Figure 5A,B). As both tumors were closely located and pathologically similar squamous cell carcinomas, they were assumed to be single origin pulmonary metastases (Figure 5C,D). However, the mutation profile was completely different between the two tumors genetically, suggesting double primary cancers (Figure 5E).
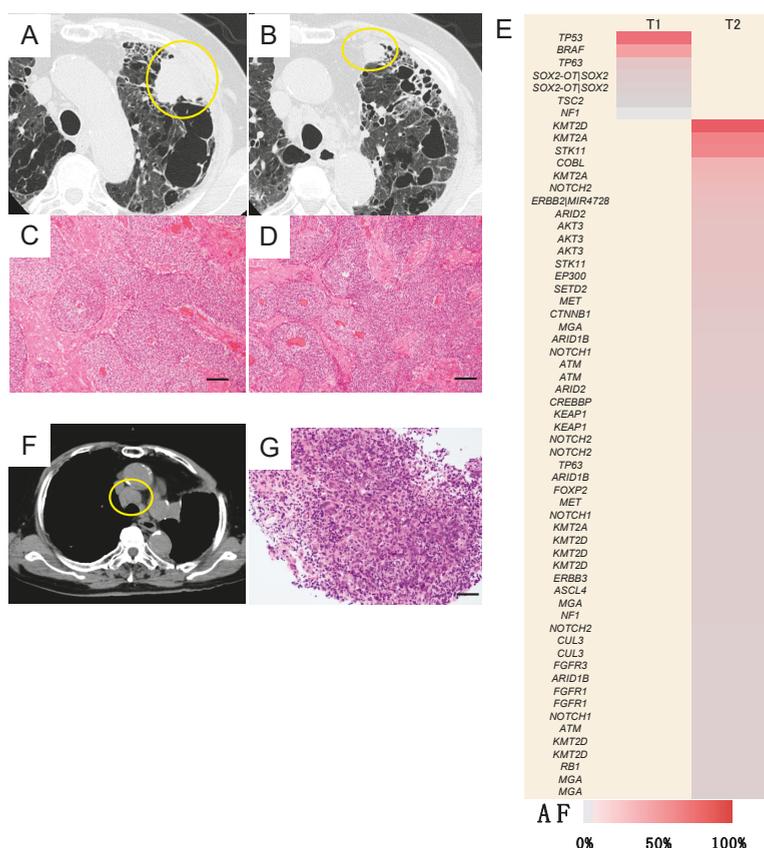
Figure 5. Radiological, histopathological and genomic findings in case C. (**A**,**B**) Two tumors, a large one (T1) and a small one (T2), were located in the left upper lobe in proximity to each other. (**C**,**D**) The tumors exhibited a similar histology of squamous cell carcinoma. Each scale bar indicates 100 μm. (**E**) Heatmap of the gene mutations of the two lung tumors. The mutation profiles of T1 and T2 were completely different. (**F**,**G**) Postoperatively, tracheobronchial lymph node enlargement was observed and the tumor was identified as a squamous cell carcinoma. Each scale bar indicates 100 μm. AF, allele fraction.

3.4. Investigation of the Discrepancies between the Clinical and/or Histopathological Diagnoses and Genetic Diagnosis

Table 1 shows the discrepancies between and among the clinical, pathological and genetic diagnoses of the primary or metastatic lesions in all 37 patients. The clinical diagnoses were comprehensively determined, mainly on the basis of imaging findings and clinical course by the cancer board of the hospital (comprised of thoracic surgeons, pulmonologists, pathologists and radiologists). The pathological diagnoses were determined on the basis of the postoperative pathological findings, especially the differences in the tissue morphology and cellular atypia detected by pathologists. The genetic diagnoses were determined on the basis of digital and statistical analyses of overlaps in the mutation profiles of individual tumors. Discrepancies between the genetic diagnosis and clinical and/or histopathological diagnoses were observed in 11 patients (29.7%). In the patients with synchronous tumors, primary and metastatic tumors were eventually diagnosed on the basis of genetic diagnosis in 24 and 2 patients, respectively. In the 11 patients with metachronous tumors, primary and metastatic

tumors were diagnosed in 5 and 6 patients, respectively, in the same manner. The distribution of primary and metastatic tumors between synchronous and metachronous tumors was significantly different; thus synchronous multiple lung tumors were deemed likely to be primary lesions.
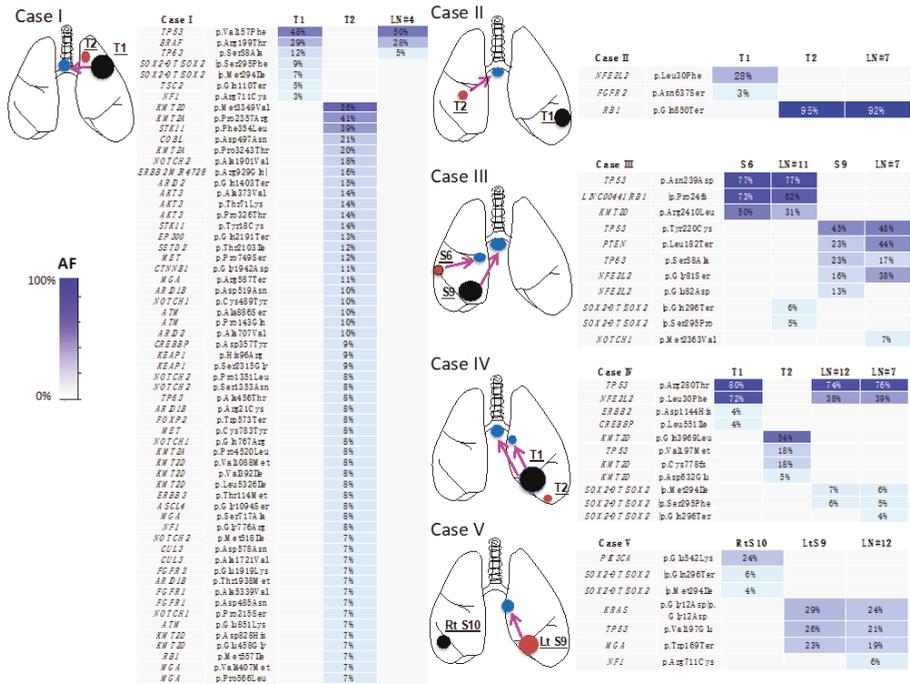
Table 1. Mutation analysis of the multiple lung cancers.

Case	Occurrence of Tumors	Interval between the 1st and 2nd Tumors	Clinical Dx	Pathological Dx	Genomic Dx
1	Synchronous	-	Double	Double	Double
2	Synchronous	-	Double	Double	Double
3	Synchronous	-	Double	Double	Double
4	Synchronous	-	Metastasis	Metastasis	Double *
5	Synchronous	-	Double	Double	Double
6	Synchronous	-	Double	Double	Double
7	Synchronous	-	Double	Double	Double
8	Synchronous	-	Double	Double	Double
9	Synchronous	-	Double	Double	Double
10	Metachronous	14 months	Metastasis	Double	Metastasis *
11	Synchronous	-	Double	Double	Double
12	Synchronous	-	Metastasis	Double	Double *
13	Synchronous	-	Double	Double	Double
14	Synchronous	-	Double	Double	Double
15	Metachronous	15 months	Double	Metastasis	Metastasis *
16	Synchronous	-	Double	Double	Double
17	Synchronous	-	Double	Double	Double
18	Synchronous	-	Metastasis	Metastasis	Double *
19	Synchronous	-	Double	Double	Double
20	Synchronous	-	Double	Double	Double
21	Metachronous	17 months	Double	Double	Double
22	Metachronous	28 months	Double	Double	Double
23	Metachronous	23 months	Double	Metastasis	Metastasis *
24	Metachronous	37 months	Double	Double	Double
25	Metachronous	37 months	Double	Double	Metastasis *
26	Synchronous	-	Double	Double	Double
27	Synchronous	-	Double	Double	Double
28	Metachronous	41 months	Double	Double	Double
29	Synchronous	-	Double	Double	Double
30	Synchronous	-	Double	Double	Metastasis *
31	Synchronous	-	Double	Double	Double
32	Metachronous	16 months	Double	Metastasis	Metastasis *
33	Synchronous	-	Double	Metastasis	Metastasis *
34	Metachronous	13 months	Double	Double	Double
35	Synchronous	-	Double	Double	Double
36	Synchronous	-	triple	triple	triple
37	Metachronous	46 months	Double	Double	Metastasis *

The cases in which the diagnoses were inconsistent in the clinicopathological and genetic examinations are indicated by *.

3.5. Genetic Diagnosis of Lymph Node Metastasis in Patients with Multiple Lung Cancers

Lymph node metastasis was detected in five patients with double primary lung cancers (Table 2). It occurred approximately at the time of surgery in three patients and was identified as postoperative lymph node recurrence in two patients (Table 2). In some patients, the route of lymph node metastasis was apparent from the timing of the metastasis as well as the location and pathological findings of the metastatic lesions (cases 4 and 5 in Table 2). In contrast, it was difficult to identify the clonal origin of lymph node metastasis on the basis of the clinical and pathological findings in the other patients, especially in those in whom the primary lesions were both squamous cell carcinomas (cases 1–3 in Table 2). However, even in these patients, a comparison of the mutation profiles of the primary and lymph node metastatic lesions revealed the route of lymph node metastasis (Figure 6).

Figure 6. Schema of lymphatic metastasis and mutation profiles in multiple lung cancers. On the basis of the coincidence and differences in the mutation profiles, the clonality of each tumor and the pathway of lymphatic progression are clearly elucidated in each case. The arrows indicate the lymphatic routes of the cancer invasion. Tumor 1 is shown in black, tumor 2 in red and lymph node metastasis in blue. #4, tracheobronchial lymph node; #7, subcarinal lymph node; #11, interlobar lymph node; and #12, hilar lymph node. S, segment; LN, lymph node; AF, allele fraction

Table 2. LN metastasis in patients with multiple lung cancers.

Case	Case No. in Table 1	Location and Histology of T1	Location and Histology of T2	Location and Histology of LN	LN Biopsy Method	Occurrence of LN Metastasis	Inconsistency between Clinical and Genomic Diagnoses
I	18	Left upper, Sq	Left upper, Sq	Right tracheobronchial, Sq	EBUS-TBNA	Postoperative	+
II	34	Left lower, Sq	Middle, Sq	Subcarinal, Sq	EBUS-TBNA	Postoperative	+
III	26	Right S9, Sq	Right S6, Sq	Interlobar and subcarinal, Sq	Surgery	Simultaneous	+
IV	12	Left S6, Sq	Left S10, small	Subcarinal, Sq	Surgery	Simultaneous	–
V	24	Right lower, acinar Ad	Left lower, solid Ad	Left lobar, solid Ad	Surgery	Simultaneous	–

S, segment; LN, lymph node; Sq, squamous cell carcinoma; Ad, adenocarcinoma; small, small cell carcinoma; EBUS-TBNA, endobronchial ultrasound-guided transbronchial needle aspiration.

3.6. Case Presentations

Three Representative Cases are Described in Detail Below

Case D (Case I in Table 2 and Figure 6)

A 74-year-old man, described as case C in the previous section, presented with paratracheal and mediastinal lymph node metastases 1 year after left upper lobectomy (Figure 5F). Although it was not possible to pathologically identify the metastasizing primary lesion (Figure 5G), the mutation profile of the metastatic lymph node was genetically consistent with that of the larger cancer. The genetic diagnosis was lymph node metastasis of the larger cancer (Figure 6).

Case E (Case II in Table 2 and Figure 6)

A 77-year-old man with lung cancer underwent left lower lobectomy (Figure 7A). One year later, a nodule appeared in the middle lobe (Figure 7B). Middle lobectomy was performed based on the assumption that the lesion was a double primary tumor. However, after 1 year, subcarinal lymph node metastasis occurred (Figure 7C). Pathologically, all three lesions were of squamous cell carcinoma type and it was impossible to determine which primary lesion had metastasized (Figure 7D–F). Given the tumor size, the tumor in the left lobe was clinically more likely to have metastasized. However, mutation analysis revealed that the two lung lesions had different mutation profiles; therefore, they were diagnosed as double primary lung cancers. Furthermore, the mutation profiles were consistent between the middle lobe lung cancer and the metastatic lymph node. Thus, lymph node metastasis of the middle lobe lung cancer was determined (Figure 6). Programmed death-ligand 1 (PD-L1) staining of tumor cells was 0% and 90% in the left lower lobe and middle lobe tumors, respectively. Treatment with an anti-PD-1 antibody (nivolumab) was administered and a complete response has been maintained for 1 year since the recurrence in the lymph node.

Case F (Case III in Table 2 and Figure 6)

A 72-year-old man presented with two tumors in the right lower lobe. Imaging findings suggested double primary lung cancers and right lower lobectomy was performed (Figure 7G,H). Postoperative pathological examination revealed metastases in the interlobar and subcarinal lymph nodes. All four lesions, including the double primary lesions and two metastatic lymph nodes, were pathologically similar squamous cell carcinomas. Therefore, it was impossible to determine which primary lesion had metastasized to the lymph nodes (Figure 7I–L). Clinically, the larger segment 9 tumor was likely to have metastasized to the two lymph nodes. However, both segment 6 and 9 tumors, which had different mutation profiles, were genetically identified as double primary lung cancers. In addition, it was found that the larger segment 9 tumor had metastasized to the interlobar lymph node, whereas the smaller segment 6 tumor had metastasized to the subcarinal lymph node (Figure 6). PD-L1 staining of tumor cells was 0% and 70% in the segment 9 and segment 6 tumors, respectively. Despite the administration of an anti-PD-1 antibody (nivolumab), the patient did not respond to the treatment and died of progression of the cancer at 17 months postoperatively.
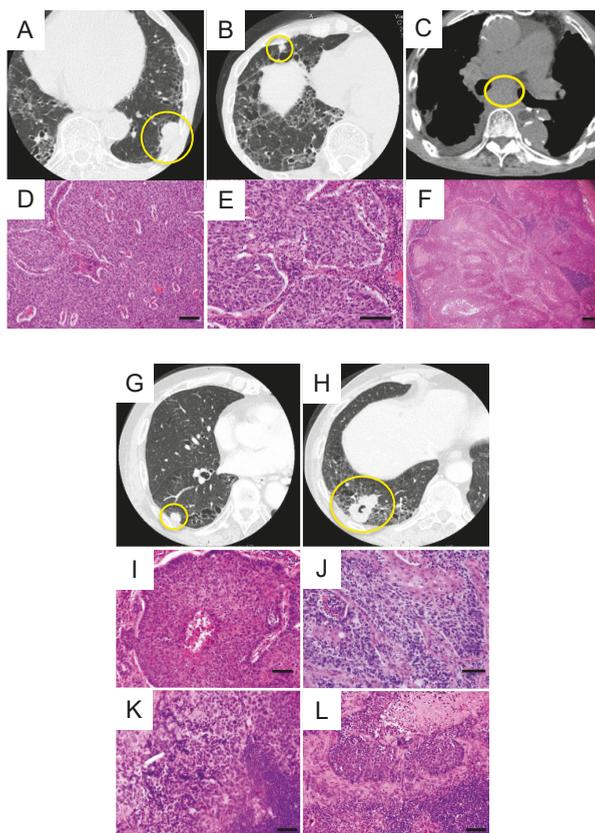
Figure 7. Radiological and histopathological findings in cases E and F. (**A–F**) Findings in case E. (**A**) Primary lesion in the left lower lobe. (**B**) Primary lesion in the middle lobe. (**C**) Subcarinal lymph node metastasis. (**D–F**) The three lesions displayed a similar histology of squamous cell carcinoma. (**G–L**) Findings in case F. (**G**) Primary lesion in right segment 6. (**H**) Primary lesion in right segment 9. (**I**) Histology of the primary lesion in segment 6. (**J**) Histology of the primary lesion in segment 9. (**K**) Histology of the subcarinal lymph node. (**L**) Histology of the interlobar lymph node. Histologically, the four lesions displayed a similar histology of squamous cell carcinoma. Each scale bar indicates 100 μm.

4. Discussion

In cases of multiple lung cancers, clinical differentiation between primary and metastatic tumors can be difficult, rendering treatment selection challenging. Furthermore, in patients with multiple lung cancers metastasized to the lymph nodes or distal sites, the focus of treatment varies depending on the cancer that has metastasized. Thus, determining the origin of the metastasizing cancer is clinically important. Therefore, we performed lung cancer mutation analysis through targeted deep sequencing and demonstrated that mutations of individual lung cancers are able to provide clonal markers, enabling discrimination of the clonal origin of multiple lung cancers and their metastases.

The consistency of mutations across multiple sites, with complete concordance in the position and patterns of base-pair substitutions or indels, cannot be a coincidental phenomenon. Although discordance between two tumors was noted in mutations with an allele fraction <20%, this can be interpreted as tumor heterogeneity [14]. In general, cancers comprise populations of cells with

various molecular and phenotypic features, a phenomenon termed intratumor heterogeneity [14,15]. This may bolster tumor adaptation, cancer progression and metastasis, and/or therapeutic failure through negative selection [14,16]. Conversely, a driver mutation triggers clonal expansion and is retained ubiquitously within the tumors of the same clone [16,17]. These theories can be interpreted as the "trunk and branch" mutation models; early somatic events that drive tumor progress in early clonal founders are represented by the "trunk" of the tumor [18,19]. Such trunk somatic mutations to be found at the early stages of tumor development are ubiquitous events occurring at all sites of disease. Meanwhile, later somatic events that occur in the wake of branched separation of subclones represent heterogeneity. Such subclonal heterogeneity may be spatially divided among regions of the same tumor or its metastatic sites [18–20]. In this context, clonally dominant mutations are important clonal markers. Primary and metastatic tumors can be differentiated by determining whether such ubiquitous driver mutations are consistent.

It is relatively straightforward to diagnose multicentric primary lung cancers of different histological type. However, it is often difficult to differentiate between multiple primary lung cancers and intrapulmonary metastases having the same histological type. In particular, in cases of multiple tumors classified as squamous cell carcinoma (such as cases C–F), differentiation based on pathological features alone is extremely difficult. Even when the morphological and immunohistological features are non-homogeneous among different parts of the tumors (e.g., cases A and B), the driver mutation is ubiquitously retained within the tumors of the same clone [16,17]. Therefore, distinction of clonality on the basis of mutation analysis is more specific and definitive than histological examination.

Detterbeck et al. reviewed the clinical and pathological criteria to distinguish second primary tumors from metastatic tumors [21]. They reported that it is impracticable to define criteria that conclusively establish the identical nature of tumors; merely finding observable similarities between tumors is insufficient. Using the method described, comprehensive mutation analysis is initially performed to identify the driver mutations in each cancer, which are subsequently compared to define their clonal origin. These criteria are definitive and reliable. Moreover, the decision criteria are generally clear and intuitive. In fact, this method yielded clear genetic diagnosis in all patients. In other words, no equivocal or ambiguous diagnosis was obtained in any of the cases. In our previous study, we had demonstrated that this method allows bronchoscopic biopsy samples and other small samples to be used for discrimination between primary and metastatic tumors [1]. Thus, our method may enable both flexible and rational decision-making based on accurate diagnosis. For example, a preoperative diagnosis of metastatic tumors may make it possible to avoid surgery, whereas a preoperative diagnosis of primary tumors would lead to surgical treatment. This novel approach may help resolve the dilemma of misdiagnosis in the clinical setting. Thus, we anticipate that it will come to be utilized as a standard diagnostic approach in daily clinical practice in the near future.

When selecting treatment methods for multiple lung cancers, it is necessary to consider the cancer type will markedly affect the prognosis. In cases D–F that have lymph node metastasis, a factor responsible for progression to an advanced stage was identified in the two tumors. Furthermore, the tumors exhibit different mutation profiles and PD-L1 staining properties. Therefore, the lesions targeted for treatment and the options selected for subsequent treatment (e.g., molecular-targeted drugs and immune checkpoint inhibitors) vary depending on the type of tumor that has metastasized to the lymph nodes. This suggests that accurate understanding of the pathology gained by performing a genetic diagnosis can exert a powerful effect on the clinical outcome. Although the use of immunotherapy has revolutionized the treatment of non-small-cell lung cancer, patterns of immunostaining with PD-L1, a biomarker for treatment response, may vary in tumor cells across individual primary tumors (e.g., (,) cases E and F) [22]. At present, molecularly targeted therapies are also rapidly evolving. The development of novel molecularly targeted therapies would enable the treatment to be specifically tailored to the features of mutations detected in individual cancers. Thus, in patients with multiple lung cancers, performing a mutation analysis helps select the medical treatment most likely to be effective.

5. Conclusions

In cases of multiple lung cancers, identifying the differences in the mutation profiles of multiple tumors will help determine their clonal origin and enable a distinction to be drawn between primary and metastatic tumors with great specificity, even in cases in which pathological distinction is impossible or equivocal. In addition, performing genetic diagnosis in addition to pathological diagnosis can help obtain a more accurate understanding of the pathology of multiple lung cancers and the lymphatic metastases. This approach may lead to the provision of treatment specifically tailored to the features of individual cases.

References

1. Goto, T.; Hirotsu, Y.; Mochizuki, H.; Nakagomi, T.; Shikata, D.; Yokoyama, Y.; Oyama, T.; Amemiya, K.; Okimoto, K.; Omata, M. Mutational analysis of multiple lung cancers: Discrimination between primary and metastatic lung cancers by genomic profile. *Oncotarget* **2017**, *8*, 31133–31143. [CrossRef] [PubMed]
2. Gibbs, A.R.; Thunnissen, F.B. Histological typing of lung and pleural tumours: Third edition. *J. Clin. Pathol.* **2001**, *54*, 498–499. [CrossRef]
3. Chansky, K.; Detterbeck, F.C.; Nicholson, A.G.; Rusch, V.W.; Vallieres, E.; Groome, P.; Kennedy, C.; Krasnik, M.; Peake, M.; Shemanski, L.; et al. The IASLC Lung Cancer Staging Project: External Validation of the Revision of the TNM Stage Groupings in the Eighth Edition of the TNM Classification of Lung Cancer. *J. Thorac. Oncol.* **2017**, *12*, 1109–1121. [CrossRef]
4. Cancer Genome Atlas Research Network. Comprehensive molecular profiling of lung adenocarcinoma. *Nature* **2014**, *511*, 543–550. [CrossRef] [PubMed]
5. Cancer Genome Atlas Research Network. Comprehensive genomic characterization of squamous cell lung cancers. *Nature* **2012**, *489*, 519–525. [CrossRef] [PubMed]
6. Clinical Lung Cancer Genome Project (CLCGP); Network Genomic Medicine (NGM). A genomics-based classification of human lung tumors. *Sci. Transl. Med.* **2013**, *5*, 209ra153.
7. Rudin, C.M.; Durinck, S.; Stawiski, E.W.; Poirier, J.T.; Modrusan, Z.; Shames, D.S.; Bergbower, E.A.; Guan, Y.; Shin, J.; Guillory, J.; et al. Comprehensive genomic analysis identifies SOX2 as a frequently amplified gene in small-cell lung cancer. *Nat. Genet.* **2012**, *44*, 1111–1116. [CrossRef]
8. Peifer, M.; Fernandez-Cuesta, L.; Sos, M.L.; George, J.; Seidel, D.; Kasper, L.H.; Plenker, D.; Leenders, F.; Sun, R.; Zander, T.; et al. Integrative genome analyses identify key somatic driver mutations of small-cell lung cancer. *Nat. Genet.* **2012**, *44*, 1104–1110. [CrossRef]
9. Imielinski, M.; Berger, A.H.; Hammerman, P.S.; Hernandez, B.; Pugh, T.J.; Hodis, E.; Cho, J.; Suh, J.; Capelletti, M.; Sivachenko, A.; et al. Mapping the hallmarks of lung adenocarcinoma with massively parallel sequencing. *Cell* **2012**, *150*, 1107–1120. [CrossRef]
10. Govindan, R.; Ding, L.; Griffith, M.; Subramanian, J.; Dees, N.D.; Kanchi, K.L.; Maher, C.A.; Fulton, R.; Fulton, L.; Wallis, J.; et al. Genomic landscape of non-small cell lung cancer in smokers and never-smokers. *Cell* **2012**, *150*, 1121–1134. [CrossRef]

11. Forbes, S.A.; Beare, D.; Boutselakis, H.; Bamford, S.; Bindal, N.; Tate, J.; Cole, C.G.; Ward, S.; Dawson, E.; Ponting, L.; et al. COSMIC: Somatic cancer genetics at high-resolution. *Nucleic Acids Res.* **2017**, *45*, D777–D783. [CrossRef]

12. Goto, T.; Hirotsu, Y.; Oyama, T.; Amemiya, K.; Omata, M. Analysis of tumor-derived DNA in plasma and bone marrow fluid in lung cancer patients. *Med. Oncol.* **2016**, *33*, 29. [CrossRef] [PubMed]

13. Nakagomi, T.; Goto, T.; Hirotsu, Y.; Shikata, D.; Yokoyama, Y.; Higuchi, R.; Otake, S.; Amemiya, K.; Oyama, T.; Mochizuki, H.; et al. Genomic Characteristics of Invasive Mucinous Adenocarcinomas of the Lung and Potential Therapeutic Targets of B7-H3. *Cancers* **2018**, *10*, 487. [CrossRef]

14. Goto, T.; Hirotsu, Y.; Amemiya, K.; Mochizuki, H.; Omata, M. Understanding Intratumor Heterogeneity and Evolution in NSCLC and Potential New Therapeutic Approach. *Cancers* **2018**, *10*, 212. [CrossRef] [PubMed]

15. Jamal-Hanjani, M.; Wilson, G.A.; McGranahan, N.; Birkbak, N.J.; Watkins, T.B.K.; Veeriah, S.; Shafi, S.; Johnson, D.H.; Mitter, R.; Rosenthal, R.; et al. Tracking the Evolution of Non-Small-Cell Lung Cancer. *N. Engl. J. Med.* **2017**, *376*, 2109–2121. [CrossRef]

16. Goto, T.; Hirotsu, Y.; Mochizuki, H.; Nakagomi, T.; Oyama, T.; Amemiya, K.; Omata, M. Stepwise addition of genetic changes correlated with histological change from "well-differentiated" to "sarcomatoid" phenotypes: A case report. *BMC Cancer* **2017**, *17*, 65. [CrossRef] [PubMed]

17. Yatabe, Y.; Matsuo, K.; Mitsudomi, T. Heterogeneous distribution of EGFR mutations is extremely rare in lung adenocarcinoma. *J. Clin. Oncol.* **2011**, *29*, 2972–2977. [CrossRef]

18. Swanton, C. Intratumor heterogeneity: Evolution through space and time. *Cancer Res.* **2012**, *72*, 4875–4882. [CrossRef]

19. Yap, T.A.; Gerlinger, M.; Futreal, P.A.; Pusztai, L.; Swanton, C. Intratumor heterogeneity: Seeing the wood for the trees. *Sci. Transl. Med.* **2012**, *4*, 127ps10. [CrossRef]

20. Gerlinger, M.; Rowan, A.J.; Horswell, S.; Larkin, J.; Endesfelder, D.; Gronroos, E.; Martinez, P.; Matthews, N.; Stewart, A.; Tarpey, P.; et al. Intratumor heterogeneity and branched evolution revealed by multiregion sequencing. *N. Engl. J. Med.* **2012**, *366*, 883–892. [CrossRef]

21. Detterbeck, F.C.; Nicholson, A.G.; Franklin, W.A.; Marom, E.M.; Travis, W.D.; Girard, N.; Arenberg, D.A.; Bolejack, V.; Donington, J.S.; Mazzone, P.J.; et al. The IASLC Lung Cancer Staging Project: Summary of Proposals for Revisions of the Classification of Lung Cancers with Multiple Pulmonary Sites of Involvement in the Forthcoming Eighth Edition of the TNM Classification. *J. Thorac. Oncol.* **2016**, *11*, 639–650. [CrossRef] [PubMed]

22. Goto, T. Radiation as an In Situ Auto-Vaccination: Current Perspectives and Challenges. *Vaccines* **2019**, *7*, 100. [CrossRef] [PubMed]

Prognostic Significance of Glucose Metabolism as GLUT1 in Patients with Pulmonary Pleomorphic Carcinoma

Hisao Imai [1], Kyoichi Kaira [2,3,*], Hideki Endoh [4], Kazuyoshi Imaizumi [5], Yasuhiro Goto [5], Mitsuhiro Kamiyoshihara [6], Takayuki Kosaka [7], Toshiki Yajima [2,8], Yoichi Ohtaki [8], Takashi Osaki [9], Yoshihito Kogure [10], Shigebumi Tanaka [11], Atsushi Fujita [12], Tetsunari Oyama [13], Koichi Minato [1], Takayuki Asao [14] and Ken Shirabe [2,8]

1   Division of Respiratory Medicine, Gunma Prefectural Cancer Center, Ota 373-8550, Japan;
      m06701014@gunma-u.ac.jp (H.I.); kminato@gunma-cc.jp (K.M.)
2   Department of Innovative Immune-Oncology Therapeutics, Gunma University Graduate School of
      Medicine, Maebashi 371-8511, Japan; yajimatos@yahoo.co.jp (T.Y.); kshirabe@gunma-u.ac.jp (K.S.)
3   Department of Respiratory Medicine, Comprehensive Cancer Center, International Medical Center, Saitama
      University Hospital, Hidaka 350-1298, Japan
4   Department of Thoracic Surgery, Saku Central Hospital Advanced Care Center, Saku 385-0051, Japan;
      hidend0509@yahoo.co.jp
5   Department of Respiratory Medicine, Fujita Health University, Toyoake 470-1192, Japan;
      jeanluc@fujita-hu.ac.jp (K.I.); gotoyasu510@gmail.com (Y.G.)
6   Department of General Thoracic Surgery, Japanese Red Cross Maebashi Hospital, Maebashi 371-0811, Japan;
      micha2005jp@yahoo.co.jp
7   Division of Thoracic Surgery, Takasaki General Medical Center, Takasaki 370-0829, Japan;
      tkosaka133@gmail.com
8   Department of General Surgical Science, Gunma University Graduate School of Medicine, Maebashi
      371-8511, Japan; yohtakiadvanced@gmail.com
9   Department of Respiratory Medicine, Shibukawa Medical Center, Shibukawa 377-0280, Japan;
      tosaki@xb4.so-net.ne.jp
10   Department of Respiratory Medicine, Nagoya Medical Center, Nagoya 460-0001, Japan;
      yo-kogure@umin.ac.jp
11   Department of Respiratory Surgery, Isesaki Municipal Hospital, Isesaki 372-0817, Japan;
      tanakasigebumi@yahoo.co.jp
12   Division of Thoracic Surgery, Gunma Prefectural Cancer Center, Ota 373-8550, Japan; afujita@gunma-cc.jp
13   Department of Diagnostic Pathology, Gunma University Graduate School of Medicine, Maebashi 371-8511,
      Japan; oyama@gunma-u.ac.jp
14   Big Data Center for Integrative Analysis, Gunma University Initiative for Advance Research,
      Maebashi 371-8511, Japan; asao@gunma-u.ac.jp
*   Correspondence: kkaira1970@yahoo.co.jp; Tel.: +81-27-220-8222; +81-42-984-4111

Abstract: Glucose metabolism is necessary for tumor progression, metastasis, and survival in various human cancers. Glucose transporter 1 (GLUT1), in particular, plays an important role in the mechanism of ^{18}F-FDG (2-[^{18}F]-fluoro-2-deoxy-d-glucose) within tumor cells. However, little is known about the clinicopathological significance of GLUT1 in patients with pulmonary pleomorphic carcinoma (PPC). Adenocarcinoma, squamous cell carcinoma, adenosquamous cell carcinoma, poorly differentiated carcinoma, large cell carcinoma, and others were identified as epithelial components, and spindle-cell type, giant-cell type, and both spindle- and giant-cell types were identified as sarcomatous components. This study was performed to determine the prognostic impact of GLUT1 expression in PPC. Patients with surgically resected PPC (n = 104) were evaluated by immunohistochemistry analysis to detect GLUT1 expression and determine the Ki-67 labeling index using specimens of the resected tumors. GLUT1 was highly expressed in 48% (50/104) of all patients, 42% (20/48) of the patients with an adenocarcinoma component, and 53% (30/56) of the patients with

a nonadenocarcinoma component. High expression of GLUT1 was significantly associated with advanced stage, vascular invasion, pleural invasion, and tumor cell proliferation as determined by Ki-67 labeling. GLUT1 expression and tumor cell proliferation were significantly correlated according to the Ki-67 labeling in all patients (Spearman's rank; r = 0.25, $p < 0.01$). In multivariate analysis, GLUT1 was identified as a significant independent marker for predicting a poor prognosis. GLUT1 is an independent prognostic factor for predicting the poor prognosis of patients with surgically resected PPC.

Keywords: pulmonary pleomorphic carcinoma; prognostic factor; glucose transporter 1

---

1. Introduction

Pulmonary pleomorphic carcinoma (PPC) is a rare disease with an incidence of 0.1%–0.4% among all lung cancers and shows a poor prognosis because of its resistance to systemic chemotherapy [1]. PPC includes carcinomatous and sarcomatoid components and is classified as a subtype of sarcomatoid carcinoma of the lung by the World Health Organization histologic classification of lung neoplasms [2,3]. Because of its rarity and low treatment efficacy, most patients with PPC exhibit recurrence even after complete surgical resection; moreover, there are no standard treatments for patients with advanced and inoperable PPC. The development of appropriate treatments and identification of predictive biomarkers are critical for improving the prognosis of patients with complex histologies, such as PPC.

Glucose metabolism is associated with tumor progression and metastases, and is used in molecular imaging, such as 2-[18F]-fluoro-2-deoxy-d-glucose (18F-FDG) positron emission tomography (PET), to detect cancers [4]. Although there are several types of glucose transporters (GLUTs), glucose transporter 1 (GLUT1) and GLUT3 are strongly expressed on the membrane of tumor cells, and a meta-analysis demonstrated GLUT1 to be a prognostic marker for predicting worse outcomes in patients with lung cancer [4]. 18F-FDG accumulates in tumor cells via GLUT1, a process closely associated with poor prognosis and tumor progression in patients with lung cancer [5]. We previously showed that 18F-FDG uptake in PPC is closely related to the presence of GLUT1 and angiogenesis, and that the accumulation of 18F-FDG and the expression level of GLUT1 were significantly higher in patients with PPC than those with other nonsmall cell lung cancer (NSCLC) [6]. This indicates that tumor glucose metabolism involving GLUT1 plays a crucial role in the carcinogenesis of PPC. 18F-FDG-PET can be used to detect primary and metastatic lesions for disease staging in patients with PPC. From a pathological perspective, studies are needed to determine how the expression of GLUT1 in cancer-specific glucose metabolism reflects the survival and metastasis of patients with PPC. However, little is known about the clinicopathological relevance of GLUT1 expression in patients with PPC.

In this clinicopathological study, we examined the prognostic role of GLUT1 expression in patients with surgically resected PPC.

2. Experimental Section

2.1. Patients

Between August 2001 and October 2015, 104 patients with histologically confirmed PPC who underwent surgical resection at multiple institutions were enrolled in this study. Pleomorphic carcinoma was diagnosed according to the 2015 World Health Organization Classification of Tumours [2]. Diagnoses were confirmed by light microscopy and immunohistochemistry. PPC was defined as NSCLC containing at least 10% sarcomatoid components. This study included 104 surgically resected primary tumors in accordance with institutional guidelines and the Declaration of Helsinki. The institutional review boards of all participating institutions approved this study. Mortality and recurrence were determined using medical records. The tumor samples were collected in our previous study [7–9].

2.2. Immunohistochemical Staining

GLUT1 expression was assessed by immunohistochemical staining using a rabbit anti-GLUT1 polyclonal antibody (Abcam, Cambridge, UK; 1:200 dilution). The reaction was visualized using the Histofine Simple Stain MAX-PO (Multi) Kit (Nichirei, Tokyo, Japan), according to the manufacturer's instructions. The detailed protocol for immunostaining has been published elsewhere [4]. Negative controls were incubated without primary antibody, and no staining was observed. GLUT1 expression was considered positive only if distinct cytoplasmic and plasma membrane staining was present. GLUT1 expression was scored as follows: 1, ≤10% of tumor area stained; 2, 11%–25% stained; 3, 26%–50% stained; 4, 51%–75% stained; and 5, ≥76% stained. Tumors in which the stained tumor cells were scored ≥4 were considered as "high-expression" tumors.

Immunohistochemical staining for Ki-67 was performed as described previously [4] using a murine monoclonal antibody against Ki-67 (Dako, Glostrup, Denmark; 1:40 dilution). Highly cellular areas of the immunostained sections were assessed for Ki-67. All epithelial cells with nuclear staining of any intensity were defined as high-expression epithelial cells. Approximately 1000 nuclei were counted on each slide. Proliferative activity was assessed as the percentage of Ki-67-stained nuclei (Ki-67 labeling index) in the sample. The median Ki-67 labeling index value was evaluated, and tumor cells with greater than median Ki-67 labeling index value were defined as high-expression tumor cells. All sections were assessed by light microscopy in a blinded manner by at least two investigators. In case of discrepancies, both investigators evaluated the slides simultaneously until reaching a final consensus. Neither of the investigators had knowledge of the patient outcomes.

2.3. Statistical Analysis

Statistical analyses were performed using Student's t- and χ^2-tests for continuous and categorical variables, respectively. Correlations were analyzed using nonparametric Spearman's rank tests. The Kaplan–Meier method was used to estimate survival as a function of time, and survival differences were analyzed by log-rank tests. Overall survival (OS) was defined as the time from tumor resection to death from any cause. Disease-free survival (DFS) was defined as the time between tumor resection and the first episode of disease progression or death. Univariate and multivariate survival analyses were performed using Cox proportional hazards models and a logistic regression model for radical surgery. $p < 0.05$ was considered to indicate statistical significance. All statistical analyses were performed using GraphPad Prism version 7 (GraphPad Software, San Diego, CA, USA) and JMP Pro version 14.0 (SAS Institute, Inc., Cary, NC, USA).

3. Results

3.1. Patient Demographics and Immunohistochemistry

GLUT1 expression was assessed in 104 patients (79 males, 25 females; median age 69 years, range 35–88 years) and correlated with patient's clinical information. All patients were diagnosed using resected primary tumors. Histologic analysis revealed that 29 patients with PPC harbored a combination of carcinomatous and sarcomatous components. In the remaining 75 primary tumors, carcinomatous components were identified in 48 patients with adenocarcinoma, 13 with squamous cell carcinoma, 8 with adenosquamous cell carcinoma, 2 with poorly differentiated carcinoma, and 4 with Pe. Of the sarcomatous components, 69 patients exhibited spindle-cell type, 10 giant-cell type, and 25 both spindle- and giant-cell types. Each percentage of epithelial and sarcomatous components is shown in Supplementary Figure S1. The day of surgery was considered the starting day for measuring postoperative survival. The median follow-up period was 476 days (range, 30–4519 days).

Patient demographics data according to GLUT1 expression are listed in Table 1. Immunohistochemical analyses were performed for 104 primary sites with PPC. GLUT1 was stained on the cell membranes of tumor specimens, and there was no evidence of normal tissue without red blood cells. Figure 1 shows the representative images of GLUT1 expression in patients with PPC. Figure 2 shows the distribution of

GLUT1 expression according to a scoring system. The frequencies of scores 1, 2, 3 4, and 5 for GLUT1 were 11%, 3%, 25%, 32%, and 19%, respectively. The percentage of samples showing high GLUT1 expression was 48% (50/104). High expression of GLUT1 was found to be significantly associated with advanced stage, vascular invasion, pleural invasion, and tumor cell proliferation, as determined by the Ki-67 index. There was a significant correlation between GLUT1 expression and tumor cell proliferation according to the Ki-67 labeling index in all patients (Spearman's rank; $r = 0.25$, $p < 0.01$).

Table 1. Patient demographics according to GLUT1 expression.

Variables	GLUT1 Expression in All Patients			
	Total (n = 104)	High (n = 50)	Low (n = 54)	*p*-Value
Age				
<69 years/≥69 years	54/50	30/20	24/30	0.12
Gender				
Male/Female	79/25	35/15	44/10	0.25
Smoking				
Yes/No	84/20	40/10	44/10	>0.99
T factor				
T1-2/T3-4	65/39	25/25	40/14	0.11
N factor				
Absent/Present	72/32	33/17	39/15	0.53
Stage				
I-II/III-IV	69/35	28/22	41/13	0.03*
Lymphatic permeation				
Absent/Present	41/63	17/33	24/30	0.31
Vascular invasion				
Absent/Present	31/73	9/41	22/32	0.02*
Pleural invasion				
Absent/Present	48/56	17/33	31/13	<0.01*
Adjuvant chemotherapy				
Absent/Present	77/27	35/15	42/12	0.38
Ki-67 labeling index				
High/Low	50/54	31/19	19/35	<0.01*
* <0.05				

* $p < 0.05$ was considered statistically significant. *t*-test score was for continuous variables, and χ^2 test for categorical variables.
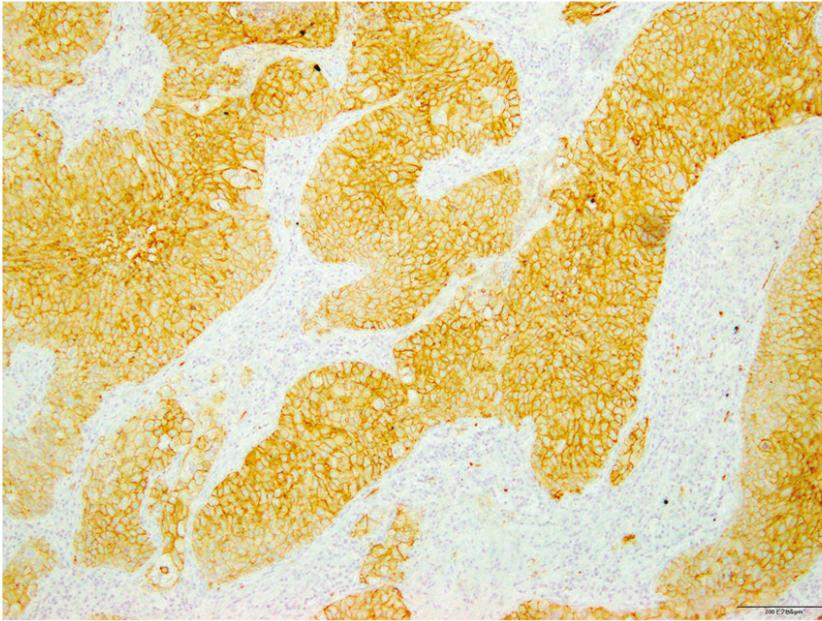
A
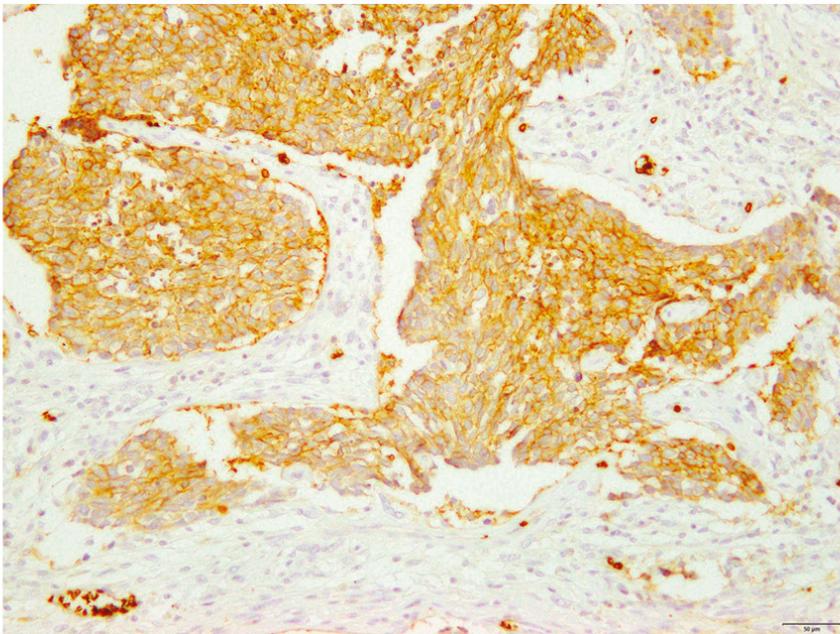
B

Figure 1. *Cont.*
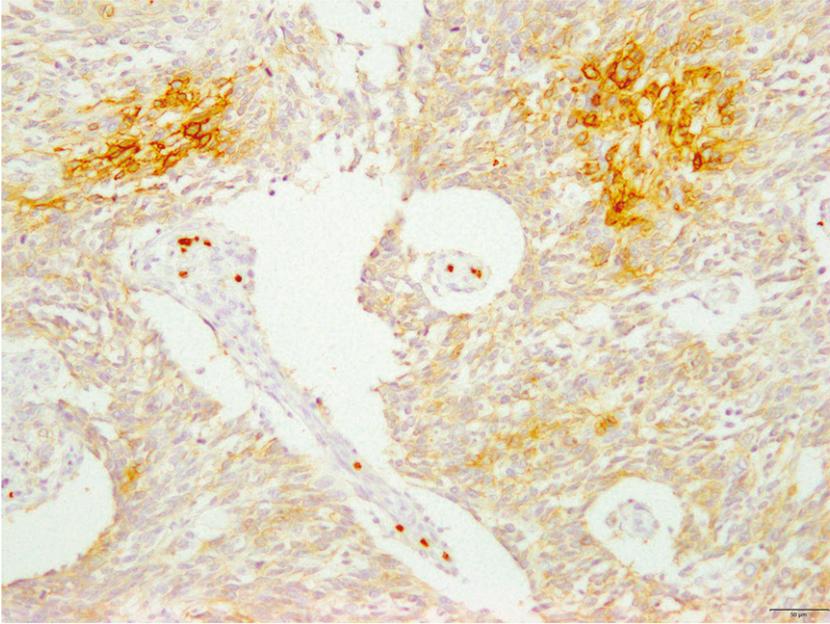
C
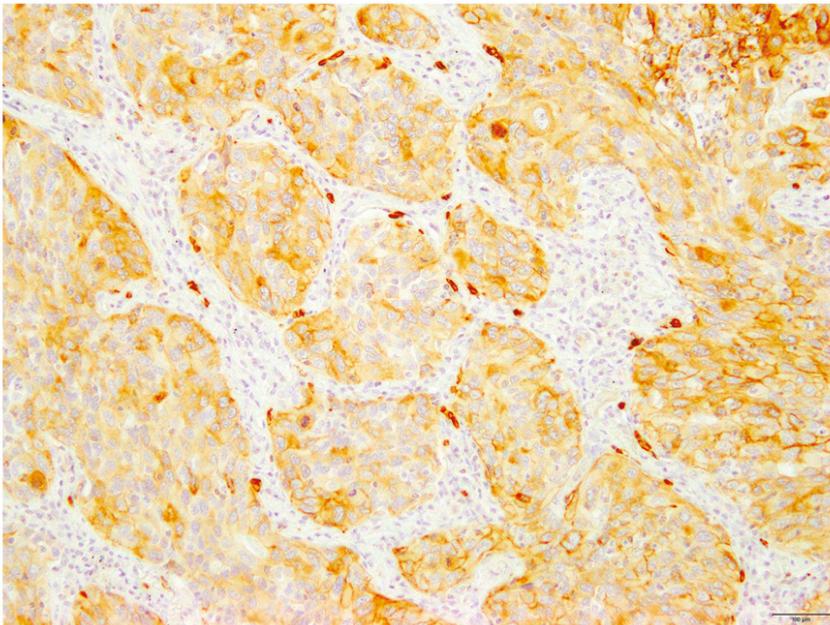
D

Figure 1. *Cont.*
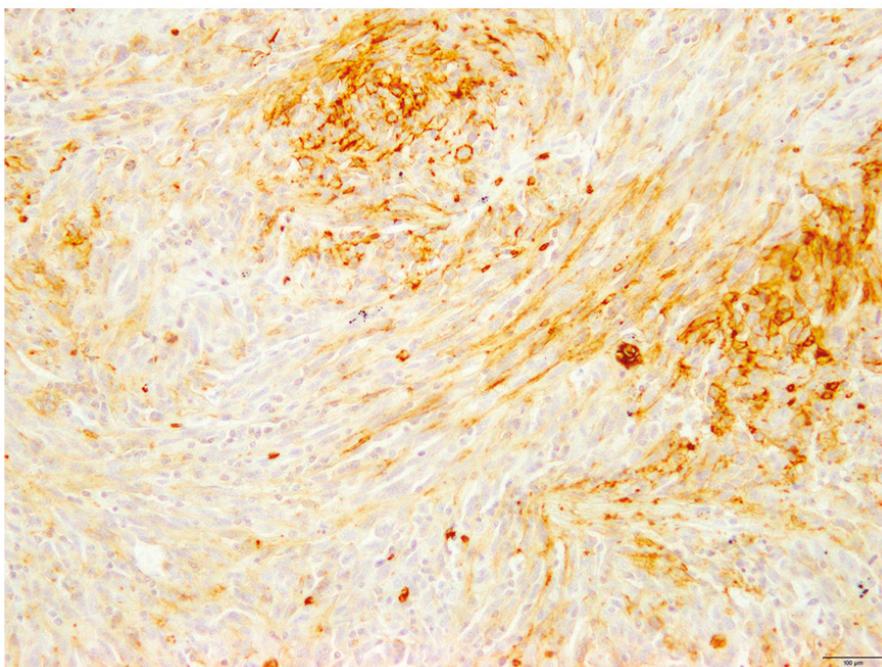
E

Figure 1. An 88-year-old male with PPC including a component of squamous cell carcinoma (**A**) GLUT1 was stained on the membrane of tumor cells, showing a score of 4. A 78-year-old female with PPC including components of squamous cell carcinoma and spindle cells: GLUT1 was stained throughout the squamous cell carcinomas (**B**) and partial lesions of spindle cells (**C**). A 77-year-old male with PPC including components of adenosquamous cell carcinoma and giant cells: GLUT1 was stained throughout the epithelial cells (**D**) and sarcomatous cells (**E**).
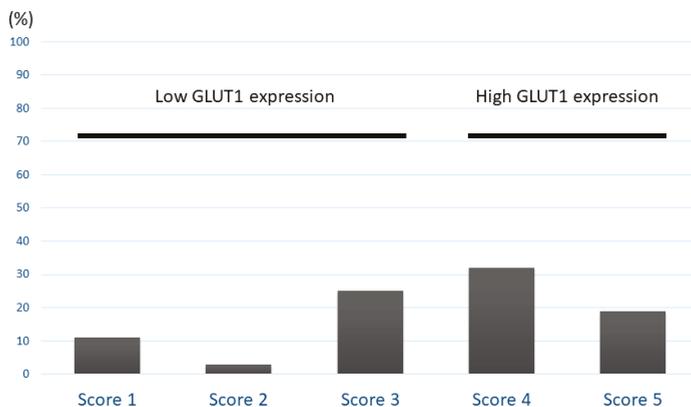

Figure 2. Distribution of GLUT1 expression according to scoring system. The frequencies of scores 1, 2, 3 4, and 5 for GLUT1 were 11%, 3%, 25%, 32%, and 19%, respectively.

Next, epithelial histological types such as adenocarcinoma (AC) and non-AC were assessed. No significant difference in the frequency of high GLUT1 expression was observed between patients with AC (20/48) and non-AC (30/56) ($p = 0.24$).

3.2. Univariate and Multivariate Survival Analysis

The median DFS and OS of all patients were 449 and 991 days, respectively. In the analysis according to the epithelial histology, the median DFS and OS of patients with AC and non-AC components were 522 and 1038 days and 336 and 507 days, respectively. In total, 60 patients died, and recurrence after initial surgery was observed in 59 patients. The above survival information has been previously described [7–9]. The results of the survival analysis are listed in Table 2. The Kaplan-Meier survival curve of all patients with high or low GLUT1 expression is shown in Figure 3. According to the univariate analysis, disease stage and GLUT1 were identified as significant factors for predicting worse OS after surgery and disease stage; pleural invasion and GLUT1 displayed a close association with poor DFS. The different variables with a cut-off of $p < 0.05$ were screened based on the results of the univariate log-rank test. In all patients, the disease stage and GLUT1 were confirmed as independent prognostic factors related to worse OS and DFS by multivariate analysis. Next, we analyzed the prognostic significance of GLUT1 expression according to the epithelial histological types of PPC (AC and non-AC component). Figure 3 shows the Kaplan-Meier survival curve of patients with AC and non-AC components. In univariate analysis, patients with a non-AC component with high GLUT1 expression showed a significantly worse OS and DFS than low GLUT1 expression compared to those with an AC component.

Table 2. Univariate and multivariate survival analysis in all patients.

Variables	Overall survival (OS) in Total Patients				
	Univariate Analysis		Multivariate Analysis		
	1-Year Rate (%)	*p*-Value	HR	95% CI	*p*-Value
Age (<69/≥69)	48/73	0.41			
Gender (female/male)	60/58	0.66			
p-stage (I-II/III-IV)	75/29	<0.01*	1.53	1.21–2.12	<0.01*
Ly (present/absent)	52/71	0.21			
v (present/absent)	59/61	0.23			
Pl (present/absent)	53/66	0.07			
Adjuvant CTx (present/absent)	66/57	0.18			
GLUT1 expression (high/low)	43/75	<0.01*	1.72	1.29–2.34	<0.01*
Ki-67 labeling index (high/low)	60/61	0.77			
	Disease-Free Survival (DFS) in Total Patients				
Age (<69/≥69)	41/69	0.12			
Gender (female/male)	58/46	0.17			
p-stage (I-II/III-IV)	67/31	<0.01*	1.58	1.19–2.09	<0.01*
ly (present/absent)	47/68	0.04			
v (present/absent)	56/62	0.08			
pl (present/absent)	43/71	<0.01*	1.15	0.57–1.02	0.07
Adjuvant CTx (present/absent)	57/52	0.97			
GLUT1 expression (high/low)	36/72	<0.01*	1.44	1.08–1.95	0.01*
Ki-67 labeling index (high/low)	51/59	0.64			

CI = confidence interval; *$p < 0.05$ is considered statistically significant, calculated with continuous variable; ly, lymphatic permeation; v, vascular invasion; pl, pleural invasion; GLUT1, glucose transporter 1; and HR, hazard ratio.
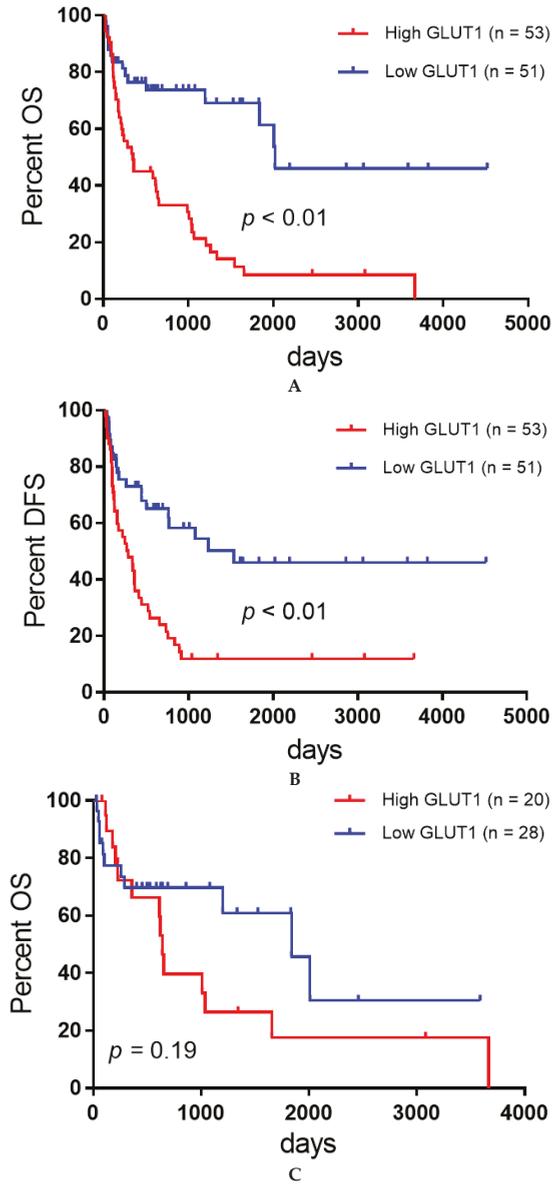
Figure 3. *Cont.*
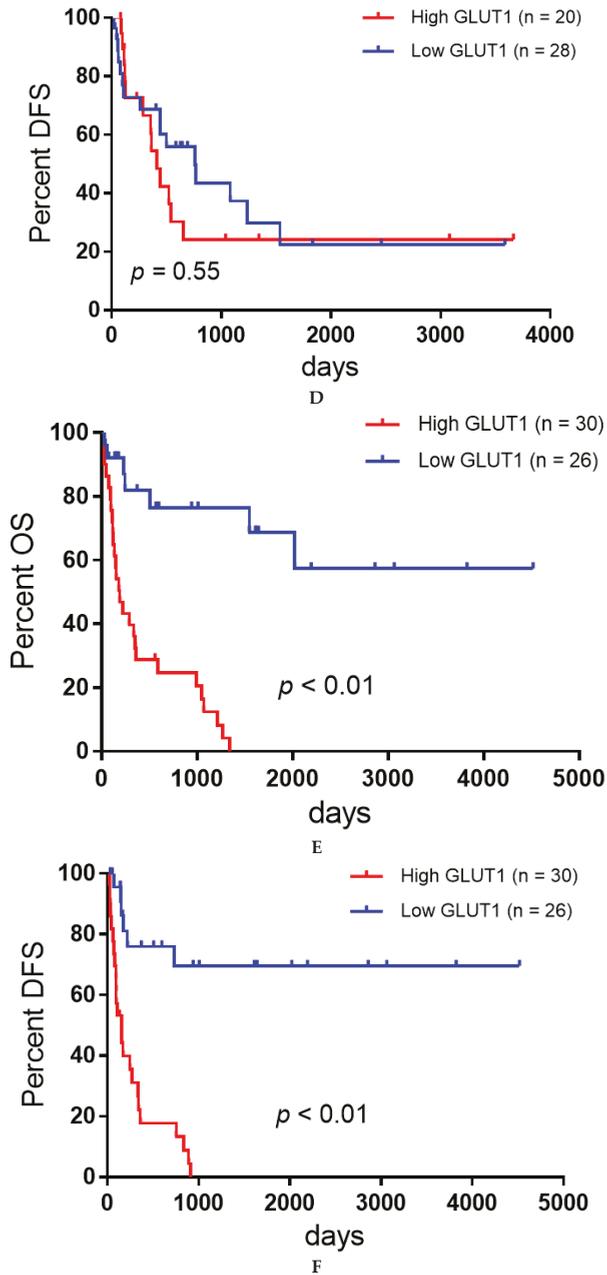
Figure 3. Kaplan-Meier survival curves for all patients (**A**,**B**), those with adenocarcinoma (**C**,**D**), and those with nonadenocarcinoma (**E**,**F**). Patients with high GLUT1 expression exhibited a significantly worse OS (A) and DFS (B) than those with low GLUT1 expression. No significant difference in the OS (C) and DFS (D) was observed between patients with adenocarcinoma with high and low GLUT1 expression, whereas the OS (E) and DFS (F) in patients with nonadenocarcinoma were significantly lower in those with high GLUT1 expression than in those low GLUT1 expression.

Figure 4 shows the forest plot of the one-year OS and DFS rates according to GLUT1 expression for each variable. Patients with high GLUT1 expression exhibited a worse OS and DFS than those with low GLUT1 expression for different variables except for stages III and IV.
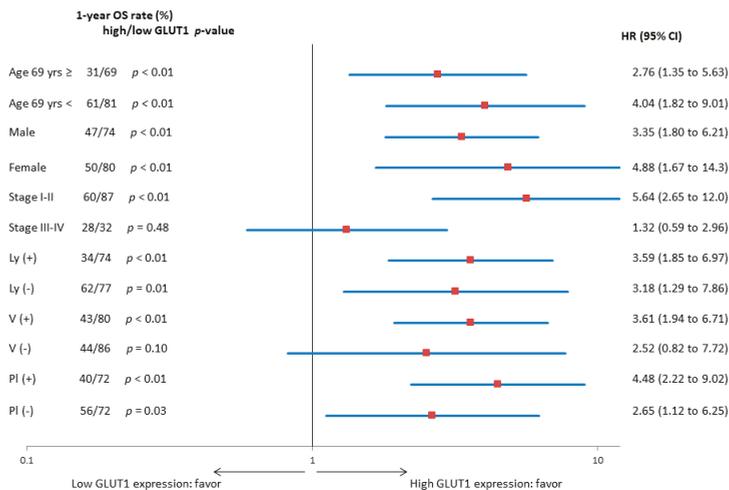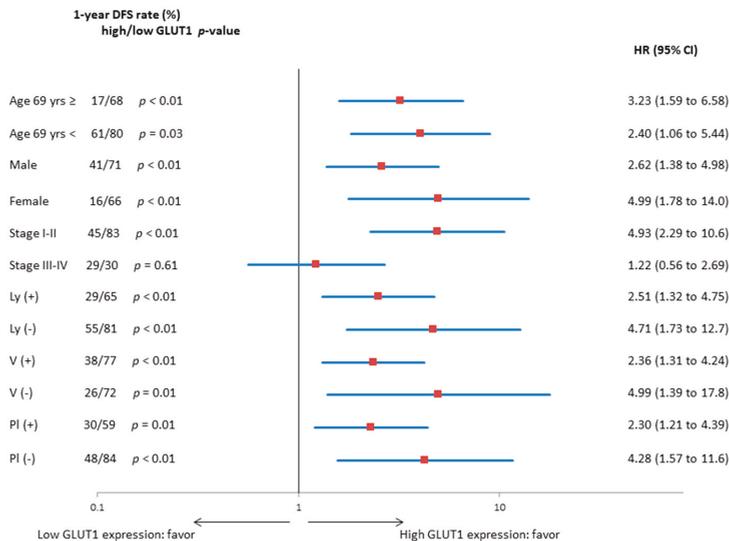
Figure 4. (**A**) Forest plot of one-year OS rate according to GLUT1 expression for each variable. (**B**) Forest plot of one-year DFS rate according to GLUT1 expression for each variable.

4. Discussion

We examined the prognostic significance of GLUT1 expression in patients with surgically resected PPC. We found that overexpression of GLUT1 is an independent factor for predicting poor outcomes

and is useful as a prognostic marker in patients with a non-AC component. In the patients with non-AC, OS and DFS showed the highest difference between low-GLUT1 and high-GLUT1 compared with all patients and subgroup patients with AC component. The value of GLUT1 as a prognostic marker differed according to the epithelial histology of PPC.

A previous meta-analysis of 1423 patients with lung cancer revealed a relationship between GLUT1 expression and clinicopathological parameters [5]. This study described that positive expression of GLUT1 was significantly associated with squamous cell carcinoma, poorly differentiated tumors, lymph node metastases, large tumor size, and advanced tumor stage. In the present study, no significant difference in the frequency of high GLUT1 expression was observed between patients with non-AC and AC components. In our analysis according to epithelial histology, however, high expression of GLUT1 was identified as a significant factor for predicting worse outcomes in patients with a non-AC component compared to those with an AC component. A previous study reported that the accumulation of FDG was closely linked to poor prognosis in patients with AC, indicating the prognostic role of glucose metabolism as a significant prognostic predictor [10]. Although the limited sample size may have biased our results, our study suggests that the role of GLUT1 as a prognostic predictor in the histology of the AC component differs between patients with PPC and NSCLC. Here, we demonstrated that high expression of GLUT1 was strongly correlated with advanced stage, vascular invasion, pleural invasion, and tumor cell proliferation. These findings correspond to those of a study on NSCLC [5].

Recently, we reported the prognostic significance of amino acid transporter 1 (LAT1) expression in patients with surgically resected NSCLC [7]. LAT1 was highly expressed in patients with PPC, and there was a close relationship between high LAT1 expression and a worse prognosis. In the analysis according to histological type, the expression of LAT1 was significantly lower in patients with an AC component than in those without an AC component; however, the role of LAT1 as a predictive marker related to poor prognosis did not differ between patients with AC and non-AC. This contradicts the findings of the current study.

There were several limitations to our study. First, the sample size was small because PPC is a rare entity, which may have biased the results. However, compared to previous studies, this was a large-scale investigation using tumor samples collected from multiple institutions. As it is difficult to definitively diagnose PPC using biopsy samples, we collected tumor samples from patients with surgically resected PPC. Second, the expression of GLUT1 has been shown to be closely associated with tumor progression, metastases, and survival of PPC; however, it remains unknown whether GLUT1 expression is correlated with the uptake of ^{18}F-FDG within PPC tumor cells. Although a previous exploratory study indicated a close relationship between GLUT1 expression and ^{18}F-FDG accumulation in patients with PPC, it is necessary to validate this correlation using different cohorts with more than 100 tumor samples. Finally, GLUT1 is found to be a targeting molecule for PPC; however, inhibition of glucose metabolism may be harmful to normal cells rather than cancer cells. Therefore, it may be difficult to administer inhibitors of GLUT1 as a treatment for PPC with a non-AC component in clinical practice. Further studies are needed to develop a selective inhibitor of GLUT1 to diminish the tumor growth and metastases of PPC.

5. Conclusions

GLUT1 is an independent predictor of poor prognosis in patients with surgically resected PPC, particularly in those with an AC component. Although GLUT1 is widely expressed in human cancers, tumor glucose metabolism was identified as an essential factor related to tumor cell proliferation, survival, and pathogenesis. Additional studies are needed to determine the therapeutic potential of GLUT1 inhibitors in patients with advanced PPC.

References

1. Chang, Y.L.; Lee, Y.C.; Shih, J.Y.; Wu, C.T. Pulmonary pleomorphic (spindle) cell carcinoma: Peculiar clinicopathologic manifestations different from ordinary non-small cell carcinoma. *Lung Cancer* **2001**, *34*, 91–97. [CrossRef]

2. Kerr, K.M.; Pelosi, G.; Austin, J.H.M. Pleomorphic, spindle cell, and giant cell carcinoma. In *WHO Classification of Tumours of the Lung, Pleura, Thymus and Heart*; Travis, W.D., Brambilla, E., Burke, A.P., Marx, A., Nicholson, A.G., Eds.; IARC Press: Lyon, France, 2015; Volume 7, pp. 88–90.

3. Fishback, N.F.; Travis, W.D.; Moran, C.A.; Guinee, D.G., Jr.; McCarthy, W.F.; Koss, M.N. Pleomorphic (spindle/giant cell) carcinoma of the lung. A clinicopathologic correlation of 78 cases. *Cancer* **1994**, *73*, 2936–2945. [CrossRef]

4. Kaira, K.; Endo, M.; Abe, M.; Nakagawa, K.; Ohde, Y.; Okumura, T.; Takahashi, T.; Murakami, H.; Tsuya, A.; Nakamura, Y.; et al. Biologic correlation of 2-[18F]-fluoro-2-deoxy-D-glucose uptake on positron emission tomography in thymic epithelial tumors. *J. Clin. Oncol.* **2010**, *28*, 3746–3753. [CrossRef] [PubMed]

5. Zhang, B.; Xie, Z.; Li, B. The clinicopathologic impacts and prognostic significance of GLUT1 expression in patients with lung cancer: A meta-analysis. *Gene* **2019**, *689*, 76–83. [CrossRef] [PubMed]

6. Kaira, K.; Endo, M.; Abe, M.; Nakagawa, K.; Ohde, Y.; Okumura, T.; Takahashi, T.; Murakami, H.; Tsuya, A.; Nakamura, Y.; et al. Biologic correlates of ^{18}F-FDG uptake on PET in pulmonary pleomorphic carcinoma. *Lung Cancer* **2011**, *71*, 144–150. [CrossRef] [PubMed]

7. Kaira, K.; Kawashima, O.; Endoh, H.; Imaizumi, K.; Goto, Y.; Kamiyoshihara, M.; Sugano, M.; Yamamoto, R.; Osaki, T.; Tanaka, S.; et al. Expression of amino acid transporter (LAT1 and 4F2hc) in pulmonary pleomorphic carcinoma. *Hum. Pathol.* **2019**, *84*, 142–149. [CrossRef] [PubMed]

8. Kaira, K.; Kamiyoshihara, M.; Kawashima, O.; Endoh, H.; Imaizumi, K.; Sugano, M.; Tanaka, S.; Fujita, A.; Kogure, Y.; Shimizu, A.; et al. Prognostic impact of β2 adrenergic receptor expression in surgically resected pulmonary pleomorphic carcinoma. *Anticancer Res.* **2019**, *39*, 395–403. [CrossRef] [PubMed]

9. Imai, H.; Shimizu, K.; Kawashima, O.; Endoh, H.; Imaizumi, K.; Goto, Y.; Kamiyoshihara, M.; Sugano, M.; Yamamoto, R.; Tanaka, S.; et al. Clinical significance of various drug-sensitivity markers in patients with surgically resected pulmonary pleomorphic carcinoma. *Cancers* **2019**, *11*, 1636. [CrossRef]

10. Kaira, K.; Shimizu, K.; Kitahara, S.; Yajima, T.; Atsumi, J.; Kosaka, T.; Ohtaki, Y.; Higuchi, T.; Oyama, T.; Asao, T.; et al. 2-Deoxy-2-[fluorine-18] fluoro-d-glucose uptake on positron emission tomography is associated with programmed death ligand-1 expression in patients with pulmonary adenocarcinoma. *Eur. J. Cancer* **2018**, *101*, 181–190. [CrossRef] [PubMed]

Article

Retrospective Efficacy Analysis of Immune Checkpoint Inhibitor Rechallenge in Patients with Non-Small Cell Lung Cancer

Yuki Katayama [1,†], Takayuki Shimamoto [1,†], Tadaaki Yamada [1,*], Takayuki Takeda [2], Takahiro Yamada [3], Shinsuke Shiotsu [4], Yusuke Chihara [5], Osamu Hiranuma [6], Masahiro Iwasaku [1], Yoshiko Kaneko [1], Junji Uchino [1] and Koichi Takayama [1]

1   Department of Pulmonary Medicine, Graduate School of Medical Science, Kyoto Prefectural University of Medicine, Kyoto 602-8566, Japan; ktym2487@koto.kpu-m.ac.jp (Y.K.); m04035ts@koto.kpu-m.ac.jp (T.S.); miwasaku@koto.kpu-m.ac.jp (M.I.); kaneko-y@koto.kpu-m.ac.jp (Y.K.); uchino@koto.kpu-m.ac.jp (J.U.); takayama@koto.kpu-m.ac.jp (K.T.)
2   Department of Pulmonary Medicine, Japanese Red Cross Kyoto Daini Hospital, Kyoto 602-8026, Japan; dyckw344@yahoo.co.jp
3   Department of Pulmonary Medicine, Matsushita Memorial Hospital, Moriguchi 570-8540, Japan; t-yamada@koto.kpu-m.ac.jp
4   Department of Pulmonary Medicine, Japanese Red Cross Kyoto Daiichi Hospital, Kyoto 605-0981, Japan; sshiotsu@gmail.com
5   Department of Pulmonary Medicine, Uji-Tokushukai Medical Center, Uji 611-0041, Japan; c1981311@koto.kpu-m.ac.jp
6   Department of Pulmonary Medicine, Otsu City Hospital, Otsu 520-0804, Japan; osamu319@true.ocn.ne.jp
*   Correspondence: tayamada@koto.kpu-m.ac.jp; Tel.: +81-75-251-5513
†   These authors contributed equally to this work and share first authorship.

Abstract: Little is known regarding the effectiveness and tolerability of immune checkpoint inhibitor (ICI) rechallenge after disease progression following initial ICI treatments. To identify eligible patients for ICI rechallenge, we retrospectively analyzed the relationship between clinical profiles and the effect of ICI rechallenge in patients with non-small cell lung cancer (NSCLC). We enrolled 35 NSCLC patients at six different institutions who were retreated with ICIs after discontinued initial ICI treatments due to disease progression. Cox proportional hazards models were used to assess the impact of clinical profiles on overall survival (OS) and progression-free survival (PFS). Median PFS and OS were 81 d (95% confidence interval, CI, 41–112 d) and 225 d (95% CI 106–361 d), respectively. The objective response rate was 2.9%, and the disease control rate was 42.9%. Multivariate analysis demonstrated that Eastern Cooperative Oncology Group Performance Score (ECOG-PS) ≥ 2 (hazard ratio, HR, 2.38; 95% CI 1.03–5.52; $p = 0.043$) and body mass index (BMI) > 20 (HR 0.43, 95% CI 0.19–0.95, $p = 0.036$) were significantly associated with PFS of ICI rechallenge. Our observations suggest that poor ECOG-PS and low BMI at intervention with ICI rechallenge may be negative predictors for ICI rechallenge treatment in patients with NSCLC.

Keywords: immunotherapy; rechallenge; non-small cell lung cancer; retrospective analysis

1. Introduction

Lung cancer is the leading cause of cancer death worldwide [1]. Current clinical studies have shown that some types of molecularly targeted therapies are able to successfully treat a subset of patients with advanced non-small cell lung cancer (NSCLC). In addition, cancer immunotherapies, such as programmed cell death protein 1 (PD-1)/programmed death ligand 1 (PD-L1) checkpoint inhibitors,

are being developed as promising alternative strategies for treating patients with advanced NSCLC. Of the current immune checkpoint inhibitors (ICIs), nivolumab, pembrolizumab, atezolizumab, and durvalumab have been approved in the United States, Japan, and other countries for the treatment of patients with NSCLC based on phase III clinical trials [2–6]. However, the majority of patients with NSCLC ultimately acquire resistance to ICI treatments. After acquiring resistance to several therapeutic regimens, ICI rechallenge is considered to be one of the therapeutic options for patients with recurrent NSCLC. Unfortunately, ICI rechallenge treatment has been clinically effective in only a small number of NSCLC patients. Therefore, it is warranted to identify predictive clinical markers for the effectiveness of ICI rechallenge. Previous retrospective studies regarding ICI rechallenge have analyzed only limited numbers of NSCLC patients [7,8]. Hence, little is currently known regarding the effectiveness and tolerability of ICI rechallenge after disease progression following initial ICI treatments. In an effort to identify the patients eligible for ICI rechallenge treatment, we retrospectively analyzed the relationship between the clinical profiles and the effect of ICI rechallenge in patients with NSCLC.

2. Experimental Section

2.1. Patients

We enrolled 35 patients with NSCLC who were retreated with ICIs after their initial ICI treatments were discontinued due to disease progression. The patients were treated between April 2017 and November 2018 at one of six different institutions, which included University Hospital Kyoto Prefectural University of Medicine (Kyoto, Japan), Japanese Red Cross Kyoto Daiichi Hospital (Kyoto, Japan), Japanese Red Cross Kyoto Daini Hospital (Kyoto, Japan), Uji-Tokushukai Medical Center (Kyoto, Japan), Matsushita Memorial Hospital (Osaka, Japan), and Otsu City Hospital (Shiga, Japan). Patient clinical data were retrospectively obtained from their medical records, including age, sex, height, weight, body mass index (BMI) at the start of ICI rechallenge, histological subtype, PD-L1 expression level in tumors, epidermal growth factor receptor (EGFR) mutation status, disease staging, metastatic site, corticosteroid administration, Eastern Cooperative Oncology Group Performance Status (ECOG-PS), smoking status, laboratory findings at the time of ICI rechallenge, and overall survival (OS), progression-free survival (PFS), response rate, and disease control rate for the patients receiving ICI treatment based on the Response Evaluation Criteria in Solid Tumors (RECIST; version 1.1). The study protocol was approved by the ethics committee of each hospital. Tumor–node–metastasis (TNM) stage was classified using the TNM stage classification system, version 8. Six received 2.5 mg to 10 mg p.o. of corticosteroids administration due to improvement in the cachexia. We have added this information in the materials and methods section. This study is an exploratory trial.

2.2. Tumor PD-L1 Analysis

PD-L1 expression was analyzed by SRL, Inc. using a PD-L1 IHC 22C3 pharmDx assay (Agilent Technologies, Santa Clara, CA, USA). The PD-L1 tumor proportion score (TPS) was calculated as a percentage of at least 100 viable tumor cells with complete or partial membrane staining. Pathologists at SRL, Inc. interpreted the TPS results.

2.3. Statistical Analysis

Statistical analyses were performed using EZR statistical software, version 1.30 [9]. All statistical tests were two-sided, and *p*-values < 0.05 were regarded as statistically significant. The cutoff values for body mass index (BMI), albumin, lactate dehydrogenase (LDH), neutrophil to lymphocyte ratio (NLR), lymphocyte to monocyte ratio (LMR), platelet to lymphocyte ratio (PLR), and C-reactive protein (CRP) following prior therapy were determined according to previous reports [10–15]. The PFS and OS were calculated using the Kaplan–Meier method, and differences were compared using the log-rank test. The hazard ratios (HRs) and their 95% confidence intervals (CIs) were estimated using the Cox

proportional hazards model in univariate analyses. The Cox proportional hazards model was also used for the multivariate analyses.

3. Results

3.1. Patient Characteristics

A total of 35 NSCLC patients treated with ICI rechallenge between April 2017 and November 2018 at six different institutions in Japan were enrolled. The median age was 70 years (range: 40–83 years), 24 patients (68.6%) were male, and 27 (77.1%) patients had a history of smoking. The histological subtypes were (23, i.e., 65.7%) adenocarcinoma and (10, i.e., 28.6%) squamous cell carcinoma. Metastatic disease was detected in the liver of five patients (14.3%) and in the brain of seven patients (20%). Of the patients, 10 (28.6%) had stage III disease, 19 (54.3%) had stage IV disease, and six (17.1%) had postoperative recurrence at the time of intervention with the initial ICI treatment. An EGFR mutation was detected in four patients (11.4%). There were no ALK-positive patients. ECOG-PS was 0–1 for 23 patients (65.7%) and 2–4 for 12 patients (34.3%). The PD-L1 TPS was ≥50% for 14 patients (50%), 1–49% for eight patients (7%), <0% for seven patients (29%), and not evaluated for six patients (17.1%). The BMI was ≥25 for 3 patients (8.6%), 20–25% for 16 patients (45.7%), and <20 for 16 patients (45.7%). Table 1 shows the baseline characteristics of patients.

Table 1. Patient characteristics at immune checkpoint inhibitor (ICI) rechallenge treatment.

Items	Group	*n* (%)
Age	Median (range)	70 (48–83)
Gender	Male	24 (68.6)
	Female	11 (31.4)
Eastern Cooperative Oncology Group Performance Score (ECOG-PS)	0–1	23 (65.7)
	2–4	12 (34.3)
Histology	Adenocarcinoma	23 (65.7)
	Squamous cell carcinoma	10 (28.6)
	Other	2 (5.7)
Smoking Status	Never smoker	8 (22.9)
	Current or former smoker	27 (77.1)
Staging	Stage III	10 (28.6)
	Stage IV	19 (54.3)
	Postoperative recurrence	6 (17.1)
Epidermal Growth Factor Receptor (EGFR) Mutations	Positive	4 (11.4)
	Negative	31 (88.6)
PD-L1 tumor proportion score (TPS)	≥50%	14 (40)
	1–49%	8 (22.9)
	<1%	7 (20)
	Not evaluated	6 (17.1)
Metastasis	Liver metastasis	5 (14.3)
	Brain metastasis	7 (20)
Body Mass Index (BMI)	BMI > 25	3 (8.6)
	25 ≥ BMI > 20	16 (45.8)
	BMI ≤ 20	16 (45.8)
Corticosteroid Administration	Yes	6 (17.1)
	No	29 (82.9)

Table 1. *Cont.*

Items	Group	n (%)
History of Treatment before ICI Rechallenge	Surgery	6 (17.1)
	Radiation therapy	12 (34.3)
	Chemotherapy (platinum)	30 (85.7)
	Chemotherapy (non-platinum)	25 (71.4)
First ICIs	Nivolumab	19 (54.3)
	Pembrolizumab	12 (34.3)
	Atezolizumab	4 (11.4)
Second ICIs	Nivolumab	5 (14.3)
	Pembrolizumab	7 (20)
	Atezolizumab	23 (65.7)
Line of First ICI	Median (range)	3 (1–15)
Line of Second ICI	Median (range)	4 (2–19)
Duration from the End of the First ICI to the Start of the Second ICI	Median (95% confidence interval; CI)	157 d (106–238)

3.2. Efficacy and Safety of ICI Treatments

The initial ICI treatment consisted of nivolumab for 19 (54.3%) patients, pembrolizumab for 12 (34.3%) patients, and atezolizumab for four (11.4%) patients. The rechallenge treatment consisted of nivolumab for five (14.3%) patients, pembrolizumab for 7 (20.0%) patients, and atezolizumab for 23 (65.7%) patients. The patients were treated with different regimens of ICIs between the initial and rechallenge treatments. In the initial ICI treatment, no patients experienced a complete response (0%), 12 experienced a partial response (34.3%), 12 experienced stable disease (34.3%), 10 experienced progressive disease (28.6%), and one was non-evaluable (2.9%). The objective response rate was 34.3%, and the disease control rate was 68.6% (Figure 1a). The PFS and OS of the initial ICI treatments were 120 d (95% CI 84–139 d) and 596 d (95% CI 455–864 d), respectively (Figure 2a,b). In the ICI rechallenge treatment, no patients experienced a complete response (0%), one experienced a partial response (2.9%), 14 experienced stable disease (40.0%), 18 experienced progressive disease (51.4%), and two were non-evaluable (5.7%). The objective response rate was 2.9% and the disease control rate was 45.7% (Figure 1b). The PFS and OS of the ICI rechallenge were 81 d (95% CI 41–112 d) and 225 d (95% CI 106–361 d), respectively (Figure 2c,d).
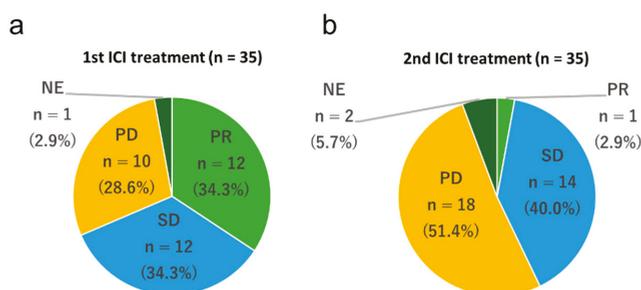
Figure 1. Frequency of the best overall response to immune checkpoint inhibitors (ICIs). (**a**) Frequency of the best overall response to first ICI treatment. (**b**) Frequency of the best overall response to ICI rechallenge treatment. PD, progressive disease; PR, partial response; SD, stable disease; NE, not evaluated.
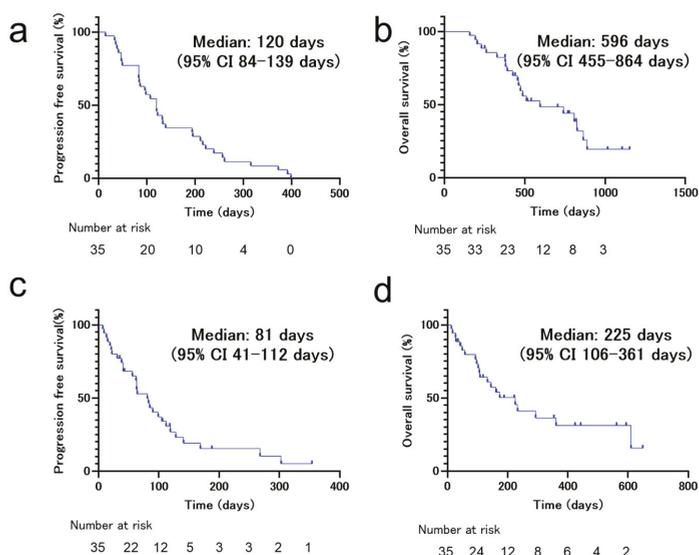
Figure 2. Kaplan–Meier survival curves of progression-free survival (PFS) and overall survival (OS) of patients who received immune checkpoint inhibitor (ICI) rechallenge treatment. (**a**) PFS of non-small cell lung cancer (NSCLC) patients (*n* = 35) on first ICI treatment. (**b**) OS of NSCLC patients (*n* = 35) on first ICI treatment. (**c**) PFS of NSCLC patients (*n* = 35) on ICI rechallenge treatment. (**d**) OS of NSCLC patients (*n* = 35) on ICI rechallenge treatment.

Univariate analyses of the patient data revealed that ECOG-PS ≥ 2 (HR 2.21, 95% CI 1.00–4.83, *p* = 0.048), BMI > 20 (HR 0.47, 95% CI 0.22–0.99, *p* = 0.047), NLR ≥ 5 (HR 2.22, 95% CI 1.02–4.84, *p* = 0.045), and LMR < 1.7 (HR 0.44, 95% CI 0.21–0.93, *p* = 0.032) were significantly associated with PFS of ICI rechallenge (Table 2). Moreover, multivariate analysis demonstrated that ECOG-PS ≥ 2 (HR 2.38, 95% CI 1.03–5.52, *p* = 0.043) and BMI > 20 (HR 0.43, 95% CI 0.19–0.95, *p* = 0.036) were significantly associated with PFS of ICI rechallenge (Table 3 and Figure 3).

Table 2. Cox proportional hazards and logistic regression models for progression-free survival (PFS) and overall survival (OS).

Items	PFS (Univariate Analysis)		OS (Univariate Analysis)	
	HR (95% CI)	***p*-Value**	**HR (95% CI)**	***p*-Value**
Age > 75 Years	0.81 (0.34–1.91)	0.63	1.45 (0.55–3.80)	0.45
Male Gender	1.47 (0.66–3.26)	0.35	2.39 (0.80–7.17)	0.12
Smoker	1.508 (0.63–3.59)	0.35	2.50 (0.73–8.58)	0.14
ECOG-PS ≥ 2	2.21 (1.00–4.83)	0.048	4.23 (1.65–10.89)	0.0028
Squamous Histology	1.08 (0.47–2.48)	0.86	0.67 (0.24–1.83)	0.43
EGFR Mutations Positive	0.83 (0.28–2.43)	0.73	1.17 (0.34–4.02)	0.80
BMI > 20	0.47 (0.22–0.99)	0.047	0.42 (0.17–1.02)	0.056
BMI > 25	0.54 (0.19–1.59)	0.27	0.92 (0.26–3.25)	0.90
Corticosteroids Administration	1.3 (0.49–3.52)	0.58	0.66 (0.19–2.27)	0.51
Alb > 3.5 g/dL	0.53 (0.25–1.11)	0.092	0.37 (0.15–0.90)	0.028
CRP > 1.0 mg/dL	1.44 (0.68–3.04)	0.34	2.92 (1.10–7.76)	0.032
LDH > 245 U/L	1.41 (0.67–2.99)	0.37	2.16 (0.89–5.24)	0.090
NLR > 5.0	2.22 (1.02–4.84)	0.045	1.98 (0.79–4.92)	0.14
LMR > 1.7	0.44 (0.21–0.93)	0.032	0.51 (0.21–1.23)	0.14
PLR > 262	2.23 (0.99–5.03)	0.054	2.80 (1.02–7.67)	0.045
Liver Metastasis	1.79 (0.61–5.28)	0.29	1.95 (0.55–6.886)	0.30

Table 2. *Cont.*

Items	PFS (Univariate Analysis)		OS (Univariate Analysis)	
	HR (95% CI)	*p*-Value	HR (95% CI)	*p*-Value
Brain Metastasis	1.17 (0.47–2.91)	0.73	0.58 (0.17–2.00)	0.39
PD-L1 TPS 1–49%	0.32 (0.096–1.05)	0.059	0.55 (0.16–1.89)	0.34
PD-L1 TPS > 50%	0.35 (0.12–1.05)	0.061	0.42 (0.12–1.49)	0.18
Lines between First and Second ICIs > 2	1.26 (0.55–2.87)	0.58	1.54 (0.59–4.04)	0.38
PFS of First ICI >120 d	1.06 (0.50–2.23)	0.89	1.30 (0.55–3.08)	0.54
Duration from the End of the First ICI to the Second ICI >157 d	0.97 (0.47–2.02)	0.94	0.77 (0.32–1.84)	0.55
Partial Response with First ICIs	0.58 (0.26–1.33)	0.20	0.99 (0.40–2.48)	0.98

Table 3. Cox proportional hazards and logistic regression models for progression-free survival (PFS) and overall survival (OS).

Items	PFS (Multivariate Analysis)		OS (Multivariate Analysis)	
	HR (95% CI)	*p*-Value	HR (95% CI)	*p*-Value
ECOG-PS ≥ 2	2.38(1.03–5.52)	0.043	3.01(1.10–8.24)	0.032
BMI > 20	0.43(0.19–0.95)	0.036		
Alb > 3.5 g/dL			0.48(0.18–1.28)	0.14
CRP > 1.0 mg/dL			1.51(0.48–4.75)	0.49
NLR > 5.0	1.08(0.22–5.18)	0.93		
LMR > 1.7	0.57(0.13–2.54)	0.46		
PLR > 262			1.93(0.68–5.43)	0.22
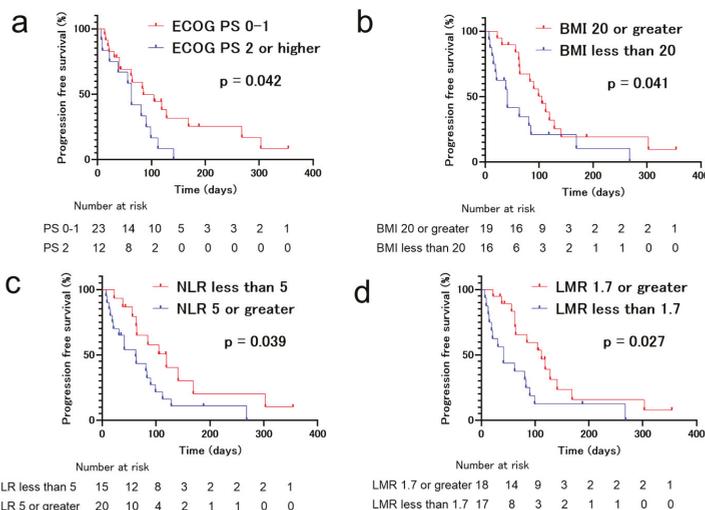
Figure 3. Kaplan–Meier survival curves for progression-free survival (PFS) of patients who received immune checkpoint inhibitor (ICI) rechallenge treatment. (**a**) Eastern Cooperative Oncology Group (ECOG-PS) ≥ 2, (**b**) body mass index (BMI) ≤ 20, (**c**) neutrophil-to-lymphocyte ratio (NLR) > 5, and (**d**) lymphocyte-to-monocyte ratio (LMR) ≤ 1.7 were significantly associated with inferior PFS.

Univariate analyses of the patient data revealed that ECOG-PS ≥ 2 (HR 4.23, 95% CI 1.65–10.89, *p* = 0.0023), CRP > 1.0 (HR 2.92, 95% CI 1.10–7.76, *p* = 0.032), albumin > 3.5 (HR 0.37, 95% CI 0.15–0.90, *p* = 0.028), and PLR > 262 (HR 2.80, 95% CI 1.02–7.67, *p* = 0.045) were significantly associated with OS of ICI rechallenge (Table 2). Multivariate analysis demonstrated that ECOG-PS ≥ 2 (HR 3.01, 95% CI 1.10–8.24, *p* = 0.032) was significantly associated with OS of ICI rechallenge (Table 3).

4. Discussion

PD-L1 expression in tumors has been used clinically as a positive predictive biomarker for the effective initial ICI treatment of patients with NSCLC [16]. However, clinically useful biomarkers have not yet been identified for predicting the efficacy of ICI rechallenge. Fujita et al. reported that objective response rate (ORR), disease control rate (DCR), and PFS values of pembrolizumab rechallenge after refractory nivolumab for 12 patients with NSCLC were 8.3%, 41.7%, and 3.1 months, respectively [8]. In addition, ORR, DCR, and PFS of atezolizumab rechallenge after refractory anti-PD-1 antibodies for 18 patients with NSCLC were 0%, 38.9%, and 2.9 months, respectively [17]. Another report showed that ORR, DCR, and PFS values of ICI rechallenge in 14 patients with ICI refractory tumors were 7.1%, 21.4%, and 1.6 months, respectively [7]. Our current observations showed that ORR, DCR, PFS, and OS values of ICI rechallenge in 35 patients with NSCLC were 2.9%, 42.9%, 2.7 months, and 7.5 months, respectively. These reproducible findings suggest that refractory NSCLC tumors for initial ICI treatments may exhibit poor responses to ICI rechallenge treatments, and the clinical benefits may be limited compared with those of the initial ICI treatment. However, a subset of patients with NSCLC demonstrate good outcomes with ICI rechallenge treatments. Therefore, there is a need for the elucidation of predictive clinical factors for re-treatment of ICI responders among patients with NSCLC.

Our multivariate analysis identified ECOG-PS and BMI as independent factors associated with poorer PFS of ICI rechallenge treatment in patients with NSCLC who were refractory to initial ICI treatment. This is the first report that identifies predictive clinical factors for the efficacy of ICI rechallenge in patients with NSCLC. The general and nutritional status of patients with NSCLC are closely related to the effects of ICI treatment. Several studies have demonstrated that poor ECOG-PS is a predictive negative factor related to clinical outcomes of initial ICI treatment in patients with NSCLC [10,13,18,19]. ECOG-PS is one of the factors that determines the tumor immune environment, and it has been reported that an imbalance of circulating T-lymphocyte subpopulations in patients with gastric cancer correlates with ECOG-PS [20]. BMI is widely used for relating weight to height, defining body size, and indicating nutritional status. In addition, a lower BMI is associated with increased mortality risk [21–24]. Our previous clinical study demonstrated that NSCLC patients with sarcopenia exhibit a significantly shorter median PFS following ICI treatment compared to that of non-sarcopenia patients [25]. Given these observations, a poor ECOG-PS and a low BMI at the time of ICI treatment intervention may be useful for predicting non-responders to initial ICI treatment, as well as ICI rechallenge treatment among patients with NSCLC. Recent clinical trials demonstrated that the ghrelin/growth hormone secretagogue receptor agonist anamorelin increases lean body mass and improves the performance status in NSCLC patients with cachexia [26,27]. Therefore, the administration of anamorelin may improve the effect of ICI rechallenge treatment.

The effectiveness of initial ICI treatments has been reported to be associated with PD-L1 expression in NSCLC tumors [28]. Our current observations show that the patients with PD-L1 expression tended to have longer PFS. This suggests that PD-L1 expression levels in pre-treatment tumors may be a factor to consider when with regard to ICI rechallenge treatment. Regardless, based on our observations, the values of blood NLR, LMR, and PLR at baseline may be useful tools for predicting responders to the ICI rechallenge treatment, which is consistent with the initial ICI treatment [10,13,15,29]. Thus, when considering ICI rechallenge treatment in patients with NSCLC, the inflammation markers, such as NLR, LMR, and PLR, may be useful to some extent for identifying responders to ICI rechallenge.

A previous report suggests that the response to initial ICI treatments correlates with the clinical response to ICI rechallenge treatment in patients with melanoma [30]. However, our results failed to indicate a relationship between clinical outcomes of initial ICI treatment and ICI rechallenge treatment in patients with NSCLC. This suggested that there may be differences between the immunological properties of NSCLC and melanoma.

The current study had several limitations. First, it consisted of a small retrospective sample. Therefore, a further large-cohort study is warranted to identify the predictive markers of ICI rechallenge

treatment. Second, although the treatment was administered at multiple centers, there may have been bias in terms of the timing of evaluating the patients using CT scanning, even though it was performed every 1–3 months after treatment.

5. Conclusions

Our observations suggest that a poor ECOG-PS and a low BMI at the time of intervention with ICI rechallenge may be useful as negative predictors for ICI rechallenge treatment in patients with NSCLC. As this retrospective study was a relatively small-scale study, further experiments are needed to validate the observations.

Abbreviations

NSCLC, non-small cell lung cancer; PD-1, programmed cell death protein 1; PD-L1, programmed death-ligand 1; ICIs, immune checkpoint inhibitors; PFS, progression-free survival; OS, overall survival; BMI, body mass index; CRP, C-reaction protein; NLR, neutrophil to lymphocyte ratio; LMR, lymphocyte to monocyte ratio; PLR, platelet to lymphocyte ratio; RECIST, Response Evaluation Criteria in Solid Tumors; CR, complete response; PR, partial response; SD, stable disease; PD, progressive disease; NE, not evaluate; PS, Eastern Cooperative Oncology Group Performance Status; CI, confidence interval; HR, hazard ratio; TPS, tumor proportion score; EGFR, epidermal growth factor receptor.

References

1. Miller, K.D.; Goding Sauer, A.; Ortiz, A.P.; Fedewa, S.A.; Pinheiro, P.S.; Tortolero-Luna, G.; Martinez-Tyson, D.; Jemal, A.; Siegel, R.L. Cancer Statistics for Hispanics/Latinos, 2018. *CA Cancer J. Clin.* **2018**, *68*, 425–445. [CrossRef] [PubMed]
2. Borghaei, H.; Paz-Ares, L.; Horn, L.; Spigel, D.R.; Steins, M.; Ready, N.E.; Chow, L.Q.; Vokes, E.E.; Felip, E.; Holgado, E.; et al. Nivolumab versus Docetaxel in Advanced Nonsquamous Non-Small-Cell Lung Cancer. *N. Engl. J. Med.* **2015**, *373*, 1627–1639. [CrossRef] [PubMed]
3. Brahmer, J.; Reckamp, K.L.; Baas, P.; Crino, L.; Eberhardt, W.E.; Poddubskaya, E.; Antonia, S.; Pluzanski, A.; Vokes, E.E.; Holgado, E.; et al. Nivolumab versus Docetaxel in Advanced Squamous-Cell Non-Small-Cell Lung Cancer. *N. Engl. J. Med.* **2015**, *373*, 123–135. [CrossRef] [PubMed]
4. Herbst, R.S.; Baas, P.; Kim, D.W.; Felip, E.; Perez-Gracia, J.L.; Han, J.Y.; Molina, J.; Kim, J.-H.; Arvis, C.D.; Ahn, M.-J.; et al. Pembrolizumab versus docetaxel for previously treated, PD-L1-positive, advanced non-small-cell lung cancer (KEYNOTE-010): A Randomised Controlled Trial. *Lancet* **2016**, *387*, 1540–1550. [CrossRef]
5. Rittmeyer, A.; Barlesi, F.; Waterkamp, D.; Park, K.; Ciardiello, F.; von Pawel, J.; Gadgeel, S.M.; Hida, T.; Kowalski, D.M.; Dols, M.C.; et al. Atezolizumab versus docetaxel in patients with previously treated non-small-cell lung cancer (OAK): A phase 3, open-label, multicentre randomised controlled trial. *Lancet* **2017**, *389*, 255–265. [CrossRef]
6. Antonia, S.J.; Villegas, A.; Daniel, D.; Vicente, D.; Murakami, S.; Hui, R.; Yokoi, T.; Chiappori, A.; Lee, K.H.; Wit de, M.; et al. Durvalumab after Chemoradiotherapy in Stage III Non-Small-Cell Lung Cancer. *N. Engl. J. Med.* **2017**, *377*, 1919–1929. [CrossRef]
7. Watanabe, H.; Kubo, T.; Ninomiya, K.; Kudo, K.; Minami, D.; Murakami, E.; Ochi, N.; Ninomiya, T.; Harada, D.; Yasugi, M.; et al. The effect and safety of immune checkpoint inhibitor rechallenge in non-small cell lung cancer. *Jpn. J. Clin. Oncol.* **2019**, *49*, 762–765. [CrossRef]
8. Fujita, K.; Uchida, N.; Kanai, O.; Okamura, M.; Nakatani, K.; Mio, T. Retreatment with pembrolizumab in advanced non-small cell lung cancer patients previously treated with nivolumab: Emerging reports of 12 cases. *Cancer Chemother. Pharmacol.* **2018**, *81*, 1105–1109. [CrossRef]

9.   Kanda, Y. Investigation of the freely available easy-to-use software 'EZR' for medical statistics. *Bone Marrow Transpl.* **2013**, *48*, 452–458. [CrossRef]

10.   Bagley, S.J.; Kothari, S.; Aggarwal, C.; Bauml, J.M.; Alley, E.W.; Evans, T.L.; Kosteva, J.A.; Ciunci, C.A.; Gabriel, P.E.; Thompson, J.C.; et al. Pretreatment neutrophil-to-lymphocyte ratio as a marker of outcomes in nivolumab-treated patients with advanced non-small-cell lung cancer. *Lung Cancer* **2017**, *106*, 1–7. [CrossRef]

11.   Kondo, T.; Nomura, M.; Otsuka, A.; Nonomura, Y.; Kaku, Y.; Matsumoto, S.; Muto, M. Predicting marker for early progression in unresectable melanoma treated with nivolumab. *Int. J. Clin. Oncol.* **2019**, *24*, 323–327. [CrossRef] [PubMed]

12.   Inomata, M.; Hirai, T.; Seto, Z.; Tokui, K.; Taka, C.; Okazawa, S.; Kambara, K.; Ichikawa, T.; Imanishi, S.; Yamada, T.; et al. Clinical Parameters for Predicting the Survival in Patients with Squamous and Non-squamous-cell NSCLC Receiving PD-1 Inhibitor Therapy. *Pathol. Oncol. Res.* **2018**. [CrossRef] [PubMed]

13.   Diem, S.; Schmid, S.; Krapf, M.; Flatz, L.; Born, D.; Jochum, W.; Templeton, A.J.; Fruh, M. Neutrophil-to-Lymphocyte ratio (NLR) and Platelet-to-Lymphocyte ratio (PLR) as prognostic markers in patients with non-small cell lung cancer (NSCLC) treated with nivolumab. *Lung Cancer* **2017**, *111*, 176–181. [CrossRef] [PubMed]

14.   Liu, J.; Li, S.; Zhang, S.; Liu, Y.; Ma, L.; Zhu, J.; Xin, Y.; Wang, Y.; Yang, C.; Cheng, Y. Systemic immune-inflammation index, neutrophil-to-lymphocyte ratio, platelet-to-lymphocyte ratio can predict clinical outcomes in patients with metastatic non-small-cell lung cancer treated with nivolumab. *J. Clin. Lab. Anal.* **2019**, *33*, e22964. [CrossRef] [PubMed]

15.   Failing, J.J.; Yan, Y.; Porrata, L.F.; Markovic, S.N. Lymphocyte-to-monocyte ratio is associated with survival in pembrolizumab-treated metastatic melanoma patients. *Melanoma Res.* **2017**, *27*, 596–600. [CrossRef] [PubMed]

16.   Reck, M.; Rodriguez-Abreu, D.; Robinson, A.G.; Hui, R.; Csoszi, T.; Fulop, A.; Gottfried, M.; Peled, N.; Tafreshi, A.; Cuffe, S.; et al. Pembrolizumab versus Chemotherapy for PD-L1-Positive Non-Small-Cell Lung Cancer. *N. Engl. J. Med.* **2016**, *375*, 1823–1833. [CrossRef]

17.   Fujita, K.; Uchida, N.; Yamamoto, Y.; Kanai, O.; Okamura, M.; Nakatani, K.; Sawai, S.; Mio, T. Retreatment With Anti-PD-L1 Antibody in Advanced Non-small Cell Lung Cancer Previously Treated With Anti-PD-1 Antibodies. *Anticancer Res.* **2019**, *39*, 3917–3921. [CrossRef]

18.   Mezquita, L.; Auclin, E.; Ferrara, R.; Charrier, M.; Remon, J.; Planchard, D.; Ponce, S.; Ares, L.P.; Leroy, L.; Audigier-Valette, C.; et al. Association of the Lung Immune Prognostic Index With Immune Checkpoint Inhibitor Outcomes in Patients With Advanced Non-Small Cell Lung Cancer. *JAMA Oncol.* **2018**, *4*, 351–357. [CrossRef]

19.   Katayama, Y.; Yamada, T.; Tanimura, K.; Yoshimura, A.; Takeda, T.; Chihara, Y.; Tamiya, N.; Kaneko, Y.; Uchino, J.; Takayama, K. Impact of bowel movement condition on immune checkpoint inhibitor efficacy in patients with advanced non-small cell lung cancer. *Thorac. Cancer* **2019**, *10*, 526–532. [CrossRef]

20.   Wang, L.; Shen, Y. Imbalance of circulating T-lymphocyte subpopulation in gastric cancer patients correlated with performance status. *Clin. Lab.* **2013**, *59*, 429–433.

21.   Naik, G.S.; Waikar, S.S.; Johnson, A.E.W.; Buchbinder, E.I.; Haq, R.; Hodi, F.S.; Schoenfeld, J.D.; Ott, P.A. Complex inter-relationship of body mass index, gender and serum creatinine on survival: Exploring the obesity paradox in melanoma patients treated with checkpoint inhibition. *J. Immunother. Cancer* **2019**, *7*, 89. [CrossRef] [PubMed]

22.   Cortellini, A.; Bersanelli, M.; Buti, S.; Cannita, K.; Santini, D.; Perrone, F.; Giusti, R.; Tiseo, M.; Michiara, M.; Marino, P.D. A multicenter study of body mass index in cancer patients treated with anti-PD-1/PD-L1 immune checkpoint inhibitors: When overweight becomes favorable. *J. Immunother. Cancer* **2019**, *7*, 57. [CrossRef] [PubMed]

23.   Xu, H.; Cao, D.; He, A.; Ge, W. The prognostic role of obesity is independent of sex in cancer patients treated with immune checkpoint inhibitors: A pooled analysis of 4090 cancer patients. *Int. Immunopharmacol.* **2019**, *74*, 105745. [CrossRef] [PubMed]

24.   De Giorgi, U.; Procopio, G.; Giannarelli, D.; Sabbatini, R.; Bearz, A.; Buti, S.; Basso, U.; Mitterer, M.; Ortega, C.; Bidoli, P.; et al. Association of Systemic Inflammation Index and Body Mass Index with Survival in Patients with Renal Cell Cancer Treated with Nivolumab. *Clin. Cancer Res.* **2019**, *25*, 3839–3846. [CrossRef]

25. Nishioka, N.; Uchino, J.; Hirai, S.; Katayama, Y.; Yoshimura, A.; Okura, N.; Tanimura, K.; Hirai, S.; Imabayashi, T.; Chihara, Y.; et al. Association of Sarcopenia with and Efficacy of Anti-PD-1/PD-L1 Therapy in Non-Small-Cell Lung Cancer. *J. Clin. Med.* **2019**, *8*, 450. [CrossRef]

26. Katakami, N.; Uchino, J.; Yokoyama, T.; Naito, T.; Kondo, M.; Yamada, K.; Kitajima, H.; Yoshimori, K.; Sato, K.; Saito, H.; et al. Anamorelin (ONO-7643) for the treatment of patients with non-small cell lung cancer and cachexia: Results from a randomized, double-blind, placebo-controlled, multicenter study of Japanese patients (ONO-7643-04). *Cancer* **2018**, *124*, 606–616. [CrossRef]

27. Takayama, K.; Katakami, N.; Yokoyama, T.; Atagi, S.; Yoshimori, K.; Kagamu, H.; Saito, H.; Takiguchi, Y.; Aoe, K.; Koyama, A.; et al. Anamorelin (ONO-7643) in Japanese patients with non-small cell lung cancer and cachexia: Results of a randomized phase 2 trial. *Support Care Cancer* **2016**, *24*, 3495–3505. [CrossRef]

28. Grizzi, G.; Caccese, M.; Gkountakos, A.; Carbognin, L.; Tortora, G.; Bria, E.; Pilotto, S. Putative predictors of efficacy for immune checkpoint inhibitors in non-small-cell lung cancer: Facing the complexity of the immune system. *Expert Rev. Mol. Diagn.* **2017**, *17*, 1055–1069. [CrossRef]

29. Jiang, T.; Qiao, M.; Zhao, C.; Li, X.; Gao, G.; Su, C.; Ren, S.; Zhou, C. Pretreatment neutrophil-to-lymphocyte ratio is associated with outcome of advanced-stage cancer patients treated with immunotherapy: A meta-analysis. *Cancer Immunol. Immunother.* **2018**, *67*, 713–727. [CrossRef]

30. Nomura, M.; Otsuka, A.; Kondo, T.; Nagai, H.; Nonomura, Y.; Kaku, Y.; Matsumoto, S.; Muto, M. Efficacy and safety of retreatment with nivolumab in metastatic melanoma patients previously treated with nivolumab. *Cancer Chemother. Pharmacol.* **2017**, *80*, 999–1004. [CrossRef]

Phase I/II Study of Docetaxel and S-1 in Previously-Treated Patients with Advanced Non-Small Cell Lung Cancer: LOGIK0408

Koichi Takayama [1,2], **Junji Uchino** [2,*], **Masaki Fujita** [3], **Shoji Tokunaga** [4], **Tomotoshi Imanaga** [5], **Ryotaro Morinaga** [6], **Noriyuki Ebi** [7], **Sho Saeki** [8], **Kazuya Matsukizono** [9], **Hiroshi Wataya** [10], **Tadaaki Yamada** [2] **and Yoichi Nakanishi** [1]

[1] Research Institute for Diseases of the Chest, Graduate School of Medical Sciences, Kyushu University, Fukuoka 8190395, Japan; takayama@koto.kpu-m.ac.jp (K.T.); naka24@e-mail.jp (Y.N.)

[2] Department of Respiratory Medicine, Kyoto Prefectural University of Medicine, Kyoto 6020841, Japan; tayamada@koto.kpu-m.ac.jp

[3] Department of Respiratory Medicine, Fukuoka University Hospital, Fukuoka 8140133, Japan; mfujita@fukuoka-u.ac.jp

[4] Medical Information Center, Kyushu University Hospital, Fukuoka 8190395, Japan; toksan@med.kyushu-u.ac.jp

[5] Department of respiratory disease, Nippon Steel Yawata Memorial Hospital, Kitakyushu 8058508, Japan; imanaga.t@ns.yawata-mhp.or.jp

[6] Department of Medical Oncology, Oita University Faculty of Medicine, Yuhu 8795593, Japan; r-morinaga@oitapref-hosp.jp

[7] Department of Respiratory Medicine, Iizuka Hospital, Iizuka, 8208505 Japan; nebi1@aih-net.com

[8] Department of Respiratory Medicine, Kumamoto University Hospital, Kumamoto 8608556, Japan; saeshow@wg7.so-net.ne.jp

[9] Department of Internal Medicine, Kagoshima City Hospital, Kagoshima 8908544, Japan; kmatsukiz@yahoo.co.jp

[10] Department of Internal Medicine, Saiseikai Fukuoka General Hospital, Fukuoka 8100001, Japan; h-wataya@saiseikai-hp.chuo.fukuoka.jp

* Correspondence: uchino@koto.kpu-m.ac.jp; Tel.: +81-75-251-5513

Abstract: Background: As docetaxel plus S-1 may be feasible for cancer treatment, we conducted a phase I/II trial to determine the recommended docetaxel dose and the fixed S-1 dose (phase I), as well as confirm the regimen's efficacy and safety (phase II) for previously-treated patients with advanced non-small cell lung cancer. Methods: Patients ≤75 years with performance status ≤1 and adequate organ function were treated at three-week intervals with docetaxel on day 1 and 80 mg/m^2 oral S-1 from days 1–14. The starting docetaxel dose was 45 mg/m^2 and this was escalated to a maximum of 70 mg/m^2. In phase II, response rate, progression-free survival (PFS), overall survival (OS), and safety were assessed. Results: The recommended doses were 50 mg/m^2 docetaxel (day 1) and 80 mg/m^2 S-1 (days 1–14). Grades 3 and 4 leukocytopenia and neutropenia occurred in 44% and 67% of patients, respectively. Nonhematologic toxicities were generally mild. Overall response to chemotherapy was 7.7% (95% confidence interval (CI), 1.6–20.9%), and median PFS and OS were 18.0 weeks (95% CI; 11.3–22.9 weeks) and 53.0 weeks, respectively. Conclusion: Fifty mg/m^2 docetaxel plus 80 mg/m^2 oral S-1 had a lower response rate than anticipated; however, the survival data were encouraging. A further investigation is warranted to select the optimal patient population.

Keywords: non-small cell lung cancer; previously treated patients; phase I/II trial; chemotherapy; docetaxel; S-1

1. Introduction

Previous clinical trials confirmed that docetaxel alone displays good anticancer effects when used to treat non-small cell lung cancer. Treatment with docetaxel is associated with significant prolongation of survival [1]. Docetaxel is an antineoplastic taxoid prepared by partial chemical modification of the non-cytotoxic precursor 10-deacetyl baccatin III, which is extracted from the needles of the European pine. Its mechanism of action is to promote the polymerization and depolymerization of microtubule proteins, resulting in microtubule stabilization and microtubule hyperplasia, which prevent chromosome migration and arrest cell division in the M phase of the cell cycle [2]. Docetaxel is useful as a second-line chemotherapy for patients that are refractory to conventional platinum-based chemotherapy [3]. When combined with platinum, docetaxel displays better responses and survival rates than other platinum-containing regimens [4,5]. S-1 is a novel oral anticancer drug composed of the 5-fluorouracil (5-FU) prodrug, tegafur, and two 5-FU modulators, 5-chloro-2,4-dihydroxypyridine (CDHP) and potassium oxonate. CDHP selectively antagonizes the rate-limiting enzyme dihydropyrimidine dehydrogenase in the 5-FU degradation pathway and enhances antitumor effects by increasing blood 5-FU levels. Potassium oxonate also selectively antagonizes orotate phosphoribosyltransferase in the gastrointestinal tract after oral administration and inhibits the formation of 5-fluoronucleotides from 5-FU. In a previous phase II study, monotherapy with S-1 produced a significant response in previously treated non-small cell lung cancer [6]. Because docetaxel and S-1 have different mechanisms of action and toxicity profiles, it may be feasible and efficient to combine these drugs for the treatment of advanced non-small cell lung cancer. Previously, Yoshida et al. reported the feasibility and usefulness of this combination chemotherapy in a clinical trial for advanced gastric cancer [7].

To improve the response rate in previously-treated patients with advanced non-small cell lung cancer, we conducted a phase I/II clinical study of docetaxel plus S-1. In this regimen, docetaxel was administered on day 1 while S-1 was administered on days 1 to 14, according to the potential schedule dependency previously reported by Kano et al. [8]. The primary objectives were to determine the maximum-tolerated dose (MTD) and the recommended dose for this regimen in a phase I study and confirm its efficacy and safety in the phase II study.

2. Experimental Section

2.1. Eligibility

Patients were enrolled in this study if they met the following eligibility criteria: cytologically or histologically confirmed diagnosis of incurable, previously treated non-small cell lung cancer; no previous use of docetaxel or uracil plus tegafur (UFT); age between 20–75 years; performance status of ≤1 on the Eastern Cooperative Oncology Group (ECOG) scale; an estimated life expectancy of >12 weeks; adequate bone marrow function (leukocyte count ≥4000/μL, platelet count ≥100,000/μL, and hemoglobin level ≥9.5 g/dL); adequate hepatic function (bilirubin level ≤1.5 mg/dL and a serum ratio of aspartate amino transferase to alanine amino transferase (AST/ALT) ≤2.5 × UNL); adequate renal function (serum creatinine ≤1.5 mg/dL); a measurable lesion according to the Response Evaluation Criteria in Solid Tumors (RECIST) guidelines version 1.0; and provision of written informed consent. The exclusion criteria were: active infection, massive ascites or pleural effusion, symptomatic brain metastasis, uncontrollable diabetes mellitus, or severe comorbidity such as heart disease or renal disease, interstitial pneumonia, watery diarrhea, active concomitant malignancy, pregnancy or lactation, or other medical problems that could prevent compliance with the protocol. The following conditions were necessary: an interval of at least 4 weeks after the end of final therapy and recovery from the previous treatment.

2.2. Treatment and Dose Escalation Schedules in the Phase I Study

On day 1 of each cycle, docetaxel (Sanofi-aventis K.K., Tokyo, Japan) diluted with 500 mL of normal saline was administered as a 90-min infusion. S-1 (Taiho Pharmaceutical Company, Tokyo, Japan) was orally administered twice daily on days 1–14. The dose of S-1 was determined according to the patient's body surface area as follows: <1.25 m^2, 40 mg; 1.25–1.50 m^2, 50 mg; and >1.5 m^2, 60 mg. Combination chemotherapy was repeated every 3 weeks until progressive disease (PD) occurred.

In the phase I study, the starting dose of docetaxel was 45 mg/m^2 (level 1). Docetaxel dose escalation was performed as follows: in the patient cohorts containing at least 3 patients at each dose level, if none of the patients treated at a given dose level experienced dose limiting toxicity (DLT) as defined below, patients were entered at the next dose level (50 mg/m^2 at level 2, 60 mg/m^2 at level 3, and 70 mg/m^2 at level 4). If 1 or 2 of the 3 patients in the cohort experienced DLT, 3 additional patients were entered at the same level. MTD was then fixed and dose escalation was discontinued if all 3 patients in the 3-patient cohorts or ≥3 patients in the 6-patient cohorts experienced DLT. Adverse events were assessed in the first two cycles of the phase I study.

In the phase II study, the recommended dose of docetaxel determined in phase I was used in combination with S-1 in the same manner. The treatment regimen was repeated every 21 days until PD, patient withdrawal, or the occurrence of a serious adverse event. Granulocyte colony-stimulating factor (G-CSF) could be administered when either fever ≥38 °C with grade 3 or 4 neutropenia occurred. DLT was defined as: grade 4 neutropenia lasting for ≥4 days, grade 3 febrile neutropenia lasting ≥72 h, grade 3 thrombocytopenia, ≥grade 3 nonhematologic toxicity (besides nausea, vomiting, fatigue, and alopecia), ≥grade 2 interstitial pneumonia, or interruption of the S-1 medication for ≥7 days. If a patient experienced DLT, the docetaxel dose was reduced by one level in the subsequent cycle. To receive a subsequent cycle of chemotherapy, patients had to have leukocyte counts ≥3000/mm^3, neutrophil counts ≥1500/mm^3, platelets ≥100,000/mm^3, serum creatinine <1.5 mg/dL, and reduction in any treatment-related nonhematologic toxicity to <grade 1 (besides alopecia and neuropathy).

2.3. Toxicity and Response Evaluation

Toxicity was evaluated according to the Common Terminology Criteria for Adverse Events, version 3.0. Patients' symptoms and general condition were observed periodically. Physical examinations, complete blood counts with differential counts, serum chemistry, and urine tests were carried out at least once per week during the DLT-evaluation period. Tumor response was evaluated according to RECIST version 1.0 every month until the final tumor response was determined. Progression-free survival (PFS) was defined as the time from the date of registration to the date of the first documentation of PD or death. Patients with PFS were censored at the last date when survival was verified. Overall survival (OS) was defined as the time from the date of registration to the date of death. Surviving patients were censored at the last confirmation date of survival. This phase I/II study was conducted in accordance with the Declaration of Helsinki and approved by the Institutional Review Board at each participating hospital. The study was monitored by an independent data and safety monitoring committee.

2.4. Statistical Considerations

The primary end point of the phase II study was the rate of response to combination chemotherapy. The study was powered to detect a significant improvement of 18% relative to the 5% estimated from previous studies [1,3]. Assuming a one-sided a = 0.05% and 80% power, sample size was calculated to be 39 patients, with 6 patients at the recommended dose level in the phase I study. PFS and OS were assessed by the Kaplan-Meier method and log-rank test.

3. Results

3.1. Phase I Study

In total, 12 patients were enrolled in the phase I study. None of the three patients in the cohort at level 1 developed DLT. When the docetaxel dose was elevated to level 2, one patient experienced DLT, a grade 3 nonhematologic toxicity. The patient had phenytoin intoxication, which might be due to impairment of the P450 metabolic pathway by S-1. Because the remaining three patients in the cohort at level 2 had no DLT, their docetaxel dose was elevated. At level 3, two patients had DLT, prolonged grade 3 myelosuppression, and grade 3 interstitial pneumonia. The safety committee emphasized the risk of interstitial pneumonia and recommended the termination of the phase I study at level 3. As a result, the MTD and recommended docetaxel dose were 60 mg/m^2 and 50 mg/m^2, respectively.

3.2. Patient Characteristics in Phase II Study

A total of 39 patients (31 men, 8 women; median patient age, 64 years; age range, 46 to 75 years) were enrolled in the phase II study. Patient characteristics are shown in Table 1. The Eastern Cooperative Oncology Group (ECOG) performance status was 0 for 18 patients and 1 for 21 patients. Histologically, there were 24 patients with adenocarcinoma, 11 with squamous cell carcinoma, and 4 with no specified histology. Twenty-nine and 10 patients were at the clinical stages of IV and IIIb, respectively. A total of 120 cycles of therapy were administered. Treatment delay or interruption in the administration of S-1 occurred in 27 cycles (23%). The median number of cycles administered per patient was 3 (range, 1–9). The relative dose intensities were 97.7% for docetaxel and 85.7% for S-1.

Table 1. Characteristics of patients in the phase II study.

Characteristics	N = 39
Age, years	
Median (range)	64 (46–75)
Sex	
Men	31
Women	8
ECOG PS	
0	18
1	21
Stage	
IIIb	10
IV	29
Histology	
Adenocarcinoma	24
Squamous cell carcinoma	11
Not specified	4

ECOG PS: Eastern Cooperative Oncology Group performance status.

3.3. Toxicity

All 39 patients were included in the safety assessment. As shown in Table 2, myelosuppression was the principal toxic effect observed. However, the degree of myelosuppression was generally mild. Grade 3 or 4 leukocytopenia, neutropenia, thrombocytopenia, and anemia occurred in 17 (44%), 26 (67%), 0 (0%), and 0 (0%) patients, respectively. Nonhematologic toxicity was also generally mild and less frequent. Grade 3 or 4 toxicity primarily included loss of appetite (7.7%), fever (5.1%), and interstitial pneumonia (5.1%).

Table 2. Toxicities in the phase II study.

Toxicity	Grade		
	3	4	3 + 4
Hematologic			
Leukocytopenia	15 (38.5%)	2 (5.1%)	17 (43.6%)
Neutropenia	14 (35.9%)	12 (30.8%)	26 (66.7%)
Anemia	0 (0%)	0 (0%)	0 (0%)
Thrombocytopenia	0 (0%)	0 (0%)	0 (0%)
Nonhematologic			
Loss of appetite	3 (7.7%)	0 (0%)	3 (7.7%)
Fever	2 (5.1%)	0 (0%)	2 (5.1%)
Pneumonitis	1 (2.6%)	1 (2.6%)	2 (5.1%)
Stomatitis	1 (2.6%)	0 (0%)	1 (2.6%)
Diarrhea	1 (2.6%)	0 (0%)	1 (2.6%)
Hypercalcemia	1 (2.6%)	0 (0%)	1 (2.6%)
Elevation of γGTP	1 (2.6%)	0 (0%)	1 (2.6%)

3.4. Efficacy

Tumor response was evaluated in 39 patients. The median follow-up period was 8 months (range, 1–39 months). The following results were found for treatment response: complete response (CR), 0; partial response (PR), 3; stable disease (SD), 24; PD, 5; and not evaluable (NE), 7. The overall response rate was 3/39 or 7.7% (95% confidence interval (CI), 1.6 –20.9%, $p = 0.31$), a value that was not significantly higher than the threshold response rate statistically estimated from previous studies. The rate of disease control, CR + PR + SD, was 27/39 or 69%. Median PFS and OS were 18.0 weeks (95% CI, 11.3–22.9 weeks) and 53.0 weeks (95% CI, 40.9–134.6 weeks), respectively. The survival curves are shown in Figures 1 and 2.
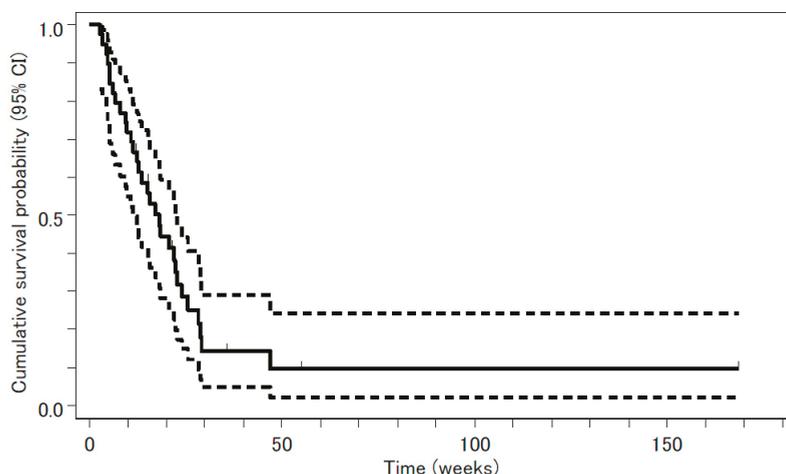
Figure 1. Progression-free survival (PFS) analyzed by the Kaplan-Meyer method is presented as a solid line. Median PFS was 18.0 weeks (95% confidence interval (CI), 11.3–22.9 weeks). The 95% CI is presented as two dashed lines.
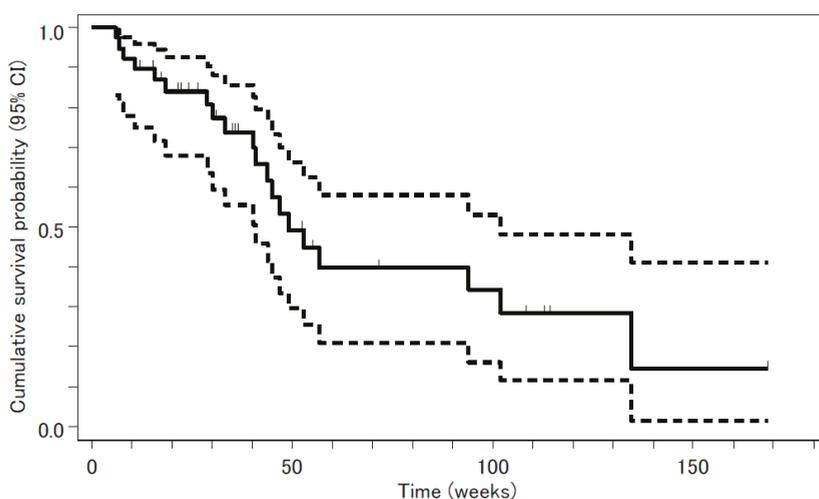
Figure 2. Overall survival (OS) analyzed by the Kaplan-Meyer method is presented as a solid line. Median OS was 53.0 weeks (95% confidence interval (CI), 40.9–134.6 weeks). The 95% CI is presented as two dashed lines.

4. Discussion

In the present study, response rate did not meet the 18% criterion needed to establish a significant improvement relative to the previously reported rate (i.e., the primary endpoint for the efficacy in the phase II study). However, combination chemotherapy was well tolerated and resulted in encouraging survival data.

Based on large-scale randomized controlled trials that compared 75 mg/m^2 docetaxel to optimal supportive care or other anticancer drugs, docetaxel monotherapy is considered to be a standard treatment for advanced non-small cell lung cancer in second-line settings [1,3]. Furthermore, S-1 was confirmed to be effective for previously treated advanced non-small cell lung cancer. Evidence for the efficacy of combination chemotherapy with docetaxel and S-1 has mainly been derived from studies on advanced gastric cancer. S-1 is one of the preferred agents for the treatment of gastric cancer. In fact, docetaxel displayed synergism with S-1 in vitro, improving the response rates in several phase II trials for advanced gastric cancer [7,9–11]. Wada et al. reported the decrease in expression of thymidylate synthase (TS) and dihydropyrimidine dehydrogenase (DPD) and an increase in expression of orotate phosphoribosyl transferase (OPRT) after co-treatment with docetaxel plus FU compared to 5-FU alone in gastric cancer cell lines [9]. DPD catalyzes the metabolic inactivation of 5-FU, while OPRT directly converts 5-FU to 5-fluorouridine-5′-monophosphate (FUMP), an active metabolite that displays anticancer effects. These changes in enzymes that metabolize 5-FU might clarify the enhanced effect of S-1 combined with docetaxel. As reported by Hasegawa et al., a similar synergistic effect is observed in castration-resistant prostate cancer [12]. Interestingly, in the xenograft model, S-1 with low-dose docetaxel could enhance the antitumor effect of S-1.

Several clinical trials have been conducted using docetaxel and S-1 for chemotherapy-naive or previously treated non-small cell lung cancer [9,13–17]. In fact, a triweekly schedule was employed with 40 mg/m^2 as the starting docetaxel dose. Previously, Oki et al. reported the usefulness of biweekly administration of docetaxel [16]. Table 3 contains a summary of results from these clinical studies. Other studies used a fixed docetaxel dose of 40 mg/m^2 + S-1 80 mg/m^2. The relatively low efficacy in these studies was perhaps due to the low fixed dose of chemotherapeutic agents. Therefore, we employed docetaxel dose escalation in the phase I part of the study, and confirmed that 50 mg/m^2 of docetaxel was effective. Moreover, S-1 dosage was determined depending on body surface area (BSA)

in each patient in this study, because the fixed dose of S-1 may be too toxic for patients with smaller BSA or ineffective for the patients with larger BSA. Although the response rate in the current study was relatively low compared to that in other studies, the disease control rate was better than those of other studies (69% in this study, 68.9% in Atagi et al., 61% in Segawa et al., 84% in Yanagihara et al., and 49% in Oki et al.) and favorable PFS and OS were obtained. In addition, the PFS was longer than that reported in a previous phase III study [18] where treatment efficacy was compared between docetaxel and gefitinib for previously treated patients with non-small cell lung cancer in Japan; the PFS in the arm treated with docetaxel was 2.0 months. For toxicity, we found that ≥grade 3 myelosuppression was more frequent in our study and may be due to the higher docetaxel dose employed relative to other studies. Nonetheless, nonhematologic toxicity was demonstrated to be mild, and 50 mg/m^2 docetaxel plus S-1 was generally well tolerated.

Table 3. Summary of the results from previous trials of docetaxel plus S-1.

	Author			
	Atagi et al. [12]	**Yanagihara et al. [14]**	**Segawa et al. [13]**	**Oki et al. [15]**
N	29	28	31	49
Docetaxel	40 mg/m^2, day 1 every 3 weeks	40 mg/m^2, day 1 every 3 weeks	40 mg/m^2, day 1 every 3 weeks	35 mg/m^2, day 1, 15 every 4 weeks
S-1	80 mg/m^2, days 1–14	80 mg/m^2, days 1–14	80 mg/m^2, days 1–15	80 mg/m^2, days 1–14
ORR	24.1%	18.4%	16.1%	16.3%
PFS (mo)	3.9	4.4	3.4	3
OS (mo)	11.8	16.1	8.7	9

ORR: overall response rate; OS: overall survival; PFS: progression-free survival.

Takeda et al. reported that in advanced non-small cell lung cancer, the expression of TS and DPD are associated with the response to S-1 and carboplatin [19]. At a low level, their expression was found to be associated with a better response and a longer survival in patients treated with S-1 and carboplatin. Altogether, the expression levels of TS and DPD may be predictive markers for the response to regimens containing S-1. Histologically, squamous cell carcinoma and high-grade carcinoma display higher expression levels for the TS protein and mRNA in non-small cell lung cancer [20,21]. Therefore, a selected patient population with lower expression levels of TS may be most suitable for treatment regimens containing TS-inhibiting agents such as the combination of docetaxel and S-1. We have a plan to conduct a study considering this in the future.

References

1. Shepherd, F.A.; Dancey, J.; Ramlau, R.; Mattson, K.; Gralla, R.; O'Rourke, M.; Levitan, N.; Gressot, L.; Vincent, M.; Burkes, R.; et al. Prospective randomized trial of docetaxel versus best supportive care in patients with non-small cell lung cancer previously treated with platinum-based chemotherapy. *J. Clin. Oncol.* **2000**, *18*, 2095–2103. [CrossRef] [PubMed]
2. Ringel, I.; Horwitz, S.B. Studies with RP 56976 (taxotere): A semisynthetic analogue of taxol. *J. Natl. Cancer Inst.* **1991**, *83*, 288–291. [CrossRef]
3. Fossella, F.V.; DeVore, R.; Kerr, R.N.; Crawford, J.; Natale, R.R.; Dunphy, F.; Kalman, L.; Miller, V.; Lee, J.S.; Moore, M.; et al. Randomized phase III trial of docetaxel versus vinorelbine or ifosfamide in patients with advanced non-small cell lung cancer previously treated with platinum-containing chemotherapy regimens. *J. Clin. Oncol.* **2000**, *18*, 2354–2362. [CrossRef] [PubMed]
4. Kubota, K.; Watanabe, K.; Kunitoh, H.; Noda, K.; Ichinose, Y.; Katakami, N.; Sugiura, T.; Kawahara, M.; Yokoyama, A.; Yokota, S.; et al. Phase III randomized trial of docetaxel plus cisplatin versus vindesine plus cisplatin in patients with stage IV non-small cell lung cancer: The Japanese Taxotere Lung Cancer Study Group. *J. Clin. Oncol.* **2004**, *22*, 254–261. [CrossRef] [PubMed]
5. Fossella, F.V.; Rigas, J. The use of docetaxel (Taxotere) in patients with advanced non-small cell lung cancer previously treated with platinum-containing chemothepy regimens. *Semin. Oncol.* **1999**, *26*, 9–12. [PubMed]
6. Kawahara, M.; Furuse, K.; Segawa, Y.; Yoshimori, K.; Matsui, K.; Kudoh, S.; Hasegawa, K.; Niitani, H.; S-1 Cooperative Study Group (Lung Cancer Working Group). Phase II study of S-1, a novel oral fluorouracil, in advanced non-small-cell lung cancer. *Br. J. Cancer* **2001**, *85*, 939–943. [CrossRef] [PubMed]
7. Yoshida, K.; Ninomiya, N.; Takakura, N.; Hirabayashi, N.; Takiyama, W.; Sato, Y.; Todo, S.; Terashima, M.; Gotoh, M.; Sakamoto, J.; et al. Phase II study of docetaxel and S-1 combination therapy for advanced or recurrent gastric cancer. *Clin. Cancer Res.* **2006**, *12*, 3402–3407. [CrossRef]
8. Kano, Y.; Akutsu, M.; Tsunoda, S.; Ando, J.; Matsui, J.; Suzuki, K.; Ikeda, T.; Inoue, Y.; Adachi, K. Schedule-dependent interaction between paclitaxel and 5-fluorouracil in human carcinoma cell lines in vitro. *Br. J. Cancer* **1996**, *74*, 704–710. [CrossRef]
9. Wada, Y.; Yoshida, K.; Suzuki, T.; Mizuiri, H.; Konishi, K.; Ukon, K.; Tanabe, K.; Sakata, Y.; Fukushima, M. Synergistic effects of docetaxel and S-1 by modulating the expression of metabolic enzymes of 5-fluorouracil in human gastric cancer cell lines. *Int. J. Cancer* **2006**, *119*, 783–791. [CrossRef]
10. Yamaguchi, K.; Shimamura, T.; Hyodo, I.; Koizumi, W.; Doi, T.; Narahara, H.; Komatsu, Y.; Kato, T.; Saitoh, S.; Akiya, T.; et al. Phase I/II study of docetaxel and S-1 in patients with advanced gastric cancer. *Br. J. Cancer* **2006**, *94*, 1803–1808. [CrossRef]
11. Park, S.R.; Kim, H.K.; Kim, C.G.; Choi, I.J.; Lee, J.S.; Lee, J.H.; Ryu, K.W.; Kim, Y.W.; Bae, J.M.; Kim, N.K. Phase I/II study of S-1 combined with weekly docetaxel in patients with metastatic gastric carcinoma. *Br. J. Cancer* **2008**, *98*, 1305–1311. [CrossRef] [PubMed]
12. Hasegawa, M.; Miyajima, A.; Kosaka, T.; Yasumizu, Y.; Tanaka, N.; Maeda, T.; Shirotake, S.; Ide, H.; Kikuchi, E.; Oya, M. Low-dose docetaxel enhances the sensitivity of S-1 in a xenograft model of human castration resistant prostate cancer. *Int. J. Cancer* **2012**, *130*, 431–442. [CrossRef] [PubMed]
13. Atagi, S.; Kawahara, M.; Kusunoki, Y.; Takada, M.; Kawaguchi, T.; Okishio, K.; Kubo, A.; Uehira, K.; Yumine, K.; Tomizawa, Y.; et al. Phase I/II study of docetaxel and S-1 in patients with previously treated non-small cell lung cancer. *J. Thorac. Oncol.* **2008**, *3*, 1012–1017. [CrossRef] [PubMed]
14. Segawa, Y.; Kiura, K.; Hotta, K.; Takigawa, N.; Tabata, M.; Matsuo, K.; Yoshioka, H.; Hayashi, H.; Kawai, H.; Aoe, K.; et al. A randomized phase II study of a combination of docetaxel and S-1 versus docetaxel monotherapy in patients with non-small cell lung cancer previously treated with platinum-based chemotherapy. *J. Thorac. Oncol.* **2010**, *5*, 1430–1434. [CrossRef] [PubMed]
15. Yanagihara, K.; Yoshimura, K.; Niimi, M.; Yasuda, H.; Sasaki, T.; Nishimura, T.; Ishiguro, H.; Matsumoto, S.; Kitano, T.; Kanai, M.; et al. Phase II study of S-1 and docetaxel for previously treated patients with locally advanced or metastatic non-small cell lung cancer. *Cancer Chemother. Pharmacol.* **2010**, *66*, 913–918. [CrossRef]
16. Oki, Y.; Hirose, T.; Yamaoka, T.; Kusumoto, S.; Shirai, T.; Sugiyama, T.; Okuda, K.; Nakashima, M.; Murata, Y.; Ohmori, T.; et al. Phase II study of S-1, a novel oral fluoropyrimidine, and biweekly administration of docetaxel for previously treated advanced non-small-cell lung cancer. *Cancer Chemother. Pharmacol.* **2011**, *67*, 791–797. [CrossRef]

17.   Takiguchi, Y.; Tada, Y.; Gemma, A.; Kudoh, S.; Hino, M.; Yoshimori, K.; Yoshimura, A.; Nagao, K.; Niitani, H. Phase I/II study of docetaxel and S-1, an oral fluorinated pyrimidine, for untreated advanced non-small cell lung cancer. *Lung Cancer* **2010**, *68*, 409–414. [CrossRef]

18.   Maruyama, R.; Nishiwaki, Y.; Tamura, T.; Yamamoto, N.; Tsuboi, M.; Nakagawa, K.; Shinkai, T.; Negoro, S.; Imamura, F.; Eguchi, K.; et al. Phase III study, V-15-32, of gefitinib versus docetaxel in previously treated Japanese patients with non-small cell lung cancer. *J. Clin. Oncol.* **2008**, *26*, 4244–4252. [CrossRef]

19.   Takeda, M.; Okamoto, I.; Hirabayashi, N.; Kitano, M.; Nakagawa, K. Thymidiylate synthase and dihydropyrimidine dehydrogenase expression levels are associated with response to S-1 plus carboplatin in advanced non-small cell lung cancer. *Lung Cancer* **2011**, *73*, 103–109. [CrossRef]

20.   Ceppi, P.; Volante, M.; Saviozzi, S.; Rapa, I.; Novello, S.; Cambieri, A.; Lacono, M.L.; Cappia, S.; Papotti, M.; Scagliotti, G.V. Squamous cell carcinoma of the lung compared with other histotypes shows higher messenger RNA and protein levels for thymidylate synthase. *Cancer* **2006**, *107*, 1589–1596. [CrossRef]

21.   Chen, C.Y.; Chang, Y.L.; Shih, J.Y.; Lin, J.W.; Chen, K.Y.; Yang, C.H.; Yu, C.J.; Yang, P.C. Thymidylate synthase and dihydrofolate reductase expression in non-small cell lung carcinoma: The association with treatment efficacy of pemetrexed. *Lung Cancer* **2011**, *74*, 132–138. [CrossRef] [PubMed]

Review

Role of Surgical Intervention in Unresectable Non-Small Cell Lung Cancer

Shigeki Suzuki [1] and Taichiro Goto [2],*

[1] General Thoracic Surgery, Sagamihara Kyodo Hospital, Kanagawa 252-5188, Japan;
shigeki.suzuki@sagamiharahp.com
[2] Lung Cancer and Respiratory Disease Center, Yamanashi Central Hospital, Kofu 400-8506, Japan
* Correspondence: taichiro@1997.jukuin.keio.ac.jp; Tel.: +81-55-253-7111

Abstract: With the development of systemic treatments with high response rates, including tyrosine kinase inhibitors and immune checkpoint inhibitors, some patients with unresectable lung cancer now have a chance to undergo radical resection after primary treatment. Although there is no general consensus regarding the definition of "unresectable" in lung cancer, the term "resectable" refers to technically resectable and indicates that resection can provide a favorable prognosis to some extent. Unresectable lung cancer is typically represented by stage III and IV disease. Stage III lung cancer is a heterogeneous disease, and in some patients with technically resectable non-small cell lung cancer (NSCLC), multimodality treatments, including induction chemoradiotherapy followed by surgery, are the treatments of choice. The representative surgical intervention for unresectable stage III/IV NSCLC is salvage surgery, which refers to surgical treatment for local residual/recurrent lesions after definitive non-surgical treatment. Surgical intervention is also used for an oligometastatic stage IV NSCLC. In this review, we highlight the role of surgical intervention in patients with unresectable NSCLC, for whom an initial complete resection is technically difficult. We further describe the history of and new findings on salvage surgery for unresectable NSCLC and surgery for oligometastatic NSCLC.

Keywords: non-small cell lung cancer; immunotherapy; unresectable; salvage surgery; oligometastasis; targeted therapy

1. Introduction

Treatment of patients with lung cancer depends on the histology, tumor stage, molecular characteristics, and assessment of a patient's overall medical condition. Currently, various guidelines for lung cancer treatment, including those from the American Society of Clinical Oncology, European Society of Medical Oncology, National Comprehensive Cancer Network (NCCN), and The Japan Lung Cancer Society, have been used [1,2]. Patients with stage I-II non-small cell lung cancer (NSCLC) are generally treated with curative-intent surgery if they are operable. Patients with stage III NSCLC are generally treated with a multimodality approach, including surgery, chemotherapy, and radiation therapy (RT). Those with stage IV or recurrent NSCLC are treated with systemic drug therapies, including chemotherapy, tyrosine kinase inhibitors (TKIs), and immune checkpoint inhibitors (ICIs). Molecular-targeted therapies such as TKI are selected if the epidermal growth factor receptor (*EGFR)* gene is mutated, while an ICI and/or cytotoxic chemotherapy is selected if this gene is not mutated.

In general, surgical treatment is selected for tumors that can be completely resected, whereas RT or drug therapy is offered for patients whose tumors cannot be completely resected or who cannot tolerate surgery. In practice, the term "resectable" not only applies to technically resectable, which is "resectable" in a narrow sense, but also refers to cases when resection can be expected to have a favorable prognosis to some extent, which is "resectable" in a broad sense. Although "unresectable" is

defined as "unable to be removed using surgery" in the National Cancer Institute dictionary, there is no general consensus regarding the definition of "unresectable" in lung cancer.

Unresectable lung cancer is considered to be represented by stage III and IV disease. Unresectable factors in stage III lung cancer are direct invasion to unresectable organs (T4) or mediastinal/extrathoracic lymph node metastasis (N2/N3). An unresectable feature of stage IV lung cancer is distant metastasis (M1). Regarding mediastinal lymph node metastasis, the 2013 American College of Chest Physicians (ACCP) guidelines defined N2 nodes that have extranodal progression and an invasive nature as infiltrative nodes, while other nodes were defined as discrete nodes. Discrete nodes were considered to likely benefit from surgical therapy [3]. In general, bulky/multi-station/infiltrative nodes are regarded as unresectable, while T4 tumors are tumors sized >7 cm or those invading the mediastinum/heart/diaphragm/carina/trachea/great vessels/recurrent nerve/esophagus/spine, or separate tumor nodule(s) in a different ipsilateral lobe. In patients with unresectable stage III lung cancer, the current standard treatment is concurrent chemoradiotherapy (CRT) [4,5], which provides a median overall survival (OS) of 22–25 months and a 5-year OS of 20% [6]. In this review, we describe the role of surgical intervention in patients with NSCLCs for whom complete resection is technically difficult ("unresectable" in the narrow sense).

2. Role of Surgical Intervention in Unresectable Lung Cancer

Stage III lung cancer is a heterogeneous disease, and in some patients with technically resectable NSCLC, including some with cT4/cN2 NSCLC, multimodality treatments, including induction CRT followed by surgery, are a treatment of choice [7]. In practice, induction therapy is used for patients with lung cancer in whom radical resection is difficult at the time of diagnosis but may be expected later owing to therapeutic intervention. The representative surgical intervention for unresectable lung cancer is salvage surgery [8,9]. Although the term "salvage (or "rescue") surgery" is not clearly defined, it refers to surgical treatment for local residual/recurrent lesions after definitive non-surgical treatment. As a type of surgical intervention for unresectable stage III lung cancer, we describe salvage surgery after definitive CRT or RT.

Although the standard treatment for stage IV lung cancer is drug therapy, there is another choice of treatment for patients with an oligometastatic state. In this state, local therapy for metastatic lesions results in favorable prognosis that is comparable with that in non-metastatic disease. The concept that patients with only a limited number of metastases from a malignant tumor can potentially be cured was developed in 1995 and was termed "oligometastasis," which describes an intermediate stage between localized and metastasized cancer [10,11]. There is currently no consensus regarding the definition of oligometastatic disease; however, most clinical trial protocols and clinicians accept a definition of 1–3 or 1–5 metastatic lesions [12,13]. Furthermore, in rare cases when definitive systemic therapy is successful, an opportunity for radical resection as salvage surgery is achieved even for stage IV lung cancer [14]. Thus, there are two situations for surgical intervention for stage IV NSCLC: surgery for oligometastatic cases and salvage surgery after definitive systemic therapy (especially, TKI or ICI). The role of surgical intervention for unresectable lung cancer is summarized in Figure 1.
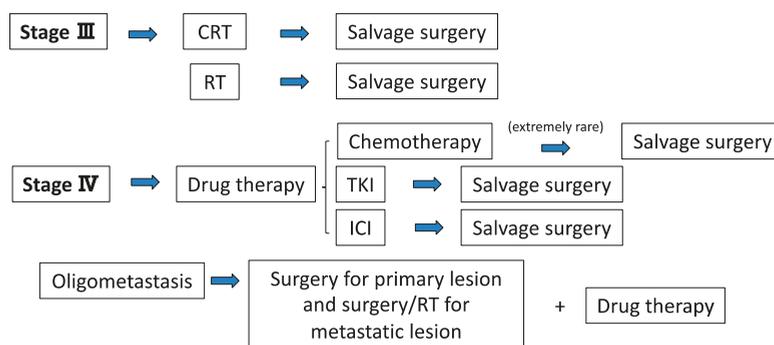
Figure 1. Current treatment strategies with surgery for unresectable stage III/IV NSCLC. CRT: chemoradiotherapy, ICI: immune-checkpoint inhibitor, NSCLC: non-small cell lung cancer, RT: radiotherapy, TKI: tyrosine kinase inhibitor.

3. Salvage Surgery for Stage III NSCLC

3.1. Salvage Surgery after Definitive CRT

The incidence of local recurrence after definitive CRT in patients with stage III NSCLC was 24–35% [15], and the survival rates after CRT were as low as 5–25% [16]. In 2019, Grass et al. showed a high relapse rate after CRT (64%) [17]. Salvage surgery for residual/recurrent tumors is almost the only treatment that can provide a cure. Compared with upfront surgery, salvage surgery after definitive CRT has greater surgical difficulty and a greater possibility of perioperative complications because a high dose of RT strongly affects the target tissue, resulting in more tissue changes [8,9].

To date, there have been limited reports of salvage surgery after definitive CRT for primary lung cancer. Dickhoff et al. reported a systematic review of the literature concerning salvage surgery after definitive CRT for locally advanced NSCLC in 2018 [18]. They reviewed eight papers including 158 patients. For patients undergoing resection ($n = 152$), a total of 44 pneumonectomies, 11 bilobectomies, 89 lobectomies, 6 segmentectomies, and 3 wedge resections were performed. Complete resection was achieved in 85–100%, with vital tumors in 61–100%. Where reported, the 90-day mortality rate was 0–11.4%. The reported survival metrics varied but included a median survival time (MST) 9–46 months and a 5-year OS rate of 20–75%. Recently, Romero et al. reported about 27 patients who underwent surgical resection after CRT. Complications were observed in 5 (18.5%) patients. The 3-and 5-year OS rates were 57.8% and 53.3%, respectively [19]. Furthermore, Kobayashi et al. reported 23 cases that underwent salvage surgery after CRT in a single center, with no perioperative death, a 5-year recurrence-free survival rate of 17.3%, and a 5-year OS rate of 41.9% [20]. Based on this evidence regarding salvage surgery after CRT, perioperative mortality appears to be acceptable, and long-term survival is possible in selected patients.

3.2. Salvage Surgery after Definitive Radiotherapy

Radiation monotherapy is indicated for patients with stage III NSCLC who are unsuitable for CRT. Stereotactic body radiotherapy (SBRT) is a good indication, especially for local lesions such as stage I NSCLC. Salvage surgery after definitive radiotherapy is more localized than definitive CRT. Since there is minimal effect on normal tissues, especially in SBRT and heavy-ion radiotherapy, the incidence of complications is expected to be low. In 2018, Dickhoff et al. performed a systematic review of salvage surgery after local recurrence of NSCLC after SBRT (7 case series with a total of 47 patients) [21]. The 5-year local recurrence rate after SBRT was approximately 10% and surgery was performed as salvage surgery in selected patients. The morbidity rate was 29–50%, and the 90-day mortality rate was 0–11%. MST ranged between 13.6 and 82.7 months. In addition, 12 patients who underwent salvage

surgery after heavy-ion radiotherapy were reported by Mizobuchi et al. in 2015 [22]. There were no serious complications in any of the cases, and the 3-year survival rate after surgery was 82%. Although there is only limited evidence regarding salvage surgery after radiotherapy for locally relapsed NSCLC, this treatment can be considered feasible and can provide acceptable morbidity and mortality rates for selected patients.

3.3. Salvage Surgery after Combination Therapy with CRT and Immunotherapy

In the phase III PACIFIC study, eligible patients received durvalumab after CRT, and this combination therapy significantly prolonged progression-free survival (PFS) compared with that in the placebo group (16.8 months versus 5.6 months) [23].

Regarding the addition of surgery to this combination therapy, the significance of surgical intervention after CRT followed by ICI remains unclear. Recently, a clinical trial (JCOG1807C) was initiated to clarify the safety and efficacy of multimodality treatment of pre- and postoperative durvalumab therapy after preoperative CRT for resectable superior sulcus tumor (SST) and durvalumab maintenance therapy after CRT for unresectable SST. In this study, eligible patients were assigned to two groups: concurrent CRT (cisplatin+S-1+radiotherapy 66 Gy) + two courses of durvalumab followed by surgery and adjuvant durvalumab for resectable SST and CRT followed by maintenance durvalumab for unresectable SST. The primary end-point is 3-year OS. We await the results of this trial.

4. Surgical Intervention for Stage IV Lung Cancer

4.1. Surgical Intervention for Patients with Oligometastatic NSCLC

Considering the indications for surgical intervention in oligometastatic NSCLC cases, brain and adrenal metastases as oligometastatic organs have been reported to have a relatively good prognosis with 5-year OS rates of 20% and 20–30% [24]. The ACCP guidelines state that in cases of single brain metastasis and adrenal metastasis, cN0–1 is indicated for local treatment of metastatic lesions and resection of the primary lesion [3]. In addition, the NCCN guidelines recommend local treatment for metastatic lesions and multidisciplinary treatments, including systemic treatment, for primary lesions in cases of single brain metastases [1]. There are two strategies including surgery for treating oligometastasis: (1) resection of the primary tumor in advance and then control of distant tumors using surgery/RT and micrometastasis with drug therapy, and (2) addition of local treatment (surgery/RT) for patients with residual tumors that responded to drug therapy and became localized; i.e., a salvage approach.

The efficacy of upfront resection of a primary lesion of oligometastatic NSCLC was reported by Wang et al. in 2018. They conducted a retrospective study of patients with oligometastatic NSCLC, and 172 patients were divided into two groups: group A underwent primary surgical treatment and adjuvant chemotherapy, while group B was treated with systematic chemotherapy and local RT. The MSTs in groups A and B were 48 months and 18 months, respectively, and the 5-year survival rates were 21.1% and 7.6%, respectively ($p < 0.05$). They concluded that the local surgical treatment of primary lesions of NSCLC significantly increased OS and the 5-year survival rates of patients with oligometastatic NSCLC [25].

Gomez et al. reported the efficacy of a salvage approach (the addition of local treatment after definitive drug therapy) for oligometastatic NSCLC in their phase II RCT. First-line therapy was four or more cycles of platinum doublet therapy or 3 or more months of EGFR or anaplastic lymphoma kinase (ALK) inhibitors. The locations of oligometastases were as follows: 13 brain, 10 bone, 8 adrenal gland, 7 pleura, 6 lung, 4 cervical lymph node, 2 liver, 2 spleen, 1 retroperitoneal lymph node, 1 paraspinal mass, and 1 kidney. After receiving first-line therapy, patients were randomly assigned to either a local consolidative therapy group (RT and/or surgery) or a maintenance treatment group. This study was terminated early after randomization of 49 patients. Among patients administered local consolidative therapies, 96% underwent some form of RT. The median PFS in the local consolidative therapy group

was 11.9 months versus 3.9 months in the maintenance treatment group (hazard ratio 0.35, *p* = 0.0054). Furthermore, no grade 4 or 5 toxicities were reported. They suggested that the addition of local therapy after first-line therapy might improve PFS of patients with oligometastatic NSCLC [26].

With regard to the optimal modality of local treatment for oligometastatic NSCLC, to date, no RCTs have compared SBRT and surgery. Otake and Goto reviewed salvage SBRT for oligometastatic NSCLC and concluded that SBRT appeared to provide a high level of local control with minimal associated toxicity [27]. Although surgery is a powerful local treatment, pre-treatment and/or post-treatment as a combined-modality approach is often required for oligometastatic NSCLC. It is necessary to carefully select surgery or RT as local treatment, considering the patient's ability to tolerate total therapies.

4.2. Salvage Surgery after Definitive Systemic Therapy

4.2.1. Salvage Surgery after Treatment with TKIs

For patients with stage IV NSCLC, chemotherapy resulted in only approximately a 7% improvement in 1-year survival compared with survival with best supportive care [28]. Compared with chemotherapy, EGFR-TKI administration results in a high response rate in patients with *EGFR* mutation-positive lung cancer; in particular, osimertinib has a response rate of 80% [29]. Among patients in whom TKI has a dramatic effect, salvage surgery for local residual/recurrent lesions is a possible treatment strategy.

Hishida et al. reported nine patients with stage IV NSCLC who underwent tumor resection after gefitinib administration. Surgery was performed for local tumor persistence, recurrence, or re-growth after treatment with gefitinib (duration of administration, 2–36 months), and the median OS after resection was 32 months. The median recurrence-free period was reported to be 6 months [30]. In another study, Hishida et al. reported the long-term outcome of 4 patients who underwent pulmonary resection for residual/regrown primary lesion of NSCLC treated with gefitinib. Recurrence was observed in three of four cases; however, all of them survived for 5 years or more after surgery. The remaining case continued to receive TKI administration for 4 years after surgery without cancer relapse [31]. Based on these reports, although no large-scale data are available, it is quite possible that salvage surgery after EGFR-TKI can be expected to have local control effects. A similar significance of salvage surgery has been reported in a case report on the use of ALK inhibitors for NSCLC with *ALK* gene translocations [32].

Recently, the effectiveness of osimertinib as a postoperative adjuvant therapy for resectable *EGFR* mutation-positive NSCLC was reported as the result of a phase III trial (ADAURA Clinical Trials, NCT02511106) [33]. In that trial, disease-free survival was significantly longer among patients who were administered osimertinib than among those who received placebo (90% versus 44%). It was unclear whether TKI should be continued after salvage surgery following treatment using TKI. However, considering the result of the ADAURA trials, it is possible that the prognosis will be improved if TKI is continued even after complete resection by salvage surgery.

4.2.2. Salvage Surgery after Treatment with ICIs

Recently, the effectiveness of the PD-1 inhibitor pembrolizumab in patients with stage IV lung NSCLC was reported as the result of a phase III trial (KEYNOTE-407). The estimated 6-month OS rate was 80.2% with pembrolizumab administration. Moreover, the median PFS with pembrolizumab of 10.3 months (not reached) was superior to that with platinum doublet chemotherapy (6 months) [34].

Furthermore, ICI combined with chemotherapy for stage IV NSCLC was reported to significantly improve OS and PFS compared with chemotherapy alone as reported in phase III trials (KEYNOTE-189 [35,36] and KEYNOTE-407 [37]). The median OS and PFS were 15.9–22 months and 6.4–8.8 months, respectively. These survival benefits were consistent regardless of the level of programmed death-ligand 1 expression. Based on this evidence, ICI or ICI combined with chemotherapy is recommended as standard therapy for stage IV NSCLC without a driver mutation.

Although there have been few reports concerning salvage surgery after ICI, Bott retrospectively examined 19 patients who underwent lung resection after ICI for metastatic or unresectable cancer, including lung cancer (47%) and metastatic melanoma (37%). Of patients who underwent resection, R0 resection was achieved in 95% and 68% of patients with viable tumor remaining. Complications occurred in 32% of patients. The 2-year OS was 77% [38]. In NSCLC, the frequency of salvage surgery has been increasing in recent years, and with the spread of ICI, salvage surgery after ICI may increase in the future. Salvage surgery after ICI is possibly a feasible and effective treatment; however, to date, it has only been described in one case report [39]. It is necessary to accumulate further evidence regarding salvage surgery after ICI.

Although there is no evidence that salvage surgery after definitive therapy confers a survival benefit compared with other non-surgical radical therapy, here, we show selected studies regarding current standard first-line therapy for stage III/IV NSCLC and limited reports on salvage surgery (Table 1).

Table 1. Selected studies on salvage surgery and first-line therapy for stage III/IV NSCLC.

Stage	Modality	OS (%), MST (m)	mPFS (m)	RR (%)	Ref.
Stage III	CRT only	5-y OS: 5–25, 26	-	-	[6,15]
	CRT → ICI	3-y OS: 66.3, 38.4	16.8	28.4	[22]
	CRT → SS	5-y OS: 20–75, 9–46	-	-	[18]
	RT → SS	N.A., 13.6–82.7	-	-	[21]
Stage IV	EGFR-TKI only(osimertinib)	1.5-y OS: 83, N.A.	8.9	80	[28]
	ICI only(pembrolizumab)	0.5-y OS: 80.2, 14–19.2	10.3	44.8	[33]
	ICI + CT	2-y OS: 45.7, 15.9–22	6.4–9	48	[34–36]
	EGFR-TKI → SS	3-y OS: 50, 32	-	-	[29]
	ICI → SS	2-y OS: 77, N.A.	-	-	[37]
(Oligometastasis)	CT + RT (all lesions)	5-y OS: 7.6, 18	-	-	[24]
	Surgery (all lesions) → CT	5-y OS: 21.1, 48	-	-	

CRT: chemoradiotherapy, CT: chemotherapy, EGFR-TKI: epidermal growth factor receptor-tyrosine kinases inhibitor, ICI: immune-checkpoint inhibitor, mPFS: median progression-free survival, MST: median survival time, N.A.: not available, NSCLC: non-small cell lung cancer, OS: overall survival, Ref.: reference, RR: response rate, RT: radiotherapy, SS: salvage surgery, y: year.

5. Future Perspectives

Several clinical questions, such as whether surgery or RT is better as a local salvage treatment after definitive systemic therapy or as the first-line local treatment for oligometastatic NSCLC, remain unanswered. The significance of surgical intervention after CRT followed by ICI treatment is also unknown. The use of adjuvant therapy was not described in this review; furthermore, the chronological time of TKI/ICI addition to surgery remains yet to be demonstrated (adjuvant or neoadjuvant). In addition, it is possible that the definition of "unresectable" may change, and R1/R2 resection or even volume reduction may turn out significant in the future. Prospective and comparative trials need to be performed to clarify these issues in the future.

6. Conclusions

This review covered the role of surgical intervention for unresectable NSCLC. Although many problems still need to be solved, while systemic treatments with high response rates such as TKI and/or ICI are being developed further, the importance of surgical treatment is expected to expand.

References

1. Bironzo, P.; Di Maio, M. A review of guidelines for lung cancer. *J. Thorac. Dis.* **2018**, *10* (Suppl. 13), 1556–1563. [CrossRef]

2. Postmus, P.E.; Kerr, K.M.; Oudkerk, M.; Senan, S.; Waller, D.A.; Vansteenkiste, J.; Escriu, C.; Peters, S.; Committee, E.G. Early and locally advanced non-small-cell lung cancer (NSCLC): ESMO Clinical Practice Guidelines for diagnosis, treatment and follow-up. *Ann. Oncol. Off. J. Eur. Soc. Med. Oncol.* **2017**, *28* (Suppl. 4), iv1–iv21. [CrossRef]

3. Silvestri, G.A.; Gonzalez, A.V.; Jantz, M.A.; Margolis, M.L.; Gould, M.K.; Tanoue, L.T.; Harris, L.J.; Detterbeck, F.C. Methods for staging non-small cell lung cancer: Diagnosis and management of lung cancer, 3rd ed: American College of Chest Physicians evidence-based clinical practice guidelines. *Chest* **2013**, *143* (Suppl. 5), e211S–e250S. [CrossRef] [PubMed]

4. Furuse, K.; Fukuoka, M.; Kawahara, M.; Nishikawa, H.; Takada, Y.; Kudoh, S.; Katagami, N.; Ariyoshi, Y. Phase III study of concurrent versus sequential thoracic radiotherapy in combination with mitomycin, vindesine, and cisplatin in unresectable stage III non-small-cell lung cancer. *J. Clin. Oncol. Off. J. Am. Soc. Clin. Oncol.* **1999**, *17*, 2692–2699. [CrossRef] [PubMed]

5. Jeremic, B.; Shibamoto, Y.; Acimovic, L.; Milisavljevic, S. Hyperfractionated radiation therapy with or without concurrent low-dose daily carboplatin/etoposide for stage III non-small-cell lung cancer: A randomized study. *J. Clin. Oncol. Off. J. Am. Soc. Clin. Oncol.* **1996**, *14*, 1065–1070. [CrossRef] [PubMed]

6. Hanna, N.; Neubauer, M.; Yiannoutsos, C.; McGarry, R.; Arseneau, J.; Ansari, R.; Reynolds, C.; Govindan, R.; Melnyk, A.; Fisher, W.; et al. Phase III study of cisplatin, etoposide, and concurrent chest radiation with or without consolidation docetaxel in patients with inoperable stage III non-small-cell lung cancer: The Hoosier Oncology Group and U.S. Oncology. *J. Clin. Oncol. Off. J. Am. Soc. Clin. Oncol.* **2008**, *26*, 5755–5760. [CrossRef] [PubMed]

7. Hung, M.S.; Wu, Y.F.; Chen, Y.C. Efficacy of chemoradiotherapy versus radiation alone in patients with inoperable locally advanced non-small-cell lung cancer: A meta-analysis and systematic review. *Med. Baltim.* **2019**, *98*, e16167. [CrossRef]

8. Dickhoff, C.; Dahele, M.; Paul, M.A.; van de Ven, P.M.; de Langen, A.J.; Senan, S.; Smit, E.F.; Hartemink, K.J. Salvage surgery for locoregional recurrence or persistent tumor after high dose chemoradiotherapy for locally advanced non-small cell lung cancer. *Lung Cancer* **2016**, *94*, 108–113. [CrossRef]

9. Sonobe, M.; Yutaka, Y.; Nakajima, D.; Hamaji, M.; Menju, T.; Ohsumi, A.; Chen-Yoshikawa, T.F.; Sato, T.; Date, H. Salvage Surgery After Chemotherapy or Chemoradiotherapy for Initially Unresectable Lung Carcinoma. *Ann. Thorac. Surg.* **2019**, *108*, 1664–1670. [CrossRef]

10. Hellman, S.; Weichselbaum, R.R. Oligometastases. *J. Clin. Oncol. Off. J. Am. Soc. Clin. Oncol.* **1995**, *13*, 8–10. [CrossRef]

11. Palma, D.A.; Louie, A.V.; Rodrigues, G.B. New Strategies in Stereotactic Radiotherapy for Oligometastases. *Clin. Cancer Res.* **2015**, *21*, 5198–5204. [CrossRef] [PubMed]

12. Palma, D.A.; Salama, J.K.; Lo, S.S.; Senan, S.; Treasure, T.; Govindan, R.; Weichselbaum, R. The oligometastatic state—separating truth from wishful thinking. *Nat. Rev. Clin. Oncol.* **2014**, *11*, 549–557. [CrossRef] [PubMed]

13. Levy, A.; Hendriks, L.E.L.; Berghmans, T.; Faivre-Finn, C.; GiajLevra, M.; GiajLevra, N.; Hasan, B.; Pochesci, A.; Girard, N.; Greillier, L.; et al. EORTC Lung Cancer Group survey on the definition of NSCLC synchronous oligometastatic disease. *Eur. J. Cancer* **2019**, *122*, 109–114. [CrossRef] [PubMed]

14. Uramoto, H. Current Topics on Salvage Thoracic Surgery in Patients with Primary Lung Cancer. *Ann. Thorac. Cardiovasc. Surg.* **2016**, *22*, 65–68. [CrossRef] [PubMed]

15. Edelman, M.J.; Gandara, D.R.; Roach, M., 3rd; Benfield, J.R. Multimodality therapy in stage III non-small cell lung cancer. *Ann. Thorac. Surg.* **1996**, *61*, 1564–1572. [CrossRef]

16. Albain, K.S.; Swann, R.S.; Rusch, V.W.; Turrisi, A.T., 3rd; Shepherd, F.A.; Smith, C.; Chen, Y.; Livingston, R.B.; Feins, R.H.; Gandara, D.R.; et al. Radiotherapy plus chemotherapy with or without surgical resection for stage III non-small-cell lung cancer: A phase III randomised controlled trial. *Lancet* **2009**, *374*, 379–386. [CrossRef]

17. Grass, G.D.; Naghavi, A.O.; Abuodeh, Y.A.; Perez, B.A.; Dilling, T.J. Analysis of Relapse Events After Definitive Chemoradiotherapy in Locally Advanced Non-Small-Cell Lung Cancer Patients. *Clin. Lung Cancer* **2019**, *20*, e1–e7. [CrossRef]

18. Dickhoff, C.; Otten, R.H.J.; Heymans, M.W.; Dahele, M. Salvage surgery for recurrent or persistent tumour after radical (chemo)radiotherapy for locally advanced non-small cell lung cancer: A systematic review. *Ther. Adv. Med. Oncol.* **2018**, *10*, 1758835918804150. [CrossRef]

19. Romero-Vielva, L.; Viteri, S.; Moya-Horno, I.; Toscas, J.I.; Maestre-Alcacer, J.A.; Ramon, Y.C.S.; Rosell, R. Salvage surgery after definitive chemo-radiotherapy for patients with Non-Small Cell Lung Cancer. *Lung Cancer* **2019**, *133*, 117–122. [CrossRef]

20. Kobayashi, A.K.; Horinouchi, H.; Nakayama, Y.; Ohe, Y.; Yotsukura, M.; Uchida, S.; Asakura, K.; Yoshida, Y.; Nakagawa, K.; Watanabe, S.I. Salvage surgery after chemotherapy and/or radiotherapy including SBRT and proton therapy: A consecutive analysis of 38 patients. *Lung Cancer* **2020**, *145*, 105–110. [CrossRef]

21. Dickhoff, C.; Rodriguez Schaap, P.M.; Otten, R.H.J.; Heymans, M.W.; Heineman, D.J.; Dahele, M. Salvage surgery for local recurrence after stereotactic body radiotherapy for early stage non-small cell lung cancer: A systematic review. *Ther. Adv. Med. Oncol.* **2018**, *10*, 1758835918787989. [CrossRef] [PubMed]

22. Mizobuchi, T.; Yamamoto, N.; Nakajima, M.; Baba, M.; Miyoshi, K.; Nakayama, H.; Watanabe, S.; Katoh, R.; Kohno, T.; Kamiyoshihara, M.; et al. Salvage surgery for local recurrence after carbon ion radiotherapy for patients with lung cancer. *Eur. J. Cardio Thorac. Surg. Off. J. Eur. Assoc. Cardio Thorac. Surg.* **2016**, *49*, 1503–1509. [CrossRef] [PubMed]

23. Antonia, S.J.; Villegas, A.; Daniel, D.; Vicente, D.; Murakami, S.; Hui, R.; Yokoi, T.; Chiappori, A.; Lee, K.H.; de Wit, M.; et al. Durvalumab after Chemoradiotherapy in Stage III Non-Small-Cell Lung Cancer. *N. Engl. J. Med.* **2017**, *377*, 1919–1929. [CrossRef] [PubMed]

24. Suzuki, H.; Yoshino, I. Approach for oligometastasis in non-small cell lung cancer. *Gen. Thorac. Cardiovasc. Surg.* **2016**, *64*, 192–196. [CrossRef]

25. Wang, Z.; Gao, S.G.; Xue, Q.; Guo, X.T.; Wang, L.X.; Yu, X.; Yang, Y.K.; Mu, J.W. Surgery of primary non-small cell lung cancer with oligometastasis: Analysis of 172 cases. *J. Thorac. Dis.* **2018**, *10*, 6540–6546. [CrossRef]

26. Gomez, D.R.; Blumenschein, G.R., Jr.; Lee, J.J.; Hernandez, M.; Ye, R.; Camidge, D.R.; Doebele, R.C.; Skoulidis, F.; Gaspar, L.E.; Gibbons, D.L.; et al. Local consolidative therapy versus maintenance therapy or observation for patients with oligometastatic non-small-cell lung cancer without progression after first-line systemic therapy: A multicentre, randomised, controlled, phase 2 study. *Lancet Oncol.* **2016**, *17*, 1672–1682. [CrossRef]

27. Otake, S.; Goto, T. Stereotactic Radiotherapy for Oligometastasis. *Cancers* **2019**, *11*, 133. [CrossRef]

28. Baggstrom, M.Q.; Stinchcombe, T.E.; Fried, D.B.; Poole, C.; Hensing, T.A.; Socinski, M.A. Third-generation chemotherapy agents in the treatment of advanced non-small cell lung cancer: A meta-analysis. *J. Thorac. Oncol. Off. Publ. Int. Assoc. Study Lung Cancer* **2007**, *2*, 845–853. [CrossRef]

29. Soria, J.C.; Ohe, Y.; Vansteenkiste, J.; Reungwetwattana, T.; Chewaskulyong, B.; Lee, K.H.; Dechaphunkul, A.; Imamura, F.; Nogami, N.; Kurata, T.; et al. Osimertinib in Untreated EGFR-Mutated Advanced Non-Small-Cell Lung Cancer. *N. Engl. J. Med.* **2018**, *378*, 113–125. [CrossRef]

30. Hishida, T.; Nagai, K.; Mitsudomi, T.; Yokoi, K.; Kondo, H.; Horinouchi, H.; Akiyama, H.; Nagayasu, T.; Tsuboi, M.; Japan Clinical Oncology Group. Salvage surgery for advanced non-small cell lung cancer after response to gefitinib. *J. Thorac. Cardiovasc. Surg.* **2010**, *140*, e69–e71. [CrossRef]

31. Hishida, T.; Yoshida, J.; Aokage, K.; Nagai, K.; Tsuboi, M. Long-term outcome of surgical resection for residual or regrown advanced non-small cell lung carcinomas following EGFR-TKI treatment: Report of four cases. *Gen. Thorac. Cardiovasc. Surg.* **2014**, *64*, 429–433. [CrossRef] [PubMed]

32. Horio, Y.; Mizuno, T.; Sakao, Y.; Inaba, Y.; Yatabe, Y.; Hida, T. Successful salvage surgery following multimodal therapy in a patient who harboured ALK-rearranged advanced lung adenocarcinoma with multiple organ metastases. *Respirol. Case Rep.* **2019**, *7*, e00451. [CrossRef] [PubMed]

33. Wu, Y.L.; Tsuboi, M.; He, J.; John, T.; Grohe, C.; Majem, M.; Goldman, J.W.; Laktionov, K.; Kim, S.W.; Kato, T.; et al. Osimertinib in Resected EGFR-Mutated Non-Small-Cell Lung Cancer. *N. Engl. J. Med.* **2020**, *383*, 1711–1723. [CrossRef] [PubMed]

34. Reck, M.; Rodriguez-Abreu, D.; Robinson, A.G.; Hui, R.; Csoszi, T.; Fulop, A.; Gottfried, M.; Peled, N.; Tafreshi, A.; Cuffe, S.; et al. Pembrolizumab versus Chemotherapy for PD-L1-Positive Non-Small-Cell Lung Cancer. *N. Engl. J. Med.* **2016**, *375*, 1823–1833. [CrossRef]

35. Gandhi, L.; Rodriguez-Abreu, D.; Gadgeel, S.; Esteban, E.; Felip, E.; De Angelis, F.; Domine, M.; Clingan, P.; Hochmair, M.J.; Powell, S.F.; et al. Pembrolizumab plus Chemotherapy in Metastatic Non-Small-Cell Lung Cancer. *N. Engl. J. Med.* **2018**, *378*, 2078–2092. [CrossRef]

36. Gadgeel, S.; Rodriguez-Abreu, D.; Speranza, G.; Esteban, E.; Felip, E.; Domine, M.; Hui, R.; Hochmair, M.J.; Clingan, P.; Powell, S.F.; et al. Updated Analysis From KEYNOTE-189: Pembrolizumab or Placebo Plus Pemetrexed and Platinum for Previously Untreated Metastatic Nonsquamous Non-Small-Cell Lung Cancer. *J. Clin. Oncol. Off. J. Am. Soc. Clin. Oncol.* **2020**, *38*, 1505–1517. [CrossRef]

37. Paz-Ares, L.; Luft, A.; Vicente, D.; Tafreshi, A.; Gumus, M.; Mazieres, J.; Hermes, B.; Cay Senler, F.; Csoszi, T.; Fulop, A.; et al. Pembrolizumab plus Chemotherapy for Squamous Non-Small-Cell Lung Cancer. *N. Engl. J. Med.* **2018**, *379*, 2040–2051. [CrossRef]

38. Bott, M.J.; Cools-Lartigue, J.; Tan, K.S.; Dycoco, J.; Bains, M.S.; Downey, R.J.; Huang, J.; Isbell, J.M.; Molena, D.; Park, B.J.; et al. Safety and Feasibility of Lung Resection After Immunotherapy for Metastatic or Unresectable Tumors. *Ann. Thorac. Surg.* **2018**, *106*, 178–183. [CrossRef]

39. Sumi, T.; Uehara, H.; Masaoka, T.; Tada, M.; Keira, Y.; Kamada, K.; Shijubou, N.; Yamada, Y.; Nakata, H.; Mori, Y.; et al. Lung adenocarcinoma with tumor resolution and dystrophic calcification after salvage surgery following immune checkpoint inhibitor therapy: A case report. *Thorac. Cancer* **2020**, *11*, 3396–3400. [CrossRef]

Review

Nivolumab for Previously Treated Patients with Non-Small-Cell Lung Cancer—Daily Practice versus Clinical Trials

Magdalena Knetki-Wróblewska *, Dariusz M. Kowalski and Maciej Krzakowski

Department of Lung Cancer and Chest Tumors, Maria Sklodowska-Curie National Research Institute of Oncology, 02-781 Warsaw, Poland; Dariusz.Kowalski@pib-nio.pl (D.M.K.); Maciej.Krzakowski@pib-nio.pl (M.K.)
* Correspondence: magdalena.knetki-wroblewska@pib-nio.pl

Abstract: Based on the results of the CheckMate 017 and CheckMate 057 studies, nivolumab therapy has become a new standard treatment for both squamous and non-squamous non-small-cell lung cancer (NSCLC). However, due to the specific inclusion criteria of these clinical trials, the efficacy and safety of nivolumab in real-world practice were not certain. In general, the real-world results of nivolumab treatment have been consistent with those obtained in clinical trials. Additional analyses of the real-world data have made the identification of prognostic factors possible. Good performance status is the most significant predictor of clinical benefit. Brain metastases, liver metastases, *EGFR* mutation, malignant pleural effusion, and a high number of metastatic sites were identified as negative prognostic factors. By contrast, a longer time to disease progression (>6 months) from the beginning of prior chemotherapy and an objective response to chemotherapy seem to have positive prognostic value in the case of nivolumab treatment. In terms of patient age, the data are inconclusive. Some blood biomarkers can also be considered significant prognostic factors.

Keywords: non-small-cell lung cancer; nivolumab; Expanded Access Program; real-world data; daily practice; prognostic factors

1. Introduction

Immune checkpoint inhibitors targeting programmed death 1 (PD-1) and its ligand (PD-L1) have significantly changed the management of advanced non-small-cell lung cancer (NSCLC) in recent years [1]. Nivolumab, a fully human antibody directed against PD-1, has been approved for previously treated advanced NSCLC. Nivolumab was associated with significantly longer overall survival (OS) than docetaxel and had a good safety profile in squamous and non-squamous NSCLC in two pivotal phase III clinical trials (CheckMate 017 and CheckMate 057) [2,3]. Pooled analysis of long-term outcomes confirmed the significant clinical efficacy of nivolumab compared with that of docetaxel [4,5]. The value of nivolumab was assessed in prospective clinical trials, the results of which were required for drug registration. However, further real-world NSCLC population studies and evaluation of the value of nivolumab in clinical practice are necessary to select a subgroup of patients in whom clinical benefits are most likely. The patient population is much more diverse in clinical practice than in clinical trials. Negative prognostic factors are frequent issues in many cases, with poor performance status, brain or liver metastases, and elderly age being the most common. Real-world data can also be used to identify additional prognostic factors that may be helpful in treatment decision-making. Some real-world data concerning nivolumab have recently been published, including those derived from the Expanded Access Program (EAP) and post-registration studies (data for nivolumab are more frequently published than data for atezolizumab and pembrolizumab). This paper aims to provide an

overview of the selected real-world studies on nivolumab and to describe predictive factors of value in clinical practice.

2. Nivolumab in Clinical Trials

The CheckMate 057 trial was designed for patients with non-squamous NSCLC. Eligible patients had primary CS IIIB/IV NSCLC or recurrent NSCLC after radiation therapy or surgical resection and documented disease progression during or after one platinum-based doublet chemotherapy regimen [3]. Patients with an acceptable general condition and adequate organ function without major comorbidities were included [3]. In all, 582 patients were randomized: 292 were assigned to receive nivolumab at a dose of 3 mg/kg every 2 weeks, and 290 to receive docetaxel at a dose of 75 mg/m^2 every 3 weeks. OS was the primary endpoint. The key secondary endpoints were investigator-assessed confirmed objective response rate and progression-free survival (PFS). Tumor response was assessed with the use of the Response Evaluation Criteria in Solid Tumors, version 1.1 (RECIST 1.1), at week 9 and then every 6 weeks until disease progression. Safety was assessed with the Cancer Institute Common Terminology Criteria for Adverse Events (CTCAE), version 4.0.

The median OS was longer in the nivolumab group than in the docetaxel group (12.2 months, 95% confidence interval (CI) 9.7–15.0, versus 9.4 months, 95% CI 8.1–10.7; hazard ratio (HR) 0.73, 95% CI 0.59–0.89; $p = 0.002$). The objective response rate was 19% with nivolumab versus 12% with docetaxel ($p = 0.02$). Treatment-related adverse events (AEs) of any grade were reported in 69% of patients in the nivolumab group and in 88% in the docetaxel group, while grade 3–4 AEs occurred in 10% of the nivolumab group and in 54% of the docetaxel group [3]. The most important data from that study are presented in Table 1.

Table 1. Nivolumab for previously treated non-small-cell lung cancer—CheckMate 017/057 [2,3].

	CheckMate 017			CheckMate 057		
	Nivolumab	Docetaxel	HR	Nivolumab	Docetaxel	HR
Number of patients	135	137		292	290	
ORR (%)	20	9	2.6; $p = 0.008$	19	12	$p = 0.02$
PFS (months)	3.5	2.8	0.62; $p < 0.001$	2.3	4.2	0.92; $p = 0.39$
OS (months)	9.2	6.0	0.59; $p < 0.001$	12.2	9.4	0.73; $p = 0.002$
AE (any grade, %)	58	86		69	88	
AE (grade 3–4, %)	7	55		10	54	

HR—hazard ratio, ORR—overall response rate, PFS—progression-free survival, OS—overall survival, AE—adverse event.

The CheckMate 017 trial was designed for patients with squamous NSCLC. Eligible patients had CS IIIB/IV NSCLC and documented disease progression after one platinum-based doublet chemotherapy [4]. The main inclusion or exclusion criteria and treatment outline were similar to those for the CheckMate 057 trial. In all, 272 patients underwent randomization: 135 patients were assigned to receive nivolumab and 137 to receive docetaxel [4].

The median OS was longer with nivolumab than with docetaxel (9.2 months, 95% CI 7.3–13.3, versus 6.0 months, 95% CI 5.1–7.3; HR 0.59, 95% CI 0.44–0.79; $p < 0.001$). The response rate was 20% with nivolumab versus 9% with docetaxel ($p = 0.008$). Treatment-related AEs of any grade occurred in 58% of patients in the nivolumab group and in 86% in the docetaxel group. Grade 3–4 AEs occurred in 7% of the nivolumab group and in 55% of the docetaxel group. The most important data from that study are presented in Table 1.

A pooled analysis of long-term outcomes confirmed the efficacy of nivolumab [4,5]. The 4-year OS rate was 14% in patients treated with nivolumab, compared with 5% in patients treated with docetaxel (14.9% for patients with non-squamous NSCLC and 9.4% for patients with squamous NSCLC in the nivolumab population); the 5-year OS rate was 13.4% with nivolumab versus 2.6% with docetaxel (HR 0.68, 95% CI 0.59–0.78) [4,5]. Patients in the nivolumab group who achieved an objective response

had the best long-term results. Median OS in patients with an objective response was not reached in the nivolumab group (95% CI 25.6–not reached) versus 17.1 months (95% CI 11.1–28.7) in the docetaxel group. The 4-year OS rate in patients with an objective response was 58% with nivolumab and 12% with docetaxel [4].

3. Nivolumab in Daily Practice

Patients likely to participate in clinical trials have to meet strictly defined, challenging criteria. Inclusion criteria usually only allow for the treatment of patients with Eastern Cooperative Oncology Group (ECOG) 0–1, without significant comorbidities, and with normal laboratory results. However, in clinical practice, the population of pretreated patients with NSCLC is very diverse. Poor performance status (ECOG 2–3), brain metastases, liver metastases, and elderly age, as well as rapid disease progression after chemotherapy are the most common problems. Real-world data can be used to assess the efficacy of nivolumab in clinical practice. Some real-world data have recently been published, including those derived from the EAP, which made it possible for many patients to be treated before the medicine was reimbursed in their countries. In total, data regarding 4800 patients have been published.

3.1. Efficacy

The Italian cohort is the largest reported group from the nivolumab EAP [6,7]. Inclusion criteria included CS IIIB/IV NSCLC, ECOG 0–2, adequate organ function, life expectancy of at least 6 weeks, and progression after at least one line of systemic treatment for advanced or metastatic disease. Patients with progression within 6 months after radical treatment for locally advanced disease were also eligible. Unstable brain metastases and active known or suspected autoimmune disease (with some exceptions) were contraindications for nivolumab treatment. For 1588 patients with non-squamous NSCLC, the median OS was 11.3 months, the 1-year OS rate was 48%, and the median PFS was 3.0 months, with a 1-year PFS rate of 22% [6]. The median OS was 7.9 months and the 1-year OS rate was 39% in the 371 patients with squamous NSCLC [7]. The overall response rate (ORR) was 18% for both the squamous and non-squamous NSCLC patient groups. Similar efficacy data from other countries are also available. In a group of 901 Japanese patients treated in an observational post-registration study, the median OS was 14.6 months for the entire patient population and the 1-year OS rate was 54.3% [8]. The median OS was 15.1 months for patients with non-squamous NSCLC and 12.3 months for patients with squamous NSCLC [8]. The median PFS for the entire patient population was 2.1 months and the ORR was 20.5% [8]. Survival and ORR data reported in other publications (patients in the EAP and in routine clinical practice) are summarized in Table 2.

Table 2. Survival in patients treated with nivolumab in real-world practice.

	Number of Patients	OS all Patients (Months)	OS Non-Squamous (Months)	OS Squamous (Months)	PFS (Months)	ORR (%)
Grossi [6]	1588	11.3	11.3	na	3	18
Crino [7]	371	7.9	na	7.9	nd	18
Morita [8]	901	14.6	15.1	12.3 **	2.1	20.5
Dudnik [9]	260	5.9	Squamous vs. non-squamous HR 1.12; *p* = 0.61		2.8	35 *
Schouten [10]	248	10.0	7.8	NR	2.6	21.8
Almazán [11]	221	9.7	12.8	6.9	5.3	17.6
Juergens [12]	472	12.0	11.8	13.1 **	3.5	nd
Figueiredo [13]	229	13.2	Squamous vs. non-squamous HR 0.72; *p* = 0.14		4.9	22.4
Manrique [14]	188	12.85	11.7	14.8 **	4.83	25.5
Brustugun [15]	58	11.7	nd	nd	4.0	nd

OS—overall survival, PFS—progression-free survival, ORR—overall response rate, NR—not reached, na—not applicable, nd—no data, HR—hazard ratio. * 49/260 patients were evaluated for response, ** Statistically non-significant.

3.2. Prognostic Factors in Real-World Practice

The clinical benefit of nivolumab, as shown in registration trials, applies to the entire patient population, but further analysis of the data suggests that some patients may benefit more than others. However, unfavorable responses to nivolumab treatment can be also observed. Therefore, it is important to identify additional prognostic factors that can be used in treatment decision-making. The real-world data are helpful in this regard.

3.2.1. Performance Status

Performance status is a crucial factor in treatment decision-making for patients with NSCLC. ECOG 0–1 is required in clinical trials, but the patient population is much more diverse in clinical practice. According to the real-world data, the prevalence of patients with ECOG ≥ 2 who are treated with nivolumab ranges from 3% to 46% [6–15]. The prognostic value of performance status has been well documented.

Multivariate survival analysis in the Italian EAP cohort of patients with non-squamous NSCLC showed that ECOG 2 performance status is an independent prognostic factor for early death ($p < 0.0001$) [6]. Poor performance status (ECOG 2), compared with ECOG 0, was also identified as an independent prognostic factor for death in the Italian EAP squamous NSCLC cohort (HR 2.76, 95% CI 1.65–4.62; $p < 0.0001$) [7]. In this cohort, the risk of death was also higher in patients with ECOG 1 than in patients with ECOG 0 (HR 1.57, 95% CI 1.17–2.11; $p = 0.003$) [7]. Similar results were obtained in the analysis of a group of 901 Japanese patients, in which 17.4% of the patients had an ECOG score of 2, 3, or 4 (HR 0.39, 95% CI 0.51–0.8; $p < 0.0001$) [8]. Poor performance status was also a risk factor for short PFS (HR 0.64, 95% CI 0.51–0.8; $p < 0.0001$) [8]. Multivariate analysis of the Portuguese EAP data identified performance status as the only independent prognostic factor ($p < 0.0006$) [13]. In a univariate analysis, the risk of death was much lower in patients with ECOG 0–1 than in patients with ECOG 2 (HR 3.8, 95% CI 2.3–6.07; $p < 0.0001$) [13]. Another univariate analysis reported an OS of 3.4 months (95% CI 2.3–4.4) in patients with ECOG 2 versus 11.79 months (95% CI 8.5–15.07) in patients with ECOG 1. The median OS for patients with ECOG 0 was not reached [14]. Some data related to the prognostic value of performance status are summarized in Table 3.

Table 3. Prognostic value of performance status in patients treated with nivolumab—real-world data.

	% of Patients ECOG ≥ 2	**OS (Months)**	
		ECOG 0–1	**ECOG ≥ 2**
Manrique [14]	10	11.79	3.4
Juergens [12]	8.9	12.91	6.77
Almazán [11]	13.6	12.8	2.9
Crino [7]	6	-	HR 2.76 * (2 vs. 0)
Figueiredo [13]	13.2	-	HR 3.8 * (≥2 vs. 0–1)
Schouten [10]	16.1	12.5	4.5
Dudnik [9]	46	9.5	3.5

OS—overall survival, ECOG—Eastern Cooperative Oncology Group, HR—hazard ratio. * Multivariate analysis.

3.2.2. Liver Metastases

A pooled analysis of the CheckMate 017 and CheckMate 057 trials with updated results from more than 3 years of follow-up included a subgroup analysis of patients with liver metastases [16]. Liver metastases were found in 23% of 854 patients at baseline. Although nivolumab had a confirmed OS benefit in patients with liver metastases (HR 0.68, 95% CI 0.50–0.91), the median OS for patients with liver metastases was 6.8 months in the nivolumab group and 5.9 months in the docetaxel group (HR 0.68, 95% CI 0.50–0.91), while for the entire patient population the median OS was 11.1 months for the nivolumab group and 8.1 months for the docetaxel group (HR 0.70, 95% CI 0.61–0.81) [16]. Patients with and without liver metastases were not directly compared.

Liver metastases were determined to be an independent negative prognostic factor for OS in multivariate analyses of some real-world data [6–8]. For Italian patients with squamous NSCLC, the HR was 1.44 (95% CI 1.04–1.98; $p = 0.03$) [7], and for non-squamous NSCLC the odds ratio (OR) for early death was 0.47 (95% CI 0.35–0.61; $p < 0.0001$) [6]. However, in another publication, the negative prognostic value of liver metastases was not confirmed [9]. In a retrospective analysis of 215 patients with NSCLC who received nivolumab, atezolizumab, or pembrolizumab (19.1% of patients had liver metastases), there was a higher risk of death in patients with liver metastasis than in those without (HR 2.04, 95% CI 1.33–3.13) [17]. Additional negative prognostic factors for patients with NSCLC and liver metastases were low albumin level, poor performance status, driver mutation, and having five or more liver metastases.

3.2.3. Brain Metastases

About 10% of non-oncogene addicted patients with NSCLC have brain metastases at diagnosis and 25–40% develop brain metastasis during the course of the disease. A pooled analysis of the CheckMate 017 and CheckMate 057 trials showed that 11% of the included patients had brain metastasis at baseline, but no detailed information about the intracranial efficacy of nivolumab were provided in the primary publications [4]. However, nivolumab was more effective than docetaxel in terms of OS in the entire analyzed patient population [4]. CheckMate 012 (NCT01454102) was a phase I, multicohort study evaluating nivolumab alone or in combination with other therapies for the treatment of patients with advanced NSCLC and untreated brain metastases (12 patients, arm M) [18]. Intracranial response was evaluated with magnetic resonance imaging [18]. The ORR was 16.7% (two patients) in that small study group; however, progressive disease was observed in the majority of patients [18].

Nivolumab therapy is routinely used in patients who have undergone primary resection or irradiation for brain metastases and whose clinical condition improved after receiving local treatment. Retrospective analyses of real-world data showed that nivolumab has intracranial activity [19–21]. Twenty-six percent of patients with non-squamous NSCLC in the Italian EAP had asymptomatic or controlled brain metastases [19]. The disease control rate was 40% and the ORR was 17%. The median OS in patients with asymptomatic or controlled brain metastases was 8.6 months (95% CI 6.4–10.8) compared with 11.3 months (95% CI 10.2–12.4) for the entire cohort [20]. In the cohort with squamous NSCLC, 10% of 372 patients had asymptomatic brain metastases. The median OS was 5.8 months (95% CI 1.9–9.8) [21]. A direct comparison of the efficacy of nivolumab in patients with and without brain metastases showed significant differences in OS [14]. In a group of 188 patients, 22% had brain metastases. The median OS was 5.09 months (95% CI 0.3–9.8) in the patients with brain metastases versus 14.8 months (95% CI 11.5–17.3) in patients without brain metastases [14]. In another cohort, in which 14.8% of 472 patients had brain metastases, the median OS reached 9 months (95% CI 5.5–13.3) in patients with brain metastases and 13.1 months (95% CI 11.5–17.1; $p = 0.007$) in patients without brain metastases [12]. Some studies have identified brain metastases as an independent negative prognostic factor [8], but others have not [6,7,9,10].

3.2.4. Elderly Patients

More than 40% of patients in the CheckMate 017 and CheckMate 057 populations were over 65 years of age, including about 7% of patients who were over 75 years of age [2,3]. Nivolumab was effective in the whole group, although for patients over 75 years of age the clinical benefit was uncertain (HR 0.9; 95% CI 0.43–1.87) [3]. The findings of the phase II CheckMate 171 trial have been published recently [22]. Overall, 811 patients with previously treated advanced squamous NSCLC were included, of whom 278 were aged over 70 years and 125 were aged over 75 years [22]. The median OS was similar in all age groups: 10.0 months (95% CI 9.2–11.2) in all patients, 10.0 months (95% CI 8.3–11.4) in those aged over 70 years, and 11.2 months (95% CI 7.9–14.2) in those aged over 75 years. The safety profile was similar across age-determined populations; however, low-grade diarrhea was more common in patients over 70 years of age than in those aged 70 or younger [22]. AEs were reported

in 13.9% of all patients, in 15.8% of those aged over 70 years, and in 18.4% of those aged over 75 years [22]. In an Italian population of 371 patients with squamous NSCLC, OS was reduced in patients aged 75 years or older (5.8 months, 95% CI 3.5–8.1) versus patients aged under 65 years (8.6 months, 95% CI 5.2–11.9), patients aged 65 to less than 75 years (8.0 months, 95% CI 5.6–10.4), and the overall population (7.9 months, 95% CI 6.2–9.6) [23]. Discontinuation rates due to treatment-related AEs were low irrespective of age (4–5%) [24]. However, a retrospective analysis of 324 Belgian patients with NSCLC showed no significant difference between older (≥70) and younger (<70 years) patients in terms of PFS (4 months versus 3.7 months, $p = 0.483$) and OS (9.3 months versus 8.4 months, $p = 0.638$) [25]. The incidence of AEs of all grades and of grade 3–4 AEs was also similar between age groups [25]. Similarly, in a group of Italian patients with non-squamous NSCLC, 522 of 1588 patients were over 70 years of age; these patients reached a median OS of 11.5 months (95% CI 10.0–13.0), while for the 232 patients aged over 75 years OS was 12.0 months (95% CI 9.2–14.8) [6]. There were no significant differences in the incidence of treatment-related AEs in the subgroups defined by age (6–7% of AEs were grade 3–4) [6]. Some studies have confirmed that treatment outcomes in clinical practice are not affected by age [11,12,26,27], whereas others have reported nivolumab treatment to have less favorable results in patients aged over 75 years [9].

3.2.5. *EGFR* Status

Of the patients in the CheckMate 057 trial, 15% had an *EGFR* mutation. Nivolumab was not better than docetaxel in that subset of patients (HR 1.18, 95% CI 0.69–2.0) [3].

In an Italian cohort of patients with non-squamous NSCLC, 102 patients (6.4%) had an *EGFR* mutation [28]. No statistically significant difference in OS was observed in patients with an *EGFR* mutation versus that in those without. OS reached 11 months in patients with *EGFR* wild-type tumors versus 8.3 months in patients with *EGFR*-mutant tumors (HR 1.11, 95% CI 0.84–1.47; $p = 0.4$) [28]. A study by the Galician Lung Cancer Group showed that OS was higher in patients without an *EGFR* mutation than in patients with *EGFR*-mutated NSCLC (12.8 versus 4.8 months, $p = 0.12$) [14]. Although univariate (HR 1.11, 95% CI 0.84–1.45; $p = 0.46$) and multivariate (HR 1.13, 95% CI 0.82–1.56; $p = 0.45$) analysis of 901 Japanese patients (12.9% with *EGFR* mutation) failed to determine the prognostic value of *EGFR* mutation [8], most reports are in line with the CheckMate 057 results and confirmed the negative prognostic value of *EGFR* mutation in patients treated with nivolumab. OS in 25 Canadian patients with *EGFR* mutation was 3.38 months, while in 229 patients with wild-type *EGFR* it was 13.37 months (HR 2.32, 95% CI 1.37–3.93; $p = 0.002$) [12]. A multivariate analysis of 613 patients (15% of whom had an *EGFR* mutation) showed *EGFR* mutation or *ALK* translocation to have negative prognostic value in terms of PFS (HR 1.45, 95% CI 1.12–1.86) [26].

3.2.6. Sensitivity to Previous Chemotherapy

A post hoc exploratory multivariate analysis of the CheckMate 057 population suggested that some patients might be at a higher risk of death within the first 3 months of treatment. The following known negative prognostic factors were considered: less than 3 months since last treatment, progressive disease as best response to prior treatment, and an ECOG score of 1 [29].

Real-life experience with nivolumab has shown that sensitivity to previous chemotherapy could have prognostic value. The Netherlands Cancer Institute published the results of 248 patients treated with nivolumab [10]. Of the 189 patients who had a documented response to prior platinum-based doublet therapy, 38.6% had progressive disease as the best response. OS was 13.1 months in patients who had been sensitive to the chemotherapy and only 5.0 months in chemotherapy-refractory patients (HR 1.7, 95% CI 1.108–2.642; $p = 0.015$). An analysis of 221 patients showed that time to progression could also have prognostic value [11]. Patients who had disease progression within 6 months of platinum therapy did worse than those who had a longer PFS than 6 months on platinum therapy (3.7 months versus 11.8 months; HR 0.39, 95% CI 0.26–0.6; $p < 0.0001$) [11]. The positive prognostic

value of both ORR and PFS of more than 6 months since the beginning of prior chemotherapy was presented in another publication [30].

3.3. Safety

In the CheckMate 057 study, the frequency of any-grade AEs related to nivolumab treatment was 69%, while the frequency of grade 3–4 AEs was 10% [3]. The most common any-grade AEs were fatigue (16%), nausea (12%), decreased appetite (10%), and asthenia (10%). The rate of discontinuation due to nivolumab-related AEs was 5% [3]. In the CheckMate 017 study, any-grade AEs were reported in 58% of patients, while grade 3–4 AEs were reported in 7% of patients, and treatment was discontinued due to nivolumab-related AEs in 3% of patients [2]. The safety profile established in clinical practice seems to be consistent with that determined in clinical trials. The relevant data are summarized in Table 4. The differences in the frequency of any-grade AEs between some publications could be associated with less precise reporting of AEs outside clinical trials.

Table 4. Incidence of adverse events (AEs) in patients treated with nivolumab—real-world data.

	All (%)	Grade 3–4 (%)	Discontinuation of Therapy Due to an AE (%)
Grossi [6]	32	6	5
Manrique [14]	78	4.8	4.8
Schouten [10]	18	6	nd
Dudnik [9]	62	7	3.5
Crino [7]	29	6	9
Garassino [28]	33	6	2.6
Kobayashi [27]	45	13.3	nd
Figueiredo [13]	76	nd	16

nd—no data.

4. Summary

Based on the results of the CheckMate 017 and CheckMate 057 studies, nivolumab therapy has become a new standard of care for both squamous and non-squamous NSCLC. Due to the specific inclusion criteria of the clinical trials, the efficacy and safety of nivolumab in real-world practice were not certain. However, some data from the EAP and from post-registration studies have recently been published, which allows for further evaluation.

In general, the real-world results are consistent with those obtained in clinical trials. From a practical point of view, the important question is how to select a subgroup of patients in whom clinical benefits are most likely. Additional analyses of the real-world data made the identification of prognostic factors possible.

Performance status is the most important prognostic factor. Several multivariate analyses showed ECOG 0–1 to be the most significant predictor of clinical benefit [6,7,13,30,31]. An analysis that focused on negative prognostic factors in response to nivolumab therapy clearly identified the following risk factors of early death: ECOG $\geq$ 2 (OR 5.66, 95% CI 2.01–15.61; $p < 0.001$), C-reactive protein to albumin ratio >0.3 (OR 10.56, 95% CI 3.61–3086; $p < 0.001$), and poor response to first-line chemotherapy (OR 2.06, 95% CI 1.03–4.14; $p < 0.001$) [31]. Additionally, many authors suggest that liver metastases, brain metastases, and *EGFR* mutation are negative prognostic factors associated with a higher risk of death. Malignant pleural effusion and a high number of metastatic sites were also identified as negative prognostic factors [30,32]. By contrast, a longer PFS on platinum therapy (>6 months) and an objective response to chemotherapy seem to have positive prognostic value in the case of nivolumab treatment. In terms of patient age, the data are inconclusive.

Blood biomarkers can also be considered in treatment decision-making. The use of the lung immune prognostic index (LIPI) based on the baseline derived neutrophil to lymphocyte ratio (dNLR) and lactate dehydrogenase (LDH) was suggested [33,34]. A high LIPI value was indicated as an independent negative prognostic factor (HR 3.67, 95% CI 1.96–6.86; $p < 0.0001$) [33]. Several other

inflammatory-related markers, such as the neutrophil to lymphocyte ratio (NLR), dNLR, LDH, interleukin 8, and indoleamine 2,3 dioxygenase activity were also found to be important [35,36].

It is noteworthy that some of these prognostic factors are also relevant to chemotherapy [37,38]. The negative prognostic value of parameters such as poor performance status, liver or brain metastases, the number of metastatic sites, and an elevated leukocyte count was demonstrated [37,38].

To summarize—the efficacy and safety of nivolumab in the second-line setting of advanced NSCLC have been established in clinical trials and confirmed in real-world practice. Long-term clinical benefit can be obtained in some patients. Good performance status (ECOG 0–1) is crucial, but other clinical variables such as site and number of metastatic lesions, time to failure of first-line chemotherapy, chemotherapy response status, and specific laboratory results should also be considered. There is a further need to collect data on the efficacy of immunotherapy in real-world clinical practice.

References

1. Planchard, D.; Popat, S.; Kerr, K.; Novello, S.; Smit, E.F.; Faivre-Finn, C.; Mok, T.S.; Reck, M.; Van Schil, P.E.; Hellmann, M.D.; et al. Metastatic non-small cell lung cancer: ESMO Clinical Practice Guidelines for diagnosis, treatment and follow-up. *Ann. Oncol.* **2018**, *29* (Suppl. 4), 192–237. [CrossRef]

2. Brahmer, J.; Reckamp, K.L.; Baas, P.; Crinò, L.; Eberhardt, W.E.; Poddubskaya, E.; Antonia, S.; Pluzanski, A.; Vokes, E.E.; Holgado, E.; et al. Nivolumab versus docetaxel in advanced squamous-cell non-small-cell lung cancer. *N. Engl. J. Med.* **2015**, *373*, 123–135. [CrossRef]

3. Borghaei, H.; Paz-Ares, L.; Horn, L.; Spigel, D.R.; Steins, M.; Ready, N.E.; Chow, L.Q.; Vokes, E.E.; Felip, E.; Holgado, E.; et al. Nivolumab versus docetaxel in advanced nonsquamous non-small-cell lung cancer. *N. Engl. J. Med.* **2015**, *373*, 1627–1639. [CrossRef] [PubMed]

4. Antonia, S.; Borghaei, H.; Ramalingam, S.; Horn, L.; De Castro Carpeño, J.; Pluzanski, A.; Burgio, M.A.; Garassino, M.; Chow, L.Q.M.; Gettinger, S.; et al. Four-year survival with nivolumab in patients with previously treated advanced non-small-cell lung cancer: A pooled analysis. *Lancet Oncol.* **2019**, *10*, 1395–1408. [CrossRef]

5. Lind, M.; Gettinger, S.; Borghei, H.; Brahmer, J.; Chow, L.; Burgio, M.; De Castro Carpeno, J.; Pluzanski, A.; Arrieta, O.; Frontera, O.A.; et al. Five-year outcomes from the randomized, phase 3 trials CheckMate 017/057: Nivolumab vs docetaxel in previously treated NSCLC. *Lung Cancer* **2020**, *139*, 1–113.

6. Grossi, F.; Genova, C.; Crino, L.; Delmonte, A.; Turci, D.; Signorelli, D.; Passaro, A.; Soto Parra, H.; Catino, A.; Landi, L.; et al. Real-life results from the overall population and key subgroups within the Italian cohort of nivolumab expanded access program in non-squamous non-small cell lung cancer. *Eur. J. Cancer.* **2019**, *123*, 72–80. [CrossRef] [PubMed]

7. Crino, L.; Bidoli, P.; Delmonte, A.; Grossi, F.; De Marinis, F.; Ardizzoni, A.; Vitiello, F.; Lo Russo, G.; Soto Parra, H.; Cortesi, E.; et al. Italian cohort of nivolumab expanded access program in squamous non-small cell lung cancer: Results from a real-world population. *Oncologist* **2019**, *24*, 1165–1171. [CrossRef] [PubMed]

8. Morita, R.; Okishio, K.; Shimizu, J.; Saito, H.; Sakai, H.; Kim, Y.H.; Hataji, O.; Yomota, M.; Nishio, M.; Aoe, K.; et al. Real-world effectiveness and safety of nivolumab in patients with non-small cell lung cancer: A multicenter retrospective observational study in Japan. *Lung Cancer* **2020**, *140*, 8–18. [CrossRef]

9. Dudnik, E.; Moskovitz, M.; Daher, S.; Shamai, S.; Hanovich, E.; Grubstein, A.; Shochat, T.; Wollner, M.; Bar, J.; Merimsky, O.; et al. Effectiveness and safety of nivolumab in advanced non-small cell lung cancer. *Lung Cancer* **2018**, *126*, 217–223. [CrossRef] [PubMed]

10. Schouten, R.; Muller, M.; de Gooijer, C.; Baas, P.; van den Heuvel, M. Real life experience with nivolumab for the treatment of non-small cell lung carcinoma. Data from the expanded access program and routine clinical care in a tertiary cancer centre-The Netherlands Cancer Institute. *Lung Cancer* **2018**, *126*, 210–216. [CrossRef] [PubMed]

11. Merino Almazán, M.; Duarte Pérez, J.M.; Marín Pozo, J.F.; Ortega Granados, A.L.; De Muros Fuentes, B.; Quesada Sanz, P.; Gago Sánchez, A.I.; Rodríguez Gómez, P.; Jurado García, J.M.; Artime Rodríguez-Hermida, F.; et al. A multicentre observational study of the effectiveness, safety and economic impact of nivolumab on non-smallcell lung cancer. *Int. J. Clin. Pharm.* **2019**, *41*, 272–279. [CrossRef] [PubMed]

12. Juergens, R.; Mariano, C.; Jolivet, J.; Finn, N.; Rothenstein, J.; Reaume, M.N.; Faghih, A.; Labbé, C.; Owen, S.; Shepherd, F.A.; et al. Real-world benefit of nivolumab in a Canadian non-small-cell lung cancer cohort. *Curr. Oncol.* **2018**, *25*, 384–392. [CrossRef] [PubMed]

13. Figueiredo, A.; Almeida, M.A.; Almodovar, M.; Alves, P.; Araújo, A.; Araújo, D.; Barata, F.; Barradas, F.; Barroso, A.; Brito, U.; et al. Real-world data from the Portuguese Nivolumab Expanded Access Program (EAP) in previously treated nonsmallcell lung cancer. *Pulmonology* **2020**, *26*, 10–17. [CrossRef]

14. Areses Manrique, M.C.; Mosquera Martínez, J.; García González, J.; Afonso Afonso, F.J.; Lázaro Quintela, M.; Fernández Núñez, N.; Azpitarte Raposeiras, C.; Amenedo Gancedo, M.; Santomé Couto, L.; García Campelo, M.R.; et al. Real world data of nivolumab for previously treated non-small cell lung cancer patients: A Galician lung cancer group clinical experience. *Transl Lung Cancer Res.* **2018**, *7*, 404–415. [CrossRef] [PubMed]

15. Brustugun, O.; Sprauten, M.; Helland, A. Real-world data on nivolumab treatment of non-small cell lung cancer. *Acta Oncol.* **2017**, *56*, 438–440. [CrossRef] [PubMed]

16. Vokes, E.E.; Ready, N.; Felip, E.; Horn, L.; Burgio, M.A.; Antonia, S.J.; Arén Frontera, O.; Gettinger, S.; Holgado, E.; Spigel, D.; et al. Nivolumab versus docetaxel in previously treated advanced non-small-cell lung cancer (CheckMate 017 and CheckMate 057): 3-year update and outcomes in patients with liver metastases. *Ann. Oncol.* **2018**, *1*, 959–965. [CrossRef] [PubMed]

17. Kitadai, R.; Okuma, Y.; Hakozaki, T.; Hosomi, Y. The efficacy of immune checkpoint inhibitors in advanced non-small-cell lung cancer with liver metastases. *J. Cancer Res. Clin. Oncol.* **2020**, *146*, 777–785. [CrossRef] [PubMed]

18. Goldman, J.; Crino, L.; Vokes, E.; Holgado, E.; Reckamp, K.; Pluzanski, A.; Spigel, D.; Kohlhaeufl, M.; Garassino, M.; Chow, L.; et al. Nivolumab in Patients With Advanced NSCLC and Central Nervous System Metastases. *J. Clin. Oncol.* **2016**, *34*, 9038. [CrossRef]

19. Dudnik, E.; Yust-Katz, S.; Nechushtan, H.; Goldstein, D.A.; Zer, A.; Flex, D.; Siegal, T.; Peled, N. Intracranial response to nivolumab in NSCLC patients with untreated or progressing CNS metastases. *Lung Cancer* **2016**, *98* (Suppl 4), 114–117. [CrossRef]

20. Crinòa, L.; Brontea, G.; Bidoli, P.; Cravero, P.; Minenza, E.; Cortesi, E.; Garassino, M.C.; Proto, C.; Cappuzzo, F.; Grossi, F.; et al. Nivolumab and brain metastases in patients with advanced non-squamous non-small cell lung cancer. *Lung Cancer* **2019**, *129*, 35–40. [CrossRef]

21. Cortinovis, D.; Chiari, R.; Catino, A.; Grossi, F.; De Marinis, F.; Sperandi, F.; Piantedosi, F.; Vitali, M.; Soto Parra, H.J.; Migliorino, M.R.; et al. Italian Cohort of the Nivolumab EAP in Squamous NSCLC: Efficacy and Safety in Patients With CNS Metastases. *Anticancer Res.* **2019**, *39*, 4265–4271. [CrossRef] [PubMed]

22. Felip, E.; Ardizzoni, A.; Ciuleanu, T.; Cobo, M.; Laktionov, K.; Szilasi, M.; Califano, R.; Carcereny, E.; Griffiths, R.; Paz-Ares, L.; et al. CheckMate 171: A phase 2 trial of nivolumab in patients with previously treated advanced squamous non-small cell lung cancer, including ECOG PS 2 and elderly populations. *Eur. J. Cancer* **2020**, *127*, 160–172. [CrossRef] [PubMed]

23. Grossi, F.; Crino, L.; Logroscino, A.; Canova, S.; Delmonte, A.; Melotti, B.; Proto, C.; Gelibter, A.; Cappuzzo, F.; Turci, D.; et al. Use of nivolumab in elderly patients with advanced squamous non-small-cell lung cancer: Results from the Italian cohort of an expanded access programme. *Eur. J. Cancer* **2018**, *100*, 126e34. [CrossRef] [PubMed]

24. Zhang, G.; Cheng, R.; Wang, H.; Zhang, Y.; Yan, X.; Li, P.; Zhang, M.; Zhang, X.; Yang, J.; Niu, Y.; et al. Comparable outcomes of nivolumab in patients with advanced NSCLC presenting with or without brain metastases: A retrospective cohort study. *Cancer Immunol. Immunother.* **2020**, *69*, 399–405. [CrossRef] [PubMed]

25. Joris, S.; Pieters, T.; Sibille, A.; Bustin, F.; Jacqmin, L.; Kalantari, H.R.; Surmont, V.; Goeminne, J.-C.; Clinckart, F.; Pat, K.; et al. Real life safety and effectiveness of nivolumab in older patients with non-small cell lung cancer: Results from the Belgian compassionate use program. *J. Geriatr. Oncol.* **2019**, 796–801.

26. Fujimoto, D.; Yoshioka, H.; Kataoka, Y.; Morimoto, T.; Kim, Y.H.; Tomii, K.; Ishida, T.; Hirabayashi, M.; Hara, S.; Ishitoko, M.; et al. Efficacy and safety of nivolumab in previously treated patients with non-small cell lung cancer. A multicenter retrospective cohort study. *Lung Cancer* **2018**, *119*, 14–20. [CrossRef] [PubMed]

27. Kobayashi, K.; Nakachi, I.; Naoki, K.; Satomi, R.; Nakamura, M.; Inoue, T.; Tateno, H.; Sakamaki, F.; Sayama, K.; Terashima, T.; et al. Real-world Efficacy and Safety of Nivolumab for Advanced Non-Small-Cell Lung Cancer: A retrospective multicenter analysis. *Clin. Lung Cancer* **2018**, *19*, 349–358. [CrossRef] [PubMed]

28. Garassino, M.C.; Gelibter, A.J.; Grossi, F.; Chiari, R.; Soto Parra, H.; Cascinu, S.; Cognetti, F.; Turci, D.; Blasi, L.; Bengala, C.; et al. Italian Nivolumab Expanded Access Program in Nonsquamous Non–Small Cell Lung Cancer Patients: Results in Never-Smokers and EGFR Mutant Patients. *J. Thorac. Oncol.* **2018**, *13*, 1146–1155. [CrossRef]

29. Peters, S.; Cappuzzo, F.; Horn, L.; Paz-Ares, L.; Borghaei, H.; Barlesi, F.; Steins, M.; Felip, E.; Spigel, D.; Dorange, C.; et al. Analysis of Early Survival in Patients With Advanced Non-Squamous NSCLC Treated With Nivolumab vs Docetaxel in CheckMate 057. In Proceedings of the IASLC 17th World Conference on Lung Cancer, Vienna, Austria, 4−7 December 2016.

30. Tournoy, K.; Thomeer, M.; Germonpré, P.; Derijcke, S.; De Pauw, R.; Galdermans, D.; Govaert, K.; Govaerts, E.; Schildermans, R.; Declercq, I.; et al. Does nivolumab for progressed metastatic lung cancer fulfill its promises? An efficacy and safety analysis in 20 general hospitals. *Lung Cancer* **2018**, *115*, 49–55. [CrossRef]

31. Inoue, T.; Tamiya, M.; Tamiya, A.; Nakahama, K.; Taniguchi, Y.; Shiroyama, T.; Isa, S.I.; Nishino, K.; Kumagai, T.; Kunimasa, K.; et al. Analysis of early death in japanese patients with advanced non-small cell lung cancer treated with nivolumab. *Clin. Lung Cancer* **2017**, *19*, 171–176. [CrossRef]

32. Pantano, F.; Russano, M.; Berruti, A.; Mansueto, G.; Migliorino, M.R.; Adamo, V.; Aprile, G.; Gelibter, A.; Falcone, A.; Russo, A.; et al. Prognostic clinical factors in patients affected by non-smallcell lung cancer receiving Nivolumab. *Expert Opin. Biol.* **2020**, *20*, 319–326. [CrossRef]

33. Ruiz-Bañobre, J.; Areses-Manrique, M.; Mosquera-Martínez, J.; Cortegoso, A.; Afonso-Afonso, F.J.; Dios-Álvarez, N.; Fernández-Núñez, N.; Azpitarte-Raposeiras, C.; Amenedo, M.; Santomé, L.; et al. Evaluation of the lung immune prognostic index in advanced non-small cell lung cancer patients under nivolumab monotherapy. *Transl Lung Cancer Res.* **2019**, *8*, 1078–1085. [CrossRef]

34. Mezquita, L.; Auclin, E.; Ferrara, R.; Charrier, M.; Remon, J.; Planchard, D.; Ponce, S.; Ares, L.P.; Leroy, L.; Audigier-Valette, C.; et al. Association of the Lung Immune Prognostic Index With Immune Checkpoint Inhibitor Outcomes in Patients With Advanced Non-Small Cell Lung Cancer. *JAMA Oncol.* **2018**, *4*, 351–357. [CrossRef]

35. Agulló-Ortuño, M.; Gómez-Martín, Ó.; Ponce, S. Blood Predictive Biomarkers for Patients With Non-smallcell Lung Cancer Associated With Clinical Response to Nivolumab. *Clin. Lung Cancer* **2020**, *21*, 75–85. [CrossRef]

36. Dusselier, M.; Deluche, E.; Delacourt, N. Neutrophil-to-lymphocyte ratio evolution is an independent predictor of early progression of second-line nivolumab-treated patients with advanced non-small-cell lung cancers. *PLoS ONE* **2019**, *14*, e0219060. [CrossRef] [PubMed]

37. Hoang, T.; Xu, R.; Schiller, J.; Bonomi, P.; Johnson, D.H. Clinical model to predict survival in chemonaive patients with advanced non-small-cell lung cancer treated with third-generation chemotherapy regimens based on eastern cooperative oncology group data. *J. Clin. Oncol.* **2005**, *23*, 175–183. [CrossRef]

38. Tibaldi, C.; Vasile, E.; Bernardini, I.; Orlandini, C.; Andreuccetti, M.; Falcone, A. Baseline elevated leukocyte count in peripheral blood is associated with poor survival in patients with advanced non-small cell lung cancer: A prognostic model. *J. Cancer Res. Clin. Oncol.* **2008**, *134*, 1143–1149. [CrossRef]

PD-(L)1 Inhibitors in Combination with Chemotherapy as First-Line Treatment for Non-Small-Cell Lung Cancer: A Pairwise Meta-Analysis

Jorge García-González [1,*,†], Juan Ruiz-Bañobre [1,*,†], Francisco J. Afonso-Afonso [2], Margarita Amenedo-Gancedo [3], María del Carmen Areses-Manrique [4], Begoña Campos-Balea [5], Joaquín Casal-Rubio [6], Natalia Fernández-Núñez [5], José Luis Fírvida Pérez [4], Martín Lázaro-Quintela [6], Diego Pérez Parente [7], Leonardo Crama [7], Pedro Ruiz-Gracia [7], Lucía Santomé-Couto [8] and Luis León-Mateos [1,*]

[1] Medical Oncology Department, University Clinical Hospital of Santiago de Compostela and Translational Medical Oncology Group (Oncomet), Health Research Institute of Santiago de Compostela (IDIS), CIBERONC, 15706 Santiago de Compostela, Spain

[2] Medical Oncology Department, Complexo Hospitalario Universitario de Ferrol, 15405 A Coruña, Spain; francisco.javier.afonso.afonso@sergas.es

[3] Medical Oncology Department, Centro Oncológico de Galicia, 15009 A Coruña, Spain; margarita.amenedo@cog.es

[4] Medical Oncology Department, Complexo Hospitalario Universitario de Ourense, 32005 Ourense, Spain; karmeleareses@hotmail.com (M.d.C.A.-M.); jlfirvidap@gmail.com (J.L.F.P.)

[5] Medical Oncology Department, Hospital Universitario Lucus Augusti, 27003 Lugo, Spain; bcamposbalea@hotmail.com (B.C.-B.); fernandeznunez.ntalia@gmail.com (N.F.-N.)

[6] Medical Oncology Department, Complexo Hospitalario Universitario de Vigo, 36213 Vigo, Spain; joaquin.casal.rubio@sergas.es (J.C.-R.); martin.lazaro.quintela@sergas.es (M.L.-Q.)

[7] Lung Cancer Medical Department, Roche Farma S.A., 28042 Madrid, Spain; diego.perez@roche.com (D.P.P.); leonardo.crama@roche.com (L.C.); pedro.ruiz.pr1@roche.com (P.R.-G.)

[8] Medical Oncology Department, Hospital POVISA, 36211 Vigo, Spain; lsantome@povisa.es

*   Correspondence: jorgejose.garcia.gonzalez@sergas.es (J.G.-G.); jurruba@gmail.com (J.R.-B.); luis.leon.mateos@sergas.es (L.L.-M.); Tel.: +34-981-951-470 (J.G.-G.); +34-981-951-470 (J.R.-B.); +34-981-951-470 (L.L.-M.)

†   Shared first authors.

Abstract: The combination of programmed cell death-1 (PD-1)/programmed death ligand-1 (PD-L1) inhibitors with chemotherapy has emerged as a promising therapeutic option for advanced non-small-cell lung cancer (NSCLC). The aim of this meta-analysis was to evaluate the efficacy of the combined strategy in this setting. For this purpose, we performed a literature search of randomized controlled trials comparing PD-(L)1 inhibitors plus platinum-based chemotherapy versus chemotherapy alone in stage IV NSCLC patients. Seven clinical trials with 4562 patients were included. In the intention-to-treat wildtype population, PD-(L)1 inhibitor plus chemotherapy was significantly associated with improved progression-free survival (PFS) (Hazard ratio (HR) = 0.61, 95% confidence interval (CI): 0.57–0.65, $p < 0.001$) and overall survival (OS) (HR = 0.76, 95% CI: 0.67–0.86; $p < 0.001$) compared to chemotherapy. A significantly higher overall response rate (ORR) was also observed with the combined strategy (Odds ratio (OR) = 2.12, 95% CI: 1.70–2.63, $p < 0.001$). Furthermore, in all the analyzed subgroups, addition of PD-(L)1 inhibitors to chemotherapy significantly improved efficacy endpoints. Specifically, stratification according to PD-L1 expression revealed a benefit across all patients, regardless of their PFS status. In conclusion, PD-(L)1 blockade added to standard platinum-based chemotherapy significantly improved PFS, OS, and ORR in the up-front treatment of advanced NSCLC.

1. Introduction

Lung cancer remains the leading cause of cancer-related death worldwide among men and the second among women [1]. Non-small-cell lung cancer (NSCLC), which is the most common type, accounts for 80% to 85% of all lung cancer diagnoses [2]. It is frequently diagnosed in the advanced stage, with 5-year survival rates ranging from 0% to 5% with chemotherapy, the only systemic therapeutic strategy available for decades [3]. In this regard, blockade of the programmed cell death-1 (PD-1)/programmed death ligand-1 (PD-L1) axis in particular has opened up a new horizon in the lung cancer therapeutic landscape, increasing overall survival (OS) not only in patients with advanced NSCLC but also in patients with stage III NSCLC and extensive-stage small-cell lung cancer [4–6].

Since 2015, three different PD-(L)1 inhibitors have been approved by the European Medicines Agency (EMA) and/or the U.S. Food and Drug Administration (FDA) for the treatment of metastatic NSCLC (mNSCLC) [7]: two anti-PD-1 antibodies (nivolumab and pembrolizumab) and one anti-PD-L1 antibody (atezolizumab), indicated for patients regardless of their PD-L1 expression status (nivolumab and atezolizumab) or for PD-L1-positive patients only (pembrolizumab). All of them have demonstrated an improvement in OS compared to docetaxel in second-line therapy [8–10]. In the first-line setting, results from the KEYNOTE 024 trial demonstrated that, compared with platinum-based chemotherapy, OS, progression-free survival (PFS), and overall response rate (ORR) were significantly improved in patients with PD-L1 expression on at least 50% of tumor cells and without oncogenic driver mutations [11,12]. Interestingly, an additional study assessing pembrolizumab efficacy versus chemotherapy using a PD-L1 tumor proportion score (TPS) of 1% or greater (KEYNOTE-042 [13]) demonstrated improved OS for the full cohort, which, despite being higher for higher PD-L1 expression, supported a potential extended role of pembrolizumab monotherapy as a standard first-line treatment for PD-L1-expressing advanced/metastatic NSCLC [14]. In contrast, nivolumab did not demonstrate statistically significant survival benefits in previously untreated PD-L1-positive mNSCLC (CheckMate-026 [15]).

Nevertheless, many patients with advanced NSCLC do not benefit from PD-(L)1 inhibitors, either in the first line or in the second or successive lines of treatment. The search for reliable predictive biomarkers of response to these drugs is therefore essential to improve patient outcomes.

The potential synergistic effects of combining chemotherapy and immunotherapy to improve the antitumor activity of anti-PD-(L)1 monotherapy were initially suggested in preclinical studies [16] (Apetoh, 2015 #16) and were further demonstrated in several clinical trials [4–6,17–25]. However, although promising outcomes have been reported, several questions remain unanswered, such as the potential real benefit for all patients at the expense of increased toxicity or the possible molecular factors that could predict the benefit of this combined therapeutic strategy.

The objective of this study was to evaluate the efficacy of the combined strategy by conducting a pairwise meta-analysis (MA) of the available information on PD-(L)1 inhibitors in combination with chemotherapy in the first-line treatment of patients with advanced NSCLC.

2. Materials and Methods

2.1. Search Strategies and Study Selection

We conducted a systematic search in PubMed to identify all eligible trials from inception until 1 January 2020, with no start date limit applied. Literature search terms used were "non-small cell lung cancer" (or "NSCLC"), "chemotherapy", "pembrolizumab", "nivolumab", "atezolizumab", "durvalumab", and all terms related to clinical trial registration (ClinicalTrials.gov, EU Clinical Trials Register, ISRCTN, and ANZCTR). An additional search of abstracts presented at the American Society

of Clinical Oncology (ASCO), European Society for Medical Oncology (ESMO), American Association for Cancer Research for Medical Oncology (AACR), and World Conference on Lung Cancer (WCLC) was also performed.

2.2. Selection Criteria

Only phase III trials conducted in patients with advanced/metastatic stage IV NSCLC not previously treated for their metastatic disease and receiving at least one PD-(L)1 inhibitor in combination with a chemotherapeutic agent were eligible for inclusion. Efficacy outcomes regarding combinations of immunotherapy plus chemotherapy expressed as PFS or OS had to be provided. Observational studies, editorials, reviews, and commentaries were excluded.

2.3. Statistical Analysis

The DerSimonian–Laird random effects models for main and subgroup analyses was implemented, assessing heterogeneity of effect-size estimates from the individual studies by Cochran's Q test and the I^2 statistic. Additionally, MA corresponding to analysis of binary data of proportions was also performed using a DerSimonian–Laird random effects model without transformation of the proportion. A high level of heterogeneity was considered if I^2 was greater than 50%. Due to the relatively low number of trials involved in this MA, values and significance of heterogeneity must be considered as guidance only [26]. Statistical significance was reached for *p*-values less than 0.05. Analyses were not controlled for multiplicity; no alpha was assigned to the different analyses. The nature of this study is therefore exploratory, mainly in the subgroup analysis. Hazard ratios (HRs) and 95% confidence intervals (CIs) for OS and PFS from the overall population and subgroups from each individual trial of advanced NSCLC were calculated. For dichotomous data, odds ratios (ORs) were estimated. The MA was performed using Open Meta Analyst v. 10 (Center for Evidence Synthesis in Health, Brown University). Recommendations of the Cochrane Collaboration and the Preferred Reporting Items for Systematic Reviews and Meta-Analyses (PRISMA) guidelines were followed for this MA [27].

For the ORR, different endpoints, including complete response (CR), partial response (PR), stable disease (SD), and progressive disease (PD), were alternately modeled. These sensitivity analyses along with those for OS and PFS did not quantitatively alter the results and conclusions of the main analyses.

3. Results

3.1. Studies Included in the Meta-Analysis

A total of 80 records from PubMed were screened. Three additional studies presented at the WCLC and/or ESMO were also included. Study selection and exclusion criteria are summarized in Figure 1. Finally, seven clinical trials carried out with 4562 patients met the inclusion criteria and were included in the MA [17,20–25,28,29]. In the specific case of CheckMate-227, part 1 [30] was excluded because immunotherapy-plus-chemotherapy efficacy evaluation was not part of the main objectives; only part 2 was considered for this MA [21].

3.2. Study Characteristics

The specific characteristics of the studies included in the MA are summarized in Table 1. The control arm in all studies was platinum-based chemotherapy with pemetrexed (three studies [17,20,21,28]) or with nab-paclitaxel/paclitaxel (five studies [21–25,29]). In one three-arm trial (IMpower150 [24]), bevacizumab was added in the control and experimental arm. This study included two experimental arms: carboplatin, paclitaxel, and atezolizumab (arm A) and carboplatin, paclitaxel, bevacizumab, and atezolizumab (arm B) versus carboplatin, paclitaxel, and bevacizumab (arm C). No comparisons between arms A and C were performed because the HR may not reflect the actual effect of add-on immunotherapy (atezolizumab plus chemotherapy vs. bevacizumab plus chemotherapy).
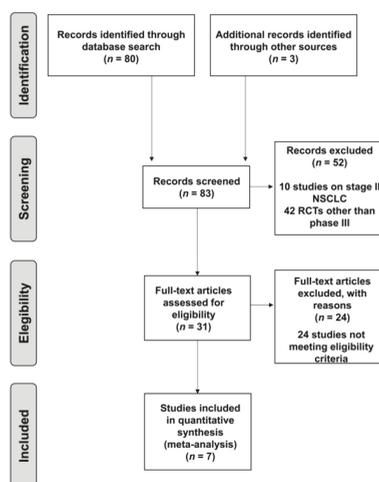
Figure 1. Flow chart of study selection (up to 1 January 2020). NSCLC, non-small-cell lung cancer; RCTs, randomized controlled trials.

Table 1. Characteristics and main outcomes of the studies included in the meta-analysis.

Study	Histology Expression	PD-L1 Expression	Primary Endpoint	Experimental Arm	Control Arm	Analysis Timing
IMpower130 [25]	Nonsquamous	All	PFS (ITT-WT *) OS (ITT-WT *)	Atezolizumab + (carboplatin + nab-paclitaxel) (*n* = 451)	Carboplatin + nab-paclitaxel (*n* = 228)	PFS: Final OS: Interim
IMpower150 [23,24]	Nonsquamous	All	PFS (ITT-WT *) OS (ITT-WT *)	Atezolizumab + (carboplatin + paclitaxel + bevacizumab) (*n* = 356)	Carboplatin + paclitaxel + bevacizumab (*n* = 336)	PFS: Final OS: Interim
KEYNOTE-189 [17,28]	Nonsquamous	All	PFS (ITT) OS (ITT)	Pembrolizumab + (carboplatin or cisplatin + pemetrexed) (*n* = 410)	Carboplatin or cisplatin + pemetrexed (*n* = 206)	PFS: Final OS: Interim
IMpower132 [20]	Nonsquamous	All	PFS (ITT) OS (ITT)	Atezolizumab + (carboplatin or cisplatin + pemetrexed) (*n* = 292)	Carboplatin or cisplatin + pemetrexed (*n* = 286)	PFS: Final OS: Interim
IMpower131 [29]	Squamous	All	PFS (ITT) OS (ITT)	Atezolizumab + (carboplatin + nab-paclitaxel) (*n* = 343)	Carboplatin + nab-paclitaxel (*n* = 340)	PFS: Final OS: Interim
KEYNOTE-407 [22]	Squamous	All	PFS (ITT) OS (ITT)	Pembrolizumab + (carboplatin + paclitaxel or nab-paclitaxel) (*n* = 278)	Carboplatin + paclitaxel or nab-paclitaxel (*n* = 281)	PFS: Final OS: Interim

* Patients with epidermal growth factor receptor (EGFR) or anaplastic lymphoma kinase (ALK) mutations excluded. PD-L1, programmed cell death-ligand 1; PFS, progression-free survival; OS, overall survival; ITT, intention-to-treat; WT, wildtype; +, plus (combination therapy).

Three studies tested anti-PD1 antibodies [17,21,22,28], and four studies tested anti-PD-L1 antibodies [20,23–25,29]. Patients with epidermal growth factor receptor (EGFR) or anaplastic lymphoma kinase (ALK) mutations were included in two clinical trials assessing atezolizumab [24,25]. Regarding the histology, four studies included patients with nonsquamous NSCLC [20,21,24,25], two included patients with squamous NSCLC [22,29], and one evaluated patients presenting both histological types [21] (note that the primary endpoint in CheckMate-227 part 2 was OS in nonsquamous mNSCLC patients only; however, both histological types were considered for this MA).

An all-comers design was used in all the studies, with NSCLC patients entering the trial regardless of their PD-L1 expression status. Stratification was performed based on this biomarker in all trials. Thus, subjects were classified as PD-L1-negative or PD-L1-positive, and within this group, investigators distinguished patients with high or low expression levels [20,25,29]. In the atezolizumab trials [20,23–25,29], levels were considered high (TC3 or IC3) when PD-L1 expression was recorded on at least 50% of tumor cells or at least 10% of tumor-infiltrating immune cells (TIICs) by immunohistochemistry; levels were considered low–intermediate, or TC1/2 or IC1/2, when expression was reported on at least 1% of tumor cells or TIICs and less than 50% of tumor cells or less than 10% of TIICs by immunohistochemistry; and PD-L1-negative status, or TC0 and IC0, was determined when expression was reported on less than 1% of tumor cells and TIICs. Similar criteria were followed in trials assessing pembrolizumab or nivolumab, but PD-L1 expression was only measured in tumor cells [17,21,22,28].

According to the eligibility criteria, none of the studies included patients who had received prior treatment for metastatic disease. However, in terms of therapy for nonmetastatic disease, although most of the studies included treatment-naïve patients, in those evaluating pembrolizumab (KEYNOTE-189 [17,28] and KEYNOTE-407 [22]) or atezolizumab [20,23–25,29], subjects had received previous therapies (Supplementary Table S1).

Coprimary endpoints for six clinical trials were PFS and OS [17,20,22–25,28,29]. The primary endpoint for CheckMate-227 part 2 was OS in nonsquamous NSCLC patients; PFS was assessed as a secondary endpoint [21]. Mature PFS data were reported in all the studies included in this MA [17,20–25,28,29], while final data for OS were available for only one of them [21]. Interim analyses were provided for the other six studies [17,20,22–25,28,29]. Both endpoints were evaluated in the intention-to-treat (ITT) population and specifically in the wildtype population (without EGFR or ALK mutations) in the IMpower130 [25] and IMpower150 studies [23,24] (see Supplementary Table S2 for the available information on patients with mutations in IMpower150). IMpower150 was the only study in which a subsequent subgroup analysis in patients with EGFR mutations or baseline liver metastasis was performed [23]. Additionally, one or both coprimary endpoints were analyzed according to different subgroups in all the studies included in the MA (PFS in six clinical trials [17,22–25,28,29] and OS in five studies [17,21,22,25,28,29]).

Patient population characteristics of all the studies included in the MA are shown in Supplementary Table S3.

3.3. Efficacy Endpoints in the Overall Population

Median PFS ranged from 4.8 to 6.8 months in the control arms and from 6.3 to 8.8 months in the treatment arms. Median OS ranged from 10.7 to 14.7 months in the control arms and from 14.2 to 22.0 months in the treatment arms. MA results demonstrated that the addition of a PD-(L)1 to chemotherapy was associated with improved PFS (PFS: $HR_{pooled} = 0.61$, 95% CI: 0.57–0.65, $p < 0.001$, Figure 2A) and OS (OS: $HR_{pooled} = 0.76$, 95% CI: 0.67–0.86; $p < 0.001$, Figure 2B) compared with chemotherapy alone. The objective response rate (ORR) was also significantly improved with the PD-(L)1 inhibitor–chemotherapy combination (odds ratio (OR_{pooled}) = 2.12, 95% CI: 1.70–2.63, $p < 0.001$, Supplementary Figure S1). The best ORR values were obtained in the IMpower150 (ORR = 56.4%) trial for nonsquamous NSCLC and KEYNOTE-407 for squamous NSCLC (57.9%). Notably, in terms of both OS and ORR, there was significant heterogeneity across the six trials ($I^2 = 52.07\%$, $p = 0.03$; $I^2 = 67.42\%$, $p = 0.005$).
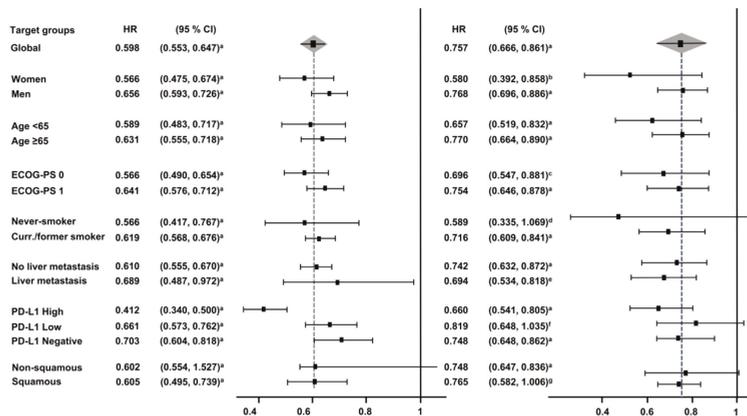
3.4. Subgroup Analysis

Subgroup analyses according to sex (women vs. men), age (<65 years vs. ≥65 years), Eastern Cooperative Oncology Group performance status (ECOG-PS = 0 vs. ECOG-PS = 1), smoking status (never-smoker vs. current/former smoker), liver metastasis (yes vs. no), and PD-L1 expression (high vs. low vs. negative) were carried out. As shown in Figure 3, overall, the addition of PD-(L)1 blockade to chemotherapy significantly improved PFS in all the subgroups. Specifically, stratification according

to PD-L1 expression revealed a benefit across all PD-L1 strata with a strong reduction in the risk of disease progression in those patients showing high expression levels (HR_{pooled} = 0.412, 95% CI: 0.34–0.5, p < 0.001). In terms of OS (Figure 3), although almost all subgroups benefited from the use of the PD-(L)1 inhibitor–chemotherapy combination, in certain cases, such as in never-smokers and PD-L1-low patients, results did not achieve statistical significance (HR_{pooled} = 0.589, 95% CI: 0.335–1.069, p = 0.082; HR_{pooled} = 0.819, 95% CI: 0.648–1.035, p = 0.093, respectively).
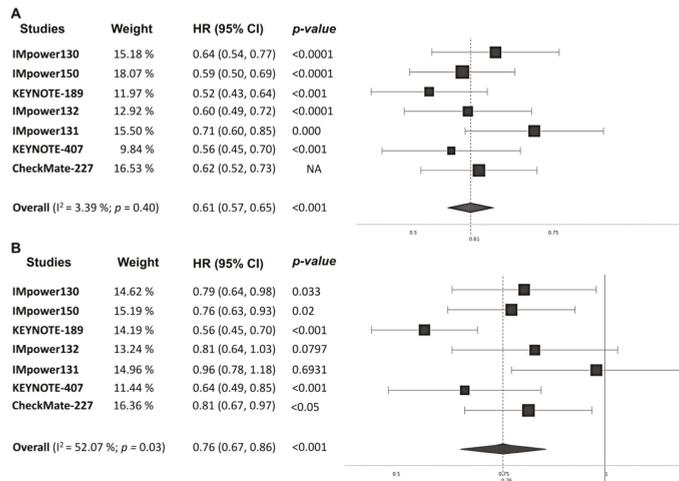
Figure 2. Forest plot of pooled hazard ratios for (**A**) progression-free survival (PFS) and (**B**) overall survival (OS) in patients who received programmed cell death-1 (PD-1)/programmed death ligand-1 (PD-L1) inhibitors plus chemotherapy vs. chemotherapy alone. HR, hazard ratio; CI, confidence interval.
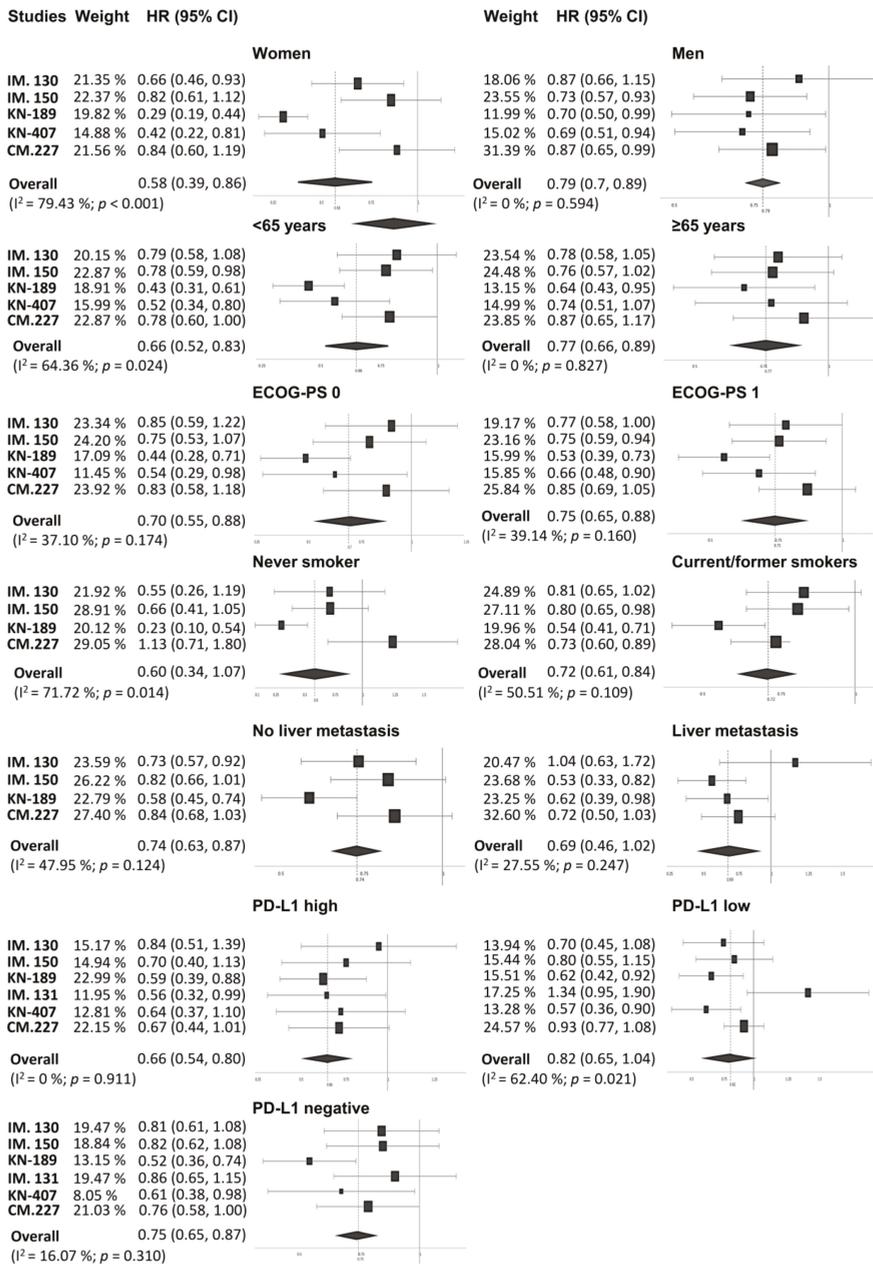

Figure 3. Forest plot of hazard ratios for progression-free survival (PFS) and overall survival (OS) in the subgroup analysis. PFS, progression-free survival; OS, overall survival. HR, hazard ratio; CI, confidence interval; Curr., current.; [a] p < 0.001; [b] p = 0.006; [c] p = 0.003; [d] p = 0.082; [e] p = 0.007; [f] p = 0.093; [g] p = 0.055.

Regarding patients with liver metastasis, a specific benefit with atezolizumab plus bevacizumab was observed both in terms of OS and PFS. Further details on the OS and PFS subgroup analyses are shown in Figures 4 and 5, respectively. Additional subgroup analyses based on the histology are available only for PFS and OS in Supplementary Figure S2.
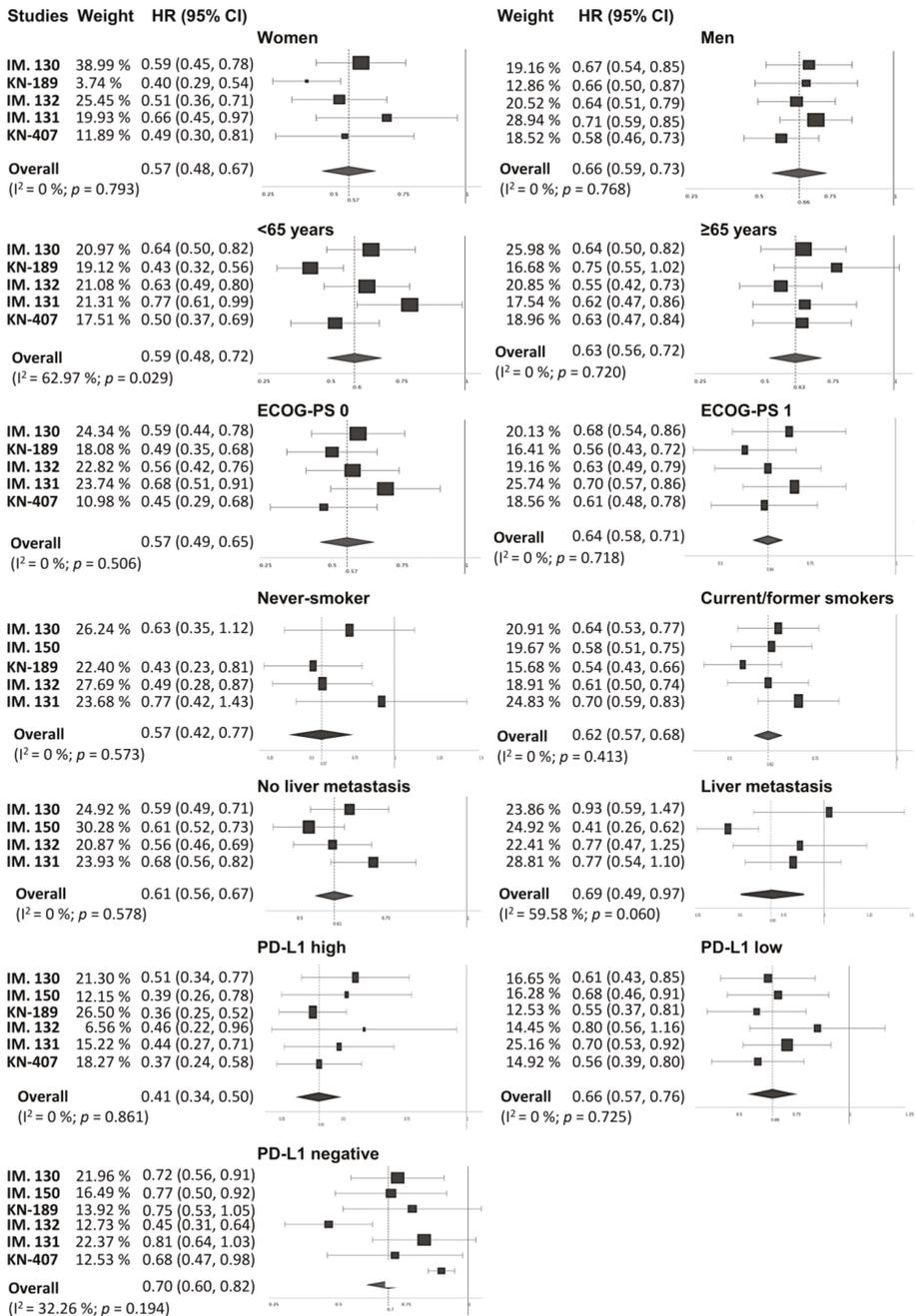
Figure 4. Forest plot of hazard ratios for progression-free survival (PFS) in the different patient subgroups. CI, confidence interval; ECOG-PS, Eastern Cooperative Oncology Group performance status; HR, hazard ratio; IM., IMpower; KN, KEYNOTE.

Figure 5. Forest plot of hazard ratios for overall survival (OS) in the different patient subgroups. CI, confidence interval; HR, hazard ratio; ECOG-PS, Eastern Cooperative Oncology Group performance status; IM., IMpower; KN, KEYNOTE; CM., CheckMate.

4. Discussion

The optimal treatment strategy for advanced NSCLC has been the focus of several randomized clinical trials. Promising immunotherapy results in the second or later lines of therapy resulted

in the approval of atezolizumab, pembrolizumab, and nivolumab [31–35]. Several clinical trials subsequently evaluated PD-(L)1 inhibitor–chemotherapy strategies in front-line treatment, some of which are included in this MA.

Our results demonstrate an overall benefit—both in terms of PFS and OS—of the addition of PD-(L)1 blockade. Although statistical significance was reached for the pooled HR for OS, substantial heterogeneity (I^2 of 52.07%) across the seven trials was also identified. Furthermore, it is worth mentioning that the most recent data were considered for this MA in the vast majority of cases and that, to date, this is the first analysis to include results from CheckMate-227 part 2 [21]. Positive efficacy results have also been reported by Tun et al. [36], who included almost the same trials as those analyzed in this study (CheckMate-227 data were collected from part 1 [37]). Other meta-analyses have also reported improvements in the efficacy of the combined strategy. Differences in these may be explained by the trials included therein, such as the study by Chen et al., in which comparisons of immune checkpoint inhibitors against chemotherapy were also considered [38]; the study by Shen et al. [39] with broader inclusion criteria (e.g., studies that directly or indirectly investigated the ORR, the disease control response (DCR), or some safety endpoints); or the meta-analysis by Addeo et al. [40], in which studies using avelumab and durvalumab were also considered. Thus, our results support the evidence that a combination strategy of PD-(L)1 inhibitor plus chemotherapy may be beneficial compared to chemotherapy alone. Indeed, to date, the combination of pembrolizumab or atezolizumab with platinum-based chemotherapy, with or without bevacizumab, are EMA-approved options available for first-line treatment of advanced/metastatic NSCLC wildtype tumors.

With respect to subgroup analyses, overall benefits were reported across the different categories. Specifically, analysis in terms of PD-L1 marker yielded a statistically significant improvement in PFS regardless of the level of PD-L1 expression. In the case of OS, improvements were observed in patients with high PD-L1 expression and patients negative for this biomarker, but not in those with low levels, probably because of the moderate–high heterogeneity recorded in the pooled analysis ($I^2 = 67.01\%$; $p = 0.016$). It is also important to note that the studies included utilized different PD-L1 assay methods, possibly representing an additional confounding factor to be considered. Other subgroup analyses also resulted in important outcomes. Thus, this meta-analysis demonstrated that patients benefited from additional immunotherapy regardless of their age. It should be noted that the impact of advanced age on the effectiveness of immune checkpoint inhibitors has not been strongly established so far, highlighting the importance of these findings. Interestingly, combinations with pembrolizumab yielded the lowest HR values in terms of both PFS and OS in several subgroups, including women, patients <65 years, and patients with ECOG-PS = 0, pointing to a potential benefit in these individuals. With respect to liver metastasis, in the IMpower150 trial [23,24], improvements were reported both in terms of PFS and OS, suggesting a specific benefit with the atezolizumab and bevacizumab combination. Indeed, although other atezolizumab trials previously reported outcomes in patients with liver metastases, data from IMpower130 [41] and IMpower132 [42] showed no survival benefit with atezolizumab plus chemotherapy, supporting the benefits of adding the antiangiogenic agent in the combination [23]. Despite the fact that the updated KEYNOTE-189 analysis showed a clinical benefit of pembrolizumab-containing regimens over chemotherapy alone in patients with liver metastases (median OS 12.6 vs. 6.6, OS HR 0.62, 12-month OS rate 51% vs. 3%) [43], this baseline characteristic, in contrast with the IMpower trials, was not a stratification factor in the study.

Most clinical trials do not include advanced NSCLC patients with driver mutations. IMpower150 was the only study to include this type of patient, showing a positive trend in OS probably due to the addition of bevacizumab to the combination strategy, as previously discussed [43]. However, this therapeutic strategy for patients with EGFR/ALK mutations should be further confirmed in prospective, randomized studies.

This meta-analysis also has some limitations. First, as mentioned, the PD-L1 assay methods were not consistent across different studies. Thus, while PD-L1 immunohistochemistry was read on both tumor cells and tumor-infiltrating cells in the atezolizumab studies (IMpower) [20,24,25,29,43], PD-L1

expression was only measured on tumor cells in the trials assessing pembrolizumab (KEYNOTE) and nivolumab (CheckMate-227), [17,21,22,28]. Second, six of the included trials only provided interim analysis of the OS [17,20,22,24,25,28,29,43], which may misrepresent overall efficacy. Finally, the subgroup analysis was limited by the available information (PFS subgroup analyses were not assessed in CheckMate-227), and consequently caution must be exercised when interpreting the results. In this regard, certain limitations were also found with the available data of three of the studies, IMpower131, IMpower132, and CheckMate-227 part 2, whose results have only been published as congress abstracts and personal communications to date [20,21,29]. Despite these limitations, our results confirm those obtained in individual studies and are in line with the outcomes obtained in similar meta-analyses.

In conclusion, treatment with PD-(L)1 inhibitors resulted in significantly longer OS and PFS in stage IV NSCLC patients compared with chemotherapy alone. As a result, immunotherapy–chemotherapy combinations may be considered as a first-line strategy for these patients.

References

1. Torre, L.A.; Siegel, R.L.; Jemal, A. Lung Cancer Statistics. *Adv. Exp. Med. Biol.* **2016**, *893*, 1–19.
2. Planchard, D.; Popat, S.; Kerr, K.; Novello, S.; Smit, E.F.; Faivre-Finn, C.; Mok, T.S.; Reck, M.; Van Schil, P.E.; Hellmann, M.D.; et al. Metastatic non-small cell lung cancer: ESMO Clinical Practice Guidelines for diagnosis, treatment and follow-up. *Ann. Oncol.* **2018**, *29*, iv192–iv237. [CrossRef] [PubMed]
3. Goldstraw, P.; Chansky, K.; Crowley, J.; Rami-Porta, R.; Asamura, H.; Eberhardt, W.E.; Nicholson, A.G.; Groome, P.; Mitchell, A.; Bolejack, V. The IASLC Lung Cancer Staging Project: Proposals for Revision of the TNM Stage Groupings in the Forthcoming (Eighth) Edition of the TNM Classification for Lung Cancer. *J. Thorac. Oncol.* **2016**, *11*, 39–51. [CrossRef] [PubMed]
4. Antonia, S.J.; Villegas, A.; Daniel, D.; Vicente, D.; Murakami, S.; Hui, R.; Yokoi, T.; Chiappori, A.; Lee, K.H.; de Wit, M.; et al. Durvalumab after Chemoradiotherapy in Stage III Non-Small-Cell Lung Cancer. *N. Engl. J. Med.* **2017**, *377*, 1919–1929. [CrossRef] [PubMed]
5. Horn, L.; Mansfield, A.S.; Szczesna, A.; Havel, L.; Krzakowski, M.; Hochmair, M.J.; Huemer, F.; Losonczy, G.; Johnson, M.L.; Nishio, M.; et al. First-Line Atezolizumab plus Chemotherapy in Extensive-Stage Small-Cell Lung Cancer. *N. Engl. J. Med.* **2018**, *379*, 2220–2229. [CrossRef]
6. Paz-Ares, L.; Dvorkin, M.; Chen, Y.; Reinmuth, N.; Hotta, K.; Trukhin, D.; Statsenko, G.; Hochmair, M.J.; Ozguroglu, M.; Ji, J.H.; et al. Durvalumab plus platinum-etoposide versus platinum-etoposide in first-line treatment of extensive-stage small-cell lung cancer (CASPIAN): A randomised, controlled, open-label, phase 3 trial. *Lancet* **2019**, *394*, 1929–1939. [CrossRef]
7. Lu, M.; Su, Y. Immunotherapy in non-small cell lung cancer: The past, the present, and the future. *Thorac. Cancer* **2019**, *10*, 585–586. [CrossRef]
8. Fehrenbacher, L.; von Pawel, J.; Park, K.; Rittmeyer, A.; Gandara, D.R.; Ponce Aix, S.; Han, J.Y.; Gadgeel, S.M.; Hida, T.; Cortinovis, D.L.; et al. Updated Efficacy Analysis Including Secondary Population Results for OAK: A Randomized Phase III Study of Atezolizumab versus Docetaxel in Patients with Previously Treated Advanced Non-Small Cell Lung Cancer. *J. Thorac. Oncol.* **2018**, *13*, 1156–1170. [CrossRef]
9. Font, E.; Gettinger, S.N.; Burgio, M.; Antonia, S.J.; Holgado, E.; Spigel, D.R.; Arrieta, O.; Domine, M.; Aren, O.; Brahmer, J.; et al. 1301PD Three-year follow-up from CheckMate 017/057: Nivolumab versus docetaxel in patients with previously treated advanced non-small cell lung cancer (NSCLC). *Ann. Oncol.* **2017**. [CrossRef]
10. Herbst, R.; Baas, P.; Kim, D.-S.; Felip, E.; Perez-Gracia, J.L.; Han, J.-Y.; Molina, J.; Kim, J.-P.; Arvis, C.; Ahn, M.-J.; et al. Factors associated with better overall survival (OS) in patients with previously treated, PD-L1–expressing, advanced NSCLC: Multivariate analysis of KEYNOTE-010. *J. Clin. Oncol.* **2017**, *35*, 9090. [CrossRef]
11. Reck, M.; Rodriguez-Abreu, D.; Robinson, A.G.; Hui, R.; Csoszi, T.; Fulop, A.; Gottfried, M.; Peled, N.; Tafreshi, A.; Cuffe, S.; et al. Pembrolizumab versus Chemotherapy for PD-L1-Positive Non-Small-Cell Lung Cancer. *N. Engl. J. Med.* **2016**, *375*, 1823–1833. [CrossRef] [PubMed]
12. Reck, M.; Rodriguez-Abreu, D.; Robinson, A.G.; Hui, R.; Csoszi, T.; Fulop, A.; Gottfried, M.; Peled, N.; Tafreshi, A.; Cuffe, S.; et al. Updated Analysis of KEYNOTE-024: Pembrolizumab Versus Platinum-Based Chemotherapy for Advanced Non-Small-Cell Lung Cancer With PD-L1 Tumor Proportion Score of 50% or Greater. *J. Clin. Oncol.* **2019**, *37*, 537–546. [CrossRef] [PubMed]
13. Mok, T.S.K.; Wu, Y.L.; Kudaba, I.; Kowalski, D.M.; Cho, B.C.; Turna, H.Z.; Castro, G., Jr.; Srimuninnimit, V.; Laktionov, K.K.; Bondarenko, I.; et al. Pembrolizumab versus chemotherapy for previously untreated, PD-L1-expressing, locally advanced or metastatic non-small-cell lung cancer (KEYNOTE-042): A randomised, open-label, controlled, phase 3 trial. *Lancet* **2019**, *393*, 1819–1830. [CrossRef]
14. Lopes, G.; Wu, Y.-L.; Kudaba, I.; Kowalski, D.; Cho, B.C.; Castro, G.; Srimuninnimit, V.; Bondarenko, I.; Kubota, K.; Lubiniecki, G.M.; et al. Pembrolizumab (pembro) versus platinum-based chemotherapy (chemo) as first-line therapy for advanced/metastatic NSCLC with a PD-L1 tumor proportion score (TPS) ≥ 1%: Open-label, phase 3 KEYNOTE-042 study. *J. Clin. Oncol.* **2018**, *36*. [CrossRef]
15. Carbone, D.P.; Reck, M.; Paz-Ares, L.; Creelan, B.; Horn, L.; Steins, M.; Felip, E.; van den Heuvel, M.M.; Ciuleanu, T.E.; Badin, F.; et al. First-Line Nivolumab in Stage IV or Recurrent Non-Small-Cell Lung Cancer. *N. Engl. J. Med.* **2017**, *376*, 2415–2426. [CrossRef] [PubMed]
16. Apetoh, L.; Ladoire, S.; Coukos, G.; Ghiringhelli, F. Combining immunotherapy and anticancer agents: The right path to achieve cancer cure? *Ann. Oncol.* **2015**, *26*, 1813–1823. [CrossRef]

17. Gadgeel, S.M.; Garassino, M.C.; Esteban, E.; Speranza, G.; Felip, E.; Hochmair, M.J.; Powell, S.F.; Cheng, S.Y.; Bischoff, H.; Peled, N.; et al. KEYNOTE-189: Updated OS and progression after the next line of therapy (PFS2) with pembrolizumab (pembro) plus chemo with pemetrexed and platinum vs placebo plus chemo for metastatic nonsquamous NSCLC. *J. Clin. Oncol.* **2019**, *37*, 9013. [CrossRef]

18. Jotte, R.; Cappuzzo, F.; Vynnychenko, I.; Stroyakovskiy, D.; Rodriguez-Abreu, D.; Hussein, M.; Soo, R.; Conter, H.J.; Kozuki, T.; Huang, K.; et al. Atezolizumab in Combination With Carboplatin and Nab-Paclitaxel in Advanced Squamous Non-Small-Cell Lung Cancer (IMpower131): Results From a Randomized Phase III Trial. *J. Thorac. Oncol.* **2020**. [CrossRef]

19. Langer, C.J.; Gadgeel, S.M.; Borghaei, H.; Papadimitrakopoulou, V.A.; Patnaik, A.; Powell, S.F.; Gentzler, R.D.; Martins, R.G.; Stevenson, J.P.; Jalal, S.I.; et al. Carboplatin and pemetrexed with or without pembrolizumab for advanced, non-squamous non-small-cell lung cancer: A randomised, phase 2 cohort of the open-label KEYNOTE-021 study. *Lancet Oncol.* **2016**, *17*, 1497–1508. [CrossRef]

20. Papadimitrakopoulou, V.; Cobo, M.; Bordoni, R.; Dubray-Longeras, P.; Szalai, Z.; Ursol, G.; Novello, S.; Orlandi, F.; Ball, S.; Goldschmidt, J.; et al. OA05.07 IMpower132: PFS and Safety Results with 1L Atezolizumab + Carboplatin/Cisplatin + Pemetrexed in Stage IV Non-Squamous NSCLC. *J. Thorac. Oncol.* **2018**, *13*, S332–S333. [CrossRef]

21. Paz-Ares, L.; Ciuleanu, T.E.; Yu, X.; Salman, P.; Pluzanski, A.; Nagrial, A.; Havel, L.; Kowalyszyn, R.; Audigier-Valette, C.; Wu, Y.L.; et al. LBA3 Nivolumab (NIVO) + platinum-doublet chemotherapy (chemo) vs chemo as first-line (1L) treatment (tx) for advanced non-small cell lung cancer (aNSCLC): CheckMate 227 - part 2 final analysis. *Ann. Oncol.* **2019**, *30*, xi67–xi68. [CrossRef]

22. Paz-Ares, L.; Luft, A.; Vicente, D.; Tafreshi, A.; Gumus, M.; Mazieres, J.; Hermes, B.; Cay Senler, F.; Csoszi, T.; Fulop, A.; et al. Pembrolizumab plus Chemotherapy for Squamous Non-Small-Cell Lung Cancer. *N. Engl. J. Med.* **2018**, *379*, 2040–2051. [CrossRef]

23. Reck, M.; Mok, T.S.K.; Nishio, M.; Jotte, R.M.; Cappuzzo, F.; Orlandi, F.; Stroyakovskiy, D.; Nogami, N.; Rodriguez-Abreu, D.; Moro-Sibilot, D.; et al. Atezolizumab plus bevacizumab and chemotherapy in non-small-cell lung cancer (IMpower150): Key subgroup analyses of patients with EGFR mutations or baseline liver metastases in a randomised, open-label phase 3 trial. *Lancet Respir. Med.* **2019**, *7*, 387–401. [CrossRef]

24. Socinski, M.A.; Jotte, R.M.; Cappuzzo, F.; Orlandi, F.; Stroyakovskiy, D.; Nogami, N.; Rodriguez-Abreu, D.; Moro-Sibilot, D.; Thomas, C.A.; Barlesi, F.; et al. Atezolizumab for First-Line Treatment of Metastatic Nonsquamous NSCLC. *N. Engl. J. Med.* **2018**, *378*, 2288–2301. [CrossRef] [PubMed]

25. West, H.; McCleod, M.; Hussein, M.; Morabito, A.; Rittmeyer, A.; Conter, H.J.; Kopp, H.G.; Daniel, D.; McCune, S.; Mekhail, T.; et al. Atezolizumab in combination with carboplatin plus nab-paclitaxel chemotherapy compared with chemotherapy alone as first-line treatment for metastatic non-squamous non-small-cell lung cancer (IMpower130): A multicentre, randomised, open-label, phase 3 trial. *Lancet Oncol.* **2019**, *20*, 924–937. [CrossRef]

26. Cochrane Collaboration. *Cochrane Handbook for Systematic Reviews of Interventions*; John Wiley & Sons: Chichester, UK; Hoboken, NJ, USA, 2008.

27. Moher, D.; Liberati, A.; Tetzlaff, J.; Altman, D.G. Preferred reporting items for systematic reviews and meta-analyses: The PRISMA statement. *J. Clin. Epidemiol.* **2009**, *62*, 1006–1012. [CrossRef]

28. Gandhi, L.; Rodríguez-Abreu, D.; Gadgeel, S.; Esteban, E.; Felip, E.; Angelis, F.D.; Domine, M.; Clingan, P.; Hochmair, M.J.; Powell, S.; et al. Abstract CT075: KEYNOTE-189: Randomized, double-blind, phase 3 study of pembrolizumab (pembro) or placebo plus pemetrexed (pem) and platinum as first-line therapy for metastatic NSCLC. *Cancer Res.* **2018**, *78*, CT075.

29. Jotte, R.M.; Cappuzzo, F.; Vynnychenko, I.; Stroyakovskiy, D.; Rodriguez Abreu, D.; Hussein, M.A.; Soo, R.A.; Conter, H.J.; Kozuki, T.; Silva, C.; et al. IMpower131: Primary PFS and safety analysis of a randomized phase III study of atezolizumab + carboplatin + paclitaxel or nab-paclitaxel vs carboplatin + nab-paclitaxel as 1L therapy in advanced squamous NSCLC. *J. Clin. Oncol.* **2018**, *36*, LBA9000. [CrossRef]

30. Hellmann, M.D.; Ciuleanu, T.E.; Pluzanski, A.; Lee, J.S.; Otterson, G.A.; Audigier-Valette, C.; Minenza, E.; Linardou, H.; Burgers, S.; Salman, P.; et al. Nivolumab plus Ipilimumab in Lung Cancer with a High Tumor Mutational Burden. *N. Engl. J. Med.* **2018**, *378*, 2093–2104. [CrossRef]

31. Conforti, F.; Pala, L.; Bagnardi, V.; De Pas, T.; Martinetti, M.; Viale, G.; Gelber, R.D.; Goldhirsch, A. Cancer immunotherapy efficacy and patients' sex: A systematic review and meta-analysis. *Lancet Oncol.* **2018**, *19*, 737–746. [CrossRef]

32. Tan, P.S.; Aguiar, P.; Haaland, B.; Lopes, G. Comparative effectiveness of immune-checkpoint inhibitors for previously treated advanced non-small cell lung cancer—A systematic review and network meta-analysis of 3024 participants. *Lung Cancer* **2018**, *115*, 84–88. [CrossRef]

33. You, W.; Liu, M.; Miao, J.D.; Liao, Y.Q.; Song, Y.B.; Cai, D.K.; Gao, Y.; Peng, H. A Network Meta-analysis Comparing the Efficacy and Safety of Anti-PD-1 with Anti-PD-L1 in Non-small Cell Lung Cancer. *J. Cancer* **2018**, *9*, 1200–1206. [CrossRef]

34. Zhou, G.-W.; Xiong, Y.; Chen, S.; Xia, F.; Li, Q.; Hu, J. Anti-PD-1/PD-L1 antibody therapy for pretreated advanced nonsmall-cell lung cancer: A meta-analysis of randomized clinical trials. *Medicine* **2016**, *95*, e4611. [CrossRef] [PubMed]

35. Zhao, Q.; Xie, R.; Lin, S.; You, X.; Weng, X. Anti-PD-1/PD-L1 Antibody Therapy for Pretreated Advanced or Metastatic Nonsmall Cell Lung Carcinomas and the Correlation between PD-L1 Expression and Treatment Effectiveness: An Update Meta-Analysis of Randomized Clinical Trials. *BioMed. Res. Int.* **2018**, *2018*, 3820956. [CrossRef] [PubMed]

36. Tun, A.M.; Thein, K.Z.; Thein, W.L.; Guevara, E. Checkpoint inhibitors plus chemotherapy for first-line treatment of advanced non-small cell lung cancer: A systematic review and meta-analysis of randomized controlled trials. *Future Sci. OA* **2019**, *5*, Fso421. [CrossRef]

37. Hellmann, M.D.; Paz-Ares, L.; Bernabe Caro, R.; Zurawski, B.; Kim, S.W.; Carcereny Costa, E.; Park, K.; Alexandru, A.; Lupinacci, L.; de la Mora Jimenez, E.; et al. Nivolumab plus Ipilimumab in Advanced Non-Small-Cell Lung Cancer. *N. Engl. J. Med.* **2019**, *381*, 2020–2031. [CrossRef]

38. Chen, Y.; Zhou, Y.; Tang, L.; Peng, X.; Jiang, H.; Wang, G.; Zhuang, W. Immune-Checkpoint Inhibitors as the First Line Treatment of Advanced Non-Small Cell Lung Cancer: A Meta-Analysis of Randomized Controlled Trials. *J. Cancer* **2019**, *10*, 6261–6268. [CrossRef]

39. Shen, K.; Cui, J.; Wei, Y.; Chen, X.; Liu, G.; Gao, X.; Li, W.; Lu, H.; Zhan, P.; Lv, T.; et al. Effectiveness and safety of PD-1/PD-L1 or CTLA4 inhibitors combined with chemotherapy as a first-line treatment for lung cancer: A meta-analysis. *J. Thorac. Dis.* **2018**, *10*, 6636–6652. [CrossRef] [PubMed]

40. Addeo, A.; Banna, G.L.; Metro, G.; Di Maio, M. Chemotherapy in Combination with Immune Checkpoint Inhibitors for the First-Line Treatment of Patients With Advanced Non-small Cell Lung Cancer: A Systematic Review and Literature-Based Meta-Analysis. *Front. Oncol.* **2019**, *9*, 264. [CrossRef] [PubMed]

41. Cappuzzo, F.M.M.; Hussein, M.; Morabito, A.; Rittmeyer, A.; Conter, H.J.; Kopp, H.; Daniel, D.; McCune, S.; Mekhail, T.; Zer, A.; et al. IMpower130: Progression-free survival (PFS) and safety analysis from a randomised phase 3 study of carboplatin + nab-paclitaxel (CnP) with or without atezolizumab (atezo) as first-line (1L) therapy in advanced non-squamous NSCLC. *Ann. Oncol.* **2018**, *29*, mdy424-065. [CrossRef]

42. Barlesi, F.N.M.; Cobo, M.; Steele, N.; Paramonov, V.; Parente, B.; Dear, R.; Berard, H.; Peled, N.; Seneviratne, L.C.; Baldini, E.; et al. IMpower132: Efficacy of atezolizumab (atezo)+carboplatin (carbo)/cisplatin (cis)+pemetrexed (pem) as 1L treatment in key subgroups with stage IV non-squamous non-small cell lung cancer (NSCLC). *Ann. Oncol.* **2018**, *29*, mdy424-066. [CrossRef]

43. Garassino, M.C.; Gadgeel, S.; Esteban, E.; Felip, E.; Speranza, G.; Angelis, F.D.; Domine, M.; Clingan, P.; Hochmair, M.J.; Powell, S.F.; et al. Abstract CT043: Outcomes among patients (pts) with metastatic nonsquamous NSCLC with liver metastases or brain metastases treated with pembrolizumab (pembro) plus pemetrexed-platinum: Results from the KEYNOTE-189 study. *Cancer Res.* **2019**, *79*, CT043.

Endocrinopathies Associated with Immune Checkpoint Inhibitor Cancer Treatment: A Review

Naoko Okura [1], Mai Asano [2], Junji Uchino [1,*], Yoshie Morimoto [1], Masahiro Iwasaku [1], Yoshiko Kaneko [1], Tadaaki Yamada [1], Michiaki Fukui [2] and Koichi Takayama [1]

[1]   Department of Pulmonary Medicine, Graduate School of Medical Science, Kyoto Prefectural University of Medicine, Kyoto 602-8566, Japan; ku-n07@koto.kpu-m.ac.jp (N.O.); yoshie-m@koto.kpu-m.ac.jp (Y.M.); miwasaku@koto.kpu-m.ac.jp (M.I.); kaneko-y@koto.kpu-m.ac.jp (Y.K.); tayamada@koto.kpu-m.ac.jp (T.Y.); takayama@koto.kpu-m.ac.jp (K.T.)

[2]   Department of Endocrinology and Metabolism, Graduate School of Medical Science, Kyoto Prefectural University of Medicine, Kyoto 602-8566, Japan; maias@koto.kpu-m.ac.jp (M.A.); michiaki@koto.kpu-m.ac.jp (M.F.)

*   Correspondence: uchino@koto.kpu-m.ac.jp; Tel.: +81-75-251-5513

Abstract: Treatment with immune checkpoint inhibitors has shown efficacy against a variety of cancer types. The effects of nivolumab and pembrolizumab on lung cancer have been reported, and further therapeutic advances are ongoing. The side effects of immune checkpoint inhibitors are very different from those of conventional cytocidal anticancer drugs and molecular targeted drugs, and they involve various organs such as the digestive and respiratory organs, thyroid and pituitary glands, and skin. The generic term for such adverse events is immune-related adverse events (irAEs). They are relatively infrequent, and, if mild, treatment with immune checkpoint inhibitors can be continued with careful control. However, early detection and appropriate treatment are critical, as moderate-to-severe irAEs are associated with markedly reduced organ function and quality of life, with fatal consequences in some cases. Of these, endocrinopathies caused by immune checkpoint inhibitors are sometimes difficult to distinguish from nonspecific symptoms in patients with advanced cancer and may have serious outcomes when the diagnosis is delayed. Therefore, it is necessary to anticipate and appropriately address the onset of endocrinopathies during treatment with immune checkpoint inhibitors. Here, we present a review of endocrine disorders caused by immune checkpoint inhibitor treatment.

Keywords: immune checkpoint inhibitors; immune-related adverse events; endocrine disorders; tumor-bearing patients

1. Introduction

In 2011, the Food and Drug Administration (FDA) approved the immune checkpoint inhibitor (ICI) ipilimumab, an anti-cytotoxic T-lymphocyte antigen-4 (anti-CTLA-4) antibody, for the treatment of malignant melanoma. Since then, anti-programmed cell death 1 (anti-PD-1) antibodies, such as nivolumab and pembrolizumab, and anti-programmed death ligand 1 (PD-L1) antibodies, such as atezolizumab and durvalumab, have been developed and approved for lung cancer treatment [1]. The effectiveness of cancer immunotherapy using these drugs can also be observed in cases receiving combined treatment with cytotoxic anticancer drugs and radiotherapy, and further expansion of the indications is expected in future.

CTLA-4 is a protein expressed on the surfaces of activated T-cells, and it inhibits T-cell activation after binding to antigen-presenting cells [2,3]. Anti-CTLA-4 antibodies bind to CTLA-4 and block the inhibitory receptors of activated T-cells, thus exerting antitumor effects. They also bind to the surface

CTLA-4 in regulatory T-cells (Tregs), thus reducing the immunosuppressive function of Tregs and enhancing tumor immune responses [4]. Furthermore, they are thought to reduce Tregs in tumor tissue via antibody-dependent cellular cytotoxicity (ADCC) and induce tumor cell death [5–7].

PD-1 is expressed on the surfaces of activated T-cells, and its binding with one of its ligands, PD-L1, inhibits T-cell activation [8]. Anti-PD-1 and anti-PD-L1 antibodies block the inhibitory system's signal to T-cells by obstructing such bindings, thus exerting antitumor effects. Therefore, while ICIs exhibit antitumor effects via a novel mechanism, immune adjustments do not work correctly in all cases, and side effects resembling autoimmune and inflammatory diseases have been reported. These types of adverse events, termed immune-related adverse events (irAEs), are characteristic side effects of ICI treatment, being distinct from the side effects of conventional anticancer drug treatment [9]. IrAEs involve almost the entire body, including the skin, gastrointestinal tract, and liver. In particular, endocrinopathy is a relatively frequent irAE [10,11].

Hypopituitarism, adrenocortical dysfunction, thyroid dysfunction, and type 1 diabetes mellitus are common endocrine disorders caused by ICI treatment [12]. Moreover, a small association between hypoparathyroidism and ICI treatment has been reported [13–16]. Pituitary dysfunction is frequent in patients receiving anti-CTLA-4 antibodies, while thyroid dysfunction is prevalent in patients receiving anti-PD-1/anti-PD-L1 antibodies [9,12]. Adrenal insufficiency is infrequent in patients treated with either drug [9,12]. Many symptoms of adrenal insufficiency, such as anorexia and malaise, are nonspecific and often observed in tumor-bearing patients. However, adrenal insufficiency can progress to fatal disease states such as adrenal crisis, and early detection and treatment according to the cause are necessary. Finally, although the frequency of type I diabetes mellitus associated with ICI treatment is small, clinicians should be aware that some cases can develop fulminant disease and should take the necessary actions in the early stages. It is important to be aware that symptoms such as fatigue caused by endocrinopathy may be misidentified as caused by the underlying cancer, and that endocrinopathy may occur with this drug when using immune checkpoint inhibitors. Table 1 shows the major ICIs indications and irAEs.

Table 1. Indication and major endocrinopathies of immune checkpoint inhibitors (ICIs).

Target	Drug	Indication	Major Endocrinopathies
Anti CTLA-4 antibody	Ipilimumab	Malignant melanoma	Hypopituitarism
		Renal cell cancer	
Anti-PD-1 antibody	Nivolumab	Malignant melanoma	Hypothyroidism Hyperthyroidism
		Non-small cell lung cancer	
		Renal cell cancer	
		Hodgkin lymphoma	
		Head and neck cancer	
		Gastric cancer	
		Malignant mesothelioma	
		Colorectal cancer with high-frequency microsatellite instability (MSI-High)	
		Esophageal cancer	
	Pembrolizumab	Non-small cell lung cancer	Hypothyroidism Hyperthyroidism
		Hodgkin lymphoma	
		Urothelial cancer	
		Solid cancers with high-frequency microsatellite instability (MSI-High)	
		Renal cell cancer	
		Head and neck cancer	
Anti PD-L1 antibody	Atezolizumab	Non-small cell lung cancer	Hypothyroidism
		Small cell lung cancer	
		Breast cancer	
	Durvalumab	Non-small cell lung cancer	Hypothyroidism Hyperthyroidism
	Avelumab	Merkel cell carcinoma renal cell cancer	Hypothyroidism

PD-1, programmed cell death 1; PD-L1, programmed death ligand 1; CTLA-4, cytotoxic T-lymphocyte antigen-4.

Here we present a review of endocrine disorders caused by ICI treatment.

2. Hypopituitarism

Hypopituitarism as an irAE is more common in patients receiving anti-CTLA-4 antibodies than in those receiving anti-PD-1/anti-PD-L1 antibodies, with the reported incidences being approximately 10% and ≤1% [17–22]. In addition, it has been reported that the incidence of hypophituitarism is higher with the concomitant use of anti-CTLA-4, and anti-PD-1/PD-L1 antibodies are more common than the use of a single agent [12]. Hypopituitarism caused by ICI treatment is classified into hypophysitis and isolated adrenocorticotropic (ACTH) deficiency. Pituitary gland enlargement is seen in hypophysitis, which causes hyposecretion of several anterior pituitary hormones, including thyroid-stimulating hormone (TSH), gonadotropins, and ACTH. On the other hand, the pituitary gland does not enlarge in ACTH deficiency, wherein the secretory capacity of only ACTH is reduced. There are very few reports of posterior pituitary dysfunction [17,23]. Although both patterns of dysfunction can occur in patients receiving anti-CTLA-4 antibodies, the use of anti-PD-1/anti-PD-L1 antibodies has been associated with ACTH deficiency in most cases [17,20,24]. Hypopituitarism often develops 4–10 weeks after treatment initiation due to anti-CTLA-4 antibodies [12]. An association between the incidence and the dose has also been noted, with one report showing a two-fold higher incidence in patients receiving high-dose ipilimumab (10 mg/kg) than in those receiving low-dose ipilimumab (3 mg/kg) [19]. Moreover, the higher dose (10 mg/kg) resulted in more adverse events than did the lower dose (3 mg/kg). However, significantly longer survival associated with the higher dose has been documented in some reports, and an association between irAE development and treatment efficacy has been pointed out [18,24]. Hypopituitarism also occurs within months to 1 year after treatment initiation due to anti-PD-1/anti-PD-L1 antibodies, and it may even develop after discontinuation of the drug [25–27]. It should be noted that ACTH hyposecretion always develops in all cases of hypopituitarism due to ICI treatment. The symptoms of ICI-induced hypopituitarism include anorexia and malaise due to secondary adrenal insufficiency, weight loss, gastrointestinal symptoms (nausea, vomiting, and diarrhea), hypotension, and hypoglycemia. In addition, headache, visual field impairment, and visual impairment occur in cases of hypophysitis with high-grade enlargement of the pituitary gland. In blood examination, abnormal findings such as hyponatremia and eosinophilia are recognized.

If hypopituitarism is suspected, it is necessary to measure the hormones secreted by the anterior pituitary gland and target organs. With regard to hypophysitis, diffuse enlargement and swelling of the pituitary gland and pituitary stalk with enhancement on contrast-enhanced magnetic resonance imaging are observed in more than half of the cases [17]. Subsequently, the enlarged pituitary gland gradually shrinks in the acute phase, and pituitary function is partially or completely lost [28,29]. During long-term observations, (median follow-up, 33 months) in one study, many of the thyroid and gonadal dysfunctions were found to be reversible, whereas ACTH hyposecretion was irreversible in most cases [29]. The pathogenesis of hypopituitarism due to ICI treatment remains unclear. In autopsied cases of pituitary dysfunction caused by tremelimumab, anti-CTLA-4 antibody, necrotic changes, and lymphocytic infiltrates with fibrosis were observed in the anterior pituitary gland. In addition, complement component 4 fragment (C4d) deposition associated with complement activation was observed; this suggested the involvement of both type IV and type II allergic reactions [17].

3. Adrenal Insufficiency

Adrenal insufficiency caused by ICI treatment includes primary and secondary adrenal insufficiency caused by hypopituitarism. Most cases are considered to have secondary adrenal insufficiency, and primary adrenal insufficiency is thought to be less frequent, with a reported incidence of 1.4% (95% confidence interval (CI): 0.9–2.2) for ipilimumab, 2.0% (95% CI: 0.9–4.3) for nivolumab, and 5.2% (95% CI: 2.9–9.2) to 7.6% (95% CI: 1.2–36.8) for nivolumab or pembrolizumab combined with ipilimumab [12]. The time of onset is estimated as one to several months after the start of treatment [22,30]. The symptoms of adrenal insufficiency are nonspecific and include fatigue, anorexia, abdominal pain, nausea, weight loss, hypotension, and hypoglycemia. The appearance of hyponatremia,

eosinophilia, and neutropenia suggests the development of adrenal insufficiency. A low morning serum cortisol level despite an elevated plasma ACTH level suggests primary adrenal insufficiency, whereas a low plasma ACTH level suggests secondary adrenal insufficiency. Serum cortisol levels of ≥18 μg/dL are considered to indicate the absence of adrenal dysfunction, while adrenal dysfunction is represented by serum cortisol levels of <4 μg/dL. When the serum cortisol level is ≥4 μg/dL and <18 μg/dL, a rapid ACTH tolerance test or an insulin-hypoglycemia test can confirm the diagnosis [31]. Bilateral adrenal enlargement on abdominal computed tomography (CT) and fluorodeoxyglucose (FDG) uptake in the bilateral adrenal glands on positron emission tomography (PET) have been reported; however, similar findings may be observed in cases of adrenal metastasis, which warrant careful judgment [32]. With regard to the pathogenesis of primary adrenal insufficiency caused by ICI treatment, adrenal autoantibodies have been detected in one case of pembrolizumab-induced adrenal insufficiency, although several points remain to be clarified [31].

4. Thyroid Dysfunction

Among endocrinopathies occurring as irAEs, thyroid dysfunction is the most frequent. Although thyroid dysfunction is mainly caused by thyrotoxicosis, while hypothyroidism is caused by destructive thyroiditis, the occurrence of Basedow's disease after the administration of anti CTLA-4 antibodies has also been reported [33,34]. The reported incidence of thyroid dysfunction with the use of anti-PD-1 antibodies is 5–10%. The incidence of thyroid dysfunction is higher with the use of anti-PD-L1 antibodies (0–5%) and anti-CTLA-4 antibodies (0–5%) [19–21]. In a previous systematic review and meta-analysis, increased use of combination treatment was observed, with hypothyroidism occurring in 16.4% cases treated with nivolumab combined with ipilimumab [12]. Moreover, the incidence of hypothyroidism was significantly higher with ICI treatment than with chemotherapy and placebo treatment [12]. In other studies, thyroid dysfunction was more frequent in cases treated with anti-thyroglobulin (Tg) antibody (anti-TgAb) and anti-thyroid peroxidase antibody (anti-TPOAb) than in cases treated without these antibodies before nivolumab treatment initiation; this finding may be beneficial for predicting the onset of thyroid dysfunction [35,36]. Destructive thyroiditis occurs within a few weeks after ICI treatment initiation in many cases, and it may present with thyrotoxicosis [37–39]. Subsequently, patients may exhibit a transition to hypothyroidism within 3–6 weeks [37–40]. In a previous study, 12 of 99 patients who received pembrolizumab developed thyrotoxicosis, and transition to hypothyroidism occurred in nine of the 12 patients [39]. Another study found thyrotoxicosis in six of 10 patients who developed indolent thyroiditis after pembrolizumab treatment initiation; all six patients exhibited a transition to hypothyroidism after four weeks [38].

Symptoms of thyrotoxicosis include palpitations, sweating, fever, diarrhea, tremors, weight loss, and general fatigue. Neck pain is generally not observed. Blood tests show a decreased serum TSH level, elevated serum free T3 (FT3) and free T4 (FT4) levels, and negativity for thyroid receptor antibody (TRAb). Quite often, anti-TgAb and anti-TPOAb are positive [30,36]. In addition, there are many cases in which the increased serum Tg level is recognized by destruction of the thyroid gland, and it is said that the Tg level normalizes upon transitioning to hypothyroidism [40]. Thyroid echography frequently shows decreased blood flow and an internal heterogeneous low signal intensity. FDG-PET also shows increased uptake, while thyroid scintigraphy shows decreased iodine uptake [38].

Hypothyroidism may develop after thyrotoxicosis or simultaneously with the onset of thyroiditis. If the latter occurs, positivity for anti-TgAb and anti-TPOAb is seen in several cases [37]. Major symptoms include general fatigue, loss of appetite, constipation, bradycardia, and weight gain. Blood tests show elevated serum TSH and decreased serum FT4 and FT3 levels. In mild cases, a slightly high TSH level may result in a state of occult hypothyroidism. Thyroid echography may show decreased blood flow, parenchymal hypointensity, and atrophy. Hypothyroidism secondary to hypopituitarism must be ruled out in patients showing hypothyroidism. Hypopituitarism can be suspected when serum FT4 levels are low and TSH levels are low to normal. Differentiation should be cautious because low serum FT3 levels also occur in the end stages of malignancy and in low T3 syndrome complicating

severe infections. In low T3 syndrome, the serum FT3 level is low and the serum FT4 level is normal or slightly decreased, while the serum TSH level is normal.

The mechanism by which ICIs cause thyroid dysfunction has not been clarified, but it has been suggested that the expression of PD-L1 and programmed death ligand 2 in the thyroid tissue plays a role [41].

5. Type 1 Diabetes Mellitus

Type 1 diabetes induced by ICI treatment results from the destruction of β-cells by ICIs and is reportedly more frequent with the use of anti-PD1/anti-PD-L1 antibodies. However, the reported incidences are 2.0% and 0.4% with nivolumab and pembrolizumab; thus, it seems to be a less common irAE [12]. The incidence of type I diabetes after ipilimumab treatment is even lower [20,42]. However, fulminant type I diabetes mellitus can worsen rapidly and prove fatal, and it is necessary to consider the possibility of this complication when administering ICIs. The time from anti-PD-1 therapy initiation to the onset of type 1 diabetes has been reported to be 13–504 days [43]. Symptoms include dry mouth, polydipsia, and polyuria due to hyperglycemia in mild-to-moderate cases. Severe disease is associated with ketosis, ketoacidosis, general fatigue, and disturbed consciousness, with further progression resulting in coma.

Fulminant type I diabetes mellitus exhibits a hyperacute onset over several days, and endogenous insulin is depleted at the time of diagnosis [44]. On the other hand, type I diabetes mellitus develops relatively slowly over the course of several weeks.

Because β-cell dysfunction is generally irreversible, it is important to make a diagnosis and initiate treatment before the development of ketoacidosis. Diabetes mellitus should be suspected when symptoms of hyperglycemia appear and fasting blood sugar and random blood sugar levels exceed 126 and 200 mg/mL, respectively. In such cases, definite diagnosis and diagnosis of the disease type should be performed.

Blood glucose levels may be elevated to approximately 200–300 mg/dL, although elevation to approximately 1000 mg/dL is also possible. The HbA1c level is also elevated, notwithstanding it is lower relative to the blood glucose level. The C peptide level gradually decreases in serum and urine, and anti-glutamic acid decarboxylase antibodies are generally absent.

6. Treatment

6.1. Hypopituitarism

Table 2 presents management strategies for hypopituitarism according to the Common Terminology Criteria for Adverse Events (CTCAE) grade. Treatment generally involves hormone replacement therapy. ACTH deficiency is treated with hydrocortisone (10 to 20 mg/day). High doses of glucocorticoids have been reported to improve pituitary enlargement [24,45]. On the other hand, it has been reported that high doses of glucocorticoids do not contribute to restoration of the secretory capacity of ACTH and are associated with relatively high mortality [24,45]. High-dose glucocorticoids are recommended only if the condition is associated with headache and pituitary enlargement with visual field damage. When both TSH and ACTH secretion disorders are present, hydrocortisone replacement therapy must be preceded by hormone replacement therapy. The use of ICIs in patients with treatment-induced hypopituitarism should be discontinued until treatment stabilizes their general condition.

Table 2. Management of hypopituitarism induced by immune checkpoint inhibitors.

CTCAE Grade	Management	Treatment of Adverse Event
Grade 1	• Hormone supplementation as needed	• Consider consultation with an endocrinologist • If adrenal insufficiency is suspected, start hydrocortisone 10–20 mg BID • Start testosterone or estrogen replacement therapy if needed
Grade 2	• Stop ICI treatment until symptoms stabilize by hormone supplementation • After amelioration of symptoms, resume administration of ICI	• Consult an endocrinologist • Consider pituitary imaging • Perform hormone replacement therapy as performed for Grade 1 events • Perform frequent thyroid function and other hormonal tests until baseline levels are achieved
Grade 3	• Same as above	• Consult an endocrinologist • Consider pituitary imaging • Perform a pituitary function test on hospitalization • If adrenal insufficiency is present, start hydrocortisone 15–30 mg BID • Perform hormone replacement therapy as performed for Grade 1 events • Perform frequent thyroid function and other hormonal tests until baseline levels are achieved
Grade 4	• Stop ICI treatment • Resume administration after recovery from crisis and stabilization of symptoms	• Perform full-body management during hospitalization • Consult an endocrinologist • Immediately start administration of hydrocortisone 100–200 mg BID • Physiological saline infusion under cardiac function monitoring • Consider pituitary imaging • Perform frequent thyroid function and other hormonal tests until baseline levels are achieved

CTCAE, Common Terminology Criteria for Adverse Events; ICI, immune checkpoint inhibitor; BID, bis in die

6.2. Adrenal Insufficiency

Table 3 presents management strategies for adrenal insufficiency according to the CTCAE grade. The condition should be managed according to its severity. Hydrocortisone (10–20 mg/day) replacement therapy should be initiated for patients with only laboratory abnormalities or mild symptoms that permit activities of daily living [46]. In case of adrenal crisis, systemic management and early administration of hydrocortisone are necessary. In all cases, consultation with an endocrinologist is recommended for medical care. If primary adrenal insufficiency due to ICI treatment occurs, the drugs should be discontinued and administered after stabilization of the patient's general condition by treatment.

Table 3. Management of adrenal insufficiency induced by immune checkpoint inhibitors.

CTCAE Grade	Management	Treatment of Adverse Event
Grade 1	• Hormone supplementation as needed • After amelioration of symptoms, resume administration of ICI	• Consult an endocrinologist • If adrenal insufficiency is suspected, start hydrocortisone 10–20 mg BID
Grade 2	• Stop ICI treatment until symptoms stabilize by hormone supplementation • After amelioration of symptoms, resume administration of ICI	• Consult an endocrinologist • Perform hormone replacement therapy as performed for Grade 1 events • Perform frequent hormonal tests until baseline levels are achieved
Grade 3	• Same as above	• Consult an endocrinologist • Perform an adrenal function test on hospitalization • If adrenal insufficiency is present, start hydrocortisone 15–30 mg BID
Grade 4	• Stop ICI treatment • Resume administration after recovery from crisis and stabilization of symptoms	• Perform full-body management during hospitalization • Consult an endocrinologist • Immediately start administration of hydrocortisone 100–200 mg BID • Physiological saline infusion under cardiac function monitoring • Perform an adrenal function test after the general condition has stabilized

CTCAE, Common Terminology Criteria for Adverse Events; ICI, immune checkpoint inhibitor.

6.3. Thyroid Dysfunction

Tables 4 and 5 show the management strategies for hyperthyroidism and hypothyroidism, respectively, according to the CTCAE grade. For thyrotoxicosis caused by destructive thyroiditis, antithyroid drugs are not necessary because the duration of symptoms is usually short. When symptoms

such as tremors and motivation are recognized, symptomatic treatment with a β-blocker is required. Antithyroid drugs are reserved for patients with Basedow's disease.

Table 4. Management of hyperthyroidism induced by immune checkpoint inhibitors.

CTCAE Grade	Management	Treatment of Adverse Event
Grade 1	• Continue ICI treatment	• Continue to monitor TSH and FT4 levels until hyperthyroidism disappears
Grade 2	• Stop ICI treatment until the symptoms ameliorate or test values become normal • After amelioration of symptoms, resume administration of ICI	• Consult an endocrinologist • Perform a thyroid function test every 2–3 weeks • If the thyroid poisoning does not resolve after 6–8 weeks, Graves' disease is differentiated
Grade 3 or 4	• Same as above	• Consult an endocrinologist • Start administration of β-blocker • Conduct clinical tests every 1–3 weeks • In case of thyroid crisis, treat the patient in the intensive care unit

CTCAE, Common Terminology Criteria for Adverse Events; ICI, immune checkpoint inhibitor; TSH, thyroid-stimulating hormone; FT4, free T4.

Table 5. Management of hypothyroidism induced by immune checkpoint inhibitors.

CTCAE Grade	Management	Treatment of Adverse Event
Grade 1	• Continue ICI treatment	• Continue to monitor TSH, FT3, and FT4 levels every 2–3 weeks
Grade 2	• Stop ICI treatment until the symptoms ameliorate or test values become normal • After amelioration of symptoms, resume administration of ICI	• Consult an endocrinologist • Start thyroid hormone replacement therapy if symptoms are present or the TSH level is high • If thyroid function is stable, perform a thyroid function test every 6 weeks
Grade 3 or 4	• Same as above	• Consult an endocrinologist • Start administration of β-blocker • In case of myxedema coma, treat the patient in the intensive care unit • Following stabilization of symptoms, treat as per the protocol for Grade 2 events

CTCAE, Common Terminology Criteria for Adverse Events; ICI, immune checkpoint inhibitor; TSH, thyroid-stimulating hormone; FT4, free T4; FT3, free T3.

In case of hypothyroidism, if the TSH level is <10 mIU/L and no symptoms are observed, ICI administration is continued and serum TSH, FT4, and FT3 levels are monitored. If the TSH level is ≥10 mIU/L and moderate symptoms are present, thyroid hormone replacement therapy is planned [37]. In case of concomitant adrenal insufficiency, careful monitoring is required, and thyroid hormone replacement should be preceded by the administration of hydrocortisone if the adrenal insufficiency worsens.

ICI treatment can be resumed when treatment with or without thyroid hormone replacement therapy results in amelioration of symptoms.

6.4. Type 1 Diabetes Mellitus

Insulin therapy is the mainstay of treatment for type 1 diabetes mellitus due to ICI treatment, and immediate treatment must be initiated. If ketosis or ketoacidosis is present, immediate-acting insulin should be continuously administered, along with intravenous saline infusion and electrolyte management. After the ketosis or ketoacidosis has improved, the patient can be switched to insulin therapy. Once insulin treatment reduces the blood glucose levels, ICI treatment can be resumed.

7. Adrenal Insufficiency in Tumor-Bearing Patients

As noted above, primary/secondary adrenal insufficiency is a less common but potentially fatal irAE, and it often includes adrenal crisis, in patients receiving ICIs. On the other hand, symptoms are often nonspecific, such as anorexia and malaise, which are also common symptoms in cancer patients. Adrenal insufficiency is also a common condition in cancer patients, and efforts must be made to detect it at an early stage.

Causes of adrenal insufficiency other than ICI treatment in cancer patients include steroid withdrawal syndrome, adrenal metastases from primary disease, and autoimmune adrenalitis.

Long-term corticosteroid treatment may be used for various purposes in cancer patients, including palliation of symptoms such as fatigue, resolution of cerebral edema, and treatment of drug-induced or radioactive organ damage. In addition, they are often administered during anticancer drug therapy. Long-term corticosteroid use causes hypothalamic–pituitary–adrenal suppression and adrenal atrophy. Steroid withdrawal syndrome may occur when steroids are suddenly reduced or discontinued, and many patients present with clinical features of acute adrenal insufficiency. It is necessary to pay attention to sudden dose reduction and discontinuation in patients who have been receiving long-term steroid treatment, and steroid withdrawal syndrome should be suspected when symptoms indicating adrenal insufficiency are observed. In case of steroid withdrawal syndrome, the symptoms rapidly disappear when the steroid dose is increased in most cases.

Moreover, when physical stresses such as diarrhea, trauma, and dehydration occur in patients receiving long-term corticosteroid treatment, relative steroid deficiency may develop and result in adrenal insufficiency symptoms. The causative disease should be treated, and the dose of the steroid drug should be increased. Failure to take appropriate measures may result in adrenal crisis and potentially fatal conditions. On the other hand, in cancer patients, metastatic adrenal tumors may cause adrenal insufficiency. A previous study involving autopsy of malignant tumors found adrenal metastasis in approximately 3% cases [47]. Further, chronic primary adrenocortical insufficiency due to metastatic adrenal tumors is rare and has been reported to occur in approximately 1% patients [47]. Even in cases of metastatic adrenal tumors, cortisol secretion is preserved until approximately 90% of the bilateral adrenal glands are destroyed, and the typical symptoms may not appear in many cases, which complicates diagnosis [48].

8. Adrenal Crisis

Adrenal crisis can occur when infection and injury are complicated by adrenocortical insufficiency, and it progresses to a fatal disease state via absolute and relative steroid deficiency. Primary/secondary adrenal insufficiency due to ICI treatment may also lead to adrenal crisis, and early diagnosis and appropriate measures should be implemented at onset. The initial symptoms of adrenal crisis, like those of adrenal insufficiency, are nonspecific and include general malaise, anesthesia, loss of appetite, weight loss, nausea, abdominal pain, and fever. However, after >12 h, consciousness disturbance and hypotension can occur.

Blood tests often show hyponatremia, hyperkalemia, hypoglycemia, dehydration, and eosinophilia. When adrenal crisis is suspected on the basis of the medical history and test results, immediate measures should be taken while excluding other conditions such as sepsis. Initial treatment includes infusion of a large volume of saline, glucose solution, and hydrocortisone. Measurements of blood cortisol and ACTH are useful for diagnosis.

9. Conclusions

In summary, endocrine dysfunction is a frequent irAE associated with ICI treatment. Anti-CTLA-4 antibodies often cause hypopituitarism, while anti-PD-1/anti-PD-L1 antibodies cause thyroid dysfunction. Primary adrenal insufficiency and type I diabetes mellitus are less frequent with all ICIs. Hypopituitarism may also cause secondary adrenal insufficiency via ACTH hyposecretion. Symptoms of adrenal insufficiency are nonspecific and common also in cancer patients; therefore, diagnosis may be difficult. Moreover, symptoms of adrenal insufficiency in cancer patients often have a background other than irAE caused by ICI in tumor bearing patients. While adrenal insufficiency leads to adrenal crisis in severe cases, type 1 diabetes mellitus may progress to fulminant disease; thus, both conditions should be detected and treated at the early stages. As the indications of ICIs expand, the number of irAEs episodes also tends to increase as shown in Figure 1. In the future, early detection

and proper management of endocrine dysfunction should be considered important for the treatment using ICI as mentioned above.
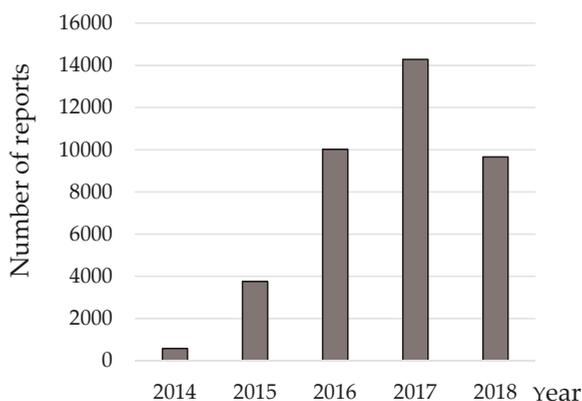
Figure 1. Adopted from Reference [49]. Food and Drug Administration (FDA)-reported numbers of immune-related Adverse Events (irAEs) with anti programmed cell death 1 (PD-1)/ programmed death ligand 1 (PD-L1) antibody monotherapy versus anti PD-1/PD-L1 antibody plus anti cytotoxic T-lymphocyte antigen-4 (CTLA-4) antibody combination treatment. (Number of reports up to June in 2018).

Author Contributions: Writing—original draft preparation, N.O., M.A., and J.U.; writing—review and editing, J.U., Y.M., M.I., Y.K., and T.Y.; supervision, M.F. and K.T. All authors have read and agreed to the published version of the manuscript.

Conflicts of Interest: The authors declare no conflict of interest.

References

1. Ribas, A.; Wolchok, J.D. Cancer immunotherapy using checkpoint blockade. *Science* **2018**, *359*, 1350–1355. [CrossRef]
2. Salomon, B.; Bluestone, J.A.C. Omplexities of Cd28/B7: Ctla-4 C Ostimulatory P Athways In A Utoimmunity And T Ransplantation. *Annu. Rev. Immunol.* **2001**, *19*, 225–252. [CrossRef] [PubMed]
3. Teft, W.A.; Kirchhof, M.G.; Madrenas, J. A molecular perspective of ctla-4 function. *Annu. Rev. Immunol.* **2006**, *24*, 65–97. [CrossRef] [PubMed]
4. Quezada, S.A.; Simpson, T.R.; Peggs, K.S.; Merghoub, T.; Vider, J.; Fan, X.; Blasberg, R.; Yagita, H.; Muranski, P.; Antony, P.A.; et al. Tumor-reactive CD4+ T cells develop cytotoxic activity and eradicate large established melanoma after transfer into lymphopenic hosts. *J. Exp. Med.* **2010**, *207*, 637–650. [CrossRef] [PubMed]
5. Bulliard, Y.; Jolicoeur, R.; Windman, M.; Rue, S.M.; Ettenberg, S.; Knee, D.A.; Wilson, N.S.; Dranoff, G.; Brogdon, J.L. Activating fc γ receptors contribute to the antitumor activities of immunoregulatory receptor-targeting antibodies. *J. Exp. Med.* **2013**, *210*, 1685–1693. [CrossRef]
6. Selby, M.J.; Engelhardt, J.J.; Quigley, M.; Henning, K.A.; Chen, T.; Srinivasan, M.; Korman, A.J. Anti-CTLA-4 antibodies of IgG2a isotype enhance antitumor activity through reduction of intratumoral regulatory T cells. *Cancer Immunol. Res.* **2013**, *1*, 32–42. [CrossRef] [PubMed]
7. Simpson, T.R.; Li, F.; Montalvo-Ortiz, W.; Sepulveda, M.A.; Bergerhoff, K.; Arce, F.; Roddie, C.; Henry, J.Y.; Yagita, H.; Wolchok, J.D.; et al. Fc-dependent depletion of tumor-infiltrating regulatory t cells co-defines the efficacy of anti-CTLA-4 therapy against melanoma. *J. Exp. Med.* **2013**, *210*, 1695–1710. [CrossRef]

8. Freeman, G.J.; Long, A.J.; Iwai, Y.; Bourque, K.; Chernova, T.; Nishimura, H.; Fitz, L.J.; Malenkovich, N.; Okazaki, T.; Byrne, M.C.; et al. Engagement of the PD-1 immunoinhibitory receptor by a novel B7 family member leads to negative regulation of lymphocyte activation. *J. Exp. Med.* **2000**, *192*, 1027–1034. [CrossRef]

9. Chang, L.S.; Barroso-Sousa, R.; Tolaney, S.M.; Hodi, F.S.; Kaiser, U.B.; Min, L. Endocrine toxicity of cancer immunotherapy targeting immune checkpoints. *Endocr. Rev.* **2018**, *40*, 17–65. [CrossRef]

10. Davies, M.; Duffield, E.A. Safety of checkpoint inhibitors for cancer treatment: Strategies for patient monitoring and management of immune-mediated adverse events. *ImmunoTargets Ther.* **2017**, *6*, 51–71. [CrossRef]

11. Postow, M.A. Managing Immune Checkpoint-Blocking Antibody Side Effects. *Am. Soc. Clin. Oncol. Educ. B* **2015**, 76–83. [CrossRef] [PubMed]

12. De Filette, J.; Andreescu, C.E.; Cools, F.; Bravenboer, B.; Velkeniers, B. A Systematic Review and Meta-Analysis of Endocrine-Related Adverse Events Associated with Immune Checkpoint Inhibitors. *Horm. Metab. Res.* **2019**, *51*, 145–156. [CrossRef] [PubMed]

13. Win, M.A.; Thein, K.Z.; Qdaisat, A.; Yeung, S.C.J. Acute symptomatic hypocalcemia from immune checkpoint therapy-induced hypoparathyroidism. *Am. J. Emerg. Med.* **2017**, *35*, 1039.e5–1039.e7. [CrossRef]

14. Umeguchi, H.; Takenoshita, H.; Inoue, H.; Kurihara, Y.; Sakaguchi, C.; Yano, S.; Hasuzawa, N.; Sakamoto, S.; Sakamoto, R.; Ashida, K. Autoimmune-Related Primary Hypoparathyroidism Possibly Induced by the Administration of Pembrolizumab: A Case Report. *J. Oncol. Pract.* **2018**, *14*, 449–451. [CrossRef] [PubMed]

15. Trinh, B.; Sanchez, G.O.; Herzig, P.; Läubli, H. Inflammation-induced hypoparathyroidism triggered by combination immune checkpoint blockade for melanoma. *J. Immunother. Cancer* **2019**, *7*. [CrossRef] [PubMed]

16. Piranavan, P.; Li, Y.; Brown, E.; Kemp, E.H.; Trivedi, N. Immune Checkpoint Inhibitor-Induced Hypoparathyroidism Associated with Calcium-Sensing Receptor-Activating Autoantibodies. *J. Clin. Endocrinol. Metab.* **2018**, *104*, 550–556. [CrossRef] [PubMed]

17. Caturegli, P.; Di Dalmazi, G.; Lombardi, M.; Grosso, F.; Larman, H.B.; Larman, T.; Taverna, G.; Cosottini, M.; Lupi, I. Hypophysitis Secondary to Cytotoxic T-Lymphocyte–Associated Protein 4 Blockade: Insights into Pathogenesis from an Autopsy Series. *Am. J. Pathol.* **2016**, *186*, 3225–3235. [CrossRef]

18. Bertrand, A.; Kostine, M.; Barnetche, T.; Truchetet, M.E.; Schaeverbeke, T. Immune related adverse events associated with anti-CTLA-4 antibodies: Systematic review and meta-analysis. *BMC Med.* **2015**, *13*. [CrossRef]

19. Byun, D.J.; Wolchok, J.D.; Rosenberg, L.M.; Girotra, M. Cancer immunotherapy-immune checkpoint blockade and associated endocrinopathies. *Nat. Rev. Endocrinol.* **2017**, *13*, 195–207. [CrossRef]

20. Barroso-Sousa, R.; Barry, W.T.; Garrido-Castro, A.C.; Hodi, F.S.; Min, L.; Krop, I.E.; Tolaney, S.M. Incidence of endocrine dysfunction following the use of different immune checkpoint inhibitor regimens a systematic review and meta-analysis. *JAMA Oncol.* **2018**, *4*, 173–182. [CrossRef]

21. González-Rodríguez, E.; Rodríguez-Abreu, D. Immune Checkpoint Inhibitors: Review and Management of Endocrine Adverse Events. *Oncologist* **2016**, *21*, 804–816. [CrossRef] [PubMed]

22. Cukier, P.; Santini, F.C.; Scaranti, M.; Hoff, A.O. Endocrine side effects of cancer immunotherapy. *Endocr. Relat. Cancer* **2017**, *24*, T331–T347. [CrossRef] [PubMed]

23. Zhao, C.; Tella, S.H.; Rivero, J.D.e.l.; Kommalapati, A.; Ebenuwa, I.; Gulley, J.; Strauss, J.; Brownell, I. Anti-PD-L1 treatment induced central diabetes insipidus. *J. Clin. Endocrinol. Metab.* **2018**, *103*, 365–369. [CrossRef] [PubMed]

24. Faje, A.; Reynolds, K.; Zubiri, L.; Lawrence, D.; Cohen, J.V.; Sullivan, R.J.; Nachtigall, L.; Tritos, N. Hypophysitis secondary to nivolumab and pembrolizumab is a clinical entity distinct from ipilimumab-associated hypophysitis. *Eur. J. Endocrinol.* **2019**, *181*, 211–219. [CrossRef]

25. Kanie, K.; Iguchi, G.; Bando, H.; Fujita, Y.; Odake, Y.; Yoshida, K.; Matsumoto, R.; Fukuoka, H.; Ogawa, W.; Takahashi, Y. Two Cases of Atezolizumab-Induced Hypophysitis. *J. Endocr. Soc.* **2018**, *2*, 91–95. [CrossRef]

26. Cho, K.Y.; Miyoshi, H.; Nakamura, A.; Kurita, T.; Atsumi, T. Hyponatremia can be a powerful predictor of the development of isolated ACTH deficiency associated with nivolumab treatment. *Endocr. J.* **2017**, *64*, 235–236. [CrossRef]

27. Okano, Y.; Satoh, T.; Horiguchi, K.; Toyoda, M.; Osaki, A.; Matsumoto, S.; Tomaru, T.; Nakajima, Y.; Ishii, S.; Ozawa, A.; et al. Nivolumab-induced hypophysitis in a patient with advanced malignant melanoma. *Endocr. J.* **2016**, *63*, 905–912. [CrossRef]

28. Albarel, F.; Gaudy, C.; Castinetti, F.; Carré, T.; Morange, I.; Conte-Devolx, B.; Grob, J.J.; Brue, T. Long-term follow-up of ipilimumab-induced hypophysitis, a common adverse event of the anti-CTLA-4 antibody in melanoma. *Eur. J. Endocrinol.* **2015**, *172*, 195–204. [CrossRef]

29. Ryder, M.; Callahan, M.; Postow, M.A.; Wolchok, J.; Fagin, J.A. Endocrine-related adverse events following ipilimumab in patients with advanced melanoma: A comprehensive retrospective review from a single institution. *Endocr. Relat. Cancer* **2014**, *21*, 371–381. [CrossRef]

30. Trainer, H.; Hulse, P.; Higham, C.E.; Trainer, P.; Lorigan, P. Hyponatraemia secondary to nivolumab-induced primary adrenal failure. *Endocrinol. Diabetes Metab. Case Rep.* **2016**, *2016*. [CrossRef]

31. Paepegaey, A.-C.; Lheure, C.; Ratour, C.; Lethielleux, G.; Clerc, J.; Bertherat, J.; Kramkimel, N.; Groussin, L. Polyendocrinopathy Resulting From Pembrolizumab in a Patient With a Malignant Melanoma. *J. Endocr. Soc.* **2017**, *1*, 646–649. [CrossRef]

32. Min, L.; Ibrahim, N. Ipilimumab-induced autoimmune adrenalitis. *Lancet Diabetes Endocrinol.* **2013**, *1*, e15. [CrossRef]

33. Inaba, H.; Ariyasu, H.; Okuhira, H.; Yamamoto, Y.; Akamatsu, H.; Katsuda, M.; Jinnin, M.; Hara, I.; Akamizu, T. Endocrine dysfunctions during treatment of immune-checkpoint inhibitors. *Trends Immunother.* **2018**, *2*. [CrossRef]

34. Gan, E.H.; Mitchell, A.L.; Plummer, R.; Pearce, S.; Perros, P. Tremelimumab-Induced Graves Hyperthyroidism. *Eur. Thyroid J.* **2017**, *6*, 167–170. [CrossRef] [PubMed]

35. Kimbara, S.; Fujiwara, Y.; Iwama, S.; Ohashi, K.; Kuchiba, A.; Arima, H.; Yamazaki, N.; Kitano, S.; Yamamoto, N.; Ohe, Y. Association of antithyroglobulin antibodies with the development of thyroid dysfunction induced by nivolumab. *Cancer Sci.* **2018**, *109*, 3583–3590. [CrossRef]

36. Kobayashi, T.; Iwama, S.; Yasuda, Y.; Okada, N.; Tsunekawa, T.; Onoue, T.; Takagi, H.; Hagiwara, D.; Ito, Y.; Morishita, Y.; et al. Patients With Antithyroid Antibodies Are Prone To Develop Destructive Thyroiditis by Nivolumab: A Prospective Study. *J. Endocr. Soc.* **2018**, *2*, 241–251. [CrossRef]

37. Alhusseini, M.; Samantray, J. Hypothyroidism in Cancer Patients on Immune Checkpoint Inhibitors with anti-PD1 Agents: Insights on Underlying Mechanisms. *Exp. Clin. Endocrinol. Diabetes* **2017**, *125*, 267–269. [CrossRef]

38. Orlov, S.; Salari, F.; Kashat, L.; Walfish, P.G. Induction of painless thyroiditis in patients receiving programmed death 1 receptor immunotherapy for metastatic malignancies. *J. Clin. Endocrinol. Metab.* **2015**, *100*, 1738–1741. [CrossRef]

39. De Filette, J.; Jansen, Y.; Schreuer, M.; Everaert, H.; Velkeniers, B.; Neyns, B.; Bravenboer, B. Incidence of thyroid-related adverse events in melanoma patients treated with pembrolizumab. *J. Clin. Endocrinol. Metab.* **2016**, *101*, 4431–4439. [CrossRef]

40. Delivanis, D.A.; Gustafson, M.P.; Bornschlegl, S.; Merten, M.M.; Kottschade, L.; Withers, S.; Dietz, A.B.; Ryder, M. Pembrolizumab-induced thyroiditis: Comprehensive clinical review and insights into underlying involved mechanisms. *J. Clin. Endocrinol. Metab.* **2017**, *102*, 2770–2780. [CrossRef]

41. Yamauchi, I.; Sakane, Y.; Fukuda, Y.; Fujii, T.; Taura, D.; Hirata, M.; Hirota, K.; Ueda, Y.; Kanai, Y.; Yamashita, Y.; et al. Clinical Features of Nivolumab-Induced Thyroiditis: A Case Series Study. *Thyroid* **2017**, *27*, 894–901. [CrossRef] [PubMed]

42. Shiba, M.; Inaba, H.; Ariyasu, H.; Kawai, S.; Inagaki, Y.; Matsuno, S.; Iwakura, H.; Yamamoto, Y.; Nishi, M.; Akamizu, T. Fulminant type 1 diabetes mellitus accompanied by positive conversion of anti-insulin antibody after the administration of anti-CTLA-4 antibody following the discontinuation of anti-PD-1 antibody. *Intern. Med.* **2018**, *57*, 2029–2034. [CrossRef]

43. Baden, M.Y.; Imagawa, A.; Abiru, N.; Awata, T.; Ikegami, H.; Uchigata, Y.; Oikawa, Y.; Osawa, H.; Kajio, H.; Kawasaki, E.; et al. Characteristics and clinical course of type 1 diabetes mellitus related to anti-programmed cell death-1 therapy. *Diabetol. Int.* **2019**, *10*, 58–66. [CrossRef] [PubMed]

44. Imagawa, A.; Hanafusa, T.; Awata, T.; Ikegami, H.; Uchigata, Y.; Osawa, H.; Kawasaki, E.; Kawabata, Y.; Kobayashi, T.; Shimada, A.; et al. Report of the Committee of the Japan Diabetes Society on the Research of Fulminant and Acute-onset Type 1 Diabetes Mellitus: New diagnostic criteria of fulminant type 1 diabetes mellitus (2012). *J. Diabetes Investig.* **2012**, *3*, 536–539. [CrossRef] [PubMed]

45. Min, L.; Hodi, F.S.; Giobbie-Hurder, A.; Ott, P.A.; Luke, J.J.; Donahue, H.; Davis, M.; Carroll, R.S.; Kaiser, U.B. Systemic high-dose corticosteroid treatment does not improve the outcome of ipilimumab-related hypophysitis: A retrospective cohort study. *Clin. Cancer Res.* **2015**, *21*, 749–755. [CrossRef] [PubMed]

46. Yanase, T.; Tajima, T.; Katabami, T.; Iwasaki, Y.; Tanahashi, Y.; Sugawara, A.; Hasegawa, T.; Mune, T.; Oki, Y.; Nakagawa, Y.; et al. Diagnosis and treatment of adrenal insufficiency including adrenal crisis: A Japan endocrine society clinical practice guideline. *Endocr. J.* **2016**, *63*, 765–784. [CrossRef] [PubMed]

47. Lam, K.-Y.; Lo, C.-Y. Metastatic tumours of the adrenal glands: A 30-year experience in a teaching hospital. *Clin. Endocrinol. (Oxf).* **2002**, *56*, 95–101. [CrossRef]

48. Barker, N.W. The pathologic anatomy in twenty-eight cases of Addison's disease. *Arch. Pathol.* **1929**, *8*, 432–450.

49. Raschi, E.; Mazzarella, A.; Antonazzo, I.C.; Bendinelli, N.; Forcesi, E.; Tuccori, M.; Moretti, U.; Poluzzi, E.; De Ponti, F. Toxicities with Immune Checkpoint Inhibitors: Emerging Priorities From Disproportionality Analysis of the FDA Adverse Event Reporting System. *Target Oncol.* **2019**, *14*, 205–221. [CrossRef]

Immune Checkpoint Inhibitors for Lung Cancer Treatment: A Review

Keisuke Onoi, Yusuke Chihara, Junji Uchino *, Takayuki Shimamoto, Yoshie Morimoto, Masahiro Iwasaku, Yoshiko Kaneko, Tadaaki Yamada and Koichi Takayama

Department of Pulmonary Medicine, Graduate School of Medical Science, Kyoto Prefectural University of Medicine, Kyoto 602-8566, Japan; onoi@koto.kpu-m.ac.jp (K.O.); c1981311@koto.kpu-m.ac.jp (Y.C.); m04035ts@koto.kpu-m.ac.jp (T.S.); yoshie-m@koto.kpu-m.ac.jp (Y.M.); miwasaku@koto.kpu-m.ac.jp (M.I.); kaneko-y@koto.kpu-m.ac.jp (Y.K.); tayamada@koto.kpu-m.ac.jp (T.Y.); takayama@koto.kpu-m.ac.jp (K.T.)
* Correspondence: uchino@koto.kpu-m.ac.jp; Tel.: +81-75-251-5513

Abstract: The treatment of lung cancer has changed drastically in recent years owing to the advent of immune checkpoint inhibitors (ICIs). A 1992 study reported that programmed cell death-1 (PD-1), an immune checkpoint molecule, is upregulated during the induction of T cell death. Since then, various immunoregulatory mechanisms involving PD-1 have been clarified, and the successful use of PD-1 blockers in anticancer therapy eventually led to the development of the current generation of ICIs. Nivolumab was the first ICI approved for treating lung cancer in 2014. Since then, various ICIs such as pembrolizumab, atezolizumab, and durvalumab have been successively introduced into clinical medicine and have shown remarkable efficacy. The introduction of ICIs constituted a major advancement in lung cancer treatment, but disease prognosis continues to remain low. Therefore, new molecular-targeted therapies coupled with existing anticancer drugs and radiotherapy have recently been explored. This review encompasses the current status, challenges, and future perspectives of ICI treatment in lung cancer.

Keywords: immune checkpoint inhibitors; non-small-cell lung cancer; PD-1; biomarker

1. Introduction

Among all malignancies, lung cancer showed the highest reported incidence and mortality in 2018 [1]. The prognosis of advanced and recurrent lung cancer is poor, and standard treatments with cytotoxic anticancer drugs have limited therapeutic effects. Recently, with the development of molecularly targeted drugs based on the results of genetic testing and immunotherapies for cancer, treatments for non-small cell lung cancer have undergone remarkable development. Molecularly targeted drugs for cancer can differentiate between cancer cells and normal cells at the genome and molecule levels and act by specifically suppressing the molecules required for cancer growth and metastasis. Cytotoxic drugs are different as they have defined molecular targets from the stage of drug discovery and therapy design, and their targets are often biomarkers, especially those predicted for treatment. In non-small cell lung cancer (NSCLC), driver oncogene mutations, which confer advantages to the growth and viability of cancer cells, are the mainstay of biomarkers. EGFR gene mutations, ALK gene translocations, ROS1 gene translocations, and BRAF gene mutations have been used, and tyrosine kinase inhibitors targeting these aberrations have elicited high response rates.

Since around 1970, immunotherapy has been initiated for lung cancer with nonspecific treatments such as OK-432, and has progressed to specific immunotherapies such as peptide vaccine therapy. However, no treatment has shown apparent efficacy beyond the standard of care with cytotoxic anticancer drugs. In recent years, as the detailed mechanism of tumor immunotherapy is understood, and anti PD-1 antibodies, one of the immune checkpoint inhibitors, have shown good results in

clinical trials with increasing insurance support, the treatment of lung cancer has entered a new era. Several trials in advanced NSCLC have reported improved survival with anti-PD-1/PD-L1 antibodies treatment, both when used alone and in combination with chemotherapy (Table 1). This article thus elaborates on the immune checkpoint inhibitors used for treating lung cancer.

Table 1. Trials of ICIs for advanced stage NSCLC.

Trial	Patient Population	Treatment Regimen	Primary Outcome Results
CheckMate 017	Stage IIIB/IV squamous NSCLC; disease recurrence after platinum-based chemotherapy	Nivolumab	Median OS: 9.2 months (95% CI: 7.3–13.3); 12 months OS: 42% (95% CI: 34–50%)
CheckMate 057	Stage IIIB/IV non-squamous NSCLC; disease recurrence after platinum-based chemotherapy	Nivolumab	Median OS: 12.2 months (95% CI: 9.7–15.1); 18 months OS: 39% (95% CI: 34–45%)
OAK	Stage IIIB/IV; disease progression after platinum-based chemotherapy	Atezolizumab	Median OS: 13.8 months (95% CI: 11.8–15.7); PP-ITT; improved OS/PFS in patients with PD-L1 expression > 1%
IMpower 150	Stage IIIB/IV; untreated metastatic non-squamous NSCLC	Chemotherapy + Bevacizumab ± Atezolizumab	Median PFS: 8.3 months (95% CI: 7.7–9.8); Median OS: 19.8 months (95% CI: 17.4–24.2)
KEYNOTE 024	Stage IV; untreated disease; PD-L1 expression > 50%	Pembrolizumab	Median PFS: 10.3 months (95% CI: 6.7–NR); 6 months PFS: 62.1% (95% CI: 53.8–69.4%)
KEYNOTE 189	Stage IIIB/IV; untreated metastatic non-squamous NSCLC	Chemotherapy ± Pembrolizumab	Median OS: 22.0 months (95% CI: 19.5–25.2); 12 months OS: 69.2% (95% CI: 64.1–73.8%)
KEYNOTE 407	Stage IIIB/IV; untreated metastatic squamous NSCLC	Chemotherapy ± Pembrolizumab	Median OS: 15.9 months (95% CI: 13.2–NR); 12 months OS: 65.2% (95% CI: 57.7–71.6%)

ICIs: Immune checkpoint inhibitors; NSCLC: non-small cell lung cancer; PD-L1: programmed cell-death ligand 1; OS: overall survival; PFS: progression-free survival; NR: not reached.

2. Mechanism of Action of Immune Checkpoint Inhibitors (ICIs)

Although cancer cells are formed daily, almost all of them are properly eliminated through the host immune response. Immune responses to cancer cells are called cancer-immunity cycles and comprise seven phases: (1) release of cancer antigens by the death of cancer cells, (2) presentation of cancer antigens to T cells by antigen-presenting cells such as dendritic cells, (3) T cell activation (priming phase), (4) T cell migration, (5) T cell infiltration, (6) cancer cell recognition, and (7) attack and elimination of cancer cells (effector phase) [2]. However, cancer cells with low immunogenicity, which do not present cancer antigens, may evade this autoimmune response and survive for a longer duration (equilibrium phase) [2,3]. Further, immunosuppressive mechanisms activated upon the accumulation of mutations in cancer cells, the induction of regulatory T cells (Tregs) and immunosuppressive cells including myeloid-derived suppressor cells (MDSCs), and the expression of immune checkpoint molecules such as PD-L1 result in uncontrolled tumor growth (escape phase) [2,3]. Thus, certain cancers are detected only after the cancer cells approach the escape phase and undergo uncontrolled proliferation, having already established a system preventing them from being eliminated through the autoimmune response.

ICIs are drugs that block the immunosuppressive mechanisms of cancer cells (Figure 1). ICIs exert their antitumor effects by harnessing host autoimmune functions, as opposed to cytocidal anticancer drugs, which inhibit the cell cycle, and agents that directly attack cancer cells, such as molecularly targeted drugs that specifically bind to gene mutation sites and suppress proliferative signals. Currently, anti-PD-1/PD-L1 antibodies are clinically used to treat lung cancer and various other cancers. In lung cancer, PD-L1 expression is used as one of the biomarkers to distinguish the treatment indication cases. Microsatellite instability has also been used as a potential anti-PD-1/PD-L1 antibodies treatment biomarker in gastric cancer, mainly as a second-line treatment after standard treatment, in triple-negative breast cancer, and as a biomarker candidate in colorectal cancer. In 2011, monotherapy with ipilimumab, an anticytotoxic T-lymphocyte antigen 4 (CTLA-4) antibody, was approved by the food and drug administration (FDA) for advanced-stage malignant melanoma, and in 2015, the combination of nivolumab and ipilimumab was approved by the FDA for use in clinical practice. Studies comparing ipilimumab+nivolumab with sunitinib alone in renal cell carcinoma and the combination of ipilimumab+nivolumab in non-small cell lung cancer have shown favorable results [4,5]. Regarding the significance of ipilimumab in combination therapy, future results are awaited as to whether two-drug combinations of immune checkpoint inhibitors (ipilimumab and nivolumab combination therapy) can contribute to higher survival rates than either immune checkpoint inhibitors alone or immune checkpoint inhibitors in combination with chemotherapy. Since numerous aspects of the mechanism of action of ICIs in vivo are unclear, this review discusses the generally considered mechanisms.
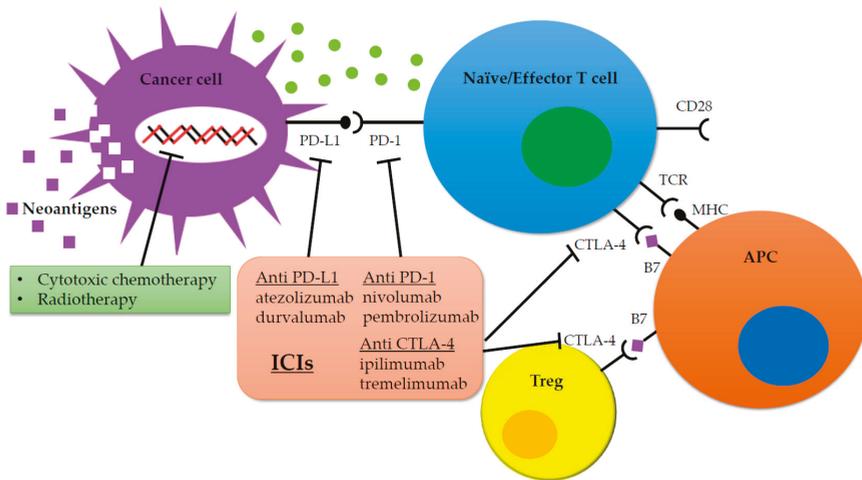
Figure 1. Immune checkpoint inhibitors in cancer treatment. Notes: Inability to activate T cells in the tumor microenvironment through the suppressive effect of Tregs or through immune checkpoints allows cancer cells to escape immune attack, survive, and grow. B7 ligands expressed on antigen-presenting cells bind to TCR and induce T cell amplification and immune response. Alternatively, binding of B7 ligands to CTLA-4 expressed on T cells suppresses their activity. CTLA-4 also enhances the activity of Tregs leading to immunosuppressive activity. PD-1 is expressed on activated T cells. PD-1 binds to its PD-L1 leading to the anergy of T cells, further promoting inhibitory signals. Pharmacological inhibition of immune checkpoints with monoclonal antibodies restores T cell antitumor activity and relieves immunosuppression. Abbreviations: CTLA-4: cytotoxic T-lymphocyte antigen 4; MHC: major histocompatibility complex; PD-1: programmed cell death-1; PD-L1: programmed cell death-1 ligand; TCR: T cell receptor; Tregs: regulatory T cells; APC: antigen presenting cell.

Anti-PD-1/PD-L1 antibodies act in the effector phase of the cancer-immunity cycle. In the effector phase, effector T cells attack cancer cells. However, binding of PD-L1 expressed on the cancer cell surface to PD-1 expressed on the surface of effector T cells suppresses the attack by effector T cells on cancer cells. Anti-PD-1/PD-L1 antibodies pharmacologically prevent the PD-1/PD-L1 interaction, thus facilitating the attack by T cells. Furthermore, these antibodies are thought to inhibit the immune response in the priming phase of the cancer-immunity cycle [6].

In contrast, anti-CTLA-4 antibodies act during antigen presentation in the priming phase, wherein dendritic cells present antigens to and activate T cells. T-cell activation requires both T-cell receptors (TCRs) and the MHCI-cancer antigen complex on the dendritic cells (principal stimulation), accompanied by the interaction between B7 (CD80/86) and CD28 on dendritic and T cells, respectively (costimulation) [7]. CTLA-4, like CD28, is expressed on the T cell surface and binds B7 with a stronger affinity than that of CD28. Thus, when CTLA-4 is upregulated, it remains bound to B7 and the costimulatory signal is not transmitted, resulting in the suppression of T cell activation [8]. Anti-CTLA-4 antibodies inhibit the binding of CTLA-4 and B7, resulting in enhanced binding of CD28 and B7, which stimulates T-cell activation and exerts antitumor effects (Figure 1) [9]. Furthermore, CTLA-4 is present on Treg surfaces, induced by cancer cells, and inhibits T-cell activation by binding to B7 on dendritic cells [10]. Thus, anti CTLA-4 antibodies are also thought to exert antitumor effects by facilitating the binding of Tregs to CTLA-4 and directly eliminating Tregs.

3. Changes in Treatment of Lung Cancer without Driver-Oncogene Mutations

Second-line therapy following platinum-based chemotherapy has long been cytotoxic therapies such a docetaxel (DTX).

In 2014, nivolumab, the world's first ICI targeting PD-1, emerged as a novel therapeutic agent for malignant melanoma. In 2015, a phase-III comparative study of DTX and nivolumab as secondary treatments for squamous and non-squamous lung cancers was conducted in the CheckMate017 (NCT01642004) and CheckMate057 (NCT01673867) studies, respectively; both studies reported that nivolumab significantly prolonged overall survival (OS) compared to DTX (CheckMate017: 6.0 mo vs. 9.2 mo, Hazard Ratio (HR) 0.59; CheckMate057: 9.4 mo vs. 12.2 mo, HR 0.73) [11,12]. Considering these findings, the indication of nivolumab was also expanded to the second-line treatment of NSCLC, and ICIs were approved for the first time for lung cancer treatment.

In 2016, another anti-PD-1 antibody, pembrolizumab, has been reported, and a phase-III comparative study of DTX and pembrolizumab as second-line therapy in NSCLC with PD-L1 ≥ 1% reported that pembrolizumab significantly prolonged patient survival compared to DTX (8.5 mo vs. 10.4 mo (pembro 2 mg/kg) /12.7 mo (pembro 10 mg/kg) [13]. Furthermore, the OAK trial (NCT02008227) compared the second-line NSCLC anti PD-L1 antibodies atezolizumab and DTX, and showed that atezolizumab prolonged survival significantly (9.6 mo vs. 13.8 mo, HR 0.73) [14]. Based on these results, pembrolizumab and atezolizumab, in addition to nivolumab, were introduced as the second-line treatment for NSCLC.

Subsequent to being established as a standard-of-care treatment for second-line therapy, in the KEYNOTE-024 study (NCT02142738) (2016), pembrolizumab significantly prolonged the overall survival (OS) of patients (10.3 mo vs. 6.0 mo, HR 0.60) [15] upon platinum-based chemotherapy as first-line therapy in a PD-L1 ≥ 50% NSCLC without driver mutations, and was approved for the first time as first-line treatment for NSCLC. In 2018, KEYNOTE-189 trial (NCT02578680) and KEYNOTE-407 trials (NCT02775435) assessed the efficacy of the combination of platinum-based chemotherapy and ICIs and approved this combination therapy as first-line treatment of lung cancer, as it significantly prolonged the OS compared to platinum-based chemotherapy alone (KEYNOTE-189 not reached (NR) vs. 11.3 mo, HR 0.49; KEYNOTE-407 15.9 mo vs. 11.3 mo, HR 0.64) [16,17] by combining pembrolizumab with platinum-based chemotherapy for non-squamous-cell lung cancer and squamous cell lung cancer, respectively. In the same year, maintenance therapy with chemoradiotherapy (CRT) followed by durvalumab drastically improved the progression-free survival (PFS) in comparison with CRT alone in unresectable stage III NSCLC in the PACIFIC study among patients with locally advanced lung cancer (16.8 mo vs. 5.6 mo, HR 0.52) [18], and thus, ICIs contributed to advancements in the standard-of-care treatment for locally advanced NSCLC for the first time in 20 y.

In 2019, the IMpower133 trial (NCT02763579) reported that the combination of atezolizumab with platinum-based chemotherapy, as first-line treatment of small-cell lung cancer (SCLC), prolonged both the PFS and OS (PFS 4.3 mo vs. 5.2 mo, HR 0.77; OS 10.3 mo vs. 12.3 mo, HR 0.70) [19]. ICIs are expected to be used to treat SCLC.

Thus, since 2016, ICIs have been widely used therapeutics in different settings from first-line to second-line and onwards, for locally advanced to advanced-stage NSCLC and SCLC and lung cancer.

4. Immune Combination Therapy

4.1. Combination with Chemotherapy

To enhance the efficacy of immunotherapy, the combination of platinum-based chemotherapy and ICIs has already been validated and introduced into actual clinical practice (Figure 1). As one of them, a comparative study of CDDP or CBDCA+Pemetrexed (PEM) plus pembrolizumab vs. CDDP or CBDCA+PEM was conducted in the KEYNOTE-189 trial, and the PFS was significantly higher in the ICI-combined group than in the chemotherapy group in PFS (8.8 mo vs. 4.9 mo, HR 0.52) and OS (NR vs. 11.3 mo, HR 0.49) [16], and this regimen was approved as first-line treatment for advanced-stage NSCLC. This study included a platinum-combination therapy, which has not been directly compared with ICI alone, and it thus remains controversial whether pembrolizumab alone or ICI plus chemotherapy is beneficial for patients with high PD-L1 expression levels. Upon ICI monotherapy, cases presenting

with cancer progression at an early stage pose a problem, whereas during combination therapy, it is advantageous to reduce progressive disease at early stages in combination treatment with cytotoxic anticancer drugs.

The therapeutic efficacy of atezolizumab as first-line therapy for NSCLC was reported in an IMpower150 trial (NCT02366143) in combination with CBDCA+paclitaxel (PTX)+bevacizumab (BEV) [19]. In this study, subgroup analyses confirmed the efficacy of ICIs among patients with hepatic metastases and driver mutations, which were previously poor responders to ICIs, suggesting the potential effects of the concomitant use of angiogenesis inhibitors. Combination therapy with angiogenesis inhibitors is expected in this regimen in cases with complications including cerebral edema and pleural effusion caused by brain metastasis.

Subsequently, the efficacy of CBDCA+nabPTX in combination with pembrolizumab was also reported in squamous cell carcinoma in a KEYNOTE-407 trial (NCT02775435) [17]; furthermore, the combination treatment with CBDCA+nabPTX and atezolizumab [20] yielded better outcomes than chemotherapy during first-line treatment of squamous cell lung cancer in the IMpower130 trial (NCT02367781). Clinical trials are currently underway for numerous combinations of ICIs and chemotherapy, including the IMpower132 trial (NCT02657434; CBDCA+PEM+ atezolizumab versus CBDCA+PEM in non-squamous lung cancer), TORG1630 trial (UMIN000021813; DTX+nivolumab versus DTX alone in NSCLC), KEYNOTE-604 trial (NCT03066778; pembrolizumab+ etoposide+carboplatin/cisplatin (EP) versus placebo+EP in SCLC), and CASPIAN trial (NCT03043872; durvalumab+tremelimumab+EP versus durvalumab+EP in SCLC).

Based on these results, various combinations of ICI plus platinum-based chemotherapy, ICI alone, and chemotherapy alone seemed appropriate as first-line treatment of advanced-stage NSCLC at present. It is thus important to examine the optimum treatment for each case on the basis of the factors including the performance status, PD-L1 expression rate, presence of driver gene mutations, and medical history.

4.2. Combination of ICIs

Combination therapy with different ICIs is currently being assessed, and the promising regimens include nivolmab+ipilimumab and durvalumab+tremelimumab. These studies have attempted to enhance the antitumor efficacy of immune cells by combining the inhibitors of PD-1/PD-L1 in the effector phase, using inhibitors of CTLA-4 in the priming phase.

In the CheckMate227 trial, a controlled trial involving combination therapy with nivolumab+ipilimumab and chemotherapy was conducted in 2019, and nivolumab+ipilimumab resulted in a significantly better OS among patients with PD-L1 $\geq$ 1% (17.1 mo vs. 14.9 mo, HR 0.79) [21]. Accordingly, combination therapy with an anti PD-1 antibody and anti CTLA-4 antibody can be clinically introduced for the first time. The POSEIDON trial (NCT03164616; durvalumab+tremelimumab+platinum-based chemotherapy) examining is also ongoing.

Alternatively, higher rates of immune-related adverse events (irAE) have been reported upon ICIs combination therapy. In studies including other carcinomas, anti CTLA-4 antibodies are reportedly associated with a higher incidence of grade-III or higher irAE (31% vs. 10%) compared to anti PD-1 antibodies [22]. In particular, colitis (odds ratio (OR) 8.7) and hypophysitis (OR 6.5) were primarily observed with anti-CTLA-4 antibody preparations, pneumonitis (OR 6.4) and thyroiditis (OR 4.3) observed with anti-PD-1 antibody preparation [22]. In the CheckMate227 study, AEs were more prevalent in the nivolumab+ipilimumab group than in the nivolumab monotherapy group in groups with both all grades/grade-III and above (all grades 75.2% vs. 64.2%, grade-III and above 31.2% vs. 18.9%), and AEs for which treatment could not be continued were also reported in the combination group (12% vs. 6.9%) [23]. Other study has reported that the concomitant use of nivolumab+ipilimumab results in an earlier onset of irAE (particularly within 12 weeks) in comparison with nivolumab alone [24]. Thus, on using ICIs, more prudent measures for irAE are required than those used before.

4.3. Combination with Radiation Therapy

In 2019, ICIs with high efficacy were reported for the treatment of unresectable stage III NSCLC. As noted above, in a PACIFIC study (NCT02125461) testing the efficacy of CRT followed by continued durvalumab treatment as consolidation, durvalumab treatment drastically improved the PFS and OS in comparison with the control group (PFS: 16.8 mo vs. 5.6 mo, HR 0.52, The 24-month overall survival rate: 66.3% vs. 55.6%, HR 0.68), leading to a major development of locally advanced-stage standard-of-care in the first 20 y [25]. In terms of the frequency of pneumonitis concerns associated with concomitant use of radiation therapy (RT) and ICIs, although pneumonitis was more common in the durvalumab group in all grades (13.1% vs. 7.7%), only a slight difference was observed between the two groups in ≥ grade-III NSCLC (4.4% vs. 3.8%, respectively), resulting in no apparent increase in the risk of serious pneumonitis [18]. The PACIFIC trial was designed to use durvalumab as a consolidation therapy in the first 42 d after the completion of CRT, whereas the ongoing PACIFIC2 trial is testing the efficacy of combination therapy with CRT and durvalumab, rather than sequential therapy (NCT03519971). The JCOG1508 studies have compared platinum-based chemotherapy + RT + durvalumab vs. platinum-based chemotherapy + RT → surgical resection + durvalumab in unresectable stage III NSCLC with N2 nodal involvement and have tested the effectiveness of durvalumab in the combined modality therapy including surgery.

5. Effects on SCLC

SCLC is a smoking-associated cancer type accounting for 10%–15% of all lung cancers. The median overall survival is 15–20 mo for limited-stage disease and 8–13 mo for extensive-stage disease, and the 5-y survival rate is 20–25% for limited-stage disease and 2% for extensive-stage disease among patients. In a phase-2 study on advanced SCLC conducted in 2011, the effectiveness of combination therapy with ipilimumab and chemotherapy was explored; however, the primary endpoint, i.e., OS prolongation, was not achieved [26]. Although ICIs for SCLC have yielded less encouraging results; the results of an IMpower133 trial published in 2019 led to the approval of CBDCA+etoposide+atezolizumab for untreated extensive-stage SCLC, as described previously [27]. The KEYNOTE-604 trial also compared pembrolizumab+EP vs. placebo+EP for untreated extensive-stage SCLC; this trial reported a significant prolongation in the PFS but not OS. In the ongoing CASPIAN trial, a three-arm comparative trial of durvalumab+tremelimumab+EP or durvalumab+EP vs. EP for untreated extensive-stage SCLC, among 268 patients receiving combination therapy with durvalumab and standard chemotherapy and 269 patients receiving standard chemotherapy alone, the median OS was significantly prolonged from 10.3 mo in the standard chemotherapy group to 13.0 mo in the combination therapy group [28]. Thus, future studies are required to develop more combination therapies with ICIs for SCLC.

Moreover, SCLC, unlike NSCLC and malignant melanoma, is generally characterized by a lower rate of PD-L1 expression [29]; however, the association between PD-L1 incidence and ICI efficacy has not been determined in SCLC. Nonetheless, TMBs are reportedly associated with the efficacy of ICIs in CheckMate026 trial [5]. The CheckMate032 trial compared the efficacy of nivolumab monotherapy with that of combination therapy with nivolumab+ipilimumab for previously treated SCLC, and the overall OS was 5.7 mo vs. 4.7 mo with no significant difference in efficacy between the combination therapy and monotherapy [30]. However, subgroup analysis revealed that combination therapy with nivolumab+ipilimumab displayed a higher efficacy than nivolumab monotherapy [30]. However, few studies have investigated the therapeutic utility of PD-L1 and the TMB in SCLC, warranting further validation in future studies.

6. Biomarkers

Although the efficacy of ICIs has been confirmed, the response rate to single agents is not as high as that of molecular-targeting agents, and the establishment of biomarkers to predict effective responses to ICIs remains challenging.

As a biomarker for therapeutic efficacy, PD-L1 has been recently used in actual clinical practice. The KEYNOTE-001 (NCT01295827) trial reported that pembrolizumab was more effective in decreasing the incidence of PD-L1 by ≥ 50%, by 1% to 49%, and by < 1% [31]. Particularly in the ≥ 50% group, patients with very high PD-L1 levels (≥ 90%) presented an even higher response rate than those with 50%–89% expression levels and presented prolonged PFS (objective response rate (ORR) 60.0% vs. 32.7%, PFS 14.5 mo vs. 4.1 mo, HR 0.50) [32]. Other studies have reported that PD-L1 upregulation, regardless of monotherapy or combination therapy, is associated with an increased efficacy of pembrolizumab [16,17,33]. Furthermore, the efficacy of ICIs other than pembrolizumab are also associated with PD-L1 upregulation [19,34], and generally, PD-L1 upregulation is associated with a higher ICI efficacy. Based on these results, we recommend using pembrolizumab monotherapy as the first-line therapy for PD-L1 positive (≥ 1%) advanced-stage NSCLC. It is also recommended to use PD-1/PD-L1 inhibitors for advanced-stage NSCLC in immune-checkpoint inhibitor-naïve patients as the second-line therapy.

However, the incidence and effects do not necessarily coincide, suggesting that tumor cell heterogeneity is one of the causes along with the potential involvement of host immune evasion mechanisms not mediated by PD-1/PD-L1 [35]. PD-L1 is often debated to be an incomplete biomarker, and several studies have as attempted to develop new biomarkers and to combine PD-L1 with other biomarkers.

While ICIs exert antitumor effects by activating immune cells, tumor infiltrating lymphocytes (TILs) are important in mediating these effects, along with PD-L1 [36]. T cells included in TILs may be enriched with clones specific for tumor antigens, but are suppressed by an immunosuppressive tumor microenvironment, and so on, and thus, they are believed to be incapable of exerting effective anti-tumor responses [37]. Results from a KEYNOTE-061 trial (NCT02370498) examining the usefulness of pembrolizumab as a second-line treatment for advanced gastric cancer reported that the effect of pembrolizumab may be predicted by the combined positive score, the number of PD-L1 positive cells among tumor cells, lymphocytes, and macrophages divided by the total number of tumor cells multiplied by 100 [38]. When the tumor microenvironment is subtyped into four types according to the presence or absence of PD-L1 expression and the presence or absence of TILs, TIL-positive/PD-L1 positive Type I and TIL-positive/PD-L1 negative Type IV are considered as "Hot tumors" in which anti-PD-1 antibodies are effective alone or in combination [36]. The usefulness of PD-L1 as a TIL biomarker has been reported in breast cancer [39], and similar studies are expected in future.

Other potential biomarkers include the total number of genetic mutations in cells, called tumor mutation burden (TMB). Mutated genes invariably yield mutated proteins, which are recognized as non-self by immune cells; hence, cells containing numerous mutated proteins are more susceptible to be attacked by immune cells, and cells with a high TMB are considered to display a more effective response to ICIs. In general, the TMB tends to be higher among smokers [40], and the relatively higher efficacy of ICI among smokers is speculated to result from the TMB [12,41]. In the 2017 CheckMate026 trial (NCT02041533), nivolumab was compared with platinum-based chemotherapy for first-line treatment of advanced-stage NSCLC with PD-L1 ≥ 5%, and nivolumab did not demonstrate superiority for the primary endpoint, PFS [5]. However, this study on exploratory TMB stratification analysis suggested that ICIs may be more effective in the high TMB group (TMB ≥ 243 nonsynonymous mutations) than in the low TMB group (TMB < 243 nonsynonymous mutations) (9.7 mo vs. 5.8 mo HR 0.62). A CheckMate227 trial (NCT02477826) (2019) comparing the efficacy of nivolumab+ipilimumab combination therapy vs. nivolumab monotherapy vs. platinum-based chemotherapy with TMB as a biomarker demonstrated the superiority of nivolumab+ipilimumab combination therapy to that of platinum-based chemotherapy; however, this tendency was stronger in the group with a high TMB (≥10 Mut/Mb) (global high: 23.0 mo vs. 16.4 mo, HR 0.68; low: 16.2 mo vs. 12.6 mo, HR 0.7, PD-L1 < 1% high: 20.4 mo vs. 11.2 mo, HR 0.51, low: 15.5 mo vs. 13.0 mo, HR 0.69) [23]. A CheckMate568 trial (NCT02659059) evaluated the safety and efficacy of concomitant nivolumab+ipilimumab combination therapy in the same year, reporting that the high-TMB group had a significantly prolonged PFS (7.1 mo

vs. 2.6 mo) [42]. Again, the results showed that TMBs and ORRs were predominantly associated in the group with PD-L1 < 1% (AUC 0.90) [42]. Consistent with the results of CheckMate568, the ORR with nivolumab plus ipilimumab in CheckMate227 was higher for tumors with PD-L1 > 1% compared with that for tumors with PD-L1 < 1% [21,42]. However, the relationship between the PD-L1 biomarker and efficacy of the combination of nivolumab and low-dose ipilimumab is complex, as in CheckMate227, there was a similar survival advantage for nivolumab and low-dose ipilimumab compared with that for standard chemotherapy in PD-L1-positive and PD-L1-negative tumors. Thus, the TMB (particularly in cases with PD-L1 < 1%) is reportedly associated with the efficacy of ICIs. At present, clinical trials considering TMBs as biomarkers are underway for atezolizumab (BFAST study: NCT03178552), and future studies are expected to yield clinically significant results.

The other reported potential benefits of these biomarkers include the prognostic nutritional index (PNI) and its association with the frequency of irAEs, neutrophil-to-lymphocyte ratio (NLR) [43], enterobacterial status [44,45], and early reduction in tumor markers [46].

Although the PNI was proposed as a predictor of surgical risk in the 1980s, it has been subsequently considered a useful marker to predict the efficacy of drugs to treat malignant diseases. Studies have reported that ICIs are more effective among patients with a high PNI, i.e., high nutritional status [47]. Further, numerous studies have reported that ICIs are more effective among patients with irAE [22,48], and that the management of adverse events is potentially important for the continuation of effective treatment.

7. Long-Term Survival

A major difference between ICIs and previously reported anticancer drugs is a substantial increase in long-term survival. On pooled analysis of the CheckMate017 and CheckMate057 trials (2019), both of which compared the efficacy of DTX and nivolumab as second-line therapy for NSCLC, the 5-y survival rate of nivolumab was 13.4%; DTX, 2.6% [49]. A 5-y survival rate of > 10% has not yet been achieved using previously reported cytocidal anticancer drugs, and ICIs resulted in a more prolonged long-term survival than conventional anticancer drugs. Furthermore, at 5 y, nivolumab treatment resulted in a response among 32.2% of patients, while no patients responded to DTX.

A follow-up report from the KEYNOTE-001 trial, a phase-I study on pembrolizumab, also reported a 5-y survival rate of 29.6% in the untreated, high PD-L1 group [50]. Notwithstanding a high long-term survival rate, the expression of PD-L1 and the frequency of TMBs are considered suitable predictors. Rizvi et al. reported that 62 patients with NSCLC, who received an ICI and acquired a PFS of ≥18 mo, presented significantly better outcomes on the basis of both PD-L1 and TMB in comparison with untreated patients (rate of PD-L1 TPS ≥ 50%: 43% vs. 23% TMB: 12.24 vs. 6.34 Mut/Mb) [51].

Though not observed in a majority of patients, treatment with immune checkpoint inhibitors may result in long-term survival, and establishment of biomarkers on long-term surviving cases is desirable.

8. Challenges Associated with ICIs

The development of ICIs is not without its challenges. Other than the aforementioned biomarkers, the following challenges may be considered.

8.1. Treatment of Patients Harboring a Driver Mutation

ICIs are clearly less effective among patients harboring driver mutations. Among other EGFR mutations, exon del19 is reported to result in a lower PFS than L858R on ICI treatment (del19 HR 0.449 p < 0.001, L858R HR 0.578 p = 0.001) [52]. Among these, the PFS, among patients harboring these mutations, was significantly higher when the PD-L1 expression rate was compared between the negative group (0%) and the positive group (≥1%) (2.8 mo vs. 1.7 mo) results [52], suggesting that PD-L1 expression rate may be related to the efficacy of ICIs, even among patients harboring driver mutations. Regimens combining atezolizumab with CBDCA+PTX+BEV in the IMpower150 trial were also effective among patients harboring driver mutations upon subgroup analysis [19], and we believe

that they hold promise as second-line treatment candidates upon using molecular-targeted agents. WJCOG8515L trial (UMIN000021133) have compared nivolumab with CBDCA+PEM in EGFR-TKI post-treatment NSCLC resistant cases through mechanisms other than T790M, and we believe that use of ICI for patients harboring driver mutations would be a future challenge.

8.2. Applicability Among Patients with a History of Interstitial Pneumonia or Autoimmune Disease

Managing irAE is of great importance with the use of ICIs. Characteristic adverse events that are less common but not experienced with cytotoxic anticancer drugs or molecular-targeted agents have become evident. Regarding disease management after manifestation, close cooperation among medical care departments is important as the AEs seem to be caused by immune activity in all organs.

Regarding the risk factors for irAE, ICIs activate the autoimmune system and induce antitumor effects. In patients with a history of autoimmune disease or interstitial pneumonitis, exacerbation of these underlying diseases or an increased incidence of irAE are worrisome and thus, cautious administration is recommended.

Furthermore, a higher incidence of smoking, and numerous cases with complications of smoking-related interstitial pneumonia have been reported. The use of ICIs among patients with interstitial pneumonia or autoimmune diseases is often excluded in clinical trials, and a few retrospective data have been reported.

Fujimoto et al. reported that 2 of 18 patients with mild-to-moderate idiopathic interstitial pneumonia had grade-II pneumonitis and that pneumonitis was alleviated in 6 patients with moderate pneumonitis upon nivolumab treatment [53]. The incidence of pneumonitis with previous ICIs did not significantly increase as the all-grade incidence of pneumonitis in ICIs ranged from 5% to 10%. On the contrary, Kanai et al. reported that the incidence of pneumonitis upon nivolumab treatment was significantly higher in the group with a history of interstitial pneumonia (31% vs. 12%), and 62% vs. 45% for grade-III or higher was associated with higher risks in the group with a history of interstitial pneumonia [54]. No deaths due to pneumonitis were recorded in these reports.

Leonardi et al. reported that treatment with ICIs alone among patients with autoimmune diseases resulted in disease exacerbation in 23% of patients, of which 32% required treatment with steroids [55]. Moreover, 38% developed some form of irAE, of which 26% were grade-III or higher [55]. Overall, 55% of patients experienced exacerbations of irAE, autoimmune disease, or both, and the incidence of irAE was similar to that in patients without autoimmune disease [55].

These reports on patients with a history of interstitial pneumonia or autoimmune disease provide retrospective data; however, it is considered necessary to exclude patients who judge the use of ICIs to be inappropriate based on their condition.

Studies wherein patients with interstitial pneumonia or autoimmune disease were administered ICIs have not provided adequate data on their safety and efficacy, and caution should be exercised with their use. In particular, the benefit for patients with high PD-L1 expression levels seems to be non-negligible, and individualized correspondence is required considering the balance with risk.

8.3. Co-Administration of Steroids

Tumor-bearing patients often receive steroids as symptomatic treatment for worsening systemic symptoms and symptoms due to cancer progression. In general, steroids are routinely administered as antiemetics during platinum-based chemotherapy. However, steroids may reduce the effects of ICIs by suppressing immune responses induced by IL-2 and CD8-positive T cells [56,57], and increasing Tregs [58,59].

Ricciuti et al. reported that patients receiving PSL-equivalent steroids at ≥10 mg on the initiation of ICI therapy had a significantly shorter survival (PFS 2.0 mo vs. 3.4 mo, HR 1.3; OS 4.9 mo vs. 11.2 mo, HR 1.7) than those receiving ICI-equivalent steroids at ≤10 mg [60]. On the contrary, the use of steroids for therapeutic purposes to counter irAE occurring during ICI treatment does not impair the efficacy

of ICI [61,62]. Thus, co-administration of steroids during ICI therapy remains a future challenge for lung cancer treatment.

9. Conclusions

ICIs have transformed the treatment of lung cancer. Although the number of patients with long-term survival after ICI treatment is significantly greater than that with previous therapies, such cases are limited, and novel therapies such as methods of selection and combination therapies that enhance efficacy remain an important issue to be resolved. The development of predictive factors for immunotherapy is crucial with regard to the efficacy of future treatment gains. Although both PD-L1 and TMBs may be helpful in case selection, it is now clear that resistance can develop by more than one mechanism. In future, further optimized treatments can be expected by combining cancer genomic information with the assessment results of cellular components from the tumor microenvironment. Although immunochemotherapy has shown great success in the treatment of lung cancer, it is expected that treatment will be individualized further on a case-by-case basis in future and will be improved by the development of combination treatments with targeted or cellular therapies, or new combinations of immunotherapies. Future challenges will likely involve targeting the correct immunotherapy to the correct immune microenvironment at an appropriate time. On the contrary, although not detailed in this article, the side effects of immune checkpoint inhibitors are very different from those of conventional cytocidal anticancer drugs and molecularly targeted drugs, spanning various organs including the skin and the digestive, respiratory, thyroid, and pituitary glands. These are considered side effects due to excessive autoimmune reactions, which are relatively infrequent and if present, are usually mild, allowing continued treatment with immune checkpoint inhibitors under careful management. However, adverse event management during treatment requires caution, as moderate to high immune-related adverse events are associated with markedly reduced organ function and quality of life, and fatal consequences have also been reported. Establishment of more appropriate usage methods such as the development of biomarkers and of combined immunotherapy is highly desired in the future.

References

1. Bray, F.; Ferlay, J.; Soerjomataram, I.; Siegel, R.L.; Torre, L.A.; Jemal, A. Global cancer statistics 2018: GLOBOCAN estimates of incidence and mortality worldwide for 36 cancers in 185 countries. *CA A Cancer J. Clin.* **2018**, *68*, 394–424. [CrossRef] [PubMed]
2. Chen, D.; Mellman, I. Oncology Meets Immunology: The Cancer-Immunity Cycle. *Immunity* **2013**, *39*, 1–10. [CrossRef] [PubMed]
3. Schreiber, R.D.; Old, L.J.; Smyth, M.J. Cancer Immunoediting: Integrating Immunity's Roles in Cancer Suppression and Promotion. *Science* **2011**, *331*, 1565–1570. [CrossRef] [PubMed]
4. Motzer, R.J.; Tannir, N.M.; McDermott, D.F.; Frontera, O.A.; Melichar, B.; Choueiri, T.K.; Plimack, E.R.; Barthelemy, P.; Porta, C.; George, S.; et al. Nivolumab plus Ipilimumab versus Sunitinib in Advanced Renal-Cell Carcinoma. *N. Engl. J. Med.* **2018**, *378*, 1277–1290. [CrossRef]
5. Carbone, D.P.; Reck, M.; Paz-Ares, L.; Creelan, B.; Horn, L.; Steins, M.; Felip, E.; Heuvel, M.M.V.D.; Ciuleanu, T.-E.; Badin, F.; et al. First-Line Nivolumab in Stage IV or Recurrent Non–Small-Cell Lung Cancer. *N. Engl. J. Med.* **2017**, *376*, 2415–2426. [CrossRef]
6. Hui, E.; Cheung, J.; Zhu, J.; Su, X.; Taylor, M.J.; Wallweber, H.A.; Sasmal, D.K.; Huang, J.; Kim, J.M.; Mellman, I.; et al. T cell costimulatory receptor CD28 is a primary target for PD-1–mediated inhibition. *Science* **2017**, *355*, 1428–1433. [CrossRef]

7. Sansom, D. CD28, CTLA-4 and their ligands: Who does what and to whom? *Immunology* **2000**, *101*, 169–177. [CrossRef]

8. Rowshanravan, B.; Halliday, N.; Sansom, D. CTLA-4: A moving target in immunotherapy. *Blood* **2018**, *131*, 58–67. [CrossRef]

9. Malas, S.; Harrasser, M.; Lacy, K.E.; Karagiannis, S.N. Antibody therapies for melanoma: New and emerging opportunities to activate immunity (Review). *Oncol. Rep.* **2014**, *32*, 875–886. [CrossRef]

10. Walunas, T.L.; Lenschow, D.J.; Bakker, C.Y.; Linsley, P.S.; Freeman, G.J.; Green, J.M.; Thompson, C.B.; Bluestone, J.A. CTLA-4 can function as a negative regulator of T cell activation. *Immunity* **1994**, *1*, 405–413. [CrossRef]

11. Brahmer, J.; Reckamp, K.L.; Baas, P.; Crino, L.; Eberhardt, W.E.; Poddubskaya, E.V.; Antonia, S.; Pluzanski, A.; Vokes, E.E.; Holgado, E.; et al. Nivolumab versus Docetaxel in Advanced Squamous-Cell Non-Small-Cell Lung Cancer. *N. Engl. J. Med.* **2015**, *373*, 123–135. [CrossRef] [PubMed]

12. Borghaei, H.; Paz-Ares, L.; Horn, L.A.; Spigel, D.R.; Steins, M.; Ready, N.E.; Chow, L.Q.; Vokes, E.E.; Felip, E.; Holgado, E.; et al. Nivolumab versus Docetaxel in Advanced Nonsquamous Non-Small-Cell Lung Cancer. *N. Engl. J. Med.* **2015**, *373*, 1627–1639. [CrossRef] [PubMed]

13. Herbst, R.S.; Baas, P.; Kim, N.-W.; Felip, E.; Pérez-Gracia, J.L.; Han, J.-Y.; Molina, J.; Kim, J.-H.; Arvis, C.D.; Ahn, M.-J.; et al. Pembrolizumab versus docetaxel for previously treated, PD-L1-positive, advanced non-small-cell lung cancer (KEYNOTE-010): A randomised controlled trial. *Lancet* **2016**, *387*, 1540–1550. [CrossRef]

14. Rittmeyer, A.; Barlesi, F.; Waterkamp, D.; Park, K.; Ciardiello, F.; Von Pawel, J.; Gadgeel, S.M.; Hida, T.; Kowalski, D.; Dols, M.C.; et al. Atezolizumab versus docetaxel in patients with previously treated non-small-cell lung cancer (OAK): A phase 3, open-label, multicentre randomised controlled trial. *Lancet* **2017**, *389*, 255–265. [CrossRef]

15. Reck, M.; Rodríguez-Abreu, D.; Robinson, A.G.; Hui, R.; Csőszi, T.; Fülöp, A.; Gottfried, M.; Peled, N.; Tafreshi, A.; Cuffe, S.; et al. Pembrolizumab versus Chemotherapy for PD-L1–Positive Non–Small-Cell Lung Cancer. *N. Engl. J. Med.* **2016**, *375*, 1823–1833. [CrossRef]

16. Gandhi, L.; Rodríguez-Abreu, D.; Gadgeel, S.; Esteban, E.; Felip, E.; De Angelis, F.; Dómine, M.; Clingan, P.; Hochmair, M.J.; Powell, S.F.; et al. Pembrolizumab plus Chemotherapy in Metastatic Non–Small-Cell Lung Cancer. *N. Engl. J. Med.* **2018**, *378*, 2078–2092. [CrossRef]

17. Paz-Ares, L.; Luft, A.; Vicente, D.; Tafreshi, A.; Gümüş, M.; Mazieres, J.; Hermes, B.; Çay Şenler, F.; Csőszi, T.; Fülöp, A.; et al. Pembrolizumab plus Chemotherapy for Squamous Non–Small-Cell Lung Cancer. *N. Engl. J. Med.* **2018**, *379*, 2040–2051. [CrossRef]

18. Antonia, S.J.; Villegas, A.; Daniel, D.; Vicente, D.; Murakami, S.; Hui, R.; Yokoi, T.; Chiappori, A.; Lee, K.H.; De Wit, M.; et al. Durvalumab after Chemoradiotherapy in Stage III Non-Small-Cell Lung Cancer. *N. Engl. J. Med.* **2017**, *377*, 1919–1929. [CrossRef]

19. Socinski, M.A.; Jotte, R.M.; Cappuzzo, F.; Orlandi, F.; Stroyakovskiy, D.; Nogami, N.; Rodríguez-Abreu, D.; Moro-Sibilot, D.; Thomas, C.A.; Barlesi, F.; et al. Atezolizumab for First-Line Treatment of Metastatic Nonsquamous NSCLC. *N. Engl. J. Med.* **2018**, *378*, 2288–2301. [CrossRef]

20. West, H.; McCleod, M.; Hussein, M.; Morabito, A.; Rittmeyer, A.; Conter, H.J.; Kopp, H.-G.; Daniel, D.; McCune, S.; Mekhail, T.; et al. Atezolizumab in combination with carboplatin plus nab-paclitaxel chemotherapy compared with chemotherapy alone as first-line treatment for metastatic non-squamous non-small-cell lung cancer (IMpower130): A multicentre, randomised, open-label, phase 3 trial. *Lancet Oncol.* **2019**, *20*, 924–937. [CrossRef]

21. Hellmann, M.D.; Paz-Ares, L.; Caro, R.B.; Zurawski, B.; Kim, S.-W.; Costa, E.C.; Park, K.; Alexandru, A.; Lupinacci, L.; Jimenez, E.D.L.M.; et al. Nivolumab plus Ipilimumab in Advanced Non–Small-Cell Lung Cancer. *N. Engl. J. Med.* **2019**, *381*, 2020–2031. [CrossRef] [PubMed]

22. Khoja, L.; Day, D.; Chen, T.W.-W.; Siu, L.L.; Hansen, A. Tumour- and class-specific patterns of immune-related adverse events of immune checkpoint inhibitors: A systematic review. *Ann. Oncol.* **2017**, *28*, 2377–2385. [CrossRef] [PubMed]

23. Hellmann, M.D.; Ciuleanu, T.-E.; Pluzanski, A.; Lee, J.S.; Otterson, G.A.; Audigier-Valette, C.; Minenza, E.; Linardou, H.; Burgers, S.; Salman, P.; et al. Nivolumab plus Ipilimumab in Lung Cancer with a High Tumor Mutational Burden. *N. Engl. J. Med.* **2018**, *378*, 2093–2104. [CrossRef] [PubMed]

24. Haanen, J.B.A.G.; Carbonnel, F.; Robert, C.; Kerr, K.M.; Peters, S.; Larkin, J.; Jordan, K.; ESMO Guidelines Committee. Management of toxicities from immunotherapy: ESMO Clinical Practice Guidelines for diagnosis, treatment and follow-up. *Ann. Oncol.* **2017**, *28*, iv119–iv142. [CrossRef]

25. Antonia, S.J.; Villegas, A.; Daniel, D.; Vicente, D.; Murakami, S.; Hui, R.; Kurata, T.; Chiappori, A.; Lee, K.H.; De Wit, M.; et al. Overall Survival with Durvalumab after Chemoradiotherapy in Stage III NSCLC. *N. Engl. J. Med.* **2018**, *379*, 2342–2350. [CrossRef]

26. Reck, M.; Luft, A.; Szczesna, A.; Havel, L.; Kim, S.-W.; Akerley, W.; Pietanza, M.C.; Wu, Y.-L.; Zielinski, C.; Thomas, M.; et al. Phase III Randomized Trial of Ipilimumab Plus Etoposide and Platinum Versus Placebo Plus Etoposide and Platinum in Extensive-Stage Small-Cell Lung Cancer. *J. Clin. Oncol.* **2016**, *34*, 3740–3748. [CrossRef]

27. Horn, L.; Mansfield, A.; Szczęsna, A.; Havel, L.; Krzakowski, M.; Hochmair, M.J.; Huemer, F.; Losonczy, G.; Johnson, M.L.; Nishio, M.; et al. First-Line Atezolizumab plus Chemotherapy in Extensive-Stage Small-Cell Lung Cancer. *N. Engl. J. Med.* **2018**, *379*, 2220–2229. [CrossRef]

28. Paz-Ares, L.; Dvorkin, M.; Chen, Y.; Reinmuth, N.; Hotta, K.; Trukhin, D.; Statsenko, G.; Hochmair, M.J.; Özgüroğlu, M.; Ji, J.H.; et al. Durvalumab plus platinum–etoposide versus platinum–etoposide in first-line treatment of extensive-stage small-cell lung cancer (CASPIAN): A randomised, controlled, open-label, phase 3 trial. *Lancet* **2019**, *394*, 1929–1939. [CrossRef]

29. Yoshimura, A.; Yamada, T.; Miyagawa-Hayashino, A.; Sonobe, Y.; Imabayashi, T.; Yamada, T.; Okada, S.; Shimamoto, T.; Chihara, Y.; Iwasaku, M.; et al. Comparing three different anti-PD-L1 antibodies for immunohistochemical evaluation of small cell lung cancer. *Lung Cancer* **2019**, *137*, 108–112. [CrossRef]

30. Ready, N.; Ott, P.A.; Hellmann, M.D.; Zugazagoitia, J.; Hann, C.L.; De Braud, F.; Antonia, S.J.; Ascierto, P.A.; Moreno, V.; Atmaca, A.; et al. Nivolumab Monotherapy and Nivolumab Plus Ipilimumab in Recurrent Small Cell Lung Cancer: Results From the CheckMate 032 Randomized Cohort. *J. Thorac. Oncol.* **2020**, *15*, 426–435. [CrossRef] [PubMed]

31. Hui, R.; Garon, E.B.; Goldman, J.W.; Leighl, N.B.; Hellmann, M.D.; Patnaik, A.; Gandhi, L.; Eder, J.P.; Ahn, M.-J.; Horn, L.; et al. Pembrolizumab as first-line therapy for patients with PD-L1-positive advanced non-small cell lung cancer: A phase 1 trial. *Ann. Oncol.* **2017**, *28*, 874–881. [CrossRef] [PubMed]

32. Aguilar, E.; Ricciuti, B.; Gainor, J.; Kehl, K.; Kravets, S.; Dahlberg, S.; Nishino, M.; Sholl, L.; Adeni, A.; Subegdjo, S.; et al. Outcomes to first-line pembrolizumab in patients with non-small-cell lung cancer and very high PD-L1 expression. *Ann. Oncol.* **2019**, *30*, 1653–1659. [CrossRef] [PubMed]

33. Mok, T.S.; Wu, Y.-L.; Kudaba, I.; Kowalski, D.M.; Cho, B.C.; Turna, H.Z.; Castro, G.; Srimuninnimit, V.; Laktionov, K.P.; Bondarenko, I.; et al. Pembrolizumab versus chemotherapy for previously untreated, PD-L1-expressing, locally advanced or metastatic non-small-cell lung cancer (KEYNOTE-042): A randomised, open-label, controlled, phase 3 trial. *Lancet* **2019**, *393*, 1819–1830. [CrossRef]

34. Park, S.; Choi, Y.-D.; Kim, J.; Kho, B.-G.; Park, C.-K.; Oh, I.-J.; Kim, Y.-C. Efficacy of immune checkpoint inhibitors according to PD-L1 tumor proportion scores in non-small cell lung cancer. *Thorac. Cancer* **2019**, *11*, 408–414. [CrossRef]

35. McGranahan, N.; Furness, A.J.S.; Rosenthal, R.; Ramskov, S.; Lyngaa, R.; Saini, S.K.; Jamal-Hanjani, M.; Wilson, G.A.; Birkbak, N.J.; Hiley, C.; et al. Clonal neoantigens elicit T cell immunoreactivity and sensitivity to immune checkpoint blockade. *Science* **2016**, *351*, 1463–1469. [CrossRef]

36. Teng, M.W.; Ngiow, S.F.; Ribas, A.; Smyth, M.J. Classifying Cancers Based on T-cell Infiltration and PD-L1. *Cancer Res.* **2015**, *75*, 2139–2145. [CrossRef]

37. Rosenberg, S.A.; Restifo, N.P. Adoptive cell transfer as personalized immunotherapy for human cancer. *Science* **2015**, *348*, 62–68. [CrossRef]

38. Shitara, K.; De Braud, F.; Mandalà, M.; Fornaro, L.; Olesiński, T.; Caglevic, C.; Muro, K.; Mansoor, W.; McDermott, R.; Chen, X.; et al. Pembrolizumab versus paclitaxel for previously treated, advanced gastric or gastro-oesophageal junction cancer (KEYNOTE-061): A randomised, open-label, controlled, phase 3 trial. *Lancet* **2018**, *392*, 123–133. [CrossRef]

39. Adams, S.; Schmid, P.; Rugo, H.; Winer, E.; Loirat, D.; Awada, A.; Cescon, D.; Iwata, H.; Campone, M.; Nanda, R.; et al. Pembrolizumab monotherapy for previously treated metastatic triple-negative breast cancer: Cohort A of the phase II KEYNOTE-086 study. *Ann. Oncol.* **2019**, *30*, 397–404. [CrossRef]

40. Gibbons, D.L.; Byers, L.A.; Kurie, J.M. Smoking, p53 mutation, and lung cancer. *Mol. Cancer Res.* **2014**, *12*, 3–13. [CrossRef]

41. Gainor, J.F.; Shaw, A.T.; Sequist, L.V.; Fu, X.; Azzoli, C.G.; Piotrowska, Z.; Huynh, T.G.; Zhao, L.; Fulton, L.; Schultz, K.R.; et al. EGFR Mutations and ALK Rearrangements Are Associated with Low Response Rates to PD-1 Pathway Blockade in Non-Small Cell Lung Cancer: A Retrospective Analysis. *Clin. Cancer Res.* **2016**, *22*, 4585–4593. [CrossRef] [PubMed]

42. Ready, N.; Hellmann, M.D.; Awad, M.M.; Otterson, G.A.; Gutierrez, M.; Gainor, J.F.; Borghaei, H.; Jolivet, J.; Horn, L.; Mates, M.; et al. First-Line Nivolumab Plus Ipilimumab in Advanced Non–Small-Cell Lung Cancer (CheckMate 568): Outcomes by Programmed Death Ligand 1 and Tumor Mutational Burden as Biomarkers. *J. Clin. Oncol.* **2019**, *37*, 992–1000. [CrossRef] [PubMed]

43. Jeyakumar, G.; Kim, S.; Bumma, N.; Landry, C.; Silski, C.; Suisham, S.; Dickow, B.; Heath, E.I.; Fontana, J.; Vaishampayan, U. Neutrophil lymphocyte ratio and duration of prior anti-angiogenic therapy as biomarkers in metastatic RCC receiving immune checkpoint inhibitor therapy. *J. Immunother. Cancer* **2017**, *5*, 82. [CrossRef] [PubMed]

44. Gopalakrishnan, V.; Spencer, C.N.; Nezi, L.; Reuben, A.; Andrews, M.C.; Karpinets, T.V.; Prieto, P.A.; Vicente, D.; Hoffman, K.; Wei, S.C.; et al. Gut microbiome modulates response to anti–PD-1 immunotherapy in melanoma patients. *Science* **2017**, *359*, 97–103. [CrossRef] [PubMed]

45. Sears, C.; Pardoll, E.M. The intestinal microbiome influences checkpoint blockade. *Nat. Med.* **2018**, *24*, 254–255. [CrossRef]

46. Lang, D.; Horner, A.; Brehm, E.; Akbari, K.; Hergan, B.; Langer, K.; Asel, C.; Scala, M.; Kaiser, B.; Lamprecht, B. Early serum tumor marker dynamics predict progression-free and overall survival in single PD-1/PD-L1 inhibitor treated advanced NSCLC—A retrospective cohort study. *Lung Cancer* **2019**, *134*, 59–65. [CrossRef]

47. Shoji, F.; Takeoka, H.; Kozuma, Y.; Toyokawa, G.; Yamazaki, K.; Ichiki, M.; Takeo, S. Pretreatment prognostic nutritional index as a novel biomarker in non-small cell lung cancer patients treated with immune checkpoint inhibitors. *Lung Cancer* **2019**, *136*, 45–51. [CrossRef]

48. Maher, V.E.; Fernandes, L.L.; Weinstock, C.; Tang, S.; Agarwal, S.; Brave, M.; Ning, Y.-M.; Singh, H.; Suzman, D.; Xu, J.; et al. Analysis of the Association Between Adverse Events and Outcome in Patients Receiving a Programmed Death Protein 1 or Programmed Death Ligand 1 Antibody. *J. Clin. Oncol.* **2019**, *37*, 2730–2737. [CrossRef]

49. Gettinger, S.; Borghaei, H.; Brahmer, J.; Chow, L.; Burgio, M.; Carpeno, J.D.C.; Pluzanski, A.; Arrieta, O.; Frontera, O.A.; Chiari, R.; et al. OA14.04 Five-Year Outcomes From the Randomized, Phase 3 Trials CheckMate 017/057: Nivolumab vs. Docetaxel in Previously Treated NSCLC. *J. Thorac. Oncol.* **2019**, *14*, 244–245. [CrossRef]

50. Garon, E.B.; Hellmann, M.D.; Rizvi, N.A.; Carcereny, E.; Leighl, N.B.; Ahn, M.-J.; Eder, J.P.; Balmanoukian, A.S.; Aggarwal, C.; Horn, L.; et al. Five-Year Overall Survival for Patients With Advanced Non-Small-Cell Lung Cancer Treated With Pembrolizumab: Results From the Phase I KEYNOTE-001 Study. *J. Clin. Oncol.* **2019**, *37*, 2518–2527. [CrossRef]

51. Rizvi, H.; Plodkowski, A.J.; Tenet, M.; Halpenny, D.; Long, N.; Sauter, J.L.; Sanchez-Vega, F.; Chatila, W.; Schultz, N.; Ladanyi, M.; et al. Clinical and molecular features predicting long-term response (LTR) to anti-PD-(L)1 based therapy in patients with NSCLC. *J. Clin. Oncol.* **2018**, *36*, 9022. [CrossRef]

52. Hastings, K.; Yu, H.; Wei, W.; Sanchez-Vega, F.; Deveaux, M.; Choi, J.; Rizvi, H.; Lisberg, A.; Truini, A.; Lydon, C.; et al. EGFR mutation subtypes and response to immune checkpoint blockade treatment in non-small-cell lung cancer. *Ann. Oncol.* **2019**, *30*, 1311–1320. [CrossRef] [PubMed]

53. Fujimoto, D.; Yomota, M.; Sekine, A.; Morita, M.; Morimoto, T.; Hosomi, Y.; Ogura, T.; Tomioka, H.; Tomii, K. Nivolumab for advanced non-small cell lung cancer patients with mild idiopathic interstitial pneumonia: A multicenter, open-label single-arm phase II trial. *Lung Cancer* **2019**, *134*, 274–278. [CrossRef] [PubMed]

54. Kanai, O.; Kim, Y.H.; Demura, Y.; Kanai, M.; Ito, T.; Fujita, K.; Yoshida, H.; Akai, M.; Mio, T.; Hirai, T. Efficacy and safety of nivolumab in non-small cell lung cancer with preexisting interstitial lung disease. *Thorac. Cancer* **2018**, *9*, 847–855. [CrossRef] [PubMed]

55. Leonardi, G.C.; Gainor, J.F.; Altan, M.; Kravets, S.; Dahlberg, S.E.; Gedmintas, L.; Azimi, R.; Rizvi, H.; Riess, J.W.; Hellmann, M.D.; et al. Safety of Programmed Death–1 Pathway Inhibitors Among Patients With Non–Small-Cell Lung Cancer and Preexisting Autoimmune Disorders. *J. Clin. Oncol.* **2018**, *36*, 1905–1912. [CrossRef] [PubMed]

56. Bianchi, M.; Meng, C.; Ivashkiv, L.B. Inhibition of IL-2-induced Jak-STAT signaling by glucocorticoids. *Proc. Natl. Acad. Sci. USA* **2000**, *97*, 9573–9578. [CrossRef]

57. Im, S.J.; Hashimoto, M.; Gerner, M.Y.; Lee, J.; Kissick, H.T.; Burger, M.C.; Shan, Q.; Hale, J.S.; Lee, J.; Nasti, T.H.; et al. Defining CD8+ T cells that provide the proliferative burst after PD-1 therapy. *Nature* **2016**, *537*, 417–421. [CrossRef] [PubMed]
58. Chen, X.; Murakami, T.; Oppenheim, J.J.; Howard, O. Differential response of murine CD4+CD25+and CD4+CD25-T cells to dexamethasone-induced cell death. *Eur. J. Immunol.* **2004**, *34*, 859–869. [CrossRef]
59. Chen, X.; Oppenheim, J.J.; Ortaldo, J.R.; Howard, O.; Winkler-Pickett, R.T. Glucocorticoid amplifies IL-2-dependent expansion of functional FoxP3+CD4+CD25+ T regulatory cellsin vivo and enhances their capacity to suppress EAE. *Eur. J. Immunol.* **2006**, *36*, 2139–2149. [CrossRef]
60. Ricciuti, B.; Dahlberg, S.E.; Adeni, A.; Sholl, L.M.; Nishino, M.; Awad, M.M. Immune Checkpoint Inhibitor Outcomes for Patients with Non–Small-Cell Lung Cancer Receiving Baseline Corticosteroids for Palliative Versus Nonpalliative Indications. *J. Clin. Oncol.* **2019**, *37*, 1927–1934. [CrossRef]
61. Santini, F.C.; Rizvi, H.; Plodkowski, A.J.; Ni, A.; Lacouture, M.E.; Gambarin-Gelwan, M.; Wilkins, O.; Panora, E.; Halpenny, D.F.; Long, N.M.; et al. Safety and Efficacy of Re-treating with Immunotherapy after Immune-Related Adverse Events in Patients with NSCLC. *Cancer Immunol. Res.* **2018**, *6*, 1093–1099. [CrossRef] [PubMed]
62. Horvat, T.; Adel, N.G.; Dang, T.-O.; Momtaz, P.; Postow, M.A.; Callahan, M.K.; Carvajal, R.D.; Dickson, M.A.; D'Angelo, S.P.; Woo, K.M.; et al. Immune-Related Adverse Events, Need for Systemic Immunosuppression, and Effects on Survival and Time to Treatment Failure in Patients With Melanoma Treated With Ipilimumab at Memorial Sloan Kettering Cancer Center. *J. Clin. Oncol.* **2015**, *33*, 3193–3198. [CrossRef] [PubMed]

MDPI